



Special Issue Reprint

---

# Obstetrics and Gynecology Medicine

Go From Bench to Bedside

---

Edited by  
Stefano Canosa and Anna Maria Nuzzo

[mdpi.com/journal/life](https://mdpi.com/journal/life)



# **Obstetrics and Gynecology Medicine: Go from Bench to Bedside**



# **Obstetrics and Gynecology Medicine: Go from Bench to Bedside**

Guest Editors

**Stefano Canosa**

**Anna Maria Nuzzo**



Basel • Beijing • Wuhan • Barcelona • Belgrade • Novi Sad • Cluj • Manchester



*Guest Editors*

Stefano Canosa  
IVIRMA Global Research  
Alliance  
Livet  
Turin  
Italy

Anna Maria Nuzzo  
Department of Surgical  
Sciences, Gynecology and  
Obstetrics 2  
University of Turin  
Turin  
Italy

*Editorial Office*

MDPI AG  
Grosspeteranlage 5  
4052 Basel, Switzerland

This is a reprint of the Special Issue, published open access by the journal *Life* (ISSN 2075-1729), freely accessible at: <https://www.mdpi.com/journal/life/special-issues/8MJ427ATRD>.

For citation purposes, cite each article independently as indicated on the article page online and as indicated below:

Lastname, A.A.; Lastname, B.B. Article Title. <i>Journal Name</i> <b>Year</b> , <i>Volume Number</i> , Page Range.
--------------------------------------------------------------------------------------------------------------------

**ISBN 978-3-7258-4396-1 (Hbk)**

**ISBN 978-3-7258-4395-4 (PDF)**

**<https://doi.org/10.3390/books978-3-7258-4395-4>**

© 2025 by the authors. Articles in this book are Open Access and distributed under the Creative Commons Attribution (CC BY) license. The book as a whole is distributed by MDPI under the terms and conditions of the Creative Commons Attribution-NonCommercial-NoDerivs (CC BY-NC-ND) license (<https://creativecommons.org/licenses/by-nc-nd/4.0/>).

# Contents

About the Editors . . . . .	ix
Preface . . . . .	xi
<b>Stefano Canosa and Anna Maria Nuzzo</b> Obstetrics and Gynecology Medicine: Go from Bench to Bedside Reprinted from: <i>Life</i> <b>2025</b> , <i>15</i> , 233, <a href="https://doi.org/10.3390/life15020233">https://doi.org/10.3390/life15020233</a> . . . . .	
	1
<b>Max T. Dufford, Tracey C. Fleischer, Laura J. Sommerville, Md. Bahadur Badsha, Ashoka D. Polpitiya, Jennifer Logan, et al.</b> Clock Proteins Have the Potential to Improve Term Delivery Date Prediction: A Proof-of-Concept Study Reprinted from: <i>Life</i> <b>2025</b> , <i>15</i> , 224, <a href="https://doi.org/10.3390/life15020224">https://doi.org/10.3390/life15020224</a> . . . . .	
	9
<b>Barbara Petra Kovács, Júlia Balog, Barbara Sebők, Márton Keszthelyi and Szabolcs Várbíró</b> Unlocking Female Fertility with a Specific Reproductive Exercise Program: Protocol of a Randomized Controlled Clinical Trial Reprinted from: <i>Life</i> <b>2025</b> , <i>15</i> , 18, <a href="https://doi.org/10.3390/life15010018">https://doi.org/10.3390/life15010018</a> . . . . .	
	27
<b>Inês Guerra de Melo, Valéria Tavares, Joana Savva-Bordalo, Mariana Rei, Joana Liz-Pimenta, Deolinda Pereira and Rui Medeiros</b> Endothelial Dysfunction Markers in Ovarian Cancer: VTE Risk and Tumour Prognostic Outcomes Reprinted from: <i>Life</i> <b>2024</b> , <i>14</i> , 1630, <a href="https://doi.org/10.3390/life14121630">https://doi.org/10.3390/life14121630</a> . . . . .	
	39
<b>Tibor Elekes, Gyula Csermely, Krisztina Kádár, László Molnár, Gábor Keszthelyi, Andrea Hozsdora, et al.</b> Learning Curve of First-Trimester Detailed Cardiovascular Ultrasound Screening by Moderately Experienced Obstetricians in 3509 Consecutive Unselected Pregnancies with Fetal Follow-Up Reprinted from: <i>Life</i> <b>2024</b> , <i>14</i> , 1632, <a href="https://doi.org/10.3390/life14121632">https://doi.org/10.3390/life14121632</a> . . . . .	
	56
<b>Alessandro Rolfo, Stefano Cosma, Anna Maria Nuzzo, Laura Moretti, Annalisa Tancredi, Stefano Canosa, et al.</b> Assessment of Placental Antioxidant Defense Markers in Vaccinated and Unvaccinated COVID-19 Third-Trimester Pregnancies Reprinted from: <i>Life</i> <b>2024</b> , <i>14</i> , 1571, <a href="https://doi.org/10.3390/life14121571">https://doi.org/10.3390/life14121571</a> . . . . .	
	70
<b>Balázs Vida, Balázs Lintner, Szabolcs Várbíró, Petra Merkely, Lotti Lúcia Lőczy, Nándor Ács, et al.</b> Assessing the Comparative Efficacy of Sentinel Lymph Node Detection Techniques in Vulvar Cancer: Protocol for a Systematic Review and Meta-Analysis Reprinted from: <i>Life</i> <b>2024</b> , <i>14</i> , 1538, <a href="https://doi.org/10.3390/life14121538">https://doi.org/10.3390/life14121538</a> . . . . .	
	81
<b>Danilo Cimadomo, Samuele Trio, Tamara Canosi, Federica Innocenti, Gaia Saturno, Marilena Taggi, et al.</b> Quantitative Standardized Expansion Assay: An Artificial Intelligence-Powered Morphometric Description of Blastocyst Expansion and Zona Thinning Dynamics Reprinted from: <i>Life</i> <b>2024</b> , <i>14</i> , 1396, <a href="https://doi.org/10.3390/life14111396">https://doi.org/10.3390/life14111396</a> . . . . .	
	86
<b>Victoria Psomiadou, Alexandros Fotiou and Christos Iavazzo</b> Mediastinal Metastasis Isolated in Ovarian Cancer: A Systematic Review Reprinted from: <i>Life</i> <b>2024</b> , <i>14</i> , 1098, <a href="https://doi.org/10.3390/life14091098">https://doi.org/10.3390/life14091098</a> . . . . .	
	104

<b>Ramona Coca, Andrei Moisin, Rafaela Coca, Atasie Diter, Mihaela Racheriu, Denisa Tanasescu, et al.</b> Exploring Therapeutic Challenges in Patients with HER2-Positive Breast Cancer— A Single-Center Experience Reprinted from: <i>Life</i> <b>2024</b> , <i>14</i> , 1025, <a href="https://doi.org/10.3390/life14081025">https://doi.org/10.3390/life14081025</a> . . . . .	<b>113</b>
<b>Chun-Gu Cheng, Sheng-Hua Su, Wu-Chien Chien, Ryan Chen, Chi-Hsiang Chung and Chun-An Cheng</b> Diabetes Mellitus and Gynecological and Inflammation Disorders Increased the Risk of Pregnancy Loss in a Population Study Reprinted from: <i>Life</i> <b>2024</b> , <i>14</i> , 903, <a href="https://doi.org/10.3390/life14070903">https://doi.org/10.3390/life14070903</a> . . . . .	<b>127</b>
<b>Carlos Delgado-Miguel, Javier Arredondo-Montero, Julio César Moreno-Alfonso, María San Basilio, Raquel Peña Pérez, Noela Carrera, et al.</b> The Role of Neutrophyl-to-Lymphocyte Ratio as a Predictor of Ovarian Torsion in Children: Results of a Multicentric Study Reprinted from: <i>Life</i> <b>2024</b> , <i>14</i> , 889, <a href="https://doi.org/10.3390/life14070889">https://doi.org/10.3390/life14070889</a> . . . . .	<b>140</b>
<b>Irinel-Gabriel Dicu-Andreescu, Marian-Augustin Marincas, Anca-Angela Simionescu, Ioana Dicu-Andreescu, Virgiliu-Mihail Prunoiu, Sânziana-Octavia Ionescu, et al.</b> Abdominal Parietal Metastasis from Cervical Cancer: A Review of One of the Most Uncommon Sites of Recurrence Including a Report of a New Case Reprinted from: <i>Life</i> <b>2024</b> , <i>14</i> , 667, <a href="https://doi.org/10.3390/life14060667">https://doi.org/10.3390/life14060667</a> . . . . .	<b>149</b>
<b>Leonard Jung, Gilbert Georg Klamming, Bert Bier and Elke Eltze</b> From Satirical Poems and Invisible Poisons to Radical Surgery and Organized Cervical Cancer Screening—A Historical Outline of Cervical Carcinoma and Its Relation to HPV Infection Reprinted from: <i>Life</i> <b>2024</b> , <i>14</i> , 307, <a href="https://doi.org/10.3390/life14030307">https://doi.org/10.3390/life14030307</a> . . . . .	<b>162</b>
<b>Dionysios Vrachnis, Alexandros Fotiou, Aimilia Mantzou, Vasilios Pergialiotis, Panagiotis Antsaklis, George Valsamakis, et al.</b> Second Trimester Amniotic Fluid Angiotensinogen Levels Linked to Increased Fetal Birth Weight and Shorter Gestational Age in Term Pregnancies Reprinted from: <i>Life</i> <b>2024</b> , <i>14</i> , 206, <a href="https://doi.org/10.3390/life14020206">https://doi.org/10.3390/life14020206</a> . . . . .	<b>177</b>
<b>Iuliana-Alina Enache, Cătălina Iovoaica-Rănescu, Ștefan Gabriel Ciobanu, Elena Iuliana Anamaria Berbecaru, Andreea Vochin, Ionuț Daniel Băluță, et al.</b> Artificial Intelligence in Obstetric Anomaly Scan: Heart and Brain Reprinted from: <i>Life</i> <b>2024</b> , <i>14</i> , 166, <a href="https://doi.org/10.3390/life14020166">https://doi.org/10.3390/life14020166</a> . . . . .	<b>187</b>
<b>Andreea Florea, Lavinia Caba, Ana-Maria Grigore, Lucian-Mihai Antoci, Mihaela Grigore, Mihaela I. Gramescu and Eusebiu Vlad Gorduza</b> Hydatidiform Mole—Between Chromosomal Abnormality, Uniparental Disomy and Monogenic Variants: A Narrative Review Reprinted from: <i>Life</i> <b>2023</b> , <i>13</i> , 2314, <a href="https://doi.org/10.3390/life13122314">https://doi.org/10.3390/life13122314</a> . . . . .	<b>204</b>
<b>Alessandro Bartolacci, Francesca Tondo, Alessandra Alteri, Lisett Solano Narduche, Sofia de Girolamo, Giulia D'Alessandro, et al.</b> The Task Matters: A Comprehensive Review and Proposed Literature Score of the Effects of Chemical and Physical Parameters on Embryo Developmental Competence Reprinted from: <i>Life</i> <b>2023</b> , <i>13</i> , 2161, <a href="https://doi.org/10.3390/life13112161">https://doi.org/10.3390/life13112161</a> . . . . .	<b>216</b>
<b>Yuting Xue, Nan Yang, Xunke Gu, Yongqing Wang, Hua Zhang and Keke Jia</b> Risk Prediction Model of Early-Onset Preeclampsia Based on Risk Factors and Routine Laboratory Indicators Reprinted from: <i>Life</i> <b>2023</b> , <i>13</i> , 1648, <a href="https://doi.org/10.3390/life13081648">https://doi.org/10.3390/life13081648</a> . . . . .	<b>230</b>

Vigneshwaran Subramaniam, Beng Kwang Ng, Su Ee Phon, Hamizan Muhammad Rafi'uddin, Abd Razak Wira Sorfan, Abd Azman Siti Hajar and Mohamed Ismail Nor Azlin	
Outcomes of Pregnancy in COVID-19-Positive Mothers in a Tertiary Centre	
Reprinted from: <i>Life</i> <b>2023</b> , <i>13</i> , 1491, <a href="https://doi.org/10.3390/life13071491">https://doi.org/10.3390/life13071491</a> . . . . .	<b>242</b>



# About the Editors

## **Stefano Canosa**

Stefano Canosa was educated at the University of Turin (Italy) where he received his Master's degree in Molecular Biotechnology and PhD in Biomedical Sciences, where his thesis was based on the development of a novel machine learning framework able to select human embryos based on their morphokinetic patterns. At the same University, he obtained his MMedSci degree in Human Reproductive Medicine and In Vitro Fertilization Techniques, and he is resident in Medical Genetics. He also earned an Advanced Training Certificate in Prenatal and Reproductive Genetics at the University of Padova. Currently, he is Senior Embryologist and Research Manager at IVIRMA Global Research Alliance, LIVET, Turin, Italy. In parallel, he actively contributes to prominent national and international societies: he is the Deputy Scientific Coordinator of the Italian Society of Embryology, Reproduction and Research (SIERR), Junior Deputy of the SIG Embryology of the European Society of Human Reproduction and Embryology (ESHRE), member of the ESHRE Young Talent Group, and member of the Working Group in Reproductive Genetics of the Italian Society of Human Genetics (SIGU). He has published over forty peer-reviewed papers (h-index = 15, >620 citations in Scopus) on clinical embryology, cryopreservation, time-lapse microscopy, reproductive genetics, and artificial intelligence as the main research topics

## **Anna Maria Nuzzo**

Anna Maria Nuzzo is a Doctor in Molecular Biotechnology and has a PhD in Biomedical Sciences and Oncology. She is trained in basic and molecular human pregnancy patho-physiology, with a particular interest in fetal-placental biology. During her PhD, she further focused her research interest on pre-eclampsia and placental-derived mesenchymal stromal cells (PDMSCs). In 2015, she moved to the University of Cambridge (UK) under the supervision of Prof. Dino Giussani, where she studied the role of the antioxidant MitoQ in animal models of pre-eclampsia. In September 2016, she moved back as a Post-Doctoral Fellow at the Department of Surgical Sciences of the University of Turin, where she actually works as a Research Scientist. Her current main research interest is the role of PDMSCs in patho-physiological placentation and their use as a new therapeutic tool for reproductive and women's health. She is a recipient of national and international awards from Fetal and Neonatal Physiological Society (FNPS), International Federation of Placental Association (IFPA), Società Italiana di Medicina Perinatale (SIMP) and "Madre e Feto" society. She is a member of the Fetal and Neonatal Society (FNPS) Executive Board.

She is the author of 24 peer-reviewed papers on feto-maternal medicine, pregnancy-related disorders and reproductive medicine (h-index = 13; 729 citations in Scopus).



# Preface

The field of obstetrics and gynecology stands at a pivotal moment, where the convergence of basic scientific research and clinical innovation is unlocking new opportunities to transform women's health. "Obstetrics and Gynecology Medicine: From Bench to Bedside" arises from a growing recognition of the need to bridge the divide between laboratory discoveries and clinical application. This volume reflects the dynamic evolution of reproductive healthcare and our collective commitment to translating scientific insights into meaningful patient outcomes.

In recent decades, remarkable progress has been made in understanding the intricate biology underlying reproductive function, pregnancy, and gynecologic disorders. Advances in molecular genetics, immunology, and biotechnology have deepened our understanding of complex conditions such as endometriosis, polycystic ovarian syndrome, infertility, and pregnancy-related complications. Yet, despite these strides, many challenges remain. The disease mechanisms are not fully understood, outcome predictions are often imprecise, and truly personalized treatment strategies remain an aspirational goal.

This reprint brings together a diverse and distinguished group of contributors, researchers and clinicians, who are leading the way in innovating obstetrics and gynecology. The chapters cover a broad spectrum of topics, ranging from foundational research to clinical trials and emerging therapies. Our aim is to present not only the current state of knowledge but also the ongoing challenges and future directions in the field.

By emphasizing both scientific rigor and clinical applicability, we hope to inspire a more integrated approach to research and care. We also hope that this volume will be a valuable resource for clinicians, researchers, and students who share a commitment to advancing women's health.

We extend our heartfelt thanks to all the contributors for their insights and dedication, and to our readers for joining us on this journey toward a more evidence-based, patient-centered future in obstetrics and gynecology.

**Stefano Canosa and Anna Maria Nuzzo**

*Guest Editors*





# Obstetrics and Gynecology Medicine: Go from Bench to Bedside

Stefano Canosa <sup>1,\*</sup> and Anna Maria Nuzzo <sup>2</sup>

<sup>1</sup> IVIRMA Global Research Alliance, LIVET, 10126 Turin, Italy

<sup>2</sup> Department of Surgical Sciences, Gynecology and Obstetrics 2, City of Health and Science-S. Anna University Hospital, University of Turin, 10126 Turin, Italy; a.nuzzo@unito.it

\* Correspondence: s.canosa88@gmail.com

## 1. Recalling the Special Issue Aims and Scope

As we reach the conclusion of this Special Issue, Obstetrics and Gynecology Medicine: Go From Bench to Bedside, it is evident that the dynamic intersection between basic science and clinical practice continues to drive the evolution of care in women's health. Over the last few decades, we have witnessed remarkable advancements in the understanding of reproductive biology, pregnancy complications, and gynecologic disorders. From the molecular mechanisms underlying endometriosis to breakthroughs in fertility preservation, these developments have reshaped the landscape of obstetrics and gynecology. Yet, despite significant strides, there remain critical gaps in our knowledge. We continue to face challenges in understanding the full etiology of many common conditions and how to treat them. Consequently, translating discoveries from the laboratory into widespread clinical applications remains a persistent obstacle, hindering the development of personalized treatments for patients. This Special Issue has sought to address some of these gaps by highlighting cutting-edge research that bridges the divide between basic science and clinical application. Through a curated collection of studies, we have explored innovative approaches in areas such as diagnoses, obstetrics, gynecological cancers, placental pathology, pregnancy loss, and assisted reproduction. These contributions underscore the importance of collaborative, interdisciplinary research in shaping the future of obstetrics and gynecology.

## 2. An Overview of Published Articles

The contributions to this Special Issue are listed in the section *List of Contributions* and are hereafter briefly overviewed.

The first contribution, from Elekes T et al. (Contribution 1), assessed the learning curve and the effectiveness of first-trimester fetal cardiovascular ultrasound screenings, providing that the curve may reach as high as 90% in terms of major congenital heart defects from an unselected pregnant population.

The second contribution, from Guerra de Melo I et al. (Contribution 2), investigated the impact of endothelial dysfunction (ED)-related genes and single-nucleotide polymorphisms (SNPs) on ovarian cancer (OC)-related venous thromboembolism (VTE) and patient thrombogenesis-independent prognosis. The authors observed that *NOS3* upregulation was linked to lower VTE incidence, while *SELP* upregulation was associated with shorter overall survival. Dismissing patients with VTE before OC diagnosis, *SELP rs6136 T* allele carriers presented lower progression-free survival.

The third contribution, from Rolfo A et al. (Contribution 3), investigated the impact of COVID-19 vaccination on third-trimester placental antioxidant defense markers. They

observed that SARS-CoV-2 infection induced placental oxidative stress (OxS), which is countered by a placental adaptive antioxidant response. Vaccination during pregnancy enhanced the placental defense, further supporting the safety and benefits of the COVID-19 vaccination in preventing complications and protecting fetal development.

The fourth contribution, from Cimadomo D et al. (Contribution 4), applied artificial intelligence to time-lapse microscopy to picture the association between embryo and inner-cell-mass (ICM) area, the ICM/Trophectoderm ratio, and the zona pellucida thickness at sequential blastocyst expansion stages, with (i) euploidy and (ii) live-birth per transfer. A quantitative standardized expansion assay (qSEA) was developed, outlining that faster and more consistent zp thinning processes can be observed among euploid blastocysts implanted versus not implanted blastocysts. qSEA can represent a promising objective, quantitative, and user-friendly strategy to predict embryo competence.

A fifth contribution, from Coca R et al. (Contribution 5), evaluated the status of *HER2* overexpression among new cases of breast neoplasia with an impact on the natural history of breast cancer disease and therapeutic personalization according to staging. Anti-*HER2* therapy in any therapeutic stage has shown increased efficiency in blocking tyrosine kinase receptors, evidenced by the high percentage of complete pathological responses, as well as the considerable percentage of complete remissions and stationary disease, in relation to the *HER2*-positive patient group.

A sixth contribution, from Cheng C et al. (Contribution 6), aimed to determine whether diabetes mellitus (DM) increases the risk of pregnancy loss and to identify other potential risk factors. The study concluded that DM together with older age, gynecological disorders, and inflammation disorders represent factors for greater risk of experiencing pregnancy loss. Healthcare providers should proactively manage and educate diabetic patients to reduce their risk of pregnancy loss.

A seventh contribution, from Delgado-Miguel C et al. (Contribution 7), aimed to determine the diagnostic value of clinical, ultrasound, and inflammatory laboratory markers in pediatric ovarian torsion (OT). It was established that the neutrophil-to-lymphocyte ratio (NLR) can be considered as a useful predictor of pediatric OT in cases with clinical and ultrasound suspicion. Values above 2.57 may help to anticipate urgent surgical treatment in these patients.

An eighth contribution, from Vrachnis D et al. (Contribution 8), investigated the associations of the amniotic fluid angiotensinogen of the renin–angiotensin system with fetal growth abnormalities. Multiple regression analysis revealed a statistically significant negative correlation between the angiotensinogen levels and gestational age and a statistically significant positive correlation between the birth weight and angiotensinogen levels. These findings suggest that fetal growth abnormalities did not correlate with differences in the amniotic fluid levels of angiotensinogen in early second-trimester pregnancies. However, increased angiotensinogen levels were found to be consistent with a smaller gestational age at birth and increased BMI of neonates.

A ninth contribution, from Xue Y et al. (Contribution 9), aimed to establish an early-onset pre-eclampsia prediction model by clinical characteristics, risk factors, and routine laboratory indicators from pregnant women at 6 to 10 gestational weeks. They observed that the performance of 12 clinical risk factors alone (among them, rates of diabetes, antiphospholipid syndrome (APS), kidney disease, obstructive sleep apnea (OSAHS), primipara, history of pre-eclampsia, and assisted reproductive technology (ART)) in predicting early-onset PE is poor, and the performance significantly improved when combining risk factors with the other 38 routine laboratory indicators. The support vector machine (SVM) model showed the best  $AUC^{ROC}$ , specificity, and sensitivity compared with a logistic regression model and decision tree model.

A tenth contribution, from Subramaniam V et al. (Contribution 10), aimed to determine the adverse maternal and fetal outcomes due to COVID-19 infection. Comparing early vs. severe stages of COVID-19 infection, it was shown that the severe-stage disease increased the risk of preterm birth and preterm birth before 34 weeks. The severe-stage disease also increased the Neonatal Intensive Care Unit (NICU) admission with lower birth weight. Moreover, the unvaccinated mothers had an increased risk of preterm birth before 34 weeks.

An eleventh contribution, from Dicu-Andreescu I et al. (Contribution 11), reviewed cases of abdominal parietal metastasis in recent decades, including a new case of a 4.5 cm abdominal parietal metastasis at the site of the scar of the former drain tube 28 months after the diagnosis of stage IIB cervical cancer (adenosquamous carcinoma), treated by external radiotherapy with concurrent chemotherapy and intracavitary brachytherapy and subsequent surgery (type B radical hysterectomy). The discussion explored the potential pathways for parietal metastasis and the impact of incomplete surgical procedures on the development of metastases.

A twelfth contribution, from Jung L et al. (Contribution 12), performed a literature search on cervical carcinoma and its relation to HPV infection. The diagnosis, the presence of HPV, and its role in cancer screening, together with the detection of new therapeutic options, were assessed across the history to continuously optimize cervical carcinoma diagnosis and treatment.

A thirteenth contribution, from Enache I et al. (Contribution 13), aimed to review the most relevant studies based on deep learning in ultrasound anomaly scan evaluation of the most complex fetal systems (heart and brain), which enclose the most frequent anomalies. AI can provide a more accurate and efficient method for identifying and diagnosing fetal anomalies, offering a promising avenue for future improvements in fetal healthcare.

A fourteenth contribution, from Flore A et al. (Contribution 14), describes the different types of hydatidiform moles and their subsequent mechanisms, which is useful to calculate the recurrence risk and estimate the method of progression to a malign form. This review synthesizes the heterogeneous mechanisms and their implications in genetic counseling.

A fifteenth contribution from Bartolacci A et al. (Contribution 15), provides a comprehensive review and proposed literature score of the effects of chemical and physical parameters on embryo developmental competence. Particularly, a prevalence of studies suggested a favor of the embryo culture performed at 37 °C and 5% oxygen.

A sixteenth contribution from Kovács BP et al. (Contribution 16), developed a 70 min full body “reproductive gymnastics”, including strengthening, stretching, and relaxation exercises combined with yoga-inspired moves and diaphragmatic breathing with meditation elements to activate the parasympathetic pathway and stress relief. In this way, fertility can be improved through the combination of natural supplements and our targeted, moderate physiotherapy program in women with an age-related decline of ovarian reserve.

A seventeenth contribution, from Vida B et al. (Contribution 17), represents a systematic review and meta-analysis protocol aiming to provide insights into the optimal sentinel lymph node (SLN) detection method with potential implications for clinical practice guidelines in vulvar cancer management.

An eighteenth contribution, from Psomiadou V et al. (Contribution 18), is a systematic review suggesting that solitary mediastinal metastasis from ovarian cancer is a very rare condition. Physicians should pay close attention when routinely evaluating thoracic scans from patients with ovarian malignancy as well as individualizing the management in such patients, since surgical resection can also be performed.

### 3. Discussion

Recent advances in translational research in obstetrics and gynecology have significantly impacted clinical practice, improved patient care, and introduced innovative approaches in the treatment of various conditions. Translational research plays a crucial role in bridging the gap between laboratory discoveries and their practical application in clinical settings. The rapid development of new diagnostic tools, therapeutic strategies, and improved clinical outcomes in this field can be attributed to the synergy between academic research and clinical practice, often supported by collaborations between public and private institutions.

#### 3.1. Recent Developments

Research has led to a better understanding and treatment of gynecological cancers, including ovarian, cervical, and endometrial cancers. New therapies that target specific molecular pathways are improving treatment outcomes and minimizing side effects. The integration of targeted therapies and immunotherapies has been a notable achievement, especially for advanced cancers. Personalized medicine, based on genetic profiling, is another example where research has been translated into more effective, individualized treatment plans [1]. Research into the molecular mechanisms behind conditions linked to placental pathology has provided insights into potential diagnostic biomarkers and novel therapeutic approaches. For instance, the identification of specific biomarkers that could predict the onset of pre-eclampsia earlier allows for timely interventions that improve maternal and fetal outcomes [2]. The discovery of new biomarkers for diagnosing and predicting outcomes in obstetrics and gynecology is transforming patient care. In ovarian cancer, for example, novel biomarkers are being explored to improve early detection and prognosis [3]. The automation of assisted reproductive technologies, such as in vitro fertilization (IVF), has made great strides, thanks to translational research. New automated systems for embryo culture, genetic screening, and embryo selection based on genetic and phenotypic characteristics are improving success rates and reducing human error. Furthermore, artificial intelligence (AI) and machine learning models are now being used to predict the success of IVF treatments more accurately, offering patient-tailored treatment plans based on a deeper understanding of their individual circumstances [4]. Consequently, personalized medicine is emerging as a powerful tool in obstetrics and gynecology, with translational research uncovering genetic, epigenetic, and environmental factors that influence disease progression and treatment responses.

#### 3.2. Gap in Knowledge

The process of transforming research innovations into new health products, as well as diagnostic and therapeutic strategies, remains a major issue of contemporary biomedical medicine due to several interconnected challenges. While significant advancements in scientific research have led to a deeper understanding of disease mechanisms and potential treatments, translating these findings into tangible, clinically effective products often takes years, if not decades. Addressing these hurdles—ranging from regulatory and financial obstacles to collaboration and accessibility issues—requires coordinated efforts among researchers, policymakers, industry leaders, and healthcare professionals.

#### 3.3. Special Issue Results

The contributions included in this Special Issue provided significant findings across oncology, prenatal care, and reproductive health.

The care of cancer patients is an extremely important issue in modern medicine. Optimizing diagnostic and treatment protocols will ensure a better prognosis and quality of

life for these patients. Recent advances in ovarian and breast cancer research have brought new hope for improved treatments and early detection. In ovarian cancer, researchers are making progress in identifying new genetic and molecular markers that will allow for earlier diagnoses and more precise targeting of therapies [5]. In this context, Guerra de Melo I et al. found that endothelial dysfunction-related genes and SNPs, in particular *NOS3* and *SELP*, significantly influenced the incidence of venous thromboembolism and overall survival in ovarian cancer patients, with the upregulation of certain genes correlating with better or worse outcomes (Contribution 2). In addition, Psomiadou V et al. highlighted the rarity of solitary mediastinal metastases in ovarian cancer, emphasizing the need for individualized treatment due to the unique challenges of this disease (Contribution 18). In breast cancer, ongoing research is focused on refining targeted therapies, particularly for specific subtypes such as *HER2*-positive and triple-negative breast cancer. New drug combinations, as well as innovations in immunotherapy and hormone therapy, are showing potential to improve outcomes and reduce resistance to treatment [6]. In our Special Issue, *HER2* overexpression in breast cancer was shown to be a critical factor in determining therapeutic strategies, with anti-*HER2* therapies showing high efficacy in reducing tumor progression (Contribution 5). Research into cervical cancer is currently focusing on the role of HPV (human papillomavirus) in the pathogenesis of the disease. On the treatment front, research is exploring new therapies, including targeted treatments and immunotherapies, to more effectively combat advanced cervical cancer [7]. The review published by Dicu-Andreescu I et al. discussed abdominal parietal metastasis in cervical cancer, noting that incomplete surgery may contribute to metastatic spread (Contribution 11), while Jung L et al. highlighted the importance of HPV in cervical cancer, advancing diagnostic and therapeutic strategies to optimize outcomes (Contribution 12). Vulvar cancer was another topic, as sentinel lymph node detection methods were reviewed with the aim of refining clinical guidelines for more accurate diagnoses and treatments (Contribution 17). Finally, Delgado-Miguel C et al. demonstrated that the neutrophil-to-lymphocyte ratio (NLR) could serve as an effective predictor of pediatric ovarian torsion, aiding in early diagnosis and intervention (Contribution 7).

Advances in prenatal screening are an example of translational medicine efforts, as the use of first-trimester fetal cardiovascular ultrasound screenings has been shown to detect up to 90% of major congenital heart defects (Contribution 1). In addition, the use of AI has demonstrated its potential in the detection of fetal anomalies, particularly heart and brain anomalies (Contribution 13). Biochemical markers such as amniotic fluid angiotensinogen levels also showed a significant correlation with both birth weight and gestational age, suggesting its potential role in understanding fetal growth (Contribution 8).

Placental pathology is the study of diseases or abnormalities that affect the placenta during pregnancy. The placenta is a vital organ that provides nutrients and oxygen to the developing fetus, removes waste products and plays a key role in hormone production. If the placenta is diseased or damaged, it can lead to complications for both mother and baby [8]. The protective effects of the COVID-19 vaccination during pregnancy were evaluated by Rolfo A et al. (Contribution 3), who showed that it enhanced placental antioxidant defenses and supported fetal development by counteracting oxidative stress induced by SARS-CoV-2. In line with these findings, Subramaniam V et al. found that severe COVID-19 infection during pregnancy was associated with an increased risk of preterm birth and neonatal intensive care unit admission, while the vaccination reduced these risks (Contribution 10). In contrast, Xue Y et al. developed a predictive model for early-onset pre-eclampsia that significantly improved predictive accuracy when clinical risk factors were combined with laboratory indicators (Contribution 9).

Human embryo culture is a critical component of successful in vitro fertilization (IVF) in the field of assisted reproductive technology (ART). The process of human pre-implantation development is complex and requires a highly controlled environment to ensure success. During embryo culture, both chemical and physical factors are essential to support proper embryo growth and maintain viability [9]. Bartolacci A et al. identified optimal culture conditions for embryo development, suggesting that embryo culture at 37 °C and 5% oxygen improves outcomes (Contribution 15). In another area of research, the application of artificial intelligence (AI) to reproductive medicine has revolutionized the way healthcare professionals approach fertility, pregnancy, and related conditions. AI has been particularly influential in areas such as in vitro fertilization (IVF), where it helps to select and prioritize embryos, predict pregnancy success, and optimize the decision-making process. Cimadomo D et al. developed the qSEA AI tool, which can predict embryo implantation success based on specific characteristics such as zona pellucida thinning, providing a more reliable method for selecting competent embryos (Contribution 4). On another topic related to infertility, Kovács BP et al. proposed a 70 min exercise program combining physiotherapy and relaxation techniques to improve fertility, especially in women with age-related decline in ovarian reserve (Contribution 16). Cheng C et al. identified diabetes, advanced age, and gynecological and inflammatory disorders as major risk factors for pregnancy loss and emphasized the importance of managing these factors to reduce the risk (Contribution 6). Finally, Flore A et al. synthesized the mechanisms behind hydatidiform moles, providing important insights into recurrence risk and genetic counseling (Contribution 14).

These findings collectively contribute to advancements in diagnostic tools, therapies, and personalized care across a range of medical fields.

### 3.4. Future Work

Looking ahead, the path to further progress will require a focused effort in several key research areas. One priority is the need for more robust longitudinal studies to better understand how environmental and genetic factors interact across the lifespan to influence conditions such as endometriosis, infertility, and pre-eclampsia. Further investment is also needed in precision medicine, where individualized treatments based on genetic profiles and other biomarkers could significantly improve outcomes for women. Research in maternal–fetal medicine, particularly in areas such as immune modulation during pregnancy and placental function, offers exciting potential to advance treatment strategies. In addition, as we move from bench to bedside, the integration of technology—such as artificial intelligence and machine learning—into obstetrics and gynecology will offer new opportunities for early detection, diagnosis and personalized care. Ensuring equitable access to these innovations, especially for underserved populations, will be critical to addressing disparities in maternal and reproductive health outcomes.

## 4. Conclusions

Translational research is transforming obstetrics and gynecology, making it an exciting and rapidly evolving field. From new cancer treatments to stem cell therapies and automated IVF, basic science is being translated into practical applications that improve patient outcomes. The collaboration between academia, clinical practice, and industry is essential to ensure that these innovations reach the bedside efficiently, ultimately improving patient care and quality of life for women worldwide. In conclusion, while we have made significant progress in the field of obstetrics and gynecology, the journey from bench to bedside is still a work in progress. The future of women's health will be shaped by continued interdisciplinary collaboration, innovation, and a commitment to translating scientific

discoveries into tangible, life-changing clinical applications. As researchers, clinicians, and policymakers, we must prioritize these areas to ensure that every woman benefits from the advances that lie ahead.

**Conflicts of Interest:** The authors declare no conflict of interest.

#### List of Contributions:

1. Elekes, T.; Csermely, G.; Kádár, K.; Molnár, L.; Keszthelyi, G.; Hozsdora, A.; Vizer, M.; Török, M.; Merkely, P.; Várbiro, S. Learning Curve of First-Trimester Detailed Cardiovascular Ultrasound Screening by Moderately Experienced Obstetricians in 3509 Consecutive Unselected Pregnancies with Fetal Follow-Up. *Life* **2024**, *14*, 1632.
2. Guerra de Melo, I.G.; Tavares, V.; Savva-Bordalo, J.; Rei, M.; Liz-Pimenta, J.; Pereira, D.; Medeiros, R. Endothelial Dysfunction Markers in Ovarian Cancer: VTE Risk and Tumour Prognostic Outcomes. *Life* **2024**, *14*, 1630.
3. Rolfo, A.; Cosma, S.; Nuzzo, A.M.; Moretti, L.; Tancredi, A.; Canosa, S.; Revelli, A.; Benedetto, C. Assessment of Placental Antioxidant Defense Markers in Vaccinated and Unvaccinated COVID-19 Third-Trimester Pregnancies. *Life* **2024**, *14*, 1571.
4. Cimadomo, D.; Trio, S.; Canosi, T.; Innocenti, F.; Saturno, G.; Taggi, M.; Soscia, D.M.; Albricci, L.; Kantor, B.; Dvorkin, M.; et al. Quantitative Standardized Expansion Assay: An artificial intelligence-powered morphometric description of blastocyst expansion and zona thinning dynamics. *Life* **2024**, *14*, 1396.
5. Coca, R.; Moisin, A.; Coca, R.; Diter, A.; Rachieru, M.; Tanasescu, D.; Popa, C.; Cerghedeian-Florea, M.E.; Boicean, A.; Tanasescu, C. Exploring therapeutic challenges in patients with Her2-positive breast cancer—A single-center experience. *Life* **2024**, *14*, 1025.
6. Cheng, C.G.; Su, S.H.; Chien, W.C.; Chen, R.; Chung, C.H.; Cheng, C.A. Diabetes Mellitus and Gynecological and Inflammation Disorders Increased the Risk of Pregnancy Loss in a Population Study. *Life* **2024**, *14*, 903.
7. Delgado-Miguel, C.; Arredondo-Montero, J.; Moreno-Alfonso, J.C.; San Basilio, M.; Peña Pérez, R.; Carrera, N.; Aguado, P.; Fuentes, E.; Díez, R.; Hernández-Oliveros, F. The Role of Neutrophil-to-Lymphocyte Ratio as a Predictor of Ovarian Torsion in Children: Results of a Multicentric Study. *Life* **2024**, *14*, 889.
8. Vrachnis, D.; Fotiou, A.; Mantzou, A.; Pergialiotis, V.; Antsaklis, P.; Valsamakis, G.; Stavros, S.; Machairiotis, N.; Iavazzo, C.; Kanaka-Gantenbein, C.; et al. Second Trimester Amniotic Fluid Angiotensinogen Levels Linked to Increased Fetal Birth Weight and Shorter Gestational Age in Term Pregnancies. *Life* **2024**, *14*, 206.
9. Xue, Y.; Yang, N.; Gu, X.; Wang, Y.; Zhang, H.; Jia, K. Risk prediction model of early-onset preeclampsia based on risk factors and routine laboratory indicators. *Life* **2023**, *13*, 1648.
10. Subramaniam, V.; Ng, B.K.; Phon, S.E.; Muhammad Rafi'uddin, H.; Wira Sorfan, A.R.; Siti Hajar, A.A.; Nor Azlin, M.I. Outcomes of Pregnancy in COVID-19-Positive Mothers in a Tertiary Centre. *Life* **2023**, *13*, 1491.
11. Dicu-Andreescu, I.G.; Marincas, M.A.; Simionescu, A.A.; Dicu-Andreescu, I.; Prunoiu, V.M.; Ionescu, S.O.; Neicu, S.A.; Radu, G.M.; Brătu, E.; Simion, L. Abdominal Parietal Metastasis from Cervical Cancer: A Review of One of the Most Uncommon Sites of Recurrence Including a Report of a New Case. *Life* **2024**, *14*, 667.
12. Jung, L.; Klamminger, G.G.; Bier, B.; Eltze, E. From Satirical Poems and Invisible Poisons to Radical Surgery and Organized Cervical Cancer Screening—A Historical Outline of Cervical Carcinoma and Its Relation to HPV Infection. *Life* **2024**, *14*, 307.
13. Enache, I.A.; Iovoaica-Rănescu, C.; Ciobanu, S.G.; Berbecaru, E.I.A.; Vochin, A.; Băluță, I.D.; Istrate-Ofițeru, A.M.; Comănescu, C.M.; Nagy, R.D.; Iliescu, D.G. Artificial intelligence in obstetric anomaly scan: Heart and brain. *Life* **2024**, *14*, 166.
14. Florea, A.; Caba, L.; Grigore, A.M.; Antoci, L.M.; Grigore, M.; Gramescu, M.I.; Gorduza, E.V. Hydatidiform Mole—Between Chromosomal Abnormality, Uniparental Disomy and Monogenic Variants: A Narrative Review. *Life* **2023**, *13*, 2314.



15. Bartolacci, A.; Tondo, F.; Alteri, A.; Solano Narduche, L.; de Girolamo, S.; D'Alessandro, G.; Rabellotti, E.; Papaleo, E.; Pagliardini, L. The task matters: A comprehensive review and proposed literature score of the effects of chemical and physical parameters on embryo developmental competence. *Life* **2023**, *13*, 2161.
16. Kovács, B.P.; Balog, J.; Sebők, B.; Keszthelyi, M.; Várbió, S. Unlocking Female Fertility with a Specific Reproductive Exercise Program: Protocol of a Randomized Controlled Clinical Trial. *Life* **2025**, *15*, 18.
17. Vida, B.; Lintner, B.; Várbió, S.; Merkely, P.; Lőczy, L.L.; Ács, N.; Tóth, R.; Keszthelyi, M. Assessing the Comparative Efficacy of Sentinel Lymph Node Detection Techniques in Vulvar Cancer: Protocol for a Systematic Review and Meta-Analysis. *Life* **2024**, *14*, 1538.
18. Psomiadou, V.; Fotiou, A.; Iavazzo, C. Mediastinal Metastasis Isolated in Ovarian Cancer: A Systematic Review. *Life* **2024**, *14*, 1098.

## References

1. Boire, A.; Burke, K.; Cox, T.R.; Guise, T.; Jamal-Hanjani, M.; Janowitz, T.; Kaplan, R.; Lee, R.; Swanton, C.; Vander Heiden, M.G.; et al. Why do patients with cancer die? *Nat. Rev. Cancer* **2024**, *24*, 578–589. [CrossRef] [PubMed]
2. Aplin, J.D.; Myers, J.E.; Timms, K.; Westwood, M. Tracking placental development in health and disease. *Nat. Rev. Endocrinol.* **2020**, *16*, 479–494. [CrossRef] [PubMed]
3. Gadducci, A.; Cosio, S. Screening for Ovarian Cancer in the General Population: State of Art and Perspectives of Clinical Research. *Anticancer. Res.* **2022**, *42*, 4207–4216. [CrossRef] [PubMed]
4. Zhang, Q.; Liang, X.; Chen, Z. A review of artificial intelligence applications in in vitro fertilization. *J. Assist. Reprod. Genet.* **2024**. [CrossRef] [PubMed]
5. Feng, F.; Liu, T.; Hou, X.; Lin, X.; Zhou, S.; Tian, Y.; Qi, X. Fine modulo Targeting the FSH/FSHR axis in ovarian cancer: Advanced treatment using nanotechnology and immunotherapy. *Front. Endocrinol.* **2024**, *15*, 1489767. [CrossRef] [PubMed]
6. Srivastava, T.P.; Dhar, R.; Karmakar, S. Looking beyond the ER, PR, and HER2: What's new in the ARsenal for combating breast cancer? *Reprod. Biol. Endocrinol.* **2025**, *23*, 9. [CrossRef]
7. Yousaf, S.; Shehzadi, A.; Ahmad, M.; Asrar, A.; Ahmed, I.; Iqbal, H.M.N.; Hussien Bule, M. Recent advances in HPV biotechnology: Understanding host-virus interactions and cancer progression—A review. *Int. J. Surg.* **2024**, *110*, 8025–8036. [CrossRef] [PubMed]
8. Todros, T.; Piccoli, E.; Rolfo, A.; Cardaropoli, S.; Guiot, C.; Gaglioti, P.; Oberto, M.; Vasario, E.; Caniggia, I. Review: Feto-placental vascularization: A multifaceted approach. *Placenta* **2011**, *32* (Suppl. S2), S165–S169. [CrossRef] [PubMed]
9. Wale, P.L.; Gardner, D.K. The effects of chemical and physical factors on mammalian embryo culture and their importance for the practice of assisted human reproduction. *Hum. Reprod. Update* **2016**, *22*, 2–22. [CrossRef]

**Disclaimer/Publisher's Note:** The statements, opinions and data contained in all publications are solely those of the individual author(s) and contributor(s) and not of MDPI and/or the editor(s). MDPI and/or the editor(s) disclaim responsibility for any injury to people or property resulting from any ideas, methods, instructions or products referred to in the content.

## Article

# Clock Proteins Have the Potential to Improve Term Delivery Date Prediction: A Proof-of-Concept Study

Max T. Dufford, Tracey C. Fleischer, Laura J. Sommerville, Md. Bahadur Badsha, Ashoka D. Polpitiya, Jennifer Logan, Angela C. Fox, Sharon R. Rust, Charles B. Cox, Thomas J. Garite, J. Jay Boniface and Paul E. Kearney \*

Sera Prognostics, Inc., Salt Lake City, UT 84109, USA; tfleischer@sera.com (T.C.F.); afox@sera.com (A.C.F.); tgarite@sera.com (T.J.G.)

\* Correspondence: pkearney@sera.com; Tel.: +1-801-990-6605

**Abstract:** Our ability to accurately predict the delivery date of term pregnancies is limited by shortcomings of modern-day clinical tools and due date estimation methods. The pregnancy clock is a series of coordinated and harmonized signals between mother, fetus, and placenta that regulate the length of gestation. Clock proteins are thought to be important mediators of these signals, yet few studies have investigated their potential utility as predictors of term delivery date. In this study, we performed a cross-sectional proteome analysis of 2648 serum samples collected between 18 and 28 weeks of gestation from mothers who delivered at term. The cohort included pregnancies both with and without complications. A total of 15 proteins of diverse functionalities were shown to have a direct association with time to birth (TTB), 11 of which have not been previously linked to gestational age. The protein A Disintegrin and Metalloproteinase 12 (ADA12) was one of the 15 proteins shown to have an association with TTB. Mothers who expressed the highest levels of ADA12 in the cohort (90th percentile) gave birth earlier than mothers who expressed the lowest levels of ADA12 (10th percentile) at a statistically significant rate (median gestational age at birth  $39^{0/7}$  weeks vs.  $39^{3/7}$  weeks,  $p < 0.001$ ). Altogether, these findings suggest that ADA12, as well as potentially other clock proteins, have the potential to serve as clinical predictors of term delivery date in uncomplicated pregnancies and represent an important step towards characterizing the role(s) of clock proteins in mediating pregnancy length.

**Keywords:** clock proteins; term delivery date; time to birth; prediction; gestational age; a disintegrin and metalloproteinase 12

## 1. Introduction

Having the capability to predict the date of term delivery (>37 weeks gestation) with certainty is an unmet need in obstetrics. Knowing precisely when labor will begin could avoid preterm birth from the mistimed scheduling of cesarian section or labor induction [1–3]. It could also mitigate delivery complications by allowing women who live in rural settings or maternity care deserts adequate time to reach hospital facilities [4–6]. Outside of a clinical setting, better estimation of when a baby will deliver has lifestyle applications since planning for this milestone affects a long list of preparative activities for the mother, their family, friends, and employer, to name a few.

In accordance with clinical guidelines, delivery date is estimated as 280 days after the woman's last menstrual period. However, only 5% of births occur on this estimated delivery

date (EDD), and 30% of births occur more than 10 days outside the EDD [7,8]. The accuracy of the EDD can be improved by a few days if it is calculated based on the fetal crown-rump length as measured by ultrasound between 8 and 12 weeks of gestation [9]. Even in developed countries, many women either lack access to ultrasounds in the first trimester or miss this crucial timing window when ultrasounds can inform gestational age [10], showing that clinical tools other than ultrasounds are needed to improve the accuracy of term delivery date prediction.

The pregnancy clock refers to a biological phenomenon in which harmonized and chronologic signals from the fetus, fetal membrane, placenta, decidua, and myometrium modulate the length of gestation [11–14]. It includes various biomarkers that comprise an immune clock, a proteomic clock, and temporal changes to the transcriptome and metabolome that correlate to gestational age based on ultrasound [14–18]. Some studies have shown that various biomarker components of the pregnancy clock, including protein activators of the Janus kinase and signal transducer pathways [16], lipid and steroid hormone metabolites [17], and cell-free DNA corresponding to placental genes [18], could potentially distinguish pregnancies of normal gestational length from those delivering preterm or late term and may have the capability to identify fetal maladaptations before symptoms appear.

It is recognized that maternal, paternal, and fetal factors also influence gestational length in normal pregnancies. Maternal age > 35 years and late-term birth in previous pregnancies correlate with longer gestation [19,20]. The length of pregnancy is also influenced by the body mass index (BMI) of the mother and father [21–23] and by the weight of the fetus in the first trimester [18]. Additionally, conceptions that take longer than 24 h to implant or that have a rapid, rather than gradual, progesterone rise during corpus luteum rescue are also associated with a longer gestational period [22].

Despite our present-day understanding of the pregnancy clock and other factors that influence gestational length, there has been little investigation into its potential utility as a clinical tool to improve the accuracy of delivery date prediction. The goal of this discovery study was to test the hypothesis that clock proteins are associated with the time to birth (TTB) and may have the capability to serve as predictors of term delivery date.

## 2. Materials and Methods

### 2.1. Materials and Reagents

Trypsin was purchased from Promega (#V5280) (Madison, WI, USA). Custom stable isotope standards were purchased from Biosynth (Staad, Switzerland). Human 14 multiple affinity removal columns (MARS-14) were purchased from Agilent (#5190-7995) (Santa Clara, CA, USA).

### 2.2. Study Design and Participants

We retrospectively analyzed 2648 banked serum samples and associated clinical and demographic data collected for an institutional-review-board-approved 11-site study in the United States (NCT01371019), which took place from April 2011 to April 2015. Inclusion and exclusion criteria for participation in the study and sample selection are shown in Table 1.

The original study aimed to characterize proteome differences in women with asymptomatic singleton pregnancies who deliver at term (>37 weeks) versus those who experience spontaneous preterm birth [24]. Prior to sample collection, enrolled individuals provided written informed consent to participate in the study and for their samples and clinical information to be used in future studies. A list of the institutions with subjects consenting to biobanking is shown in Supplementary Table S1. The samples used in the

current study included term births only and were collected from 18<sup>0/7</sup> through 28<sup>6/7</sup> weeks of gestation at a single time point for each participant.

**Table 1.** Study inclusion and exclusion criteria.

Inclusion Criteria	Exclusion Criteria
<ul style="list-style-type: none"> <li>• Subject is 18 years or older</li> <li>• Subject has a singleton pregnancy</li> <li>• Subject can provide consent</li> <li>• Subject consented to use of their specimens and data for future research</li> </ul>	<ul style="list-style-type: none"> <li>• Subject is pregnant with more than one fetus</li> <li>• There is a known or suspected fetal anomaly</li> <li>• Early discontinued (consent errors, duplicate enrollment, unable to complete blood draw, gestational age (GA) window violation, inclusion/exclusion violations, sample handling errors, etc.)</li> <li>• Early withdraw, lost to follow-up</li> <li>• Insufficient sample amount</li> </ul>

### 2.3. Proteomic Analysis

Whole blood samples were processed to serum at the study sites within 2.5 h of collection. Then, 0.5 mL serum aliquots were frozen at  $-80^{\circ}\text{C}$ , shipped to Sera Prognostics, Inc. on dry ice, and stored at  $-80^{\circ}\text{C}$  until analyzed. Maternal serum samples were analyzed in Sera Prognostics' Clinical Laboratory Improvement Amendment (CLIA)-certified and College of American Pathologists (CAP)-accredited laboratory according to a prespecified laboratory analysis plan and standard operating protocols [25,26]. Serum samples were randomized and allocated into batches that contained both study samples and quality controls and processed, as described in [25]. Briefly, after thawing samples on ice, equal volumes of serum from each subject were depleted of high-abundance proteins on MARS-14 columns run on an Agilent 1260 liquid chromatography system. Depleted serum samples were reduced, alkylated, and digested with trypsin. They were then spiked with stable isotope standard (SIS) peptides corresponding to each measured endogenous peptide, and then desalted and analyzed by coupled liquid chromatography–multiple-reaction- monitoring mass spectrometry (LC-MRM-MS) on an Agilent 1290 UHPLC system coupled to an Agilent 6490 triple quadrupole mass spectrometer. We used a multiple-reaction- monitoring (MRM) assay to measure 150 peptides from 110 proteins that were either (1) of placental origin, (2) maternal serum proteins with reported roles in pregnancy, or (3) used as quality controls. Peptides were quantified as the peak area of the endogenous peptide divided by the peak area of its corresponding SIS peptide counterpart, generating a response ratio (RR). Pooled serum from either non-pregnant or pregnant women served as quality control samples and were used to monitor batch quality throughout the depletion and LC/MS/MS process, as described in [25]. Quality control samples were not used to normalize samples.

### 2.4. Statistical Analyses

A Wilcoxon test was performed to identify proteotypic peptides with mean response ratios that changed significantly between 18 and 20 weeks and 26 and 28 weeks of gestation. The results were visualized using a volcano plot. Significant difference was defined as  $p < 0.05$  and a minimum log2 fold change of  $+/-0.25$  in relative abundance. A subset of these proteins were smoothed using a generalized additive model and plotted relative to gestational age at blood draw (GABD). Confidence intervals were included to show 95% overall population values across GABD for each model. Separately, we performed a protein association study using Mendelian randomization (MR), a statistical approach to identifying causal genes that has also been applied to proteomic data [26–29]. We applied an

MR-based machine learning algorithm (MRPC) with 50 iterations of bootstrapping [27,28] to identify proteins that have an association with time to birth (TTB) among individuals delivering at term. MRPC conducts a series of statistical tests for marginal and conditional independence between pairs of nodes. If the null hypothesis (i.e., no association between two nodes) of the marginal independence test fails to reject, then the corresponding edge (i.e., association between two nodes) is removed. Otherwise, the edge is retained for subsequent conditional independence test to determine if the association persists after accounting for other nodes. We used a 10% level of significance threshold (type I error rate) for each test. Finally, we compared differences in gestational age at birth (GAB) in participants having the highest (90th percentile) and lowest (10th percentile) amounts of the placental protein a distintegrin and metalloproteinase 12 (ADA12). Prior to comparing the GAB distributions, the relative abundances of ADA12 were normalized for GABD by regressing ADA12 levels against GABD and then removing any trend. The significance of the GAB mean difference was assessed using the Welch two sample *t*-test. This analysis was limited to term pregnancies with vaginal deliveries ( $n = 1839$ ). We eliminated cesarean section deliveries because those are often scheduled prior to the natural onset of labor. It is unclear how many of the vaginal deliveries in the analysis were scheduled inductions, as induction data were only captured for preterm deliveries. In addition, a subset analysis of the 1839 subjects was performed to compare GAB in the highest and lowest percentiles of ADA12 levels in complicated and uncomplicated pregnancies separately. Complicated pregnancies were defined as pregnancies with diabetes (gestational or preexisting), preeclampsia, pregnancy-induced or pre-existing hypertension, incompetent cervix, polyhydramnios, chorioamnionitis, and non-reassuring fetal status. Uncomplicated pregnancies excluded the conditions listed above. All analyses and visualizations were performed using the statistical program R, version 4.4.2 [30].

### 3. Results

#### 3.1. Patient Characteristics

In this retrospective study, all 2648 banked serum samples from term pregnancies were selected based on inclusion and exclusion criteria for NCT01371019 and sample selection (Table 1). Demographics of the study population were collected at the same time as blood samples and are shown in Table 2. The population was characterized by diverse clinical and demographic characteristics and pregnancy histories. While only term pregnancies were analyzed, the diverse population and the presence of pregnancy complications, including gestational diabetes, preeclampsia, and pregnancy-induced hypertension, among others, support the generalizability of these study results.

**Table 2.** Demographics of study participants.

Demographic/Clinical Variable	Value	All Subjects (n = 2648)
Maternal Age	Median (IQR)	28 years (23–32)
Maternal Pre-pregnancy BMI	Median (IQR)	25.90 (22.3–31.4) *
Gravida	Primigravida	710 (26.8 %)
	Multigravida	1938 (73.2 %)
Race	Black	414 (15.6%)
	White	1998 (75.5%)
	Other	236 (8.9%)
Ethnicity	Hispanic	942 (35.6%)
	Not Hispanic	1706 (64.4%)

Table 2. Cont.

Demographic/Clinical Variable	Value	All Subjects (n = 2648)
Gestational age at blood draw (GABD)	Median (IQR)	166 days (141–184)
Gestational age at birth (GAB)	Median (IQR)	274 days (270–280)
Diabetes **	Gestational	183 (6.9%)
	Type I	19 (0.7%)
	Type II	55 (2.1%)
	None	2391 (90.3%)
Pre-eclampsia	No	2516 (95.0%)
	Yes	132 (5.0%)
Pregnancy-Induced Hypertension	No	2580 (97.4%)
	Yes	68 (2.6%)
Other Complications ***	No	2455 (92.7%)
	Yes	193 (7.3%)
Delivery	Cesarean Section: Primary	405 (15.3%)
	Cesarean Section: Repeat	404 (15.3%)
	Vaginal	1839 (69.4%)

\* A total of 45 values for maternal pre-pregnancy BMI were missing from the dataset. \*\* Type I and type II diabetes indicate study participants who were diagnosed with diabetes before pregnancy. \*\*\* Other complications include incompetent cervix, polyhydramnios, chorioamnionitis, and non-reassuring fetal status.

### 3.2. Clock Protein Expression

To identify proteins with levels that change during pregnancy, we first compared maternal serum protein expression at 18–20 weeks' gestation to that at 26–28 weeks' gestation. Changes were considered significant if protein levels satisfied both a minimum change of  $\log_2\text{FC} = 0.25$  and achieved a  $p\text{-value} < 0.05$ . Several growth factors, glycoproteins, adhesion proteins, and immune regulators known to play a role in fetal growth and development demonstrated significant changes in expression (Figure 1A) that largely agree with reported findings. Both linear and non-linear expression changes were seen among samples taken between 18 and 20 weeks and 26–28 weeks of gestation. Representative changes are shown in Figure 1B, and a full listing of proteins shown in Figure 1A is provided in Supplementary Table S2.

### 3.3. Association Between Proteins and Time to Birth

The time to birth is defined as  $TTB = (GAB - GABD)$ , where GAB is gestational age at birth and GABD is gestational age at blood draw. To characterize associations between the proteins analyzed and TTB, we applied an MRPC [27,28] to the full protein dataset. Of the proteins analyzed (Supplementary Table S2), 15 were shown to have a direct association with TTB (Figure 2). Among these were growth hormones, adhesion molecules, glycoproteins, enzymes, and lipid-binding proteins that are involved in proliferation, migration, adhesion, fetal and placental growth, immune modulation during pregnancy, pattern recognition, and lipid metabolism (Table 3). Growth hormone 2 (SOM2), chorionic somatomammotropin (CSH), chorionic gonadotropin subunit  $\beta 1$  (CGB1), and sushi, von Willebrand Factor type A, EGF, and pentraxin domain-containing protein (SVEP1), are known markers of gestational age [16,31–34]. Several others, including cell adhesion molecule L1 (CHL1), lymphocyte adhesion molecule 1 (LYAM1, i.e., L-selectin),

a distintegrin and metalloproteinase 12 (ADA12), ectonucleotide pyrophosphatase/phosphodiesterase 2 (ENPP2, i.e., autotaxin), apolipoprotein C-III (APOC3), and pregnancy-specific  $\beta$ 1 glycoprotein 1 (PSG1) have been proposed as markers of certain fetal abnormalities and/or pregnancy complications [35–45] but have not been linked to TTB. The remaining proteins have not been previously associated with either pregnancy complications or TTB. Overall, these results identify both known and novel biomarkers that may have practical applications in predicting the probability of delivery by week in the term period.

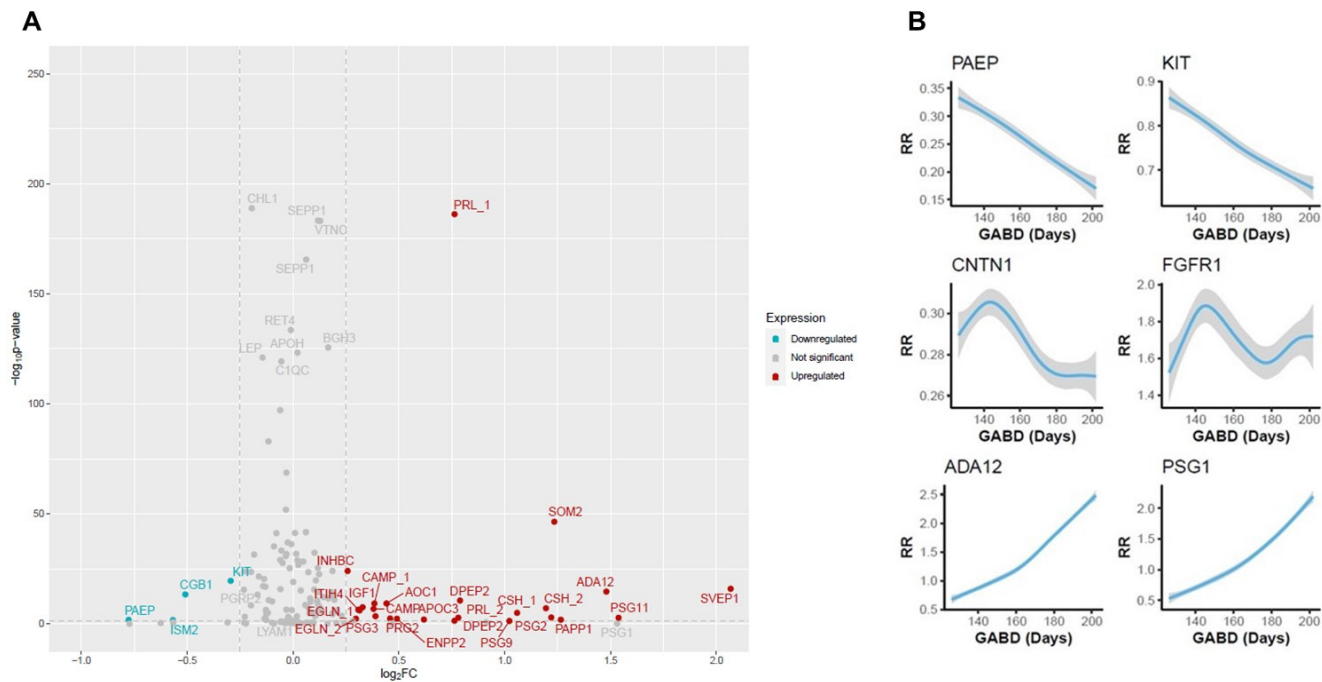


**Figure 1.** Changes in protein expression between 18 and 20 weeks of gestation and 26 to 28 weeks of gestation. **(A)** Volcano plot showing significantly upregulated (red) and downregulated (blue) proteins. Gray proteins demonstrated no significant change. Significance is represented on the *y*-axis as the  $-\log_{10}$  *p*-value, while the magnitude of change is shown on the *x*-axis is the  $\log_2$  fold-change. When a protein is depicted more than once (denoted by \_1 and \_2), it was measured using two distinct peptides. **(B)** Smoothing plots showing expression changes in representative proteins that were significantly upregulated (ADA12 and PSG1), downregulated (PAEP and KIT), or demonstrated no significant change (CNTN1 and FGFR1). The 95% CI between expression (response ratio (RR)) and gestational age at blood draw (GABD) is represented by the width of the gray-shaded area.

**Table 3.** Summary of proteins shown to have a direct association with TTB. NS = not significant.

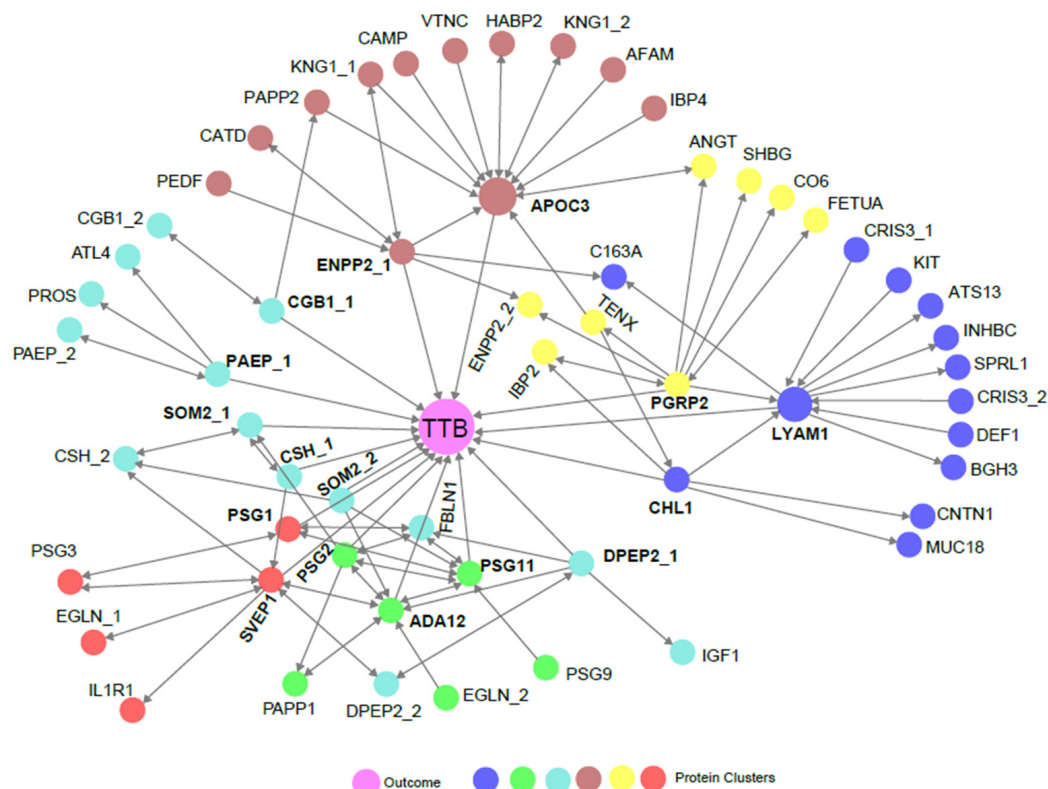
Protein (UniProt ID)	Expression Change Between 18 and 20 Weeks of Gestation and 26 and 28 Weeks of Gestation, Wilcoxon Test	Placentally Expressed [46]	Protein Type	Role in Pregnancy	Previously Reported Associations with TTB or Pregnancy Complications
Peptidoglycan Recognition Protein 2 (PGRP2)	Downregulated NS	Yes	Hydrolase enzyme	Pattern recognition protein	None
Cell Adhesion Molecule L1 Like (CHL1)	Downregulated NS	No	Cell adhesion molecule	Negative regulator of proliferation	Brain malformation and neurodevelopmental delay [37,38,42]

Table 3. Cont.

Protein (UniProt ID)	Expression Change Between 18 and 20 Weeks of Gestation and 26 and 28 Weeks of Gestation, Wilcoxon Test	Placentally Expressed [46]	Protein Type	Role in Pregnancy	Previously Reported Associations with TTB or Pregnancy Complications
Lymphocyte Adhesion Molecule 1 (LYAM1)	Downregulated NS	No	Cell adhesion molecule	Cell adhesion and migration	Preeclampsia [35]
Dipeptidase 2 (DPEP2)	Upregulated	Yes	Hydrolase enzyme	Cell differentiation	None
Growth Hormone 2 (SOM2)	Upregulated	Yes	Growth hormone	Cell differentiation and proliferation	Marker of gestational age [31]
Chorionic somatomammotropin (CSH) *	Upregulated	Yes	Growth hormone	Stimulates lactation and fetal growth	Marker of gestational age [16]
Progestogen-associated endometrial protein (PAEP)	Downregulated	Yes	Glycoprotein	Regulates uterine environment/immune cell inhibitor	None
Chorionic Gonadotropin Subunit Beta 1 (CGB1)	Downregulated	Yes	$\beta$ -subunit of human chorionic gonadotropin	Stimulates uterine and fetal growth/immune modulator	Marker of gestational age [33]
Pregnancy-Specific $\beta$ 1 Glycoprotein 11 (PSG11)	Upregulated	Yes	Placental glycoprotein	Immune cell and angiogenesis modulator	None
Disintegrin and metalloproteinase domain-containing protein 12 (ADA12)	Upregulated	Yes	Placental glycoprotein	Placental growth and differentiation	Preterm birth, fetal growth restriction, preeclampsia, Down Syndrome, small for gestational age [36,41,47]
Pregnancy-Specific $\beta$ 1 Glycoprotein 2 (PSG2)	Upregulated	Yes	Placental glycoprotein	Immune cell and angiogenesis modulator	None
Sushi, von Willebrand Factor type A, EGF, and pentraxin domain-containing protein (SVEP1)	Upregulated	Yes	Cell adhesion molecule	Facilitates cell alignment and migration	Marker of gestational age [32]
Pregnancy-Specific $\beta$ 1 Glycoprotein 1 (PSG1)	Upregulated NS	Yes	Placental glycoprotein	Immune cell and angiogenesis modulator	Preeclampsia [48]
Ectonucleotide Pyrophosphatase/ Phosphodiesterase 2 (ENPP2)	Upregulated	Yes	Phosphodiesterase and phospholipase	Cell proliferation and migration	Preeclampsia [39,40]
Apolipoprotein C-III (APOC3)	Upregulated	No	Lipid binding protein	Modulator of lipid metabolism	Gestational Diabetes Mellitus [44]

\* Since their protein sequences differ by only one amino acid, our methods cannot distinguish CSH1 from CSH2.





**Figure 2.** An MRPC analysis showing statistical directional relationships between proteins and TTB. Colors represent groups of proteins that are clustered based on hierarchical clustering. The outcome (TTB) is indicated by the center purple circle. Single direction arrowheads indicate statistically causal relationships where the protein or outcome being touched by the arrowhead is statistically dependent on the protein being touched by the blunt end of the arrow. Bidirectional arrows indicate indeterminate statistical causality. When a protein is depicted more than once (denoted by \_1 and \_2), it was measured on two distinct peptides. Proteins with a direct association to TTB are bold.

### 3.4. Biological Association of Biomarkers with TTB

We next sought to visualize the impact of biomarker levels on the distribution of births. To this end, we performed a proof-of-concept analysis based on the expression of ADA12. We chose ADA12 because it had one of the largest fold changes in any protein we analyzed in this study (Figure 1A) and a near-linear association with GABD with tight confidence intervals (Figure 1B). We compared the gestational age at birth (GAB) distributions of women with the highest ADA12 levels (90th percentile) and lowest ADA12 levels (10th percentile) in all term vaginal deliveries, after normalizing for GABD, to determine if there was a difference in delivery dates. Subjects in the bottom decile of ADA12 levels had a right-skewed GAB distribution, while those in the top decile were left-skewed (Figure 3, top and middle panels). This skew was further demonstrated by significantly different mean GABs between the two groups. In the 10th percentile, the mean GAB was  $39^{3/7}$  weeks, whereas the mean GAB in the 90th percentile was  $39^{0/7}$  weeks,  $p < 0.001$  (Figure 3, bottom panel).

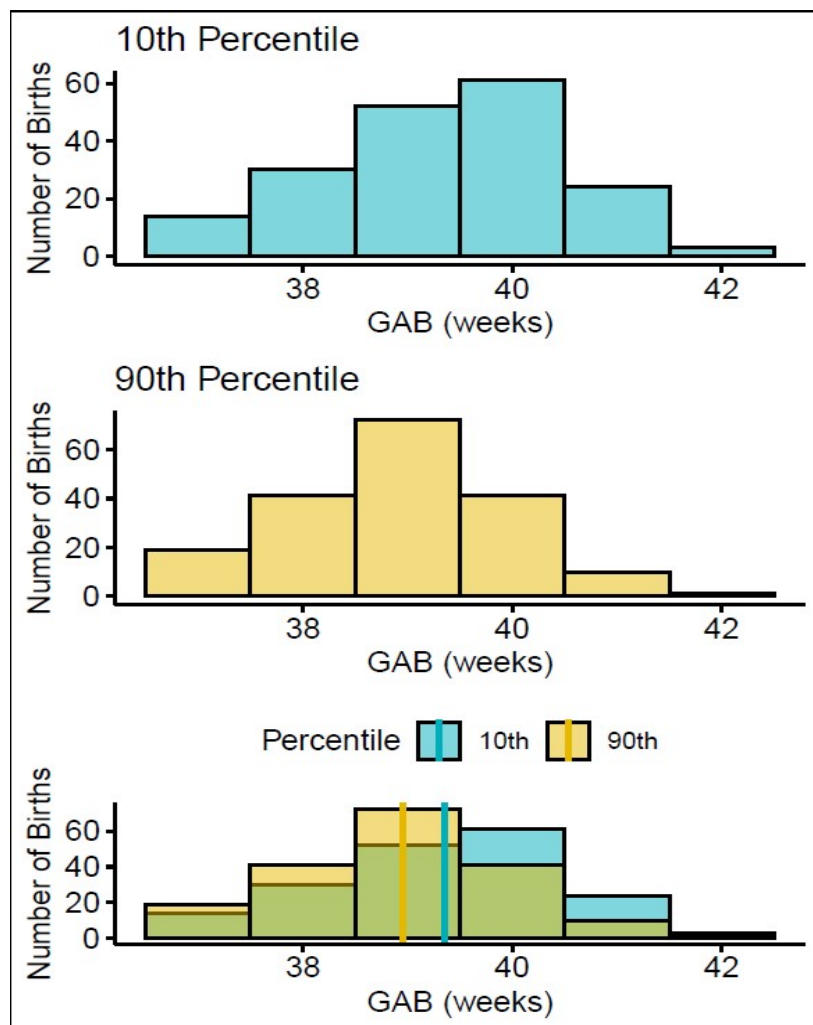


**Figure 3.** Association between GAB and ADA12 expression in all term vaginal deliveries. Graphs showing the distribution of GAB in mothers who expressed the lowest levels of ADA12 (**top**) and highest levels of ADA12 (**middle**). The combined number of births in both groups (**bottom**, green shading), shows how many more births from each group (yellow = 90th percentile, blue = 10th percentile) occurred in each week relative to the other. The solid lines indicate the mean GABs for each group: yellow = 90th percentile, blue = 10th percentile.

To better understand how pregnancy complications might impact the predictive capability of clock proteins, we analyzed complicated and uncomplicated pregnancies separately. All complicated pregnancies, defined as those with diabetes (pre-existing or gestational), preeclampsia, pre-existing or pregnancy-induced hypertension, incompetent cervix, polyhydramnios, chorioamnionitis, or non-reassuring fetal status, were analyzed as a single group to both better power the study, and because some participants reported more than one complication. In uncomplicated pregnancies alone ( $n = 1242$ ), defined as pregnancies without the above outcomes, the mean GAB of the lowest (10th percentile) ADA12 expressors was  $39^{5/7}$  weeks compared to the mean GAB of  $39^{0/7}$  weeks in the highest (90th percentile) ADA12 expressors. The separation of GABs in uncomplicated pregnancies alone was increased by 2 days relative to all term vaginal deliveries. In complicated pregnancies alone ( $n = 597$ ), the mean GAB of both highest and lowest ADA12 expressors were both  $39^{0/7}$  weeks. Altogether, this suggests that ADA12, and potentially other clock proteins, could aid in the prediction of TTB in uncomplicated term pregnancies.

#### 4. Discussion

Having a means to accurately predict the date of term delivery could improve pregnancy outcomes by avoiding the mistimed scheduling of labor induction or cesarian section and by allowing mothers adequate time to reach hospital facilities. The pregnancy clock is understood to be a series of chronological and harmonized signals among the mother, fetus, and placenta that regulate the length of gestation. Although our understanding of the pregnancy clock proteome has advanced in recent years, the potential clinical utility of clock proteins as predictors of delivery date has not been thoroughly evaluated.

Most of the information that leads to the prediction of the timing of the normal onset of labor and delivery at term comes from dating of the mother's last menstrual period and/or early examination and ultrasound. Often such information is unavailable, poorly remembered, or unreliable, so any surrogate means of predicting the time of delivery has great clinical and socioeconomic value. To date, most efforts to improve gestational age dating have used ultrasound, but this approach has technical limitations, and often women are unable to seek care early enough in pregnancy to provide the accurate measurements that make this tool reliable [10]. Further, our physiologic understanding of the processes leading to the timing of normal onset of labor at term is incomplete [49,50]. For these reasons, having additional means to predict when normal term labor and delivery will occur is highly important.

In this retrospective, cross-sectional study, we discovered proteins that demonstrated significant changes in expression between two gestational age windows, separated by only five weeks (Figure 1). Using MRPC analysis, we identified 15 proteins that had a direct association to the TTB, 11 of which have not been previously linked to gestational age (Figure 2). We investigated the potential clinical utility of ADA12 as a term delivery date predictor by comparing the mean and distribution of GAB between the cohort's highest (90th percentile) and lowest (10th percentile) expressors of ADA12 at blood draw. Results showed the mean GAB to be significantly earlier in the highest ADA12 expressors compared to the lowest expressors (Figure 3). Separate analyses of complicated and uncomplicated pregnancies demonstrated an even greater separation in GAB between the highest and lowest ADA12 expressors among mothers with uncomplicated pregnancies. No separation in GAB was observed in complicated pregnancies.

Our findings on ADA12 suggest that uncomplicated pregnancies characterized by higher levels of this protein (i.e., the highest expressors in the cohort analyzed in this study) are farther advanced (shorter TTB) than those with lower levels (the lowest expressors in the study cohort). A pregnancy that is more advanced based on higher ADA12 levels and short TTB could reflect more rapid fetal development compared to pregnancies characterized by lower ADA12 levels and longer TTB. Alternatively, biomarker differences and their ability to indicate the actual TTB of pregnancy, could be a reflection of pregnancy misdating due to inaccurate recollection of when the last menstrual period occurred, limitations in fetal ultrasound measures, or lack of these measures entirely [51,52].

Regardless, based on its functional roles in pregnancy and association between its expression levels and various pregnancy complications, ADA12 may serve as an accurate predictor of term delivery date. ADA12 plays a key role in regulating trophoblast migration and invasion during early pregnancy and helps anchor trophoblast columns in the placenta during the first trimester [53]. It also cleaves insulin-like growth factor (IGF)-binding proteins that regulate the concentration of IGF, which is important for fetal growth [54]. The decreased expression of ADA12 during the first or second trimester of pregnancy has been linked to preterm birth, fetal growth restriction, preeclampsia, Down syndrome, and an increased likelihood of the fetus being small for gestational age at birth [36,41,47,55].

These observations suggest that ADA12 expression is carefully regulated in normal pregnancies and that deviation from normal levels at certain points during gestation may reflect abnormal or delayed fetal development and pregnancy complications. The direct association that we found between ADA12 and TTB and the difference in the mean GAB between the highest and lowest ADA12 expressors in our study cohort supports a role for this protein as a delivery date predictor in uncomplicated term pregnancies.

In agreement with previous studies, our findings showed a direct association between TTB and CSH, SOM2, CGB1, and SVEP1. Maternal circulating CSH increases as pregnancy progresses and correlates with STAT-5 signaling activity in CD4 T cells, an event that strongly predicts gestational age [16]. SOM2, a placentally derived hormone, is a key driver of fetal growth and placental development. It steadily increases through pregnancy, peaking around week 37 of gestation. The gestational age at peak placental SOM2 levels is associated with pregnancy length and, thus, is also an indicator of delivery date [31]. CGB1 is the subunit that gives human chorionic gonadotropin (hCG) its functional specificity. hCG is critical for fetal viability as it plays a central role in thickening the uterine lining, stimulating progesterone production, stopping menstruation, and enhancing embryo implantation and survival [56]. Quantitative measurements of hCG are currently used in clinical practice to calculate gestational age [33]. In addition, one study showed that, when the CGB transcript was included in a model that contained measurements of eight cfRNAs, it was predictive of delivery within 14 days of the actual date with an accuracy ranging from 23 to 45% depending on trimester, roughly comparable to ultrasound with an accuracy of 48% [18]. SVEP1, which is also upregulated in pregnancy, has been shown to correlate with gestational age of chorionic villi [32]. Each of these proteins is placentally derived, and placental–fetal signaling plays a crucial role in the pregnancy clock and triggering of parturition.

Many of the 15 proteins shown to have a direct association with TTB have placental expression, including pregnancy-specific  $\beta$ 1 glycoprotein 1 (PSG1). PSG1 binds to heparin sulfate proteoglycans, the latency-associated peptide of TGF- $\beta$ 1, and the platelet integrin  $\alpha$ IIb $\beta$ 3 [57,58]. Through interactions with these ligands, PSG1 helps mediate the shift away from innate immunity in pregnancy [59,60] and dampens platelet aggregation and thrombosis to counterbalance the prothrombotic maternal environment of pregnancy [58]. PSG1 expression gradually increases throughout pregnancy, reaching its peak around 36 weeks of gestation [61]. In our study, PSG1 expression increased during the 8–10-week timeframe studied but not to statistical significance. Since the smoothing plot shows a linear association with GABD and small confidence intervals, this was likely due to the gestational timeframe for blood draw being too narrow to reach significance. Other PSG proteins measured in our study had similar linear associations with GABD. Interestingly, the transcript for PSG7 was included in the 8-cfRNA model described above.

Another placental protein identified here, PAEP, helps modulate the immune system in pregnancy. During the second trimester, a tightly regulated suppression of the immune system occurs to prevent the mother from rejecting the fetus. This suppression is characterized by a shift towards a Th2 immune response, which decreases the number of several types of innate immune cells including natural killer (NK) cells [62,63]. PAEP has been shown to facilitate this natural immune shift by mediating apoptosis of NK cells [64,65]. Our findings suggest that PAEP and other proteins involved in the immune system shift may also serve as a type of signaling molecule to indicate the progress of gestation.

The abnormal expression or disrupted function of several of the other identified proteins has been associated with pregnancy complications and/or fetal abnormalities, but, to our knowledge, none of these have previously been associated with TTB. For

instance, CHL1 is an adhesion molecule that is expressed on the surface of neurons and plays a role in their migration and organization. Mutations in the *CHL1* gene result in brain malformation and neurodevelopmental delay [42], and neurological phenotypes attributed to fetal alcohol syndrome have been partially attributed to disruption of functions mediated by CHL1 [37,38,66]. CHL1 is highly expressed in the developing fetal spinal cord and in extracellular vesicles, suggesting that during pregnancy it serves as an extracellular signaling molecule to support axon outgrowth. [67]. Our study suggests that CHL1-mediated activity may also serve as a clock signal that influences TTB.

LYAM1 (L-selectin) is an adhesion molecule expressed on the surface of leukocytes, blastocysts and in cytotrophoblast aggregates. This protein facilitates blastocyst adhesion to the endometrium during pregnancy to enable embryo implantation and is essential for the proper anchoring of the fetus to the decidua [68,69]. LYAM1 is highly expressed at the beginning of pregnancy, then tapers during the second trimester [70]. Its levels may remain elevated in preeclampsia, likely because of increased leukocyte activation stemming from inflammatory signaling [35]. The novel association between LYAM1 and TTB reported in this study aligns with its role as a mediator of implantation and protector of fetal placement during pregnancy.

One protein identified in our study has not been associated with normal pregnancy processes, pregnancy complications, or gestational age. PGRP2 is a pattern recognition molecule, expressed mainly in gut epithelial cells, that recognizes and hydrolyzes bacterial peptidoglycan (PGN) [71,72]. Bacterial PGN derived from the gut microbiota has been shown to influence brain development [73], and PGRP2 has been implicated as a mediator of this phenomenon, owing to its influence on expression of brain-derived neurotropic factor and the autism risk gene *c-Met* [74]. Our findings suggest a novel role for this protein as an indicator of pregnancy timing.

Although these findings are intriguing, we acknowledge this study's limitations. Since only 110 proteins were measured in the MRM assay, it is possible that the direct associations we report between certain proteins and TTB may include protein intermediates, which could be identified in a larger analysis. This study was not based on longitudinal sampling; therefore, we could not make direct associations between changes in protein expression and outcome in the same study participant. However, since the proteins shown to be associated with TTB were identified in a large cross-sectional cohort, the associations we found are likely applicable to the general population. This study did not investigate the contribution of clinical variables to the prediction of TTB. For example, in our cohort, there was a significant difference in GAB between primigravida vs. multigravida women (276.1 vs. 274.0 days, respectively,  $p < 0.001$ ). The cohort was not well annotated regarding reasons for labor induction/augmentation so some gestational ages at delivery may have been a result of scheduled delivery. Additionally, although medications were noted in the Case Report Form, there was not sufficient granularity to know which medications were present at the time of blood draw. The observation that the mean GABs were not different between the highest and lowest ADA12 expressors in complicated pregnancies, suggests that pregnancy complications may impact the predictive capability of ADA12 or other clock proteins. However, our ability to evaluate the impact of these variables is unfortunately limited because clinical decision-making and the response and adherence to treatment for study participants who experienced complicated pregnancies are unknown. Further investigation is needed to better characterize the relationship(s) between pregnancy complications and gestational length. In the future, any algorithm utilizing clock proteins to predict TTB may need to include the existence of certain demographic or clinical factors, such as maternal BMI or age, or require updating predictions as complications develop in the index pregnancy.

## 5. Conclusions

This study demonstrated proof-of-concept for ADA12 as a potential biomarker for predicting the delivery date of uncomplicated term pregnancy and identified a direct association between TTB and 15 proteins, 11 of which have not been previously linked to delivery date prediction or gestational age. Overall, this discovery work represents an important first step towards characterizing the relationship between clock protein behavior and the duration of pregnancy and determining their clinical utility as predictors of delivery date in term pregnancies.

**Supplementary Materials:** The following supporting information can be downloaded at: <https://www.mdpi.com/article/10.3390/life15020224/s1>, Table S1: Study cites that agreed to biobanking; Table S2: Proteins identified as regulated or identified as directly or indirectly associated with time to birth.

**Author Contributions:** Conceptualization, M.T.D., T.C.F., L.J.S., C.B.C., J.J.B. and P.E.K.; Methodology, M.T.D., M.B.B., A.D.P., C.B.C., J.J.B. and P.E.K.; Formal analysis, M.T.D., T.C.F. and A.D.P.; Investigation, M.T.D., T.C.F., M.B.B. and A.D.P.; Data curation, M.T.D., T.C.F., M.B.B., A.C.F. and S.R.R.; Writing—original draft preparation, M.T.D., T.C.F., L.J.S., M.B.B., A.D.P. and T.J.G.; Writing—review and editing, M.T.D., T.C.F., L.J.S., M.B.B., A.D.P., J.L., A.C.F., S.R.R., C.B.C., T.J.G., J.J.B. and P.E.K.; Visualization, M.T.D., M.B.B. and A.D.P.; Supervision, C.B.C., J.J.B. and P.E.K.; Project administration, J.L. All authors have read and agreed to the published version of the manuscript.

**Funding:** This research was funded by Sera Prognostics, Inc.

**Institutional Review Board Statement:** The PAPR study (NCT01371019) was conducted according to International Conference on Harmonization Good Clinical Practice Guidelines and approved by the Institutional Review Boards/Ethics Committees of all 10 participating study sites. The following is a list of approvals: Office of Human Research Ethics, University of North Carolina (11-1641, 13 September 2011), Institutional Review Board for Human Research, Office of Research Integrity, Medical University of South Carolina (Pro00012552, 11 October 2011), Maricopa Integrated Health System Institutional Review Board (2011-078, 18 October 2011), Western IRB (used by Ohio State University (20112063, 13 December 2011), Baystate Medical Center Institutional Review Board (BH-12-020, 23 December 2011), Research Integrity Office, Oregon Health and Science University (IRB00008131, 7 February 2012), San Diego Perinatal Center (20112063, 10 February 2012), University of Texas Medical Branch Institutional Review Board (12-046, 29 March 2012), Regional Obstetrical Consultants (20112063, 20 November 2012), and Christiana Care Institutional Review Board (32234, 28 December 2012). All necessary patient/participant consent was obtained, and the appropriate institutional forms have been archived.

**Informed Consent Statement:** Informed consent was obtained from all subjects involved in the study.

**Data Availability Statement:** Data supporting the results presented here are available upon request from the corresponding author. Data will not be made publicly available or in any format that may violate a subject's right to privacy.

**Acknowledgments:** The authors thank the Principal Investigators of the PAPR clinical trial (NCT01371019): Scott A. Sullivan, Glenn R. Markenson, Jay D. Iams, Dean V. Coonrod, Leonardo M. Pereira, M. Sean Esplin, Larry M. Cousins, Garrett K. Lam, and Matthew K. Hoffman for contributing samples and clinical data. We wish to acknowledge the study coordinators and research personnel at the study sites, the participants in the PAPR study, and the Sera Prognostics, Inc. clinical laboratory and clinical operations teams.

**Conflicts of Interest:** All authors are employees or consultants of Sera Prognostics, Inc. Sera Prognostics employees and consultants played a role in the study design, data collection and analysis, manuscript preparation, and the decision to submit.

## Abbreviations

The following abbreviations are used in this manuscript:

ADA12	Disintegrin and metalloproteinase domain-containing protein 12
AFAM	Afamin
ANGT	Angiotensinogen
AOC1	Amiloride-sensitive amine oxidase [copper-containing]
APOC3	Apolipoprotein C-III
APOH	Beta-2-glycoprotein 1
ATL4	ADAMTS-like protein 4
ATS13	A disintegrin and metalloproteinase with thrombospondin motifs 13
BGH3	Transforming growth factor-beta-induced protein ig-h3
BMI	Body mass index
C163A	Scavenger receptor cysteine-rich type 1 protein M130
C1QC	Complement C1q subcomponent subunit C
CAMP	Cathelicidin antimicrobial peptide
CAP	College of American Pathologists
CATD	Cathepsin D
CGB1	Choriogonadotropin subunit beta variant 1
CHL1	Neural cell adhesion molecule L1-like protein
CLIA	Clinical Laboratory Improvement Amendment
CNTN1	Contactin-1
CO6	Complement component C6
CRIS3	Cysteine-rich secretory protein 3
CSH	Chorionic somatomammotropin hormone 1
CSH	Chorionic somatomammotropin hormone 2
DEF1	Neutrophil defensin 1
DPEP2	Dipeptidase 2
EDD	Estimated delivery date
EGLN	Endoglin
ENPP2	Ectonucleotide pyrophosphatase/phosphodiesterase family member 2
FBLN1	Fibulin-1
FETUA	Alpha-2-HS-glycoprotein
HABP2	Hyaluronan-binding protein 2
GAB	Gestational age at birth
GABD	Gestational age at blood draw
IBP2	Insulin-like growth factor-binding protein 2
IBP4	Insulin-like growth factor-binding protein 4
IGF1	Insulin-like growth factor I
IL1R	Interleukin-1 receptor type 1
INHBC	Inhibin beta C chain
ISM2	Isthmin-2
ITIH4	Inter-alpha-trypsin inhibitor heavy chain H4
KIT	Mast/stem cell growth factor receptor Kit
KNG1	Kininogen-1
LC-MRM-MS	Liquid chromatography–multiple reaction monitoring–mass spectrometry
LEP	Leptin
LYAM1	L-selectin
MARS	Multiple affinity removal system
MR	Mendelian randomization
MRPC	Mendelian randomization-based machine learning algorithm
MRM	Multiple reaction monitoring
MUC18	Cell surface glycoprotein MUC18

PAEP	Glycodelin
PAPP1	Pappalysin-1
PAPP2	Pappalysin-2
PEDF	Pigment epithelium-derived factor
PGRP2	<i>n</i> -acetylmuramoyl-L-alanine amidase
PRG2	Bone marrow proteoglycan
PRL	Prolactin
PROS	Vitamin K-dependent protein S
PSG1	Pregnancy-specific beta-1-glycoprotein 1
PSG11	Pregnancy-specific beta-1-glycoprotein 11
PSG2	Pregnancy-specific beta-1-glycoprotein 2
PSG3	Pregnancy-specific beta-1-glycoprotein 3
PSG9	Pregnancy-specific beta-1-glycoprotein 9
RET4	Retinol-binding protein 4
RR	Response ratio
SEPP1	Selenoprotein P
SHBG	Sex hormone-binding globulin
SOM2	Growth hormone variant
SPRL1	SPARC-like protein 1
SIS	Stable isotope standard
SVEP1	Sushi, von Willebrand factor type A, EGF and pentraxin domain-containing protein 1
TENX	Tenascin-X
TTB	Time to birth
UHPLC	Ultra-high-performance liquid chromatography
VTNC	Vitronectin

## References

- Engle, W.A.; Kominiarek, M.A. Late preterm infants, early term infants, and timing of elective deliveries. *Clin. Perinatol.* **2008**, *35*, 325–341. [CrossRef] [PubMed]
- Hong, J.; Atkinson, J.; Roddy Mitchell, A.; Tong, S.; Walker, S.P.; Middleton, A.; Lindquist, A.; Hastie, R. Comparison of Maternal Labor-Related Complications and Neonatal Outcomes Following Elective Induction of Labor at 39 Weeks of Gestation vs Expectant Management: A Systematic Review and Meta-analysis. *JAMA Netw. Open* **2023**, *6*, e2313162. [CrossRef]
- Khasawneh, W.; Alyousef, R.; Akawi, Z.; Al-Dhoun, A.; Odat, A. Maternal and Perinatal Determinants of Late Hospital Discharge Among Late Preterm Infants; A 5-Year Cross-Sectional Analysis. *Front. Pediatr.* **2021**, *9*, 685016. [CrossRef] [PubMed]
- Pearson, J.; Siebert, K.; Carlson, S.; Ratner, N. Patient perspectives on loss of local obstetrical services in rural northern Minnesota. *Birth* **2018**, *45*, 286–294. [CrossRef] [PubMed]
- Sonenberg, A.; Mason, D.J. Maternity Care Deserts in the US. *JAMA Health Forum* **2023**, *4*, e225541. [CrossRef] [PubMed]
- Tanne, J.H. Nearly six million women in the US live in maternity care deserts. *BMJ* **2023**, *382*, 1878. [CrossRef] [PubMed]
- Vos, S.C.; Anthony, K.E.; O’Hair, H.D. Constructing the uncertainty of due dates. *Health Commun.* **2014**, *29*, 866–876. [CrossRef] [PubMed]
- Naidu, K.; Fredlund, K.L. Gestational Age Assessment. In *StatPearls*; StatPearls Publishing: Treasure Island, FL, USA, 2025.
- Committee on Obstetric Practice American Institute of Ultrasound in Medicine Society for Maternal–Fetal Medicine. Committee Opinion No 700: Methods for Estimating the Due Date. *Obstet Gynecol* **2017**, *129*, e150–e154. [CrossRef]
- Osterman, M.J.K.; Hamilton, B.E.; Martin, J.A.; Driscoll, A.K.; Valenzuela, C.P. Births: Final Data for 2022. *Natl. Vital Stat. Rep.* **2024**, *73*, 1–56. [PubMed]
- Menon, R.; Bonney, E.A.; Condon, J.; Mesiano, S.; Taylor, R.N. Novel concepts on pregnancy clocks and alarms: Redundancy and synergy in human parturition. *Hum. Reprod. Update* **2016**, *22*, 535–560. [CrossRef]
- McLean, M.; Bisits, A.; Davies, J.; Woods, R.; Lowry, P.; Smith, R. A placental clock controlling the length of human pregnancy. *Nat. Med.* **1995**, *1*, 460–463. [CrossRef] [PubMed]
- Norwitz, E.R.; Bonney, E.A.; Snegovskikh, V.V.; Williams, M.A.; Phillippe, M.; Park, J.S.; Abrahams, V.M. Molecular Regulation of Parturition: The Role of the Decidual Clock. *Cold Spring Harb. Perspect. Med.* **2015**, *5*, a023143. [CrossRef] [PubMed]
- Peterson, L.S.; Stelzer, I.A.; Tsai, A.S.; Ghaemi, M.S.; Han, X.; Ando, K.; Winn, V.D.; Martinez, N.R.; Contrepois, K.; Moufarrej, M.N.; et al. Multiomic immune clockworks of pregnancy. *Semin. Immunopathol.* **2020**, *42*, 397–412. [CrossRef] [PubMed]



15. Aghaeepour, N.; Ganio, E.A.; McIlwain, D.; Tsai, A.S.; Tingle, M.; Van Gassen, S.; Gaudilliere, D.K.; Baca, Q.; McNeil, L.; Okada, R.; et al. An immune clock of human pregnancy. *Sci. Immunol.* **2017**, *2*, eaan2946. [CrossRef] [PubMed]
16. Aghaeepour, N.; Lehallier, B.; Baca, Q.; Ganio, E.A.; Wong, R.J.; Ghaemi, M.S.; Culos, A.; El-Sayed, Y.Y.; Blumenfeld, Y.J.; Druzin, M.L.; et al. A proteomic clock of human pregnancy. *Am. J. Obstet. Gynecol.* **2018**, *218*, 347.e1–347.e14. [CrossRef] [PubMed]
17. Liang, L.; Rasmussen, M.H.; Piening, B.; Shen, X.; Chen, S.; Rost, H.; Snyder, J.K.; Tibshirani, R.; Skotte, L.; Lee, N.C.; et al. Metabolic Dynamics and Prediction of Gestational Age and Time to Delivery in Pregnant Women. *Cell* **2020**, *181*, 1680–1692.e15. [CrossRef] [PubMed]
18. Ngo, T.T.M.; Moufarrej, M.N.; Rasmussen, M.H.; Camunas-Soler, J.; Pan, W.; Okamoto, J.; Neff, N.F.; Liu, K.; Wong, R.J.; Downes, K.; et al. Noninvasive blood tests for fetal development predict gestational age and preterm delivery. *Science* **2018**, *360*, 1133–1136. [CrossRef]
19. Mitao, M.; Mwita, W.C.; Antony, C.; Adinan, H.; Shayo, B.; Amour, C.; Mboya, I.B.; Mahande, M.J. Recurrence of post-term pregnancy and associated factors among women who delivered at Kilimanjaro Christian Medical Centre in northern Tanzania: A retrospective cohort study. *PLoS ONE* **2023**, *18*, e0282078. [CrossRef]
20. Lancaster, E.E.; Lapato, D.M.; Jackson-Cook, C.; Strauss, J.F., 3rd; Roberson-Nay, R.; York, T.P. Maternal biological age assessed in early pregnancy is associated with gestational age at birth. *Sci. Rep.* **2021**, *11*, 15440. [CrossRef] [PubMed]
21. Campbell, J.M.; McPherson, N.O. Influence of increased paternal BMI on pregnancy and child health outcomes independent of maternal effects: A systematic review and meta-analysis. *Obes. Res. Clin. Pract.* **2019**, *13*, 511–521. [CrossRef]
22. Jukic, A.M.; Baird, D.D.; Weinberg, C.R.; McConaughy, D.R.; Wilcox, A.J. Length of human pregnancy and contributors to its natural variation. *Hum. Reprod.* **2013**, *28*, 2848–2855. [CrossRef]
23. Mekonen, M.W.; Bayew, A.T.; Lakew, T.J. Factors affecting the duration of gestation among women taking prenatal care at Gondar referral hospital, Ethiopia. *Health Sci. Rep.* **2022**, *5*, e676. [CrossRef] [PubMed]
24. Saade, G.R.; Boggess, K.A.; Sullivan, S.A.; Markenson, G.R.; Iams, J.D.; Coonrod, D.V.; Pereira, L.M.; Esplin, M.S.; Cousins, L.M.; Lam, G.K.; et al. Development and validation of a spontaneous preterm delivery predictor in asymptomatic women. *Am. J. Obstet. Gynecol.* **2016**, *214*, 633.e1–633.e24. [CrossRef] [PubMed]
25. Bradford, C.; Severinsen, R.; Pugmire, T.; Rasmussen, M.; Stoddard, K.; Uemura, Y.; Wheelwright, S.; Mentinova, M.; Chelsky, D.; Hunsucker, S.W.; et al. Analytical validation of protein biomarkers for risk of spontaneous preterm birth. *Clin. Mass Spectrom.* **2017**, *3*, 25–38. [CrossRef]
26. Davey Smith, G.; Hemani, G. Mendelian randomization: Genetic anchors for causal inference in epidemiological studies. *Hum. Mol. Genet.* **2014**, *23*, R89–R98. [CrossRef]
27. Badsha, M.B.; Fu, A.Q. Learning Causal Biological Networks With the Principle of Mendelian Randomization. *Front. Genet.* **2019**, *10*, 460. [CrossRef]
28. Badsha, M.B.; Martin, E.A.; Fu, A.Q. MRPC: An R Package for Inference of Causal Graphs. *Front. Genet.* **2021**, *12*, 651812. [CrossRef] [PubMed]
29. Khanam, R.; Fleischer, T.C.; Boghossian, N.S.; Nisar, I.; Dhingra, U.; Rahman, S.; Fox, A.C.; Ilyas, M.; Dutta, A.; Naher, N.; et al. Performance of a validated spontaneous preterm delivery predictor in South Asian and Sub-Saharan African women: A nested case control study. *J. Matern. Fetal Neonatal Med.* **2022**, *35*, 8878–8886. [CrossRef] [PubMed]
30. R Core Team. *R: A Language and Environment for Statistical Computing, Version 4.4.2*; R Foundation for Statistical Computing: Vienna, Austria, 2024.
31. Chellakooty, M.; Vangsgaard, K.; Larsen, T.; Scheike, T.; Falck-Larsen, J.; Legarth, J.; Andersson, A.M.; Main, K.M.; Skakkebaek, N.E.; Juul, A. A longitudinal study of intrauterine growth and the placental growth hormone (GH)-insulin-like growth factor I axis in maternal circulation: Association between placental GH and fetal growth. *J. Clin. Endocrinol. Metab.* **2004**, *89*, 384–391. [CrossRef] [PubMed]
32. Hannibal, R.L.; Cardoso-Moreira, M.; Chetty, S.P.; Lau, J.; Qi, Z.; Gonzalez-Maldonado, E.; Cherry, A.M.; Yu, J.; Norton, M.E.; Baker, J.C. Investigating human placentation and pregnancy using first trimester chorionic villi. *Placenta* **2018**, *65*, 65–75. [CrossRef] [PubMed]
33. Korevaar, T.I.; Steegers, E.A.; de Rijke, Y.B.; Schalekamp-Timmermans, S.; Visser, W.E.; Hofman, A.; Jaddoe, V.W.; Tiemeier, H.; Visser, T.J.; Medici, M.; et al. Reference ranges and determinants of total hCG levels during pregnancy: The Generation R Study. *Eur. J. Epidemiol.* **2015**, *30*, 1057–1066. [CrossRef] [PubMed]
34. Velegrakis, A.; Sfakiotaki, M.; Sifakis, S. Human placental growth hormone in normal and abnormal fetal growth. *Biomed. Rep.* **2017**, *7*, 115–122. [CrossRef] [PubMed]
35. Acar, A.; Altinbas, A.; Ozturk, M.; Kosar, A.; Kirazli, S. Selectins in normal pregnancy, pre-eclampsia and missed abortus. *Haematologia* **2001**, *31*, 33–38. [CrossRef] [PubMed]
36. Andres, F.; Wong, G.P.; Walker, S.P.; MacDonald, T.M.; Keenan, E.; Cannon, P.; Nguyen, T.V.; Hannan, N.J.; Tong, S.; Kaitu'u-Lino, T.J. A disintegrin and metalloproteinase 12 (ADAM12) is reduced at 36 weeks' gestation in pregnancies destined to deliver small for gestational age infants. *Placenta* **2022**, *117*, 1–4. [CrossRef] [PubMed]

37. Arevalo, E.; Shanmugasundararaj, S.; Wilkemeyer, M.F.; Dou, X.; Chen, S.; Charness, M.E.; Miller, K.W. An alcohol binding site on the neural cell adhesion molecule L1. *Proc. Natl. Acad. Sci. USA* **2008**, *105*, 371–375. [CrossRef] [PubMed]
38. Bearer, C.F. Mechanisms of brain injury: L1 cell adhesion molecule as a target for ethanol-induced prenatal brain injury. *Semin. Pediatr. Neurol.* **2001**, *8*, 100–107. [CrossRef] [PubMed]
39. Erenel, H.; Yilmaz, N.; Cift, T.; Bulut, B.; Sozen, I.; Aslan Cetin, B.; Gezer, A.; Ekmekci, H.; Kaya, B.; Tuten, A. Maternal serum autotaxin levels in early- and late-onset preeclampsia. *Hypertens. Pregnancy* **2017**, *36*, 310–314. [CrossRef] [PubMed]
40. Kremer, A.E.; Bolier, R.; Dixon, P.H.; Geenes, V.; Chambers, J.; Tolenaars, D.; Ris-Stalpers, C.; Kaess, B.M.; Rust, C.; van der Post, J.A.; et al. Autotaxin activity has a high accuracy to diagnose intrahepatic cholestasis of pregnancy. *J. Hepatol.* **2015**, *62*, 897–904. [CrossRef] [PubMed]
41. Laigaard, J.; Spencer, K.; Christiansen, M.; Cowans, N.J.; Larsen, S.O.; Pedersen, B.N.; Wewer, U.M. ADAM 12 as a first-trimester maternal serum marker in screening for Down syndrome. *Prenat. Diagn.* **2006**, *26*, 973–979. [CrossRef]
42. Li, Y.T.; Chen, J.S.; Jian, W.; He, Y.D.; Li, N.; Xie, Y.N.; Wang, J.; Zhang, V.W.; Huang, W.R.; Jiang, F.M.; et al. L1CAM mutations in three fetuses diagnosed by medical exome sequencing. *Taiwan. J. Obstet. Gynecol.* **2020**, *59*, 451–455. [CrossRef] [PubMed]
43. Tuzluoglu, S.; Ustunyurt, E.; Karasin, S.S.; Karasin, Z.T. Investigation of Serum Pregnancy-Specific Beta-1-Glycoprotein and Relationship with Fetal Growth Restriction. *JBRA Assist. Reprod.* **2022**, *26*, 267–273. [CrossRef] [PubMed]
44. Ramanjaneya, M.; Butler, A.E.; Bashir, M.; Bettahi, I.; Moin, A.S.M.; Ahmed, L.; Elrayess, M.A.; Hunt, S.C.; Atkin, S.L.; Abou-Samra, A.B. apoA2 correlates to gestational age with decreased apolipoproteins A2, C1, C3 and E in gestational diabetes. *BMJ Open Diabetes Res. Care* **2021**, *9*, e001925. [CrossRef] [PubMed]
45. Dou, X.; Menkari, C.; Mitsuyama, R.; Foroud, T.; Wetherill, L.; Hammond, P.; Suttie, M.; Chen, X.; Chen, S.Y.; Charness, M.E.; et al. L1 coupling to ankyrin and the spectrin-actin cytoskeleton modulates ethanol inhibition of L1 adhesion and ethanol teratogenesis. *FASEB J.* **2018**, *32*, 1364–1374. [CrossRef]
46. The Human Protein Atlas. Available online: <https://www.proteinatlas.org/> (accessed on 10 December 2024).
47. Kasimis, C.; Evangelinakis, N.; Rotas, M.; Georgitsi, M.; Pelekanos, N.; Kassanos, D. Predictive value of biochemical marker ADAM-12 at first trimester of pregnancy for hypertension and intrauterine growth restriction. *Clin. Exp. Obstet. Gynecol.* **2016**, *43*, 43–47. [CrossRef]
48. Toprak, K.; Yildiz, Z.; Akdemir, S.; Esen, K.; Kada, R.; Can Gulec, N.; Omar, B.; Bicer, A.; Demirbag, R. Low pregnancy-specific beta-1-glycoprotein is associated with nondipper hypertension and increased risk of preeclampsia in pregnant women with newly diagnosed chronic hypertension. *Scand. J. Clin. Lab. Investig.* **2023**, *83*, 479–488. [CrossRef]
49. Ilicic, M.; Zakar, T.; Paul, J.W. The Regulation of Uterine Function During Parturition: An Update and Recent Advances. *Reprod. Sci.* **2020**, *27*, 3–28. [CrossRef] [PubMed]
50. Bonney, E.A. Demystifying animal models of adverse pregnancy outcomes: Touching bench and bedside. *Am. J. Reprod. Immunol.* **2013**, *69*, 567–584. [CrossRef]
51. Wegienka, G.; Baird, D.D. A comparison of recalled date of last menstrual period with prospectively recorded dates. *J. Womens Health* **2005**, *14*, 248–252. [CrossRef] [PubMed]
52. Barr, W.B.; Pecci, C.C. Last menstrual period versus ultrasound for pregnancy dating. *Int. J. Gynaecol. Obstet.* **2004**, *87*, 38–39. [CrossRef] [PubMed]
53. Christians, J.K.; Beristain, A.G. ADAM12 and PAPP-A: Candidate regulators of trophoblast invasion and first trimester markers of healthy trophoblasts. *Cell Adhes. Migr.* **2016**, *10*, 147–153. [CrossRef] [PubMed]
54. Myers, J.E.; Thomas, G.; Tuytten, R.; Van Herreweghe, Y.; Djiokep, R.O.; Roberts, C.T.; Kenny, L.C.; Simpson, N.A.; North, R.A.; Baker, P.N. Mid-trimester maternal ADAM12 levels differ according to fetal gender in pregnancies complicated by preeclampsia. *Reprod. Sci.* **2015**, *22*, 235–241. [CrossRef]
55. Gaccioli, F.; Aye, I.; Sovio, U.; Charnock-Jones, D.S.; Smith, G.C.S. Screening for fetal growth restriction using fetal biometry combined with maternal biomarkers. *Am. J. Obstet. Gynecol.* **2018**, *218*, S725–S737. [CrossRef]
56. Montagnana, M.; Trenti, T.; Aloe, R.; Cervellin, G.; Lippi, G. Human chorionic gonadotropin in pregnancy diagnostics. *Clin. Chim. Acta* **2011**, *412*, 1515–1520. [CrossRef] [PubMed]
57. Blois, S.M.; Sulkowski, G.; Tirado-González, I.; Warren, J.; Freitag, N.; Klapp, B.F.; Rifkin, D.; Fuss, I.; Strober, W.; Dveksler, G.S. Pregnancy-specific glycoprotein 1 (PSG1) activates TGF-beta and prevents dextran sodium sulfate (DSS)-induced colitis in mice. *Mucosal Immunol.* **2014**, *7*, 348–358. [CrossRef] [PubMed]
58. Shanley, D.K.; Kiely, P.A.; Golla, K.; Allen, S.; Martin, K.; O’Riordan, R.; Ball, M.; Aplin, J.D.; Singer, B.B.; Caplice, N.; et al. Pregnancy-specific glycoproteins bind integrin alphaIIb beta3 and inhibit the platelet-fibrinogen interaction. *PLoS ONE* **2013**, *8*, e57491. [CrossRef] [PubMed]
59. Martinez, F.F.; Cervi, L.; Knubel, C.P.; Panzetta-Dutari, G.M.; Motran, C.C. The role of pregnancy-specific glycoprotein 1a (PSG1a) in regulating the innate and adaptive immune response. *Am. J. Reprod. Immunol.* **2013**, *69*, 383–394. [CrossRef] [PubMed]
60. Martinez, F.F.; Knubel, C.P.; Sanchez, M.C.; Cervi, L.; Motran, C.C. Pregnancy-specific glycoprotein 1a activates dendritic cells to provide signals for Th17-, Th2-, and Treg-cell polarization. *Eur. J. Immunol.* **2012**, *42*, 1573–1584. [CrossRef] [PubMed]

61. Zhou, G.Q.; Baranov, V.; Zimmermann, W.; Grunert, F.; Erhard, B.; Mincheva-Nilsson, L.; Hammarstrom, S.; Thompson, J. Highly specific monoclonal antibody demonstrates that pregnancy-specific glycoprotein (PSG) is limited to syncytiotrophoblast in human early and term placenta. *Placenta* **1997**, *18*, 491–501. [CrossRef] [PubMed]
62. Sargent, I.L.; Borzychowski, A.M.; Redman, C.W. NK cells and human pregnancy—An inflammatory view. *Trends Immunol.* **2006**, *27*, 399–404. [CrossRef]
63. Mahajan, D.; Sharma, N.R.; Kancharla, S.; Kolli, P.; Tripathy, A.; Sharma, A.K.; Singh, S.; Kumar, S.; Mohanty, A.K.; Jena, M.K. Role of Natural Killer Cells during Pregnancy and Related Complications. *Biomolecules* **2022**, *12*, 68. [CrossRef]
64. Okamoto, N.; Uchida, A.; Takakura, K.; Kariya, Y.; Kanzaki, H.; Riittinen, L.; Koistinen, R.; Seppala, M.; Mori, T. Suppression by human placental protein 14 of natural killer cell activity. *Am. J. Reprod. Immunol.* **1991**, *26*, 137–142. [CrossRef] [PubMed]
65. Mukhopadhyay, D.; Sundereshan, S.; Rao, C.; Karande, A.A. Placental protein 14 induces apoptosis in T cells but not in monocytes. *J. Biol. Chem.* **2001**, *276*, 28268–28273. [CrossRef]
66. Licheri, V.; Brigman, J.L. Altering Cell-Cell Interaction in Prenatal Alcohol Exposure Models: Insight on Cell-Adhesion Molecules During Brain Development. *Front. Mol. Neurosci.* **2021**, *14*, 753537. [CrossRef]
67. Cau, F.; Fanni, D.; Manchia, M.; Gerosa, C.; Piras, M.; Murru, R.; Paribello, P.; Congiu, T.; Coni, P.; Pichiri, G.; et al. Expression of L1 Cell Adhesion Molecule (L1CAM) in extracellular vesicles in the human spinal cord during development. *Eur. Rev. Med. Pharmacol. Sci.* **2022**, *26*, 6273–6282. [CrossRef] [PubMed]
68. Prakobphol, A.; Genbacev, O.; Gormley, M.; Kapidzic, M.; Fisher, S.J. A role for the L-selectin adhesion system in mediating cytotrophoblast emigration from the placenta. *Dev. Biol.* **2006**, *298*, 107–117. [CrossRef] [PubMed]
69. Feng, Y.; Ma, X.; Deng, L.; Yao, B.; Xiong, Y.; Wu, Y.; Wang, L.; Ma, Q.; Ma, F. Role of selectins and their ligands in human implantation stage. *Glycobiology* **2017**, *27*, 385–391. [CrossRef] [PubMed]
70. Genbacev, O.D.; Prakobphol, A.; Foulk, R.A.; Krtolica, A.R.; Ilic, D.; Singer, M.S.; Yang, Z.Q.; Kiessling, L.L.; Rosen, S.D.; Fisher, S.J. Trophoblast L-selectin-mediated adhesion at the maternal-fetal interface. *Science* **2003**, *299*, 405–408. [CrossRef]
71. Gelius, E.; Persson, C.; Karlsson, J.; Steiner, H. A mammalian peptidoglycan recognition protein with N-acetylmuramoyl-L-alanine amidase activity. *Biochem. Biophys. Res. Commun.* **2003**, *306*, 988–994. [CrossRef]
72. Lo, D.; Tynan, W.; Dickerson, J.; Mendy, J.; Chang, H.W.; Scharf, M.; Byrne, D.; Brayden, D.; Higgins, L.; Evans, C.; et al. Peptidoglycan recognition protein expression in mouse Peyer’s Patch follicle associated epithelium suggests functional specialization. *Cell. Immunol.* **2003**, *224*, 8–16. [CrossRef]
73. Tosoni, G.; Conti, M.; Diaz Heijtz, R. Bacterial peptidoglycans as novel signaling molecules from microbiota to brain. *Curr. Opin. Pharmacol.* **2019**, *48*, 107–113. [CrossRef] [PubMed]
74. Arentsen, T.; Qian, Y.; Gkatzis, S.; Femenia, T.; Wang, T.; Udekwu, K.; Forssberg, H.; Diaz Heijtz, R. The bacterial peptidoglycan-sensing molecule Pglyrp2 modulates brain development and behavior. *Mol. Psychiatry* **2017**, *22*, 257–266. [CrossRef] [PubMed]

**Disclaimer/Publisher’s Note:** The statements, opinions and data contained in all publications are solely those of the individual author(s) and contributor(s) and not of MDPI and/or the editor(s). MDPI and/or the editor(s) disclaim responsibility for any injury to people or property resulting from any ideas, methods, instructions or products referred to in the content.

Protocol

# Unlocking Female Fertility with a Specific Reproductive Exercise Program: Protocol of a Randomized Controlled Clinical Trial

Barbara Petra Kovács <sup>1,2,\*</sup>, Júlia Balog <sup>3</sup>, Barbara Sebők <sup>2,4</sup>, Márton Keszthelyi <sup>2,5</sup> and Szabolcs Várbíró <sup>2,5,6</sup>

<sup>1</sup> Doctoral College, Semmelweis University, 1085 Budapest, Hungary

<sup>2</sup> Workgroup for Science Management, Semmelweis University Doctoral College, 1085 Budapest, Hungary; sebok.barbara23@gmail.com (B.S.); keszthelyi.marton@semmelweis.hu (M.K.); varbiro.szabolcs@semmelweis.hu (S.V.)

<sup>3</sup> Department of Metabolism, Digestion and Reproduction, Imperial College London, London W12 0NN, UK; j.balog@imperial.ac.uk

<sup>4</sup> Dr. Manninger Jenő Trauma Center, 1081 Budapest, Hungary

<sup>5</sup> Department of Obstetrics and Gynecology, Faculty of Medicine, Semmelweis University, 1082 Budapest, Hungary

<sup>6</sup> Department of Obstetrics and Gynecology, Faculty of Medicine, Szeged University, 6720 Szeged, Hungary

\* Correspondence: kovacs.barbara@phd.semmelweis.hu

**Abstract:** According to World Health Organization (WHO) data, 16% of people are affected by infertility across the globe. One underlying factor is the age-related decline of ovarian reserve (DOR), which can lead to a higher chance of infertility and has no widely accepted treatment currently. Specific supplements and moderate exercise have been shown to improve fertility; however, there is no consensus to date on the type of exercise providing the best results. Our goal is to develop a novel exercise program combined with natural supplements for the improvement of fertility. We also propose a single-centered, randomized, open-label clinical trial using our newly developed exercise in the intervention group, compared to walking and no exercise in the other groups, to investigate the benefits of this exercise program in the future. In this study, we developed a structured, novel combination of exercises focusing on the pelvic and ovarian regions, core strengthening and improvement of blood circulation in this region. The 70 min full body “reproductive gymnastics”, includes strengthening, stretching, and relaxation exercises combined with yoga-inspired moves and diaphragmatic breathing with meditation elements to activate the parasympathetic pathway and stress relief. We believe we can improve fertility through the combination of natural supplements and our targeted, moderate physiotherapy program in women with DOR.

**Keywords:** infertility treatment; physiotherapy; targeted exercise; DOR; fertility improvement; FSH; AMH; randomized controlled clinical trial; combined supplements; ovarian rejuvenation

## 1. Introduction

Infertility is a growing concern worldwide, marked by the inability to achieve clinical pregnancy after a year of regular, unprotected intercourse [1]. Its global prevalence is significantly increasing, concurrently with the rising trend of delayed parenthood, and it affects an estimated 186 million people [2,3]. With increased maternal age, patients have to confront the decline in age-related ovarian reserve (DOR), which is well defined by the current determination of Anti-Müllerian Hormone (AMH), Antral Follicle Count (AFC), and basal FSH levels [4]. According to the American Society for Reproductive Medicine,

the use of AMH and AFC as screening tests is most suitable for detecting poor ovarian response [5]. Since no single measure of ovarian reserve has 100% specificity in diagnosing DOR, a combination of biochemical and transvaginal ultrasound measurements (including FSH, LH, E2, AMH, and AFC) is utilized in this study to evaluate changes in ovarian reserve. Diminished ovarian reserve (DOR) is characterized by poor fertility indicators, even with the application of assisted reproductive techniques (ARTs), posing a significant challenge in reproductive medicine [6].

It has been shown that supplements have a high impact on the restoration of fertility. Myo-inositol has been demonstrated to improve ovarian function and increase the quality of oocytes, particularly in women with polycystic ovary syndrome (PCOS), leading to higher pregnancy rates [7,8]. In particular, several clinical trials demonstrate that its administration can have therapeutic effects in infertile women, and that it can also be useful as a preventive treatment during pregnancy [9].

Folic acid is essential for DNA synthesis and repair, and its supplementation is crucial for proper fetal development and reducing the risk of neural tube defects [10]. Melatonin not only regulates sleep but also acts as a potent antioxidant, protecting oocytes from oxidative damage and improving their quality [11–13]. Vitamins C and E, both powerful antioxidants, have been shown to reduce oxidative stress in the reproductive organs, thereby enhancing fertility, not only in woman [14,15]. Vitamin D3 plays a critical role in the modulation of the immune system and the regulation of reproductive processes, with deficiencies linked to adverse fertility outcomes [16]. Coenzyme Q10 is vital for mitochondrial function and energy production in oocytes, with studies indicating that its supplementation improves ovarian response and embryo quality [17,18]. Collectively, these supplements contribute to a comprehensive approach to restoring and enhancing fertility, addressing both physiological and biochemical factors involved in reproductive health.

The World Health Organization (WHO), and the American College of Obstetricians and Gynecologists (ACOG) suggests that women planning pregnancy should engage in at least 150 min of moderate physical activity per week, to reduce reproductive risks [19,20]. Not only does engaging in regular exercise improve fertility outcomes, but the specific type of physical activity plays a major role in enhancing reproductive health.

The coordinated, optimal functioning of the muscles involved in pelvic-lumbar (core) stabilization (diaphragm, pelvic floor muscles, transversus abdominis muscle (TVA), multifidus muscles) is of paramount importance for spinal protection, efficient breathing and movement, injury prevention, force transmission, optimal function and support of the pelvic floor and pelvic organs (ovaries, uterus), and proper regulation of sexual function. Pelvic-lumbar (core) stabilization is developed by strengthening the deep stabilization system of the spine, in coordination with the correct breathing pattern [21]. The proper muscle function of the TVA is of paramount importance for pelvic and lumbar stability, the restoration of physiological breathing patterns, and the efficient functioning of the pelvic floor muscles that work in co-contraction with it. Rehabilitation of the pelvic region and pelvic floor is essential to improving fertility. Exercises that improve pelvic-lumbar (core) stabilization have been shown to improve the function of the pelvic floor muscles, which play a crucial role in supporting the reproductive organs and improving blood supply to the ovaries and uterus [22]. Several authors agree that through breathing exercises, the complex trunk stabilization system can be directly affected [23–25]. Normal breathing mechanics play a key role in posture, optimal pelvic floor muscle function, and spinal stabilization.

Prolonged mental and physical stress, postural and lifestyle habits, and improper breathing patterns all contribute to diaphragmatic dysfunction. These factors also stimulate the sympathetic nervous system and stimulate the secretion of the stress hormone (cortisol),

which also has a negative impact on fertility [26]. Additionally, diaphragmatic breathing has been shown to reduce stress, which is crucial for enhancing fertility, as chronic stress can disrupt hormone balance and menstrual cycles [27]. Yoga and diaphragmatic breathing, in particular, have demonstrated stress-reducing benefits, activating the parasympathetic nervous system and promoting a state of relaxation conducive to reproductive health [28,29].

These professional aspects should be combined in a targeted and comprehensive multidimensional exercise program.

Despite these promising findings, further research is needed to confirm these effects due to the limited number and sample size of previous studies and the current ambiguity in exercise recommendations for improving fertility outcomes.

In this study, we present a novel and innovative therapeutic exercise protocol specifically designed for pelvic region rehabilitation and ovarian rejuvenation. The therapeutic exercises focus on improving fertility, rehabilitation of the pelvic region (including re-education of the pelvic floor muscles), teaching correct posture, improving the pelvic-lumbar core stabilization system, restoring optimal muscular function of the diaphragm, and activating the parasympathetic nervous system through learning stress-relieving breathing and relaxation. These exercises are expected to enhance pelvic circulation and improve muscle function, which are crucial for reproductive health, especially in patients with diminished ovarian reserve (DOR).

The primary objective of this study is to assess the ovarian rejuvenating effect of this specific exercise program before IVF/ICSI cycles or spontaneous pregnancy, confirming the reproductive efficacy of this regimen. We also aim to improve stimulation and oocyte quality in patients who meet the inclusion criteria, partly by improving pelvic and ovarian circulation (ovarian rejuvenation exercise, the subject of this study) and partly by enhancing cumulus corona radiata and granulosa cell function (per os rejuvenation therapy).

It is expected that our results will show that AMH will be increased, basal FSH levels will be decreased, cycle length will be optimized (getting closer to 28–30 days), fertility rates and stimulation will be improved, and spontaneous pregnancy will be detected at the end of the process. If this investigation confirms the efficacy of the specific exercise program in DOR patients, this could make a useful contribution to fertility treatment in this poorly manageable patient population.

## 2. Experimental Design

This protocol was written in accordance with the Standard Protocol Items: Recommendations for Interventional Trials (SPIRIT) reporting template [30]. This was a single-center, randomized (1:1:1), open-label clinical trial, with three treatment groups: per os therapy (Group A), per os therapy and walking (Group B), per os therapy and special exercise (Group C). The purpose of randomization is to eliminate selection bias. The study protocol was approved and registered by the Human Reproduction Committee of Hungarian Medical Research Council (25489-8/2021/EÜIG).

### 2.1. Study Setting

This study will involve women aged 20–42 diagnosed with diminished ovarian reserve (DOR) who meet the following criteria: (1) AMH levels  $< 1.1$  ng/mL at the beginning of the cycle, (2) BMI between 18.5 and 30 kg/m<sup>2</sup>, (3) regular and normal menstruation, and (4) specified hormone levels (TSH  $< 2.5$  mIU/mL, vitamin D3  $> 75$  nmol/L, Prolactin  $< 24$  ng/mL). We plan to enroll 120 patients between January 2025 and December 2025.

## 2.2. Eligibility Criteria

### 2.2.1. Inclusion Criteria

Participants who meet the following inclusion criteria will be included: (1) female of reproductive age 20–42 years; (2) BMI: 18.5–30 kg/m<sup>2</sup>; (3) regular menstruation; (4) anti-Müllerian hormone (AMH) < 1.1 ng/mL; (5) hormone levels: TSH < 2.5 mIU/mL, vitamin D3: >75 nmol/L, Prolactin: <24 ng/mL; (6) understanding the study design, risks, and benefits, and providing informed consent; and (7) the ability to comply with the study protocol.

### 2.2.2. Exclusion Criteria

Participants meeting any of the following criteria will be excluded: (1) age > 42 years old; (2) antral follicle count (AFC) < 3 measured on day 2 of the cycle; (3) multiple unsuccessful stimulation cycles ending with cancellation; (4) allergy to medications used for ovarian rejuvenation; (5) three or more ovarian surgeries result in significant ovarian reserve depletion (iatrogenic POI, iatrogenic DOR); (6) secondary amenorrhea; (7) uterine developmental abnormalities; and (8) inability to engage in physical activity.

## 2.3. Objectives

The primary objective of this study is to assess the efficacy of specific exercise routine on ovarian function compared with a standard of care and low intensity walking in patients with diminished ovarian reserve, by optimizing hormone levels for better stimulation possibilities.

### 2.3.1. Primary Outcome

The primary outcome is the change in FSH and AMH levels compared with the levels before. Spontaneous pregnancy during the study period will be recorded as a primary outcome measure.

### 2.3.2. Secondary Outcomes

The secondary outcomes include: optimization of E2 and LH levels; optimization of menstrual cycle length; change in BMI level; improvement in quality of life using the FSFI questionnaire; and comparing the effectiveness between the 3 study groups.

## 2.4. Sample Size

A parallel, 3-group design will be used. We determined the sample size using G\*Power 3.1.9.7 software. We employed one-way analysis of variance (ANOVA) due to consideration of three different therapies. The effect size was estimated at 0.4. We set alpha to 0.05 and power to 0.95. Consequently, the software provided an estimated total sample size of 102, resulting in 34 cases per group. To account for a potential dropout rate of 15%, we increased the sample size to 40 participants per group. Therefore, the total sample size needed for the study is 120 participants [31].

## 2.5. Statistical Methods

Descriptively, we intend to calculate the mean, standard deviation, minimum, maximum, and range of data, while the occurrence of spontaneous pregnancy will be presented as a percentage. For the evaluation of results, after conducting the Shapiro–Wilk normality test, paired T-tests or Wilcoxon tests will be used to compare baseline and three-month laboratory results within each group, and one-way analysis of variance (ANOVA) or Kruskal–Wallis’s test, along with Tukey’s post hoc test, will be used for comparison among the three groups. Chi-square tests or Fisher’s exact tests are planned to be applied for comparing the numbers or percentages between groups.

## 2.6. Recruitment

Patients meeting the eligibility criteria will be recruited from the Assisted Reproduction Center of Semmelweis University, Hungary. Detailed information about the study will be provided verbally and in writing by the examining physician. Research subjects are informed that in this clinical trial we intend to compare three groups of infertile women. The group receiving only per os complementary therapy, the group receiving per os complementary therapy and walking, and the group receiving per os complementary therapy and a specific exercise program will be tested. We will also inform prospective participants that participation in the research is voluntary and that the anonymized data obtained will be summarized and subjected to statistical analysis. Participation in the study will take approximately 12 weeks.

## 2.7. Implementation

The principal investigator or a designated sub-investigator will input the required data into a web-based allocation system for eligible patients. Subsequently, the system will allocate participants to the three investigated groups. The required data include personal data, demographic data, medical and family history, body composition assessment (weight, height, BMI), menstrual cycle (length and days of menstruation), hormone levels (AMH, FSH, LH, E2, PRL, TSH, vitamin 25-OH-D3), progesterone levels, and the FSFI questionnaire, as shown in Table 1.

**Table 1.** Study Assessments and Procedures.

	Screening	Baseline (2–4. Day of Menstrual Cycle)	Baseline (21–22. Day of the Same Cycle)	3 Months (2–4. Day of Cycle)	3 Months (21–22. Day of the Same Cycle)
<b>Assessment</b>					
Investigator meetings	✓				
Informed consent	✓				
Demographics, medical, and family history	✓				
Body composition assessment (Weight, Height, BMI)	✓			✓	
Menstrual cycle	✓			✓	
Hormone levels (AMH, FSH, LH, E2, PRL, TSH, 25-OH-D3 vitamin)		✓		✓	
Progesteron		✓	✓		✓
FSFI questionnaire		✓		✓	
Spontaneous pregnancy				✓	

## 3. Materials and Equipment

The per os therapy consists of the following supplementation and amounts: daily 3 mg of melatonin (Pharma Nord, Vejle, Denmark) before bedtime in addition to daily intake of 1000 mg of vitamin C (slow release), 400 mg of vitamin E, 2500 IU/day of vitamin D3, and 200 mg of Coenzyme Q10 (Pharma Nord, Vejle, Denmark); and twice daily a preparation containing 2000 mg of myo-inositol, 50 mg of alpha-lactalbumin, and 200 µg of folic acid (Inofolic premium, Exeltis Hungary, Budapest, Hungary). For the rejuvenation



exercise, there is no mandatory equipment, although an exercise mat and a pillow or ball are recommended.

## 4. Detailed Procedures

### 4.1. Intervention

The standard dietary supplement/vitamin oral therapy for all three groups includes the intake of a preparation containing myo-inositol + folic acid orally twice a day. Participants in the study are asked to take 3 mg of melatonin before bedtime in addition to daily intake of 1000 mg of vitamin C (slow release), 400 mg of vitamin E, 2500 IU/day of vitamin D3, and 200 mg of Coenzyme Q10.

Combined with the supplement therapy, patients in Arm B will be asked to perform low intensity walking 3 times per week for 1 h each session.

For Arm C (per os therapy and special exercise), our special 70 min moderate-intensity exercise program is available 3 times a week for at least 3 months. This therapeutic exercise program is designed to combine several professional aspects in all exercises including postural correction, pelvic-lumbar stabilization, rehabilitation of the pelvic region, re-education of the pelvic floor muscles, restoration of optimal diaphragm function, dynamic mobilization and stretching exercises, use of the relaxation and therapeutic effects of costo-diaphragmatic breathing, optimization of joint range of motion, and development of balance and coordination. There is a large emphasis on the combination of exercises with relaxation-type exercises of costo-diaphragmatic breathing. The constant attention on breathing helps the patients relax, activates the parasympathetic nervous system, and ensures the strengthening of multiple muscle groups by contraction and relaxation.

The therapeutic movement program begins with a 15 min warm-up focused on teaching active elongation and correct posture, diaphragmatic breathing, hip joint–shoulder joint–thoracic spine mobilization exercises and activating the gluteal group to prepare the pelvic region and the whole body for exercise. The warm-up is followed by a 15 min active core strengthening session, designed to develop the pelvic-lumbar stabilization system and optimize hip joint range of motion, in coordination with proper breathing technique. Proper mobility of the lumbar–pelvic–hip complex and optimal functioning of the core muscles are also necessary for optimal functioning of the pelvic organs (ovaries, uterus). In this session, exercises use coordinated activation of the TVA and pelvic floor muscles along with breathing. The third 15 min section focuses on costo-diaphragmatic breathing in various yoga postures to activate the parasympathetic nervous system, promoting relaxation and stress relief and improving fertility. The other aim of this phase is to restore muscle balance around the pelvis through stretching exercises and to relax the PF through relaxation breathing techniques. The next 15 min session before the cool-down presents the therapeutic objectives of the previous sessions in a complex way, including postural correction, dynamic stretching, and core stabilization exercises, together with correct breathing techniques. Our goal is to compensate for mobility problems due to a sedentary lifestyle, relieve pelvic floor muscles, improve pelvic organ circulation, and correct fertility problems due to restricted hip movements. The final 10 min session is an active pelvic mobilization through dance movements in a vertical position. The aim of this phase is to optimize the movements of the hypomobile lumbar–pelvic–hip complex (LPHC). This is achieved by hip rotations, pelvic tilts, and a combination of these movements. If there is not adequate range of motion in the lumbar spine–pelvic–hip joint, sexual function is significantly affected and limited, and this also has a negative impact on fertility. The stress-relieving effects of music and dance are used to release female energy and mobilize the pelvic girdle.

The workout can be tailored to specific needs by offering multiple levels and incorporating weights. All the exercises will be conducted by a women's reproductive health physiotherapist.

#### 4.2. Randomization

Patients will be randomly assigned to Arm A (per os therapy), Arm B (per os therapy and walking), or Arm C (per os therapy and special exercise) in a 1:1:1 ratio by an internet-based distant third-party statistician blinded to the study and participant details. The recruiting physician will be trained and provided with detailed instructions on the recruitment protocol. The objective of randomization is to eliminate selection bias. The trial design is summarized in Figure 1.

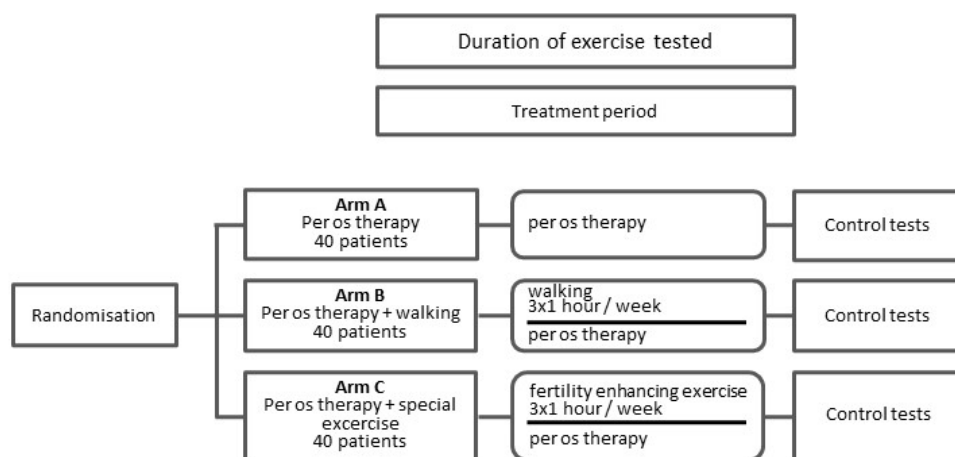


**Figure 1.** Trial design.

#### 4.3. Treatments of Adverse Events

Local investigators will handle any adverse events in accordance with current good clinical practice guidelines. Each adverse event will be documented in a case report form, detailing its nature, onset and resolution times, severity, treatment, and outcome. Follow-up examinations will be conducted as needed to ensure patient safety.

Should the monitoring physician observe any harm to a participant or signs of ineffectiveness during the trial, the participant will be removed from the study.

#### 4.4. Criteria for Discontinuation of Trial Treatment

The criteria for the discontinuation of a trial are as follows:

(1) The participant refuses further participation or withdraws consent; (2) termination of the entire study; (3) occurrence of a spontaneous pregnancy; (4) failure to adhere to the study rules; (5) attendance of fewer than 75% of the exercise sessions by the participant in the intervention group; (6) occurrence of any other intervention or surgery during the study period that may alter the study outcome; (7) undesirable events related to the treatment, such as acute pain, musculoskeletal complaints, or acute mental or physical trauma preventing continuation of the study; (8) presence of a newly diagnosed malignancy; (9) any situation where oral therapy or physiotherapy is deemed unfit to continue according to the decision of the physician and physiotherapist.

#### 4.5. Discontinuation of the Study

The study will be terminated early if the Institutional Review Board (IRB) identifies any of the following: serious adverse drug effects; a newly diagnosed malignancy; or participants encountering unexpected, significant, or unacceptable risks (such as death).

#### 4.6. Baseline Assessments

Baseline assessments will adhere to the trial's standard operating procedure (SOP). During the first visit, between days 2 and 4 of the cycle, a laboratory examination will be conducted, including hormone levels of AMH, FSH, LH, E2, PRL, TSH, 25-OH-D3 vitamin, and progesterone. Baseline progesterone will be measured between days 21 and 22 of the same cycle. The FSFI questionnaire will also commence during this phase.

#### 4.7. Efficacy Assessments

The efficacy of the trial treatment will be evaluated using a comprehensive set of parameters measured at the 3-month follow-up. Participants' weight, height, and BMI will be recorded. This will help in assessing any changes in body composition resulting from the intervention. The regularity and characteristics of participants' menstrual cycles will be monitored from the start to the end of the study. This continuous observation aims to identify any improvements or alterations in menstrual health. Hormonal evaluations, including levels of AMH, FSH, LH, E2, PRL, TSH, and 25-OH-D3 vitamin, will be conducted at the conclusion of the study as well. As a primary outcome, the change in FSH and AMH levels will be administered. The measurement of progesterone will help evaluate the sufficiency of the luteal phase, which is critical for reproductive health. These measures will provide insights into the hormonal balance and ovarian function of the participants. The FSFI questionnaire will be administered to assess changes in sexual function. This self-reported measure will provide valuable data on the impact of the intervention on participants' sexual health. The occurrence of spontaneous pregnancy during the study period will be recorded as a primary outcome measure. This will directly indicate the effectiveness of the intervention in improving fertility. These comprehensive assessments will collectively provide a thorough evaluation of the intervention's efficacy.

#### 4.8. Data Monitoring Committee

An oversight committee comprising clinical trial experts, including a biostatistician, will be established. The oversight committee will analyze unblinded outcome data to assess safety and efficacy, determining whether there are indications of unsafe treatments warranting the discontinuation of the trial. Additionally, the committee will alert the Trial Steering Committee to any instances of unethical treatment or serious adverse events.

To manage the data for this study, the IBM Clinical Development Management System (IBM Corporation, Somers, NY, USA), utilizing an Electronic Data Capture (EDC) system, will be employed.

### 5. Expected Results

This clinical trial aims to explore whether our therapeutic exercise program designed to rejuvenate the ovaries and rehabilitate the pelvic region is effective in improving ovarian reserve in women with DOR. The exercise aims to show the effects of increased pelvic region circulation on ovarian reserve. We are not aware of any other studies aiming to discover the effects of pelvic-specific physical therapy on the fertility of women with DOR. Our study is the first to investigate the multifaceted impact of specially combined physical activity compared with walking and no physical activity at all on female fertility in patients with infertility diagnosed with diminished ovarian reserve (DOR). Improving assisted reproductive outcomes has become a critical issue for both infertile couples and clinicians. Considering the strong desire of patients and the urgent need for treatment, per os rejuvenation therapy combined with walking and per os rejuvenation therapy "without exercise" were selected as a control method rather than placebo. Targeted exercise of the pelvic region and the relaxation and therapeutic effects of costo-diaphragmatic breathing

may be an important factor besides lifestyle changes and nutritional factors, which are among the most valuable and promising interventions in preserving and restoring human health and fertility, representing an area of medical research that remains to be fully explored [32].

Data on the association between physical activity and female fertility are subject to debates. Several studies have previously investigated the therapeutic effects of exercise on fertility, but no clear consensus has emerged. In many studies, researchers have reported mixed results, which is probably one of the reasons why the factors affecting fertility are multifactorial. Several studies show that regular, moderate physical activity can help achieve optimal hormonal balance and regular ovulation, thereby improving fertility [33,34]. Some clinical and experimental studies have also revealed that regular moderate intensity exercise is beneficial for maintaining and improving ovarian reserve and positively influences the ovarian reserve profile [35,36]. There is also evidence available that physical activity combined with other psychosocial and metabolic stressors can trigger a stress response, inhibiting ovulation and the production of key hormones for conception [34]. Frequent high-intensity physical activity (PA) increases subfertility and infertility, especially ovulatory infertility [37]. Athletes have been observed to have a higher incidence of reproductive dysfunction and ovulatory infertility than non-athletes [38,39]. However, there are also studies showing the opposite effect, i.e., that vigorous PA may be associated with improved fertility, although this has only been shown in women with low physical activity, overweight, and obesity [33,40]. There is also no consensus among researchers on the effect of physical activity before ART on pregnancy outcomes [41–43]. In a systematic review of 34 studies published in 2023, researchers concluded that there was insufficient evidence to determine the relationship between physical activity and male and female fertility [44]. This review also examined the association between daily walking duration and female fertility. Conflicting results were found when examining this relationship.

The recommendation of the World Health Organization (WHO) and the American College of Obstetricians and Gynecologists (ACOG) that women planning a pregnancy should do at least 150 min of moderate physical activity per week to reduce reproductive risk [19] is in accordance with our study recommendations. Despite a large number of studies on the curative relationship between physical activity and fertility, in fact, we still know very little about the optimal duration, intensity, and form of PA in reducing infertility risk. The goal of our study is to optimize and rigorously test the effect of a reproductive, targeted exercise on ovarian function in a controlled environment, and possibly include specific exercises in the treatment options for DOR and infertility.

In conclusion, our study addresses the type of physical activity in enhancing various aspects of female fertility, including body composition, hormonal balance, menstrual regularity, sexual function, and spontaneous pregnancy rates. These findings advocate for the integration of regular therapeutic exercise into fertility treatment plans to optimize reproductive health outcomes. Our preliminary three volunteer patients had a promising change in their FSH and AMH levels after 3 months of exercise, further supporting the possible success of the study. Our study results may provide high-quality evidence for evaluating the effectiveness of reproductive physiotherapy in the treatment of DOR patients and in the evaluation of outcomes following IVF-ET. This study will contribute to providing a therapeutic option for DOR patients.

**Author Contributions:** Conceptualization, B.P.K. and S.V.; methodology, B.P.K. and S.V.; validation, S.V.; formal analysis, B.S.; investigation, B.P.K.; resources, S.V.; data curation, J.B.; writing—original draft preparation, B.P.K. and M.K.; writing—review and editing, J.B. and S.V.; visualization, B.S.; supervision, S.V.; project administration, S.V. All authors have read and agreed to the published version of the manuscript.

**Funding:** This research and APC were funded by Government PhD fellowship fund (Simmelweis University, DA9CGI-2021) (BPK) and Semmelweis Science and Innovation Fund (STIA-OTKA-2021), Semmelweis University (S.V.).

**Institutional Review Board Statement:** The study protocol was approved and registered by the Human Reproduction Committee of Hungarian Medical Research Council (25489-8/2021/EÜIG), dated 12 July 2021.

**Informed Consent Statement:** Informed consent was obtained from all subjects in the study.

**Data Availability Statement:** Data are available at the request from the authors.

**Acknowledgments:** We would like to thank to the late Tamás Kőrösi, the Hungarian infertility specialist who inspired the invention of this new ovarian rejuvenation therapy program.

**Conflicts of Interest:** The authors do not declare any conflicts of interest.

## References

1. Vander Borgh, M.; Wyns, C. Fertility and infertility: Definition and epidemiology. *Clin. Biochem.* **2018**, *62*, 2–10. [CrossRef] [PubMed]
2. Inhorn, M.C.; Patrizio, P. Infertility around the globe: New thinking on gender, reproductive technologies and global movements in the 21st century. *Hum. Reprod. Updat.* **2015**, *21*, 411–426. [CrossRef]
3. Ombelet, W.; Cooke, I.; Dyer, S.; Serour, G.; Devroey, P. Infertility and the provision of infertility medical services in developing countries. *Hum. Reprod. Updat.* **2008**, *14*, 605–621. [CrossRef] [PubMed]
4. La Marca, A.; Sighinolfi, G.; Radi, D.; Argento, C.; Baraldi, E.; Artenisio, A.C.; Stabile, G.; Volpe, A. Anti-Müllerian hormone (AMH) as a predictive marker in assisted reproductive technology (ART). *Hum. Reprod. Updat.* **2010**, *16*, 113–130. [CrossRef] [PubMed]
5. Tal, R.; Seifer, D.B. Ovarian reserve testing: A user's guide. *Am. J. Obstet. Gynecol.* **2017**, *217*, 129–140. [CrossRef] [PubMed]
6. Cohen, J.; Chabbert-Buffet, N.; Darai, E. Diminished ovarian reserve, premature ovarian failure, poor ovarian responder—A plea for universal definitions. *J. Assist. Reprod. Genet.* **2015**, *32*, 1709–1712. [CrossRef] [PubMed]
7. Katyal, G.; Kaur, G.; Ashraf, H.; Bodapati, A.; Hanif, A.; Okafor, D.K.; Khan, S. Systematic Review of the roles of Inositol and Vitamin D in improving fertility among patients with Polycystic Ovary Syndrome. *Clin. Exp. Reprod. Med.* **2024**, *51*, 181–191. [CrossRef] [PubMed]
8. Unfer, V.; Carlomagno, G.; Dante, G.; Facchinetti, F. Effects of myo-inositol in women with PCOS: A systematic review of randomized controlled trials. *Gynecol. Endocrinol.* **2012**, *28*, 509–515. [CrossRef]
9. Gambioli, R.; Forte, G.; Buzzaccarini, G.A.-O.; Unfer, V.; Laganà, A.A.-O. Myo-Inositol as a Key Supporter of Fertility and Physiological Gestation. *Pharmaceuticals* **2021**, *14*, 504. [CrossRef]
10. Greenberg, J.A.; Bell, S.J.; Guan, Y.; Yu, Y.H. Folic Acid supplementation and pregnancy: More than just neural tube defect prevention. *Rev. Obstet. Gynecol.* **2011**, *4*, 52–59.
11. Tamura, H.; Jozaki, M.; Tanabe, M.; Shirafuta, Y.; Mihara, Y.; Shinagawa, M.; Tamura, I.; Maekawa, R.A.-O.X.; Sato, S.; Taketani, T.; et al. Importance of Melatonin in Assisted Reproductive Technology and Ovarian Aging. *Int. J. Mol. Sci.* **2020**, *21*, 1135. [CrossRef]
12. Espino, J.A.-O.; Macedo, M.; Lozano, G.; Ortiz, Á.; Rodríguez, C.; Rodríguez, A.B.; Bejarano, I. Impact of Melatonin Supplementation in Women with Unexplained Infertility Undergoing Fertility Treatment. *Antioxidants* **2019**, *8*, 338. [CrossRef]
13. Wang, Y.; Liu, S.; Gan, F.; Xiong, D.; Zhang, X.; Zheng, Z. Melatonin levels and embryo quality in IVF patients with diminished ovarian reserve: A comparative study. *Reprod. Biol. Endocrinol.* **2024**, *22*, 127. [CrossRef]
14. Kopa, Z.; Keszthelyi, M.; Sofikitis, N. Administration of Antioxidants in the Infertile Male: When it may have a Beneficial Effect? *Curr. Pharm. Des.* **2021**, *27*, 2665–2668. [CrossRef]
15. Md Amin, N.A.; Sheikh Abdul Kadir, S.A.-O.; Arshad, A.A.-O.; Abdul Aziz, N.; Abdul Nasir, N.A.-O.; Ab Latip, N.A.-O. Are Vitamin E Supplementation Beneficial for Female Gynaecology Health and Diseases? *Molecules* **2022**, *27*, 1896. [CrossRef] [PubMed]
16. Iervolino, M.; Lepore, E.; Forte, G.; Laganà, A.A.-O.; Buzzaccarini, G.A.-O.; Unfer, V. Natural Molecules in the Management of Polycystic Ovary Syndrome (PCOS): An Analytical Review. *Nutrients* **2021**, *13*, 1677. [CrossRef]
17. Bentov, Y.; Casper, R.F. The aging oocyte—Can mitochondrial function be improved? *Fertil. Steril.* **2013**, *99*, 18–22. [CrossRef] [PubMed]

18. Florou, P.A.-O.; Anagnostis, P.A.-O.; Theocharis, P.; Chourdakakis, M.A.-O.; Goulis, D.A.-O. Does coenzyme Q<sub>10</sub> supplementation improve fertility outcomes in women undergoing assisted reproductive technology procedures? A systematic review and meta-analysis of randomized-controlled trials. *J. Assist. Reprod. Genet.* **2020**, *37*, 2377–2387. [CrossRef] [PubMed]
19. American College of Obstetricians and Gynecologists. Committee Opinion No. 762: Prepregnancy Counseling. *Obstet. Gynecol.* **2019**, *133*, e178–e189. [CrossRef]
20. Bull, F.A.-O.; Al-Ansari, S.S.; Biddle, S.; Borodulin, K.; Buman, M.A.-O.; Cardon, G.; Carty, C.; Chaput, J.A.-O.; Chastin, S.A.-O.; Chou, R.; et al. World Health Organization 2020 guidelines on physical activity and sedentary behaviour. *Br. J. Sports Med.* **2020**, *54*, 1451–1462. [CrossRef]
21. Ki, C.; Heo, M.; Kim, H.Y.; Kim, E.J. The effects of forced breathing exercise on the lumbar stabilization in chronic low back pain patients. *J. Phys. Ther. Sci.* **2016**, *28*, 3380–3383. [CrossRef]
22. Thabet, A.A.; Alshehri, M.A. Efficacy of deep core stability exercise program in postpartum women with diastasis recti abdominis: A randomised controlled trial. *J. Musculoskelet. Neuronal Interact.* **2019**, *19*, 62–68. [PubMed]
23. Chaitow, L. Breathing pattern disorders, motor control, and low back pain. *J. Osteopath. Med.* **2004**, *7*, 33–40. [CrossRef]
24. Roussel, N.; Nijs, J.; Truijzen, S.; Vervecken, L.; Mottram, S.; Stassijns, G. Altered breathing patterns during lumbopelvic motor control tests in chronic low back pain: A case-control study. *Eur. Spine J.* **2009**, *18*, 1066–1073. [CrossRef]
25. Vostatek, P.; Novák, D.; Rychnovský, T.; Rychnovská, S. Diaphragm postural function analysis using magnetic resonance imaging. *PLoS ONE* **2013**, *8*, e56724. [CrossRef] [PubMed]
26. Ma, X.; Yue, Z.-Q.; Gong, Z.-Q.; Zhang, H.; Duan, N.-Y.; Shi, Y.-T.; Wei, W.; Li, Y.-F. The Effect of Diaphragmatic Breathing on Attention, Negative Affect and Stress in Healthy Adults. *Front. Psychol.* **2017**, *8*, 234806. [CrossRef]
27. Jerath, R.; Crawford, M.W.; Barnes, V.A.; Harden, K. Self-regulation of breathing as a primary treatment for anxiety. *Appl. Psychophysiol. Biofeedback* **2015**, *40*, 107–115. [CrossRef] [PubMed]
28. Khajuria, A.; Kumar, A.; Joshi, D.; Kumaran, S.S. Reducing Stress with Yoga: A Systematic Review Based on Multimodal Biosignals. *Int. J. Yoga* **2023**, *16*, 156–170. [CrossRef]
29. Vempati, R.P.; Telles, S. Yoga-based guided relaxation reduces sympathetic activity judged from baseline levels. *Psychol. Rep.* **2002**, *90*, 487–494. [CrossRef]
30. Chan, A.W.; Tetzlaff, J.M.; Gøtzsche, P.C.; Altman, D.G.; Mann, H.; Berlin, J.A.; Dickersin, K.; Hróbjartsson, A.; Schulz, K.F.; Parulekar, W.R.; et al. SPIRIT 2013 explanation and elaboration: Guidance for protocols of clinical trials. *BMJ* **2013**, *346*, e7586. [CrossRef] [PubMed]
31. Schulz, K.F.; Grimes, D.A. Sample size calculations in randomised trials: Mandatory and mystical. *Lancet* **2005**, *365*, 1348–1353. [CrossRef] [PubMed]
32. Fontana, R.; Della Torre, S. The Deep Correlation between Energy Metabolism and Reproduction: A View on the Effects of Nutrition for Women Fertility. *Nutrients* **2016**, *8*, 87. [CrossRef] [PubMed]
33. Cong, J.; Li, P.; Zheng, L.; Tan, J. Prevalence and Risk Factors of Infertility at a Rural Site of Northern China. *PLoS ONE* **2016**, *11*, e0155563. [CrossRef]
34. Hakimi, O.A.-O.; Cameron, L.C. Effect of Exercise on Ovulation: A Systematic Review. *Sports Med.* **2017**, *47*, 1555–1567. [CrossRef] [PubMed]
35. Kiranmayee, D.; Praveena, T.; Himabindu, Y.; Sriharibabu, M.; Kavya, K.; Mahalakshmi, M. The Effect of Moderate Physical Activity on Ovarian Reserve Markers in Reproductive Age Women Below and Above 30 Years. *J. Hum. Reprod. Sci.* **2017**, *10*, 44–48. [CrossRef]
36. Surekha, T.; Himabindu, Y.; Sriharibabu, M.; Pandey, A.K. Impact of physical activity on ovarian reserve markers in normal, overweight and obese reproductive age women. *Indian J. Physiol. Pharmacol.* **2014**, *58*, 162–165.
37. Joseph, D.N.; Whirledge, S. Stress and the HPA Axis: Balancing Homeostasis and Fertility. *Int. J. Mol. Sci.* **2017**, *18*, 2224. [CrossRef] [PubMed]
38. Otis, C.L.; Drinkwater, B.; Johnson, M.; Loucks, A.; Wilmore, J. ACSM Position Stand: The Female Athlete Triad. *Med. Sci. Sports Exerc.* **1997**, *29*, 1–9. [CrossRef] [PubMed]
39. Warren, M.P.; Perlroth, N.E. The effects of intense exercise on the female reproductive system. *J. Endocrinol.* **2001**, *170*, 3–11. [CrossRef] [PubMed]
40. McKinnon, C.J.; Hatch, E.E.; Rothman, K.J.; Mikkelsen, E.M.; Wesselink, A.K.; Hahn, K.A.; Wise, L.A. Body mass index, physical activity and fecundability in a North American preconception cohort study. *Fertil. Steril.* **2016**, *106*, 451–459. [CrossRef] [PubMed]
41. Foucaut, A.A.-O.; Faure, C.; Julia, C.; Czernichow, S.; Levy, R.; Dupont, C. Sedentary behavior, physical inactivity and body composition in relation to idiopathic infertility among men and women. *PLoS ONE* **2019**, *14*, e0210770. [CrossRef]
42. Läänelaid, S.A.-O.; Ortega, F.A.-O.; Kunovac Kallak, T.A.-O.; Joelsson, L.; Ruiz, J.A.-O.; Hreinsson, J.; Wänggren, K.A.-O.; Stavreus-Evers, A.; Kalda, R.; Salumets, A.A.-O.; et al. Physical and Sedentary Activities in Association with Reproductive Outcomes among Couples Seeking Infertility Treatment: A Prospective Cohort Study. *Int. J. Environ. Res. Public Health* **2021**, *18*, 2718. [CrossRef]

43. Sõritsa, D.; Mäestu, E.; Nuut, M.; Mäestu, J.; Migueles, J.H.; Läänelaid, S.; Ehrenberg, A.; Sekavin, A.; Sõritsa, A.; Salumets, A.; et al. Maternal physical activity and sedentary behaviour before and during in vitro fertilization treatment: A longitudinal study exploring the associations with controlled ovarian stimulation and pregnancy outcomes. *J. Assist. Reprod. Genet.* **2020**, *37*, 1869–1881. [CrossRef]
44. Brinson, A.A.-O.; da Silva, S.A.-O.; Hesketh, K.A.-O.; Evenson, K.A.-O. Impact of Physical Activity and Sedentary Behavior on Spontaneous Female and Male Fertility: A Systematic Review. *J. Phys. Act. Health* **2023**, *20*, 600–615. [CrossRef] [PubMed]

**Disclaimer/Publisher’s Note:** The statements, opinions and data contained in all publications are solely those of the individual author(s) and contributor(s) and not of MDPI and/or the editor(s). MDPI and/or the editor(s) disclaim responsibility for any injury to people or property resulting from any ideas, methods, instructions or products referred to in the content.

Article

# Endothelial Dysfunction Markers in Ovarian Cancer: VTE Risk and Tumour Prognostic Outcomes

Inês Guerra de Melo <sup>1,2</sup>, Valéria Tavares <sup>1,2,3</sup>, Joana Savva-Bordalo <sup>4</sup>, Mariana Rei <sup>5</sup>, Joana Liz-Pimenta <sup>2,6</sup>, Deolinda Pereira <sup>4</sup> and Rui Medeiros <sup>1,2,3,7,8,\*</sup>

- <sup>1</sup> Molecular Oncology and Viral Pathology Group, Research Centre of IPO Porto (CI-IPOP), Pathology and Laboratory Medicine Department, Clinical Pathology SV/RISE@CI-IPOP (Health Research Network), Portuguese Oncology Institute of Porto (IPO Porto)/Porto Comprehensive Cancer Centre (Porto. CCC), 4200-072 Porto, Portugal; ines.melo@ipoporto.min-saude.pt (I.G.d.M.); valeria.tavares@ipoporto.min-saude.pt (V.T.)
- <sup>2</sup> Faculty of Medicine, University of Porto (FMUP), 4200-072 Porto, Portugal; joanalizpimenta@gmail.com
- <sup>3</sup> ICBAS—Instituto de Ciências Biomédicas Abel Salazar, Universidade do Porto, 4050-313 Porto, Portugal
- <sup>4</sup> Department of Medical Oncology, Portuguese Institute of Oncology of Porto (IPO Porto), 4200-072 Porto, Portugal; joana.sa@ipoporto.min-saude.pt (J.S.-B.); dpereira@ipoporto.min-saude.pt (D.P.)
- <sup>5</sup> Department of Gynaecology, Portuguese Institute of Oncology of Porto (IPO Porto), 4200-072 Porto, Portugal; marianacruzrei@gmail.com
- <sup>6</sup> Department of Medical Oncology, Centro Hospitalar de Trás-os-Montes e Alto Douro (CHTMAD), 5000-508 Vila Real, Portugal
- <sup>7</sup> Faculty of Health Sciences, Fernando Pessoa University, 4200-150 Porto, Portugal
- <sup>8</sup> Research Department, Portuguese League Against Cancer (NRNorte), 4200-172 Porto, Portugal
- \* Correspondence: ruimedei@ipoporto.min-saude.pt; Tel.: +351-22-508-4000

**Abstract:** Ovarian cancer (OC) presents daunting lethality rates worldwide, with frequent late-stage diagnosis and chemoresistance, highlighting the need for improved prognostic approaches. Venous thromboembolism (VTE), a major cancer mortality factor, is partially driven by endothelial dysfunction (ED). ED's pro-inflammatory state fosters tumour progression, suggesting a VTE-independent link between ED and cancer. Given this triad's interplay, ED markers may influence OC behaviour and patients' prognosis. Thus, the impact of ED-related genes and single-nucleotide polymorphisms (SNPs) on OC-related VTE and patient thrombogenesis-independent prognosis was investigated. *NOS3* upregulation was linked to lower VTE incidence ( $\chi^2$ ,  $p = 0.013$ ), while *SELP* upregulation was associated with shorter overall survival (log-rank test,  $p = 0.048$ ). Dismissing patients with VTE before OC diagnosis, *SELP* rs6136 T allele carriers presented lower progression-free survival (log-rank test,  $p = 0.038$ ). Nevertheless, due to the SNP minor allele underrepresentation, further investigation is required. Taken together, ED markers seem to exhibit roles that depend on the clinical context, such as tumour-related thrombogenesis or cancer prognosis. Validation with larger cohorts and more in-depth functional studies are needed for data clarification and potential therapeutic strategies exploitation to tackle cancer progression and thrombosis in OC patients.

**Keywords:** ovarian neoplasms; venous thrombosis; polymorphism; endothelium; nitric oxide; von Willebrand factor; P-selectin; prognosis

## 1. Introduction

Tumour heterogeneity and therapy resistance remain the major obstacles to effective treatment of malignant diseases [1]. This is particularly evident in ovarian cancer (OC), displaying five-year survival rates below 50% in most countries, particularly when considering advanced stages [2,3]. Indeed, late-stage diagnosis combined with the common acquisition of chemoresistance makes OC the most lethal gynaecological tumour on a global scale [2,4–6]. The histological subtype primarily accountable for gynaecological cancer-related deaths is serous carcinoma (SC), particularly high-grade tumours [7,8].



Beyond the International Federation of Gynaecology and Obstetrics (FIGO) staging, histological and grade classification, prognosis assessment also relies on baseline serum cancer antigen 125 (CA-125) levels, the extent of debulking surgery and chemotherapy regimens, as independent key factors [2,9]. However, these prognostic determinants alone are not sufficient to fully capture the complexity of the disease [10,11]. Thus, more reliable biomarkers are crucial for improving prognostic accuracy, treatment strategies and disease monitoring, enabling a more personalised and effective OC management.

Venous thromboembolism (VTE), including deep vein thrombosis (DVT) and pulmonary embolism (PE), is a common cardiovascular complication among patients with cancer, also representing their second leading cause of death [6,12,13]. These patients face a fourfold to ninefold heightened vulnerability to venous thrombogenesis compared with the general population, which can be explained by factors related to the patient (e.g., patient's advanced age), tumour (e.g., cancer primary site) and antineoplastic treatments (e.g., chemotherapy) [13–16]. Among OC patients, beyond patient and cancer-related factors, platinum-based chemotherapy, antiangiogenic treatment, and pelvic surgery, significantly increase the incidence of VTE, ranking this malignancy among those with the highest thrombotic risk [17,18]. Indeed, the connection between cancer pathophysiology and VTE has garnered significant attention. In a bidirectional relationship, malignancy and cancer-associated thrombosis (CAT) serve as a mutual risk factor for each other and exert a significant impact on each other's mortality rates [19,20]. Given the negative effect of CAT, a better comprehension of its pathogenesis is crucial.

Whether in the general population or in cancer patients, VTE development can be elucidated by the Virchow Triad, which encompasses three key factors: stasis of blood flow, blood hypercoagulability and endothelial dysfunction (ED). The latter, defined as an alteration in the normal function of the endothelial cells (ECs) lining the interior of blood vessels, is pivotal in VTE onset [15,21]. The core of ED is an imbalance between endothelium-derived relaxing factors (EDRFs) and constricting factors (EDCFs). Among various EDRFs, nitric oxide (NO) plays the most critical role in ED [21,22]. In addition to endothelial permeability, decreased NO bioavailability induces the expression of important cell adhesion molecules (CAMs), namely P-selectin, E-selectin, von Willebrand factor (vWF), intercellular adhesion molecule 1 (ICAM-1) and vascular cell adhesion molecule-1 (VCAM-1), which facilitate cell-to-cell interaction, promoting the migration and adhesion of leucocytes [23]. Also, the TGF- $\beta$  co-receptor endoglin (ENG) is upregulated, further contributing to a pro-inflammatory state that precedes VTE [24–27].

Beyond VTE, ED is a critical factor in the pathogenesis of a vast spectrum of other metabolic and cardiovascular diseases (CVD) [22,24,28]. A relevant bridge to cancer is also formed as the pro-inflammatory state of ED promotes tumour growth and progression. Additionally, the inhibition of vasodilation supports cell proliferation and anti-apoptotic responses, reinforcing the association between ED and cancer [29,30]. Collectively, the triad formed by ED, VTE and cancer could open potential avenues for OC management, particularly from a genetic perspective. Indeed, ED is thought to have a genetic basis, with single-nucleotide polymorphisms (SNPs) being particularly valuable [31,32]. Given their frequency and relevance at a population level, investigating SNPs implicated in ED susceptibility may support CAT's prediction and early diagnosis, improve OC prognosis assessments and enable more personalised and targeted tumour treatments. In this context, this study aimed to explore the implications of ED biomarkers on the occurrence of OC-related VTE and the prognosis of OC patients, independent of thrombosis.

## 2. Materials and Methods

### 2.1. Population Description

A retrospective hospital-based cohort study was carried out enrolling epithelial OC (EOC) patients of European ancestry admitted for first-line treatment from March 2017 to December 2023 at the Department of Gynaecology and Oncology of IPO Porto. Patients were excluded when underage, only admitted for a second opinion or with follow-up

completed at other institutions. Ultimately, 98 EOC patients (cohort A) with available biological material were recruited. All participants signed a consent form according to the principles of the Helsinki Declaration before their enrolment in the research.

All EOC cases were staged using the FIGO staging system [33]. Adding to this, the Response Evaluation Criteria in Solid Tumours (RECIST) version 1.1 was considered when evaluating the tumour response to chemotherapy [34]. Follow-up records, as well as demographic and clinicopathological information, were retrieved by consulting all patients' medical data files.

In summary, the mean age of the patients was 63.2 years, and most of them were post-menopausal ( $n = 79$ , 80.6%) and had received their diagnosis at advanced cancer stages (FIGO III/IV;  $n = 74$ , 75.5%). A total of 82 (83.7%) patients were diagnosed with serous tumours. Most ( $n = 41$ , 41.8%) received standard treatment (cytoreductive surgery followed by chemotherapy with carboplatin/cisplatin combined with paclitaxel). Complete or optimal surgical resection was achieved for 45 (45.9%) patients. The median follow-up time in the study was 25.5 months.

CAT was defined as a VTE event occurring six months before to two years after OC detection [35]. Therefore, analyses involving VTE included only patients with a minimum follow-up of two years, with those who died during this period also considered. Notably, active screening is not an established clinical protocol at IPO Porto and thus it was not performed. Among the 80 OC patients with sufficient follow-up time, 17 (21.3%) developed OC-related VTE, with 6 cases occurring before and 11 after OC diagnosis. The median time interval between VTE and OC diagnosis was 3.5 months for thrombotic cases preceding OC diagnosis and 9.0 months for post-diagnosis cases. Regarding the type of VTE, ten events (58.8%) were DVT, five (29.4%) were PE, one involved both DVT and PE and one occurred in an unusual location.

This study had previously received approval from the ethics committee at IPO Porto (CES IPO: 69/021; 11 March 2021).

## 2.2. Sample Collection, Genomic DNA and RNA Extraction

Using a standard phlebotomy approach, venous peripheral blood samples of patients were collected into EDTA collection tubes prior to their first-line chemotherapy.

Following the manufacturer's instructions, the QIAamp DNA Blood Mini Kit (Cat. No. 51106, Qiagen, Hilden, Germany) was used to isolate genomic deoxyribonucleic acid (DNA) from the blood samples of each patient for SNP genotyping.

The isolation of peripheral blood components (PBCs) was conducted as described elsewhere [10]. Total ribonucleic acid (RNA) for messenger RNA (mRNA) analyses was extracted from the cellular fraction of the peripheral blood samples using the GRS RNA kit—Blood & cultured cells (#GK08.0100, Grisp Research Resolutions<sup>®</sup>, Porto, Portugal) as per the manufacturer's instructions.

The concentration and purity of the DNA and RNA samples were verified using the NanoDrop Lite spectrophotometer by Thermo Fisher Scientific<sup>®</sup> (Waltham, MA, USA). Only RNA samples with  $A_{260}/A_{280} \geq 1.90$  were admitted. Once extracted and quantified, all DNA samples were stored at  $-20\text{ }^{\circ}\text{C}$ , while the RNA samples were stored at  $-80\text{ }^{\circ}\text{C}$  until use.

## 2.3. Polymorphism Selection and Genotyping

Several criteria were used to guide the identification of relevant SNPs associated with ED. The genetic variants were selected if they: (1) were located within genes implicated in ED, (2) had a demonstrated impact on the expression or activity of the respective encoded proteins, (3) had a role in CVD and metabolic diseases and/or cancer and (4) had available TaqMan genotyping assays. Finally, SNPs related to the same gene and in strong linkage disequilibrium (LD) (meaning with a  $r^2$  value higher than 0.9) were dismissed. Applying these criteria, three SNPs were selected: *NOS3* rs2070744, *SELP* rs6136 and *VWF* rs1063856.

SNP genotyping was carried out in a StepOne Plus quantitative real-time (qRT)-PCR system (Applied Biosystems®, Foster City, CA, USA), leveraging the TaqMan® Allelic Discrimination approach. Thermal cycles for DNA amplification were the following: activation of Taq DNA-polymerase (10 min at 95 °C); denaturation of DNA chains (15 s of 45 cycles at 95 °C) and primer pairing and extension (1 min at 60 °C). Each reaction was conducted with a 6.0 µL mix, including 2.5 µL of TaqPath™ ProAmp™ Master Mix (1×), 2.375 µL of sterile water, 0.125 µL of TaqMan® Genotyping Assay (C\_\_15903863\_10 for NOS3 rs2070744, C\_\_11975277\_20 for SELP rs6136 and C\_\_3288406\_30 for VWF rs1063856), and 1.0 µL of genomic DNA, incorporating negative controls (without genetic material) to assess false positives. A double-sampling strategy of at least 10.0% randomly selected samples was performed to ensure SNP genotyping quality. StepOne Software (version 2.3 Applied Biosystems®, Foster City, CA, USA) was employed to analyse the data on DNA amplification data. The genotyping results were evaluated by two researchers with no previous knowledge regarding the demographic and clinicopathological details of patients involved in the study.

#### 2.4. Gene Selection

A comprehensive literature review on the molecular profile associated with ED was recently conducted by our research group [36]. Based on this review, genes were selected by prioritising those expressed by PBCs, particularly monocytes, neutrophils, and platelets. Furthermore, different phases of ED—immediate endothelial activation, delayed endothelial activation, and established ED—were considered, leading to the selection of the following genes: NOS3, SELP, ICAM1, ENG, and ET-1 encoding gene (EDN1).

Cohort A was subsampled by filtering out patients who: (1) had a history of other malignancies; (2) were breastfeeding or pregnant at the time of diagnosis; (3) had a history of autoimmune diseases or were undergoing immunosuppressive therapies; (4) had acute infections at cancer diagnosis; (5) were undergoing anticoagulant treatments for diseases other than VTE; and (6) possessed the polymorphisms Factor V Leiden (F5 rs6025) and F2 (Factor II encoding gene) rs1799963. The resultant cohort—cohort B—was comprised of 55 OC patients, who were subject to gene expression analysis.

#### 2.5. cDNA Conversion and Gene-Relative Quantification

Complementary DNA (cDNA) strands were generated from total RNA samples by using the High-Capacity cDNA Reverse Transcription Kit (Applied Biosystems®, Carlsbad, CA, USA) as per the manufacturer's instructions, and a Mycycler™ Thermal cycler (Bio-Rad Laboratories, Hercules, CA, USA) with the recommended cycle conditions (10 min at 25 °C, 120 min at 37 °C, and 5 min at 85 °C). All reactions incorporated negative controls.

The relative quantification of gene expression was performed with the StepOne Plus qRT-PCR system. Each reaction was executed using a 10.0 µL mixture containing: 5.0 µL of 2× TaqMan™ Gene Expression Master Mix and 0.5 µL of TaqMan™ 20× Gene Expression Assays, both by Applied Biosystems® (Foster City, CA, USA); and 3.0 µL of nuclease-free water and 1.5 µL of cDNA sample. The selected assays were the following: Hs01574665\_m1 (NOS3), Hs00923996\_m1 (ENG), Hs00174961\_m1 (EDN1), Hs00164932\_m1 (ICAM1), and Hs00927900\_m1 (SELP). Glyceraldehyde-3-phosphatedehydrogenase (GAPDH) and hypoxanthine phosphoribosyl transferase 1 (HPRT1) were tested as endogenous controls with the assays Hs03929097\_g1 and Hs02800695\_m1, respectively. All reactions followed the same thermal cycling conditions: 50 °C for 2 min, 95 °C for 10 min followed by 45 cycles of 15 s at the same temperature, and 1 min at 60 °C. Negative controls (without cDNA) were included in all reactions to assess false positives, and a triple-sampling strategy of all samples was employed. The amplification of all targets and endogenous controls of each sample was conducted on the same plate. Reactions with standard deviation (SD) values of cycle thresholds (Ct) >0.5 were excluded. Ct values were generated with the same set baseline and threshold values for each plate by using the qRT-PCR analysis software from the Thermo Fisher Connect platform (Thermo Fisher Scientific, Waltham, MA, USA).

## 2.6. Statistical Analysis

Data analysis was conducted using IBM SPSS Statistics for Windows (version 29, IBM Corp., Armonk, NY, USA). The assessment of data distribution relied on the Kolmogorov–Smirnov test. Continuous variables were dichotomised using the mean value as the cut-off for normally distributed data or the median for non-normally distributed data.

The genotype distribution of each SNP in this study was compared with that of the Iberian population (<https://www.ensembl.org/index.html>, accessed on 18 August 2024). The Hardy–Weinberg equilibrium (HWE) was tested using the chi-square test ( $\chi^2$ ). Associations of the SNPs with patients' clinical and demographic characteristics, including CAT status, as well as the expression of ED-related genes, were analysed using  $\chi^2$ .

The gene-normalised relative expression was computed using the Livak method with *GAPDH* as the endogenous control due to its stable expression when compared to *HPRT* (i.e., lower SD values). By applying the interquartile range (IQR), the most severe outliers in the levels of normalised relative expression of each gene were identified and further dismissed. Furthermore, four expression profiles categorising gene-normalised relative expression were defined: (A) low vs. high considering median value expression; (B) low vs. intermediate vs. high expression values considering the terciles; (C) low (first and second terciles) vs. high (third tercile) expression; and (D) low (first tercile) vs. high (remaining distribution) by combining the terciles.

Depending on the data distribution, the Mann–Whitney *U* test or Student–*t* test was used to evaluate the statistical differences in the gene-normalised relative expression levels according to VTE status (VTE-negative/VTE-positive). When examining these associations considering patients without VTE, those with the condition before OC diagnosis, and those after, the Kruskal–Wallis test or one-way analysis of variance followed by Dunnett's test was employed.  $\chi^2$  was further used for confirmation. The same test was employed to assess the associations of gene expression levels with ED-related SNPs and patients' clinical and demographic characteristics.

The impact of ED-related markers on the patient's progression-free survival (PFS) and overall survival (OS) was evaluated. PFS was defined as the interval between the initiation of cancer treatment and either the date of recurrence, progression, related mortality, or the patient's last clinical evaluation. OS was deemed the time from the patient's diagnosis until death (all causes included) or the last clinical evaluation. Survival curves were generated with the Kaplan–Meier method, while the survival probabilities were examined using the log-rank test. The most fitting genetic model for each variant (recessive or dominant) was established after analysing the survival curves under the additive genetic model. The risks of tumour progression and patient death were computed employing the Cox proportional hazards model.

All tests conducted were two-sided and a 5.0% significance level was established. Furthermore, *p*-values between 0.050 and 0.060 were deemed marginally significant.

## 3. Results

### 3.1. Distribution of SNP Genotypes

The distribution of the variants' genotypes is represented in Table 1. The ED-related SNPs were in HWE ( $\chi^2$ ,  $p > 0.050$ ), demonstrating no significant deviation from expected genotype frequencies.

**Table 1.** Genotype distribution of ED-related SNPs.

SNP	MAFi <sup>1</sup> (MA)	Genotype	<i>n</i> (%)	<i>n</i> Total (%)	MAFs (MA)
NOS3 rs2070744	49.5% (C)	CC	21 (21.4)	98 (100)	46.9% (C)
		CT	50 (51.0)		
		TT	27 (27.6)		

Table 1. Cont.

SNP	MAFi <sup>1</sup> (MA)	Genotype	n (%)	n Total (%)	MAFs (MA)
SELP rs6136	8.9% (G)	TT	81 (82.7)	98 (100)	9.2% (G)
		GT	16 (16.3)		
		GG	1 (1.0)		
VWF rs1063856	34.1% (C)	CC	10 (10.2)	98 (100)	36.2% (C)
		CT	51 (52.0)		
		TT	37 (37.8)		

<sup>1</sup> According to the Ensembl database accessed on 18 August 2024. Abbreviations: SNP, single-nucleotide polymorphism; MAFi, minor allele frequency in the Iberian population; MAFs, minor allele frequency in the study cohort; MA, minor allele.

### 3.2. ED Markers and Clinical Characteristics of OC Patients

While no significant associations were found for the evaluated ED-related genes [regardless of the expression profile ( $\chi^2$ ,  $p > 0.050$ )], the SNPs were associated with several demographic and clinicopathological features of the patients (Table 2). The NOS3 rs2070744 CC genotype was more prevalent among patients with a CVD and/or metabolic disease history (CC vs. CT vs. TT;  $\chi^2$ ,  $p = 0.049$ ). This association was corroborated when considering patients with both conditions (CC vs. CT/TT;  $\chi^2$ ,  $p = 0.023$ ). Furthermore, the SNP TT genotype was more frequently associated with using poly (ADP-ribose) polymerase (PARP) inhibitors (PARPi) in both the additive (CC vs. CT vs. TT;  $\chi^2$ ,  $p = 0.029$ ) and dominant (CC/CT vs. TT;  $\chi^2$ ,  $p = 0.025$ ) genetic models. A marginal association was observed between this SNP and international normalised ratio (INR) baseline levels (CC/CT vs. TT;  $\chi^2$ ,  $p = 0.059$ ).

Table 2. Associations between SNPs and clinicopathological features of the patients.

SNP	Associated Characteristic	Associated Genotype/Allele	Statistical Model	p Value
NOS3 rs2070744	Cardiovascular or metabolic disease history	CC	CC vs. CT vs. TT	0.049
	Cardiovascular and metabolic disease history	CC	CC vs. CT/TT	0.023
	Use of PARPi	TT	CC vs. CT vs. TT	0.029
		TT	CC/CT vs. TT	0.025
	Higher INR	TT	CC/CT vs. TT	0.059
SELP rs6136	Cardiovascular and/or metabolic disease history	G	GG/GT vs. TT	0.018
	Advanced (III/IV) FIGO stages	TT	GG vs. GT vs. TT	0.042
VWF rs1063856	ATE history	TT	CC/CT vs. TT	0.018
		TT	CC vs. CT vs. TT	0.021
	Anticoagulant use before OC diagnosis	TT	CC vs. CT vs. TT	0.054

Abbreviations: SNP, single-nucleotide polymorphism; PARPi, poly (ADP-ribose) polymerase (PARP) inhibitors; INR, international normalised ratio; ATE, arterial thromboembolism.

The SELP rs6136 G allele was more frequently associated with a CVD and/or metabolic disease history (GG/GT vs. TT;  $\chi^2$ ,  $p = 0.018$ ). Conversely, the T allele appeared to be more prevalent in patients at advanced FIGO stages (III/IV;  $\chi^2$ ,  $p = 0.042$ ). However, the findings should be evaluated carefully given the underrepresentation of the GG genotype, reflecting its low minor allele frequency (MAF) (8.9%) in the Iberian population.

The VWF rs1063856 TT genotype was strongly associated with a history of arterial thromboembolism (ATE) in both the dominant (CC/CT vs. TT;  $\chi^2$ ,  $p = 0.018$ ) and additive (CC vs. CT vs. TT;  $\chi^2$ ,  $p = 0.021$ ) models. Additionally, an association between this genotype and anticoagulant use before OC diagnosis yielded a marginal result ( $\chi^2$ ,  $p = 0.054$ ).

### 3.3. ED-Markers and VTE Status

Two different approaches were used to assess this association. The first approach grouped patients into two categories—those with (VTE positive) and those without VTE (VTE-free/negative). In the second approach, VTE-free patients were compared to those with the condition before OC diagnosis and those presenting VTE after tumour diagnosis. Although no significant associations were detected for the SNPs, [regardless of the approach used ( $\chi^2$ ,  $p > 0.050$ )], in the first approach, *NOS3* was marginally associated with VTE status using the Mann–Whitney *U* test on cohort B. Namely, patients without VTE were found to present higher gene expression levels compared to those with the condition ( $p = 0.057$ ). Regarding  $\chi^2$  for confirmation, *NOS3* expression levels were once again found to be significantly associated with VTE risk in both approaches (Table 3). In the first approach, higher *NOS3* expression was associated with a lower risk of VTE (profile B;  $\chi^2$ ,  $p = 0.013$ ). Notably, VTE events were only reported in the low and intermediate *NOS3* expression groups. In the second approach, VTE events were only observed in the low and intermediate expression groups, with none occurring in the high expression group (profile B;  $\chi^2$ ,  $p = 0.027$ ). The  $\chi^2$  did not reveal any additional significant association between the expression of the ED-related genes and VTE status ( $p > 0.050$ ).

**Table 3.** Significant associations of *NOS3* expression and VTE occurrence.

Gene	Profile	<i>n</i>	Expression			<i>p</i> Value
			Low	Intermediate	High	
<i>NOS3</i>	B	VTE negative	10	12	18	0.013
		VTE positive	5	4	0	
	B	VTE-free	10	12	17	0.027
		VTE before OC	2	1	0	
		VTE after OC	3	3	0	

Abbreviations: VTE, venous thromboembolism; OC, ovarian cancer.

### 3.4. SNPs' Impact on Clinical Outcome of OC Patients (Independently of VTE)

To eliminate potential confounding effects of pre-existing VTE on the relationship between SNPs and patient prognosis, the analyses were performed considering the entire cohort A ( $n = 98$ ) and the subgroup of patients excluding those who had VTE before OC diagnosis ( $n = 89$ ). In this survival analysis, only the *SELP* SNP showed a significant association with the PFS or OS of the patients. The remaining negative results are detailed in Supplementary Table S1. Considering the entire Cohort A, the *SELP* rs6136 TT genotype showed a marginal association with PFS (GG/GT vs. TT; log-rank test,  $p = 0.054$ ; Figure 1a) while being significantly associated with poorer PFS compared to the G allele genotypes (CG/GT vs. TT; mean OS of  $24.4 \pm 3.2$  months and  $43.7 \pm 8.1$  months, respectively, log-rank test,  $p = 0.038$ ; Figure 1b) in subgroup assessment. Despite the statistical significance, it is important to note the underrepresentation of the G allele genotype, which limits the robustness of these results.

### 3.5. Genes' Impact on Clinical Outcome of OC Patients (Independently of VTE)

A similar approach to cohort A was used to segment cohort B patients, resulting in a subgroup excluding patients who experienced VTE before OC diagnosis ( $n = 52$ ). In the total cohort B ( $n = 55$ ), patients with high *SELP* expression (profile D) exhibited a shorter OS compared to their counterparts (mean OS of  $41.2 \pm 5.1$  and  $57.9 \pm 9.2$  months, respectively, log-rank test,  $p = 0.048$ ; Figure 2). In the sub-analysis, *SELP* expression not only continued to show a significant association with OS but also displayed an association with PFS (Figure 3). For PFS, the high *SELP* expression (profile C) group had a mean PFS of  $14.4 \pm 1.7$  months compared to  $26.3 \pm 4.8$  months in the low expression group (log-rank test,  $p = 0.014$ , Figure 3a). Concerning OS, patients with a high expression (profile

D) had a lower survival time than their counterparts (mean OS of  $41.5 \pm 5.3$  months and  $60.6 \pm 9.5$  months, log-rank test,  $p = 0.023$ , Figure 3b). Consistent with the SNP analyses, only *SELP* showed a significant association with OC patient prognosis, further supporting its potential role as a prognostic factor in these patients, with high expression levels associated with a less favourable outcome. The negative findings from all gene analyses conducted are summarised in Supplementary Table S2.

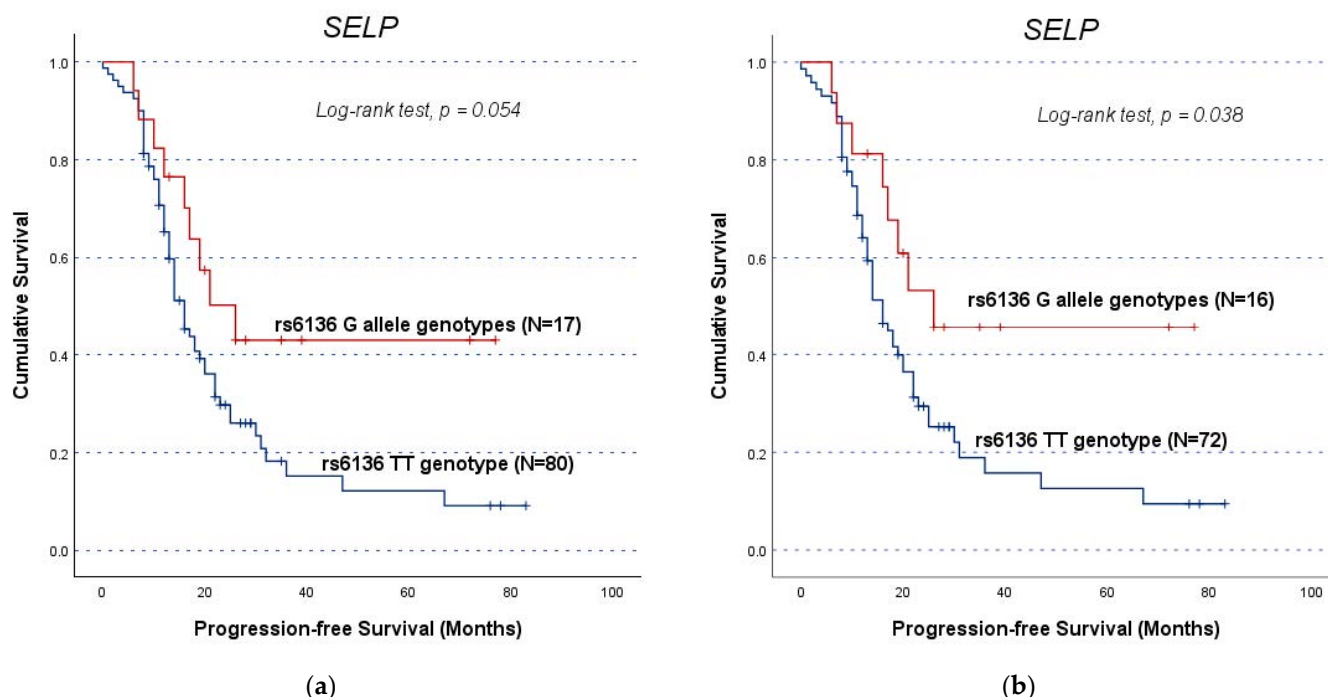


**Figure 1.** Progression-free survival (PFS) by Kaplan–Meier and log-rank test for OC patients, according to *SELP* rs6136 genotype distribution. The TT genotype carriers had lower survival times: (a) For OC patients in the entire cohort ( $n = 97$ ), the association had a marginal statistically significant result (GG/GT vs. TT; log-rank test,  $p = 0.054$ ); (b) For OC patients in the sub-cohort ( $n = 88$ ), excluding those with prior VTE, TT genotype carriers had a mean PFS of  $24.4 \pm 3.2$  months while G allele carriers had a mean PFS of  $43.7 \pm 8.1$  months (GG/GT vs. TT; log-rank test,  $p = 0.038$ ).

### 3.6. SNPs' Impact on Gene Expression

Regarding the influence of the SNPs on their respective gene expression levels in cohort B, no significant association was found (Table 4). Considering all cohort B patients ( $n = 55$ ), the *NOS3* rs2070744 T allele (TT/CT vs. CC) was significantly linked with higher levels of *ICAM1* (profile D,  $\chi^2$ ,  $p = 0.045$ ). The TT genotype showed a marginal association with higher *ENG* expression (CC/CT vs. TT; profile B,  $\chi^2$ ,  $p = 0.058$ ). Moreover, the *VWF* rs1063856 TT genotype (additive model) was significantly linked to higher *SELP* expression (profile B,  $\chi^2$ ,  $p = 0.025$ , respectively). Regarding the subgroup ( $n = 52$ ), the *NOS3* rs2070744 T allele (TT/CT vs. CC) was again associated with higher *ICAM1* expression levels (profile D,  $\chi^2$ ,  $p = 0.019$ ). The mentioned associations are resumed in Table 5.

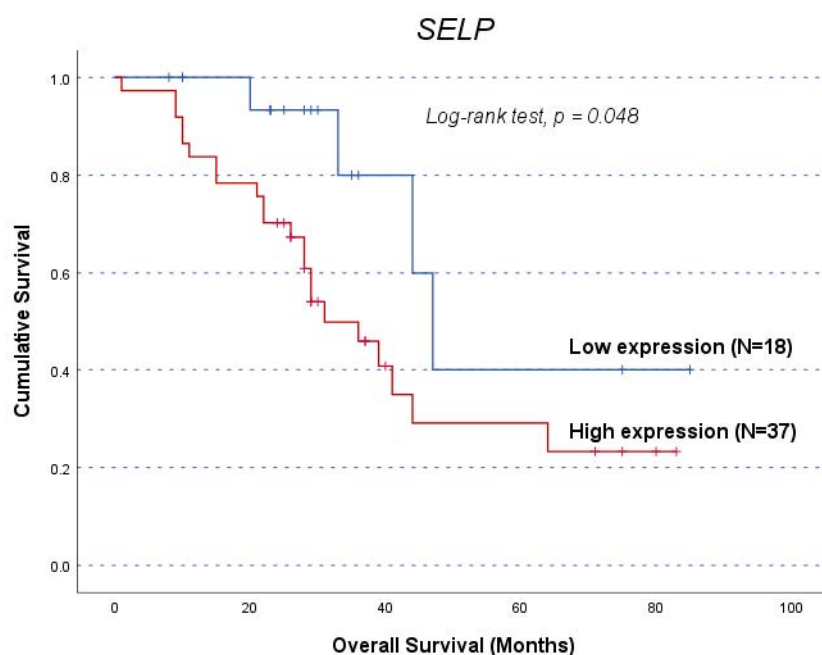
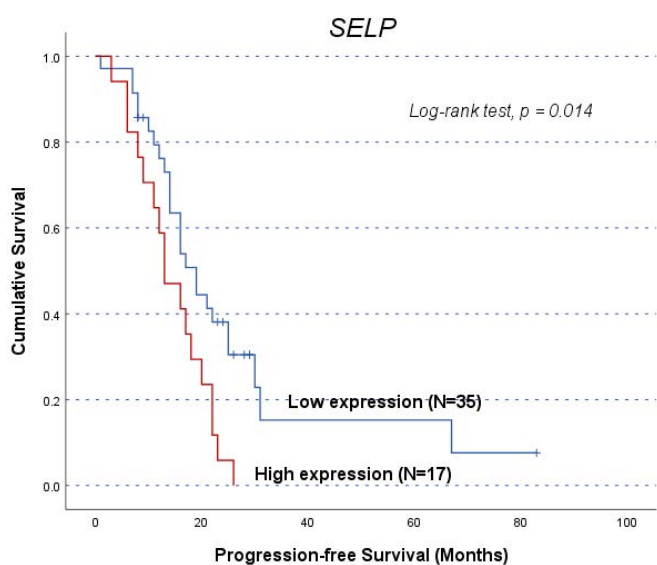
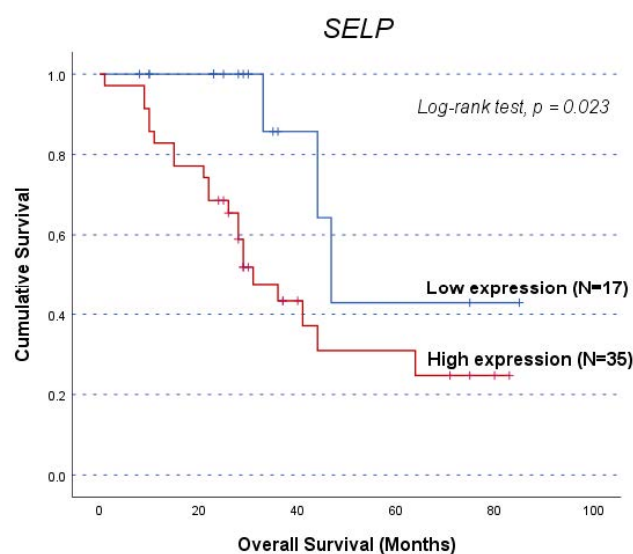


**Figure 2.** Overall survival (OS) ( $n = 55$ ) by Kaplan–Meier and log-rank test for OC patients, according to *SELP* expression levels. Patients with high *SELP* expression (profile D) had a lower OS compared to those with low *SELP* expression ( $p = 0.048$ ). The high expression group had a mean OS of  $41.2 \pm 5.1$  months, while the low expression group had a mean OS of  $57.9 \pm 9.2$  months.



(a)



(b)

**Figure 3.** Progression-free survival (PFS) and overall survival (OS) by Kaplan–Meier and log-rank test for OC patients in the sub-cohort ( $n = 52$ ), excluding those with prior VTE, according to *SELP* expression levels: (a) Patients with high *SELP* expression had a lower PFS compared to those with low *SELP* expression (profile C). The high expression group had a mean PFS of  $14.4 \pm 1.7$  months, while the low expression group had a mean PFS of  $26.3 \pm 4.8$  months (log-rank test,  $p = 0.014$ ); (b) Patients with high *SELP* expression had a lower OS compared to those with low *SELP* expression (profile D). The high expression group had a mean OS of  $41.5 \pm 5.3$  months, while the low expression group had a mean OS of  $60.6 \pm 9.5$  months (log-rank test,  $p = 0.023$ ).



**Table 4.** Genotype distribution of each SNP (additive model) in cohort B ( $n = 55$ ), according to the expression profile A of the respective gene.

SNP	Genotype	Low Gene Expression $n$ (%)	High Gene Expression $n$ (%)
NOS3 rs2070744	CC	8 (14.5)	6 (10.9)
	CT	15 (27.3)	12 (21.8)
	TT	4 (7.3)	10 (18.2)
SELP rs6136	TT	22 (40.0)	23 (41.8)
	GT	5 (9.1)	5 (9.1)

Abbreviations: SNP, single-nucleotide polymorphism.

**Table 5.** Significant associations between investigated SNPs and gene expression.

SNP	Genotype/ Allele	Statistical Model	Upregulated Gene	Gene Expression Profile	$p$ Value	Cohort
NOS3 rs2070744	T	TT/CT vs. CC	ICAM1	D	0.019	Sub-cohort ( $n = 52$ )
	TT	CC/CT vs. TT	ENG	B	0.058	
	T	TT/CT vs. CC	ICAM1	D	0.045	
VWF rs1063856	TT	CC vs. CT vs. TT	SELP	B	0.025	Entire cohort B ( $n = 55$ )

Abbreviations: SNP, single-nucleotide polymorphism.

#### 4. Discussion

Despite advancements in the treatment setting, long-term survival rates for OC remain low due to several challenges, including late-stage disease diagnosis and the frequent development of resistance to therapy allied to the high recurrence rates. Identifying effective prognostic biomarkers of OC is crucial for improving clinical management and personalising therapeutic strategies [1–3,6,37]. A growing body of evidence has underscored the crucial role of ED in the initiation and progression of cancer, with its influence extending to various hallmarks of the disease. In parallel, ED has long been recognised as one of the primary factors linked to VTE, a condition commonly observed in cancer patients [36]. The interaction between ED, VTE, and OC could enable the identification of novel biomarkers and therapeutic targets for more personalised disease management for OC patients. This study assessed the association of the ED markers with VTE occurrence and their prognostic value for OC.

Starting with NOS3 rs2070744, it involves the substitution of a thymine (T) with a cytosine (C) at position -786 in the 5'-flanking region. This alternation promotes the binding of the DNA repair, replication and recombination protein, replication protein A1 (RPA1), to the NOS3 promoter. This assembly reduces the promoter activity leading to serum NO decline, which enables proliferation pathways and inhibits tumour cell apoptosis [30,38–41]. In this study, the rs2070744 C allele was more prevalent among patients with a history of CVD and metabolic diseases (CC vs. CT vs. TT;  $\chi^2$ ,  $p = 0.049$ ), which is consistent with the literature [39,42,43]. Additionally, the SNP was marginally associated with the baseline INR (C vs. TT;  $\chi^2$ ,  $p = 0.059$ ), corroborating the effect of the SNP on haemostatic abnormalities [44]. Contrary to the observation that decreased NO levels—which define ED status—are associated with a pro-thrombotic potential, rs2070744 was not significantly associated with CAT susceptibility [21]. On the other hand, higher NOS3 expression was significantly linked to a lower risk of VTE ( $\chi^2$ ,  $p = 0.013$ ), which aligns with the protective role of NO in maintaining endothelial integrity and preventing excessive clot formation [22,28,45]. Notably, the expression of the remaining genes was not significantly associated with CAT occurrence. Collectively, these results suggest that NOS3 may have a unique and context-dependent role in CAT pathogenesis among OC patients.

The lack of association between rs2070744 and NOS3 expression may help explain why this SNP does not appear to influence CAT susceptibility. This finding should be

examined in additional studies with larger cohort sizes. Inclusively, while with no statistical significance, the C allele tended to be more common among those with low *NOS3* expression, supporting the existing evidence [30,38–41]. All in all, the interplay between NO deficiency and the activation of vasoconstrictors exacerbates ED's role in promoting a pro-thrombotic and pro-inflammatory environment, leading to enhanced cellular proliferation, angiogenesis, and metastasis—key processes in tumourigenesis. This connection further underscores the significance of ED beyond its involvement in VTE, highlighting its contribution to a wider array of pathological conditions that share common mechanistic pathways with cancer [21,22,28,36,39,46–48].

The influence of *NOS3* expression on OC may extend to treatment, particularly in the context of PARPi. The association of the rs2070744 TT genotype with higher levels of NO compared to the C allele may reflect a preserved capacity for regulating inflammatory and apoptotic processes. As an apoptosis modulator, elevated NO levels enhance apoptosis in cancer cells, which could potentially impact the effectiveness of PARPi [30,47,49]. The significant association between the TT genotype and the use of PARPi (C vs. TT;  $\chi^2$ ,  $p = 0.025$ ) suggest that this genotype is linked to a more robust apoptotic response to the treatment, possibly indicating a more favourable clinical outcome or a preferred therapeutic response in OC patients [50]. Another hypothesis suggests that NO may play a role in sensitising *BRCA1/2*-proficient tumours to PARPi by inhibiting homologous recombination repair (HRR) pathways. Briefly, *BRCA*-mutated tumours have a reduced ability to repair DNA via HRR, making them more vulnerable to treatments that further inhibit DNA repair, like PARPi. However, *BRCA1/2* mutations are only present in 10.0–15.0% of OC, meaning that for most OC patients with *BRCA1/2*-proficient tumours, PARPi is less effective. Recently, NO donors have been proposed as such efficient sensitising agents [51]. Thus, the elevated NO levels associated with the TT genotype could enhance the synthetic lethality of PARPi, even in patients without *BRCA1/2* mutations, by promoting error-prone DNA repair mechanisms.

Intriguingly, the rs2070744 T allele was associated with higher expression levels of *ICAM1* [ $\chi^2$ ,  $p = 0.045$  ( $n = 55$ );  $\chi^2$ ,  $p = 0.019$  ( $n = 52$ )], and marginally associated with the upregulation of *ENG* [ $\chi^2$ ,  $p = 0.058$  ( $n = 55$ )]. The elevated expression of *ICAM1*, a crucial marker for leukocyte adhesion and endothelial inflammation, suggests a potential exacerbation of inflammatory responses in T allele carriers [52]. Moreover, the increased expression of *ENG*, which plays a key role in EC functions, particularly in regulating proliferation, migration and angiogenesis, could indicate an altered endothelial state with potential impacts on tumour progression [53]. These findings seem to contrast with the expectation that higher NO levels associated with the T allele should mitigate ED and thrombotic risk. Instead, the presence of the T allele appears to be associated with a molecular profile suggesting persistent ED, despite elevated NO levels. Nevertheless, besides being a novel ED marker highly expressed in activated ECs, *ENG* also regulates *NOS3* expression, playing a crucial role in NO-mediated vasodilation, through the  $\text{TGF}\beta$ /activin receptor-like kinase-5 (ALK5)/mothers against decapentaplegic homolog 2 (SMAD2) pathway [26,54]. Thus, the simultaneous upregulation of *ENG* and *NOS3* (assuming the *NOS3* rs2070744 T allele association with higher *NOS3* expression) acts in line with a more preserved endothelium resultant from a regular NO bioavailability, reinforcing the vascular dynamics modulated by *ENG* [30,40,41,54]. Again, the lack of statistical significance on the association of T allele carriers and higher *NOS3* expression (regardless of the observed trend) may be a justifying factor for the mere marginally significant association of T allele carriers with higher *ENG* expression, reflecting a complex interaction between NO levels and other ED markers.

The SNP rs2070744 has been linked to the susceptibility of several tumours, including breast, prostate, bladder, gastric, and colorectal cancers, and oral squamous cell carcinoma [30,36,41,48,55–62]. However, studies reporting a clear prognostic role of rs2070744 in cancer are limited, focusing primarily on its association with survival in response to specific therapies in renal cell carcinoma, hepatocellular carcinoma, and bladder cancer [63–65]. Notably, these studies yield inconsistent results regarding which allele or genotype was

associated with a worse prognosis. In this study, no prognostic value of rs2070744 or *NOS3* expression was observed.

Regarding the *SELP* rs6136, this SNP is a missense variant resulting from a thymine (T) to guanine (G) substitution and consequent threonine (Thr) replacement by proline (Pro) at position 715, at exon 13. Adjacent to this exon, which encodes the last repeat segment of *SELP*, is the exon encoding the transmembrane domain of the protein. Under alternative splicing, a soluble *SELP* (s*SELP*) is produced, without a transmembrane domain. The reported association of the G allele with reduced s*SELP* levels suggests that this allele is linked to impaired splicing efficiency or altered protein processing, leading to decreased production or increased degradation of s*SELP* compared to the T allele [66,67].

In the present study, no statistical significance was achieved for *SELP* rs6136 and the expression of the respective gene. Nevertheless, the rs6136 G allele was significantly associated with a CVD and/or metabolic disease history (GG/GT vs. TT;  $\chi^2$ ,  $p = 0.018$ ), aligning with the literature findings, that link this allele with both higher risk of development of metabolic and CVD (including CAT) and lower s*SELP* levels [20,66,68,69]. The apparent inconsistency in the literature regarding the simultaneous association of the rs6136 G allele with these two factors remains unresolved. On one side, *SELP* is reported to facilitate leukocyte recruitment to the site of inflammation, potentially contributing to thrombosis, tumour progression and cancer cachexia [70]. Conversely, studies such as the *Etude Cas-Témoign de l'Infarctus du Myocarde* (ECTIM) have shown a protective effect of the G allele against myocardial infarction, proposing *SELP* rs6136 as a polymorphic variant with a population-dependent role. Furthermore, the alteration in the processing of the mRNA or the protein itself may be favouring the transmembrane form of *SELP* over s*SELP* as the reduction of the latter related to the increase of the former [71].

The *SELP* rs6136 T allele displayed a greater prevalence in patients with advanced FIGO stages ( $\chi^2$ ,  $p = 0.042$ ), indicating a worse prognosis associated with *SELP* upregulation. This finding was further confirmed with the observation that TT genotype carriers in this study exhibited lower PFS in the analysis of the entire cohort A (with a marginal result) and the subgroup analysis without patients that had VTE preceding their OC diagnosis (log-rank test,  $p = 0.038$ ) than patients with the G allele. Consistently, patients with higher levels of *SELP* presented a shorter OS compared to their counterparts in the total cohort B (log-rank test,  $p = 0.048$ ), and both diminished PFS and OS (log-rank test,  $p = 0.014$  and  $p = 0.023$ , respectively) in the sub-analysis cohort dismissing patients with VTE before OC diagnosis. This result aligns with previous studies regarding advanced EOC prognosis, where increased expression of *SELP* mRNA was linked to worse OS [72]. Taken together, this study's findings suggest that ED and *SELP*'s roles are not merely associated with the presence of VTE but are closely linked with their impact in the context of ongoing cancer [20]. However, this SNP should be evaluated carefully given the underrepresentation of the GG genotype in the study sample, which makes it challenging to draw definitive conclusions about its impact on cancer outcomes. Looking forward, expanding the cohort could enable wider genotype representation and consequently provide better statistical power. Also, combining the quantification of protein levels with gene expression analyses could help clarify these study's findings, such as s*SELP*'s role in the complex VTE–ED–OC triad.

As for *VWF*, the variant rs1063856 involves a thymine (T) to cytosine (C) substitution in exon 18, which leads to increased plasma levels of vWF and, consequently a higher thrombosis risk [73,74]. Elevated vWF levels are known to contribute to cancer progression, as vWF can enhance platelet adhesion and aggregation, creating a pro-thrombotic environment that favours tumour metastasis [75]. Curiously, the T allele was significantly associated with a history of ATE in this study ( $\chi^2$ ,  $p = 0.018$ ). Although controversial, this result aligns with the marginal association of the SNP TT genotype with the use of anti-coagulants before their OC diagnosis, suggesting a pro-thrombotic role for this genotype. Although no association was detected between the SNP and the expression level of *VWF* in OC patients' PBCs, the TT genotype was found to be significantly associated with a higher expression of *SELP* ( $\chi^2$ ,  $p = 0.025$ ). This finding is consistent with the SNP's association with

ATE and the use of anticoagulants before OC diagnosis. Overall, *VWF* rs1063856 seems to have a role in thrombo-inflammatory mechanisms as *SELP* is known to mediate the interaction between activated ECs, platelets, and immune cells, a key process in thrombogenesis [16]. Although previous investigations report the association of *VWF* rs1063856 with both *vWF* plasma levels and VTE incidence, the present study lacks statistical significance for both analyses [74]. Notably, there is a lack of literature assessing the prognostic value of this SNP. In this study, no prognostic value was observed for *VWF* rs1063856, which aligns with the current gap in research regarding the role of this SNP in predicting cancer progression or patient outcomes.

Future research should aim to externally validate these findings in larger cohorts and other populations and perform functional studies to better understand the molecular mechanisms underpinning the associations between ED-related markers and ovarian tumourigenesis. Additionally, it will be important to conduct active screenings of CAT and integrate the flow-mediated dilation (FMD) test into future studies to directly measure and confirm the presence of ED in OC patients. Finally, in addition to PBCs, the expression of ED-related genes should be evaluated in endothelial cells—the primary source—to gain a better understanding of the gene expression dynamics.

## 5. Conclusions

Over the last few years, the search for reliable prognostic biomarkers has become a priority to improve OC management and patient outcomes. In the cancer research field, markers related to ED have garnered significant interest due to their roles in tumour invasion, angiogenesis and metastasis. Given the dual role of ED in CAT and cancer progression (independently of VTE), the present study aimed to assess the impact of specific ED-related genetic variations and genes on OC-related VTE occurrence, OC progression, and patient survival. Among the evaluated markers, only *NOS3* expression was significantly associated with VTE occurrence. Namely, its higher expression was linked to a reduced risk of VTE, reinforcing the idea of a protective effect of NO in venous thrombogenesis. This is attributed, at least partially, to the maintenance of endothelial integrity and normal activity, a well-established role of NO in cardiovascular research. Another important finding relates to *SELP*, a crucial mediator of endothelial integrity and tumour angiogenesis. In this study, *SELP* expression was associated with poor clinical outcomes. As for the SNP, despite demonstrating a strong correlation with poorer survival, no definitive conclusions may be taken due to limiting underrepresentation of its genotypes. Although more studies with larger cohort sizes and diverse populations are needed, together the findings of this preliminary study suggest that ED-related markers have a significant yet context-dependent role in ovarian tumourigenesis, which goes beyond venous thrombogenesis. Thus, additional research could pave the way for the identification of novel prognostic biomarkers for OC management, which are currently needed to improve patient clinical outcomes. Since one biomarker is most likely to be insufficient to significantly improve the accuracy of prognosis assessment, the goal should be to identify and combine multiple ED-related markers with a prognostic value in OC into a profile. Indeed, future studies should investigate a broader spectrum of ED-related genes to aid in the development of targeted therapies that address both cancer progression and thrombosis, offering new avenues for personalised treatment of OC.

**Supplementary Materials:** The following supporting information can be downloaded at: <https://www.mdpi.com/article/10.3390/life14121630/s1>, Supplementary Table S1. Negative results on the associations between investigated SNPs and patient survival. Supplementary Table S2. Negative results on the associations between the investigated genes and patient survival.

**Author Contributions:** Conceptualisation, I.G.d.M., V.T. and R.M.; methodology, I.G.d.M.; formal analysis, I.G.d.M., V.T. and R.M.; investigation, I.G.d.M., V.T., J.S.-B., M.R. and J.L.-P.; resources, R.M.; data curation, V.T. and R.M.; writing—original draft preparation, I.G.d.M.; writing—review and editing, I.G.d.M., V.T., J.S.-B., M.R., J.L.-P., D.P. and R.M.; supervision, V.T., D.P. and R.M.;

funding acquisition, V.T. and R.M. All authors have read and agreed to the published version of the manuscript.

**Funding:** This study was funded by the Portuguese Institute of Oncology of Porto (IPO Porto) (CI-IPOP-22-2015) and the Fundação para a Ciência e Tecnologia (FCT). V.T. is a PhD scholarship holder (Grant reference: 2020.08969.BD; <https://doi.org/10.54499/2020.08969.BD>) supported by FCT, co-financed by European Social Funds (FSE) and national funds of MCTES. The institutions had no implications for writing and publishing this article.

**Institutional Review Board Statement:** The study was conducted in accordance with the Declaration of Helsinki, and approved by the Ethics Committee of the Portuguese Institute of Oncology of Porto (CES IPO: 69/021; 11 March 2021).

**Informed Consent Statement:** Informed written consent according to the principles of the Helsinki Declaration was obtained from each patient before their enrolment.

**Data Availability Statement:** The data presented in this study are available on request from the corresponding author.

**Acknowledgments:** The authors would like to thank the Ministério da Saúde de Portugal, the Portuguese Institute of Oncology of Porto (IPO Porto), the Portuguese League Against Cancer (NRNorte) and the Fundação para a Ciência e Tecnologia (FCT).

**Conflicts of Interest:** J.L.-P. has received a research grant from GESCAT-Grupo de Estudos de Cancro e Trombose. This institution had no role in the decision to conduct the study, write and publish this manuscript. The remaining authors declare that they have no known competing financial interests or personal relationships that could have appeared to influence the work reported in this paper.

## References

1. Dagogo-Jack, I.; Shaw, A.T. Tumour heterogeneity and resistance to cancer therapies. *Nat. Rev. Clin. Oncol.* **2018**, *15*, 81–94. [CrossRef] [PubMed]
2. Tavares, V.; Marques, I.S.; de Melo, I.G.; Assis, J.; Pereira, D.; Medeiros, R. Paradigm Shift: A Comprehensive Review of Ovarian Cancer Management in an Era of Advancements. *Int. J. Mol. Sci.* **2024**, *25*, 1845. [CrossRef] [PubMed]
3. Moufarrij, S.; O'cearbhaill, R.E. Novel Therapeutics in Ovarian Cancer: Expanding the Toolbox. *Curr. Oncol.* **2023**, *31*, 97–114. [CrossRef] [PubMed]
4. Sowamber, R.; Lukey, A.; Huntsman, D.; Hanley, G. Ovarian Cancer: From Precursor Lesion Identification to Population-Based Prevention Programs. *Curr. Oncol.* **2023**, *30*, 10179–10194. [CrossRef] [PubMed]
5. Sideris, M.; Menon, U.; Manchanda, R. Screening and prevention of ovarian cancer. *Med. J. Aust.* **2024**, *220*, 264–274. [CrossRef]
6. Marques, I.S.; Tavares, V.; Savva-Bordalo, J.; Rei, M.; Liz-Pimenta, J.; de Melo, I.G.; Assis, J.; Pereira, D.; Medeiros, R. Long Non-Coding RNAs: Bridging Cancer-Associated Thrombosis and Clinical Outcome of Ovarian Cancer Patients. *Int. J. Mol. Sci.* **2023**, *25*, 140. [CrossRef]
7. Gong, T.-T.; Guo, S.; Liu, F.-H.; Huo, Y.-L.; Zhang, M.; Yan, S.; Zhou, H.-X.; Pan, X.; Wang, X.-Y.; Xu, H.-L.; et al. Proteomic characterization of epithelial ovarian cancer delineates molecular signatures and therapeutic targets in distinct histological subtypes. *Nat. Commun.* **2023**, *14*, 7802. [CrossRef]
8. González-Martín, A.; Harter, P.; Leary, A.; Lorusso, D.; Miller, R.; Pothuri, B.; Ray-Coquard, I.; Tan, D.; Bellet, E.; Oaknin, A.; et al. Newly diagnosed and relapsed epithelial ovarian cancer: ESMO Clinical Practice Guideline for diagnosis, treatment and follow-up. *Ann. Oncol.* **2023**, *34*, 833–848. [CrossRef]
9. Arora, T.; Mullangi, S.; Vadakekut, E.S.; Lekkala, M.R. *Epithelial Ovarian Cancer*; StatPearls Publishing: Treasure Island, FL, USA, 2024.
10. Tavares, V.; Savva-Bordalo, J.; Rei, M.; Liz-Pimenta, J.; Assis, J.; Pereira, D.; Medeiros, R. Haemostatic Gene Expression in Cancer-Related Immunothrombosis: Contribution for Venous Thromboembolism and Ovarian Tumour Behaviour. *Cancers* **2024**, *16*, 2356. [CrossRef]
11. Matte, I.; Garde-Granger, P.; Bessette, P.; Piché, A. Ascites from ovarian cancer patients stimulates MUC16 mucin expression and secretion in human peritoneal mesothelial cells through an Akt-dependent pathway. *BMC Cancer* **2019**, *19*, 406. [CrossRef]
12. Marques, I.S.; Tavares, V.; Neto, B.V.; Mota, I.N.R.; Pereira, D.; Medeiros, R. Long Non-Coding RNAs in Venous Thromboembolism: Where Do We Stand? *Int. J. Mol. Sci.* **2023**, *24*, 12103. [CrossRef] [PubMed]
13. Tatsumi, K. The pathogenesis of cancer-associated thrombosis. *Int. J. Hematol.* **2024**, *119*, 495–504. [CrossRef] [PubMed]
14. Khorana, A.A.; Kuderer, N.M.; Culakova, E.; Lyman, G.H.; Francis, C.W. Development and validation of a predictive model for chemotherapy-associated thrombosis. *Blood* **2008**, *111*, 4902–4907. [CrossRef] [PubMed]
15. Fernandes, C.J.; Morinaga, L.T.; Alves, J.L.; Castro, M.A.; Calderaro, D.; Jardim, C.V.; Souza, R. Cancer-associated thrombosis: The when, how and why. *Eur. Respir. Rev.* **2019**, *28*, 180119. [CrossRef]

16. Yeini, E.; Satchi-Fainaro, R. The role of P-selectin in cancer-associated thrombosis and beyond. *Thromb. Res.* **2022**, *213*, S22–S28. [CrossRef]
17. Shafa, A.; Watkins, A.B.; McGree, M.E.; Weroha, S.J.; Wahner Hendrickson, A.E.; Block, M.S.; Langstraat, C.L.; McBane, R.D., 2nd; Bakkum-Gamez, J.N.; Kumar, A. Incidence of venous thromboembolism in patients with advanced stage ovarian cancer undergoing neoadjuvant chemotherapy: Is it time for thromboprophylaxis? *Gynecol. Oncol.* **2023**, *176*, 36–42. [CrossRef]
18. Glassman, D.; Bateman, N.W.; Lee, S.; Zhao, L.; Yao, J.; Tan, Y.; Ivan, C.; Rangel, K.M.; Zhang, J.; Conrads, K.A.; et al. Molecular Correlates of Venous Thromboembolism (VTE) in Ovarian Cancer. *Cancers* **2022**, *14*, 1496. [CrossRef] [PubMed]
19. Kacimi, S.E.O.; Moeinafshar, A.; Haghighi, S.S.; Saghaideh, A.; Rezaei, N. Venous thromboembolism in cancer and cancer immunotherapy. *Crit. Rev. Oncol.* **2022**, *178*, 103782. [CrossRef]
20. Zhang, X.; Zhang, C.; Ma, Z.; Zhang, Y. Soluble P-selectin level in patients with cancer-associated venous and artery thromboembolism: A systematic review and meta-analysis. *Arch. Med. Sci.* **2023**, *19*, 274–282. [CrossRef]
21. Poredos, P.; Jezovnik, M.K. Endothelial Dysfunction and Venous Thrombosis. *Angiology* **2018**, *69*, 564–567. [CrossRef]
22. Cyr, A.R.; Huckaby, L.V.; Shiva, S.S.; Zuckerbraun, B.S. Nitric Oxide and Endothelial Dysfunction. *Crit. Care Clin.* **2020**, *36*, 307–321. [CrossRef] [PubMed]
23. Deanfield, J.E.; Halcox, J.P.; Rabelink, T.J. Endothelial function and dysfunction: Testing and clinical relevance. *Circulation* **2007**, *115*, 1285–1295. [CrossRef] [PubMed]
24. Migliacci, R.; Becattini, C.; Pesavento, R.; Davi, G.; Vedovati, M.C.; Guglielmini, G.; Falcinelli, E.; Ciabattini, G.; Valle, F.D.; Prandoni, P.; et al. Endothelial dysfunction in patients with spontaneous venous thromboembolism. *Haematologica* **2007**, *92*, 812–818. [CrossRef]
25. Incalza, M.A.; D’Oria, R.; Natalicchio, A.; Perrini, S.; Laviola, L.; Giorgino, F. Oxidative stress and reactive oxygen species in endothelial dysfunction associated with cardiovascular and metabolic diseases. *Vasc. Pharmacol.* **2018**, *100*, 1–19. [CrossRef]
26. Zhang, J. Biomarkers of endothelial activation and dysfunction in cardiovascular diseases. *Rev. Cardiovasc. Med.* **2022**, *23*, 73. [CrossRef]
27. Tripska, K.; Sá, I.C.I.; Vasinova, M.; Vicen, M.; Havelek, R.; Eissazadeh, S.; Svobodova, Z.; Vitverova, B.; Theuer, C.; Bernabeu, C.; et al. Monoclonal anti-endoglin antibody TRC105 (carotuximab) prevents hypercholesterolemia and hyperglycemia-induced endothelial dysfunction in human aortic endothelial cells. *Front. Med.* **2022**, *9*, 845918. [CrossRef] [PubMed]
28. Endemann, D.H.; Schiffrin, E.L. Endothelial dysfunction J. *Am. Soc. Nephrol.* **2004**, *15*, 1983–1992. [CrossRef]
29. Franses, J.W.; Drosu, N.C.; Gibson, W.J.; Chitalia, V.C.; Edelman, E.R. Dysfunctional endothelial cells directly stimulate cancer inflammation and metastasis. *Int. J. Cancer* **2013**, *133*, 1334–1344. [CrossRef]
30. Choi, J.Y.; Lee, K.M.; Noh, D.Y.; Ahn, S.H.; Lee, J.E.; Han, W.; Jang, I.J.; Shin, S.G.; Yoo, K.Y.; Hayes, R.B.; et al. Genetic polymorphisms of eNOS, hormone receptor status, and survival of breast cancer. *Breast Cancer Res. Treat.* **2006**, *100*, 213–218. [CrossRef]
31. Lutsey, P.L.; Zakai, N.A. Epidemiology and prevention of venous thromboembolism. *Nat. Rev. Cardiol.* **2023**, *20*, 248–262. [CrossRef]
32. Chiarella, P.; Capone, P.; Sisto, R. Contribution of Genetic Polymorphisms in Human Health. *Int. J. Environ. Res. Public Heal.* **2023**, *20*, 912. [CrossRef] [PubMed]
33. Berek, J.S.; Renz, M.; Kehoe, S.; Kumar, L.; Friedlander, M. Cancer of the ovary, fallopian tube, and peritoneum. *Int. J. Gynecol. Obstet.* **2021**, *155*, 61–85. [CrossRef] [PubMed]
34. Eisenhauer, E.A.; Therasse, P.; Bogaerts, J.; Schwartz, L.H.; Sargent, D.; Ford, R.; Dancey, J.; Arbuck, S.; Gwyther, S.; Mooney, M.; et al. New response evaluation criteria in solid tumours: Revised RECIST guideline (version 1.1). *Eur. J. Cancer* **2009**, *45*, 228–247. [CrossRef] [PubMed]
35. Gran, O.V.; Smith, E.N.; Braekkan, S.K.; Jensvoll, H.; Solomon, T.; Hindberg, K.; Wilsgaard, T.; Rosendaal, F.R.; Frazer, K.A.; Hansen, J.-B. Joint effects of cancer and variants in the factor 5 gene on the risk of venous thromboembolism. *Haematologica* **2016**, *101*, 1046–1053. [CrossRef]
36. de Melo, I.G.; Tavares, V.; Pereira, D.; Medeiros, R. Contribution of Endothelial Dysfunction to Cancer Susceptibility and Progression: A Comprehensive Narrative Review on the Genetic Risk Component. *Curr. Issues Mol. Biol.* **2024**, *46*, 4845–4873. [CrossRef] [PubMed]
37. Wang, L.; Wang, X.; Zhu, X.; Zhong, L.; Jiang, Q.; Wang, Y.; Tang, Q.; Li, Q.; Zhang, C.; Wang, H.; et al. Drug resistance in ovarian cancer: From mechanism to clinical trial. *Mol. Cancer* **2024**, *23*, 1–26. [CrossRef]
38. Miyamoto, Y.; Saito, Y.; Nakayama, M.; Shimasaki, Y.; Yoshimura, T.; Yoshimura, M.; Harada, M.; Kajiyama, N.; Kishimoto, I.; Kuwahara, K.; et al. Replication protein A1 reduces transcription of the endothelial nitric oxide synthase gene containing a -786T>C mutation associated with coronary spastic angina. *Hum. Mol. Genet.* **2000**, *9*, 2629–2637. [CrossRef]
39. Filho, C.K.C.; Oliveira-Paula, G.H.; Pereira, V.C.R.; Lacchini, R. Clinically relevant endothelial nitric oxide synthase polymorphisms and their impact on drug response. *Expert Opin. Drug Metab. Toxicol.* **2020**, *16*, 927–951. [CrossRef]
40. Wang, Q.; Sun, H.; Qi, X.; Zhou, M. eNOS rs2070744 polymorphism might influence predisposition to hemorrhagic cerebral vascular diseases in East Asians: A meta-analysis. *Brain Behav.* **2020**, *10*, e01538. [CrossRef]
41. Wu, X.; Wang, Z.-F.; Xu, Y.; Ren, R.; Heng, B.-L.; Su, Z.-X. Association between three eNOS polymorphisms and cancer risk: A meta-analysis. *Asian Pac. J. Cancer Prev.* **2014**, *15*, 5317–5324. [CrossRef]

42. Sydorchuk, A.R.; Sydorchuk, L.P.; Gutnitska, A.F.; Dzhuryak, V.S.; Kryvetska, I.I.; Sydorchuk, R.I.; Ursuliak, Y.V.; Iftoda, O.M. Endothelium function biomarkers and carotid intima-media thickness changes in relation to NOS3 (rs2070744) and GNB3 (rs5443) genes polymorphism in the essential arterial hypertension. *Endocr. Regul.* **2022**, *56*, 104–114. [CrossRef] [PubMed]
43. Sydorchuk, A.; Sydorchuk, L.; Gutnitska, A.; Vasyuk, V.; Tkachuk, O.; Dzhuryak, V.; Myshkovskii, Y.; Kyfiak, P.; Sydorchuk, R.; Iftoda, O. The role of NOS3 (rs2070744) and GNB3 (rs5443) genes' polymorphisms in endothelial dysfunction pathway and carotid intima-media thickness in hypertensive patients. *Gen. Physiol. Biophys.* **2023**, *42*, 179–190. [CrossRef]
44. Yetkin, U.; Karabay, O.; Öñol, H. Effects of oral anticoagulation with various INR levels in deep vein thrombosis cases. *Curr. Control. Trials Cardiovasc. Med.* **2004**, *5*, 1. [CrossRef] [PubMed]
45. Kolluru, G.K.; Siamwala, J.H.; Chatterjee, S. eNOS phosphorylation in health and disease. *Biochimie* **2010**, *92*, 1186–1198. [CrossRef]
46. Neubauer, K.; Zieger, B. Endothelial cells and coagulation. *Cell Tissue Res.* **2022**, *387*, 391–398. [CrossRef] [PubMed]
47. Napoli, C.; Paolisso, G.; Casamassimi, A.; Al-Omran, M.; Barbieri, M.; Sommesse, L.; Infante, T.; Ignarro, L.J. Effects of nitric oxide on cell proliferation: Novel insights. *J. Am. Coll. Cardiol.* **2013**, *62*, 89–95. [CrossRef]
48. Gao, X.; Wang, J.; Wang, W.; Wang, M.; Zhang, J. eNOS Genetic Polymorphisms and Cancer Risk: A Meta-Analysis and a Case-Control Study of Breast Cancer. *Medicine* **2015**, *94*, e972. [CrossRef]
49. Vannini, F.; Kashfi, K.; Nath, N. The dual role of iNOS in cancer. *Redox Biol.* **2015**, *6*, 334–343. [CrossRef]
50. Rose, M.; Burgess, J.T.; O'byrne, K.; Richard, D.J.; Bolderson, E. PARP Inhibitors: Clinical Relevance, Mechanisms of Action and Tumor Resistance. *Front. Cell Dev. Biol.* **2020**, *8*, 564601. [CrossRef]
51. Wilson, A.; Menon, V.; Khan, Z.; Alam, A.; Litovchick, L.; Yakovlev, V. Nitric oxide-donor/PARP-inhibitor combination: A new approach for sensitization to ionizing radiation. *Redox Biol.* **2019**, *24*, 101169. [CrossRef]
52. Bui, T.M.; Wiesolek, H.L.; Sumagin, R. ICAM-1: A master regulator of cellular responses in inflammation, injury resolution, and tumorigenesis. *J. Leukoc. Biol.* **2020**, *108*, 787–799. [CrossRef] [PubMed]
53. Muñoz, T.G.; Amaral, A.T.; Puerto-Camacho, P.; Peinado, H.; de Álava, E. Endoglin in the Spotlight to Treat Cancer. *Int. J. Mol. Sci.* **2021**, *22*, 3186. [CrossRef] [PubMed]
54. Santibanez, J.F.; Letamendia, A.; Perez-Barriocanal, F.; Silvestri, C.; Saura, M.; Vary, C.P.; Lopez-Novoa, J.M.; Attisano, L.; Bernabeu, C. Endoglin increases eNOS expression by modulating Smad2 protein levels and Smad2-dependent TGF-beta signaling. *J. Cell. Physiol.* **2007**, *210*, 456–468. [CrossRef] [PubMed]
55. Lu, J.; Wei, Q.; Bondy, M.L.; Yu, T.; Li, D.; Brewster, A.; Shete, S.; Sahin, A.; Meric-Bernstam, F.; Wang, L. Promoter polymorphism (−786T > C) in the endothelial nitric oxide synthase gene is associated with risk of sporadic breast cancer in non-Hispanic white women age younger than 55 years. *Cancer* **2006**, *107*, 2245–2253. [CrossRef]
56. Zhang, L.; Chen, L.M.; Wang, M.N.; Chen, X.J.; Li, N.; Huang, Y.D.; Chen, M. The G894t, T-786c and 4b/a polymorphisms in Enos gene and cancer risk: A meta-analysis. *J. Evid. Based Med.* **2014**, *7*, 263–269. [CrossRef]
57. Nan, J.; Liu, Y.; Xu, C.; Ge, D. Effects of eNOS gene polymorphisms on individual susceptibility to cancer: A meta-analysis. *Nitric Oxide* **2019**, *84*, 1–6. [CrossRef] [PubMed]
58. Polat, F.; Turaçlar, N.; Yilmaz, M.; Bingöl, G.; Vural, H.C. eNOS gene polymorphisms in paraffin-embedded tissues of prostate cancer patients. *Turk. J. Med Sci.* **2016**, *46*, 673–679. [CrossRef] [PubMed]
59. Abedinzadeh, M.; Dastgheib, S.A.; Maleki, H.; Heiranizadeh, N.; Zare, M.; Jafari-Nedooshan, J.; Kargar, S.; Neamatzadeh, H. Association of Endothelial Nitric Oxide Synthase Gene Polymorphisms with Susceptibility to Prostate Cancer: A Comprehensive Systematic Review and Meta-Analysis. *Urol. J.* **2020**, *17*, 329–337. [CrossRef]
60. Su, C.-W.; Chien, M.-H.; Lin, C.-W.; Chen, M.-K.; Chow, J.-M.; Chuang, C.-Y.; Chou, C.-H.; Liu, Y.-C.; Yang, S.-F. Associations of genetic variations of the endothelial nitric oxide synthase gene and environmental carcinogens with oral cancer susceptibility and development. *Nitric Oxide* **2018**, *79*, 1–7. [CrossRef]
61. Jang, M.J.; Jeon, Y.J.; Kim, J.W.; Chong, S.Y.; Hong, S.P.; Oh, D.; Cho, Y.K.; Chung, K.W.; Kim, N.K. Association of eNOS polymorphisms (−786T > C, 4a4b, 894G > T) with colorectal cancer susceptibility in the Korean population. *Gene* **2012**, *512*, 275–281. [CrossRef]
62. Krishnaveni, D.; Amar Chand, B.; Shravan Kumar, P.; Uma Devi, M.; Ramanna, M.; Jyothy, A.; Pratibha, N.; Balakrishna, N.; Venkateshwari, A. Association of endothelial nitric oxide synthase gene T-786C promoter polymorphism with gastric cancer. *World J. Gastrointest. Oncol.* **2015**, *7*, 87–94. [CrossRef]
63. George, D.J.; Martini, J.-F.; Staehler, M.; Motzer, R.J.; Magheli, A.; Donskov, F.; Escudier, B.; Li, S.; Casey, M.; Valota, O.; et al. Phase III Trial of Adjuvant Sunitinib in Patients with High-Risk Renal Cell Carcinoma: Exploratory Pharmacogenomic Analysis. *Clin. Cancer Res.* **2019**, *25*, 1165–1173. [CrossRef] [PubMed]
64. Casadei-Gardini, A.; Marisi, G.; Dadduzio, V.; Gramantieri, L.; Faloppi, L.; Ulivi, P.; Foschi, F.G.; Tamburini, E.; Vivaldi, C.; Rizzato, M.D.; et al. Association of NOS3 and ANGPT2 Gene Polymorphisms with Survival in Patients with Hepatocellular Carcinoma Receiving Sorafenib: Results of the Multicenter Prospective INNOVATE Study. *Clin. Cancer Res.* **2020**, *26*, 4485–4493. [CrossRef] [PubMed]
65. Ryk, C.; Koskela, L.R.; Thiel, T.; Wiklund, N.P.; Steineck, G.; Schumacher, M.C.; de Verdier, P.J. Outcome after BCG treatment for urinary bladder cancer may be influenced by polymorphisms in the NOS2 and NOS3 genes. *Redox Biol.* **2015**, *6*, 272–277. [CrossRef] [PubMed]

66. Kaur, R.; Singh, J.; Kapoor, R.; Kaur, M. Association of SELP Polymorphisms with Soluble P-Selectin Levels and Vascular Risk in Patients with Type 2 Diabetes Mellitus: A Case–Control Study. *Biochem. Genet.* **2019**, *57*, 73–97. [CrossRef] [PubMed]
67. Barbaux, S.C.; Blankenberg, S.; Rupprecht, H.J.; Francomme, C.; Bickel, C.; Hafner, G.; Nicaud, V.; Meyer, J.; Cambien, F.; Tiret, L. Association between P-selectin gene polymorphisms and soluble P-selectin levels and their relation to coronary artery disease. *Arter. Thromb. Vasc. Biol.* **2001**, *21*, 1668–1673. [CrossRef]
68. Kou, L.; Yang, N.; Dong, B.; Li, Y.; Yang, J.; Qin, Q. Interaction between SELP genetic polymorphisms with inflammatory cytokine interleukin-6 (IL-6) gene variants on cardiovascular disease in Chinese Han population. *Mamm. Genome* **2017**, *28*, 436–442. [CrossRef]
69. Ay, C.; Jungbauer, L.V.; Sailer, T.; Tengler, T.; Koder, S.; Kaider, A.; Panzer, S.; Quehenberger, P.; Pabinger, I.; Mannhalter, C. High concentrations of soluble P-selectin are associated with risk of venous thromboembolism and the P-selectin Thr715 variant. *Clin. Chem.* **2007**, *53*, 1235–1243. [CrossRef]
70. Powrózek, T.; Mlak, R.; Brzozowska, A.; Mazurek, M.; Gołębiowski, P.; Małecka-Massalska, T. Relationship Between-2028 C/T SELP Gene Polymorphism, Concentration of Plasma P-Selectin and Risk of Malnutrition in Head and Neck Cancer Patients. *Pathol. Oncol. Res.* **2019**, *25*, 741–749. [CrossRef]
71. Tao, Y.; Zhang, Q.; Wang, H.; Yang, X.; Mu, H. Alternative splicing and related RNA binding proteins in human health and disease. *Signal Transduct. Target. Ther.* **2024**, *9*, 26. [CrossRef]
72. Singel, K.L.; Grzankowski, K.S.; Khan, A.N.M.N.H.; Grimm, M.J.; D’auria, A.C.; Morrell, K.; Eng, K.H.; Hylander, B.; Mayor, P.C.; Emmons, T.R.; et al. Mitochondrial DNA in the tumour microenvironment activates neutrophils and is associated with worse outcomes in patients with advanced epithelial ovarian cancer. *Br. J. Cancer* **2019**, *120*, 207–217. [CrossRef] [PubMed]
73. Mufti, A.H.; Ogiwara, K.; Swystun, L.L.; Eikenboom, J.C.J.; Budde, U.; Hopman, W.M.; Halldén, C.; Goudemand, J.; Peake, I.R.; Goodeve, A.C.; et al. The common VWF single nucleotide variants c.2365A > G and c.2385T > C modify VWF biosynthesis and clearance. *Blood Adv.* **2018**, *2*, 1585–1594. [CrossRef] [PubMed]
74. Smith, N.L.; Rice, K.M.; Bovill, E.G.; Cushman, M.; Bis, J.C.; McKnight, B.; Lumley, T.; Glazer, N.L.; Vlieg, A.V.H.; Tang, W.; et al. Genetic variation associated with plasma von Willebrand factor levels and the risk of incident venous thrombosis. *Blood* **2011**, *117*, 6007–6011. [CrossRef] [PubMed]
75. Comerford, C.; Glavey, S.; Quinn, J.; O’Sullivan, J.M. The role of VWF/FVIII in thrombosis and cancer progression in multiple myeloma and other hematological malignancies. *J. Thromb. Haemost.* **2022**, *20*, 1766–1777. [CrossRef]

**Disclaimer/Publisher’s Note:** The statements, opinions and data contained in all publications are solely those of the individual author(s) and contributor(s) and not of MDPI and/or the editor(s). MDPI and/or the editor(s) disclaim responsibility for any injury to people or property resulting from any ideas, methods, instructions or products referred to in the content.



## Article

# Learning Curve of First-Trimester Detailed Cardiovascular Ultrasound Screening by Moderately Experienced Obstetricians in 3509 Consecutive Unselected Pregnancies with Fetal Follow-Up

Tibor Elekes <sup>1,2</sup>, Gyula Csermely <sup>1</sup>, Krisztina Kádár <sup>1</sup>, László Molnár <sup>1</sup>, Gábor Keszthelyi <sup>1</sup>, Andrea Hozsdora <sup>1</sup>, Miklós Vizer <sup>3</sup>, Marianna Török <sup>4,5,\*</sup>, Petra Merkely <sup>4,†</sup> and Szabolcs Várbiro <sup>4,5,6,†</sup>

<sup>1</sup> RMC-Fetal Medicine Centre, Gábor Áron Street 74-78, H-1026 Budapest, Hungary; drelekestibor@gmail.com (T.E.); drcsermelygyula@gmail.com (G.C.); krisztinakadar@hotmail.com (K.K.); molnar.sumi@gmail.com (L.M.); kszimed2000@t-online.hu (G.K.); hozs.andi@gmail.com (A.H.)

<sup>2</sup> Cardiovascular Medicine and Research Division, Semmelweis University, Üllői Street 26, H-1085 Budapest, Hungary

<sup>3</sup> DaVinci Private Hospital, Mátyás Ottó Street 1, H-7635 Pécs, Hungary; vizermiklosgabor@gmail.com

<sup>4</sup> Department of Obstetrics and Gynecology, Semmelweis University, Üllői Street 78a, H-1082 Budapest, Hungary; merkely.petra@gmail.com (P.M.); varbiro.szabolcs@semmelweis.hu (S.V.)

<sup>5</sup> Workgroup of Research Management, Doctoral School, Semmelweis University, Üllői Street 22, H-1085 Budapest, Hungary

<sup>6</sup> Department of Obstetrics and Gynecology, University of Szeged, Semmelweis Street 1, H-6725 Szeged, Hungary

\* Correspondence: torok.marianna@semmelweis.hu

† These authors contributed equally to this work.

**Abstract:** Our primary objective was to assess the effectiveness of detailed cardiovascular ultrasound screening during the first trimester, which was performed by obstetricians with intermediate experience. We collected first-trimester fetal cardiac screening data from an unselected pregnant population at RMC-Fetal Medicine Center during a study period spanning from 1 January 2010, to 31 January 2015, in order to analyze our learning curve. A pediatric cardiologist performed a follow-up assessment in cases where the examining obstetrician determined that the fetal cardiac screening results were abnormal or high-risk. Overall, 42 (0.88%) congenital heart abnormalities were discovered prenatally out of 4769 fetuses from 4602 pregnant women who had at least one first-trimester cardiac ultrasonography screening. In total, 89.2% of the major congenital heart abnormalities (27 of 28) in the following fetuses were discovered (or at least highly suspected) at the first-trimester screening and subsequent fetal echocardiography by the pediatric cardiology specialist. Of these, 96.4% were diagnosed prenatally. According to our results, the effectiveness of first-trimester fetal cardiovascular ultrasound screening conducted by moderately experienced obstetricians in an unselected ('routine') pregnant population may reach as high as 90% in terms of major congenital heart defects, provided that equipment, quality assurance, and motivation are appropriate.

**Keywords:** cardiovascular ultrasound screening; learning curve; moderately experienced obstetricians; fetal follow up

## 1. Introduction

Moderate and severe congenital heart defects (CHD) requiring intensive postnatal cardiac care are the most frequent fetal malformations with an incidence of 6–8 per 1000 live births. If we consider all small-sized ventricular septal defects (VSD), bicuspid aortic valves, and other minor cardiac malformations, which potentially increase cardiac morbidity at later ages, this incidence may be as high as 7.5 per cent [1]. Fetal cardiac anomalies are responsible for 20% of intrauterine fetal demise and 20 to 30% of neonatal mortality.

Prenatal diagnosis of CHD may help the work of genetic counselors, contribute to a better understanding of the prognosis of affected fetuses, and reduce the psychological and physical risk of affected pregnant women [2–4]. In utero detection of CHD may improve neonatal morbidity and mortality as a result of prior organization of intensive postnatal cardiac care [5–9]. Fetal echocardiography in high-risk patients is usually performed by pediatric cardiologists. The high-risk pregnant population includes pregnant women with a positive family history of CHD, in vitro fertilization, maternal metabolic disorder, mainly diabetes and obesity, higher maternal age, autoimmune diseases (SLE, Sjögren), fetal teratogen exposure, and abnormal NT, TR, and DV on the first-trimester genetic ultrasound examination [10–15]. In this group of high-risk pregnant patients, the vast majority of severe CHD cases are diagnosed prenatally [16,17]. On the other hand, according to the literature, 90% of CHD is not present in the high-risk group and routine obstetric ultrasound screening of the low-risk pregnant population is generally ineffective in finding the majority of major fetal cardiac anomalies due to the time-consuming nature of the examination and the lack of the acquired expertise, which would be greatly improved after a proper learning process [18–23]. Aneuploidy screening in the 11 to 13 + 6-week window by Fetal Medicine Foundation (FMF)-certified obstetric sonographers resulted in improved detection rates of CHD in the first trimester [24].

Given the fact that it is the obstetric sonographer who initially evaluates the 11–13-week fetus, there is great demand for obstetricians to conduct early and comprehensive fetal heart scans [25–27].

Thanks to the widespread use of high-frequency ultrasound scanners and the introduction of novel Doppler techniques, obstetricians skilled in fetal cardiac scanning are able to visualize four-chamber views and ventricular outflow tracts of first-trimester fetuses in approximately 95 to 97% of cases [28–31]. A significant number of international investigational research groups have proved high effectiveness (>90% detection rate, DR) of prospective first-trimester extended fetal cardiac screening conducted by highly qualified obstetric sonographers in high-risk pregnant patients [28,32]. However, the current literature lacks sufficient information regarding the effectiveness of early fetal cardiac examinations performed by obstetricians with basic and intermediate experience in unselected (low- and high-risk), also referred to as ‘routine’ pregnant populations, and of the learning curve [31,33,34].

Our study’s primary goal was to assess the efficacy of first-trimester prolonged cardiovascular ultrasonography screening carried out by obstetricians with a moderate level of experience (an examiner experienced in the differential diagnosis of regular first-trimester heart planes but less experienced in the differential diagnosis of irregular first-trimester heart planes (i.e., has seen few abnormal cases)) in consecutive cases of an unselected pregnant population. Our investigation’s second goal was to examine and better understand the learning curve we saw throughout the course of the five-year study period with reference to the sonographic assessment of the fetal heart between weeks 11 and 13.

## 2. Materials and Methods

Our retrospective study was approved by the Scientific and Investigational-Ethical Committee of the Hungarian Medical Scientific Council (2013/EKU (588/2013)). Data from the first-trimester fetal cardiovascular screening of consecutive patients from an unselected (or “routine”) pregnant population at the RMC-Fetal Medicine Center throughout a study period from 1 January 2010 to 31 January 2015, were used to analyze the learning curve. Fetuses of pregnant women who received screening between 1 January 2011 and 30 June 2014, were monitored throughout pregnancy in order to assess the effectiveness of first-trimester cardiac screening.

Fetal cardiac scans were performed during routine first-trimester extended ultrasound screening, which included a comprehensive study of fetal sono-anatomy and aneuploidy, as well as preeclampsia screening in accordance with the protocol of the FMF (maternal age, body weight and height, maternal serum beta-hCG and PAPP-A assay combined with

fetal sonographic measurement of nuchal translucency (NT), nasal bone (NB) visualization, fetal heart rate (FHR) measurement, tricuspid regurgitation (TR), ductus venosus (DV) blood flow examination for aneuploidy, and maternal blood pressure, medical history, serum PAPP-A, and, as of 1 January 2014, serum PIGF assay combined with sonographic assessment of maternal left and right uterine artery Doppler-flow PI-value for preeclampsia screening, respectively) [33,35].

Transabdominal ultrasound examinations were conducted by using Accuvix V20 (Samsung-Medison, Seoul, Republic of Korea) and Voluson S8 (GE Medical Systems, Florence, SC, USA) ultrasound scanners both equipped with 4 to 8 MHz convex abdominal transducers. At the beginning of the study period, ultrasound examinations were performed by three obstetricians (all of them were FMF-audited sonographers for NT, NB, DV, and TR), who were experienced in the assessment of normal fetal first- and second-trimester cardiac anatomy but only moderately experienced in the final evaluation of abnormal fetal cardiac anatomy. During the last year of the study period, an FMF-audited sonographer joined the obstetric team, who pre-screened pregnant patients.

Intrauterine cardiac screening was introduced in the 1980s, which at that time only consisted of the examination of 4 cavity planes, ideally at 18–22 weeks. Subsequently, it was recognized that in many cases, CHD exists despite the normal four-cavity view; therefore, by further increasing the detection rate, in 2001, Yagel et al., added the determination of the abdominal situs, aortic arch, ventricular outflow tract, and mediastinal vessel examination as part of the screening procedure. In 2015, the three-vessel tracheal view was incorporated into the UK screening protocol. During our screenings, we used all of the aforementioned techniques in the first-trimester heart examination [36–39].

In all cases, a comprehensive medical history was taken from the patients, including maternal body weight and height, temperature, and blood pressure. As of 1 January 2011, an institutional standardized protocol was introduced for sonographic examination of the first-trimester fetal heart, according to which the following planes, structures, and functions are to be examined and archived digitally:

1. Determination of abdominal situs;
2. Cardiac size and axis;
3. Four-chamber view: crux cordis, ventricular septum in the four-chamber-plane, ventricular color inflow, tricuspid pulsed-wave Doppler, and FHR;
4. Three-vessel view, V-confluence of color flow;
5. Longitudinal view: aortic arch with color flow, ductal arch, right ventricular outflow tract, imaging of the crossing of great vessels (during first-trimester cardiac screening it is more reliable to visualize a cross-section of the aorta next to the longitudinal section of the pulmonary trunk from a median-sagittal plane rather than using an axial cardiac grand-sweep);
6. Optional examinations of the left atrial pulmonary vein (at least two) and right atrial caval vein connections (veno-atrial concordancy).

Cardiac screening according to this protocol was considered comprehensive if all of the previously mentioned structures were stored digitally. No time limitations were applied during the examinations. The examination was only interrupted when a visualization obstacle other than fetal position occurred, such as a significant distance between fetus and transducer (retroflexed uterus, thick maternal abdominal wall, previous abdominal scars, anterior placenta), and where vaginal ultrasound was also found to be inadequate [40,41]. In cases deemed to be within the normal range at first-trimester cardiac screening, if the patient returned to us later, the cardiac scan was repeated at 18 to 20 weeks and at 28 to 30 weeks. A pediatric cardiologist reevaluated all routinely screened cases that were found to be “abnormal”, as well as high-risk instances. The parents received thorough genetic counseling in the case that the prenatal cardiac screening revealed abnormalities.

Fetal karyotyping by chorionic villous sampling or amniocentesis was offered to all pregnant women who had positive first-trimester aneuploidy screening test results or if the type of CHD indicated it.

Pregnant women who underwent screening at our center received routine prenatal, genetic, and general obstetric care at various institutes of the country (221 attending physicians); therefore, data concerning the outcomes of pregnancies were collected from patients in three different methods:

1. Patients responded to our queries via email (our address appeared on the first-trimester obstetric ultrasound report);
2. Data were retrieved from the digital records of the obstetric division of our center where patients received prenatal care;
3. Verbal interviews with mothers by phone were performed by trained health personnel of our center. In the event of inconclusive outcome data, a follow-up interview via phone was repeated by the obstetrician to ascertain clear outcome results.

For statistical analysis, the Chi-Square Test was used and  $p < 0.05$  was evaluated as a significant difference. The data were evaluated using GraphPad Prism 6.0. software.

### 3. Results

Overall, 42 (0.88%) cases of congenital heart disease were identified during the 4769 fetuses (155 twins, 6 triplets, and 4441 singletons) of 4602 pregnant mothers who underwent at least one first-trimester cardiac ultrasound screening between 1 January 2010, and 31 January 2015 (the majority also underwent second and third-trimester screening).

Table 1 presents the summary of the distribution of different types of CHD according to the timing of detection and gestational age.

**Table 1.** Prenatally observed abnormal hearts during the learning curve.

	2010	2011	2012	2012	2014	Total
# of 1st-trim. examinations	228	586	872	1228	1855	4769
# of abnormal hearts (1st-trim. Dx)	2 (1)	8 (7)	6 (5)	15 (14)	11 (9)	42 (36)
HLHS		2		1	1	4
AVSD	1	1	1	1	3	7
AVSD + HRH		1				1
AVSD + HLH			1		1	2
AVSD + Heterotaxia		1				1
VSD		1	2	3	1	7
VSD + LV < RV				1		1
ASD + LV < RV			1			1
LV > RV					1	1
LV < RV					1	1
HLH + VSD				1		1
HRH + VSD		1				1
Aortic stenosis + HLH + AVSD				1		1
Aortic atresia	1	1				2
Pulmonary valve regurgitation					1	1
Pulmonary atresia + HRH				1		1
Septal fibrosis + VSD				1		1
Ventricular fibro-elastosis				1		1
Rhabdomyoma					1	1
TGA					1	1
Tetralogy of Fallot				1		1
Isolated pericardial fluid			1	1		2
CHD—non evaluated				2		2

Abbreviations: #, number; Dx, diagnosis; HLHS, hypoplastic left heart syndrome; AVSD, atrio-ventricular septal defect; HRH, hypoplastic right heart; HLH, hypoplastic left heart (LV << RH); VSD, ventricular septal defect; LV, left ventricle; RV, right ventricle; ASD, atrial septal defect; TGA, transposition of great arteries; CHD, congenital heart defect.

Considering the low case number ( $n = 228$ ) observed in the first study year (2010) and the absence of a uniformly applied examination protocol for the assessment of the fetal heart, fetuses screened during this particular time interval were not followed. In the group

of patients who underwent screening in the second half of 2014 ( $n = 1032$  fetuses), the vast majority of pregnancies were still ongoing at the time of the outcome data analysis (from the 1 February 2015 to 31 March 2015). Consequently, only fetuses screened between the 1 January 2011 and the 30 June 2014 were followed and data retrieved from the outcome of the aforementioned fetuses were used to assess the effectiveness of screening.

During this three-and-a-half-year period, 3509 fetuses (125 twins, 6 triplets, and 3241 singletons) of 3372 pregnant women underwent a comprehensive fetal cardiovascular ultrasound screening at 11–13 + 6-weeks of gestation. The ratio of followed pregnancies was 93% (3142/3372). Of the 239 fetuses from 230 pregnancies who were lost at follow-up, no abnormalities were identified by a first-trimester fetal cardiac ultrasound scan. Of the 3270 followed fetuses, 3020 were singletons, 116 were twins, and 6 were triplets. The mean maternal age at the time of first-trimester screening was 33.9 years (range: 17–45). The ratio of pregnant women aged  $> 35$  years was 46.9%. The mean fetal crown-rump length (CRL) was 64.0 mm (range: 45.0–84.0).

The mean maternal ages at the time of first-trimester screening in the entire study population and in the group of pregnancies affected with major fetal CHD were 33.9 and 35.8 years, respectively (nonsignificant,  $\chi^2 = 3.601$ ,  $df = 1$ ,  $p = 0.058$ ). The proportions of women above 35 years of age in the overall study population and in the group of pregnancies affected by major fetal CHD were 46.9% and 71.0%, respectively (significant,  $\chi^2 = 6.642$ ,  $df = 1$ ,  $p = 0.0099$ ).

The results of our NT, DV, and TR measurements (FMF software version 2.3) performed in conjunction with fetal cardiac screening revealed that 56.1% of NT values were above the median and 4.9% of them were above the 95th percentile, respectively. Simultaneously, in 54% of prenatally detected cardiac defects (20/37), NT-values were below the 99th percentile ( $< 3.5$  mm), and in 46% of them (17/37), the NT-value was less than 2.5 mm. With respect to other cardiac markers, TR was found in 0.6% of non-CHD cases and in 29% of fetuses with CHD (10/35) (significant,  $\chi^2 = 308.486$ ,  $df = 1$ ,  $p < 0.05$ ). Similarly, an abnormal DV blood flow pattern was identified in 4.3% of all examined fetuses and in 51% of fetuses affected with cardiac anomalies (18/35) (significant,  $\chi^2 = 168.282$ ,  $df = 1$ ,  $p < 0.05$ ).

### 3.1. Prenatal Diagnosis

During the first-trimester cardiac ultrasound screening of 3270 followed fetuses, 34 hearts were identified by the examining moderately experienced obstetricians as ‘abnormal’. Of the cases, two were deemed to be within the normal range (#33 and 34), the initial diagnosis was either refined or supplemented in five (#4, 14, 21, 24, and 32), and three cases were not examined (#6, 15, and 18) by the pediatric cardiology specialist. In 24 cases, the cardiologist agreed with the initial diagnosis. In the three non-examined cases by pediatric cardiology specialists, pregnant women did not comply with repeated fetal cardiac ultrasound scans because, due to the presence of other associated fetal congenital malformations, they opted for pregnancy termination. Of the 32 prenatally verified abnormal fetal hearts (examined by both moderately experienced obstetricians and a pediatric cardiology specialist), 6 cases were interpreted as ‘minor anomaly’ (#3, 10, 28, 30, 31, and 32), while the remaining cases ( $n = 26$ ) were evaluated as ‘major cardiac vitium’. CHD were considered to be ‘major anomalies’ if they required cardiac surgery during the first year of life.

Two minor anomalies that were also confirmed by the cardiologist at the first-trimester scan (#31: isolated pericardial fluid; and #32: minor inlet ventricular septal defect, VSD), which were considered as a ‘normal heart’ at the second-trimester ultrasound screening. One case of fetal septal fibrotic area detected by both the obstetrician and the cardiologist at the time of first-trimester cardiac screening was supplemented with the diagnosis of VSD during second-trimester ultrasound screening (#28). Case #30 (isolated pericardial fluid at first-trimester screening), interpreted as a ‘minor anomaly’, proved postnatally to be a major cardiac defect (complex pulmonary atresia, Table 2).

**Table 2.** Abnormal cardiac findings during the following period.

	1st-Trim. OB. Dx	1st-Trim. Card. Dx	NT	TR	Abn. DV	20-Week OB + Card.	Assoc. Malformations	Karyotype	Pregnancy Outcome
1	AVSD	idem	2.3	+	+	-		47XX, +21	Termination
2	AVSD, HeterotaxiaDextrocardia	idem	1.7	not done	+	-	-	-	Termination
3	VSD	idem	7.9	+	+	-	-	-	Termination
4	AVSD + HRH	id. + fibro-elast	2.5	-	+	-	SUA	46XY	Termination
5	AVSD + HLHS	idem	1.9	-	-	-	-	46XX, 16 polymorph.	Termination
6	LV < RV, ASD	Not examined	5.1	-	-	-	Omphalocele paklatoschisis	47XX, +13	Termination
7	Tricu. atr, HRH, VSD	idem	1.6	Flow:-	-	-	-	46XX (abortum)	Termination
8	AVSD	idem	5	+	-	-	Oligohydramnios	-	Termination
9	HLHS	idem	6	+	-	-	Holoprosencephalia Polydactylia Hydronephrosis Camptodactylia SUA	47XY, +13	Termination
10	VSD (subaortic)	idem	N/A	not done	not done	-	oligohydramnion	69XXX	Termination
11	VSD, fibro-leastosis	idem	2.1	-	-	-	-	-	Termination
12	PA atr., HRH	idem	3.9	-	-	-	-	-	Termination
13	RV fibro-elastosis	idem	5.5	not done	not done	-	-	-	Termination
14	HLHS, VSD	HLHS, AVSD Aorta stenosis	1.5	+	not done	-	-	-	Termination
15	Left rot., Abn. GA	Not examined	6	not done	+	-	cervical cyst, short bones	PCR negative Cytogenetics cannot be performed:	Termination
16	HLHS	idem	2.4	-	+	-	Alob. holoprosencephaly Palatoschisis SUA	-	Termination
17	HLHS, VSD,	idem	7	-	not done	-	Holoprosencephaly Encephalocele Omphalocele	-	Termination
18	Abn. 4-CV + outfl. tr.	Not examined	8	not done	+	-	-	-	Termination
19	LV < RV, VSD	idem	7.3	-	-	-	Cleft lip and palate	47XX, +13	Termination
20	Tetralogy of Fallot	idem	4.5	.	+	-	-	-	Termination
21	LV < RV, AVSD	only AVSD	3.6	-	+	-	-	47XX, +21	Termination
22	AVSD	idem	4.7	+	+	-	Clubfoot, short bones	-	Termination
23	LV < RV,	idem	9	not done	+	-	Strawberry shape skull	-	Termination
24	RV > LV, P. valve reg.	P.valve reg.	1.8	+	+	-	-	47XX, +17 Chr 16 polymorph.	Termination
25	AVSD	idem	5.1	+	+	-	Short bones	-	Termination
26	AVSD	idem	6.5	+	+	-	-	-	Termination
27	HLHS	idem	1.2	not done	+	-	Omphalocele Cheilo-palatoschisis	-	Termination
28	Septal fibrotic area, Rhabdomyoma	idem	1.6	-	-	idem + VSD; Swiss cheese VSD	-	46XX	Born, idem, closed VSD No VSD Ventricular septum in upper third of echo-dense terime

Table 2. Cont.

	1st-Trim. OB. Dx	1st-Trim. Card. Dx	NT	TR	Abn. DV	20-Week OB + Card.	Assoc. Malformations	Karyotype	Pregnancy Outcome
29	HLHS	idem	3.1	+	+	-	-	47XX, +21	Termination Born, complex P. atresia
30	Isol. pericard. fluid	idem	2.1	-	-	hasn't come back	-	-	1 year old with com-plex pulmonary atresia
31	Isol. pericard. fluid	idem	1.8	-	-	normal heart	-	-	Born, healthy
32	Large VSD	Min. inlet VSD	2.8	-	-	normal heart	-	46XX	Born, healthy
33	RV < LV	normal heart	4.8	+	-	normal heart	-	46XX, NT panel negative	Born, healthy
34	PA < Ao	normal heart	2.1	-	-	normal heart	-	-	Born, healthy
35	normal heart	-	2.4	-	-	VSD (subaortic) Ao. atr, LV > RV, fibr endocardialis fibrosis	Cleft lip	46XY	Born, VSD closed
36	normal heart	-	2.4	-	+	3-trim. Rhabdomyoma; Multiplex rhabdomyoma	-	46XY	Termination
37	normal heart	-	2	-	-	VSD (inlet)	-	-	Born, Dx proved
38	normal heart	-	1.9	-	+	small VSD	-	46XY	Born, Dx proved
39	normal heart	-	3.3	-	-		-	NIPT: negative	Born, cl. lip, VSD closed

Abbreviations: HLHS, hypoplastic left heart syndrome; AVSD, atrio-ventricular septal defect; HRH, hypoplastic right heart; HLH, hypoplastic left heart (LV << RH); VSD, ventricular septal defect; LV, left ventricle; RV, right ventricle; ASD, atrial septal defect; TGA, transposition of great arteries; CHD, congenital heart defect; Dx, diagnosis; OB, medium-experienced obstetrician; Card, pediatric cardiologist specialist; NT, nuchal translucency; TR, tricuspidal regurgitation, DV, ductus venosus; Abn, abnormal; Assoc, associated; Tricu atr, tricuspidal atresia; PA, pulmonary artery; Rot, rotation; GA, great arteries; 4-CV, four-chamber view; Outfl. tr., Outflow tracts; P. valve reg., Pulmonary valve regurgitation; Pericardial, pericardial; Ao, Aorta; idem (id), identical; N/A, non-available; SUA, single umbilical artery; Alob, alobar; cl. lip, cleft lip.

Of the 3238 first-trimester fetal hearts that were interpreted as ‘normal’ by moderately experienced obstetricians, second-trimester fetal echocardiography was indicated due to the presence of abnormal NT, DV, or TR, that verified three further minor anomalies (VSD; case #35, 38, and 39) and one major vitium (case #36: aortic stenosis + diffuse endocardial fibroelastosis). In one case, intensive fetal cardiologic observation and follow-up were indicated due to a positive family history; however, neither first- nor second-trimester screening found any abnormality. In the third trimester, however, multiple rhabdomyomas were detected (case #37).

### 3.2. Outcomes of Pregnancies

Of the 3270 followed fetuses, 3191 (97.6%) were born, while 79 fetuses (2.4%) were either not born or died early. Perinatal mortality was observed in 8 cases as a result of infection or for reasons that remain unclear. Major CHD was not detected in this cohort of patients. Spontaneous abortion occurred in 18 cases (0.5%) during the mid-trimester; there were no cases of major CHD in this group of patients, and first-trimester cardiac screening was negative for all of these cases. A total of 53 pregnancies (1.6%) were terminated for a genetic indication, of which 29 were found to have CHD (Table 3).

**Table 3.** Outcome of pregnancy in the follow-up period.

Number of Pregnancies Followed	n = 3270
Live births	3191 (97.6%)
Pregnancy losses	79 (2.4%)
Perinatal deaths (intrauterine demise + neonatal death)	8 (0.2%)

### 3.3. Postnatal Diagnoses

A total of 13 newly diagnosed minor cardiac anomalies were identified in the 3191 newborn infants (of which 10 cases of innocent cardiac murmurs and 2 cases of patent foramen ovale were excluded from the analysis as these are not considered cardiac anomalies, Table 4). In case #30, at one year of age, a pediatric cardiologic examination diagnosed a major cardiac malformation (complex pulmonary atresia, Table 3). In this particular case, the initial first-trimester cardiac scan showed a normal appearance of the four-chamber view and that of ventricular outflow tracts; however, the presence of isolated pericardial fluid was detected. Unfortunately, the pregnant patient did not attend the scheduled fetal echocardiography or the routine second and third-trimester obstetric ultrasound screenings.

**Table 4.** Postnatally recognized cardiac findings.

Type of Cardiac Anomaly	Number of Fetuses
Ventricular septal defect (2–5 mm)	8
Atrial septal defect II	3
Aortic valve stenosis min. grade	1
Bicuspidal aortic valve + PFO	1
Complex pulmonary atresia	1
TOTAL	14
(PFO + innocent cardiac murmurs)	(2 + 10)

Abbreviation: PFO: patent foramen ovale.

In case #32 (minor inlet VSD), second-trimester fetal echocardiography revealed that minor cardiac anomalies suspected prenatally at first-trimester screening were found to be negative, confirming a normal neonatal heart. In case #28, second-trimester fetal echocardiography augmented the diagnosis of first-trimester septal fibrotic area with VSD, and that finding was only supported partially after birth (the VSD was subsequently proved to be closed). In case #39, the initial first-trimester cardiac scan displayed a normal fetal heart, while abnormal NT was 3.3 mm, and non-invasive prenatal testing (NIPT) was negative. However, second-trimester fetal echocardiography detected a small VSD that was confirmed to be closed after birth. In the other two minor fetal cardiac anomalies diagnosed at the second-trimester fetal echocardiography, postnatal cardiac evaluation confirmed the prenatal diagnoses.

In summary, 49 (1.49%) cardiac abnormalities were observed in the 3270 fetuses followed. Thirteen new cardiac abnormalities (28.6%) were first discovered postnatally (1 major and 13 minor defects), while 35 (71.4%) of the 49 cardiac anomalies were diagnosed prenatally (27 major and 8 minor defects).

Of the four small VSDs diagnosed prenatally, only two cases were confirmed postnatally, supporting the possibility of spontaneous intrauterine closure (healing) of minor fetal cardiac septal defects.

Of the fetuses followed, 96.4% of major CHD (27 of 28) were diagnosed prenatally by moderately experienced obstetricians in collaboration with a pediatric cardiology specialist, and 89.2% of them (25 of 28) were already diagnosed (or at least highly suspected) at first-trimester screening and subsequent fetal echocardiography.

In the first year of the five-year study period (2010), our objective was to visualize and store as many clear planes of the first-trimester fetal heart as possible; therefore, our reports



were limited to fragments of a complete cardiac examination panel, including only a true four-chamber view plane. Of the 282 first-trimester cardiac scans conducted, only one abnormal fetal heart with an atrio-ventricular septal defect (AVSD) and one case of aortic stenosis were diagnosed in the second trimester (Table 1). During the 2011–2012 (already followed) study period, 11 major cardiac defects were identified from a significantly larger group of examinations ( $n = 1458$ ), and 9 of them were picked up at the first-trimester scan. In one of the two cases where CHD was not identified (case #36, aortic atresia, left ventricle >> right ventricle, fibrosis, see Table 2), the four-chamber view (at later offline analysis the aorta appeared slightly narrower) at first-trimester scan appeared to be normal and the patient had a high risk for trisomy 21 (1:4); both were both ruled out at subsequent chorionic villous sampling (CVS). At the 18-week scan, a definitive diagnosis of fetal aortic atresia was established. The second undiagnosed cardiac vitium (detailed in the ‘results’ section) was only detected after birth (complex pulmonary atresia, case #36, see Table 2).

Of the 9 diagnosed first-trimester major cardiac defects, detailed fetal echocardiography led to the diagnosis of Down’s syndrome in two cases (case #1: AVSD and case #29: hypoplastic left heart syndrome, HLHS). In cases #2, 4, 5, and 7, fetal cardiac anomalies were identified with an NT value within the normal range and the karyotype was also normal. In one case (case #2), assessment of the situs and the four-chamber view led us to the final diagnosis of AVSD combined with heterotaxy (see Table 2). During the second half of the study (2013–2014), all major cardiac defects were identified at first-trimester screening, with the exception of one case of fetal rhabdomyoma (Table 1).

#### 4. Discussion

The clinical data of unselected consecutive pregnant women screened at our center indicate that the examined population should be considered to have an intermediate-risk profile with respect to maternal age. No statistically significant difference was observed in terms of maternal age between the entire study population and the group of pregnancies affected by major fetal CHD. In contrast, the incidence of major fetal CHD was significantly higher for the subset of women aged > 35 years.

This phenomenon highlights the increased incidence of congenital malformations, including CHD associated with advanced maternal age and chromosomal abnormalities [42,43]. The present study demonstrated that an abnormal fetal karyotype was present in 24% of cases (9/37). It is important to note that older maternal age is a significant contributing factor to fetal heart development defects. Both fetal and maternal complications increase significantly with a maternal age of 35 years during pregnancy. A maternal age of greater than 35 years has recently been associated with subclinical myocardial dysfunction [44] and several obstetrical complications (gestational diabetes, gestational hypertension, pre-eclampsia) [45–47].

On the other hand, a typical tendency in Hungary over the last decade is that older pregnant women with better socio-economic status prefer to undergo high-standard screening and diagnostic obstetric examinations in well-equipped specialized private obstetric clinics (with well-trained specialists) leading to a very high detection rate of various fetal pathologies. Last but not least, primary care obstetricians tend to refer their high-risk patients immediately and directly to these perinatal centers.

According to the meta-analysis, the detection rate of congenital cardiac defects increases by up to 23% [28,48]. The newly formed high-risk group of routinely screened fetuses with NT-values above the 99th percentile (cut-off > 3.5 mm) was detected. Many studies have proved that other markers for first-trimester screening for aneuploidies, such as TR and DV, are useful for screening for congenital cardiac defects. The combination of NT measurement with TR and DV blood flow assessment reaches a detection rate of 48% for major congenital cardiac defects in the first trimester [49,50].

The NT, DV, and TR measurements of our study support the data that these novel cardiac markers (NT, TR, and DV), introduced in extended first-trimester screening, can significantly narrow and refine the cohort of pregnant patients at risk for CHD beyond

those at high baseline risk with classic indications. Nevertheless, the routine clinical use of NT, DV, and TR alone will not result in the detection of the vast majority of congenital cardiac defects [28,48,50,51]. To achieve this, it is essential that a structural evaluation of the fetal heart be performed in both maternal age-related and abnormal NT-, TR-, and DV-related risk pregnancy groups, as well as in the group of pregnant women at high baseline risk for CHD with classic indications.

The examinations were conducted using state-of-the-art ultrasound equipment; however, instead of high-frequency linear probes designed specifically for cardiac scanning, we used medium-frequency and resolution convex abdominal transducers with wide view-angle and greater tissue depth penetration, suitable for complete first-trimester ultrasound screening. Due to the limited maneuverability of transvaginal ultrasound probes, this approach was rarely used, mostly in cases with a retroflected uterus. Our experience supports the observation that optimal visualization is not dependent solely on body mass index (BMI) but rather on transducer-fetal heart distance, which is influenced by BMI, uterine, placental, and fetal position [28,31,32,34,52]. The extended first-trimester screening examinations were performed by three obstetricians, who had 4 to 8 years of mid-level sonographic experience in fetal diagnostics (mainly second-trimester), one-year FMF-TR/DV audit at the beginning of the study (2010), and little experience in assessing healthy and abnormal fetal heart. At the beginning of the study period, inexperience was offset by the time dedicated to the examination; some cases were analyzed offline for 3 to 4 h. Later on, a highly-qualified sonographer joined our team and her excellent overall performance in the pre-screening allowed the obstetricians to focus on the evaluation of pathologic findings and, subsequently, the total examination time was reduced to 20–30 min. A pre-screening ultrasound by a sonographer should always be followed by post-screening performed by an obstetrician preferably using check-lists to ensure continuous quality control.

Previously, our pediatric cardiologist was used to performing echos on fetuses over 16 weeks, but thanks to her openness, she became more and more comfortable with first-trimester ultrasounds. By the end of the study period, fetal hearts interpreted as ‘abnormal’ by moderately experienced obstetricians were rescanned by the pediatric cardiologist and pregnant mothers received a detailed fetal cardiologic second opinion within 24 h, significantly reducing their psychological distress.

Case #36 supports the novel findings that the progression of CHD may be intense, especially up to the 20th week of pregnancy.

In the initial period of the learning curve (2010–2012), the typical and common features of the nine cases of CHD detected in the first trimester were an abnormal four-chamber view and failure to demonstrate the involvement of the great vessels in the cardiac defect. (A limitation of each study, including ours, which addresses the prenatal sonographic assessment of abnormal hearts, is that subsequent histopathological evaluation of the first-trimester fetal heart is not feasible in the majority of cases). Although the assessment of outflow tracts did not contribute to the diagnosis of CHD, we believe that it was nevertheless an invaluable experience. The long timeframe available for extended first-trimester screening resulted in significantly enhanced proficiency in delicate transducer movements and empirical learning.

Table 1 shows that during the second half (2013–2014) of our study, first-trimester abnormal great-vessel diagnoses were also observed (Tetralogy of Fallot, Transposition of the Great Arteries).

## 5. Conclusions

According to our research, if appropriate equipment, quality control, and motivation are in place, the effectiveness of first-trimester fetal cardiovascular ultrasound screening by moderately experienced obstetricians in an unselected (so-called “routine”) pregnant population may reach 90% in terms of major congenital heart defects.

Our data demonstrate that early fetal echocardiography not only provides reassurance to the majority of pregnant women with regard to the absence of cardiac anomalies, as

the most common congenital birth defect, but also significantly contributes to the early diagnosis of chromosomal abnormalities. The majority of cases in which fetal cardiac anomalies were detected are usually so complex and severe that they allow couples to opt for an early termination of their pregnancies and thus decrease maternal general medical risks and the psychological burden of second-trimester elective termination.

The use of first-trimester cardiac markers (NT, TR, and DV) may draw our attention to serious complex structural heart defects and may also help in the detection of minor and major fetal cardiac anomalies that are only visualized at second-trimester screening. Subsequently, it may provide an opportunity to improve neonatal morbidity and mortality as a result of prior organization of intensive perinatal cardiac care.

Second-opinion fetal echocardiography, performed by pediatric cardiology specialists to re-assess suspected cardiac anomalies by moderately experienced obstetricians, is crucial as correction and/or augmentation of established diagnoses will help genetic counselors and couples to better understand the severity, complexity, and prognosis of the condition.

The immediate availability of a pediatric cardiologist can significantly reduce the psychological stress that parents experience as a result of the diagnostic uncertainty of the obstetricians.

In our study, we presented a 5-year learning curve, at the conclusion of which we had performed a high case number of nearly 4800 first-trimester fetal cardiac scans, identified over 40 fetal cardiac anomalies, and significantly enhanced proficiency among physicians in visualizing and assessing both four-chamber view- and outflow tract-planes, as well as large vessel relations of the 11 to 13-week fetal heart.

It may be reasonably assumed that an experienced obstetrician-sonographer performs at least 1300 first-trimester aneuploidy and cardiovascular screens annually. Consequently, in a country like Hungary, only 10–15% of moderately and highly experienced obstetrician-sonographers would require specialized training to enable them to perform detailed early fetal echocardiography, thereby ensuring that every pregnant Hungarian woman has access to this service. Provided that a structured high-quality training program is made available, this could be achieved in a shorter time span than our learning curve, and thus first-trimester fetal echocardiography might become part of routine first-trimester screening.

**Author Contributions:** Conceptualization, T.E. and S.V.; methodology, T.E.; validation, T.E., S.V., P.M. and M.T.; formal analysis, T.E., S.V., P.M. and M.T.; investigation, T.E., G.C., K.K., L.M., G.K., A.H., M.V., M.T., P.M. and S.V.; resources, S.V.; data curation, T.E., G.C., K.K., L.M., G.K., A.H., M.V., M.T., P.M. and S.V.; writing—original draft preparation, T.E., G.C., K.K., L.M., G.K., A.H., M.V., M.T., P.M. and S.V.; writing—review and editing, T.E., G.C., K.K., L.M., G.K., A.H., M.V., M.T., P.M. and S.V.; visualization, T.E. and P.M.; supervision, S.V., M.T. and P.M.; project administration, T.E., P.M. and M.T.; funding acquisition, M.T. and S.V. All authors have read and agreed to the published version of the manuscript.

**Funding:** This research was funded by the Semmelweis Science and Innovation Found (STIA-OTKA-2021 for S.V.) and the Hungarian Hypertension Society (for S.V., M.T.).

**Institutional Review Board Statement:** Our study was approved by the Scientific and Investigational-Ethical Committee of the Hungarian Medical Scientific Council (2013/EKU (588/2013)).

**Informed Consent Statement:** Informed consent was obtained from all subjects involved in the study.

**Data Availability Statement:** The published article contains all generated and analyzed data from this series.

**Conflicts of Interest:** The authors declare no conflicts of interest.

## References

1. Hoffman, J.I.; Kaplan, S. The incidence of congenital heart disease. *J. Am. Coll. Cardiol.* **2002**, *39*, 1890–1900. [CrossRef] [PubMed]
2. Yates, R.S. The influence of prenatal diagnosis on postnatal outcome in patients with structural congenital heart disease. *Prenat. Diagn.* **2004**, *24*, 1143–1149. [CrossRef] [PubMed]

3. Volpe, P.; Paladini, D.; Marasini, M.; Buonadonna, A.L.; Russo, M.G.; Caruso, G.; Marzullo, A.; Vassallo, M.; Martinelli, P.; Gentile, M. Common arterial trunk in the fetus: Characteristics, associations, and outcome in a multicentre series of 23 cases. *Heart* **2003**, *89*, 1437–1441. [CrossRef] [PubMed]
4. Corno, A.F. Introduction to the series: Pre-natal diagnosis in congenital heart defects. *Transl. Pediatr.* **2021**, *10*, 2144–2147. [CrossRef] [PubMed]
5. Bonnet, D.; Coltri, A.; Butera, G.; Fermont, L.; Le Bidois, J.; Kachaner, J.; Sidi, D. Detection of transposition of the great arteries in fetuses reduces neonatal morbidity and mortality. *Circulation* **1999**, *99*, 916–918. [CrossRef]
6. Morris, S.A.; Ethen, M.K.; Penny, D.J.; Canfield, M.A.; Minard, C.G.; Fixler, D.E.; Nembhard, W.N. Prenatal diagnosis, birth location, surgical center, and neonatal mortality in infants with hypoplastic left heart syndrome. *Circulation* **2014**, *129*, 285–292. [CrossRef]
7. Donofrio, M.T.; Levy, R.J.; Schuette, J.J.; Skurow-Todd, K.; Sten, M.B.; Stallings, C.; Pike, J.I.; Krishnan, A.; Ratnayaka, K.; Sinha, P.; et al. Specialized delivery room planning for fetuses with critical congenital heart disease. *Am. J. Cardiol.* **2013**, *111*, 737–747. [CrossRef]
8. Donofrio, M.T. Predicting the Future: Delivery Room Planning of Congenital Heart Disease Diagnosed by Fetal Echocardiography. *Am. J. Perinatol.* **2018**, *35*, 549–552. [CrossRef]
9. Toma, D.; Moldovan, E.; Gozar, L. The Impact of Prenatal Diagnosis in the Evolution of Newborns with Congenital Heart Disease. *J. Crit. Care Med. (Targu Mures)* **2023**, *9*, 6–11. [CrossRef]
10. Ye, B.; Wu, Y.; Chen, J.; Yang, Y.; Niu, J.; Wang, H.; Wang, Y.; Cheng, W. The diagnostic value of the early extended fetal heart examination at 13 to 14 weeks gestational age in a high-risk population. *Transl. Pediatr.* **2021**, *10*, 2907–2920. [CrossRef]
11. Ozyuncu, O.; Tanacan, A.; Fadiloglu, E.; Unal, C.; Ziyadova, G.; Deren, O. Impact of Increased Nuchal Translucency Values on Pregnancy Outcomes: A Tertiary Center Experience. *Fetal Pediatr. Pathol.* **2021**, *40*, 189–197. [CrossRef] [PubMed]
12. Minnella, G.P.; Crupano, F.M.; Syngelaki, A.; Zidere, V.; Akolekar, R.; Nicolaides, K.H. Diagnosis of major heart defects by routine first-trimester ultrasound examination: Association with increased nuchal translucency, tricuspid regurgitation and abnormal flow in ductus venosus. *Ultrasound Obstet. Gynecol.* **2020**, *55*, 637–644. [CrossRef] [PubMed]
13. Mokbel, A.; Attia, D.H.; Zayed, H.S.; Eesa Naem, N.; Mahmoud, G.; Riad, R.; Abou Elewa, S.; Youssef, M.; Haggag, H.; Mohamed, S.S. Pregnancy outcomes among Egyptian women with systemic lupus erythematosus: A prospective cohort study. *Lupus* **2023**, *32*, 521–530. [CrossRef] [PubMed]
14. Ingul, C.B.; Loras, L.; Tegnander, E.; Eik-Nes, S.H.; Brantberg, A. Maternal obesity affects fetal myocardial function as early as in the first trimester. *Ultrasound Obstet. Gynecol.* **2016**, *47*, 433–442. [CrossRef]
15. Pavlicek, J.; Klaskova, E.; Prochazka, M.; Dolezalkova, E.; Matura, D.; Spacek, R.; Simetka, O.; Gruszka, T.; Polanska, S.; Kacerovsky, M. Congenital heart defects according to the types of the risk factors—A single center experience. *J. Matern. Fetal Neonatal Med.* **2019**, *32*, 3606–3611. [CrossRef]
16. Allan, L.D.; Sharland, G.K.; Milburn, A.; Lockhart, S.M.; Groves, A.M.; Anderson, R.H.; Cook, A.C.; Fagg, N.L. Prospective diagnosis of 1,006 consecutive cases of congenital heart disease in the fetus. *J. Am. Coll. Cardiol.* **1994**, *23*, 1452–1458. [CrossRef]
17. Pascal, C.J.; Huggon, I.; Sharland, G.K.; Simpson, J.M. An echocardiographic study of diagnostic accuracy, prediction of surgical approach, and outcome for fetuses diagnosed with discordant ventriculo-arterial connections. *Cardiol. Young* **2007**, *17*, 528–534. [CrossRef]
18. Allan, L.D. Echocardiographic detection of congenital heart disease in the fetus: Present and future. *Br. Heart J.* **1995**, *74*, 103–106. [CrossRef]
19. LeFevre, M.L.; Bain, R.P.; Ewigman, B.G.; Frigoletto, F.D.; Crane, J.P.; McNellis, D. A randomized trial of prenatal ultrasonographic screening: Impact on maternal management and outcome. RADIUS (Routine Antenatal Diagnostic Imaging with Ultrasound) Study Group. *Am. J. Obstet. Gynecol.* **1993**, *169*, 483–489. [CrossRef]
20. McBrien, A.; Sands, A.; Craig, B.; Dornan, J.; Casey, F. Impact of a regional training program in fetal echocardiography for sonographers on the antenatal detection of major congenital heart disease. *Ultrasound Obstet. Gynecol.* **2010**, *36*, 279–284. [CrossRef]
21. Cawyer, C.R.; Kuper, S.G.; Ausbeck, E.; Sinkey, R.G.; Owen, J. The added value of screening fetal echocardiography after normal cardiac views on a detailed ultrasound. *Prenat. Diagn.* **2019**, *39*, 1148–1154. [CrossRef] [PubMed]
22. Bhambhani, A.; Mathew, A.; Varunya, M.; Uligada, S.; Kala, P. Role of routine fetal echocardiography in an unselected group of pregnant women for prenatal detection of cardiac malformations. *Indian Heart J.* **2020**, *72*, 427–430. [CrossRef] [PubMed]
23. Tegnander, E.; Williams, W.; Johansen, O.J.; Blaas, H.G.; Eik-Nes, S.H. Prenatal detection of heart defects in a non-selected population of 30,149 fetuses—detection rates and outcome. *Ultrasound Obstet. Gynecol.* **2006**, *27*, 252–265. [CrossRef] [PubMed]
24. Herghelegiu, C.G.; Duta, S.F.; Neacsu, A.; Suci, N.; Veduta, A. Operator experience impact on the evaluation of still images of a first trimester cardiac assessment protocol. *J. Matern. Fetal Neonatal Med.* **2022**, *35*, 1957–1961. [CrossRef] [PubMed]
25. Sun, H.Y. Prenatal diagnosis of congenital heart defects: Echocardiography. *Transl. Pediatr.* **2021**, *10*, 2210–2224. [CrossRef]
26. Perez, M.T.; Bucholz, E.; Asimacopoulos, E.; Ferraro, A.M.; Salem, S.M.; Schauer, J.; Holleman, C.; Sekhvat, S.; Tworetzky, W.; Powell, A.J.; et al. Impact of maternal social vulnerability and timing of prenatal care on outcome of prenatally detected congenital heart disease. *Ultrasound Obstet. Gynecol.* **2022**, *60*, 346–358. [CrossRef]
27. McBrien, A.; Hornberger, L.K. Early fetal echocardiography. *Birth Defects Res.* **2019**, *111*, 370–379. [CrossRef]

28. Makrydimas, G.; Sotiriadis, A.; Ioannidis, J.P. Screening performance of first-trimester nuchal translucency for major cardiac defects: A meta-analysis. *Am. J. Obstet. Gynecol.* **2003**, *189*, 1330–1335. [CrossRef]
29. Karim, J.N.; Bradburn, E.; Roberts, N.; Papageorgiou, A.T.; ACCEPTS Study. First-trimester ultrasound detection of fetal heart anomalies: Systematic review and meta-analysis. *Ultrasound Obstet. Gynecol.* **2022**, *59*, 11–25. [CrossRef]
30. Rustico, M.A.; Benettoni, A.; D'Ottavio, G.; Fischer-Tamaro, L.; Conoscenti, G.C.; Meir, Y.; Natale, R.; Bussani, R.; Mandruzzato, G.P. Early screening for fetal cardiac anomalies by transvaginal echocardiography in an unselected population: The role of operator experience. *Ultrasound Obstet. Gynecol.* **2000**, *16*, 614–619. [CrossRef]
31. Votino, C.; Kacem, Y.; Dobrescu, O.; Dessy, H.; Cos, T.; Foulon, W.; Jani, J. Use of a high-frequency linear transducer and MTI filtered color flow mapping in the assessment of fetal heart anatomy at the routine 11 to 13 + 6-week scan: A randomized trial. *Ultrasound Obstet. Gynecol.* **2012**, *39*, 145–151. [CrossRef] [PubMed]
32. Volpe, P.; De Robertis, V.; Campobasso, G.; Tempesta, A.; Volpe, G.; Rembouskos, G. Diagnosis of congenital heart disease by early and second-trimester fetal echocardiography. *J. Ultrasound Med.* **2012**, *31*, 563–568. [CrossRef] [PubMed]
33. Siljee, J.E.; Knekt, A.C.; Knapen, M.F.; Bekker, M.N.; Visser, G.H.; Schielen, P.C. Positive predictive values for detection of trisomies 21, 18 and 13 and termination of pregnancy rates after referral for advanced maternal age, first trimester combined test or ultrasound abnormalities in a national screening programme (2007–2009). *Prenat. Diagn.* **2014**, *34*, 259–264. [CrossRef] [PubMed]
34. Volpe, P.; Ubaldo, P.; Volpe, N.; Campobasso, G.; De Robertis, V.; Tempesta, A.; Volpe, G.; Rembouskos, G. Fetal cardiac evaluation at 11–14 weeks by experienced obstetricians in a low-risk population. *Prenat. Diagn.* **2011**, *31*, 1054–1061. [CrossRef]
35. Chaemsaihong, P.; Sahota, D.S.; Poon, L.C. First trimester preeclampsia screening and prediction. *Am. J. Obstet. Gynecol.* **2022**, *226*, S1071–S1097 e1072. [CrossRef]
36. Yagel, S.; Cohen, S.M.; Achiron, R. Examination of the fetal heart by five short-axis views: A proposed screening method for comprehensive cardiac evaluation. *Ultrasound Obstet. Gynecol.* **2001**, *17*, 367–369. [CrossRef]
37. Allan, L. Antenatal diagnosis of heart disease. *Heart* **2000**, *83*, 367. [CrossRef]
38. Bull, C. Current and potential impact of fetal diagnosis on prevalence and spectrum of serious congenital heart disease at term in the UK. British Paediatric Cardiac Association. *Lancet* **1999**, *354*, 1242–1247. [CrossRef]
39. The International Society of Ultrasound in Obstetrics & Gynecology; Carvalho, J.S.; Allan, L.D.; Chaoui, R.; Copel, J.A.; DeVore, G.R.; Hecher, K.; Lee, W.; Munoz, H.; Paladini, D.; et al. ISUOG Practice Guidelines (updated): Sonographic screening examination of the fetal heart. *Ultrasound Obstet. Gynecol.* **2013**, *41*, 348–359. [CrossRef]
40. Garcia Delgado, R.; Garcia Rodriguez, R.; Ortega Cardenes, I.; Gonzalez Martin, J.M.; De Luis Alvarado, M.; Segura Gonzalez, J.; Medina Castellano, M.; Garcia Hernandez, J.A. Feasibility and Accuracy of Early Fetal Echocardiography Performed at 13(+0)–13(+6) Weeks in a Population with Low and High Body Mass Index: A Prospective Study. *Reprod. Sci.* **2021**, *28*, 2270–2277. [CrossRef]
41. van Nisselrooij, A.E.L.; Teunissen, A.K.K.; Clur, S.A.; Rozendaal, L.; Pajkrt, E.; Linskens, I.H.; Rammeloo, L.; van Lith, J.M.M.; Blom, N.A.; Haak, M.C. Why are congenital heart defects being missed? *Ultrasound Obstet. Gynecol.* **2020**, *55*, 747–757. [CrossRef] [PubMed]
42. Best, K.E.; Rankin, J. Is advanced maternal age a risk factor for congenital heart disease? *Birth Defects Res. A Clin. Mol. Teratol.* **2016**, *106*, 461–467. [CrossRef] [PubMed]
43. Miller, A.; Riehle-Colarusso, T.; Siffel, C.; Frias, J.L.; Correa, A. Maternal age and prevalence of isolated congenital heart defects in an urban area of the United States. *Am. J. Med. Genet. A* **2011**, *155A*, 2137–2145. [CrossRef] [PubMed]
44. Sonaglioni, A.; Nicolosi, G.L.; Migliori, C.; Bianchi, S.; Lombardo, M. Usefulness of second trimester left ventricular global longitudinal strain for predicting adverse maternal outcome in pregnant women aged 35 years or older. *Int. J. Cardiovasc. Imaging* **2022**, *38*, 1061–1075. [CrossRef] [PubMed]
45. Lean, S.C.; Derricott, H.; Jones, R.L.; Heazell, A.E.P. Advanced maternal age and adverse pregnancy outcomes: A systematic review and meta-analysis. *PLoS ONE* **2017**, *12*, e0186287. [CrossRef]
46. Sheen, J.J.; Wright, J.D.; Goffman, D.; Kern-Goldberger, A.R.; Booker, W.; Siddiq, Z.; D'Alton, M.E.; Friedman, A.M. Maternal age and risk for adverse outcomes. *Am. J. Obstet. Gynecol.* **2018**, *219*, e391. [CrossRef]
47. Pinheiro, R.L.; Areia, A.L.; Mota Pinto, A.; Donato, H. Advanced Maternal Age: Adverse Outcomes of Pregnancy, A Meta-Analysis. *Acta Med. Port.* **2019**, *32*, 219–226. [CrossRef]
48. Hyett, J.; Perdu, M.; Sharland, G.; Snijders, R.; Nicolaides, K.H. Using fetal nuchal translucency to screen for major congenital cardiac defects at 10–14 weeks of gestation: Population based cohort study. *Bmj* **1999**, *318*, 81–85. [CrossRef]
49. Chelemen, T.; Syngelaki, A.; Maiz, N.; Allan, L.; Nicolaides, K.H. Contribution of ductus venosus Doppler in first-trimester screening for major cardiac defects. *Fetal Diagn. Ther.* **2011**, *29*, 127–134. [CrossRef]
50. Pereira, S.; Ganapathy, R.; Syngelaki, A.; Maiz, N.; Nicolaides, K.H. Contribution of fetal tricuspid regurgitation in first-trimester screening for major cardiac defects. *Obstet. Gynecol.* **2011**, *117*, 1384–1391. [CrossRef]

51. Becker, R.; Wegner, R.D. Detailed screening for fetal anomalies and cardiac defects at the 11–13-week scan. *Ultrasound Obstet. Gynecol.* **2006**, *27*, 613–618. [CrossRef] [PubMed]
52. Persico, N.; Moratalla, J.; Lombardi, C.M.; Zidere, V.; Allan, L.; Nicolaides, K.H. Fetal echocardiography at 11–13 weeks by transabdominal high-frequency ultrasound. *Ultrasound Obstet. Gynecol.* **2011**, *37*, 296–301. [CrossRef] [PubMed]

**Disclaimer/Publisher’s Note:** The statements, opinions and data contained in all publications are solely those of the individual author(s) and contributor(s) and not of MDPI and/or the editor(s). MDPI and/or the editor(s) disclaim responsibility for any injury to people or property resulting from any ideas, methods, instructions or products referred to in the content.

Article

# Assessment of Placental Antioxidant Defense Markers in Vaccinated and Unvaccinated COVID-19 Third-Trimester Pregnancies

Alessandro Rolfo <sup>1,\*</sup>, Stefano Cosma <sup>2</sup>, Anna Maria Nuzzo <sup>1</sup>, Laura Moretti <sup>1</sup>, Annalisa Tancredi <sup>2</sup>, Stefano Canosa <sup>2</sup>, Alberto Revelli <sup>1</sup> and Chiara Benedetto <sup>2</sup>

<sup>1</sup> Department of Surgical Sciences, Gynecology and Obstetrics 2, City of Health and Science—S. Anna University Hospital, University of Turin, 10126 Turin, Italy; a.nuzzo@unito.it (A.M.N.); l.moretti@unito.it (L.M.); alberto.revelli@unito.it (A.R.)

<sup>2</sup> Department of Surgical Sciences, Gynecology and Obstetrics 1, City of Health and Science—S. Anna University Hospital, University of Turin, 10126 Turin, Italy; stefano.cosma@unito.it (S.C.); annalisa.tancredi@unito.it (A.T.); s.canosa88@gmail.com (S.C.); chiara.benedetto@unito.it (C.B.)

\* Correspondence: alessandro.rolfo@unito.it; Tel.: +39-011-6707804

**Abstract:** Background: Pregnancy has been identified as a risk factor for severe COVID-19, leading to maternal and neonatal complications. The safety and effects of the SARS-CoV-2 vaccination during pregnancy, particularly on placental function and oxidative stress (OxS), remain underexplored. We investigated the impact of vaccination on third-trimester placental antioxidant defense markers. Methods: Ninety full-term pregnant women were divided into the following groups: vaccinated (n = 27) and unvaccinated (n = 25) COVID-19-positive pregnant women; control subgroups were composed of vaccinated (n = 19) or unvaccinated (n = 19) COVID-19-negative women with a healthy term singleton pregnancy with no signs of COVID-19. Placental samples were collected after delivery. Lipid peroxidation (TBARS), gene expression of HIF-1 $\alpha$ , and catalase (CAT), superoxide dismutase-1 (SOD1) and CAT-SOD1 enzymatic activity were measured. Results: COVID-19-positive placentae exhibited significantly higher TBARS and HIF-1 $\alpha$  levels compared to controls, regardless of vaccination status. Vaccination significantly increased placental CAT and SOD1 expression and activity in COVID-19-positive women, suggesting enhanced antioxidant defense. Unvaccinated women showed a higher incidence of COVID-19 symptoms and lower antioxidant enzyme activity. Conclusions: SARS-CoV-2 infection induced placental OxS, which is countered by a placental adaptive antioxidant response. Vaccination during pregnancy enhances placental defense, further supporting the safety and benefits of COVID-19 vaccination in preventing complications and protecting fetal development.

**Keywords:** COVID-19; SARS-CoV-2 vaccination; pregnancy; placenta; oxidative stress

## 1. Introduction

The Coronavirus Disease 2019 (COVID-19) pandemic, with more than six million deaths worldwide, has been a major source of concern over the past years. Pregnancy has been identified as an independent risk factor for severe COVID-19 disease, with implications for both the mother and the fetus [1]. Several studies have demonstrated increased rates of intensive care, invasive ventilation, extracorporeal membrane oxygenation, pre-eclampsia, premature delivery, stillbirth, neonatal and maternal mortality [2,3], that have been observed even in healthy women with no co-morbidities [4].

In late 2020, Severe Acute Respiratory Syndrome Coronavirus 2 (SARS-CoV-2) vaccines were introduced, resulting in a reduction of more than 85% in the risk of developing symptomatic disease and transmitting the virus [5]. Although the vaccines were not tested in pregnancy, the American College of Obstetricians and Gynecologists (ACOG) [6] recommended their use for pregnant women. Pregnancy-specific concerns included the potential effects of vaccination on maternal safety, fetal development and placental physiopathology.

Despite the fact that pregnancy was an exclusion criterion in early SARS-CoV-2 vaccine trials, observational data were quickly collected, demonstrating that the benefits of vaccination outweighed its potential risks, and emphasizing vaccine safety in pregnancy, its protective effect against symptomatic disease, and minimal adverse fetal outcomes [7–10]. Key findings in favor of SARS-CoV-2 vaccine safety were that there were no signs of the mRNA vaccine in the maternal blood, placenta or cord blood at delivery, and that maternal IgM was not detected in the umbilical cord blood following vaccination in pregnancy [11–13], indicating that the vaccine did not cross the placental barrier and did not elicit an immune response in the fetus. As previously demonstrated for pertussis, tetanus, and influenza [14–16], maternal IgG raised by SARS-CoV-2 vaccination crossed the placenta and was found in the umbilical cord blood at birth [11–13,17–20]. Overall, these findings indicated that a direct effect of vaccination on fetal development was unlikely. This was also confirmed by several authors whose studies showed no evidence of an increased risk of preterm birth, small size for gestational age, or stillbirth after SARS-CoV-2 vaccination [7,8,10,21–23]. In line with these data, the European Medicine Agency (EMA) COVID-19 task force (ETF) also reviewed several studies involving approximately 65,000 pregnancies at different stages, failing to find any sign of an increased risk of obstetrical complications, miscarriages, preterm births or adverse fetal effects following SARS-CoV-2 vaccination [24]. In a population-based cohort study conducted to assess neonatal safety following the COVID-19 mRNA vaccination during pregnancy, which included 196,470 newborns in Sweden and Norway, the findings indicated that infants that had pre-natal exposure to vaccination showed statistically lower odds of neonatal intracranial hemorrhage, hypoxic-ischemic encephalopathy and mortality, while there was no significant increase in adverse outcomes [25]. These findings further contribute to the evidence supporting the COVID-19 mRNA vaccine's safety during pregnancy. It must be remembered that SARS-CoV-2 vaccination is specifically endorsed to protect pregnant women from severe illness, and is advised for specific high-risk conditions, like hepatitis and meningococcal disease [26].

While vascular pathological changes associated with COVID-19 infection, such as thrombosis, malperfusion and vasculopathy, have been extensively reported on both maternal and fetal-placental sides [27], a few studies have specifically examined the placental response to SARS-CoV-2 vaccination. Morphological studies have demonstrated that vaccination did not cause placental abnormalities such as intervillitis, trophoblast necrosis, increased fibrin or MPFD (massive perivillous fibrin/fibrinoid deposition), villitis or thrombohematomas [28]. Moreover, correlations between clinical and epidemiologic data and those from placental pathology studies have suggested that a potential (and even likely) mechanism of fetal protection from COVID-19 infection could arise from maternal vaccination, preventing maternal viremia, placental infection and vasculopathy [27,29].

SARS-CoV-2 vaccination efficacy is known to be strictly dependent on the maternal immune response, and several exogenous and endogenous factors can interfere [30]. A relevant role is played by the Oxidative State (OxS), determined by the balance between pro-oxidant and antioxidant factors [30]. In this context, our group recently demonstrated increased OxS markers of TBARS and HIF-1 $\alpha$  in the placenta of women infected with COVID-19 during the third trimester of pregnancy, accompanied by increased placental antioxidant superoxide-dismutase (SOD) and catalase (CAT) enzymatic activity, suggesting a compensatory antioxidant defense adaptation aimed at protecting placental physiology and fetal growth [31]. Our previous findings indicated a placental OxS inhibition in response to COVID-19 that was able to counteract the viral cytotoxic activity. To this regard, however, nothing is known about the effect of SARS-CoV-2 vaccination on the placental response to OxS in pregnant women.

In the present study, we investigated the placental antioxidant asset, involving CAT and SOD enzymes, comparing (a) vaccinated vs. unvaccinated COVID-19-positive women during the third trimester of pregnancy, and (b) vaccinated or unvaccinated COVID-19-positive pregnant women vs. vaccinated or unvaccinated COVID-19-negative pregnant women.



## 2. Materials and Methods

### 2.1. Study Population and Tissue Collection

A total number of 90 full-term pregnant women were recruited at the Gynecology and Obstetrics 1 and 2 Units, Sant'Anna University Hospital, City of Health and Science, Turin (Italy), between 1 January and 31 March 2022. Fifty-two of them were identified as positive for COVID-19 with a nasopharyngeal swab, with the virus detected by a reverse transcriptase-polymerase chain reaction (RT-PCR) assay (Liferiver Bio-Tech, San Diego, CA, USA). These 52 COVID-19-positive pregnant women were divided into two subgroups: vaccinated (v-COVID-19;  $n = 27$ ), who received at least 1 dose of the SARS-CoV-2 mRNA vaccine (Pfizer-BioNTech, Collegeville, PA, USA; or ModernaTX, Cambridge, MA, USA); and unvaccinated (u-COVID-19;  $n = 25$ ), who did not receive any SARS-CoV-2 vaccine before delivery. The control subgroups were composed of vaccinated (v-CTRL;  $n = 19$ ) or unvaccinated (u-CTRL;  $n = 19$ ) COVID-19-negative women with a healthy term singleton pregnancy, with no signs of maternal, placental or fetal COVID-19 disease.

After delivery, four full-thickness biopsies were randomly collected from the placental basal plate (intermediate area) and immediately frozen. Calcified, necrotic and seriously damaged areas were excluded. The samples were subsequently processed for mRNA and protein isolation. Maternal anamnesis and neonatal outcome data were recorded.

### 2.2. Assessment of OxS Markers

Since ROS are highly reactive and have a very short half-life, their direct detection in tissue and body fluids with accuracy and precision is unfeasible [32]. Alternatively, a valid method to detect OxS in biological samples is to investigate ROS-mediated oxidative damage to cell lipids, proteins and nucleic acids [33]. Herein, placenta plasma membrane lipid peroxidation was estimated by determining the Thiobarbituric Acid Reactive Substances (TBARS) using a TBARS Assay Kit (Cayman chemical, Ann Arbor, MI, USA). Absorbance was measured at 535 nm on a microplate reader and TBARS values were calculated using a Malondialdehyde (MDA) standard curve, prepared by acid hydrolysis of 1,1,3,3-tetramethoxypropane. The values were expressed as MDA  $\mu\text{M}$ .

### 2.3. Placental RNA Isolation and Real-Time PCR

TRI<sup>®</sup> reagent (Sigma-Aldrich, Milan, Italy) was used to isolate total placental RNA from frozen biopsies following the manufacturer's instructions. DNase I was used to remove genomic DNA contaminations. 3  $\mu\text{g}$  of total RNA was reverse-transcribed using a random hexamers approach (Fermentas Europe, St. Leon-Rot, Germany, Cat. No k1632). Hypoxia-Inducible Factor-1 $\alpha$  (HIF-1 $\alpha$ ), CAT, and SOD1 gene expression levels were determined by real-time PCR using specific TaqMan primers and probes (Life Technologies, Carlsbad, CA, USA, Cat. No 4331182). Ribosomal 18S RNA expression was used as an internal reference (Life Technologies, Cat. No 4333760F) and relative expression was calculated according to Livak and Schmittgen [34].

### 2.4. CAT and SOD Enzymatic Activity

Placental CAT and SOD enzymatic activity were assessed using commercially available kits (Cayman Chemical, Ann Arbor, MI, USA). In brief, CAT peroxidative function was measured based on the reaction between CAT and methanol in the presence of hydrogen peroxide of optimal concentration. 4-amino-3-hydrazino-5-mercapto-1,2,4-triazole was used to spectrophotometrically quantify formaldehyde at 540 nm. The results were expressed in nmol/min/mL. Total SOD activity was measured with cytochrome C reduction by superoxide ( $\text{O}_2^{\bullet-}$ ) radicals monitored spectrophotometrically at 450 nm, using the xanthine-xanthine oxidase system. The results were expressed in U/mL.

### 2.5. Statistical Analysis

As the data did not show a normal distribution, the Kruskal–Wallis non-parametric test and the Mann–Whitney U-test with Bonferroni's correction were performed. The data

are presented as Mean  $\pm$  SE (standard error). The categorical variables are presented as percentages; the comparison between groups was performed using a chi-square test.

SPSS Version 29 statistical software (IBM Corp., Chicago, IL, USA) was used for statistical analysis. The significance was set at  $p < 0.05$ .

### 3. Results

#### 3.1. Clinical Features of the Study Population

A total of 52 pregnant women tested positive for COVID-19 infection at delivery; among them, 27 were included in the v-COVID-19 subgroup as they received at least one dose of a SARS-CoV-2 mRNA vaccine; only 8 of them (29.6%) completed the vaccination course of three doses, while 16 (59.2%) received two doses and 3 (11.1%) received one dose. The average time between the last dose of the SARS-CoV-2 vaccine and delivery was  $103.1 \pm 18.6$  days (range 14–377 days), and 83.3% of the v-COVID-19 patients received the last dose during pregnancy. The other 25 COVID-19-positive patients were included in the u-COVID-19 subgroup, as they did not receive any SARS-CoV-2 vaccine.

The control (CTRL) subgroups were composed of 38 pregnant women who tested negative for COVID-19 infection at delivery; they were categorized as vaccinated (v-CTRL;  $n = 19$ ) or unvaccinated (u-CTRL;  $n = 19$ ). In the v-CTRL group, 10 (52.6%) completed the vaccination course, 8 (42.1%) received two SARS-CoV-2 vaccine doses and 5.3% received only one dose.

The clinical features of the study population are presented in Table 1. Maternal age, gestational age at delivery, nulliparous percentage and cesarean section rate were comparable among groups. Pre-pregnancy co-morbidity did not significantly differ among the subgroups, nor was the rate of obstetrical complications significantly different. The COVID-19-positive groups presented no stillbirths and they did not require neonatal respiratory support within 24 h of birth. Among the COVID-19-positive women, symptoms like fever and anosmia, ageusia and asthenia were more frequently observed in unvaccinated women (32% and 16%, respectively) than in vaccinated women (7.4% and 0%, respectively).

**Table 1.** Clinical features of vaccinated and unvaccinated COVID-19-positive women and of COVID-19-negative control subgroups. Values are expressed as median  $\pm$  SE or percentage. Significant differences ( $p < 0.05$ ): \* significant compared with v-CTRL; ^ significant compared with u-CTRL; § significant compared with v-COVID-19; ° significant compared with u-COVID-19.

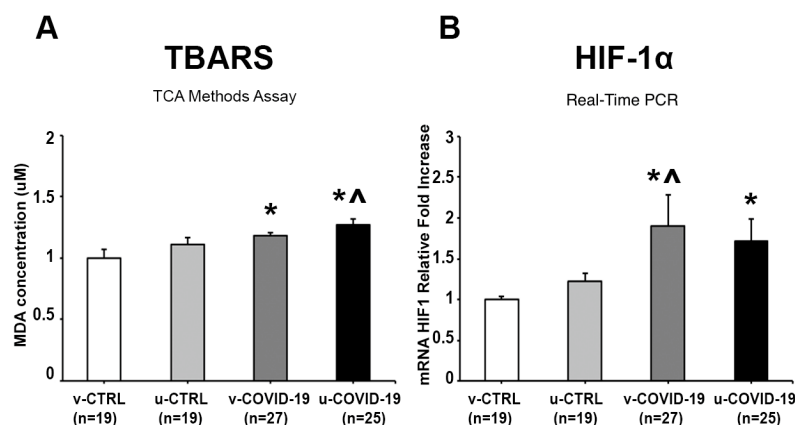
	v-CTRL (n = 19)	u-CTRL (n = 19)	v-COVID-19 (n = 27)	u-COVID-19 (n = 25)	p Value
Nulliparous (%)	42.1 (n = 8)	26.3 (n = 5)	33.3 (n = 9)	32 (n = 8)	$p > 0.05$
Maternal age at delivery (years)	$35.3 \pm 1$	$34.1 \pm 1.3$	$32.8 \pm 0.7$	$31.4 \pm 1.4$	$p > 0.05$
Gestational age at delivery (weeks)	$37.5 \pm 0.8$	$38.6 \pm 0.3$	$38.8 \pm 0.5$	$39 \pm 0.3$	$p > 0.05$
One vaccine dose (%)	5.3 (n = 1)	0	11.1 (n = 3)	0	$p > 0.05$
Two vaccine doses (%)	42.1 (n = 8)	0 *	59.2 (n = 16) *^	0 §	*§ $p < 0.001$
Three vaccine doses (%)	52.6 (n = 10)	0 *	29.6 (n = 8) ^	0 *§	* $p < 0.001$ ^ $p = 0.009$ § $p = 0.003$
<b>Pre-Pregnancy co-morbidity:</b>					
Autoimmune disease (%)	10.5 (n = 2)	10.5 (n = 2)	11.1 (n = 3)	12 (n = 3)	$p > 0.05$
Thyroid dysfunction (%)	5.3 (n = 1)	0	3.7 (n = 1)	8 (n = 2)	$p > 0.05$
Uterine myoma (%)	26.3 (n = 5)	5.3 (n = 1)	3.7 (n = 1)	8 (n = 2)	$p > 0.05$
BMI >30 (%)	0	21 (n = 4)	14.8 (n = 4)	24 (n = 6)	$p > 0.05$

Table 1. Cont.

	v-CTRL (n = 19)	u-CTRL (n = 19)	v-COVID-19 (n = 27)	u-COVID-19 (n = 25)	p Value
<b>Pregnancy complications:</b>					
Gestational Hypertension (%)	5.3 (n = 1)	5.3 (n = 1)	7.4 (n = 2)	0	$p > 0.05$
IUGR (%)	5.3 (n = 1)	0	0	0	$p > 0.05$
PE (%)	5.3 (n = 1)	0	0	0	$p > 0.05$
Preterm birth (%)	26.3 (n = 5)	10.5 (n = 2)	3.7 (n = 1)	8 (n = 2)	$p > 0.05$
Cholestasis (%)	0	10.5 (n = 2)	0	8 (n = 2)	$p > 0.05$
GDM (%)	21 (n = 4)	15.8 (n = 3)	18.5 (n = 5)	20 (n = 5)	$p > 0.05$
<b>SARS-CoV-2 symptoms:</b>					
Dyspnea (%)	0	0	7.4 (n = 2)	0	$p > 0.05$
Fever (%)	0	0	7.4 (n = 2)	32 (n = 8) * <sup>§</sup>	* <sup>^</sup> $p = 0.006$ ; <sup>§</sup> $p = 0.025$
Anosmia/Ageusia/Asthenia(%)	0	0	0	16 (n = 4) <sup>°</sup>	<sup>°</sup> $p = 0.031$
Cough (%)	0	0	11.1 (n = 3)	12 (n = 3)	$p > 0.05$
Rhinitis (%)	0	0	3.7 (n = 1)	16 (n = 4)	$p > 0.05$
<b>Obstetrics and Neonatal outcomes:</b>					
Pathological Doppler (%)	0	0	3.7 (n = 1)	4 (n = 1)	$p > 0.05$
Pathological CTG (%)	5.3 (n = 1)	5.3 (n = 1)	14.8 (n = 4)	4 (n = 1)	$p > 0.05$
Fetal Biometry:					
>95th centile (%)	15.8 (n = 3)	15.8 (n = 3)	22.2 (n = 6)	20 (n = 5)	$p > 0.05$
<5th centile (%)	5.3 (n = 1)	5.3 (n = 1)	3.7 (n = 1)	0	$p > 0.05$
Caesarean section (%)	52.6 (n = 10)	31.6 (n = 6)	63 (n = 17)	52 (n = 13)	$p > 0.05$
Birth weight (g)	2975 ± 151	3152.6 ± 75	3259.2 ± 124.8	3277 ± 96.5	$p > 0.05$
Placental weight (g)	545.8 ± 22.8	594.6 ± 22.1	535 ± 29.4	576.7 ± 24.1	$p > 0.05$
APGAR < 7 at 5 min (%)	0	0	3.7 (n = 1)	0	$p > 0.05$
Female fetus (%)	57.9 (n = 11)	31.6 (n = 6)	66.7 (n = 18) <sup>^</sup>	32 (n = 8) <sup>§</sup>	<sup>^</sup> $p = 0.019$ ; <sup>§</sup> $p = 0.012$
Male fetus (%)	42.1 (n = 8)	68.4 (n = 13)	33.3 (n = 9) <sup>^</sup>	68 (n = 17) <sup>§</sup>	<sup>^</sup> $p = 0.019$ ; <sup>§</sup> $p = 0.012$

### 3.2. OxS Markers TBARS and HIF-1 $\alpha$ in v-COVID-19 and u-COVID-19 Placentae

We found a significant TBARS increase in the v-COVID-19 ( $p = 0.05$ , 1.2-fold increase) and u-COVID-19 ( $p = 0.01$ , 1.3-fold increase) placentae compared to the v-CTRL subgroup, and in the u-COVID-19 vs. u-CTRL placentae ( $p = 0.05$ , 1.14-fold increase) (Figure 1A). No significant differences were reported between the v-COVID-19 and u-COVID-19 subgroups ( $p > 0.05$ ) (Figure 1A). Overall, these findings suggested the presence of a significantly increased placental OxS linked to COVID-19 infection.



**Figure 1.** Effects of COVID-19 infection on oxidative stress markers in the placentae of the v-COVID-19, u-COVID-19, v-CTRL and u-CTRL subgroups: (A) TBARS and (B) HIF-1 $\alpha$  gene expression. \* significant vs. v-CTRL; ^ significant vs. u-CTRL.

The gene expression level of hypoxia-inducible factors-1 $\alpha$  (HIF-1 $\alpha$ ), a main player in the cellular response to hypoxia and OxS, was significantly increased in the v-COVID-19 ( $p = 0.04$ , 1.9-fold increase) and u-COVID-19 ( $p = 0.019$ , 1.2-fold increase) placentae compared to the v-CTRL subgroup (Figure 1B), and in the v-COVID-19 subgroup relative to the u-CTRL subgroup ( $p = 0.02$ , 1.6-fold increase) (Figure 1B). No significant differences were reported between the v-COVID-19 and u-COVID-19 groups ( $p > 0.05$ ) (Figure 1B).

### 3.3. Evaluation of Placental Antioxidant Markers

Antioxidant enzymes prevent OxS-mediated tissue damage by detoxifying free radicals. SOD1 catalyzes the conversion of the O<sub>2</sub><sup>•−</sup> radical to H<sub>2</sub>O<sub>2</sub>; then, cytosolic CAT transforms H<sub>2</sub>O<sub>2</sub> into water. We reported significantly higher CAT mRNA levels in the placentae of the v-COVID-19 ( $p = 0.009$ , 2.5-fold increase) and u-COVID-19 ( $p = 0.04$ , 1.4-fold increase) subgroups compared to the v-CTRL subgroup (Figure 2A). Moreover, the v-COVID-19 placentae significantly over-expressed the CAT gene in comparison with the u-CTRL placentae ( $p = 0.007$ , 2.4-fold increase). Importantly, a significant increase in placental CAT expression was reported in the v-COVID-19 relative to the u-COVID-19 subgroup ( $p = 0.034$ , 1.5-fold increase). In line with these data, placental CAT enzymatic activity was significantly increased in the v-COVID-19 and u-COVID-19 subgroups compared to the v-CTRL ( $p < 0.001$ , 1.1-fold increase;  $p < 0.001$ , 1.1-fold increase) and u-CTRL subgroups ( $p = 0.002$ , 1.2-fold increase;  $p = 0.001$ , 1.1-fold increase) (Figure 2C). Importantly, CAT enzymatic activity was significantly increased in the v-COVID-19 placentae relative to the u-COVID-19 placentae ( $p = 0.017$ , 1.1-fold increase).

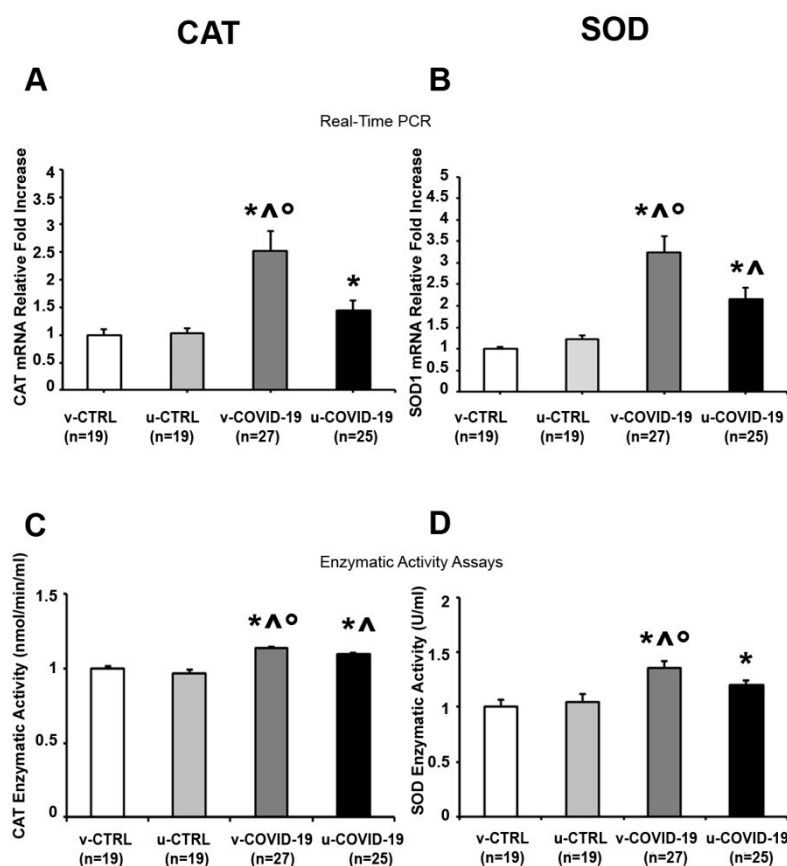


**Figure 2.** Effects of COVID-19 infection on antioxidant defense markers in the placenta from the v-COVID-19, u-COVID-19, v-CTRL and u-CTRL group: (A) mRNA expression and (C) enzymatic activities of CAT, (B) mRNA expression and (D) enzymatic activity of SOD. \* significant effect vs. v-CTRL; ^ significant effect vs. u-CTRL; ° significant effect vs. u-COVID-19.

CAT overexpression was accompanied by a significant increase in SOD1 mRNA levels in v-COVID-19 ( $p < 0.001$ , 3.2-fold increase;  $p = 0.001$ , 2.7-fold increase) and u-COVID-19 ( $p < 0.001$ , 2.1-fold increase;  $p = 0.017$ , 1.8-fold increase) placentae compared to the v-CTRL and u-CTRL subgroups (Figure 2B). Moreover, SOD1 gene expression levels were significantly over-expressed in the v-COVID-19 placentae relative to the u-COVID-19 placentae ( $p = 0.04$ , 1.5-fold increase). SOD1 gene overexpression was accompanied by a significant increase in SOD enzymatic activity in the v-COVID-19 ( $p = 0.007$ , 1.3-fold increase) and u-COVID-19 ( $p = 0.002$ , 1.2-fold increase) subgroups compared to the v-CTRL subgroup (Figure 2D). Moreover, SOD enzymatic activity was significantly increased in the v-COVID-19 placentae relative to the u-CTRL placentae ( $p = 0.001$ , 1.3-fold increase) and, importantly, the u-COVID-19 ( $p = 0.04$ , 1.1-fold increase) subgroup.

#### 4. Discussion

Despite the exclusion of pregnant women from initial phase 3 clinical trials [7], it is now well known that SARS-CoV-2 vaccination is safe in pregnancy and represents the most important intervention to protect gestation from COVID-19-related morbidity and mortality, in the meantime offering protection to the newborn at birth [35]. Most previous studies on the impact of SARS-CoV-2 vaccination during pregnancy, however, have focused on maternal and infant outcomes, without considering the possible effects on the placental tissue. Herein, in order to better understand the consequences of SARS-CoV-2 vaccination on pregnancy and fetal-placental development, we investigated obstetrical and neonatal outcomes together with placental OxS molecular markers and antioxidant activity. In accordance with our previously published data [31], we confirmed a significant increase in both the OxS markers TBARS and HIF-1 $\alpha$  and the antioxidant CAT and SOD1 enzymes in COVID-19-positive placentae compared to COVID-19-negative controls, emphasizing the placental ability to counteract COVID-19-induced OxS during pregnancy. For the first time, we also demonstrated that SARS-CoV-2 vaccination significantly increased the antioxidant enzymes CAT and SOD1 in the placentae of COVID-19-positive patients, eliciting a boost in placental protection against OxS.

From a clinical perspective, we reported herein a significantly increased incidence of COVID-19-related maternal symptoms in unvaccinated vs. vaccinated pregnant women who were positive for the virus at delivery. Our findings are in line with previous data showing that pregnant women who received at least one dose of the vaccine before COVID-19 infection had an 80% lower risk of developing severe symptoms [36]. In our study, the increased incidence of maternal symptoms in unvaccinated COVID-19-positive pregnant women was associated with a lower placental antioxidant defense, suggesting a reduced placental compensatory adaptation despite no significant changes in neonatal birth weight and/or Apgar score. While this study focused on molecular and biochemical markers of oxidative stress, collaboration with a pathologist for a detailed placental histopathological examination could have provided additional insights into potential structural changes or localized effects that might not be evident through molecular markers alone. Future studies incorporating such analyses may help to provide a more comprehensive understanding of placental responses to SARS-CoV-2 infection and vaccination.

Our results are in line with those of Smithgall et al., who also reported no differences in placental anatomopathological findings when comparing the placenta of 164 vaccinated and 267 unvaccinated women [37].

Exacerbated inflammation and OxS have been proposed as key players in COVID-19 pathophysiology [31,38,39]. Indeed, we observed a significant increase in placental lipid peroxidation and HIF-1 $\alpha$  expression in all COVID-19-positive women. COVID-19 infection, in fact, compromises mitochondrial structure and functionality, triggering the production of reactive oxygen species (ROS) [31] as well as an inflammatory response with the release of cytokines as interleukin-10 (IL-10), tumor necrosis factor-alpha (TNF- $\alpha$ ) and interferon-gamma (INF- $\gamma$ ). This inflammatory pathway further reinforces mitochondrial ROS production and OxS [39,40]. Besides being culprits of COVID-19 infection, ROS

production and OxS could also be generated as a consequence of immunization and antibody production by activated B and T immune cells, as suggested by observations of increased ROS levels after the first dose of mRNA-based SARS-CoV-2 vaccines [41].

The first line of defense against OxS consists in the overproduction of the antioxidant enzymes CAT and SOD1, which convert superoxide radicals into hydrogen peroxide and then into water plus molecular oxygen [42]. In the present study, a significant increase in CAT and SOD1 expression and activity was observed in vaccinated COVID-19-positive placentae compared to both unvaccinated and control COVID-19-negative patients. Recently, IgGs carrying CAT activity were found to be significantly increased in non-pregnant patients who had recovered from COVID-19 compared to both healthy women and patients vaccinated with the recombinant Sputnik V vaccine, opening up the hypothesis that COVID-19 infection may stimulate the production of antibodies with enzymatic activity that degrades hydrogen peroxide and counteracts ROS production [43]. The increased CAT expression and activity that we observed in the v-COVID-19 placentae suggests that vaccination further increases the ability to scavenge hydrogen peroxide; this could represent an adaptive response to the immunization, aimed at neutralizing the effect of ROS and preventing membrane lipid peroxidation.

Besides promoting inflammation and oxidative injury, increased ROS levels are able to further stimulate viral replication [44,45]. CAT is the most abundant and effective catalyst for the decomposition of  $H_2O_2$  [46], being able to breakdown 107  $H_2O_2$  molecules in 1 s. Based on this, Qin et al. recently explored the effectiveness of CAT administration as a potential treatment for COVID-19, showing that the administration of nano-encapsulated CAT to Rhesus macaques elicited cytoprotection, increased the viability of HPAEpiC human pulmonary alveolar epithelial cells, down-regulated the leukocyte production of  $TNF-\alpha$  and IL-10, and inhibited COVID-19 replication, without noticeable toxicity [47]. These data underline the therapeutic potential of exogenous CAT administration, further emphasizing the importance of endogenous placental CAT overactivation promoted by anti-SARS-CoV-2 vaccination.

In mice immunized through the administration of recombinant SARS-CoV-2 spike protein antigens, the decline in anti-COVID-19 antibodies caused by OxS and SOD decreased upon virus re-exposure, and the activation of the JAK2/STAT1 pathway was efficiently counteracted by upregulating SOD production [48]. These findings suggest that the vaccination-related boost in placental SOD expression and activity described in our work could also prolong the duration of SARS-CoV-2 immunization.

A recent in vitro study, aimed at investigating the effects of mRNA vaccines encoding for the COVID-19 S protein (mRNA-S) on the fetal–maternal interface, reported that S proteins could interact with ACE-2 receptors, triggering the production of CXCL-10 and CXCL-11 chemokines, IL-6 and IFN-Type 1alpha, molecules that are critical in regulating the immune response in pregnancy. Moreover, the authors observed higher gene expression of the ACE-2 receptor, pivotal for COVID-19 access into host cells [49], in chorionic trophoblast cells compared to other fetal membrane layers [50]. Besides its role in the viral mechanism of infection, ACE-2 activation possesses beneficial downstream effects due to its antioxidant and vasodilatory properties [50]. In accordance with this, our results corroborate these previous findings, adding the placental CAT and SOD enzymatic antioxidant boost to the positive effects of mRNA vaccination during pregnancy.

## 5. Conclusions

In conclusion, our data demonstrate that the placental antioxidant adaptation against COVID-19-induced OxS in placentae is enhanced by the SARS-CoV-2 vaccine, adding further evidence of the role of vaccination as a key and safe tool for the prevention of pregnancy complications.

**Author Contributions:** A.R. (Alessandro Rolfo): study conceptualization and design, coordination of the study, data interpretation, writing—original manuscript, writing—review and editing. S.C. (Stefano Cosma): patient recruitment coordination and sample collection, writing—original

manuscript, writing—review and editing. A.M.N.: experimental procedures, writing—original manuscript, data analysis. L.M., S.C. (Stefano Canosa) and A.T.: patient recruitment, sample collection and processing, data curation. A.R. (Alberto Revelli): supervision, writing—original manuscript. C.B.: project administration, supervision, patient selection and recruitment, writing—review and editing. All authors have read and agreed to the published version of the manuscript.

**Funding:** This research received no external funding.

**Institutional Review Board Statement:** The study was conducted in accordance with the Declaration of Helsinki, and approved by the Institutional Review Board (IRB) of the City of Health and Science of Turin (reference number: 00171/2020).

**Informed Consent Statement:** Written informed consent for placental collection and subsequent analysis was obtained.

**Data Availability Statement:** The raw data supporting the conclusions of this article will be made available by the authors without undue reservation.

**Conflicts of Interest:** The authors declare no conflicts of interest.

## References

1. Pham, A.; Aronoff, D.M.; Thompson, J.L. Maternal COVID-19, vaccination safety in pregnancy, and evidence of protective immunity. *J. Allergy Clin. Immunol.* **2021**, *148*, 728–731. [CrossRef] [PubMed]
2. Allotey, J.; Stallings, E.; Bonet, M.; Yap, M.; Chatterjee, S.; Kew, T.; Debenham, L.; Llavall, A.C.; Dixit, A.; Zhou, D.; et al. Clinical manifestations, risk factors, and maternal and perinatal outcomes of coronavirus disease 2019 in pregnancy: Living systematic review and meta-analysis. *BMJ* **2020**, *370*, m3320. [CrossRef]
3. Marchand, G.; Patil, A.S.; Masoud, A.T.; Ware, K.; King, A.; Ruther, S.; Brazil, G.; Calteux, N.; Ulibarri, H.; Parise, J.; et al. Systematic review and meta-analysis of COVID-19 maternal and neonatal clinical features and pregnancy outcomes up to 3 June 2021. *AJOG Glob. Rep.* **2022**, *2*, 100049. [CrossRef]
4. Sahin, D.; Tanacan, A.; Erol, S.A.; Yucel Yetiskin, F.D.; Besimoglu, B.; Ozden Tokalioglu, E.; Anuk, A.T.; Turgut, E.; Ayhan, S.G.; Turgay, B.; et al. Management of pregnant women with COVID-19: A tertiary pandemic center experience on 1416 cases. *J. Med. Virol.* **2022**, *94*, 1074–1084. [CrossRef] [PubMed]
5. Dagan, N.; Barda, N.; Kepten, E.; Miron, O.; Perchik, S.; Katz, M.A.; Hernán, M.A.; Lipsitch, M.; Reis, B.; Balicer, R.D. BNT162b2 mRNA COVID-19 Vaccine in a Nationwide Mass Vaccination Setting. *N. Engl. J. Med.* **2021**, *384*, 1412–1423. [CrossRef] [PubMed]
6. COVID-19 Vaccination Considerations for Obstetric–Gynecologic Care [Internet]. Available online: <https://www.acog.org/clinical/clinical-guidance/practice-advisory/articles/2020/12/covid-19-vaccination-considerations-for-obstetric-gynecologic-care> (accessed on 18 September 2024).
7. Blakeway, H.; Prasad, S.; Kalafat, E.; Heath, P.T.; Ladhani, S.N.; Le Doare, K.; Magee, L.A.; O'Brien, P.; Rezvani, A.; von Dadelszen, P.; et al. COVID-19 vaccination during pregnancy: Coverage and safety. *Am. J. Obstet. Gynecol.* **2022**, *226*, 236.e1–236.e14. [CrossRef]
8. Theiler, R.N.; Wick, M.; Mehta, R.; Weaver, A.L.; Virk, A.; Swift, M. Pregnancy and birth outcomes after SARS-CoV-2 vaccination in pregnancy. *Am. J. Obstet. Gynecol. MFM* **2021**, *3*, 100467. [CrossRef]
9. Shimabukuro, T.T.; Kim, S.Y.; Myers, T.R.; Moro, P.L.; Oduyebo, T.; Panagiotakopoulos, L.; Marquez, P.L.; Olson, C.K.; Liu, R.; Chang, K.T.; et al. Preliminary Findings of mRNA COVID-19 Vaccine Safety in Pregnant Persons. *N. Engl. J. Med.* **2021**, *384*, 2273–2282. [CrossRef]
10. Wainstock, T.; Yoles, I.; Sergienko, R.; Sheiner, E. Prenatal maternal COVID-19 vaccination and pregnancy outcomes. *Vaccine* **2021**, *39*, 6037–6040. [CrossRef]
11. Mithal, L.B.; Otero, S.; Shanes, E.D.; Goldstein, J.A.; Miller, E.S. Cord blood antibodies following maternal coronavirus disease 2019 vaccination during pregnancy. *Am. J. Obstet. Gynecol.* **2021**, *225*, 192–194. [CrossRef]
12. Prahl, M.; Golan, Y.; Cassidy, A.G.; Matsui, Y.; Li, L.; Alvarenga, B.; Chen, H.; Jigmeddagva, U.; Lin, C.Y.; Gonzalez, V.J.; et al. Evaluation of transplacental transfer of mRNA vaccine products and functional antibodies during pregnancy and infancy. *Nat. Commun.* **2022**, *13*, 4422. [CrossRef] [PubMed]
13. Beharier, O.; Plitman Mayo, R.; Raz, T.; Nahum Sacks, K.; Schreiber, L.; Suissa-Cohen, Y.; Chen, R.; Gomez-Tolub, R.; Hadar, E.; Gabbay-Benziv, R.; et al. Efficient maternal to neonatal transfer of antibodies against SARS-CoV-2 and BNT162b2 mRNA COVID-19 vaccine. *J. Clin. Investig.* **2021**, *131*, e154834. [CrossRef] [PubMed]
14. Schlaudecker, E.P.; Steinhoff, M.C.; Omer, S.B.; McNeal, M.M.; Roy, E.; Arifeen, S.E.; Dodd, C.N.; Raqib, R.; Breiman, R.F.; Zaman, K.; et al. IgA and neutralizing antibodies to influenza A virus in human milk: A randomized trial of antenatal influenza immunization. *PLoS ONE* **2013**, *8*, e70867. [CrossRef] [PubMed]
15. Blencowe, H.; Lawn, J.; Vandelaer, J.; Roper, M.; Cousens, S. Tetanus toxoid immunization to reduce mortality from neonatal tetanus. *Int. J. Epidemiol.* **2010**, *39* (Suppl. S1), i102–i109. [CrossRef]

16. Switzer, C.; D'Heilly, C.; Macina, D. Immunological and Clinical Benefits of Maternal Immunization Against Pertussis: A Systematic Review. *Infect. Dis. Ther.* **2019**, *8*, 499–541. [CrossRef]
17. Shook, L.L.; Atyeo, C.G.; Yonker, L.M.; Fasano, A.; Gray, K.J.; Alter, G.; Edlow, A.G. Durability of Anti-Spike Antibodies in Infants After Maternal COVID-19 Vaccination or Natural Infection. *JAMA* **2022**, *327*, 1087–1089. [CrossRef]
18. Gray, K.J.; Bordt, E.A.; Atyeo, C.; Deriso, E.; Akinwunmi, B.; Young, N.; Baez, A.M.; Shook, L.L.; Cvrk, D.; James, K.; et al. Coronavirus disease 2019 vaccine response in pregnant and lactating women: A cohort study. *Am. J. Obstet. Gynecol.* **2021**, *225*, 303.e1–303.e17. [CrossRef]
19. Collier, A.R.Y.; McMahan, K.; Yu, J.; Tostanoski, L.H.; Aguayo, R.; Ansel, J.; Chandrashekar, A.; Patel, S.; Apraku Bondzie, E.; Sellers, D.; et al. Immunogenicity of COVID-19 mRNA Vaccines in Pregnant and Lactating Women. *JAMA* **2021**, *325*, 2370–2380. [CrossRef]
20. Atyeo, C.G.; Shook, L.L.; Brigida, S.; De Guzman, R.M.; Demidkin, S.; Muir, C.; Akinwunmi, B.; Baez, A.M.; Sheehan, M.L.; McSweeney, E.; et al. Maternal immune response and placental antibody transfer after COVID-19 vaccination across trimester and platforms. *Nat. Commun.* **2022**, *13*, 3571. [CrossRef]
21. Rottenstreich, M.; Sela, H.Y.; Rotem, R.; Kadish, E.; Wiener-Well, Y.; Grisaru-Granovsky, S. COVID-19 vaccination during the third trimester of pregnancy: Rate of vaccination and maternal and neonatal outcomes, a multicentre retrospective cohort study. *BJOG* **2022**, *129*, 248–255. [CrossRef]
22. Fell, D.B.; Dimanlig-Cruz, S.; Regan, A.K.; Häberg, S.E.; Gravel, C.A.; Oakley, L.; Alton, G.D.; Török, E.; Dhinsa, T.; Shah, P.S.; et al. Risk of preterm birth, small for gestational age at birth, and stillbirth after covid-19 vaccination during pregnancy: Population based retrospective cohort study. *BMJ* **2022**, *378*, e071416. [CrossRef] [PubMed]
23. Bookstein Peretz, S.; Regev, N.; Novick, L.; Nachshol, M.; Goffer, E.; Ben-David, A.; Asraf, K.; Doolman, R.; Levin, E.G.; Regev Yochay, G.; et al. Short-term outcome of pregnant women vaccinated with BNT162b2 mRNA COVID-19 vaccine. *Ultrasound Obstet. Gynecol.* **2021**, *58*, 450–456. [CrossRef] [PubMed]
24. COVID-19: Latest Safety Data Provide Reassurance About Use of mRNA Vaccines During Pregnancy | European Medicines Agency (EMA) [Internet]. 2022. Available online: <https://www.ema.europa.eu/en/news/covid-19-latest-safety-data-provide-reassurance-about-use-mrna-vaccines-during-pregnancy> (accessed on 18 September 2024).
25. Norman, M.; Magnus, M.C.; Söderling, J.; Juliusson, P.B.; Navér, L.; Örtqvist, A.K.; Häberg, S.; Stephansson, O. Neonatal Outcomes After COVID-19 Vaccination in Pregnancy. *JAMA* **2024**, *331*, 396–407. [CrossRef]
26. Simionescu, A.A.; Streinu-Cercel, A.; Popescu, F.D.; Stanescu, A.M.A.; Vieru, M.; Danciu, B.M.; Miron, V.D.; Săndulescu, O. Comprehensive Overview of Vaccination during Pregnancy in Europe. *J. Pers. Med.* **2021**, *11*, 1196. [CrossRef]
27. Heeralall, C.; Ibrahim, U.H.; Lazarus, L.; Gathiram, P.; Mackraj, I. The effects of COVID-19 on placental morphology. *Placenta* **2023**, *138*, 88–96. [CrossRef]
28. Shanes, E.D.; Otero, S.; Mithal, L.B.; Mupanomunda, C.A.; Miller, E.S.; Goldstein, J.A. Severe Acute Respiratory Syndrome Coronavirus 2 (SARS-CoV-2) Vaccination in Pregnancy: Measures of Immunity and Placental Histopathology. *Obstet. Gynecol.* **2021**, *138*, 281–283. [CrossRef] [PubMed]
29. Schwartz, D.A. Stillbirth after COVID-19 in Unvaccinated Mothers Can Result from SARS-CoV-2 Placentitis, Placental Insufficiency, and Hypoxic Ischemic Fetal Demise, Not Direct Fetal Infection: Potential Role of Maternal Vaccination in Pregnancy. *Viruses* **2022**, *14*, 458. [CrossRef]
30. Bakadia, B.M.; Boni, B.O.O.; Ahmed, A.A.Q.; Yang, G. The impact of oxidative stress damage induced by the environmental stressors on COVID-19. *Life Sci.* **2021**, *264*, 118653. [CrossRef]
31. Rolfo, A.; Cosma, S.; Nuzzo, A.M.; Salio, C.; Moretti, L.; Sassoè-Pognetto, M.; Carosso, A.R.; Borella, F.; Cutrin, J.C.; Benedetto, C. Increased Placental Anti-Oxidant Response in Asymptomatic and Symptomatic COVID-19 Third-Trimester Pregnancies. *Biomedicines* **2022**, *10*, 634. [CrossRef]
32. Olowe, R.; Sandouka, S.; Saadi, A.; Shekh-Ahmad, T. Approaches for Reactive Oxygen Species and Oxidative Stress Quantification in Epilepsy. *Antioxidants* **2020**, *9*, E990. [CrossRef]
33. Katerji, M.; Filippova, M.; Duerksen-Hughes, P. Approaches and Methods to Measure Oxidative Stress in Clinical Samples: Research Applications in the Cancer Field. *Oxid. Med. Cell Longev.* **2019**, *2019*, 1279250. [CrossRef]
34. Livak, K.J.; Schmittgen, T.D. Analysis of relative gene expression data using real-time quantitative PCR and the 2<sup>(-Delta Delta C(T))</sup> Method. *Methods* **2001**, *25*, 402–408. [CrossRef] [PubMed]
35. Proto, A.; Agliardi, S.; Pani, A.; Renica, S.; Gazzaniga, G.; Giossi, R.; Senatore, M.; Di Ruscio, F.; Campisi, D.; Vismara, C.; et al. COVID-Vaccines in Pregnancy: Maternal and Neonatal Response over the First 9 Months after Delivery. *Biomolecules* **2024**, *14*, 435. [CrossRef] [PubMed]
36. Martínez-Varea, A.; Satorres, E.; Florez, S.; Domenech, J.; Desco-Blay, J.; Monfort-Pitarch, S.; Hueso, M.; Perales-Marín, A.; Diago-Almela, V. Comparison of Maternal-Fetal Outcomes among Unvaccinated and Vaccinated Pregnant Women with COVID-19. *J. Pers. Med.* **2022**, *12*, 2008. [CrossRef]
37. Smithgall, M.C.; Murphy, E.A.; Schatz-Siemers, N.; Matrai, C.; Tu, J.; Baergen, R.N.; Yang, Y.J. Placental pathology in women vaccinated and unvaccinated against SARS-CoV-2. *Am. J. Obstet. Gynecol.* **2022**, *227*, 782–784. [CrossRef] [PubMed]
38. Vollbracht, C.; Kraft, K. Oxidative Stress and Hyper-Inflammation as Major Drivers of Severe COVID-19 and Long COVID: Implications for the Benefit of High-Dose Intravenous Vitamin C. *Front. Pharmacol.* **2022**, *13*, 899198. [CrossRef]



39. Picca, A.; Calvani, R.; Coelho-Junior, H.J.; Landi, F.; Bernabei, R.; Marzetti, E. Mitochondrial Dysfunction, Oxidative Stress, and Neuroinflammation: Intertwined Roads to Neurodegeneration. *Antioxidants* **2020**, *9*, 647. [CrossRef]
40. Pliss, A.; Kuzmin, A.N.; Prasad, P.N.; Mahajan, S.D. Mitochondrial Dysfunction: A Prelude to Neuropathogenesis of SARS-CoV-2. *ACS Chem. Neurosci.* **2022**, *13*, 308–312. [CrossRef]
41. Lymperaki, E.; Kazeli, K.; Tsamesidis, I.; Nikza, P.; Poimenidou, I.; Vagdatli, E. A Preliminary Study about the Role of Reactive Oxygen Species and Inflammatory Process after COVID-19 Vaccination and COVID-19 Disease. *Clin. Pract.* **2022**, *12*, 599–608. [CrossRef]
42. Dorval, J.; Hontela, A. Role of glutathione redox cycle and catalase in defense against oxidative stress induced by endosulfan in adrenocortical cells of rainbow trout (*Oncorhynchus mykiss*). *Toxicol. Appl. Pharmacol.* **2003**, *192*, 191–200. [CrossRef]
43. Tolmacheva, A.S.; Onumere, M.K.; Sedykh, S.E.; Timofeeva, A.M.; Nevinsky, G.A. Catalase Activity of IgGs of Patients Infected with SARS-CoV-2. *Int. J. Mol. Sci.* **2023**, *24*, 10081. [CrossRef] [PubMed]
44. Vlahos, R.; Stambas, J.; Bozinovski, S.; Broughton, B.R.S.; Drummond, G.R.; Selemidis, S. Inhibition of Nox2 oxidase activity ameliorates influenza A virus-induced lung inflammation. *PLoS Pathog.* **2011**, *7*, e1001271. [CrossRef]
45. Sebastiano, M.; Chastel, O.; de Thoisy, B.; Eens, M.; Costantini, D. Oxidative stress favours herpes virus infection in vertebrates: A meta-analysis. *Curr. Zool.* **2016**, *62*, 325–332. [CrossRef] [PubMed]
46. Nishikawa, M.; Hashida, M.; Takakura, Y. Catalase delivery for inhibiting ROS-mediated tissue injury and tumor metastasis. *Adv. Drug Deliv. Rev.* **2009**, *61*, 319–326. [CrossRef]
47. Qin, M.; Cao, Z.; Wen, J.; Yu, Q.; Liu, C.; Wang, F.; Zhang, J.; Yang, F.; Li, Y.; Fishbein, G.; et al. An Antioxidant Enzyme Therapeutic for COVID-19. *Adv. Mater.* **2020**, *32*, e2004901. [CrossRef] [PubMed]
48. Mo, L.H.; Luo, X.Q.; Ma, K.; Shao, J.B.; Zhang, G.H.; Liu, Z.G.; Liu, D.B.; Zhang, H.P.; Yang, P.C. Superoxide Dismutase Prevents SARS-CoV-2-Induced Plasma Cell Apoptosis and Stabilizes Specific Antibody Induction. *Oxid. Med. Cell Longev.* **2022**, *2022*, 5397733. [CrossRef]
49. Li, M.; Chen, L.; Zhang, J.; Xiong, C.; Li, X. The SARS-CoV-2 receptor ACE2 expression of maternal-fetal interface and fetal organs by single-cell transcriptome study. *PLoS ONE* **2020**, *15*, e0230295. [CrossRef]
50. Kammala, A.K.; Tatiparthi, M.; Thomas, T.J.; Bonam, S.R.; Boldogh, I.; Haitao, H.; Sharma, S.; Menon, R. In vitro mRNA-S maternal vaccination induced altered immune regulation at the maternal-fetal interface. *Am. J. Reprod. Immunol.* **2024**, *91*, e13861. [CrossRef]

**Disclaimer/Publisher’s Note:** The statements, opinions and data contained in all publications are solely those of the individual author(s) and contributor(s) and not of MDPI and/or the editor(s). MDPI and/or the editor(s) disclaim responsibility for any injury to people or property resulting from any ideas, methods, instructions or products referred to in the content.

## Protocol

# Assessing the Comparative Efficacy of Sentinel Lymph Node Detection Techniques in Vulvar Cancer: Protocol for a Systematic Review and Meta-Analysis

Balázs Vida <sup>1</sup>, Balázs Lintner <sup>1</sup>, Szabolcs Várbiro <sup>2</sup>, Petra Merkely <sup>1</sup>, Lotti Lúcia Lőczy <sup>1</sup>, Nándor Ács <sup>1</sup>,  
Richárd Tóth <sup>1,†</sup> and Márton Keszthelyi <sup>1,\*,†</sup>

<sup>1</sup> Department of Obstetrics and Gynecology, Semmelweis University, 1082 Budapest, Hungary; vidabalazs.2000@gmail.com (B.V.); lintner.balazs.zoltan@semmelweis.hu (B.L.); merkely.petra@gmail.com (P.M.); keszthelyi.lotti.lucia@semmelweis.hu (L.L.L.); acs.nandor@semmelweis.hu (N.Á.); toth.richard@semmelweis.hu (R.T.)

<sup>2</sup> Workgroup of Research Management, Doctoral School, Semmelweis University, 1085 Budapest, Hungary; varbiro.szabolcs@semmelweis.hu

\* Correspondence: keszthelyi.marton@semmelweis.hu

† These two authors contributed equally to this work.

**Abstract:** This systematic review and meta-analysis protocol aims to evaluate the comparative efficacy of different sentinel lymph node (SLN) detection techniques in the management of vulvar cancer. Vulvar cancer, though rare, predominantly affects older women and requires effective management strategies. The SLN technique has become a standard approach for early-stage cases, offering reduced morbidity compared to complete lymphadenectomy. Currently, various SLN detection methods exist, including the use of Technetium-99m (Tc99m), Indocyanine Green (ICG), and superparamagnetic iron oxide (SPIO), but there is a lack of comprehensive comparison of their efficacy. This review will systematically search relevant databases, including PubMed, Scopus, Cochrane, Web of Science and Embase following PRISMA guidelines, to gather data from clinical trials. The primary outcome will be the detection rates of SLN techniques with secondary outcomes examining patient characteristics and procedural factors. The analysis will utilize random-effects models to compare detection rates across studies. The results of this study aim to provide insights into the optimal SLN detection method with potential implications for clinical practice guidelines in vulvar cancer management. The protocol is registered under the PROSPERO registration number CRD42024590774.

**Keywords:** vulvar cancer; sentinel lymph node; Technetium-99m; Indocyanine green

## 1. Introduction

Vulvar cancer is a rare malignancy comprising 5% of all gynecological cancers and 1% of all cancers in women. It predominantly affects patients between the ages of 65 and 75 with most cases diagnosed at an early stage [1,2]. The five-year survival rate varies significantly based on the stage at diagnosis, with early-stage (Stage I) disease offering a nearly 100% survival rate, while advanced-stage disease with lymph node metastasis reduces this figure to below 60% [2]. Prior to the introduction of sentinel lymph node (SLN) detection, complete lymphadenectomy (CL) was the standard practice. However, CL is associated with significant adverse effects (lymphocyst formation, lymphedema) that substantially impair patients' quality of life. The development of a technique capable of identifying SLNs without the severe complications associated with CL was a pivotal advancement, leading to the evolution of the sentinel technique. According to the FIGO (Fédération Internationale de Gynécologie et d'Obstétrique) guidelines, for patients with squamous cell carcinoma, unifocal tumors smaller than 4 cm, and no clinical signs of groin node involvement, SLN detection and excision is recommended [3]. The current guidelines

from the European Society of Gynecological Oncology (ESGO) mandate the use of a radiotracer, typically Technetium-99m (Tc99m), for SLN detection. These guidelines further recommend the combination of Tc99m with a colorimetric adjuvant, such as isosulfan or methylene blue dye, or an infrared imaging technique, such as ICG [4]. The success rate of SLN techniques can be affected by various factors. The earliest SLN detection methods employed blue dye, which was initially considered promising but was later surpassed by radiotracers, which offer significantly higher detection rates [5]. Tc99m is widely regarded as the gold standard in SLN detection for VC. However, Tc99m is not without its drawbacks. The requirement for a nuclear medicine facility, the need for administration around the tumor site the day before surgery, and the lack of real-time visual guidance pose logistical and practical challenges to its use [6]. A newer approach using ICG has shown promise in vulvar cancer [7]. ICG is a hydrophilic fluorescent agent that, when used with near-infrared (NIR) imaging, facilitates SLN biopsy in a single intraoperative step. Studies have demonstrated the feasibility and efficacy of ICG-guided SLN biopsy in early-stage VC [8]. Although ICG and NIR imaging have demonstrated comparable detection rates to Tc99m, the available data are often insufficient for definitive conclusions, and the supporting evidence remains limited [9–11]. An emerging approach showing promising detection rates and gaining increasing attention in vulvar cancer management is the superparamagnetic iron oxide (SPIO) method, which eliminates the need for radioactive tracers, provides high detection accuracy, and offers logistical advantages by allowing same-day procedures without the requirement for specialized nuclear medicine facilities [12,13]. Recognizing the need for a comprehensive evaluation, this study aims to conduct a systematic review comparing the detection rates of all currently used SLN techniques. By addressing this gap in the literature, we seek to provide critical insights into the comparative efficacy of these methods in the management of vulvar cancer.

## 2. Experimental Design

This systematic review will be conducted and reported following the Preferred Reporting Items for Systematic Reviews and Meta-Analyses (PRISMA) guidelines.

### 2.1. Eligibility Criteria

#### 2.1.1. Type of Studies

We will include prospective and retrospective clinical trials, as well as randomized controlled trials, without any language restrictions. The search will cover all relevant studies available in the databases from their inception up to 15 August 2024.

#### 2.1.2. Types of Participants

Eligible studies will include women diagnosed with vulvar cancer classified as FIGO stage T1a or T2, where the tumor size exceeds 2 cm but remains under 4 cm, with an invasion depth greater than 1 mm, and without detectable lymph node metastasis. While vulvar cancer predominantly affects older women, participants of all age groups will be included in the analysis.

#### 2.1.3. Type of Methods

We aim to include all currently available SLN detection methods. These will include the Tc99m isotope, blue dye, ICG, and SPIO solution.

#### 2.1.4. Type of Outcomes

The primary outcome of interest will be the detection rates (DRs). Secondary outcomes will focus on patient-specific factors such as mean and median age (year), body mass index (BMI) ( $\text{kg}/\text{m}^2$ ), tumor size (cm) and grade, tumor position (lateral, medial) and anatomical location (distance to the midline/clitoris/anus/vagina/urethra (cm)), type of surgery (wide local excision, hemivulvectomy, vulvectomy), lymph node assessment (unilateral vs. bilateral), lymphovascular space invasion (LVSI) (1–4), histotype (carcinoma vs. melanoma)

and their influence on detection rates. Additionally, we aim to assess procedure-related variables, such as the doses (activity, mg) and concentrations (mg/mL) of substances used, type of surgery, and short and long-term complications.

## 2.2. Materials and Equipment

Our search will utilize the terms “sentinel” and “vulv” across the most comprehensive online databases, including PubMed, Scopus, Cochrane, Embase, Web of Science, and Medline. The search will cover all records available up to and including 15 August 2024.

## 2.3. Detailed Procedure

We will follow the recommendations of the Cochrane Collaboration for planning, study selection, and data extraction. All relevant studies will be identified through our search strategy across the specified databases. Duplicate records will be removed using the bibliographic management tool EndNote, X 9 version: 21.4 and Rayyan will be utilized for the screening and selection process. The initial screening will be conducted based on titles and abstracts, which are followed by full-text reviews. Additional relevant articles will be manually identified by reviewing the reference lists of the included studies. Two independent reviewers will be responsible for the selection and data extraction, using a predefined standardized data collection form. Any disagreements will be resolved with the involvement of a third independent reviewer. Cohen’s kappa coefficient will be calculated to assess inter-rater reliability during both the selection and extraction phases.

## 2.4. Data Items

The extracted information will include the date, name of the author, country, type of malignancy, study design, patient number and groin number, detection rates, doses and concentrations, mean age, and the mean BMI of the patients. If any data are missing, incomplete, or unclear, the authors will be contacted for clarification.

## 2.5. Outcomes and Prioritization

Our primary outcome will be the DR of each SLN detection method, including combinations of different techniques, with a focus on comparing their effectiveness. A secondary objective will be to investigate the relationship between detection rates and patient characteristics, such as average BMI. Additionally, if sufficient data are available, we will attempt to gather information on the doses and concentrations of the substances used in these procedures.

## 2.6. Effect Measures

For dichotomous outcomes, such as successful SLN detection or adverse events, we will report risk ratios (RRs) along with risk differences (RDs) and group proportions for better clarity. For continuous variables, including patient-related data (e.g., BMI), we will present mean differences (MDs) or differences between medians (MedDs), depending on the format in which the data are provided in the studies. We will also report the group-specific means or medians to enhance the interpretability of the results.

## 2.7. Risk of Bias

Two members of the review team will assess the risk of bias via the robvis visualization tool for all of the studies. If a disagreement arises, a third reviewer will be involved. The tool evaluates five areas of potential bias: bias from the randomization process, bias due to deviations from the intended interventions, bias from missing outcome data, bias in outcome measurement, and publication bias: bias in the selection of reported results. Each domain includes signaling questions designed to gather relevant information. The answers to these questions are processed through algorithms to rate each domain as having a low risk of bias, some concerns, or a high risk of bias. These individual domain ratings are then

combined into an overall risk-of-bias judgment, which also falls into the categories of low risk, some concerns, or high risk of bias.

### 2.8. Data Synthesis

If the included studies and their results show sufficient homogeneity, we will carry out a meta-analysis using a random-effects model. Both qualitative and quantitative data synthesis will be undertaken. At least three studies will be required to conduct a meta-analysis. The random effects model will be employed to combine effect sizes using a frequentist approach. For dichotomous outcomes, we will calculate risk ratios (RRs) along with 95% confidence intervals (CIs) as the effect size measure. Proportions of events of interest will be pooled separately for each group. For continuous variables, we will use either the mean difference (MD) or the difference between medians (MedD) with 95% CI as the effect size, depending on how the data are presented. If only quartiles are provided, we will estimate the mean and standard deviation (SD) assuming the distribution is either normal or lognormal; otherwise, the median differences will be pooled. Pooled RR based on raw data will be calculated using the Mantel–Haenszel method, with the exact Mantel–Haenszel technique applied to manage zero cell counts. The inverse variance weighting method will be utilized for calculating the pooled RR and MD when raw data are not available. To enhance precision, we will adjust the pooled confidence intervals using the Hartung–Knapp method when it produces a more conservative result. The heterogeneity variance ( $\tau^2$ ) will be estimated using the restricted maximum-likelihood estimator, and the confidence interval will be derived using the Q profile method. Heterogeneity among the studies will be evaluated using Higgins and Thompson’s  $I^2$  statistic. Results will be deemed statistically significant if the confidence interval excludes the null value. The findings will be visually represented using forest plots, and prediction intervals will be reported when applicable. We will explore model-fitting parameters and identify potential outliers using various influence measures and visual plots. All statistical analyses will be performed using the R software package (R Core Team) version: 4.4.2. The confidence in effect estimates for each reported outcome will be assessed using the Grading of Recommendations, Assessment, Development, and Evaluation approach by two reviewers, and possible disagreement will be assessed by a third reviewer.

### 2.9. Ethical Concerns

Patients or members of the public will not participate in our research; therefore, ethical approval is not required for this study, as no original data will be collected

### 2.10. Registration

Prospero registration number: CRD42024590774

## 3. Expected Results

While previous meta-analyses and systematic reviews have demonstrated the efficacy of ICG in SLN detection, a direct comparison with the ESGO-recommended tracer, Tc99m, remains necessary and warrants an updated analysis. Additionally, the novel SPIO method, given its promising potential, and blue dye, one of the earlier techniques still in use, require further evaluation and comparison against established methods. By employing the RoB 2.0 tool and robvis visualization software, our study strives to minimize bias and ensure a high level of evidence quality. The findings of this systematic review may influence future clinical guidelines, as it aims to provide an up-to-date comparison of all currently employed SLN detection techniques in vulvar cancer. However, the robustness of our conclusions may be limited by the quality of the individual studies included, particularly if there are gaps or inconsistencies in the reported data.

**Author Contributions:** B.V.: conceptualization, methodology, writing—original draft, project administration; B.L.: conceptualization, resources, writing—review and editing, supervision, project administration; S.V.: resources, methodology, software, P.M.: conceptualization, methodology, software, writing—review and editing; L.L.L.: resources, writing—review and editing; N.Á.: conceptualization, writing—review and editing, R.T.: conceptualization, methodology, software, writing—review and editing, supervision.; M.K.: conceptualization, methodology, resources, writing—review and editing, supervision. M.K. is the guarantor of the review. All authors have read and agreed to the published version of the manuscript.

**Funding:** This research received no external funding.

**Institutional Review Board Statement:** Not applicable.

**Informed Consent Statement:** Not applicable.

**Data Availability Statement:** Due to this article’s nature, no original data were used.

**Conflicts of Interest:** The authors declare no conflicts of interest.

## References

- Alkatout, I.; Schubert, M.; Garbrecht, N.; Weigel, M.T.; Jonat, W.; Mundhenke, C.; Günther, V. Vulvar cancer: Epidemiology, clinical presentation, and management options. *Int. J. Womens Health* **2015**, *7*, 305–313. [CrossRef] [PubMed]
- Miljanović-Špika, I.; Madunić, M.D.; Topolovec, Z.; Kujadin Kenjereš, D.; Vidosavljević, D. Prognostic factors for vulvar cancer. *Acta Clin. Croat.* **2021**, *60*, 25–32. [CrossRef] [PubMed]
- Virarkar, M.; Vulasala, S.S.; Daoud, T.; Javadi, S.; Lall, C.; Bhosale, P. Vulvar Cancer: 2021 Revised FIGO Staging System and the Role of Imaging. *Cancers* **2022**, *14*, 2264. [CrossRef] [PubMed]
- Oonk, M.H.M.; Planchamp, F.; Baldwin, P.; Mahner, S.; Mirza, M.R.; Fischerová, D.; Creutzberg, C.L.; Guillot, E.; Garganese, G.; Lax, S.; et al. European Society of Gynaecological Oncology Guidelines for the Management of Patients with Vulvar Cancer—Update 2023. *Int. J. Gynecol. Cancer* **2023**, *33*, 1023–1043. [CrossRef] [PubMed]
- de Hullu, J.A.; Doting, E.; Piers, D.A.; Hollema, H.; Aalders, J.G.; Koops, H.S.; Boonstra, H.; van der Zee, A.G. Sentinel lymph node identification with technetium-99m-labeled nanocolloid in squamous cell cancer of the vulva. *J. Nucl. Med.* **1998**, *39*, 1381–1385. [PubMed]
- Hauspy, J.; Beiner, M.; Harley, I.; Ehrlich, L.; Rasty, G.; Covens, A. Sentinel lymph node in vulvar cancer. *Cancer* **2007**, *110*, 1015–1023. [CrossRef] [PubMed]
- Crane, L.M.; Themelis, G.; Arts, H.J.; Buddingh, K.T.; Brouwers, A.H.; Ntziachristos, V.; van Dam, G.M.; van der Zee, A.G. Intraoperative near-infrared fluorescence imaging for sentinel lymph node detection in vulvar cancer: First clinical results. *Gynecol. Oncol.* **2011**, *120*, 291–295. [CrossRef] [PubMed]
- Schaafsma, B.E.; Verbeek, F.P.; Peters, A.A.; van der Vorst, J.R.; de Kroon, C.D.; van Poelgeest, M.I.; Trimbo, J.B.; van de Velde, C.J.; Frangioni, J.V.; Vahrmeijer, A.L.; et al. Near-infrared fluorescence sentinel lymph node biopsy in vulvar cancer: A randomised comparison of lymphatic tracers. *BJOG* **2013**, *120*, 758–764. [CrossRef] [PubMed]
- Cho, H.W. 612P Sentinel lymph node detection and accuracy in vulvar cancer: Meta-analysis and systemic review. *Ann. Oncol.* **2022**, *33*, S825. [CrossRef]
- Cornel, K.; Mehta, M.; Swift, B.; Covens, A.; Vicus, D.; Kupets, R.; Gien, L. The use of Indocyanine Green (ICG) for sentinel lymph node detection in vulvar cancer (175). *Gynecol. Oncol.* **2023**, *176*, S67–S68. [CrossRef]
- Koual, M.; Benoit, L.; Nguyen-Xuan, H.T.; Bentivegna, E.; Azaïs, H.; Bats, A.S. Diagnostic value of indocyanine green fluorescence guided sentinel lymph node biopsy in vulvar cancer: A systematic review. *Gynecol. Oncol.* **2021**, *161*, 436–441. [CrossRef] [PubMed]
- Del Valle, D.; Ruiz, R.; Lekuona, A.; Cobas, P.; Jaunarena, I.; Gorostidi, M.; Cespedes, J. Superparamagnetic iron oxide (SPIO) for sentinel lymph node detection in vulvar cancer. *Gynecol. Oncol.* **2024**, *187*, 145–150. [CrossRef] [PubMed]
- Thill, M.; Kurylcio, A.; Welter, R.; van Haasteren, V.; Grosse, B.; Berclaz, G.; Polkowski, W.; Hauser, N. The Central-European SentiMag study: Sentinel lymph node biopsy with superparamagnetic iron oxide (SPIO) vs. radioisotope. *Breast* **2014**, *23*, 175–179. [CrossRef] [PubMed]

**Disclaimer/Publisher’s Note:** The statements, opinions and data contained in all publications are solely those of the individual author(s) and contributor(s) and not of MDPI and/or the editor(s). MDPI and/or the editor(s) disclaim responsibility for any injury to people or property resulting from any ideas, methods, instructions or products referred to in the content.

## Article

# Quantitative Standardized Expansion Assay: An Artificial Intelligence-Powered Morphometric Description of Blastocyst Expansion and Zona Thinning Dynamics

Danilo Cimadomo <sup>1,\*</sup>, Samuele Trio <sup>2</sup>, Tamara Canosi <sup>3</sup>, Federica Innocenti <sup>1</sup>, Gaia Saturno <sup>1</sup>, Marilena Taggi <sup>1</sup>, Daria Maria Soscia <sup>1,4</sup>, Laura Albricci <sup>1</sup>, Ben Kantor <sup>5</sup>, Michael Dvorkin <sup>5</sup>, Anna Svensson <sup>5</sup>, Thomas Huang <sup>6,7</sup>, Alberto Vaiarelli <sup>1</sup>, Gianluca Gennarelli <sup>8,9,†</sup> and Laura Rienzi <sup>1,10,†</sup>

- <sup>1</sup> IVIRMA Global Research Alliance, GENERA, Clinica Valle Giulia, 00197 Rome, Italy; federica.innocenti@ivirma.com (F.I.); gaia.saturno@generapma.it (G.S.); marilena.taggi@ivirma.com (M.T.); daria.soscia@generapma.it (D.M.S.); laura.albricci@generapma.it (L.A.); alberto.vaiarelli@gmail.com (A.V.); laura.rienzi@ivirma.com (L.R.)
  - <sup>2</sup> IVIRMA Global Research Alliance, DEMETRA, 50141 Florence, Italy; samuele.trio@gmail.com
  - <sup>3</sup> Department of Biology and Biotechnology “Lazzaro Spallanzani”, University of Pavia, 27100 Pavia, Italy; tamara.canosi01@universitadipavia.it
  - <sup>4</sup> Department of Biomedicine and Prevention, University of Tor Vergata, 00128 Rome, Italy
  - <sup>5</sup> Fairtilty Ltd., Tel Aviv 6721508, Israel; ben@fairtilty.com (B.K.); michael.dvorkin@fairtilty.com (M.D.); anna.svensson@fairtilty.com (A.S.)
  - <sup>6</sup> Pacific In Vitro Fertilization Institute, Honolulu, HI 96826, USA; huangt@hawaii.edu
  - <sup>7</sup> John A. Burns School of Medicine, University of Hawaii at Manoa, Honolulu, HI 96826, USA
  - <sup>8</sup> Gynecology and Obstetrics 1U, Physiopathology of Reproduction and IVF Unit, Department of Surgical Sciences, S. Anna Hospital, University of Turin, 10126 Turin, Italy; gennarelligl@gmail.com
  - <sup>9</sup> IVIRMA Global Research Alliance, Livet, 10126 Turin, Italy
  - <sup>10</sup> Department of Biomolecular Sciences, University “Carlo Bo” of Urbino, 61029 Urbino, Italy
- \* Correspondence: danilo.cimadomo@ivirma.com; Tel.: +39-3470182967  
† These authors contributed equally to this work.

**Abstract:** Artificial intelligence applied to time-lapse microscopy may revolutionize embryo selection in IVF by automating data collection and standardizing the assessments. In this context, blastocyst expansion dynamics, although being associated with reproductive fitness, have been poorly studied. This retrospective study (N = 2184 blastocysts from 786 cycles) exploited both technologies to picture the association between embryo and inner-cell-mass (ICM) area in  $\mu\text{m}^2$ , the ICM/Trophectoderm ratio, and the zona pellucida thickness in  $\mu\text{m}$  (zp-T) at sequential blastocyst expansion stages, with (i) euploidy and (ii) live-birth per transfer (N = 548 transfers). A quantitative-standardized-expansion-assay (qSEA) was also set-up; a novel approach involving automatic annotations of all expansion metrics every 30 min across 5 h following blastulation. Multivariate regressions and ROC curve analyses were conducted. Aneuploid blastocysts were slower, expanded less and showed thicker zp. The qSEA outlined faster and more consistent zp thinning processes among euploid blastocysts, being more or as effective as the embryologists in ranking euploid embryo as top-quality of their cohorts in 69% of the cases. The qSEA also outlined faster and more consistent blastocyst expansion and zp thinning dynamics among euploid implanted versus not implanted blastocysts, disagreeing with embryologists’ priority choice in about 50% of the cases. In conclusion, qSEA is a promising objective, quantitative, and user-friendly strategy to predict embryo competence that now deserves prospective validations.

**Keywords:** blastocyst expansion; zona pellucida thinning; euploidy; live birth; artificial intelligence

## 1. Introduction

The main tasks in the IVF laboratory are to optimize the laboratory conditions and the performance of the embryologists, as well as to score, rank, and select embryos to

maximize the possibilities to achieve a live birth (LB). An efficient embryo selection tool to identify reproductively competent embryos would significantly reduce the time-to-pregnancy by preventing unnecessary embryo transfers (ETs), with relevant economic and psychological implications [1]. Still, currently, static morphological embryo assessment is the most common selection scheme, especially in non-preimplantation genetic testing (PGT) cycles. However, morphological assessment is inconsistent across the embryologist community, especially across different IVF centers [2].

The introduction of new technologies, such as time-lapse microscopy (TLM) and artificial intelligence (AI) in clinical embryology, have provided novel and advanced information on human embryo development. TLM permits undisturbed culture conditions, allowing for continuous monitoring of embryo development dynamics. Several studies have leveraged TLM with the aim of identifying morphokinetic markers of embryonic competence [3]; however, to date, TLM-driven embryo selection has not been shown to be better than an embryologist's assessment [4,5]. Nonetheless, the implementation of TLM to investigate human preimplantation development has provided embryologists with a powerful tool to precisely evaluate the timings of cellular divisions and detect abnormal dynamics that would be impossible to assess through static assessments (e.g., trichotomous cleavage or spontaneous blastocyst collapse) [6].

Lately, AI has been subject to several studies because it holds the potential to objectify and automate embryo assessment and enhance embryo selection by extracting relevant information from embryo microscopy images and videos. AI models aim at identifying embryos with the highest chance to implant in each cohort and provide embryologists with a score to prioritize them for transfer [7]. AI-based TLM assessment represents a powerful approach to studying embryo preimplantation development with countless possibilities.

In this context, blastocyst expansion represents an interesting feature to investigate. Indeed, it has been previously reported to be associated with embryo competence through both static and dynamic morphological assessments [8,9]. Notably, blastocyst expansion is a morphogenetic process common to several species [10], regulated by trophoblast (TE) functional properties after embryonic genome activation. This phase is indeed very sensitive, being the first process occurring after inner cell mass (ICM) and TE differentiation. Several authors have indeed focused their attention on the clinical implications of blastocyst expansion, being mostly concordant in reporting a positive association [11–14].

Huang and colleagues designed a dynamic and standardized blastocyst expansion assessment scheme called quantitative standardized expansion assay (qSEA). This approach aimed at minimizing the variability across the operators in assessing blastocysts' quality by focusing instead on their expansion at well-defined timepoints. Specifically, beginning at time of blastulation (tB) for 10 h at 2 h intervals, these authors measured the cross-sectional area of the embryo cavity and its surrounding TE in  $\mu\text{m}^2$  through the Embryoscope's measurement tool. The data reported significantly associated with blastocyst competence, suggesting qSEA is a promising embryo selection tool that is less exposed to subjective evaluations and suitable for automation [9,15,16]. The recent implementation of AI-powered software for dynamic embryo assessment allowed us to slightly adapt the qSEA and enhance it with additional morphometric information (e.g., zona pellucida thickness). The aim of this retrospective study was to adopt an AI-powered version of the qSEA in a large dataset of 2184 biopsied blastocysts—of which 548 transferred—obtained during 786 PGT-A cycles. We assessed the association of the parameters extracted with this bioinformatic pipeline with embryo chromosomal competence (euploidy) and the reproductive competence (LB per euploid ET). In a clinical simulation, we also tested the putative value of this tool for embryo selection purposes.

## 2. Materials and Methods

### 2.1. Study Population and Study Design

This is a retrospective study including 2184 blastocysts obtained from 786 PGT-A cycles cultured in a time-lapse incubator (Embryoscope, Vitrolife, Gothenburg, Sweden)



between January 2013 and December 2020 at a private IVF Center in Rome (IVIRMA Global Research Alliance, Genera, Clinica Valle Giulia). Patient characteristics are summarized in Supplemental Table S1. They were mostly advanced maternal age and poor prognosis women. Of the 2184 total blastocysts included in the study, 40.5% (886/2184) were euploid and the remaining 59.5% (1298/2184) were aneuploid. The aim of the study was to evaluate the putative association between an AI-powered morphometric and morphodynamic assessment of blastocyst expansion with their chromosomal (i.e., euploidy) and/or reproductive competence (i.e., LB after vitrified-warmed euploid single embryo transfer). The analysis was conducted at each specific blastulation timings (as described below), as well as using an adapted protocol of the qSEA described by Huang previously [9,15,16] (also detailed below).

Ethical committee approval was obtained for the retrospective analysis of pseudonymized videos and data aimed at identifying patient, cycle or embryo features associated with IVF efficacy and/or efficiency.

## 2.2. IVF and PGT-A Laboratory Protocols

Ovarian stimulation was conducted with a GnRH antagonist protocol and ovulation was triggered with either GnRH-agonist or hCG based on patient characteristics and the judgment of a gynaecologist. Oocyte retrieval was conducted 35 h after trigger, and ICSI was performed according to a previously detailed protocol [17]. A continuous single culture medium (CSCM, Irvine Scientific, Santa Ana, CA, USA) was adopted, with a medium refresh on Day 5 in case of extended culture to Days 6 or 7. No laser assisted zona puncture (zp) drilling was applied on Day 3, and the embryos were left undisturbed within an intact zp throughout their development until the fully expanded blastocyst stage, when TE biopsy was conducted as thoroughly described previously [18]. The biopsied blastocysts were vitrified within 30 min from biopsy to prevent their re-expansion. Comprehensive chromosome testing (CCT) was conducted through qPCR or NGS at an external laboratory to report uniform aneuploidies [19,20]. Intermediate chromosomes copy numbers (ICN) were reported as either euploid or aneuploid [20]. Only vitrified-warmed single euploid blastocyst transfers were conducted with either a hormonal replacement therapy or a modified-natural endometrial preparation protocol. All transfers from the same oocyte retrieval were included. Blastocyst morphology was graded by the embryologists relying on Gardner's scoring system [21] as excellent if AA; good if AB or BA; average if BB, AC, or CA; and low if CC, BC, or CB.

## 2.3. Blastocyst Expansion AI-Powered Morphometric and Morphodynamic Analysis

All Embryoscope videos were analysed through an AI-powered tool (CHLOE™, Fairtility, Tel Aviv, Israel) to automate, standardize, objectify, and quantify embryo assessment. CHLOE is an AI tool based on a convolutional neural network that automatically analyses embryo videos and annotates specific events of embryo development. Here we leveraged AI to annotate the time of starting blastulation (tSB); the time of blastulation (tB); the time of expanding blastocyst (tEB) (as described in [3,22]); and the time of biopsy (t-biopsy; i.e., the end of the video, when TE biopsy was performed) in hours post insemination (hpi). We also leveraged the AI to annotate the area of the embryo including the zp (zp-A); the area of the embryo proper (emb-A); the thickness of the zona pellucida (zp-T; calculated as the largest distance between the emb-A and the zp-A edges); the area of the ICM (ICM-A); and the ratio between the area of the ICM and the area of the TE (ICM/TE ratio) (Figure 1). All of these metrics were calculated by the software at the median focal plane as the proportions of video frames occupied by each feature under investigation (single pixel = 300 µm; whole wells' area = 90,000 µm<sup>2</sup>) at each blastulation timing (Figure 1). Also, increases and decreases for all these measures were assessed between each blastulation timing and the following. All data were assessed for their association with euploidy and with LB among vitrified-warmed transferred euploid blastocysts.

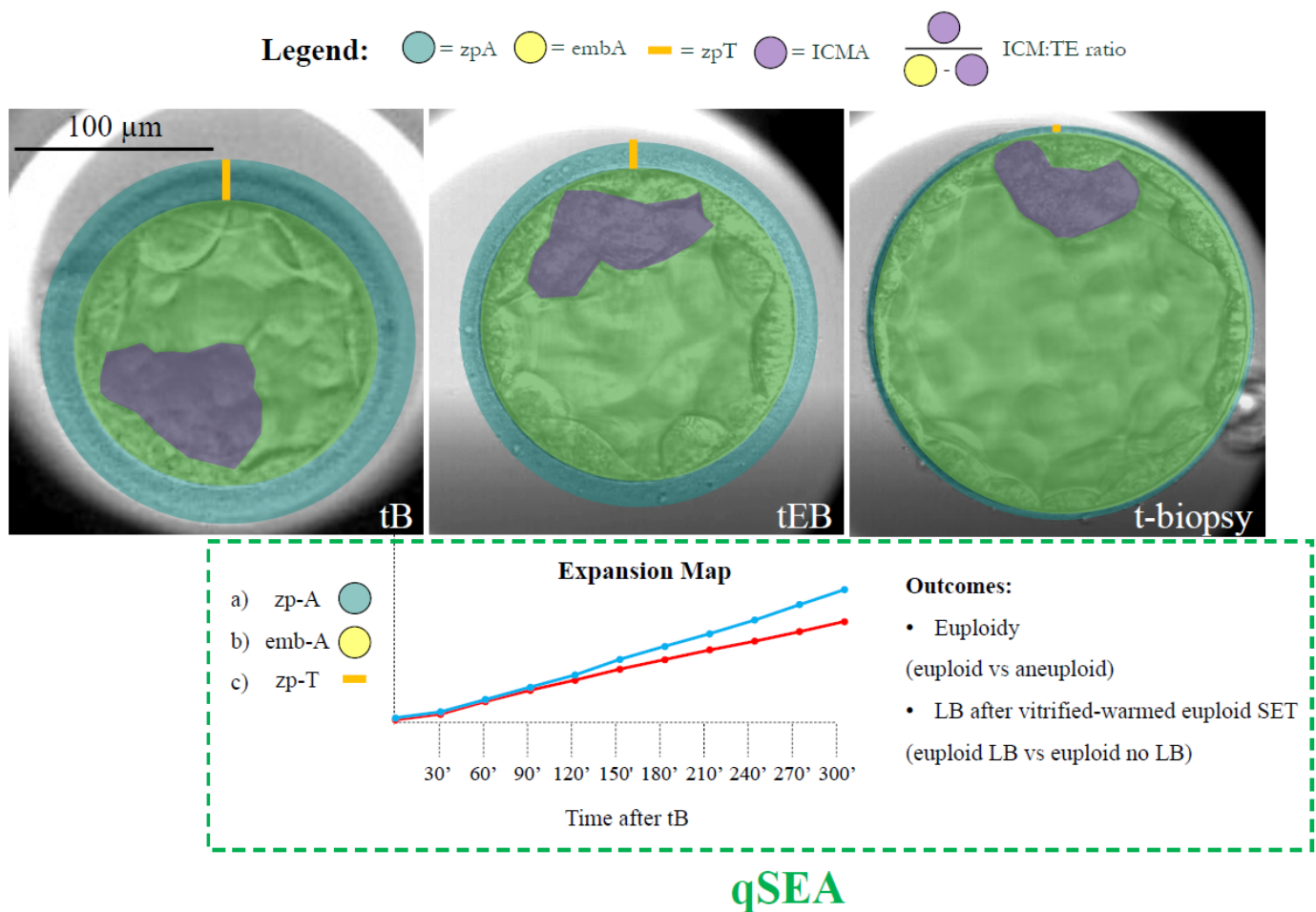


**Figure 1.** Definition of the features and timings under investigation. The AI-powered software CHLOE™ (Fairtility, Tel Aviv, Israel) was adopted to automatically annotate the time of blastulation (tB); the time of expanding blastocyst (tEB) (according to the definitions of the ESHRE TLT working group); and the time of biopsy (t-biopsy; i.e., the end of the video, when trophectoderm biopsy was performed) in hours post insemination (hpi). The same software annotated the area of embryo including the zp (zp-A; green circle); the area of the embryo proper (emb-A; yellow circle); the thickness of the zona pellucida (zp-T; calculated as the largest distance between the emb-A and the zp-A edges; orange line); the area of the ICM (ICM-A; purple shade); and the ratio between the area of ICM and the area of the trophectoderm (ICM/TE ratio). All of these metrics were calculated by the software at the median focal plane as the proportions of video frames occupied by each feature under investigation (single pixel = 300 µm; whole wells' area = 90,000 µm<sup>2</sup>) at each blastulation timing. The quantitative standardized expansion assay (qSEA) was also automatically generated for each embryo by annotating the zp-A, emb-A, and the zp-T every 30 min across the 5 h following the tB. These data were then clustered according to blastocyst chromosomal constitution (euploid versus aneuploid) and reproductive competence (transferred euploid blastocysts that resulted in a LB versus transferred euploid blastocysts that did not result in a LB). This process generated six expansion maps (like the example with the blue and red lines for the two different outcomes) that were scrutinized to assess putative differences. Scale bar, 100 µm.

#### 2.4. AI-Powered qSEA

For zp-A, emb-A, and zp-T, the qSEA was also calculated by adapting Huang's protocol [9,15,16]. In detail, these metrics were automatically annotated for each embryo by CHLOE every 30 min over the 5 h following the tB. The data were then clustered according to blastocyst chromosomal constitution (euploid versus aneuploid), and reproductive competence (transferred euploid blastocysts that resulted in a LB versus transferred euploid

blastocysts that did not result in a LB). This generated six expansion maps that were scrutinized to assess putative differences in the expansion dynamics (Figure 1).

### 2.5. Clinical Simulations

Two simulations were conducted to assess the putative value of the qSEA had we used it clinically to prioritize blastocysts for transfer (as previously done for the iDAScore v1.0 [23]).

Among the 786 PGT-A cycles with  $\geq 1$  biopsied blastocyst, 352 obtained both euploid and aneuploid embryos. In these cycles, we could assess how often the embryologists and the qSEA were concordant and discordant in blastocyst ranking, and how often the highest ranked embryos were indeed euploid (the workflow is summarized in Supplemental Figure S1A).

Among the 237 PGT-A cycles with  $\geq 2$  euploid blastocysts, 216 underwent  $\geq 1$  ET (99 performed only 1 ET, 14 performed  $>1$  ET always obtaining a LB, 50 performed  $>1$  ET never obtaining a LB, and 53 performed  $>1$  ET with both LB and implantation failures/miscarriages). In these cycles, we could assess how often the embryologists and the qSEA were concordant and discordant in ranking euploid blastocysts, and how often the highest ranked embryos indeed resulted in a LB (the workflow is summarized in Supplemental Figure S1B).

### 2.6. Statistical Analysis

The software SPSS version 29.0.1.0 (171) was used for statistics (IBM, Armonk, NY, USA). Continuous data are shown as mean  $\pm$  standard deviation (SD). The normal (Gaussian) distribution of the data was assessed with a Shapiro–Wilk test and either *t*-test/ANOVA or Mann Whitney U/Kruskal Wallis tests were adopted to assess statistically significant differences. Categorical data are shown as ratios with percentages. Fisher’s exact or chi-squared tests were adopted to assess statistically significant differences. All putative associations of the data with euploidy among biopsied blastocysts, or reproductive competence (LB) among transferred euploid blastocysts, were confirmed with either linear or logistic regression analyses. The results were adjusted for relevant confounders identified among maternal age, BMI, previous conception(s) (no/yes), cause of infertility, duration of infertility, sperm quality, and blastocyst morphology.

## 3. Results

### 3.1. Aneuploid Blastocysts Were Slower, Expanded Less and Showed a Thicker Zona Pellucida with Respect to Euploid Embryos

The first analysis conducted was a comparison of all morphometric features at the tSB, tB, tEB, and t-biopsy among euploid and aneuploid blastocysts, as well as among transferred euploid blastocysts that resulted in a LB versus not (Table 1). The data were compared among the study groups and adjusted for confounders in case of significant associations at univariate analyses. The confounders were maternal age and blastocyst morphology for the euploidy outcome, and only blastocyst morphology for the LB outcome. Aneuploid blastocysts were slower than euploid over all blastulation timings from tSB to t-biopsy, while euploid reproductively incompetent blastocysts were slower than competent from tB onwards (Table 1). Aneuploid blastocysts, while starting from a larger expansion in terms of both zp-A and emb-A at the tB, showed both smaller zp-A and emb-A than euploid blastocysts at the t-biopsy ( $24,082 \pm 5763 \mu\text{m}^2$  versus  $25,438 \pm 5968 \mu\text{m}^2$ , adjusted-*p* < 0.01; and  $23,612 \pm 5960 \mu\text{m}^2$  versus  $25,058 \pm 6212 \mu\text{m}^2$ , adjusted-*p* < 0.01) and expanded significantly less (zp-A t-biopsy/tEB:  $+38\% \pm 31\%$  versus  $+47\% \pm 33\%$ , adjusted-*p* < 0.01; zp-A t-biopsy/tB:  $+69\% \pm 39\%$  versus  $+80\% \pm 41\%$ , adjusted-*p* < 0.01; emb-A t-biopsy/tEB:  $+40\% \pm 34\%$  versus  $+48\% \pm 36$ , adjusted-*p* < 0.01; emb-A t-biopsy/tB:  $+77\% \pm 44\%$  versus  $+90\% \pm 47\%$ , adjusted-*p* < 0.01) (Table 1; Supplemental Figure S2A,B). No association was reported between both parameters and the LB (Table 1). Also, the ICM-A and

the ICM/TE ratio was comparable among euploids and aneuploids, as well as among euploids that resulted in a LB and euploids that failed to result in a LB (Table 1). Conversely, the zp-T was significantly thicker among aneuploid blastocysts versus euploids already at the tEB ( $12.9 \pm 2.4 \mu\text{m}$  versus  $12.6 \pm 2.5 \mu\text{m}$ , adjusted- $p = 0.01$ ), a difference that became even more visible at the t-biopsy ( $8.1 \pm 3.2 \mu\text{m}$  versus  $7.1 \mu\text{m} \pm 2.7$ , adjusted- $p < 0.01$ ), thereby outlining a significantly less consistent thinning (zp-T t-biopsy/tEB:  $-37\% \pm 24\%$  versus  $-43\% \pm 22\%$ , adjusted- $p = 0.01$ ; zp-T t-biopsy/tB:  $-50\% \pm 20\%$  versus  $-55\% \pm 18\%$ , adjusted- $p < 0.01$ ) (Table 1; Supplemental Figure S2C). Also in this case, no association was reported with the reproductive competence among transferred euploid blastocysts (Table 1).

**Table 1.** Summary of the main results. Area of the zona pellucida (zp-A), area of the embryo proper (emb-A), thickness of the zona pellucida (zp-T), are of the inner cell mass (ICM-A), ratio between ICM and trophoctoderm (ICM/TE ratio) at the time of blastulation (tB), at the time of blastocyst expansion (tEB) and at the time of biopsy (t-biopsy), between aneuploid versus euploid blastocysts, and between euploid not resulted and resulted in a live birth (LB). Also, the increase in all areas and the decrease in zp-T throughout consecutive timings and from tB to t-biopsy were reported and compared across the study groups.

	Aneuploid N = 1298	Euploid N = 886	p-Value	Euploid-No LB N = 315	Euploid-LB N = 233	p-Value
tSB, mean $\pm$ SD, hpi	102.5 $\pm$ 10.5	100.5 $\pm$ 9.6	$p < 0.01$	100.3 $\pm$ 9.7	99.0 $\pm$ 9.8	$p = 0.10$
tB, mean $\pm$ SD, hpi	113.0 $\pm$ 12.7	109.7 $\pm$ 11.1	$p < 0.01$	109.9 $\pm$ 11.2	107.5 $\pm$ 10.9	$p = 0.01$
tEB, mean $\pm$ SD, hpi	120.9 $\pm$ 14.5	115.9 $\pm$ 12.0	$p < 0.01$	116.7 $\pm$ 12.4	112.6 $\pm$ 11.2	$p < 0.01$
t-biopsy, mean $\pm$ SD, hpi	136.0 $\pm$ 15.2	131.6 $\pm$ 13.7	$p < 0.01$	132.4 $\pm$ 13.9	127.1 $\pm$ 12.5	$p < 0.01$
zp-A at tB, mean $\pm$ SD, $\mu\text{m}^2$	14,288 $\pm$ 1257	14,168 $\pm$ 1119	$p = 0.02^*$	14,124 $\pm$ 1071	14,263 $\pm$ 1231	$p = 0.16$
zp-A at tEB, mean $\pm$ SD, $\mu\text{m}^2$	17,435 $\pm$ 1828	17,417 $\pm$ 1955	$p = 0.82$	17,482 $\pm$ 2234	17,542 $\pm$ 1835	$p = 0.74$
Ratio tEB/tB, mean $\pm$ SD	+22% $\pm$ 10%	+23% $\pm$ 12%	$p = 0.74^*$	+24% $\pm$ 14%	+23% $\pm$ 9%	$p = 0.48$
zp-A at t-biopsy, mean $\pm$ SD, $\mu\text{m}^2$	24,082 $\pm$ 5763	25,438 $\pm$ 5968	$p < 0.01^*$	25,141 $\pm$ 5873	25,790 $\pm$ 6159	$p = 0.21$
Ratio t-biopsy/tEB, mean $\pm$ SD	+38% $\pm$ 31%	+47% $\pm$ 33%	$p < 0.01^*$	+45% $\pm$ 33%	+47% $\pm$ 33%	$p = 0.35$
Ratio t-biopsy/tB, mean $\pm$ SD	+69% $\pm$ 39%	+80% $\pm$ 41%	$p < 0.01^*$	+79% $\pm$ 42%	+81% $\pm$ 42%	$p = 0.47$
emb-A at tB, mean $\pm$ SD, $\mu\text{m}^2$	13,349 $\pm$ 1196	13,249 $\pm$ 1121	$p = 0.03^*$	13,235 $\pm$ 1107	13,309 $\pm$ 1121	$p = 0.44$
emb-A at tEB, mean $\pm$ SD, $\mu\text{m}^2$	16,900 $\pm$ 1867	16,922 $\pm$ 1986	$p = 0.79$	16,996 $\pm$ 2274	17,030 $\pm$ 1757	$p = 0.85$
Ratio tEB/tB, mean $\pm$ SD	+27% $\pm$ 11%	+28% $\pm$ 13%	$p = 0.28^*$	+29% $\pm$ 16%	+28% $\pm$ 10%	$p = 0.64$
emb-A at t-biopsy, mean $\pm$ SD, $\mu\text{m}^2$	23,612 $\pm$ 5960	25,058 $\pm$ 6212	$p < 0.01^*$	24,694 $\pm$ 6169	25,512 $\pm$ 6299	$p = 0.13$
Ratio t-biopsy/tEB, mean $\pm$ SD	+40% $\pm$ 34%	+48% $\pm$ 36%	$p < 0.01^*$	+46% $\pm$ 35%	+50% $\pm$ 34%	$p = 0.22$
Ratio t-biopsy/tB, mean $\pm$ SD	+77% $\pm$ 44%	+90% $\pm$ 47%	$p < 0.01^*$	+87% $\pm$ 48%	+92% $\pm$ 46%	$p = 0.26$
zp-T at tB, mean $\pm$ SD, $\mu\text{m}$	16.4 $\pm$ 2.9	16.2 $\pm$ 2.9	$p = 0.25$	16.5 $\pm$ 3.0	16.3 $\pm$ 3.1	$p = 0.55$
zp-T at tEB, mean $\pm$ SD, $\mu\text{m}$	12.9 $\pm$ 2.4	12.6 $\pm$ 2.5	$p = 0.01^*$	12.9 $\pm$ 2.5	12.8 $\pm$ 2.5	$p = 0.54$
Ratio tEB/tB, mean $\pm$ SD	-21% $\pm$ 11%	-22% $\pm$ 11%	$p = 0.53^*$	-21% $\pm$ 11%	-22% $\pm$ 10%	$p = 0.90$
zp-T at t-biopsy, mean $\pm$ SD, $\mu\text{m}$	8.1 $\pm$ 3.2	7.1 $\pm$ 2.7	$p < 0.01^*$	7.3 $\pm$ 2.9	6.9 $\pm$ 2.5	$p = 0.11$
Ratio t-biopsy/tEB, mean $\pm$ SD	-37% $\pm$ 24%	-43% $\pm$ 22%	$p = 0.01^*$	-43% $\pm$ 22%	-44% $\pm$ 20%	$p = 0.24$
Ratio t-biopsy/tB, mean $\pm$ SD	-50% $\pm$ 20%	-55% $\pm$ 18%	$p < 0.01^*$	-55% $\pm$ 18%	-57% $\pm$ 16%	$p = 0.21$

Table 1. Cont.

	Aneuploid N = 1298	Euploid N = 886	p-Value	Euploid-No LB N = 315	Euploid-LB N = 233	p-Value
ICM-A at tB, mean $\pm$ SD, $\mu\text{m}^2$	3458 $\pm$ 905	3414 $\pm$ 902	$p = 0.27$	3425 $\pm$ 953	3434 $\pm$ 852	$p = 0.91$
ICM-A at tEB, mean $\pm$ SD, $\mu\text{m}^2$	3497 $\pm$ 1047	3460 $\pm$ 1066	$p = 0.43$	3414 $\pm$ 1078	3468 $\pm$ 984	$p = 0.55$
Ratio tEB/tB, mean $\pm$ SD	+5% $\pm$ 35%	+5% $\pm$ 33%	$p = 0.99$	+4% $\pm$ 33%	+3% $\pm$ 25%	$p = 0.65$
ICM-A at t-biopsy, mean $\pm$ SD, $\mu\text{m}^2$	3804 $\pm$ 1471	3727 $\pm$ 1469	$p = 0.31$	3800 $\pm$ 1547	3541 $\pm$ 1212	$p = 0.08$
Ratio t-biopsy/tEB, mean $\pm$ SD	+11% $\pm$ 50%	+10% $\pm$ 45%	$p = 0.42$	+13% $\pm$ 46%	+4% $\pm$ 36%	$p = 0.17^{**}$
Ratio t-biopsy/tB, mean $\pm$ SD	+12% $\pm$ 49%	+12% $\pm$ 51%	$p = 0.97$	+16% $\pm$ 56%	+6% $\pm$ 45%	$p = 0.08$
ICM/TE ratio at tB, mean $\pm$ SD	26% $\pm$ 7%	26% $\pm$ 7%	$p = 0.61$	26% $\pm$ 7%	26% $\pm$ 7%	$p = 0.95$
ICM/TE ratio at tEB, mean $\pm$ SD	21% $\pm$ 6%	21% $\pm$ 6%	$p = 0.36$	20% $\pm$ 6%	20% $\pm$ 6%	$p = 0.50$
ICM/TE ratio at t-biopsy, mean $\pm$ SD	17% $\pm$ 8%	16% $\pm$ 7%	$p = 0.97^*$	16% $\pm$ 7%	15% $\pm$ 6%	$p = 0.47^{**}$

\* adjusted for maternal age and blastocyst morphological quality. \*\* adjusted for blastocyst morphological quality.

When adjusting for maternal age, blastocyst morphological quality, and the zp-A, the zp-A ratio t-biopsy/tB showed a more significant association with euploid constitution than the zp-A per se, with a multivariate-OR 2.2, 95%CI 1.1–4.4, and an adjusted  $p$ -value = 0.02.

When adjusting for maternal age, blastocyst morphological quality and the emb-A, the emb-A ratio t-biopsy/tB showed a more significant association with euploid constitution than the emb-A per se, with a multivariate-OR 2.2, 95%CI 1.3–4.0, and an adjusted  $p$ -value < 0.01.

When adjusting for maternal age, blastocyst morphological quality and the zp-T ratio t-biopsy/tB, the zp-T showed a more significant association with euploid constitution than the ratio itself, with a multivariate-OR 0.92, 95%CI 0.86–0.98, and an adjusted  $p$ -value < 0.01.

### 3.2. The Zona Pellucida Thinning Process in the 5 h Following the tB Was More Substantial Among Euploid Blastocysts than Aneuploid

The definition of the t-biopsy is based on embryologists' assessments, daily workload, and IVF laboratory logistics; therefore, it cannot be fully standardized. Conversely, the tB is specific to each embryo (i.e., "Time from insemination to formation of a full blastocyst; when the blastocoele filled the embryo with <10% increase in its diameter" according to [22] or "last frame before zona starts to thin" according to [3]), and it is automatically annotated by CHLOE. Moreover, blastocysts are never biopsied within 5 h following the tB, as they cannot achieve a suitable stage in such timeframe. These characteristics suggest that the qSEA is a more reliable and less biased strategy for assessing the association between blastocyst expansion dynamics and their competence.

When adopting the qSEA to compare aneuploid versus euploid blastocysts, no difference was reported for the emb-A and the zp-A (Supplemental Figures S3 and S4). Conversely, the zp-T showed a significantly slower and less consistent zona thinning among aneuploid blastocysts, which became significant already 150 min following the tB (even when adjusted for maternal age and blastocyte morphology) (Supplemental Figure S5A). The receiver operating characteristic (ROC) curve analysis showed an area under the curve (AUC) = 0.72, 95%CI 0.69–0.74,  $p < 0.01$  for the prediction of euploidy based on the zp-T qSEA adjusted for maternal age. The same value was 0.75, 95%CI 0.73–0.77,  $p < 0.01$  if

considering the zp-T along with maternal age, blastocyst morphology, and the t-biopsy (Supplemental Figure S5B).

### 3.3. zp-A, emb-A, and zp-T qSEA Were Significantly Associated with Euploid Blastocysts' Reproductive Competence

When adopting the qSEA to compare euploid blastocysts resulting in a LB versus reproductively incompetent blastocysts, all three qSEA showed a significant association (Figures 2A, 3A and 4A). The zp-A qSEA outlined significant differences already after 150 min following the tB (Figure 2A), while the emb-A and the zp-T did so after 180 min (Figures 3A and 4A). The ROC curve analyses showed AUCs to be almost superimposable for all three qSEA models, either per se (AUC = 0.61) or adjusted for confounders (AUC = 0.64–0.65) (Figures 2B and 3B).

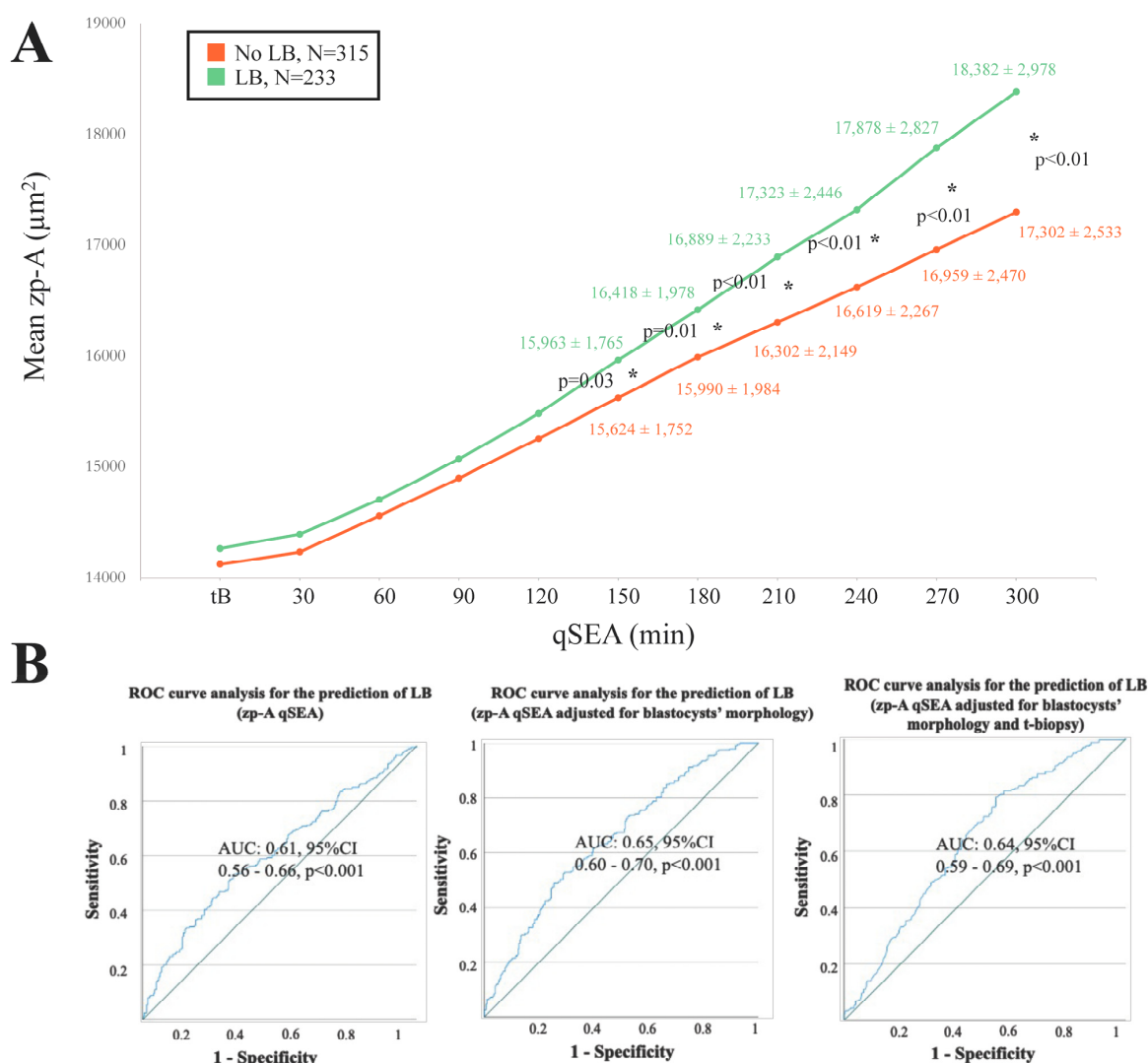


**Figure 2.** (A) The zp-A (area of the embryo including the zona pellucida in  $\mu\text{m}^2$ ) qSEA (quantitative standardized expansion assay) outlined a larger expansion among euploid blastocysts that resulted in a live birth (LB) (green line) versus euploid blastocysts that did not result in a LB (orange line), which became significant 150 min following the time of blastulation (tB). The stars (\*) identify the significant datapoints showing the mean  $\pm$  SD in the two groups at that timing. (B) Receiver Characteristics Operating (ROC) curve analyses outlined a significant association between the zp-A qSEA with a LB after euploid blastocyst transfer unadjusted, adjusted for blastocyst morphology, and adjusted for blastocyst morphology and time of biopsy (t-biopsy). AUC, area under the curve.

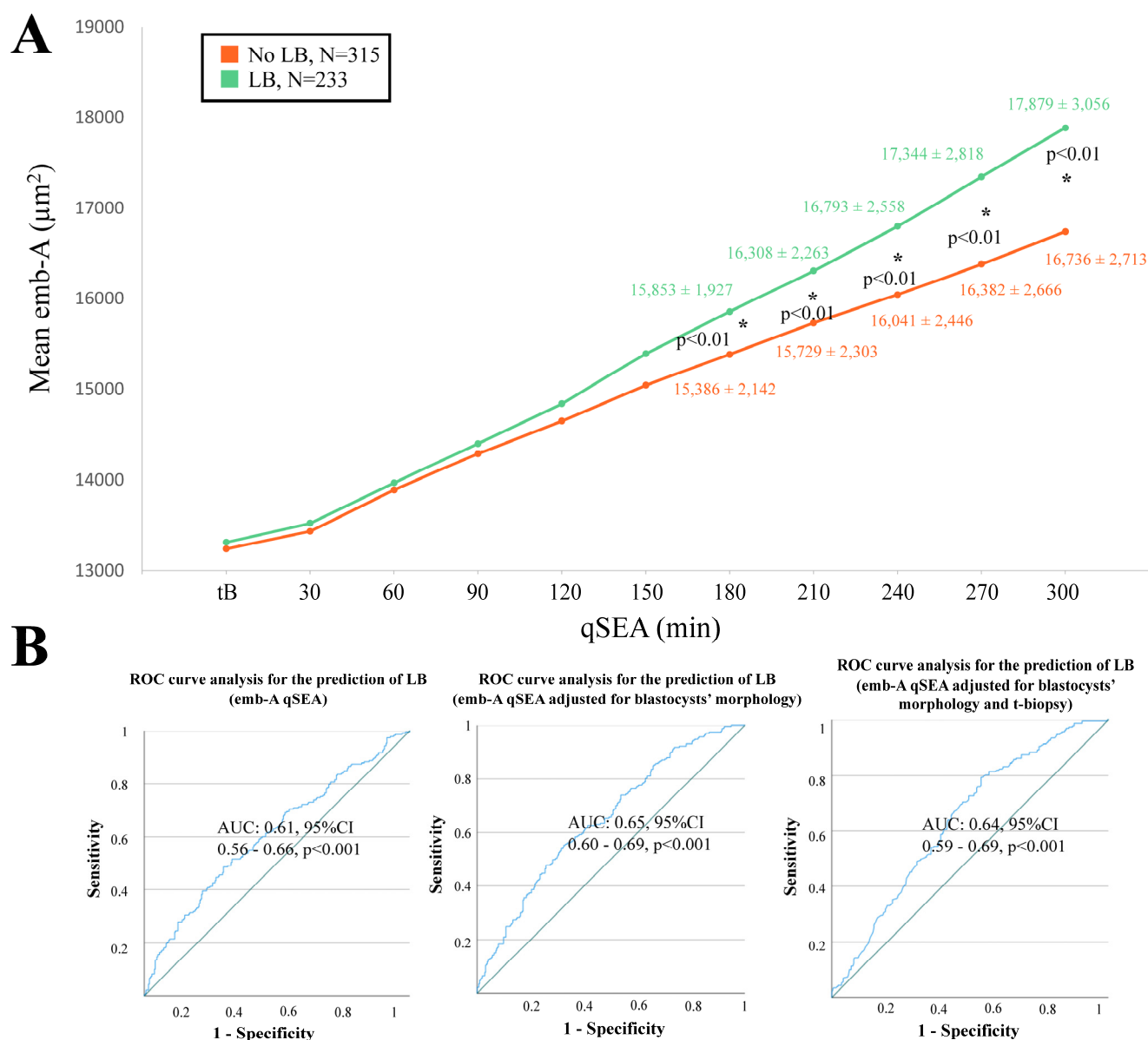


**Figure 3.** (A) The emb-A (area of the embryo proper in  $\mu\text{m}^2$ ) qSEA (quantitative standardized expansion assay) outlined a large expansion among euploid blastocysts that resulted in a live birth (LB) (green line) versus euploid blastocysts that did not result in a LB (orange line), which became significant already 180 min following the time of blastulation (tB). The stars (\*) identify the significant datapoints showing the mean  $\pm$  SD in the two groups at that timing. (B) Receiver Operating Characteristics (ROC) curve analyses outlined a significant association between the emb-A qSEA with a LB after euploid blastocyst transfer unadjusted, adjusted for blastocyst morphology, and adjusted for blastocyst morphology and time of biopsy (t-biopsy). AUC, area under the curve.

### 3.4. The zp-T qSEA Would Have Ranked a Euploid Blastocyst as Top Quality in Its Cohort in 57% of the Cycles with >1 Biopsied Blastocyst and Both Euploid and Aneuploid Embryos

As detailed previously, 352 cycles could be included in a clinical simulation to assess whether the zp-T qSEA (versus the embryologists) would have ranked a euploid blastocyst as top-quality within cohorts with >1 biopsied blastocyst and both euploid and aneuploid embryos (Supplemental Figure S1A). In 24% of the cases (N = 85/352), the embryologists and the zp-T qSEA would have agreed on the highest-ranked blastocyst; in 42% of the cases (N = 147/352), they would have disagreed; and in the remaining 34% of the cases (N = 120/352), the embryologists ranked more than one blastocyst as

top-quality in their cohort (Supplemental Figure S6). Overall, the embryologists' highest ranked blastocysts were: (i) euploid in 45% of the cases ( $N = 159/352$ ) versus 57% for the zp-T qSEA ( $N = 199/352$ ); (ii) aneuploid in 25% of the cases ( $N = 89/352$ ) versus 43% for the zp-T qSEA ( $N = 153/352$ ); and (iii) both euploid and aneuploid in 30% of the cases ( $N = 104/352$ ) versus never for the zp-T qSEA (Supplemental Figure S6). In fact, it is highly unlikely that two blastocysts would be equally ranked by the qSEA, being that this strategy is based on highly specific and objective measurements.

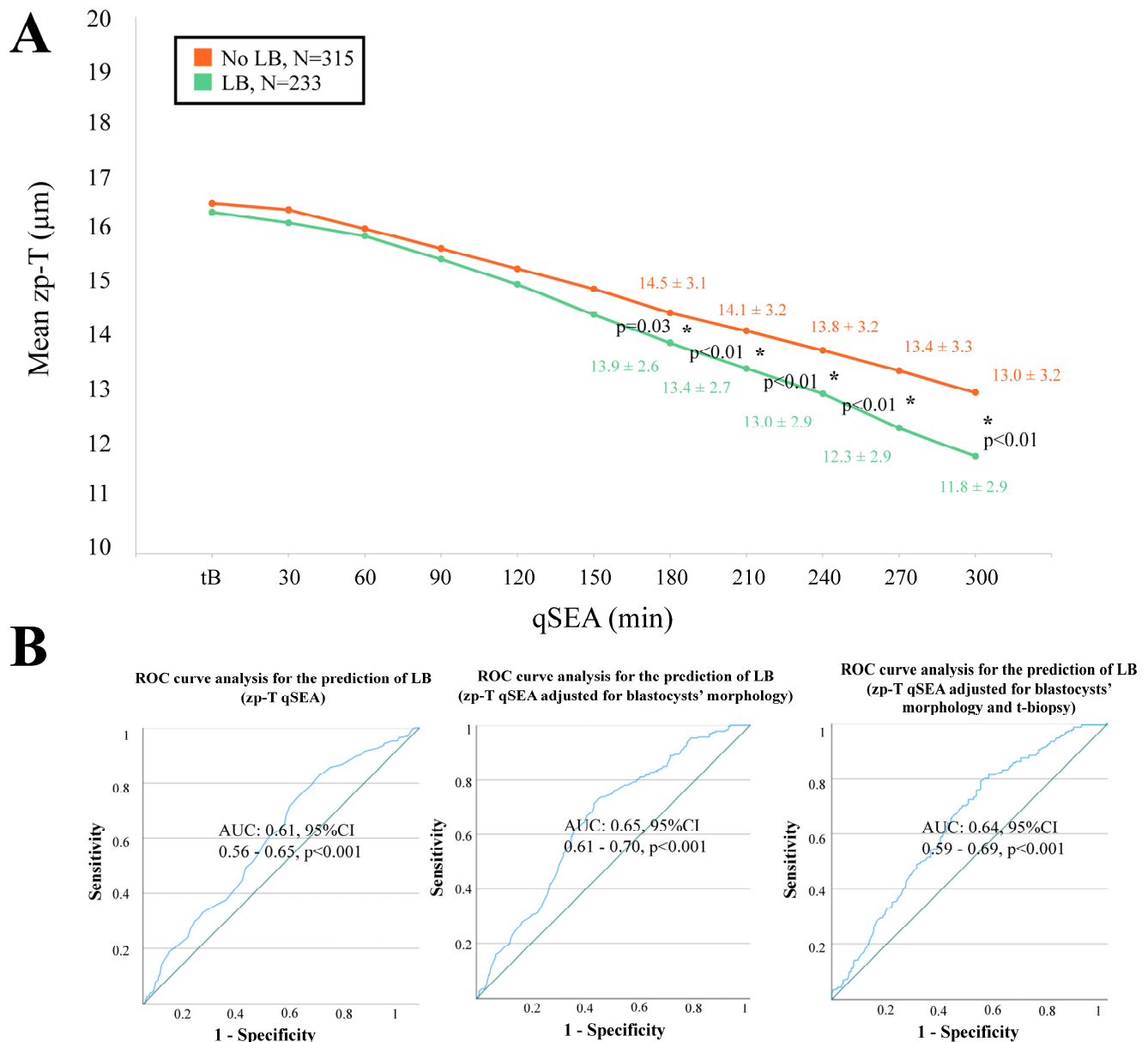


**Figure 4.** (A) The zp-T (thickness of the zona pellucida in  $\mu\text{m}$ ) qSEA (quantitative standardized expansion assay) outlined a more consistent zona thinning among euploid blastocysts that resulted in a live birth (LB) (green line) versus euploid blastocysts that did not result in a LB (orange line), which became significant already 180 min following the time of blastulation (tB). The stars (\*) identify the significant datapoints showing the mean  $\pm$  SD in the two groups at that timing. (B) Receiver Characteristics Operating (ROC) curve analyses outlined a significant association between the zp-T qSEA with a LB after euploid blastocyst transfer unadjusted, adjusted for blastocyst morphology, and adjusted for blastocyst morphology and time of biopsy (t-biopsy). AUC, area under the curve.



### 3.5. In 69% of the Cycles with >1 Biopsied Blastocyst and Both Euploid and Aneuploid Embryos, the zp-T qSEA Ranking Would Be Equal or Better than Embryologist Rankings

When embryologists and the zp-T qSEA were compared for their putative effectiveness in blindly ranking euploid blastocysts as top quality within their cohorts: (i) they would have been equally effective in 43% of the cases (being either both wrong [ $N = 47/352$ , 13%] or both right [ $N = 104/352$ , 30%]); (ii) the embryologists would have been more effective in 15% of the cases ( $N = 52/352$ ); (iii) the zp-T qSEA would have been more effective in 7% of the cases ( $N = 26/352$ ); (iv) the zp-T qSEA would have ranked a euploid on top while the embryologists both a euploid and an aneuploid in 19% of the cases ( $N = 66/352$ ); and (v) the zp-T qSEA would have ranked an aneuploid on top while the embryologists both a euploid and an aneuploid in 16% of the cases ( $N = 57/352$ ) (Supplemental Figure S6). The raw data of this clinical simulation are provided in Supplemental Table S2.

### 3.6. In 46% of the Cases, the zp-A and emb-A qSEAs Would Have Disagreed with the Embryologists in Prioritizing Euploid Blastocysts for Transfer; The zp-T qSEA, Instead, Would Have Disagreed in 60% of the Cases

As detailed previously, 216 cycles could be included in a clinical simulation to assess the zp-A, emb-A, and zp-T qSEAs performance versus the embryologists in prioritizing euploid blastocysts for transfer within cohorts with  $\geq 2$  euploid blastocysts (Figure 2B). Specifically, in 99 cycles there were  $\geq 2$  euploid blastocysts but only 1 had been transferred, in 14 cycles there were  $\geq 2$  euploid blastocysts and all resulted in a LB, in 50 cycles there were  $\geq 2$  euploid blastocysts and all did not result in a LB, and in 53 cycles there were  $\geq 2$  euploid blastocysts resulting in both LBs and implantation failures/miscarriages. In 54% of the cases ( $N = 116/216$ ), the embryologists and the zp-A or the emb-A qSEA would have agreed on euploid blastocyst prioritization for transfer, while in 46% of the cases ( $N = 100/216$ ) they would have disagreed (Supplemental Figure S7A,B). The same results for the zp-T qSEA would have been 40% ( $N = 86/216$ ) and 60% ( $N = 130/216$ ), respectively (Supplemental Figure S7C). In terms of clinical effectiveness, the embryologists prioritized for transfer a competent euploid blastocyst in 47% of the cases ( $N = 102/216$ ). In this scenario, the zp-A and the emb-A qSEA choice would have been correct in 38% of the cases ( $N = 82/216$  and  $81/216$ , respectively). However, this outcome may improve up to 61%, because in 23% of the cases ( $N = 50/216$  for both the zp-A and emb-A) the euploid blastocysts with the highest priority according to the zp-A and emb-A qSEA had not been transferred yet (Supplemental Figure S7A,B). Regarding the zp-T qSEA, instead, its choice would have been correct in 27% of the cases ( $N = 59/216$ ). However, this outcome may improve up to 63%, because in 36% of the cases ( $N = 78/216$ ) the euploid blastocysts with the highest priority according to the zp-T qSEA had not been transferred yet (Supplemental Figure S7C). The raw data of this clinical simulation are provided in Supplemental Figure S7A–C and in Supplemental Tables S3–S5).

## 4. Discussion

Blastocyst morphological quality is significantly associated with both the chromosomal and reproductive competence of embryos [24]; however, it cannot be used alone to accurately predict these outcomes. Currently, blastocyst morphological quality is primarily assessed in IVF laboratories using grading systems such as the Gardner system [21]. Nonetheless, these grading systems are subjective and often vary among clinical embryologists, particularly when they work at different IVF centers or have undergone diverse training programs [2]. To address these limitations, AI-powered tools have been developed to analyze static images or time-lapse videos of embryo development. These tools aim to objectively assess embryo quality and rank embryos within a cohort based on a standardized scoring system. Typically, a higher score indicates a greater likelihood that the embryo is euploid and/or will successfully implant after embryo transfer [7,25]. In this study, we evaluated a qSEA model, determined its association with embryo euploidy

and its potential to predict live birth outcomes. Both a comprehensive analysis and an intra-cohort clinical simulation were performed to test its effectiveness.

#### 4.1. Clinical Implications of the Evidence Produced in This Study

Blastocyst expansion dynamics might provide relevant information on embryo reproductive competence. Indeed, several studies suggested that, among blastocyst morphological characteristics, expansion represents an intriguing feature to consider when ranking embryos in terms of priority for transfer [8,26,27] in both conventional and PGT-A cycles. Based on these preliminary data from the literature, we aimed at producing objective, morphometric and reproducible information on the expansion process, to reliably assess a putative association between these embryo-specific dynamics and its chromosomal (i.e., euploidy) and/or reproductive competence (i.e., LB after euploid blastocyst transfer). Huang's former positive experience with the qSEA [9,15,16], and the possibility of integrating this method with AI-standardized and -powered analyses and PGT-A, incited us to test it for its association with blastocyst competence in our setting and patient population. Our study improved Huang's previous experience through a large sample size ( $N = 2184$ ), the use of PGT-A to assess the chromosomal constitution of all blastocysts, and the adoption of a TE biopsy protocol that does not entail assisted hatching on Day 3, thereby not affecting the process of blastocyst physiological expansion.

Besides confirming that aneuploid and euploid reproductively incompetent embryos are generally slower in reaching all blastulation timings milestones from tSB to t-biopsy [28,29], our data have highlighted an association between euploidy and larger zp-A and emb-A, as well as thinner zp at t-biopsy. Also, the zp-A and emb-A ratio t-biopsy/tB and the zp-T ratio t-biopsy/tB outlined larger expansion and more consistent zona thinning among euploid blastocysts versus aneuploid. Possibly, different issues—either chromosomal, metabolic, or structural—affect embryo timeliness in setting up TE epithelium architecture. This in turn could affect its possibility to cope with the increased hydrostatic pressure, essential for the expansion process. This hypothesis is consistent with a recent study [30], where the authors attempted to define to what extent blastocyst expansion dynamics could be affected by different classes of aneuploidies. Interestingly, all classes of aneuploidies, except for trisomies, significantly impaired the expansion process compared to euploid blastocysts. As has already been shown across several studies in the literature, TE characteristics seem more relevant than ICM in terms of association with embryo reproductive competence [8,31,32]. Indeed, the ICM-A and the ICM/TE ratio showed no association with all outcomes under investigation. This evidence might mirror the predominant role of the TE over the ICM in the process of implantation when it must establish a timely and effective dialogue with the endometrium.

Although blastocyst static morphometric evaluation before vitrification or biopsy in the absence of time-lapse incubators might also be clinically relevant, it is inherently biased by logistic issues, like daily workload, lab schedule, and embryologist decisions. The qSEA instead represents a less biased and more embryo-centred assessment, because the tB is reached by all useable blastocysts, regardless of their developmental pace, and more than 5 h always elapse from this timing and biopsy. Interestingly, consistent with Huang's previous experience, the expansion maps showed significant associations between the zp-A, emb-A, and zp-T qSEAs and euploid blastocyst reproductive competence, even when adjusted for blastocyst morphology and t-biopsy (i.e., the main embryological confounders upon euploid embryo implantation potential), already 150–180 min following the tB. The zp-T qSEA outlined significant associations with the euploidy as well. Although this overall association already has important implications in terms of basic knowledge (which we will discuss below), we were interested in defining the putative clinical relevance of qSEA had we used it clinically in our setting. In fact, to improve the performance of embryologists with embryo ranking and prioritization for transfer, the information provided by this tool (as any other embryo selection tool) must be clinically effective when used within a given cohort of embryos produced by a couple. To this end, we conducted two clinical

simulations (as previously done for iDAScore v1.0 [23]): (i) among cycles with  $\geq 2$  biopsied blastocysts, of which both euploid and aneuploid, to test zp-T qSEA euploidy prediction; and (ii) among cycles  $\geq 2$  euploid blastocysts, of which  $\geq 1$  transferred, to test all qSEA LB prediction. Notably, the zp-T qSEA would have disagreed with the embryologists in ranking embryos in 42% of cases, while it would have represented a swing vote between two blastocysts equally ranked on top by the operators in a further 34% of the cases. This information is interesting, especially considering that the zp-T qSEA ranked euploid blastocysts on top in 57% of the cases and it would have been right with the embryologists being either wrong or uncertain in 26% of the cases. In our population of advanced maternal age women, these data are even more intriguing. When tested for its prediction of a LB in the context of euploid blastocyst transfers among cohorts with  $\geq 2$  euploid embryos, the zp-A and emb-A qSEAs disagreed with the embryologists in embryo prioritization in 46% of the cases, a rate that increased to 60% for the zp-T qSEA. Again, this is interesting because it outlines a scenario where there is room for improving embryo selection when adopting this tool with respect to embryologist evaluations. In 38% and 27% of the cases, the zp-A or emb-A qSEAs and zp-T qSEA, respectively, would have correctly prioritized for transfer a competent euploid blastocyst. Both these rates may significantly increase in the future considering that in 23% and 36% of the cases, the blastocysts that would have been chosen based on the zp-A or emb-A qSEAs and the zp-T qSEA, respectively, had not been transferred yet. In the case of a positive outcome after transfer, these instances will increase the prevalence of events where the qSEA would have outperformed the embryologists (currently 8% and 10% for the zp-A or emb-A qSEAs and zp-T qSEA, respectively). Only a future RCT comparing embryologist rankings versus qSEA rankings to prioritize the first blastocyst for transfer in the context of either conventional or PGT-A cycles would ultimately unveil the true clinical benefit of this tool. Until then, these preliminary data should be considered only promising.

The main limitation of this study is inherent to its retrospective nature. Moreover, this study represents the second experience worldwide with the qSEA; confirmatory evidence should therefore be derived from further investigation at other centres and in other settings to validate these findings.

#### 4.2. Basic Science Data Supporting the Evidence Produced in This Study

The cavitation and expansion processes are regulated by several genes, including E-cadherin, catenin, tight junction proteins, and the sodium–potassium ATPase transport system [33]. The initiation of blastulation is characterized by the formation of a small cavity or multiple microlumens eventually merging. A study on mice has proposed that vesicles or vacuoles are involved in blastocoel formation as they are released by exocytosis at the level of the basal membrane, thereby producing the microlumens [34]. More recently, another group proposed a “hydro-osmotic coarsening theory” suggesting that osmotic pressure at the level of the intercellular cell junctions transiently disrupts cell–cell contact, forming numerous small lumens [35]. These lumens then undergo intercellular ion and fluid exchange, eventually coalescing into a single lumen, i.e., the blastocoel cavity. After the initial microlumen formation, further expansion results from the active Na/K-ATPase transport mechanism located on the basolateral surface of the TE epithelium. This generates a sodium gradient, in turn ensuring water influx from the external environment into the microlumen [36,37]. Along with the osmotic gradient, water channels known as aquaporins (AQPs) facilitate water influx through the outer cells. Various AQP isoforms are expressed during preimplantation development in mice, and each isoform may play a unique role because of their temporally and spatially distinct expression patterns [38]. Simultaneously, the adherens junction, tight junction, desmosomes, and gap junction, form a seal between the TE cells, which are pivotal for fluid intake and blastocoel formation and expansion [33]. From a basic cellular perspective, the chromosome instability at the origin of aneuploidies seems to universally compromise cellular fitness [39–41]. It is reasonable to hypothesize that the resulting imbalances in both transcription and translation can affect both the cellularity

and function of the emerging TE to produce and maintain the blastocoel fluid that will be critical both for hatching and for productive, sustained invasion of the endometrium. Transcription defects affecting the various players involved in these processes, as well as external environmental insults may impact the cavitation process and alter the viscoelastic properties of the blastocyst [42–44]. Throughout blastocyst expansion, the blastocyst applies hydrostatic mechanical pressure on the zp, progressively leading to its thinning up to the creation of a nick [45]. Following, expansion allows the embryo to hatch and possibly implant. In mice, this hatching process is facilitated by the timely secretion of implantation-related molecules, such as cytokines [45] and zonolytic proteases, like strypsin, hepsin, and cathepsin [46] by both TE and endometrial cells [45,47]. Proteases might be involved in this process in humans as well, according to recent data [48]. In general, the extent of zp thinning might mirror the timeliness of these finely regulated spatiotemporal processes, providing relevant information to predict blastocysts reproductive potential in mammals, including humans [49]. Previous studies have suggested that zp-T and zp-T variation may be useful additional parameters for embryo assessment, in addition to conventional morphological grading. Indeed, embryos with a thinner zp or greater zp-T variation showed a greater chance of implantation and evolution in an ongoing pregnancy than embryos with thicker zp [50–53]. In general, a thinner zp, even if localized just to some areas, might facilitate hatching, as well as the transportation and release of lytic enzymes and/or messengers (e.g., miRNAs), ultimately supporting implantation [50,54]. In summary, the process of blastulation, expansion, and hatching certainly deserve future deeper biomechanical investigations, as their characterization holds potential for generating relevant evidence for embryo selection purposes as well.

#### 4.3. Future Perspectives of Molecular Investigations

In the future, integrating molecular data, particularly transcriptomic analyses, with genomic and chromosomal assessments from a single biopsy may significantly enhance our understanding of early embryonic development and implantation processes [55]. Current clinical investigations still fail to capture the complete picture of embryonic competence. In-depth transcriptomic data could identify molecular markers that explain why certain embryos exhibit varying developmental rates, distinct levels of blastocyst expansion, and heterogeneous overall morphological quality, despite being derived from the same cohort of oocytes and exposed to the same in vitro culture conditions. These differences in gene expression may reveal underlying metabolic, cellular, or epigenetic factors with significant implications for embryo selection [56,57].

## 5. Conclusions

Blastocyst expansion dynamics, timing, and morphometrics measured by AI provide objective and quantitative data related to embryo competence. qSEA is a promising, user-friendly, and easily applicable strategy that deserves further evaluation. Basic research into the mechanisms controlling blastocyst expansion is also warranted.

**Supplementary Materials:** The following supporting information can be downloaded at: <https://www.mdpi.com/article/10.3390/life14111396/s1>, Supplemental Figure S1. Study Flowchart. The figure summarizes the study flowchart and the number of preimplantation genetic testing for aneuploidies (PGT-A) cycles that could be included in the clinical simulations for euploidy (A) and live birth (LB) (B) prediction. Supplemental Figure S2. Euploid blastocysts (green boxplots) expand more (larger zp-A and emb-A, respectively area of the embryo in  $\mu\text{m}^2$  with or without the zona pellucida) between the time of blastulation (tB) and the time of biopsy (t-biopsy) and undergo a more consistent zona pellucida thinning (zp-T, thickness of the ZP in  $\mu\text{m}$ ) than aneuploid blastocysts (red boxplots). Supplemental Figure S3. (A) The zp-A (area of the embryo including the zona pellucida in  $\mu\text{m}^2$ ) qSEA (quantitative standardized expansion assay) did not outline any significant difference between euploid (green line) and aneuploid (red line) blastocysts. Supplemental Figure S4. (A) The emb-A (area of the embryo proper in  $\mu\text{m}^2$ ) qSEA (quantitative standardized expansion assay) did not outline any significant difference between euploid (green line) and aneuploid (red line) blastocysts.

Supplemental Figure S5. (A) The zp-T (thickness of the zona pellucida in  $\mu\text{m}$ ) qSEA (quantitative standardized expansion assay) outlined a more consistent zona thinning among euploid blastocysts (green line) versus aneuploid blastocysts (red line), that became significant already 150 min following the time of blastulation (tB). The stars (\*) identify the significant datapoints showing the mean  $\pm$  SD in the two groups at that timing. (B) Receiver Characteristics Operating (ROC) curve analyses outlined a significant association between the zp-T qSEA with euploidy when adjusted only for maternal age, for maternal age blastocysts' morphology, as well as for maternal age, blastocysts' morphology and time of biopsy (t-biopsy). AUC, area under the curve. Supplemental Figure S6. Outcomes of a clinical simulation to assess zp-T (zona pellucida thickness in  $\mu\text{m}$ ) qSEA (quantitative standardized expansion assay) performance versus the embryologists (E) in ranking euploid blastocysts on top among cohorts with both euploid and aneuploid siblings. Ranking concordance was not assessable any time  $\geq 2$  embryos were ranked on top by the embryologists, among which one was the zp-T qSEA highest ranked blastocyst (black bar of the histogram). Effectiveness in prioritizing the euploid blastocyst was not assessable any time  $\geq 2$  embryos were ranked on top by the embryologists, of which  $\geq 1$  was euploid and  $\geq 1$  was aneuploid (dark grey section of the pie chart; blue and brown bars of the histogram). Raw data are shown in Supplemental Table S2. Supplemental Figure S7. Outcomes of a clinical simulation to assess (A) zp-A (area of the embryo including the zona pellucida in  $\mu\text{m}^2$ ) qSEA (quantitative standardized expansion assay), (B) emb-A (area of the embryo proper in  $\mu\text{m}^2$ ) qSEA, and (C) zp-T (zona pellucida thickness in  $\mu\text{m}$ ) qSEA performance versus the embryologists (E) in ranking euploid blastocysts resulting a live birth (LB) on top among cohorts with  $\geq 2$  euploid siblings. Effectiveness in prioritizing the competent euploid blastocyst was not assessable any time the highest ranked embryo according to the qSEA has not been transferred yet (dark grey sections of the pie charts; dark grey bars of the histograms). Raw data are shown in Supplemental Tables S3–S5. Supplemental Table S1. Patients' characteristics. Supplemental Table S2. Distribution of the PGT-A cycles in the clinical simulation for the comparison of embryologists' (E) versus zp-T qSEA's performance in ranking euploid blastocysts on top. The results are summarized in Supplementary Figure S3. \*  $\geq 2$  embryos ranked on top according to the embryologists, that included also the embryo ranked on top according to the zp-T qSEA. ^  $\geq 2$  embryos ranked on top according to the embryologists, of which  $\geq 1$  euploid and  $\geq 1$  aneuploid. Supplemental Table S3. Distribution of the PGT-A cycles in the clinical simulation for the comparison of embryologists' (E) versus zp-A qSEA's performance in ranking euploid blastocysts that resulted in a live birth (LB) on top. The results are summarized in Supplementary Figure S4A. Supplemental Table S4. Distribution of the PGT-A cycles in the clinical simulation for the comparison of embryologists' (E) versus emb-A qSEA's performance in ranking euploid blastocysts that resulted in a live birth (LB) on top. The results are summarized in Supplementary Figure S4B. Supplemental Table S5. Distribution of the PGT-A cycles in the clinical simulation for the comparison of embryologists' (E) versus zp-T qSEA's performance in ranking euploid blastocysts that resulted in a live birth (LB) on top. The results are summarized in Supplementary Figure S4C.

**Author Contributions:** Conceptualization, D.C., T.H., A.V., G.G. and L.R.; Data curation, D.C., S.T., T.C., F.I., G.S., M.T., D.M.S. and L.A.; Formal analysis, D.C., S.T., T.C., F.I. and M.T.; Investigation, D.C., S.T., T.C., F.I. and M.T.; Methodology, D.C., S.T., T.C., F.I., M.T., B.K. and T.H.; Project administration, D.C. and L.R.; Resources, D.C.; Software, B.K., M.D. and A.S.; Supervision, D.C., F.I., M.T., L.A., B.K., M.D., A.S., T.H., A.V., G.G. and L.R.; Validation, D.C., S.T., T.C., F.I., M.T., B.K., M.D., A.S., T.H. and L.R.; Visualization, F.I. and M.T.; Writing—original draft, D.C., S.T. and T.C.; Writing—review & editing, D.C., F.I., M.T., B.K., M.D., A.S., T.H., A.V., G.G. and L.R. All authors have read and agreed to the published version of the manuscript.

**Funding:** This research received no external funding.

**Institutional Review Board Statement:** The study was conducted in accordance with the Declaration of Helsinki and approved by the Comitato Etico Territoriale Lazio Area 1; Prot. 0747/2023, Rif. 7283; Date: 20 September 2023.

**Informed Consent Statement:** Data Protection approval was obtained for the retrospective analysis of pseudonymized videos and data to investigate the efficacy and efficiency of IVF protocols and strategies.

**Data Availability Statement:** The data underlying this article are available in the article and in its online Supplementary Materials.

**Conflicts of Interest:** B.K., M.D., A.S. were employed by Fairtivity. The remaining authors declare that the research was conducted in the absence of any commercial or financial relationships that could be construed as a potential conflict of interest.

## Abbreviations

IVF, in vitro fertilization; LB, live birth; ET, embryo transfer; PGT-A, preimplantation genetic testing for aneuploidies; TLM, time lapse microscopy; AI, artificial intelligence; ICM, inner cell mass; qSEA, quantitative standardized expansion assay; GnRH, gonadotrophins releasing hormone; hCG, human chorionic gonadotrophin; zp, zona pellucida; CCT, comprehensive chromosome testing; qPCR, quantitative polymerase chain reaction; NGS, next generation sequencing; ICN, intermediate copy number; tSB, time of starting blastulation; tB, time of blastulation; tEB, time of expanding blastocyst; t-biopsy, time of biopsy; TE, trophoctoderm; zp-A, are of the zona pellucida; zq-T, thickness of the zona pellucida; emb-A, area of the embryo; ICM-A, area of the inner cell mass; ICM:TE, ratio between the area of the inner cell mass and the area of the trophoctoderm; BMI, body mass index; ROC, receiver operating characteristic; AUC, area under the curve.

## References

- Gardner, D.K.; Meseguer, M.; Rubio, C.; Treff, N.R. Diagnosis of human preimplantation embryo viability. *Hum. Reprod. Update* **2015**, *21*, 727–747. [CrossRef] [PubMed]
- Khosravi, P.; Kazemi, E.; Zhan, Q.; Malmsten, J.E.; Toschi, M.; Zisimopoulos, P.; Sigaras, A.; Lavery, S.; Cooper, L.A.D.; Hickman, C.; et al. Deep learning enables robust assessment and selection of human blastocysts after in vitro fertilization. *NPJ Digit. Med.* **2019**, *2*, 21. [CrossRef]
- Apter, S.; Ebner, T.; Freour, T.; Guns, Y.; Kovacic, B.; Le Clef, N.; Marques, M.; Meseguer, M.; Montjean, D.; Sfontouris, I.; et al. Eshre Working group on Time-lapse technology: Good practice recommendations for the use of time-lapse technology. *Hum. Reprod. Open* **2020**, *2020*, hoaa008. [CrossRef]
- Armstrong, S.; Bhide, P.; Jordan, V.; Pacey, A.; Marjoribanks, J.; Farquhar, C. Time-lapse systems for embryo incubation and assessment in assisted reproduction. *Cochrane Database Syst. Rev.* **2019**, *5*, CD011320. [CrossRef] [PubMed]
- Ahlstrom, A.; Lundin, K.; Lind, A.K.; Gunnarsson, K.; Westlander, G.; Park, H.; Thurin-Kjellberg, A.; Thorsteinsdottir, S.A.; Einarsson, S.; Astrom, M.; et al. A double-blind randomized controlled trial investigating a time-lapse algorithm for selecting Day 5 blastocysts for transfer. *Hum. Reprod.* **2022**, *37*, 708–717. [CrossRef] [PubMed]
- Coticchio, G.; Barrie, A.; Lagalla, C.; Borini, A.; Fishel, S.; Griffin, D.; Campbell, A. Plasticity of the human preimplantation embryo: Developmental dogmas, variations on themes and self-correction. *Hum. Reprod. Update* **2021**, *27*, 848–865. [CrossRef]
- Kragh, M.F.; Karstoft, H. Embryo selection with artificial intelligence: How to evaluate and compare methods? *J. Assist. Reprod. Genet.* **2021**, *38*, 1675–1689. [CrossRef]
- Ahlstrom, A.; Westin, C.; Reiser, E.; Wikland, M.; Hardarson, T. Trophoctoderm morphology: An important parameter for predicting live birth after single blastocyst transfer. *Hum. Reprod.* **2011**, *26*, 3289–3296. [CrossRef]
- Huang, T.T.; Chinn, K.; Kosasa, T.; Ahn, H.J.; Kessel, B. Morphokinetics of human blastocyst expansion in vitro. *Reprod. Biomed. Online* **2016**, *33*, 659–667. [CrossRef]
- Cockburn, K.; Rossant, J. Making the blastocyst: Lessons from the mouse. *J. Clin. Investig.* **2010**, *120*, 995–1003. [CrossRef]
- Mio, Y.; Maeda, K. Time-lapse cinematography of dynamic changes occurring during in vitro development of human embryos. *Am. J. Obstet. Gynecol.* **2008**, *199*, 660.e1–660.e5. [CrossRef]
- Marcos, J.; Perez-Albala, S.; Mifsud, A.; Molla, M.; Landeras, J.; Meseguer, M. Collapse of blastocysts is strongly related to lower implantation success: A time-lapse study. *Hum. Reprod.* **2015**, *30*, 2501–2508. [CrossRef] [PubMed]
- Gazzo, E.; Pena, F.; Valdez, F.; Chung, A.; Velit, M.; Ascenzo, M.; Escudero, E. Blastocyst contractions are strongly related with aneuploidy, lower implantation rates, and slow-cleaving embryos: A time lapse study. *JBRA Assist. Reprod.* **2020**, *24*, 77–81. [CrossRef] [PubMed]
- Bodri, D.; Sugimoto, T.; Yao Serna, J.; Kawachiya, S.; Kato, R.; Matsumoto, T. Blastocyst collapse is not an independent predictor of reduced live birth: A time-lapse study. *Fertil. Steril.* **2016**, *105*, 1476–1483.e3. [CrossRef] [PubMed]
- Huang, T.T.; Huang, D.H.; Ahn, H.J.; Arnett, C.; Huang, C.T. Early blastocyst expansion in euploid and aneuploid human embryos: Evidence for a non-invasive and quantitative marker for embryo selection. *Reprod. Biomed. Online* **2019**, *39*, 27–39. [CrossRef]
- Huang, T.T.F.; Kosasa, T.; Walker, B.; Arnett, C.; Huang, C.T.F.; Yin, C.; Harun, Y.; Ahn, H.J.; Ohta, A. Deep learning neural network analysis of human blastocyst expansion from time-lapse image files. *Reprod. Biomed. Online* **2021**, *42*, 1075–1085. [CrossRef] [PubMed]
- Maggiulli, R.; Cimadomo, D.; Fabozzi, G.; Papini, L.; Dovere, L.; Ubaldi, F.M.; Rienzi, L. The effect of ICSI-related procedural timings and operators on the outcome. *Hum. Reprod.* **2020**, *35*, 32–43. [CrossRef]
- Maggiulli, R.; Giancani, A.; Cimadomo, D.; Ubaldi, F.M.; Rienzi, L. Human Blastocyst Biopsy and Vitrification. *J. Vis. Exp.* **2019**, *146*, e59625. [CrossRef]

19. Treff, N.R.; Tao, X.; Ferry, K.M.; Su, J.; Taylor, D.; Scott, R.T., Jr. Development and validation of an accurate quantitative real-time polymerase chain reaction-based assay for human blastocyst comprehensive chromosomal aneuploidy screening. *Fertil. Steril.* **2012**, *97*, 819–824. [CrossRef]
20. Capalbo, A.; Poli, M.; Rienzi, L.; Girardi, L.; Patassini, C.; Fabiani, M.; Cimadomo, D.; Benini, F.; Farcomeni, A.; Cuzzi, J.; et al. Mosaic human preimplantation embryos and their developmental potential in a prospective, non-selection clinical trial. *Am. J. Hum. Genet.* **2021**, *108*, 2238–2247. [CrossRef]
21. Gardner, D.K.; Schoolcraft, B. In vitro culture of human blastocysts. In *Toward Reproductive Certainty: Fertility and Genetics Beyond*; Parthenon Press: Carnforth, UK, 1999; pp. 378–388.
22. Campbell, A.; Fishel, S.; Bowman, N.; Duffy, S.; Sedler, M.; Hickman, C.F. Modelling a risk classification of aneuploidy in human embryos using non-invasive morphokinetics. *Reprod. Biomed. Online* **2013**, *26*, 477–485. [CrossRef] [PubMed]
23. Cimadomo, D.; Chiappetta, V.; Innocenti, F.; Saturno, G.; Taggi, M.; Marconetto, A.; Casciani, V.; Albricci, L.; Maggiulli, R.; Coticchio, G.; et al. Towards Automation in IVF: Pre-Clinical Validation of a Deep Learning-Based Embryo Grading System during PGT-A Cycles. *J. Clin. Med.* **2023**, *12*, 1806. [CrossRef] [PubMed]
24. Zhan, Q.; Sierra, E.T.; Malmsten, J.; Ye, Z.; Rosenwaks, Z.; Zaninovic, N. Blastocyst score, a blastocyst quality ranking tool, is a predictor of blastocyst ploidy and implantation potential. *F S Rep.* **2020**, *1*, 133–141. [CrossRef]
25. Salih, M.; Austin, C.; Warty, R.R.; Tiktin, C.; Rolnik, D.L.; Momeni, M.; Rezaatofghi, H.; Reddy, S.; Smith, V.; Vollenhoven, B.; et al. Embryo selection through artificial intelligence versus embryologists: A systematic review. *Hum. Reprod. Open* **2023**, *2023*, hoad031. [CrossRef]
26. Lagalla, C.; Barberi, M.; Orlando, G.; Sciajno, R.; Bonu, M.A.; Borini, A. A quantitative approach to blastocyst quality evaluation: Morphometric analysis and related IVF outcomes. *J. Assist. Reprod. Genet.* **2015**, *32*, 705–712. [CrossRef]
27. Zhao, J.; Yan, Y.; Huang, X.; Sun, L.; Li, Y. Blastocoele expansion: An important parameter for predicting clinical success pregnancy after frozen-warmed blastocysts transfer. *Reprod. Biol. Endocrinol.* **2019**, *17*, 15. [CrossRef] [PubMed]
28. Coticchio, G.; Ezoe, K.; Lagalla, C.; Zaca, C.; Borini, A.; Kato, K. The destinies of human embryos reaching blastocyst stage between Day 4 and Day 7 diverge as early as fertilization. *Hum. Reprod.* **2023**, *38*, 1690–1699. [CrossRef]
29. Bamford, T.; Barrie, A.; Montgomery, S.; Dhillon-Smith, R.; Campbell, A.; Easter, C.; Coomarasamy, A. Morphological and morphokinetic associations with aneuploidy: A systematic review and meta-analysis. *Hum. Reprod. Update* **2022**, *28*, 656–686. [CrossRef]
30. Hori, K.; Hori, K.; Kosasa, T.; Walker, B.; Ohta, A.; Ahn, H.J.; Huang, T.T.F. Comparison of euploid blastocyst expansion with subgroups of single chromosome, multiple chromosome, and segmental aneuploids using an AI platform from donor egg embryos. *J. Assist. Reprod. Genet.* **2023**, *40*, 1407–1416. [CrossRef]
31. Baatarsuren, M.; Sengebaljir, D.; Ganbaatar, C.; Tserendorj, T.; Erdenekhuyag, B.; Baljinnyam, L.; Radnaa, E.; Dorjpurev, A.; Ganbat, G.; Boris, T.; et al. The trophectoderm could be better predictable parameter than inner cellular mass (ICM) for live birth rate and gender imbalance. *Reprod. Biol.* **2022**, *22*, 100596. [CrossRef]
32. Thompson, S.M.; Onwubalili, N.; Brown, K.; Jindal, S.K.; McGovern, P.G. Blastocyst expansion score and trophectoderm morphology strongly predict successful clinical pregnancy and live birth following elective single embryo blastocyst transfer (eSET): A national study. *J. Assist. Reprod. Genet.* **2013**, *30*, 1577–1581. [CrossRef] [PubMed]
33. Watson, A.J.; Barcroft, L.C. Regulation of blastocyst formation. *Front. Biosci.* **2001**, *6*, 708–730. [CrossRef]
34. Aziz, M.; Alexandre, H. The origin of the nascent blastocoele in preimplantation mouse embryos ultrastructural cytochemistry and effect of chloroquine. *Roux Arch. Dev. Biol.* **1991**, *200*, 77–85. [CrossRef] [PubMed]
35. Le Verge-Serandour, M.; Turlier, H. A hydro-osmotic coarsening theory of biological cavity formation. *PLoS Comput. Biol.* **2021**, *17*, e1009333. [CrossRef]
36. Manejwala, F.M.; Cragoe, E.J., Jr.; Schultz, R.M. Blastocoele expansion in the preimplantation mouse embryo: Role of extracellular sodium and chloride and possible apical routes of their entry. *Dev. Biol.* **1989**, *133*, 210–220. [CrossRef]
37. Wiley, L.M. Cavitation in the mouse preimplantation embryo: Na/K-ATPase and the origin of nascent blastocoele fluid. *Dev. Biol.* **1984**, *105*, 330–342. [CrossRef] [PubMed]
38. Barcroft, L.C.; Offenberg, H.; Thomsen, P.; Watson, A.J. Aquaporin proteins in murine trophectoderm mediate transepithelial water movements during cavitation. *Dev. Biol.* **2003**, *256*, 342–354. [CrossRef]
39. Torres, E.M.; Williams, B.R.; Amon, A. Aneuploidy: Cells losing their balance. *Genetics* **2008**, *179*, 737–746. [CrossRef]
40. Williams, B.R.; Prabhu, V.R.; Hunter, K.E.; Glazier, C.M.; Whittaker, C.A.; Housman, D.E.; Amon, A. Aneuploidy affects proliferation and spontaneous immortalization in mammalian cells. *Science* **2008**, *322*, 703–709. [CrossRef]
41. Ben-David, U.; Amon, A. Context is everything: Aneuploidy in cancer. *Nat. Rev. Genet.* **2020**, *21*, 44–62. [CrossRef]
42. Vinals Gonzalez, X.; Odia, R.; Cawood, S.; Gaunt, M.; Saab, W.; Seshadri, S.; Serhal, P. Contraction behaviour reduces embryo competence in high-quality euploid blastocysts. *J. Assist. Reprod. Genet.* **2018**, *35*, 1509–1517. [CrossRef] [PubMed]
43. DiZio, S.M.; Tasca, R.J. Sodium-dependent amino acid transport in preimplantation mouse embryos. III. Na<sup>+</sup>-K<sup>+</sup>-ATPase-linked mechanism in blastocysts. *Dev. Biol.* **1977**, *59*, 198–205. [CrossRef] [PubMed]
44. Kort, J.; Behr, B. Biomechanics and developmental potential of oocytes and embryos. *Fertil. Steril.* **2017**, *108*, 738–741. [CrossRef]
45. Seshagiri, P.B.; Vani, V.; Madhulika, P. Cytokines and Blastocyst Hatching. *Am. J. Reprod. Immunol.* **2016**, *75*, 208–217. [CrossRef] [PubMed]

46. Shafei, R.A.; Syrkasheva, A.G.; Romanov, A.Y.; Makarova, N.P.; Dolgushina, N.V.; Semenova, M.L. Blastocyst Hatching in Humans. *Ontogenez* **2017**, *48*, 8–20. [CrossRef]
47. Yang, G.; Chen, J.; He, Y.; Luo, H.; Yuan, H.; Chen, L.; Huang, L.; Mao, F.; Hu, S.; Qian, Y.; et al. Neddylation Inhibition Causes Impaired Mouse Embryo Quality and Blastocyst Hatching Failure Through Elevated Oxidative Stress and Reduced IL-1 $\beta$ . *Front. Immunol.* **2022**, *13*, 925702. [CrossRef]
48. Almagor, M.; Levin, Y.; Halevy Amiran, R.; Fieldust, S.; Harir, Y.; Or, Y.; Shoham, Z. Spontaneous in vitro hatching of the human blastocyst: The proteomics of initially hatching cells. *Vitr. Cell Dev. Biol. Anim.* **2020**, *56*, 859–865. [CrossRef]
49. Seshagiri, P.B.; Sen Roy, S.; Sireesha, G.; Rao, R.P. Cellular and molecular regulation of mammalian blastocyst hatching. *J. Reprod. Immunol.* **2009**, *83*, 79–84. [CrossRef] [PubMed]
50. Cohen, J.; Inge, K.L.; Suzman, M.; Wiker, S.R.; Wright, G. Videocinematography of fresh and cryopreserved embryos: A retrospective analysis of embryonic morphology and implantation. *Fertil. Steril.* **1989**, *51*, 820–827. [CrossRef]
51. Palmstierna, M.; Murkes, D.; Csemiczky, G.; Andersson, O.; Wramsby, H. Zona pellucida thickness variation and occurrence of visible mononucleated blastomers in preembryos are associated with a high pregnancy rate in IVF treatment. *J. Assist. Reprod. Genet.* **1998**, *15*, 70–75. [CrossRef]
52. Bertrand, E.; Van den Bergh, M.; Englert, Y. Does zona pellucida thickness influence the fertilization rate? *Hum. Reprod.* **1995**, *10*, 1189–1193. [CrossRef] [PubMed]
53. Gabrielsen, A.; Bhatnager, P.R.; Petersen, K.; Lindenberg, S. Influence of zona pellucida thickness of human embryos on clinical pregnancy outcome following in vitro fertilization treatment. *J. Assist. Reprod. Genet.* **2000**, *17*, 323–328. [CrossRef] [PubMed]
54. Sun, Y.P.; Xu, Y.; Cao, T.; Su, Y.C.; Guo, Y.H. Zona pellucida thickness and clinical pregnancy outcome following in vitro fertilization. *Int. J. Gynaecol. Obstet.* **2005**, *89*, 258–262. [CrossRef] [PubMed]
55. Fuchs Weizman, N.; Wyse, B.A.; Antes, R.; Ibarrientos, Z.; Sangaralingam, M.; Motamedi, G.; Kuznyetsov, V.; Madjunkova, S.; Librach, C.L. Towards Improving Embryo Prioritization: Parallel Next Generation Sequencing of DNA and RNA from a Single Trophectoderm Biopsy. *Sci. Rep.* **2019**, *9*, 2853. [CrossRef] [PubMed]
56. Nomm, M.; Ivask, M.; Parn, P.; Reimann, E.; Koks, S.; Jaakma, U. Detecting Embryo Developmental Potential by Single Blastomere RNA-Seq. *Genes* **2023**, *14*, 569. [CrossRef]
57. Groff, A.F.; Resetkova, N.; DiDomenico, F.; Sakkas, D.; Penzias, A.; Rinn, J.L.; Eggan, K. RNA-seq as a tool for evaluating human embryo competence. *Genome Res.* **2019**, *29*, 1705–1718. [CrossRef]

**Disclaimer/Publisher’s Note:** The statements, opinions and data contained in all publications are solely those of the individual author(s) and contributor(s) and not of MDPI and/or the editor(s). MDPI and/or the editor(s) disclaim responsibility for any injury to people or property resulting from any ideas, methods, instructions or products referred to in the content.



# Mediastinal Metastasis Isolated in Ovarian Cancer: A Systematic Review

Victoria Psomiadou <sup>1,\*</sup>, Alexandros Fotiou <sup>2</sup> and Christos Iavazzo <sup>1</sup>

<sup>1</sup> Metaxa Memorial Cancer Hospital, 51 Botassi Str., 18537 Piraeus, Greece; christosiavazzo@hotmail.com

<sup>2</sup> 3rd Department of Obstetrics and Gynecology, Athens Medical School, National and Kapodistrian University, Attikon Hospital, 12462 Athens, Greece; alexandrosfotiou92@gmail.com

\* Correspondence: psomiadouvictoria@gmail.com

**Abstract:** Background: Isolated mediastinal metastases from ovarian carcinoma are considered exceptional. Since such metastases are considered advanced stage disease, systemic therapy is the indicated therapeutic approach; however, some articles report that surgical excision is also feasible. Methods: We reviewed the English-language literature to detect cases of isolated mediastinal ovarian cancer metastases and present the management applied as well as their outcomes. Results: From 1998 to 2022, 15 such cases have been reported, with 4 of those cases being primary ovarian cancer presentation and 11 being ovarian cancer recurrence. The histology of the tumor was serious in all of the cases. Regarding the management of cancer, various methods were applied. In total, 11 of the patients underwent a surgical resection of the mediastinal metastasis, 2 received systemic therapy, 1 received a combination of palliative chemotherapy and radiation and the last patient was treated with laser debulking and radiotherapy. The mean reported follow-up was 11 months. Conclusions: Solitary mediastinal metastasis from ovarian cancer is very rare; physicians should pay close attention when routinely evaluating thoracic scans from patients with ovarian malignancy as well as individualizing the management in such patients, since surgical resection can also be performed. However, definitive conclusions cannot be drawn from the small number of case reports available.

**Keywords:** ovarian cancer; isolated mediastinal metastases; ovarian metastases; surgical debulking; cytoreduction

## 1. Introduction

The rate of mediastinal dissemination in ovarian cancer (OC) is estimated at only 2.3%, which is mainly believed to occur via locoregional spread, following a specific pattern where the primary tumor spreads in the mediastinal space, located between the pleural cavities, which enclose the lungs (Figure 1) via intrathoracic lymph nodes metastases. Usually, isolated mediastinal metastases are rare and appear late in the course of the disease and when they are present, they are usually a manifestation of widely disseminated disease [1]. However, the reported cases of mediastinal involvement in ovarian cancer patients are increasing, which may be due to the progress made regarding the imaging techniques and the chemotherapeutic agents as well as the overall longer survival rate of ovarian cancer patients. Recently, thoracic cytoreduction has been proposed in such cases either with the intent to either cure or to extend the survival rates [2]. However, the estimated median survival time after extra-abdominal metastases in OC patients is unclear, since the existing literature on these cases is limited to case reports and no randomised trials exist to strongly support surgical approaches against systemic chemotherapy in these scenarios. Nevertheless, their detection and distinction from metastases from different primary sites are of huge clinical importance because the treatment and prognosis diverge significantly, although the main treatment so far as for any general metastatic cancer consists of palliative chemotherapy without curative intent. This underscores the importance for clinicians to

contemplate mediastinal metastasis during OC patient follow-ups. Successful cytoreduction surgery (CRS) for this less frequent metastatic site has been reported with promising outcomes but due to its low incidence, little data are available [3]. Metastasis to the mediastinum from OC can lead to severe complications due to direct pericardial invasion. In instances of a solitary mediastinal metastasis, surgery could be the most effective treatment option. However, a substantial number of cases need to be gathered to determine the best management strategy, and a multidisciplinary approach and individualized treatment are always crucial in managing rare gynecological cancer cases, since the importance of personalized and innovative treatment strategies in rare metastatic conditions has been emphasized in many studies, suggesting that radiotherapy or neoadjuvant chemotherapy could also be considered [4–6]. In the present review, we aim to investigate the possible role of secondary cytoreduction in patients with isolated mediastinal ovarian cancer disease to identify related needs, explore feasibility and reveal outcomes associated with different treatment approaches.

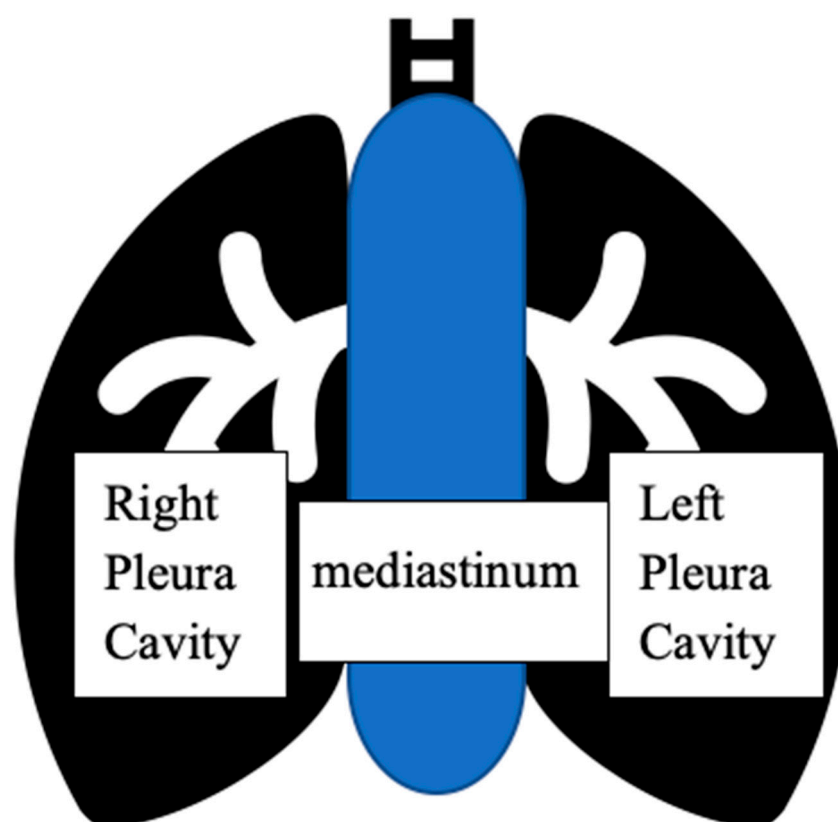


**Figure 1.** The mediastinum located between the pleural cavities, which enclose the lungs.

## 2. Materials and Methods

### 2.1. Data Sources

We searched PubMed, Google Scholar and Cochrane Library databases from inception until August 2024. To minimise the possibility of report losses, we also performed snowballing of the references of articles that we retrieved. Our search strategy included the text word (isolated mediastinal) AND (metastasis OR involvement) AND (ovarian cancer OR tubal OR peritoneal) and is schematically presented in the PRISMA flow diagram (Figure 2).

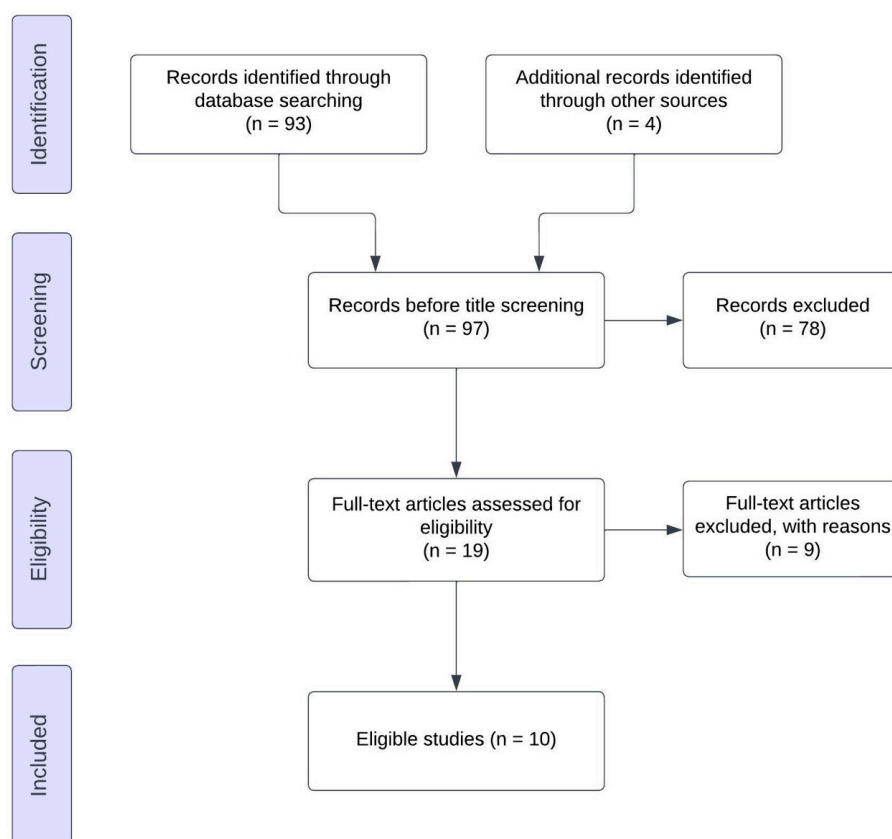


**Figure 2.** PRISMA flow diagram.

## 2.2. Study Selection Criteria

The selection of studies was conducted in three consecutive stages. After checking for duplicate publications, two authors (VP and AF) screened the titles and abstracts of electronically retrieved articles to determine if they were eligible for inclusion. The decision was finalized after retrieving and reviewing the full texts of articles that were considered to be relevant to the topic. Any discrepancies that arose among the two authors during these steps were resolved by consensus of all authors.

## 2.3. Selected Studies

Eligibility criteria were predetermined. No language restrictions were applied during the electronic search but we excluded all articles that were written in languages other than English. All studies that investigated histological or radiological diagnosis of isolated mediastinal metastasis of an ovarian, tubal or peritoneal carcinoma as well as the outcomes of various treatments that were implemented in these patients were included in the present systematic review, provided that these recurrences were isolated and no other organs were involved in disease relapse. The stage of the disease at primary diagnosis was not considered a criterion for inclusion, nor the extent of the follow-up period; however, differences in baseline characteristics of patients were recorded and tabulated when available. Conference abstracts were also considered as eligible and tabulated. Editorials, comments and reviews were not included in the present systematic review.

## 2.4. Literature Review

The literature search revealed 93 potentially relevant articles of which the abstracts and titles were screened. In total, 19 articles were included for full-text evaluation, of which 6 were excluded because they presented cases with multiple metastases or extended disease, and 3 titles referred to radiological criteria to distinguish the metastatic mediastinal disease from other entities. Studies on mediastinal metastasis in OC patients were either

retrospective case reports or case series on patients with OC. Table 1 summarizes the patients' and the disease characteristics as well as the management applied and the follow-up of reported mediastinal metastasis (MM) in these studies. Finally, 10 articles were selected for analysis. A summary of the studies included is shown in Table 1 [3,7–12].

**Table 1.** Studies reporting data on isolated mediastinal metastasis in ovarian cancer patients.

First Author Year,	Nr of Patients	Age of Patients (Range)	Serous Histology	Other Histology	Primary Disease	Recurrence	Time Period from Initial Diagnosis to Recurrence (Years)	Main Symptoms	Primary Disease Treatment		Mediastinal Resection	LN Treated with Systematic Therapy	Follow-Up (mo)
									Chemo Therapy	Surgical Debulking			
Case series													
Moran, 2005 [10]	3	Median: 40 (33–50)	3	0	0	3	NM	None	0	3	3	0	Median: 12 (6–18)
Blanchard, 2007 [8]	4	Median: 62.5 (58–67)	NM	NM	0	4	4.5	None	0	4	0	0	Median: 75.5 (19–132)
Case reports													
Oguchi, 1998 [9]	1	41	1	0	0	1		Dyspnea	0	1	1	0	5
Montero, 2000 [11]	1	46	1	0	0	1	0	None	0	1	1 (VATS)	0	6
Zannoni, 2006 [13]	1	63	1	0	1	0	20 months earlier	Dyspnea	1 (NACT)	1	1	0	1.5
Scarci, 2010 [3]	1	71	1	0	1	0		Dyspnea	1 (NACT)	1	0	1	10
Dhilon, 2016 [7]	1	61	1	0	0	1		Bilateral mass	0	1	1	0	36
Inoue, 2020 [12]	1	67	1	0	0	1	29	None	1	1	1 (VATS)	0	12
Solek, 2021 [14]	1	48	0	1	0	1		Dyspnea	0	1	0	1	7
Miura, 2022 [15]	1	88	1	0	0	1	16	None	1	1	1	0	10

Abbreviations: NM = not mentioned.

### 3. Results

In total, 10 studies with a total of 15 patients were investigated. In 10 cases (66.6%), the primary tumor was of serous histology and interestingly, in one case (6.66%), the primary tumor was a borderline tumor. By the time of the MM, 11 of the patients (73.3%) suffered from ovarian cancer recurrence, and surprisingly, the median time period between the initial diagnosis and the mediastinal recurrence was 13 years, while in 1 patient, mediastinal disease presented 20 months before the ovarian malignancy was diagnosed. Only in four patients (26.7%) was the mediastinal metastasis diagnosed simultaneously with the primary disease. The major symptoms of the patients were dyspnea in four cases (26.7%) and hemoptysis in one patient (6.66%). The median age at the time of diagnosis of the metastases was 58 years, including four patients at fertile age (26.6%). In total, 14 of the patients (93.3%) had undergone either primary or intermediate cytoreduction at the time of the diagnosis. The included studies [3–12] showed variations in the method of treatment since 10 patients (66.6%) underwent surgical resection, sometimes followed by adjuvant chemotherapy. More specifically, eight patients underwent transdiaphragmatic incision (53.3%), which

was combined in one patient with the placement of a tracheobronchial stent, in another by rigid bronchoscopy, right thoracotomy, pleural biopsy, de-roofing of the mediastinal cyst and pleurodesis in the patient with hemoptysis, where the trachea was covered with a serratus anterior flap, combined with bronchoscopic laser debulking to open up the right mainstem bronchus and to control hemoptysis. Two patients (13.3%) underwent Video-Assisted Thoracic Surgery (VATS). No surgical complication was reported. Alternative management included chemotherapy in two patients (13.3%) and expectative management with observation in another three patients (20%), since the patients lacked any symptoms and impressively remained stable and asymptomatic during the follow-up period. The median follow-up was 11 months.

#### 4. Discussion

It has been reported that the mediastinum could be the only site of metastasis when the primary tumor is in the ovaries with an incidence of up to 2.3%. [4]. The low incidence of mediastinal spread in ovarian carcinoma was attributed to locoregional dissemination mainly associated with advanced-stage disease [1]. On the other hand, Zannoni et. al. reported an interesting case of OC with mediastinal involvement as the first manifestation of the disease, 20 months before the abdominal mass could radiologically be identified [10].

Although mediastinal metastasis reports have shown favorable long-term results following repeated surgical resection, chemotherapy or even after surveillance and several reports of spreading bypassing the upper abdomen have been mentioned over the years, there has never been any postulation for the rationale associating ovarian cancer with isolated mediastinal metastases [13]. The behavior of ovarian carcinoma is distinct and differs significantly from the hematogenous metastasis commonly seen in other types of cancer. The majority of ovarian metastases are found within the peritoneal cavity. Once cancer cells have detached from the primary ovarian tumor, either as single cells or clusters, they metastasize passively through the movement of peritoneal fluid, invading the mesothelial cell layers of the peritoneum and omentum. Distribution outside of the peritoneum through the vasculature is less frequent in ovarian cancer (16%) and is typically associated with stage IV disease and a poor prognosis. The most common sites of distant metastasis are the liver (12.6%), pleura (6.6%), and lungs (4.6%) [11]. The precise mechanism accounting for this phenomenon of skip metastasis bypassing the first draining solid organ or the sentinel node through the hematogenous and lymphatics route is unclear but these features reinforced a heightened awareness at all times in detecting metastatic disease during the management of all ovarian, salpingeal and peritoneal malignancies.

When it comes to identification of such rare metastases, radiology appears to play an essential role, especially in asymptomatic patients. Typically, computer tomography (CT) is the preferable radiological method for OC patients' surveillance and staging; however, in our study, three cases (20%) were initially demonstrated in a chest X-ray. In a case report by Oguchi et. al., the diagnosis was histologically confirmed following radiological evidence of mediastinal metastasis shown in single photon emission tomography (SPECT) and Tc-99m MDP (Technetium 99m-methyl diphosphonate) [9]. Another possible method to localize suspicious is utilising photon emission tomography/computer tomography (PET/CT), as described in the cases presented by Inoue et.al. [12] and Zannoni et al. [13]. Interestingly, some of the cases lacked histological confirmation and the therapeutic management was planned based on the radiological findings [8]. However, the present review supports the hypothesis that patients with ovarian cancers should be followed up with CT scans of the thorax for staging and surveillance routinely, since only two of the metastases were synchronous with the disease diagnosis [3,11], while the majority of the lesions in the present series occurred within several years after the initial presentation [7–9,12,13].

Curative treatment of late recurrence from ovarian cancer is not typically successful, although in certain cases of late recurrence from ovarian cancer, secondary debulking surgery may be recommended for selected patients. A retrospective cohort study involving 123 patients with recurrent ovarian cancer found that complete secondary cytoreduction

had the greatest impact on overall survival throughout the treatment course [12]. This is especially true for cases where recurrent disease is localized, the patient has a good performance status, and they responded well to initial therapy, and usually, a combination of secondary debulking surgery (cytoreduction) and chemotherapy is recommended. In our study, surgical excision was successfully performed in 10 of the patients (66.6%), in 8 via thoracic surgery and in 2 via the minimal invasive technique of Video-Assisted Thoracic Surgery (VATS). Four of the patients did not receive any treatment (26.7%) [8], and in only one (6.7%) was palliative systemic therapy and immunotherapy administered [14], while Miura et al. recently reported a case of ovarian cancer mediastinal recurrence that was treated with a combination of radiotherapy and six cycles of carboplatin and paclitaxel after removing the metastatic tumor via median sternotomy and diaphragm resection [15].

The initial classification of FIGO stage IV ovarian cancer categorized patients based on the extent of the disease, prognosis, and recommended management. This included the presence of extra-peritoneal disease such as pleural effusion, liver metastases, and involvement of lymph nodes outside the abdomen, such as the supraclavicular lymph nodes. However, in the 2014 revision, patients with pleural effusion were considered as a separate category from those with parenchymal disease or metastases to extra-abdominal lymph nodes. Nasioudis et al. discovered that isolated distant lymph node metastases have a more favorable prognosis compared to stage IV disease with metastases in other sites, and are similar to those of patients with stage IIIC disease [16]. Zang et al. compared stage IV ovarian cancer patients with metastasis either outside the abdomen or in the liver and found that women with isolated supraclavicular lymphadenopathy or malignant pleural effusion had better survival rates than other stage IV patients [17]. Deng et al. conducted a study with 1481 patients and found that the site of distant metastases significantly impacts the overall prognosis in FIGO stage IV ovarian cancer patients. They observed a lower overall survival for parenchymal metastases compared to distant lymph node metastases [18]. Similarly, Herpje et al. found in a large study that women with stage IV serous ovarian cancer who only had lymph node involvement as distant metastasis lived longer than other stage IV patients [19]. A recent review by Pergalotis et al. demonstrated that ovarian cancer patients with isolated lymph node recurrence have prolonged survival compared to recurrences in other sites as well. This type of recurrence appears to be less aggressive and can be treated with a combination of secondary cytoreduction and standard chemotherapy in selected cases [20]. This aligns with previous research conducted by Uzan et al., which suggested that patients with prior isolated ovarian cancer nodal recurrence may have a more favorable prognosis when undergoing surgical resection followed by chemoradiation or radiation therapy [21].

A basic limitation of our study is that isolated mediastinal metastasis is an absolute rarity of less clinical significance, since in any patient with ovarian cancer history where a suspicious mass is identified on a full body CT scan, a biopsy is required. Additionally, in cases of singular lesions, surgical removal would likely be offered to the patients alongside systemic therapy or radiotherapy. However, our study illuminated approaches where the patients received chemotherapy alone or expectant management with observation, with some cases lacking histological confirmation as well. Despite surgical dissection being a standard procedure that does not solely depend on the localization of the lesion, our review highlights that even though the mediastinum is not usually the first region of metastasis, excision of the mass can be a viable approach for certain subsets of ovarian cancer patients with isolated mediastinal metastasis (IMM), with the goal of improving survival rates. Our findings align with a recent publication from the Memorial Sloan Kettering (MSK) Cancer Center team, which demonstrated the safety and feasibility of intrathoracic cytoreduction in 178 advanced-stage ovarian cancer patients. Their study also suggested that this approach could lead to significantly improved progression-free survival (PFS) and overall survival (OS) in carefully selected patients who can undergo tumor-free surgery, despite having extra-abdominal tumor burden. Additionally, the same study recommends evaluating the eligibility of patients with operable stage IV disease for primary debulking surgery (PDS)

instead of automatically considering neoadjuvant chemotherapy (NACT). Recent data indicate promising results when comparing NACT to PDS, suggesting that high-tumor-burden stage IV patients may not always require NACT as previously suggested in the classical approach [22]. However, further limitations include the small numbers of total cases and the use of retrospective data to acquire reports of cases of prostration. Another limitation is that our systematic review was not registered in PROSPERO; therefore, it can be crosschecked that the study was conducted as planned. Last, this is a self-funded study and due to limited access to other databases such as Embase and Scopus, only three databases (PubMed, Google and Cochrane Library) were included, thus representing a slight selection bias.

Hence, our study draws attention to an almost neglected disease entity of ovarian cancer, namely isolated mediastinal metastases. In the light of the existing literature, the different options in the treatment outcomes are presented, outspreading from surgical removal either via transdiaphragmatic incision in the majority of the cases or Video-Assisted Thoracic Surgery (VATS) to the conservative approach with chemotherapy or even expectative management with observation. The variety in the therapeutic methods is indicative of the need of highly specialized care of such rare cases and is giving credence to handling those patients in a multidisciplinary team and at tertiary centers, where highly selected patients eligible for surgical treatment might undergo curative intent cytoreduction with a fair chance of long-term disease control. Individual therapy planning is also required for patients with a desire to become pregnant, although based on the current recommendations, fertility-sparing surgery with preservation of the uterus with or without preservation of the contralateral annex is only acceptable in young patients with early-stage ovarian carcinoma and it should not be considered in patients with advanced disease [23].

## 5. Conclusions

As shown by the size of the present series and literature review, isolated mediastinal metastases with a very low incidence lack a specific treatment strategy, while systemic therapy is typically administered, based on the general recommendations for OC stage IV disease. The true incidence of isolated mediastinal metastases without abdominal metastases in ovarian cancer could be low, but this remains unclear. Nevertheless, our findings highlight the importance of including the search for mediastinal disease in the staging and surveillance stages of all patients with ovarian cancer and practically recommending to the clinician to not preclude a search for mediastinal metastases in the absence of abdominal involvement. Furthermore, although the current trend is to administer chemotherapy in patients with stage IV disease, exploring the potential feasibility of optimal disease debulking remains controversial. Our review provides a comprehensive summary of the clinical characteristics, treatment methods, and outcomes of MM in ovarian cancer patients, which is to our knowledge not extensively covered in other literature. By compiling data from 15 reported cases, our study highlights the diversity in treatment approaches and the potential for surgical intervention, adding to the body of knowledge on managing advanced-stage ovarian cancer. Multi-disciplinary team meetings during which these cases are discussed are essential to outline an optimal strategy and evaluate the option of surgical cytoreduction. Last but not least, since anterior mediastinal metastasis from OC can cause major complications, future research in the management of isolated mediastinal metastasis in a case of ovarian cancer is needed and a large number of cases must be accumulated to establish optimal management, including more detailed patient data and standardizing the outcome measures across cases to improve the robustness of the findings.

**Author Contributions:** Conceptualization, C.I.; methodology, V.P.; software, V.P.; validation, C.I.; formal analysis, V.P.; investigation, V.P.; resources, V.P.; data curation, A.F.; writing—original draft preparation, V.P.; writing—review and editing, V.P.; visualization, C.I.; supervision, C.I.; project administration, A.F.; funding acquisition, V.P. All authors have read and agreed to the published version of the manuscript.

**Funding:** This research received no external funding.

**Data Availability Statement:** Publicly available datasets were analyzed in this study. This data can be found here: <https://pubmed.ncbi.nlm.nih.gov/>; <https://scholar.google.com/>; <https://www.cochranelibrary.com/>.

**Acknowledgments:** All contributors meet the criteria for authorship (ICMJE: authorship and contributorship).

**Conflicts of Interest:** All authors declare no conflict of interest. The authors declare that no funds, grants, or other support were received during the preparation of this manuscript.

## References

1. Thomakos, N.; Diakosavvas, M.; Machairiotis, N.; Fasoulakis, Z.; Zarogoulidis, P.; Rodolakis, A. Rare Distant Metastatic Disease of Ovarian and Peritoneal Carcinomatosis: A Review of the Literature. *Cancers* **2019**, *11*, 1044. [CrossRef] [PubMed] [PubMed Central]
2. Hamaji, M.; Yamaguchi, K.; Koyasu, S.; Date, H. Thoracoscopic Resection of Fluorodeoxyglucose-Avid Mediastinal Lymph Nodes Associated with Advanced Ovarian Carcinoma. *Thorac. Cardiovasc. Surg.* **2019**, *67*, 692–696. [CrossRef] [PubMed]
3. Scarci, M.; Attia, R.; Routledge, T.; King, J. A rare case of high-grade serous ovarian epithelial carcinoma presenting as an isolated cystic mediastinal mass: A case report and brief review of the literature. *Ann. R. Coll. Surg. Engl.* **2010**, *92*, W57–W58. [CrossRef] [PubMed] [PubMed Central]
4. Dueño, S.; Stein, R.; Jamal, M.; Lewis, G.; Hew, K. Metastasis of serous ovarian carcinoma to the breast: A case report and review of the literature. *J. Med. Case Rep.* **2024**, *18*, 127. [CrossRef] [PubMed] [PubMed Central]
5. Georgescu, M.T.; Georgescu, D.E.; Georgescu, T.F.; Serbanescu, L.G. Changing the Prognosis of Metastatic Cervix Uteri Adenosquamous Carcinoma through a Multimodal Approach: A Case Report. *Case Rep. Oncol.* **2020**, *13*, 1545–1551. [CrossRef] [PubMed] [PubMed Central]
6. Chan, J.K.; Chow, S.; Bhowmik, S.; Mann, A.; Kapp, D.S.; Coleman, R.L. Metastatic gynecologic malignancies: Advances in treatment and management. *Clin. Exp. Metastasis* **2018**, *35*, 521–533. [CrossRef] [PubMed]
7. Dhillon, S.S.; Harris, K.; Pokharel, S.; Yendamuri, S. Calcified Mediastinal Metastasis of Ovarian Cancer Mimicking Broncholithiasis. *J. Bronchol. Interv. Pulmonol.* **2016**, *23*, 229–231. [CrossRef] [PubMed]
8. Blanchard, P.; Plantade, A.; Pagès, C.; Afchain, P.; Louvet, C.; Tournigand, C.; de Gramont, A. Isolated lymph node relapse of epithelial ovarian carcinoma: Outcomes and prognostic factors. *Gynecol. Oncol.* **2007**, *104*, 41–45. [CrossRef] [PubMed]
9. Oguchi, M.; Higashi, K.; Taniguchi, M.; Tamamura, H.; Okimura, T.; Yamamoto, I. Calcified mediastinal metastases from ovarian cancer imaged with Tc-99m MDP SPECT. *Clin. Nucl. Med.* **1998**, *23*, 479–481. [CrossRef] [PubMed]
10. Moran, C.A.; Suster, S.; Silva, E.G. Low-grade serous carcinoma of the ovary metastatic to the anterior mediastinum simulating multilobar thymic cysts: A clinicopathologic and immunohistochemical study of 3 cases. *Am. J. Surg. Pathol.* **2005**, *29*, 496–499. [CrossRef] [PubMed]
11. Montero, C.A.; Gimferrer, J.M.; Baldo, X.; Ramirez, J. Mediastinal metastasis of ovarian carcinoma. *Eur. J. Obstet. Gynecol. Reprod. Biol.* **2000**, *91*, 199–200. [CrossRef] [PubMed]
12. Inoue, E.; Yotsumoto, T.; Inoue, Y.; Fukami, T.; Kitani, M.; Hirano, Y.; Nagase, M.; Morio, Y. Mediastinal metastasis from ovarian serous carcinoma 29 years after initial treatment. *Respir. Med. Case Rep.* **2020**, *29*, 101003. [CrossRef] [PubMed] [PubMed Central]
13. Zannoni, G.F.; Vellone, V.G.; Distefano, M.G.; Fadda, G.; Scambia, G. Ovarian serous carcinoma presenting with mediastinal lymphadenopathy 20 months before the intraabdominal mass: Role of immunohistochemistry. *Gynecol. Oncol.* **2007**, *104*, 497–500. [CrossRef] [PubMed]
14. Sołek, J.M.; Zielińska, A.; Sobczak, M.; Czernek, U.; Kubiak, R.; Kordek, R.; Jesione-Kupnicka, D. Serous borderline tumor with distant mediastinal metastasis? An Exceptional presentation of ovarian tumor. *Pol. J. Pathol.* **2021**, *72*, 272–276. [CrossRef] [PubMed]
15. Miura, H.; Miura, J.; Goto, S.; Yamamoto, T. Ovarian serous carcinoma in which mediastinal recurrence of the cancer was resected 16 years after surgery: A case report. *Respirol. Case Rep.* **2022**, *10*, e0988. [CrossRef] [PubMed] [PubMed Central]
16. Nasioudis, D.; Ko, E.M.; Haggerty, A.F.; Giuntoli, R.L.; Burger, R.A.; Morgan, M.A.; Latif, N.A. Isolated distant lymph node metastases in ovarian cancer. Should a new substage be created? *Gynecol. Oncol. Rep.* **2019**, *28*, 86–90. [CrossRef] [PubMed] [PubMed Central]
17. Zang, R.Y.; Zhang, Z.Y.; Cai, S.M.; Tang, M.Q.; Chen, J.; Li, Z.T. Epithelial ovarian cancer presenting initially with extraabdominal or intrahepatic metastases: A preliminary report of 25 cases and literature review. *Am. J. Clin. Oncol.* **2000**, *23*, 416–419. [CrossRef] [PubMed]
18. Deng, K.; Yang, C.; Tan, Q.; Song, W.; Lu, M.; Zhao, W.; Lou, G.; Li, Z.; Li, K.; Hou, Y. Sites of distant metastases and overall survival in ovarian cancer: A study of 1481 patients. *Gynecol. Oncol.* **2018**, *150*, 460–465. [CrossRef] [PubMed]
19. Hjerpe, E.; Staf, C.; Dahm-Kähler, P.; Ståhlberg, K.; Bjurberg, M.; Holmberg, E.; Borgfeldt, C.; Tholander, B.; Hellman, K.; Kjølhed, P.; et al. Lymph node metastases as only qualifier for stage IV serous ovarian cancer confers longer survival than other sites of distant disease—A Swedish Gynecologic Cancer Group (SweGCG) study. *Acta Oncol.* **2018**, *57*, 331–337. [CrossRef] [PubMed]



20. Pergialiotis, V.; Androutsou, A.; Papoutsi, E.; Bellos, I.; Thomakos, N.; Haidopoulos, D.; Rodolakis, A. Survival outcomes of ovarian cancer patients treated with secondary cytoreductive surgery for isolated lymph node recurrence: A systematic review of the literature. *Int. J. Surg.* **2019**, *69*, 61–66. [CrossRef] [PubMed]
21. Uzan, C.; Morice, P.; Rey, A.; Pautier, P.; Camatte, S.; Lhommé, C.; Haie-Meder, C.; Duvillard, P.; Castaigne, D. Outcomes after combined therapy including surgical resection in patients with epithelial ovarian cancer recurrence(s) exclusively in lymph nodes. *Ann. Surg. Oncol.* **2004**, *11*, 658–664. [CrossRef] [PubMed]
22. Fotopoulou, C. Intrathoracic surgery as part of primary cytoreduction for advanced ovarian cancer: The evolution of a “pelvic” surgeon. *Gynecol. Oncol.* **2023**, *170*, A1–A3. [CrossRef] [PubMed]
23. Pessini, S.A.; Carvalho, J.P.; dos Reis, R.; Filho, A.L.d.S.; Primo, W.Q.S.P. Fertility preservation in gynecologic cancer patients. *Rev. Bras. Ginecol. Obs.* **2023**, *45*, 161–168. [CrossRef] [PubMed] [PubMed Central]

**Disclaimer/Publisher’s Note:** The statements, opinions and data contained in all publications are solely those of the individual author(s) and contributor(s) and not of MDPI and/or the editor(s). MDPI and/or the editor(s) disclaim responsibility for any injury to people or property resulting from any ideas, methods, instructions or products referred to in the content.

Article

# Exploring Therapeutic Challenges in Patients with HER2-Positive Breast Cancer—A Single-Center Experience

Ramona Coca <sup>1,2</sup>, Andrei Moisin <sup>3,4,\*</sup>, Rafaela Coca <sup>1,2</sup>, Atasie Diter <sup>1</sup>, Mihaela Racheriu <sup>3,5</sup>, Denisa Tanasescu <sup>6</sup>, Carmen Popa <sup>5</sup>, Maria-Emilia Cerghedean-Florea <sup>3</sup>, Adrian Boicean <sup>1</sup> and Ciprian Tanasescu <sup>3,4</sup>

<sup>1</sup> Clinical Medical Department, Faculty of General Medicine, “Lucian Blaga” University of Sibiu, Str. Lucian Blaga nr. 2A, 550169 Sibiu, Romania; ramona.coca@ulbsibiu.ro (R.C.); rafaela.coca@ulbsibiu.ro (R.C.); diter.atasie@ulbsibiu.ro (A.D.); adrian.boicean@ulbsibiu.ro (A.B.)

<sup>2</sup> Department of Oncology, Sibiu County Emergency Clinical Hospital, B-dul Corneliu Coposu nr. 2-4, 550245 Sibiu, Romania

<sup>3</sup> Surgical Clinical Department, Faculty of General Medicine, “Lucian Blaga” University of Sibiu, Str. Lucian Blaga nr. 2A, 550169 Sibiu, Romania; mihaela.racheriu@ulbsibiu.ro (M.R.); mariaemilia.florea@ulbsibiu.ro (M.-E.C.-F.); ciprian.tanasescu@ulbsibiu.ro (C.T.)

<sup>4</sup> Department of Surgery, Sibiu County Emergency Clinical Hospital, B-dul Corneliu Coposu nr. 2-4, 550245 Sibiu, Romania

<sup>5</sup> Department of Radiology and Medical Imaging, Sibiu County Emergency Clinical Hospital, B-dul Corneliu Coposu nr. 2-4, 550245 Sibiu, Romania; carmen.0306@yahoo.com

<sup>6</sup> Department of Nursing and Dentistry, Faculty of General Medicine, “Lucian Blaga” University of Sibiu, Str. Lucian Blaga nr. 2A, 550169 Sibiu, Romania; denisa.tanasescu@ulbsibiu.ro

\* Correspondence: andreicatalin.moisin@ulbsibiu.ro

**Abstract:** Breast cancer is one of the most common forms of neoplasia worldwide. The purpose of our observational study was to evaluate the status of HER2 overexpression among new cases of breast neoplasia with an impact on the natural history of breast cancer disease and therapeutic personalization according to staging. This study included 45 breast cancer patients which have an overexpression of HER2 through the mutation of the EGFR-ERBB2 receptor. Immunohistochemical staining was performed on sections of formalin-fixed paraffin-embedded breast tissue. The patients were evaluated demographically and therapeutically in all stages. The post-surgical histopathological examination revealed complete pathological responses in 19 patients and pathological responses with residual disease either at the tumor level or lymphatic or both variants in a percentage of 44% (15 cases). The disease-free interval (DFI) under anti-HER2 therapy was recorded in 41 patients, representing 91% of the study group. Anti-HER2 therapy in any therapeutic stage has shown increased efficiency in blocking these tyrosine kinase receptors, evidenced by the high percentage of complete pathological responses, as well as the considerable percentage (47%) of complete remissions and stationary disease, in relation to the HER2-positive patient group.

**Keywords:** HER2; ERBB2 protein; breast cancer; tyrosine kinase receptors

## 1. Introduction

The increased incidence of breast cancer and the presence of various malignant phenotypes require the search for an optimal, systematic strategy for the diagnosis and treatment of this neoplasia [1,2]. The current oncological therapeutic concept is to customize the therapy in order to increase the disease-free interval (for early stages) and progression-free survival (in metastatic disease) as well as the overall survival [2,3]. The decision making process in breast cancer management should include a detailed discussion with the patient regarding the need for essential genetic testing [4,5]. Multigenic test panels have a positive impact on establishing an individualized therapeutic approach, both for patients and their descendants (knowledge of and reduction in neoplasia risk) [6,7]. Limited testing of BReast CAncer gene 1 (BRCA 1) and BReast CAncer gene 2 (BRCA 2) mutations may lead to the

omission of other genetic changes that radically influence the therapeutic approach, with negative implications for increasing overall survival [7,8]. BRCA 1/2 germ mutation testing as well as multigenic panels do not have settlement systems (full or co-payment) through the National Health Insurance House [9]. The price of these genetic determinations is high, which is why, due to the current socioeconomic conditions, only a small percentage of patients can afford BRCA testing [9–12].

In HER2-positive breast cancer, the overexpression of HER2 is identified in a percentage range of 15–20% of all cases of invasive breast carcinomas and in approximately 10% of breast cancers with positive estrogenic receptors [13,14]. In the neoadjuvant setting, the standard of care is represented by the double anti-HER2 blockade: Pertuzumab + Trastuzumab associated with chemotherapy with Taxanes, according to the guidelines from the ESMO (European Society of Medical Oncology) and NCCN (National Comprehensive Cancer Network) [15,16].

The addition of anti-HER2 therapy to the neoadjuvant management of early-stage HER2-positive breast cancer has yielded substantial clinical benefits, dramatically improving patient outcomes in HER2-positive (HER2+) early breast cancer, as recently proven by the 2021 EBCTCG (Early Breast Cancer Trialists' Collaborative Group) meta-analysis of Trastuzumab in HER2-positive early breast cancer [17,18]. Although pCR (pathological complete response) patients have a very favorable outcome with adjuvant trastuzumab (+/– pertuzumab), adjuvant T-DM1 (Trastuzumab–Emtansine) offers an important escalation strategy in non-pCR patients in the adjuvant setting [17,18].

For recurrent metastatic disease, anti-HER2 therapy includes several treatment lines, depending on the progression of the disease [19,20]. The pretherapeutic diagnostic evaluation of relapsed metastatic breast cancer includes the revision of the HER2 protein positivity (tumor genetic instability) by a biopsy of metastatic lesions and the identification of PIK3CA genetic mutations as well as the PD-L1 immune receptor [21,22]. Immunotherapy has recently been reimbursed in Romania, in triple negative metastatic breast cancer [21,22].

In the treatment of HER2-negative metastatic breast cancer (Figure 1), the metastatic site is important, because it can be both a detectable marker and a therapeutic target [23–25]. The presence or absence of estrogen and progesterone receptors (ER;PR) and HER2, mitotic activity, the site of metastases, and cancer recurrence, determines the treatment for metastatic breast cancer [25,26]. According to recent guidelines, endocrine therapy should be the treatment of choice for most patients with advanced or metastatic ER+, PR+/HER2 (–) breast cancer unless there is evidence of rapidly progressive visceral disease with organ dysfunction or imminent organ failure [27,28]. The association of targeted therapy with endocrine therapy has shown an improved overall survival compared to endocrine therapy alone [29,30]. The use of poly (ADP-ribose) polymerase (PARP) inhibitors as monotherapy has shown significant improvements in the PFS (progression-free survival) compared to chemotherapy in metastatic HER2-mutated germline BRCA breast cancer [31,32]. Olaparib is a selective inhibitor of the poly (ADP-ribose) polymerase (PARP) enzymes (PARP1 and PARP2), which works by taking advantage of the defect in DNA repair in cancer cells with BRCA mutations and inducing cell death [33]. In breast cancer, it is used as an adjuvant treatment for HER2-negative neoplasia, as well as in the triple negative intrinsic subtype [34,35]. Alpelisib is an inhibitor of phosphatidylinositol 3-kinase (PI3K) with strong anti-tumor activity [36,37]. In addition to Fulvestrant, it is indicated for the treatment of women with postmenopausal breast neoplasm and men with advanced or metastatic breast cancer with positive hormone receptors (ER+, PR+), negative HER2, and mutated-PIK3CA [38,39].

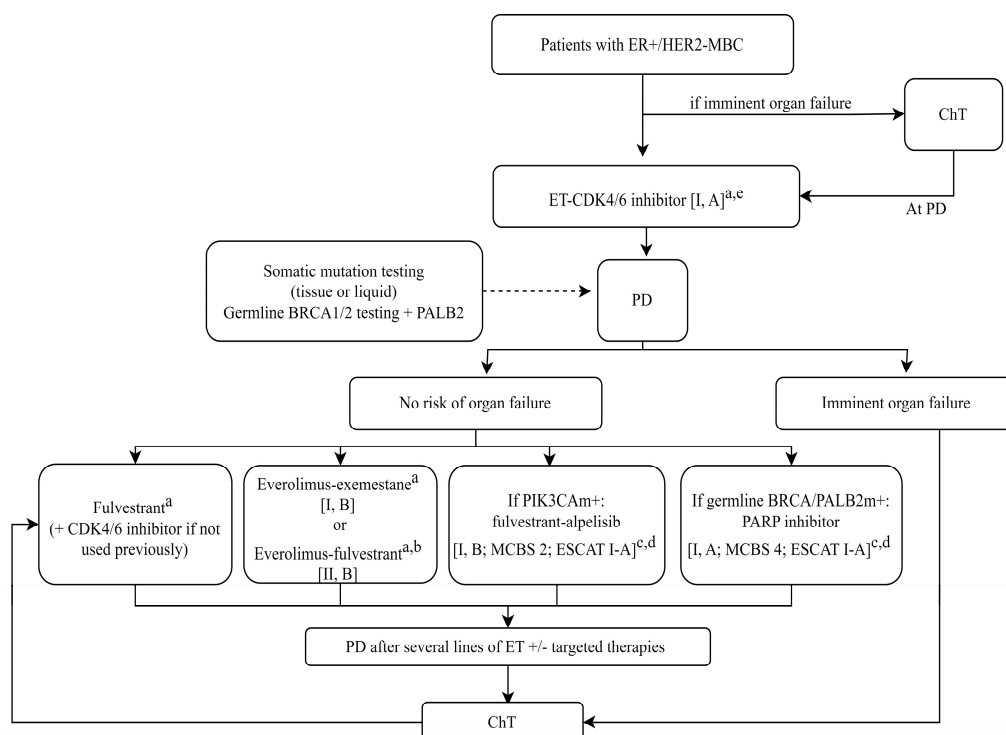


**Figure 1.** Treatment of metastatic breast cancer with positive estrogenic receptors, HER2–negative, but with BRCA 1 and BRCA2 mutations, +/– MUTATIONS of PIK3CA [23]. Figure legend: CDK4/6, cyclin–dependent kinase 4 and 6; ChT, chemotherapy; ER, estrogen receptor; ESCAT, ESMO Scale for Clinical Actionability of Molecular Targets; ESR1, estrogen receptor 1; ET, endocrine therapy; HER2, human epidermal growth factor receptor 2; m, mutation; MBC, metastatic breast cancer; MCBS, ESMO–Magnitude of Clinical Benefit Scale; PALB2, partner and localiser of BRCA2; PARP, poly (ADP–ribose) polymerase; PD, progressive disease; PIK3CA, phosphatidylinosi–tol–4,5-bisphosphate 3–kinase catalytic subunit alpha.

In our Romanian National Health Care Program PN 3, PIK3CA mutation therapy is not settled, while testing and treatment are received by patients who can afford it. In our clinic, only one young patient with recurrent metastatic disease benefited from self-purchased anti-PIK3CA therapy. The purpose of our retrospective observational study is to demonstrate the importance of genetic determinations in the management of patients with breast cancer. Our main objective was to assess HER2 overexpression among newly diagnosed breast carcinomas, related to clinical, diagnostic, and personalized therapeutic management according to the stage. Secondary objectives were to assess HER2 positivity related to demographic, therapeutic, and evolutionary criteria (the time interval in which relapses occurred after the first line of targeted treatment and the number of subsequent therapeutic lines). We focused on assessing the aggressive behaviors of breast cancer in HER2-positive women included in the study by assessing the DFI (disease-free interval), i.e., the onset of remission, without the occurrence of a loco-regional or remote relapse for the non-metastatic stages and the PFS (progression-free survival), respectively, regarding the appearance of new metastatic lesions or the resumption of evolution through the progression of old lesions for the metastatic stages. We limited ourselves to assess the disease-free interval (DFI) of the patients that were temporarily enrolled for a period of our study, associated with successive anti-HER2 therapeutic lines administered in accordance with the existing approvals in the Romanian National Health Program PN3. In this paper, we focused on the study of drug combinations in oncology patients diagnosed with breast cancer and treated at the Sibiu Emergency County Clinical Hospital and the therapeutic impact on the PFS and DFI. The combination of Pertuzumab + Trastuzumab was a major breakthrough in the management of HER2-positive breast cancer patients.

## 2. Materials and Methods

### 2.1. Patient Selection

The patient selection in this study included all patients who presented a complete medical history since the diagnosis of breast cancer. The following were investigated for each patient included in the study:

- Histopathological and immunohistochemical results, as well as immunofluorescence tests for HER2 equivocal tissue samples collected by surgical biopsies (incisional or excisional) or ultrasound-guided biopsies using breast biopsy needles;
- BRCA tests or multigene tests on serum samples from patients who have funded themselves financially (the tests not being settled by the Romanian National Health Program), an insignificant number within the selected group of patients;
- The patient's electronic observation sheet (the ATLAS computer program of the Sibiu County Emergency Clinical Hospital);
- Paper-based medical records (inpatient care and day care observation sheets from the hospital's archive);
- Onc2 record sheets from the outpatient/Oncology department of the Sibiu County Emergency Clinical Hospital).

### 2.2. Study Design

This retrospective study was conducted over a 3-year period (January 2021–December 2023) at the Sibiu County Emergency Clinical Hospital. A total of 237 patients with breast carcinoma were diagnosed and admitted to the Oncology department, of which 45 had histopathologically confirmed breast cancer with HER2 overexpression through the mutational process of the EGFR-ERBB2 receptor.

Informed consent was obtained from all subjects involved in the study, and the study was conducted in accordance with the Declaration of Helsinki and by the Ethics Committee of the Sibiu County Emergency Clinical Hospital (approval no. 4952; Sibiu, Romania). This study focused on genetic determinations in the management of patients with breast cancer, specifically assessing HER2 overexpression among newly diagnosed breast neoplasias.

The study was limited in determining genetic susceptibility of patients included in the study by mutations in BRCA 1/2 repairing genes or other genes determined by multiple panels, considering financial constraints. The main objective was to assess HER2 overexpression related to clinical, diagnostic, and personalized therapeutic management according to the stage of breast cancer.

### 2.3. Inclusion and Exclusion Criteria

- Inclusion Criteria
  - Patients with suspected breast tumors assessed through clinical examination and mammogram.
  - Patients with histopathologically confirmed breast cancer showing HER2 overexpression.
  - Patients who provided informed consent and were included in the study conducted at the Sibiu County Emergency Clinical Hospital.
- Exclusion Criteria
  - Patients with negative HER2 status (0, 1+).
  - Patients with HER2 equivocal (2+) status/FISH- or DISH-negative.
  - Patients not meeting the criteria for genetic susceptibility testing due to financial limitations.

### 2.4. Follow-Up Details

Each patient included in this study was followed-up with every 6 months, over a period of 3 years, until December 2023. The evaluation was carried out both clinically and through imaging to assess the therapeutic response and the disease-free interval

(DFI). For the imaging evaluation, magnetic resonance imaging (MRI), Computerized Tomography (CT) and Positron Emission Tomography-Computed Tomography scans (PET-CT) were included.

### 2.5. Immunohistochemical Detection of Hormone Receptors KI67 and HER2

Immunohistochemical staining for ER, PR, HER2, and KI67 was performed on sections of formalin-fixed paraffin-embedded breast tissue from core biopsies and subsequent surgical specimens. The thickness of breast tissue sections was 3  $\mu\text{m}$ . After heating in the drying oven, the sections were stained using the Ventana BenchMark<sup>®</sup>GX in automatic mode (Ventana Medical Systems Inc., Tucson, AZ, USA) for the assessment of ER, PR, HER2, and KI67. The assessment of ER and PR was based on the staining intensity (weak, moderate, intense) and the percentage of tumor cells showing nuclear immunostaining for ER and PR with a range between 0 and 100%. Breast tissue sections were considered positive for ER and PR if >1% of tumor cells showed positive nuclear staining [40]. KI67 was expressed as the percentage of the number of immunostained nuclei among the total number of nuclei of tumor cells. The evaluation criteria of HER2 status were based on the intensity of cell membrane immunostaining and the percentage of membrane-positive cells by using a score range from 0 to 3+ [13]. HER2 negativity (score 0 or 1+) was concluded when no staining or membrane staining in <10% of tumor cells or weakly partial membrane staining in more than 10% of tumor cells was observed. HER2 equivocal status (score 2+) was concluded when weak to moderate complete membrane staining in >10% of tumor cells and HER2-positive status (score 3+) was concluded when strong complete membrane staining in more than 10% of tumor cells was observed [13,41].

After performing the immunohistochemistry and immunofluorescence tests, 45 HER2-positive patients ( $n = 45$ ) were identified, who were evaluated demographically and therapeutically (anti-HER2 treatment alone, double therapy, first-line, and post-progression of the disease) in all stages (I–IV). In patients whose result showed HER2 equivocal status (2+), the tissue samples were sent to an accredited genetics laboratory in the country, where immunofluorescence tests (FISH/DISH) were performed. By this method, the amplification/non-amplification of the gene encoding the HER2 protein was established.

The 2 multigene panel tests, for the patients who accepted and could financially afford to perform them, were collected in the Oncology department along with signed informed consent and sent to the accredited genetics laboratories in the country. The tests were performed with a new generation sequencing method based on the PCR reaction. In addition, 4 cases of BRCA mutations in young patients were also identified. Another 9 tests were performed only for the identification of BRCA mutations. This was the choice of each patient who preferred to know the mutant or wild-type status of these genes with prophylactic therapeutic utility for bilateralization and ovarian neoplasia.

### 2.6. Statistical Analysis

Data were statistically analyzed using the Microsoft Office Excel application (Microsoft Corp., Redmond, DC, USA) and SPSS Statistics 23.0 software (SPSS, Inc., Chicago, IL, USA). For the statistical analysis performed, two qualitative variables were used to compare the association table (Crosstabs). A significance level ( $p$ ) of the Likelihood ratio test of  $p < 0.05$  was considered statistically significant.

### 2.7. Characteristics of the Group

Demographic characteristics, hormonal status, comorbidities, and family history of breast cancer of the patients included in the study group are described in Table 1. Forty-four (44) female patients and one HER2-positive male patient with a median age of 58 years (32–73 years) were included in our study. Regarding the environment of origin, it is observed that the majority of patients were from an urban environment (34 vs. 11 cases) compared to a rural one. The hormonal status of the patients included in the study group was balanced, 21 patients being identified in the premenopausal stage (47%) and 24 in the

menopausal stage (53%). From the total number of patients included in the study group, 53% (24 cases) presented comorbidities, namely, hypertension and type II diabetes, at the time of diagnosis, while 21 of them did not present any comorbidities.

**Table 1.** Demographic characteristics and main clinical features of HER2-positive patients.

Total Number of Patients with HER2-Positive Breast Cancer (2021–2023) N * (%)	Environment of Origin in HER2-Positive Patients N (%)	Hormonal Status of HER2-Positive Patients N (%)	Comorbidities N (%)
45 (100%)	Urban 34 (76%)	Premenopause 21 (47%)	Hypertension and type II diabetes 24 (53%)
Age of patients: ≤45 years: 3 (7%) 45–73 years: 42 (93%)	Rural 11 (24%)	Menopause 24 (53%)	Absent 21 (47%)
Stage at diagnosis N (%)	Tumor size (T) N (%)	Palpable axillary lymph nodes (N) N (%)	Metastatic disease (M) N (%)
I 2 (4%)	T1 5 (11%)	N0 8 (18%)	M0 36 (80%)
II 14 (31%)	T2 19 (40%)	N1 22 (49%)	M1 9 (20%)
III 20 (45%)	T3 11 (25%)	N2 13 (29%)	
IV 9 (20%)	T4a 0	N3 2 (4%)	
	T4b 8 (20%)		
	T4c 2 (4%)		

\* N = Number of patients.

### 3. Results

Although the current study is based on a group of only 45 patients, it highlighted important characteristics in patients with HER2-positive breast cancer. Main clinical features of HER2-positive breast cancer patients and those with a family history of cancer are described in Table 2. Analyzing the presence of right versus left tumors, we note the more frequent location in the right breast in 27 cases (60%), compared to 18 cases in the left mammary gland (40%). In most cases (82%), the tumors were singular, followed by six cases with bifocal tumors (14%) and only two cases of multifocal tumors (4%). Regarding the site of the breast tumors, the most frequent location was in the outer-upper quadrant (42%), followed by the inner-upper quadrant (18%) and the union of the upper quadrants (18%). Four patients had a tumor located in the central quadrant (9%) and three patients had a tumor in the inner lower quadrant (6%). In addition, three cases with occult breast carcinoma were identified (axillary adenopathy confirmed histologically and immunohistochemically, without clinically detectable mammary tumor, respectively, or imaging).

**Table 2.** Main clinical features of HER2-positive breast cancer patients.

Localization of HER2-Positive Tumors Depending on the Right/Left Breast N * (%)	The Incidence of HER2-Positive Breast Tumors Depending on the Quadrant N (%)	Types of HER2-Positive Tumors N (%)	Family History of Cancer N (%)	Positivity of ER ***** and PR ***** in HER2-Positive Patients
Right breast 27 (60%)	UOQ ** 19 (42%)	Single 37 (82%)	First-degree relatives with breast cancer 5 (11%)	(ER+, PR+) 26 (58%) (ER+, PR−) 3 (7%) (ER−, PR−) 16 (35%)
Left breast 18 (40%)	UIQ *** 8 (18%) UUQ **** 8 (18%) ILQ ***** 3 (6%) CQ ***** 4 (9%) Occult (Tx) 3 (7%)	Bifocal 6 (14%) Multifocal 2 (4%)	Other neoplasia 4 (9%)	

\* N = number of patients. \*\* UOQ = upper-outer quadrant. \*\*\* UIQ = upper-inner quadrant. \*\*\*\* UUQ = union of the upper quadrant. \*\*\*\*\* ILQ = inner-lower quadrant. \*\*\*\*\* CQ = central quad-rant, \*\*\*\*\* ER = estrogen receptor, \*\*\*\*\* PR = progesterone receptor.

The immunohistochemical determination of hormone receptors (Table 2) revealed positivity at different degrees of estrogen receptors (ERs) and progesterone receptors (PRs). Most of the HER2-positive patients had both positive hormone receptors (58%), followed by patients with both negative hormone receptors (35%). Only 7% of the patients (three cases) had positive estrogen receptors associated with negative progesterone receptors.

Regarding the immunohistochemical analysis related to the relevant breast, the HER2-positive patients with negative estrogenic receptors and negative progesterone receptors (ER−, PR−) are associated with right breast location ( $p < 0.05$ ).

The histopathological and immunohistochemical characteristics of the HER2-positive patients are described in Table 3. The histopathological subtype NST (no special type) or invasive ductal carcinoma predominated in 41 cases (91%), compared to lobular carcinoma, which was identified in only 3 cases (7%). A single case (2%) of metaplastic carcinoma with squamous differentiation was detected ( $p = 0.633$ ).

**Table 3.** Histopathological and immunohistochemical characteristics of HER2-positive patients.

Histopathological Type of Breast Cancer N * (%)	HER2 Overexpression N (%)	KI67 N (%)	Tumor Grade N (%)
Ductal invasive carcinoma (NST **) 41 (91%)	HER2-positive (3+) for IHC *** 40 (89%)	<30% 8 (18%)	G1 1 (2%)
Invasive lobular carcinoma 3 (7%)	HER2-equivocal (2+) 5 (11%)	30–50% 20 (44%)	G2 27 (60%)
Metaplastic carcinoma with squamous differentiation 1 (2%)		50–90% 17 (38%)	G3 17 (38%)

\* N = number of patients; \*\* NST = no special type; \*\*\* IHC = immunohistochemistry.

The HER2 status of the patients included in our study was immunohistochemically strongly positive in a percentage of 89% (40 cases), the remaining 11%, equating to five



patients, displayed amplification in the immunofluorescence tests, being initially identified with equivocal HER2 (2+).

The value of the KI67 proliferation index was 82%. An increased value of this index corresponds to a higher tumor aggressiveness. Thus, from all the patients included in the study, 17 patients (38%) presented KI67 between 50 and 90%, 20 patients (44%) between 30 and 50% and only 8 cases (18%) had KI67 reduced by below 30%.

We decided to analyze the value of KI67 in relation to hormone receptors. By using the Likelihood ratio test, a highly significant association was found between patients with RE+ RE− and a KI67 index < 30% ( $p = 0.001$ ).

In terms of tumor grading, 38% (17 cases) had poorly differentiated tumors (G3), 27 patients (60%) had tumors with intermediate grading (G2), and only 1 patient (2%) had well-differentiated tumors ( $p = 0.649$ ). These data correlate with the value of the proliferation index presented above and by the predominance of G2+G3 (98%). The KI67 index was 82%, with over 30% of values considered high. There is a percentage difference of mathematical association between the KI67 value and G2 + G3 of about 16%, which can be explained by the lack of a gold standard for assessing the percentage tumor aggression in terms of the KI67 value. Regarding the classification of intrinsic HER2-positive subtypes, 31 patients (69%) were identified with LUMINAL B-HER2-positive tumors (positive estrogenic hormone receptors, KI67 over 20%), and 14 patients (31%) displayed enriched HER2 tumors (hormone receptor-negative). The intrinsic subtype Luminal B HER2-positive refers to a malignant phenotype characterized by positive estrogenic receptors (ERs), positive or negative progesterone receptors (PRs), a KI67 value over 30%, and HER2 positivity. The enriched HER2 subtype is immunohistochemically characterized by the negativity of hormonal receptors and HER2 positivity.

We decided to analyze patients with HER2-positive breast cancer according to the stage of the disease (Table 1). Nine patients (20%) were diagnosed as HER2-positive in stage IV, only two in stage I (4%), fourteen cases in stage II (31%), and twenty cases in stage III (45%). The data presented show that the majority of the patients (65%) had advanced loco-regional and metastatic disease at diagnosis.

The patients included in the study group were analyzed according to the cTNM staging system (Table 1), which revealed important features. The prevalence of T2 tumors was 40% (19 cases), being the most frequent, followed by 11 cases with T3 tumors (25%) and 10 patients (24%) with T4 tumors (T4b and T4c). Only five patients (11%) presented small tumors classified as T1. The T category (tumor size) was established by clinical ruler measurement of the palpable dimensions of two perpendicular diameters, taking into account the maximum diameter. Statistical analysis does not show an association between HER2 overexpression and tumor size ( $p = 0.053$  in Likelihood ratio test).

On clinical palpation of the peripheral lymph nodes, 22 cases (49%) were identified in the N1 stage and 13 patients (29%) in the N2 stage. Two cases (4%) were categorized as N3 and only 18% (eight cases) had clinically negative axilla ( $p = 0.173$ ). The clinical status N (node) was established by palpation, without being histopathologically confirmed by biopsy. Currently, there is a reluctance of some surgeons to perform a biopsy (post-diagnosis) on any palpable peripheral adenopathy, a very important diagnostic element in achieving correct staging.

Regarding the presence of metastases (M), 36 of the HER2-positive patients (80%) did not have metastatic disease at diagnosis after performing imaging investigations (abdominal-pelvic CT scan, bone scintigraphy as appropriate, brain or bone MRI). A proportion of 20% of patients had distant metastases.

Neoadjuvant anti-HER2 treatment in combination with sequential chemotherapy (Table 4) was administered to 32 HER2-positive patients (71%) as a double blockade of anti-EGFR monoclonal antibodies (Pertuzumab + Trastuzumab), and to 2 patients (4%), following monotherapy with Trastuzumab. Of the total number of patients included in the study, 11 (25%) did not benefit from neoadjuvant anti-HER2 therapy for various reasons (patient preference, metastatic stage, per primam surgery with presentation to the Oncological

Commission after surgery, cardiovascular comorbidities that risked decompensation by administering the anti-HER2 therapy).

**Table 4.** Oncological treatment of HER2-positive patients.

Anti-HER2-NaT + ChT ***** N * (%)	Anti-HER2-AT *****, 1st Line N (%)	Surgery N (%)	RT *** N (%)
(No) NaT **** 11 (25%)	Trastuzumab alone 3 (8%)	RM with ALND ***** 28 (62%)	No RT 14 (31%)
Double anti-HER2 blockade 32 (71%)	TDM-1 ** alone 12 (34%)	RM ***** with subsequent reconstruction and prophylactic oophorectomy 1 (2%)	Adjuvant RT 31 (69%)
Anti-HER2 monotherapy 2 (4%)	Double anti-HER2 blockade 21 (58%)	Sectorectomy with ALND 7 (16%) No surgery 9 (20%)	

\* N = number of patients; \*\* TDM-1 = Trastuzumab emtansine; \*\*\* RT = radiation therapy; \*\*\*\* NaT = neoadjuvant treatment; \*\*\*\*\* AT = adjuvant treatment; \*\*\*\*\* ALND = axillary lymph node dissection; \*\*\*\*\* ChT = chemotherapy; \*\*\*\*\* RM = radical mastectomy.

After the end of the neoadjuvant treatment, as well as the clinical and imaging evaluation of the therapeutic response, the patients were directed to the surgical sequence. A total of 28 patients (62%) underwent radical surgery, performing radical Madden mastectomy with axillary lymph node dissection, and 16% (7 cases) benefited from conservative surgery (sectorectomy with axillary lymph node dissection). Mandatory postoperative adjuvant radiotherapy for conservative surgery and residual tumor from the breast and/or lymphatic (axillary) nodes was indicated in 31 cases, representing a rate of 69%. In one case with the identified BRCA mutation, bilateral mastectomy with homolateral axillary lymph node dissection was performed followed by subsequent breast reconstruction, which was performed in a plastic surgery center in the country. This case benefited from informed consent and prophylactic oophorectomy. In the Sibiu County Emergency Clinical Hospital, at the time of performing the mentioned surgical sequences, the sentinel lymph node technique was not possible.

The post-surgical histopathological examination (Table 5) revealed complete pathological responses (pCRs) in 19 patients (56%), without residual tumor or microscopic lymphatic invasion (yT0N0M0) and in a percentage of 44% (15 cases), pathological responses with residual disease either at the tumor level or lymphatic or both variants.

According to the postoperative therapeutic guidelines, the first anti-HER2 treatment line was performed according to the postoperative histopathological response and the presence of axillary adenopathy (cN+) at diagnosis. Twelve cases (34%) received monotherapy with TDM-1 for residual disease ( $ypT \neq ypT0 + / - ypN \neq ypN0 + M0$ ). A proportion of 44% (20 cases) of HER2-positive patients who were treated with neoadjuvant or adjuvant anti-HER2 therapy relapsed after first-line, while 56% had complete remission or stable disease (without progression). The disease-free interval (DFI) or the time period in which we recorded a stable disease at most, in other words without progression, was recorded in 41 patients, representing 91% of the study group. The remaining four patients did not reach DFI, still having disease progression despite anti-HER2 therapy. For progressive disease (single or repeated progression), follow-up lines of anti-HER2 treatment have been established. A total of 14 patients (31%) followed two lines of anti-HER2 drugs, while for 10 patients (22%), a third line of therapy was necessary.

**Table 5.** The relationship between anti-HER2 positivity and the evolution of breast cancer.

The Occurrence of Relapse after 1st Anti-HER2 Therapeutic Line N * (%)	Disease-Free Interval (DFI) N (%)	Anti-HER2 Treatment Lines N (%)	Histopathological Response after Neoadjuvant Anti-HER2 Therapy N (%)
With relapse 20 (44%)	Without DFI 4 (9%)	Single treatment line 21 (47%)	pCR ** 19 (56%)
No relapse 25 (56%)	With DFI 41 (91%)	Two lines of treatment 14 (31%)	Partial response 15 (44%)
		Three lines of treatment 10 (22%)	

\* N = number of patients; \*\* pCR = pathological complete response.

The types of tumor relapse were either bilateralization (1 case), or remote, as single metastasis (7 cases) or multiple metastases in different sites (12). Out of the total number of patients who presented relapse in the form of metastases, the majority of the cases presented liver and bone metastases each at a percentage of 61%, followed by regional lymph node metastases in 45% of cases, lungs and brain metastases were detected in 22%, while skin and retroorbital metastases were the rarest, being identified in one patient each (5%). The BRCA status was determined in a small number of cases (13 patients) given the financial aspects represented by the high cost of BRCA or multigene testing. Four BRCA mutations were identified in young patients, less than 45 years of age, and in nine other cases, the wild-type (non-mutant) profile was determined. In a number of 32 patients, the determination of mutations was not performed either because testing was no longer recommended at their age, or because of financial inconveniences.

#### 4. Discussion

Out of 237 newly diagnosed breast cancer cases during the period January 2021–December 2023 in our clinic, only 45 (19%) were HER2-positive tumors and were therefore included in our research. Most of them, 36 cases (80%), were in the early stages, and benefited from neoadjuvant management with the anti-HER2 standard of care plus chemotherapy. pCR was performed in 19 patients (56%), who continued the same anti-HER2 treatment in the adjuvant setting as well. The remaining 15 cases had residual tumor burden and received, therefore, adjuvant second-line anti-HER2 therapy. On the other hand, 9 patients were diagnosed at stage IV and benefited from several anti-HER2 treatment lines depending on the PFS. Overall, the DFI was reached in a significant number of patients, namely, 91% (41 out of 45 cases).

The multimodal treatment of breast cancer has made substantial progress in recent years [42,43]. The involvement of modern oncology and surgical treatment options have led to a substantial benefit to patients, defining the multidisciplinary treatment of breast cancer [42,43]. The introduction of immunohistochemical testing and genetic screening has led to the prioritization of therapy and a correct approach to initiating treatment [42,44].

The difference in the HER2 positivity rate of 19% for the 237 new cases diagnosed at the Sibiu County Emergency Clinical Hospital, compared to the study of Rüschoff J. et al., is probably due to the small group of patients included in our retrospective study, compared to the 15,992 histopathological samples collected from 160 oncological centers in Germany [45]. However, the 19% obtained in our group of patients diagnosed with breast cancer falls within the range mentioned also by international studies and guidelines [46–48].

The histopathological gradings G2 and G3 and the KI67 proliferation index, both variables characterizing the malignant phenotype specific to the tumor, correlate with aggressive evolution, translating into the increased risk of loco-regional and remote relapse.

An unfavorable influence on the evolution of the disease is the stage of the disease and the lymph node status (palpable) at diagnosis; 82% of the HER2-positive patients had cN+. The HER2-positive patients mainly were at advanced stages at presentation (III and IV), equating to 65% of all the women included in our study group. A proportion of 11% were identified as having a family history of breast cancer, which correlates with a high susceptibility to breast neoplasia.

HER2-positive breast cancer has an unfavorable prognosis, with an amplified risk of relapse and a more aggressive course of the disease, which is shown by the 44% of relapses after the first line of treatment with monoclonal antibodies.

The percentage of complete post-neoadjuvant pathological responses (targeted anti-HER2 combination therapy and sequential chemotherapy) reveals the effectiveness of the targeted treatment. The discovery and implementation of the National Health Program for new molecules directed against HER2 has allowed for the administration of follow-up lines of targeted treatment so that the overall survival is prolonged. A total of 14 patients benefited from two lines of therapy, and 10 patients received three lines of anti-HER2 therapy.

The most widely used anti-HER2 treatment was double blockade with Pertuzumab and Trastuzumab both as a neoadjuvant (71%) and adjuvant (58%) as well as in the first line of therapy of metastatic disease (100%). The double blockade confers superior therapeutic efficiency by blocking two loci of the EGFR/ERBB 2 receptor.

Our retrospective study, conducted over a limited period of time, did not allow for the correlation of the tumor aggressiveness conferred by HER2 overexpression with the status of the hormone receptors. The patients underwent radical surgical treatment (mastectomy) over conservative surgery (64% versus 16%), possibly due to the preferences of women with breast neoplasia and/or the surgeon. All the patients who underwent the surgical sequence benefited from axillary lymphodissection, the sentinel lymph node technique not being available in the Sibiu County Emergency Clinical Hospital during the period of our study. At the end of the three-year follow-up analysis, there were no deaths among the patients enrolled in our study. This is to highlight once again the effectiveness of treatment and a rapidly evolving era of oncology therapies aimed at increasing survival and quality of life.

More than half of the patients included in this study achieved pCR and continued with the same anti-HER2 therapy in the neoadjuvant setting. The outcomes suggest the importance of neoadjuvant therapy in prolonged DFS. Patients with HER2-positive stage IV breast cancer have benefited from several subsequent lines of anti-HER2 therapy with a prolonged PFS. It is important to emphasize once again that following the correct treatment strategies in HER2-positive patients in the neoadjuvant–surgery–adjuvant settings led to high pCR rates and favorable survival outcomes. Although the recommendations of the international guidelines were followed, the chemotherapeutic regimens were personalized, with the aim of increasing treatment compliance and maintaining the intensity of the doses.

## 5. Conclusions

The HER2 biomarker is a predictive prognostic indicator for the evolution of neoplastic disease, which gives it an augmented aggressiveness, marked in the results of our study by the reduction in the disease-free interval (DFI) and by the occurrence of relapses or by the evolution of metastatic disease.

Anti-HER2 therapy in any therapeutic stage (neoadjuvant, adjuvant, first line in metastatic disease) has shown increased efficiency in blocking these tyrosine kinase receptors, evidenced by the high percentage of complete pathological responses, as well as the considerable percentage (47%) of complete remissions and stationary disease, in relation to the HER2-positive patient group. The errors in our observational study can be derived from the short follow-up interval. This was chosen as a result of the introduction, in recent years, of double anti-HER2 blockade in the targeted therapy of these patients. Until recently, monotherapy with Trastuzumab was used. This is the reason why a correlation with the

overall survival and mortality was not achieved, these variables requiring a much longer evaluation period.

BRCA testing with the aim of prophylaxis of contralateral recurrence and oophorectomy to decrease the risk of ovarian carcinoma failed for socioeconomic reasons due to the high cost of these tests, which cannot be borne by most of our patients.

Due to the short time period in which the research was conducted, aspects such as the correlation between tumor aggressiveness due to HER2 overexpression could not be studied. A detailed analysis of survival data should also be considered, becoming a goal of a future update of our research. We are very interested in the DFS rates of our HER2-positive breast cancer patients, evaluated as the time to recurrence and recurrence sites. Whether the immunohistochemical characteristics will change at relapse remains a question to be answered in the future. Every relapse should undergo biopsy whenever possible, since therapeutic strategies rely on pathological characteristics. In the future, we intend to continue the current study, being part of another prospective study that envisages a thorough follow-up of patients over a longer period of time.

**Author Contributions:** Conceptualization, R.C. (Ramona Coca), A.M., M.-E.C.-F. and C.T.; methodology, A.D.; software, C.P.; validation, C.P., A.B. and C.T.; formal analysis, M.R. and D.T.; investigation, R.C. (Ramona Coca) and A.D.; resources, R.C. (Ramona Coca) and R.C. (Rafaela Coca); data curation, D.T. and A.B.; writing—original draft preparation, R.C. (Rafaela Coca), A.M. and C.T.; writing—review and editing, A.M. and C.P.; visualization, A.D. and M.R.; supervision, D.T.; project administration, R.C. (Rafaela Coca) and C.T.; funding acquisition, M.R. and A.B. All authors have read and agreed to the published version of the manuscript.

**Funding:** Project financed by Lucian Blaga University of Sibiu (Knowledge Transfer Center) and Hasso Plattner Foundation research grants LBUS-HPI-ERG-2023-05.

**Institutional Review Board Statement:** The present study followed international regulations under the Declaration of Helsinki. The present study was approved by the Ethics Committee of the Sibiu County Emergency Clinical Hospital (approval no. 4952; Sibiu, Romania).

**Informed Consent Statement:** Written informed consent has been obtained from the patients to publish this paper.

**Data Availability Statement:** The datasets used and/or analyzed during the current study are available from the corresponding author on reasonable request.

**Conflicts of Interest:** The authors declare no conflicts of interest.

## References

1. Sung, H.; Ferlay, J.; Siegel, R.L.; Laversanne, M.; Soerjomataram, I.; Jemal, A.; Bray, F. Global Cancer Statistics 2020: GLOBOCAN Estimates of Incidence and Mortality Worldwide for 36 Cancers in 185 Countries. *CA Cancer J. Clin.* **2021**, *71*, 209–249. [CrossRef] [PubMed]
2. Pulumati, A.; Pulumati, A.; Dwarakanath, B.S.; Verma, A.; Papineni, R.V.L. Technological advancements in cancer diagnostics: Improvements and limitations. *Cancer Rep.* **2023**, *6*, e1764. [CrossRef] [PubMed]
3. Debela, D.T.; Muzazu, S.G.; Heraro, K.D.; Ndalama, M.T.; Mesele, B.W.; Haile, D.C.; Kitui, S.K.; Manyazewal, T. New approaches and procedures for cancer treatment: Current perspectives. *SAGE Open Med.* **2021**, *9*, 20503121211034366. [CrossRef]
4. Paul, J.; Metcalfe, S.; Stirling, L.; Wilson, B.; Hodgson, J. Analyzing communication in genetic consultations—a systematic review. *Patient Educ. Couns.* **2015**, *98*, 15–33. [CrossRef]
5. Pashayan, N.; Antoniou, A.C.; Ivanus, U.; Esserman, L.J.; Easton, D.F.; French, D.; Sroczynski, G.; Hall, P.; Cuzick, J.; Evans, D.G.; et al. Personalized early detection and prevention of breast cancer: ENVISION consensus statement. *Nat. Rev. Clin. Oncol.* **2020**, *17*, 687–705. [CrossRef]
6. Niraula, S. Tumor Genomic Sequencing as an Impetus to Screen for Germline Mutations: Primum Non Nocere. *J. Oncol. Pract.* **2019**, *15*, 474–475. [CrossRef]
7. Reid, S.; Pal, T. Update on multi-gene panel testing and communication of genetic test results. *Breast J.* **2020**, *26*, 1513–1519. [CrossRef]
8. Beitsch, P.D.; Whitworth, P.W.; Hughes, K.; Patel, R.; Rosen, B.; Compagnoni, G.; Baron, P.; Simmons, R.; Smith, L.A.; Grady, I.; et al. Underdiagnosis of Hereditary Breast Cancer: Are Genetic Testing Guidelines a Tool or an Obstacle? *J. Clin. Oncol. Off. J. Am. Soc. Clin. Oncol.* **2019**, *37*, 453–460. [CrossRef]

9. Vidra, R.; Ciuleanu, T.E.; Nemeş, A.; Pascu, O.; Heroiu, A.M.; Antone, N.; Vidrean, A.I.; Oprean, C.M.; Pop, L.A.; Ber-indan-Neagoe, I.; et al. Spectrum of BRCA1/2 Mutations in Romanian Breast and Ovarian Cancer Patients. *Int. J. Environ. Res. Public Health* **2022**, *19*, 4314. [CrossRef] [PubMed]
10. Manchanda, R.; Sun, L.; Patel, S.; Evans, O.; Wilschut, J.; De Freitas Lopes, A.C.; Gaba, F.; Brentnall, A.; Duffy, S.; Cui, B.; et al. Economic Evaluation of Population-Based BRCA1/BRCA2 Mutation Testing across Multiple Countries and Health Systems. *Cancers* **2020**, *12*, 1929. [CrossRef]
11. Cătană, A.; Trifa, A.P.; Achimas-Cadariu, P.A.; Bolba-Morar, G.; Lisencu, C.; Kutasi, E.; Chelaru, V.F.; Muntean, M.; Martin, D.L.; Antone, N.Z.; et al. Hereditary Breast Cancer in Romania-Molecular Particularities and Genetic Counseling Challenges in an Eastern European Country. *Biomedicines* **2023**, *11*, 1386. [CrossRef]
12. Chakravarty, D.; Johnson, A.; Sklar, J.; Lindeman, N.I.; Moore, K.; Ganesan, S.; Lovly, C.M.; Perlmutter, J.; Gray, S.W.; Hwang, J.; et al. Somatic Ge-nomic Testing in Patients With Metastatic or Advanced Cancer: ASCO Provisional Clinical Opinion. *J. Clin. Oncol. Off. J. Am. Soc. Clin. Oncol.* **2022**, *40*, 1231–1258. [CrossRef]
13. Wolff, A.C.; Hammond, M.E.H.; Hicks, D.G.; Dowsett, M.; McShane, L.M.; Allison, K.H.; Allred, D.C.; Bartlett, J.M.; Bilous, M.; Fitzgibbons, P.; et al. College of American Pathologists. Recommendations for human epidermal growth factor receptor 2 testing in breast cancer: American Society of Clinical Oncology/College of American Pathologists clinical practice guideline update. *J. Clin. Oncol. Off. J. Am. Soc. Clin. Oncol.* **2013**, *31*, 3997–4013. [CrossRef] [PubMed]
14. Patani, N.; Martin, L.A.; Dowsett, M. Biomarkers for the clinical management of breast cancer: International perspective. *Int. J. Cancer* **2013**, *133*, 1–13. [CrossRef]
15. Cardoso, F.; Kyriakides, S.; Ohno, S.; Penault-Llorca, F.; Poortmans, P.; Rubio, I.T.; Zackrisson, S.; Senkus, E.; ESMO Guidelines Committee. Early breast cancer: ESMO Clinical Practice Guidelines for diagnosis, treatment and follow-up. *Ann. Oncol. Off. J. Eur. Soc. Med. Oncol.* **2019**, *30*, 1194–1220. [CrossRef]
16. Theriault, R.L.; Carlson, R.W.; Allred, C.; Anderson, B.O.; Burstein, H.J.; Edge, S.B.; Farrar, W.B.; Forero, A.; Giordano, S.H.; Goldstein, L.J.; et al. National Comprehensive Cancer Network. Breast cancer, version 3.2013: Featured updates to the NCCN guidelines. *J. Natl. Compr. Cancer Netw.* **2013**, *11*, 753–761. [CrossRef]
17. Harbeck, N. Neoadjuvant and adjuvant treatment of patients with HER2-positive early breast cancer. *Breast* **2022**, *62* (Suppl. S1), S12–S16. [CrossRef]
18. Bradley, R.; Braybrooke, J.; Gray, R.; Hills, R.; Liu, Z.; Peto, R.; Davies, L.; Dodwell, D.; McGale, P.; Pan, H.; et al. Trastuzumab for early-stage, HER2-positive breast cancer: A meta-analysis of 13,864 women in seven randomised trials. *Lancet. Oncol.* **2021**, *22*, 1139–1150. [CrossRef] [PubMed]
19. Mandó, P.; Waisberg, F.; Pasquinelli, R.; Rivero, S.; Ostinelli, A.; Perazzo, F. HER2-Directed Therapy in Advanced Breast Cancer: Benefits and Risks. *OncoTargets Ther.* **2023**, *16*, 115–132. [CrossRef]
20. Savard, M.F.; Khan, O.; Hunt, K.K.; Verma, S. Redrawing the Lines: The Next Generation of Treatment in Metastatic Breast Cancer. American Society of Clinical Oncology educational book. *Am. Soc. Clin. Oncol. Annu. Meet.* **2019**, *39*, e8–e21.
21. Cho, Y.A.; Ko, S.Y.; Suh, Y.J.; Kim, S.; Park, J.H.; Park, H.R.; Seo, J.; Choi, H.G.; Kang, H.S.; Lim, H.; et al. PIK3CA Mutation as Potential Poor Prognostic Marker in Asian Female Breast Cancer Patients Who Received Adjuvant Chemotherapy. *Curr. Oncol.* **2022**, *29*, 2895–2908. [CrossRef]
22. Rosin, J.; Svegrup, E.; Valachis, A.; Zerdes, I. Discordance of PIK3CA mutational status between primary and metastatic breast cancer: A systematic review and meta-analysis. *Breast Cancer Res. Treat.* **2023**, *201*, 161–169. [CrossRef] [PubMed]
23. Gennari, A.; André, F.; Barrios, C.H.; Cortés, J.; de Azambuja, E.; DeMichele, A.; Dent, R.; Fenlon, D.; Gligorov, J.; Hurvitz, S.A.; et al. ESMO Clinical Practice Guideline for the diagnosis, staging and treatment of patients with metastatic breast cancer. *Ann. Oncol. Off. J. Eur. Soc. Med. Oncol.* **2021**, *32*, 1475–1495. [CrossRef] [PubMed]
24. Marino, N.; Woditschka, S.; Reed, L.T.; Nakayama, J.; Mayer, M.; Wetzel, M.; Steeg, P.S. Breast cancer metastasis: Issues for the personalization of its prevention and treatment. *Am. J. Pathol.* **2013**, *183*, 1084–1095. [CrossRef]
25. Caswell-Jin, J.L.; Plevritis, S.K.; Tian, L.; Cadham, C.J.; Xu, C.; Stout, N.K.; Sledge, G.W.; Mandelblatt, J.S.; Kurian, A.W. Change in Survival in Metastatic Breast Cancer with Treatment Advances: Meta-Analysis and Systematic Review. *JNCI Cancer Spectr.* **2018**, *2*, pky062. [CrossRef] [PubMed]
26. Park, M.; Kim, D.; Ko, S.; Kim, A.; Mo, K.; Yoon, H. Breast Cancer Metastasis: Mechanisms and Therapeutic Implications. *Int. J. Mol. Sci.* **2022**, *23*, 6806. [CrossRef] [PubMed]
27. Ditsch, N.; Untch, M.; Kolberg-Liedtke, C.; Jackisch, C.; Krug, D.; Friedrich, M.; Janni, W.; Müller, V.; Albert, U.S.; Banyś-Paluchowski, M.; et al. AGO Recommendations for the Diagnosis and Treatment of Patients with Locally Advanced and Metastatic Breast Cancer: Update 2020. *Breast Care* **2020**, *15*, 294–309. [CrossRef] [PubMed]
28. Vieira, C.; Piperis, M.N.; Sagkriotis, A.; Cottu, P. Systemic treatment for hormone receptor-positive/HER2-negative advanced/metastatic breast cancer: A review of European real-world evidence studies. *Crit. Rev. Oncol. Hematol.* **2022**, *180*, 103866. [CrossRef] [PubMed]
29. Gao, J.J.; Cheng, J.; Bloomquist, E.; Sanchez, J.; Wedam, S.B.; Singh, H.; Amiri-Kordestani, L.; Ibrahim, A.; Sridhara, R.; Goldberg, K.B.; et al. CDK4/6 inhibitor treatment for patients with hormone receptor-positive, HER2-negative, advanced or metastatic breast cancer: A US Food and Drug Administration pooled analysis. *Lancet Oncol.* **2020**, *21*, 250–260. [CrossRef] [PubMed]

30. Piezzo, M.; Chiodini, P.; Riemma, M.; Cocco, S.; Caputo, R.; Cianniello, D.; Di Gioia, G.; Di Lauro, V.; Rella, F.D.; Fusco, G.; et al. Progression-Free Survival and Overall Survival of CDK 4/6 Inhibitors Plus Endocrine Therapy in Metastatic Breast Cancer: A Systematic Review and Meta-Analysis. *Int. J. Mol. Sci.* **2020**, *21*, 6400. [CrossRef]
31. Cortesi, L.; Rugo, H.S.; Jackisch, C. An Overview of PARP Inhibitors for the Treatment of Breast Cancer. *Target. Oncol.* **2021**, *16*, 255–282. [CrossRef] [PubMed]
32. Gradishar, W.J.; Moran, M.S.; Abraham, J.; Abramson, V.; Aft, R.; Agnese, D.; Allison, K.H.; Anderson, B.; Burstein, H.J.; Chew, H.; et al. NCCN Guidelines® Insights: Breast Cancer, Version 4.2023. *J. Natl. Compr. Cancer Netw.* **2023**, *21*, 594–608. [CrossRef]
33. Sachdev, E.; Tabatabai, R.; Roy, V.; Rimel, B.J.; Mita, M.M. PARP Inhibition in Cancer: An Update on Clinical Development. *Target. Oncol.* **2019**, *14*, 657–679. [CrossRef]
34. Tutt, A.N.J.; Garber, J.E.; Kaufman, B.; Viale, G.; Fumagalli, D.; Rastogi, P.; Gelber, R.D.; de Azambuja, E.; Fielding, A.; Balmaña, J.; et al. OlympiA Clinical Trial Steering Committee and Investigators. Adjuvant Olaparib for Patients with BRCA1- or BRCA2-Mutated Breast Cancer. *N. Engl. J. Med.* **2021**, *384*, 2394–2405. [CrossRef] [PubMed]
35. Caulfield, S.E.; Davis, C.C.; Byers, K.F. Olaparib: A Novel Therapy for Metastatic Breast Cancer in Patients With a BRCA1/2 Mutation. *J. Adv. Pract. Oncol.* **2019**, *10*, 167–174. [PubMed]
36. Rodon, J.; Curigliano, G.; Delord, J.P.; Harb, W.; Azaro, A.; Han, Y.; Wilke, C.; Donnet, V.; Sellami, D.; Beck, T. A Phase Ib, open-label, dose-finding study of alpelisib in combination with paclitaxel in patients with advanced solid tumors. *Oncotarget* **2018**, *9*, 31709–31718. [CrossRef]
37. Nguyen, P.; Musa, A.; Samantray, J. Alpelisib-Induced Diabetic Ketoacidosis. *Cureus* **2021**, *13*, e14796. [CrossRef]
38. Schwartzberg, L.; Greene, H. Hormone Receptor-Positive, HER2-Negative Breast Cancer: Recent Advances and Best Practices. *J. Adv. Pract. Oncol.* **2020**, *11*, 275–279.
39. Narayan, P.; Prowell, T.M.; Gao, J.J.; Fernandes, L.L.; Li, E.; Jiang, X.; Qiu, J.; Fan, J.; Song, P.; Yu, J.; et al. FDA Approval Summary: Alpelisib Plus Fulvestrant for Patients with HR-positive, HER2-negative, PIK3CA-mutated, Advanced or Metastatic Breast Cancer. *Clin. Cancer Res. Off. J. Am. Assoc. Cancer Res.* **2021**, *27*, 1842–1849. [CrossRef]
40. Hammond, M.E.H.; Hayes, D.F.; Dowsett, M.; Allred, D.C.; Hagerty, K.L.; Badve, S.; Fitzgibbons, P.L.; Francis, G.; Goldstein, N.S.; Hayes, M.; et al. American Society of Clinical Oncology/College Of American Pathologists guideline recommendations for immunohistochemical testing of estrogen and progesterone receptors in breast cancer. *J. Clin. Oncol.* **2010**, *28*, 2784–2795. [CrossRef]
41. Cong, T.D.; Thanh, T.N.; Phan, Q.A.N.; Thi, A.P.H.; Tran, B.S.N.; Vu, Q.H.N. Correlation between HER2 Expression and Clinicopathological Features of Breast Cancer: A Cross-Sectional Study in Vietnam. *Asian Pac. J. Cancer Prev.* **2020**, *21*, 1135–1142. [CrossRef] [PubMed]
42. Tănăsescu, C.; Serban, D.; Moisin, A.; Popa, C.; Coca, R.; Iancu, G.; Tudosie, M.S.; Costea, D.O.; Socea, B.; Tudor, C.; et al. Impact of modern personalized treatment of breast cancer on surgical attitude and outcomes. *Exp. Ther. Med.* **2022**, *23*, 57. [CrossRef]
43. Moisin, A.; Manda, G.; Bratu, D.G.; Serban, D.; Smarandache, C.G.; Motofei, C.; Tanasescu, C. Efficiency of modified radical mastectomy in the therapeutic conduct of breast cancer. *Rom. Biotechnol. Lett.* **2021**, *26*, 2331–2339. [CrossRef]
44. Teodoru, C.A.; Roman, M.D.; Dura, H.; Cerghedeian-Florea, M.-E. Orbital Metastases of Breast Cancer in Males. *Diagnostics* **2023**, *13*, 780. [CrossRef] [PubMed]
45. Rüschhoff, J.; Lebeau, A.; Kreipe, H.; Sinn, P.; Gerharz, C.D.; Koch, W.; Morris, S.; Ammann, J.; Untch, M.; Nicht-interventionelle Untersuchung (NIU) HER2 Study Group. Assessing HER2 testing quality in breast cancer: Variables that influence HER2 positivity rate from a large, multicenter, observational study in Germany. *Mod. Pathol. Off. J. U. S. Can. Acad. Pathol.* **2017**, *30*, 217–226. [CrossRef] [PubMed]
46. Wolff, A.C.; Hammond, M.E.H.; Allison, K.H.; Harvey, B.E.; Mangu, P.B.; Bartlett, J.M.; Bilous, M.; Ellis, I.O.; Fitzgibbons, P.; Hanna, W.; et al. Human Epidermal Growth Factor Receptor 2 Testing in Breast Cancer: American Society of Clinical Oncology/College of American Pathologists Clinical Practice Guideline Focused Update. *J. Clin. Oncol. Off. J. Am. Soc. Clin. Oncol.* **2018**, *36*, 2105–2122. [CrossRef] [PubMed]
47. Singh, J.C.; Lichtman, S.M. Targeted Agents for HER2-Positive Breast Cancer: Optimal Use in Older Patients. *Drugs Aging* **2021**, *38*, 829–844. [CrossRef]
48. Tarantino, P.; Viale, G.; Press, M.F.; Hu, X.; Penault-Llorca, F.; Bardia, A.; Batistatou, A.; Burstein, H.J.; Carey, L.A.; Cortes, J.; et al. ESMO expert consensus statements (ECS) on the definition, diagnosis, and management of HER2-low breast cancer. *Ann. Oncol. Off. J. Eur. Soc. Med. Oncol.* **2023**, *34*, 645–659. [CrossRef]

**Disclaimer/Publisher’s Note:** The statements, opinions and data contained in all publications are solely those of the individual author(s) and contributor(s) and not of MDPI and/or the editor(s). MDPI and/or the editor(s) disclaim responsibility for any injury to people or property resulting from any ideas, methods, instructions or products referred to in the content.

Article

# Diabetes Mellitus and Gynecological and Inflammation Disorders Increased the Risk of Pregnancy Loss in a Population Study

Chun-Gu Cheng <sup>1,2,†</sup>, Sheng-Hua Su <sup>3,†</sup>, Wu-Chien Chien <sup>4,5</sup>, Ryan Chen <sup>6</sup>, Chi-Hsiang Chung <sup>4,5</sup> and Chun-An Cheng <sup>7,\*</sup>

<sup>1</sup> Department of Emergency Medicine, Taoyuan Armed Forces General Hospital, Taoyuan 32549, Taiwan; doc50015@yahoo.com.tw

<sup>2</sup> Department of Emergency Medicine, Tri-Service General Hospital, National Defense Medical Center, Taipei 11490, Taiwan

<sup>3</sup> Department of Pulmonary Medicine, Cheng-Hsin General Hospital, Taipei 11220, Taiwan; chgh9241@gmail.com

<sup>4</sup> School of Public Health, National Defense Medical Center, Taipei 11490, Taiwan

<sup>5</sup> Department of Medical Research, Tri-Service General Hospital, National Defense Medical Center, Taipei 11490, Taiwan

<sup>6</sup> Upper School, Taipei American School, Taipei 111039, Taiwan; 666rcthepro@gmail.com

<sup>7</sup> Department of Neurology, Tri-Service General Hospital, National Defense Medical Center, Taipei 11490, Taiwan

\* Correspondence: cca@ndmctsgh.edu.tw; Tel.: +886-2-87927173

† These authors contributed equally to this work.

**Abstract:** (1) Background: Diabetes mellitus (DM) induces oxidative stress and inflammation with negative effect on pregnancy outcomes. This study aimed to determine whether DM increases the risk of pregnancy loss and to identify other potential risk factors; (2) Methods: We identified female patients diagnosed with DM from 2000–2015 in the Taiwanese National Health Insurance Research Database according to the *International Classification of Diseases*, Ninth Edition, Clinical Modification (ICD-9 CM) code 250. The event was pregnancy loss, defined as ICD-9 CM codes 630–639, which was tracked until 31 December 2015. The control group included 4-fold more non-DM female patients who were matched for age and disease severity. Multivariate Cox regression was employed to determine the risk factors associated with pregnancy loss; (3) Results: The hazard ratio (HR) for the risk of pregnancy loss due to DM was 1.407 (95% confidence interval: 1.099–1.801,  $p = 0.007$ ), and the risk factors for older age, gynecological disorders and inflammation disorders were included. (4) Conclusions: The study concluded that women with DM have a greater risk of experiencing pregnancy loss. Healthcare providers should proactively manage and educate diabetic patients to reduce their risk of pregnancy loss. Understanding other probable risk factors can help in developing targeted interventions and support systems for women to improve pregnancy outcomes.

**Keywords:** diabetes mellitus; pregnancy loss; risk

## 1. Introduction

Pregnancy loss is a non-viable pregnancy, defined as the natural termination of a pregnancy before the fetus is viable outside the uterus, and remains a significant clinical concern with complex etiological factors [1]. It is a complex process with various potential underlying mechanisms, including genetic abnormalities, uterine anatomical abnormalities, progesterone deficiency [2], immunological factors, and environmental factors, such as infections or toxicity [1].

There were more pregnancy outcomes in the Asian group. with a 5-fold greater risk of poor pregnancy outcomes, including abortion and malformation, in pregnant Asian women



with diabetes mellitus (DM) than in pregnant Caucasian women in a study conducted in England [3]. A previous study reported an odds ratio (OR) of 1.11 for the risk of pregnancy loss in mothers with higher fasting blood sugar than in mothers with normal fasting blood sugar among pregnant women in China [4]. Compared with all live births in the USA, women with recurrent pregnancy loss are associated with prediabetes, with an adjusted OR of 1.9 [5]. Previous studies have indicated an increased risk of pregnancy loss in diabetic women, highlighting the multifaceted interplay among metabolic dysfunction, endocrine abnormalities, oxidative stress, and placental impairment [6].

Successful pregnancy relies on immune adaptations that allow fetal survival and development while protecting the mother. The initial phase of pregnancy is characterized by an inflammatory environment that supports embryo implantation, followed by an immunotolerant phase for fetal development. Trophoblast invasion requires inflammatory activity to invade the uterine cavity via decidual dendritic cells, uterine-natural killer cells, and T helper 1 cells with interleukin (IL)-1, 6 and 8. Estrogen and progesterone are critical for regulating endometrial receptivity [7]. Estrogen induces proliferation and prepares the endometrium, whereas progesterone drives decidualization and maintains the window of implementation. The blastocyst and endometrium secrete various factors (e.g., leukemia inhibitory factor, integrins, and adhesion molecules) to synchronize their development and facilitate implantation [8]. Endometrial glands produce histotrophs to support embryo survival and implantation. Decidualization supports embryo implantation and controls embryo quality. The maternal immune system creates an immunotolerant environment at the maternal-embryo interface via immunoregulatory cells, including T helper 2 cells with IL-10 and regulatory T cells, which are crucial for maintaining tolerance to paternal antigens to maintain fetal development in the cavity after implementation [7].

Chronic hyperglycemia in DM can cause hypothalamic–pituitary–ovarian (HPO) dysfunction with hormone impairment, DNA damage, oxidative and endoplasmic reticulum stress, and mitochondrial dysfunction [9]. High blood sugar causes protein misfolding in the endoplasmic reticulum, which can trigger apoptosis and inflammation [10]. Oxidative stress and inflammation disrupt normal cellular functions and induce damage to placental tissues, increasing trophoblast differentiation and glycogen accumulation and dysregulating glucose metabolism, and angiogenesis affects nutrient and oxygen delivery to the fetus, which are crucial for fetal development.

Pregnancy loss in a hyper-inflammatory state increases the risk of cardiovascular events [11], chronic obstructive pulmonary disease [12] and rheumatoid arthritis [13] within several years. Psychological morbidity is common after pregnancy loss, including increases in the risk of anxiety, depression, posttraumatic stress disorder, and suicide [1]. There is little evidence that pre-pregnancy DM is related to pregnancy loss in the Asian population. We retrospectively utilized data from Taiwan’s National Health Insurance Research Database (NHIRD). By analyzing a large cohort of women of childbearing age, we sought to elucidate the impact of DM on pregnancy outcomes and identify potential comorbid conditions that may increase the risk of pregnancy loss.

This study aimed to evaluate the association between maternal DM and the risk of pregnancy loss in the Chinese population. This study underscores the importance of effective diabetes management and the need for targeted interventions to mitigate the risk of pregnancy loss in women with DM. Therefore, healthcare staff need to develop clinical strategies that can improve maternal and fetal health outcomes, comprehensively manage diabetes, and address associated comorbidities to increase pregnancy viability.

## 2. Materials and Methods

The National Health Insurance system was implemented in 1995 for citizens’ health-care and covers more than 99.9% of citizens in Taiwan. Each healthcare institution must provide data for the payment of insurance claims every month. The NHIRD is a comprehensive dataset provided by the National Insurance Administration that includes patients’

birthdays, visit dates, disease codes, procedure codes, medication codes and insurance payments [14].

DM patients were identified from the Taiwanese NHIRD by the *International Classification of Diseases*, 9th Revision, Clinical Modification (ICD-9 CM) code 250. The childbearing age of women was defined as between 20 and 50 years. Females of childbearing age who had been diagnosed with DM and had more than 3 visits from 2001–2015 were included in the study group. The exclusion criteria were being male, having fewer than 3 visits, being below or above childbearing age, being diagnosed with DM before 2001, and experiencing pregnancy loss before inclusion. The control group included 4-fold more females who were matched for sex, age, and disease severity according to the Charlson Comorbidity Index (CCI) and index date. The event was pregnancy loss, defined as in ICD-9 CM codes 630–639, which was tracked until 31 December 2015.

Comorbidities were determined by ICD-9-CM codes and included polycystic ovary syndrome (256.4), pelvic inflammatory disease (616), urinary tract infection (599), premenstrual syndrome (625.4), endometriosis (617), autoimmune disease (710, 714), obesity (278), hypertension (401–405), hyperlipidemia (272), chronic kidney disease (580–589), hyperthyroidism (242), fibromyalgia (729.1), chronic fatigue syndrome (780.71), chronic obstructive pulmonary disease (491, 492, 494, 496), asthma (493), alcohol use disorders (291, 303, 305.1, 571.0–571.4), depression (296, 300.4, 311), anxiety (300.1–300.3, 300.5–300.9), irritable bowel syndrome (564.1), bladder disorder (596), and polyneuropathy (diabetic: 250.6 and 357.2; other: 729.2). The flowchart of this study is shown in Figure 1. To understand the risk of different types of DM, the ICD-9-CM code of 250.01 was used to define as type 1 DM, and the others (250 except 250.01) were used to define type 2 DM. This study was approved by the Ethics Institutional Review Board of Tri-Service General Hospital (TSGHIRB: B-110-051).

The descriptive statistics, compared between groups for continuous variables, were analyzed with Student's *t* test, and categorical variables were analyzed with the chi-square test. The significant difference in cumulative incidence was determined via Kaplan–Meier curve with log rank test. Multivariate Cox regression was employed to determine the risk factors associated with pregnancy loss. A *p* value less than 0.05 indicated a significant difference. The analysis was performed with SPSS version 21 (Asia Analytics Taiwan Ltd., Taipei, Taiwan).

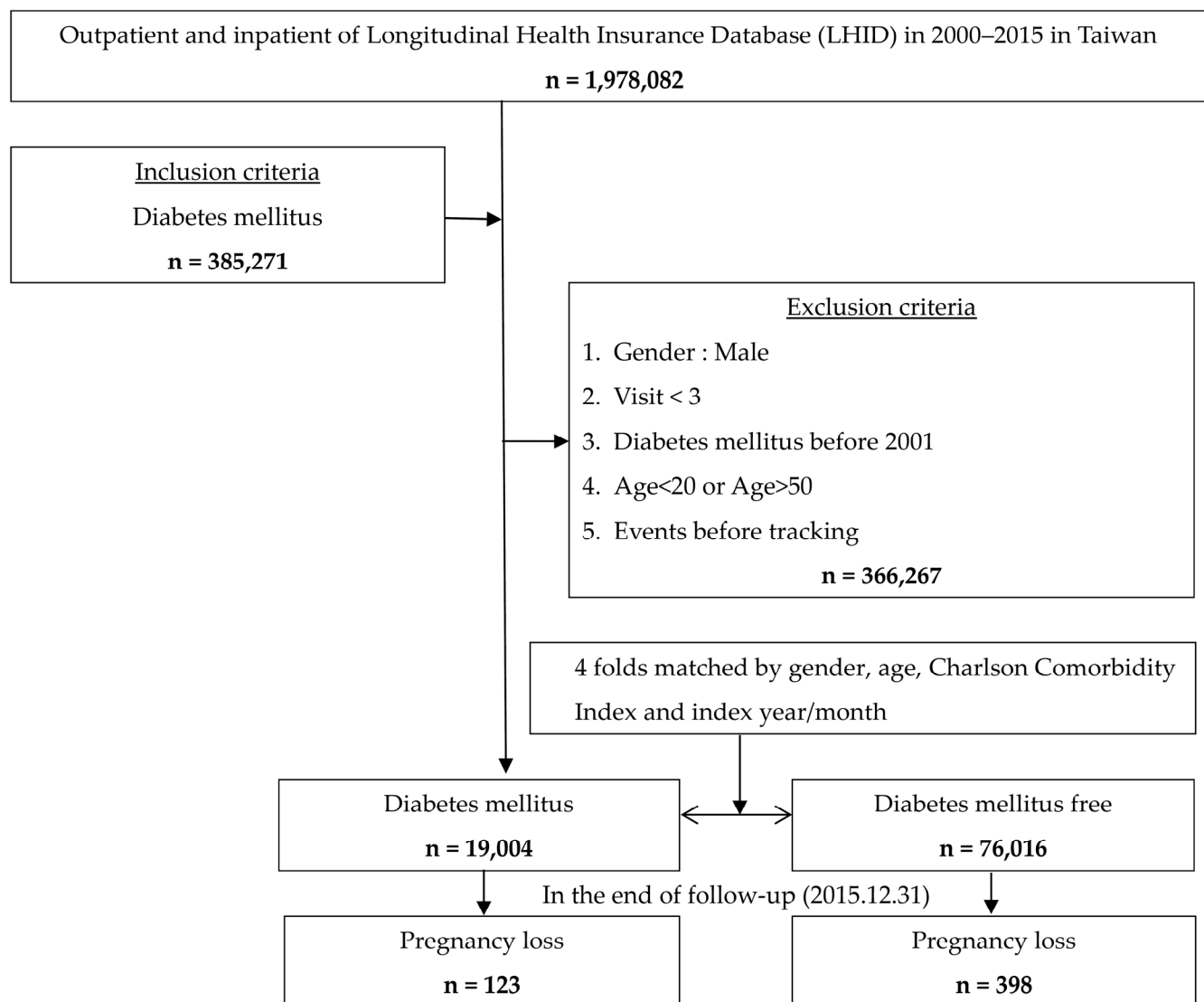


**Figure 1.** Flowchart of study sample selection from the National Health Insurance Research Database in Taiwan.

### 3. Results

There were 19,004 females with DM and 76,016 females without DM included in this study. There were 123 pregnancy losses (cumulative incidence of 2.29%) in the DM group and 398 pregnancy losses (1.7%) in the control group at the 14-year follow-up ( $p = 0.031$ ) (Figure 2). The rate of pregnancy loss was 87.53 per hundred thousand in patients with DM and 71.06 per hundred thousand in patients without DM.

There was a greater prevalence of polycystic ovary syndrome, obesity, hypertension, hyperlipidemia, hyperthyroidism, alcohol use disorder, polyneuropathy, low income and hospital visits in females with DM. Premenstrual syndrome, endometriosis, autoimmune disease, chronic kidney disease, fibromyalgia, chronic obstructive pulmonary disease, asthma, depression, anxiety, irritable bowel disease, and bladder disorders were less common in females with DM (Table 1).

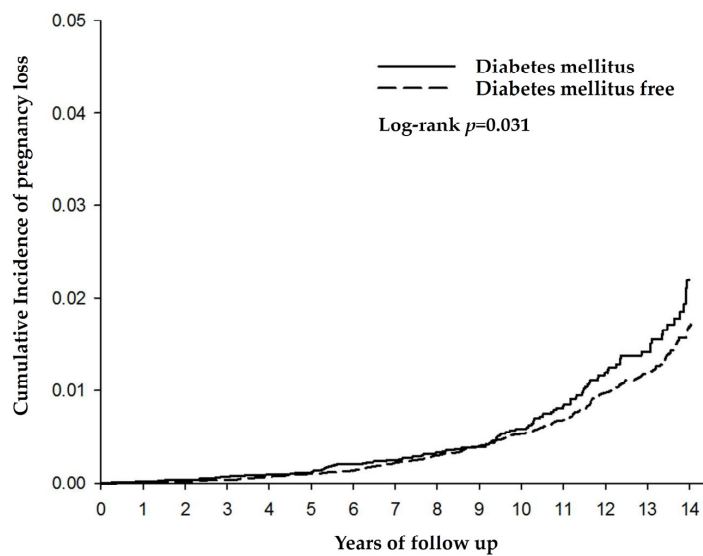


**Figure 2.** The cumulative incidence of pregnancy loss in the two groups.

**Table 1.** Baseline data of women with and without diabetes mellitus.

Variables	Total	Diabetes Mellitus	Without Diabetes Mellitus	<i>p</i>
Number	95,020	19,004	76,016	1
Low-income	1294 (1.4%)	383 (2%)	911 (1.2%)	<0.001 *
Polycystic ovary syndrome	2968 (3.1%)	1081 (5.7%)	1887 (2.5%)	<0.001 *
Pelvis inflammation disorder	63,262 (66.6%)	12,238 (64.4%)	51,024 (67.1%)	<0.001 *
Urinary tract infection	31,863 (33.5%)	6460 (34%)	25,403 (33.4%)	0.144
Premenstrual syndrome	2786 (2.9%)	410 (2.2%)	2376 (3.1%)	<0.001 *
Endometriosis	10,925 (11.5%)	2007 (10.6%)	8918 (11.7%)	<0.001 *
Autoimmune disease	9531 (10%)	1163 (6.1%)	8368 (11%)	<0.001 *
Obesity	3321 (3.5%)	1727 (9.1%)	1594 (2.1%)	<0.001 *
Hypertension	17,705 (18.6%)	7565 (39.8%)	10,140 (13.3%)	<0.001 *
Hyperlipidemia	21,161 (22.3%)	9319 (49%)	11,842 (15.6%)	<0.001 *
Chronic kidney disease	7815 (8.2%)	1407 (7.4%)	6408 (8.4%)	<0.001 *
Hyperthyroidism	7583 (8%)	1797 (9.5%)	5786 (7.6%)	<0.001 *
Fibromyalgia	39,543 (41.6%)	7505 (39.5%)	32,038 (42.1%)	<0.001 *
Chronic fatigue syndrome	1345 (1.4%)	277 (1.5%)	1068 (1.4%)	0.5907
Chronic obstructive pulmonary disease	15,567 (16.4%)	2085 (11%)	13,482 (17.7%)	<0.001 *
Asthma	17,032 (17.9%)	2406 (12.7%)	14,626 (19.2%)	<0.001 *
Alcoholic disorder	1658 (1.7%)	431 (2.3%)	1227 (1.6%)	<0.001 *
Depression	10,722 (11.3%)	2006 (10.6%)	8716 (11.5%)	0.003 *
Anxiety	10,141 (10.7%)	1804 (9.5%)	8337 (11%)	<0.001 *
Irritable bowel disorder	13,057 (13.7%)	2063 (10.9%)	10,994 (14.5%)	<0.001 *
Bladder disorder	2517 (2.6%)	455 (2.4%)	2062 (2.7%)	0.01 *
Polyneuropathies	471 (0.5%)	430 (2.3%)	41 (0.1%)	<0.001 *
Urbanization levels				0.773
1 (The highest)	29,386 (30.9%)	5564 (29.3%)	23,822 (31.3%)	
2	31,769 (33.4%)	6235 (32.8%)	25,534 (33.6%)	
3	26,916 (28.3%)	5600 (29.5%)	21,316 (28%)	
4 (The lowest)	6593 (6.9%)	1546 (8.1%)	5047 (6.6%)	
Missing	356 (0.4%)	59 (0.3%)	297 (0.4%)	
Hospital levels				<0.001 *
Medical center	15,775 (16.6%)	3479 (18.3%)	12,296 (16.2%)	
Regional hospital	18,644 (19.6%)	4851 (25.5%)	13,793 (18.1%)	
Local hospital	14,649 (15.4%)	3901 (20.5%)	10,748 (14.1%)	
Clinic	45,952 (48.4%)	6773 (35.6%)	39,179 (51.5%)	

\*  $p < 0.05$ .

The hazard ratio (HR) for the risk of pregnancy loss in DM patients was 1.407 (95% confidence interval (C.I.): 1.099–1.801,  $p = 0.007$ ). The risk associated with different types of DM had an adjusted HR of 1.498 (95% C.I.: 1.124–1.895,  $p = 0.001$ ) in women with type 2 DM and 1.256 (95% C.I.: 1.058–1.762,  $p = 0.015$ ) in women with type 1 DM. The risk factors were age, with an HR of 1.020 (95% C.I.: 1.004–1.063,  $p = 0.002$ ); pelvic inflammatory disease, with an HR of 2.145 (95% C.I.: 1.911–2.22,  $p < 0.001$ ); premenstrual syndrome, with an HR of 2.067 (95% C.I.: 1.486–2.763,  $p < 0.001$ ); polycystic ovary syndrome, with an HR of 1.792 (95% C.I.: 1.403–2.121,  $p < 0.001$ ); endometriosis, with an HR of 1.42 (95% C.I.: 1.197–1.683,  $p < 0.001$ ); autoimmune disease, with an HR of 1.29 (95% C.I.: 1.111–1.543,  $p < 0.001$ ); urinary tract infection, with an HR of 1.803 (95% C.I.: 1.529–1.88,  $p < 0.001$ ); hyperthyroidism, with an HR of 1.234 (95% C.I.: 1.056–1.503,  $p = 0.001$ ); fibromyalgia, with an HR of 1.353 (95% C.I.: 1.204–1.579,  $p < 0.001$ ); chronic fatigue syndrome, with an HR of 1.835 (95% C.I.: 1.106–2.978,  $p < 0.001$ ); asthma, with an HR of 1.382 (95% C.I.: 1.204–1.595,  $p < 0.001$ ); alcohol use disorder, with an HR of 1.562 (95% C.I.: 1.303–2.701,  $p < 0.001$ ); depression, with an HR of 1.528 (95% C.I.: 1.131–1.735,  $p < 0.001$ ); irritable bowel syndrome, with an HR of 1.340 (95% C.I.: 1.104–1.532,  $p < 0.001$ ); a high CCI score, with an HR of 1.221 (95% C.I.: 1.133–1.468,  $p < 0.001$ ); and fewer visits to medical centers, with an HR of 0.678 (95% C.I.: 0.586–0.917,  $p = 0.001$ ) (Table 2). The risk of pregnancy loss in the first trimester (HR of 1.296 (95% C.I.: 1.089–1.792)) and after the first trimester (HR of 1.724 (95% C.I.: 1.250–1.996)) were noted.

**Table 2.** Risk of pregnancy loss according to multivariate Cox regression.

	Crude Hazard Ratio	<i>p</i>	Adjusted Hazard Ratio	<i>p</i>
Diabetes mellitus	1.682 (95% C.I.: 1.423–1.971)	<0.001 *	1.407 (95% C.I.: 1.099–1.801)	0.007 *
Age	1.034 (95% C.I.: 1.025–1.073)	<0.01 *	1.020 (95% C.I.: 1.004–1.063)	0.002 *
Post CCI	1.311 (95% C.I.: 1.164–1.571)	<0.001 *	1.221 (95% C.I.: 1.133–1.468)	<0.001 *
Low-income	1.567 (95% C.I.: 0.795–1.798)	0.246	1.268 (95% C.I.: 0.575–1.483)	0.387
Polycystic ovary syndrome	6.765 (95% C.I.: 4.282–8.835)	<0.01 *	1.792 (95% C.I.: 1.403–2.121)	<0.001 *
Pelvis inflammation disorder	2.245 (95% C.I.: 2.013–2.498)	<0.001 *	2.145 (95% C.I.: 1.911–2.220)	<0.001 *
Urinary tract infection	1.894 (95% C.I.: 1.625–1.972)	<0.001 *	1.803 (95% C.I.: 1.529–1.880)	<0.001 *
Premenstrual syndrome	2.701 (95% C.I.: 1.941–3.177)	<0.001 *	2.067 (95% C.I.: 1.486–2.763)	<0.001 *
Endometriosis	1.443 (95% C.I.: 1.202–1.694)	<0.001 *	1.420 (95% C.I.: 1.197–1.683)	<0.001 *
Autoimmune disease	1.382 (95% C.I.: 1.125–1.553)	<0.001 *	1.290 (95% C.I.: 1.111–1.543)	<0.001 *
Obesity	1.843 (95% C.I.: 1.354–2.241)	<0.001 *	1.068 (95% C.I.: 0.867–1.798)	0.465
Hypertension	1.006 (95% C.I.: 0.435–1.972)	0.904	0.986 (95% C.I.: 0.421–1.933)	0.804
Hyperlipidemia	1.343 (95% C.I.: 0.791–1.597)	0.803	1.146 (95% C.I.: 0.682–1.371)	0.201
Chronic kidney disease	1.262 (95% C.I.: 0.679–1.486)	0.797	1.135 (95% C.I.: 0.597–1.337)	0.663
Hyperthyroidism	1.680 (95% C.I.: 1.423–1.986)	<0.001 *	1.234 (95% C.I.: 1.056–1.503)	0.001 *
Fibromyalgia	1.403 (95% C.I.: 1.276–1.688)	<0.001 *	1.353 (95% C.I.: 1.204–1.579)	<0.001 *
Chronic fatigue syndrome	2.561 (95% C.I.: 1.897–3.808)	<0.001 *	1.835 (95% C.I.: 1.106–2.978)	<0.001 *
Chronic obstructive pulmonary disease	1.264 (95% C.I.: 0.925–1.440)	0.703	1.116 (95% C.I.: 0.875–1.438)	0.069
Asthma	1.467 (95% C.I.: 1.303–1.765)	<0.001 *	1.382 (95% C.I.: 1.204–1.595)	<0.001 *
Alcoholic disorder	2.016 (95% C.I.: 1.513–2.897)	<0.001 *	1.562 (95% C.I.: 1.303–2.701)	<0.001 *
Depression	1.680 (95% C.I.: 1.27–1.864)	<0.001 *	1.528 (95% C.I.: 1.131–1.735)	<0.001 *
Anxiety	1.065 (95% C.I.: 0.755–1.279)	0.301	0.972 (95% C.I.: 0.734–1.186)	0.702
Irritable bowel disorder	1.513 (95% C.I.: 1.331–1.792)	<0.001 *	1.340 (95% C.I.: 1.104–1.532)	<0.001 *
Bladder disorder	1.030 (95% C.I.: 0.681–1.156)	0.333	0.972 (95% C.I.: 0.513–1.097)	0.498
Polyneuropathies	0.998 (95% C.I.: 0.425–1.201)	0.505	0.706 (95% C.I.: 0.342–1.084)	0.488
Urbanization level				
1 (The highest)	Reference		Reference	
2	1.098 (95% C.I.: 0.511–1.584)	0.465	1.003 (95% C.I.: 0.408–1.438)	0.565
3	1.145 (95% C.I.: 0.562–1.601)	0.43	1.072 (95% C.I.: 0.492–1.483)	0.551
4 (The lowest)	1.246 (95% C.I.: 0.678–1.65)	0.301	1.125 (95% C.I.: 0.533–1.572)	0.48

Table 2. Cont.

	Crude Hazard Ratio	<i>p</i>	Adjusted Hazard Ratio	<i>p</i>
Hospital levels				
Medical Center	0.655 (95% C.I.: 0.512–0.834)	<0.001 *	0.687 (95% C.I.: 0.586–0.917)	0.001 *
Regional hospital	0.724 (95% C.I.: 0.409–0.978)	0.014 *	0.782 (95% C.I.: 0.432–1.034)	0.132
Local hospital	0.832 (95% C.I.: 0.335–1.106)	0.505	0.89 (95% C.I.: 0.356–1.297)	0.202
Clinic	Reference		Reference	

\* *p* < 0.05; C.I.: confidence interval; CCI: Charlson Comorbidity Index.

#### 4. Discussion

Patients with DM experience a greater rate of pregnancy loss than patients without DM, and patients with DM have a 1.4-fold greater risk of pregnancy loss. Effective management of blood sugar levels is crucial for minimizing these risks and improving pregnancy outcomes for women with DM. Several other conditions also increase the risk of pregnancy loss. Gynecological disorders, autoimmune diseases, mood disorders, irritable bowel syndrome, chronic fatigue syndrome, and fibromyalgia are also risk factors for pregnancy loss, and healthcare professionals need to be aware of these risks and manage patients according to the findings of this study.

A total of 4.9% of these cases occurred in India, which is a developing country [15]. The rate of pregnancy loss was 2.6% in type 1 DM patients and 3.7% in type 2 diabetes patients in New Zealand [16]. Mothers with diabetes mellitus receive more healthcare related to metabolism and obstetrics. DM care programs and pregnancy care programs have been developed for several decades, hence the lower incidence of pregnancy loss in Taiwan. The risk ratio was 1.6 for spontaneous pregnancy loss, whereas HbA1c levels  $\geq 5.6\%$  and for risk ratio of 2.1 in every 1 mmol/L increase in fasting blood sugar levels in non-DM mothers were reported [17].

More fetal chromosomal abnormalities occur with increasing maternal age, increasing the likelihood of miscarriage [18]. The most common cause of early pregnancy loss is chromosomal abnormalities in the fetus. A decrease in uterine and hormonal function in older mothers increases the risk of abortion. Older women had a greater risk of abortion than women aged 15–19 years in Ethiopia, with an adjusted OR of 6.13 for women aged 45–49 years [19]. Advanced maternal age showed an adjusted OR of 5.83 in Syrian refugee women [20]. Women who married at more than 26 years of age in Iran were found to have an increased risk of abortion [21]. Our study revealed a 2% increase in pregnancy loss risk with every one-year increase in maternal age.

Polycystic ovary syndrome (POCS) is often associated with insulin resistance, the prevalence of which is increasing in patients with DM. Patients with polycystic ovary syndrome exhibit impaired trophoblast differentiation, increased placental glycogen accumulation, and reduced placental angiogenesis. A mouse study revealed that hyperandrogenism and insulin resistance negatively affect fetal survival through alterations in the mitochondria–ROS–SOD1/Nrf2 axis in the placenta [22]. Our study revealed a 1.8-fold greater risk in women with polycystic ovary syndrome.

Women with endometriosis exhibit a greater inflammatory state. Successful implantation requires a transient increase in proinflammatory cytokines (T helper 1 cells) via immunomodulation, followed by a switch to an anti-inflammatory state (Th2 profile). Recurrent pregnancy loss is linked to immune dysregulation with an increase in proinflammatory cytokines and a decreased anti-inflammatory state [23]. Endometriosis increases the risk of gestational diabetes with an OR of 1.23 [24]. Patients with endometriosis suffer from uncomfortable pain when nonsteroidal anti-inflammatory drugs are used, with an OR of 2.45 spontaneous abortion [25]. The risk of miscarriage in endometriosis had an OR of 1.27 [26]. Our study showed similar results.

DM increased the risk of premenstrual dysphoric disorder (PMDD) in a previous study [27]. Women with PMDD have higher cortisol levels in the late-luteal stage than women without PMDD [28]. Sympathetic overactivity and parasympathetic dysfunction

were noted in young females with premenstrual dysphoric syndrome. Depression symptoms decreased the levels of brain-derived neurotrophic factor in a previous study [29]. Sympathetic activity increases inflammation, and parasympathetic dysfunction decreases anti-inflammatory function, increasing the risk of pregnancy loss. Our study revealed an HR of 2.1.

The expression of apoptosis-related Fas and Fas-L and inflammation-related cytokines was seen in the ovaries and uterus in mice treated with lipid polysaccharides [30]. Bacterial lipopolysaccharide induces apoptosis by decreasing Bcl-2 and increasing caspase-3 in the ovaries [31]. Dysbiosis of the vaginal microbiota was related to proinflammatory cytokine levels in a previous study [32]. In our study, women with pelvic inflammatory disease had a 2.1% risk, and those with urinary tract infection had a 1.8% risk of pregnancy loss.

Autoimmune diseases included systemic lupus erythematosus (SLE) and rheumatoid arthritis. Patients with arthritis exhibit sympathetic overactivity with chronic inflammation. There was a greater risk of autoimmune diseases in patients who experienced pregnancy loss with higher proinflammatory cytokine levels with TH1/TH2 imbalance, atherosclerosis, hormone decreases and complement products influencing placental development [7]. Women with Sjögren's syndrome have a greater risk of pregnancy loss with an RR of 8.85, and of systemic lupus erythematosus with OR 4.90 [33]. Women with rheumatoid arthritis have an increased incidence of PCOS and endometriosis [34]. In a Danish study, women with rheumatoid arthritis had a 1.25-fold increased risk of pregnancy loss [35]. Thyroid antibodies were related to increased risk of gestational diabetes mellitus with a pooled RR of 1.12 [36]. Our study revealed a lower risk of pregnancy loss in women with autoimmune diseases due to the use of regular anti-inflammatory medication.

Hyperthyroidism leads to increased ROS production in mitochondria with oxidative stress [37]. Inadequate treatment for hyperthyroidism in early pregnancy was the main risk factor for pregnancy loss, with an adjusted HR of 1.28 for women who were not treated in early pregnancy and 1.18 for women treated with antithyroid agents in early pregnancy in a Danish population-based study [38]. Our study showed similar results.

Alcohol use during pregnancy is a serious public health issue since it has several detrimental impacts on mothers' and unborn children's health. Alcohol consumption during pregnancy is related to the amount of alcohol consumed before pregnancy, the number of pregnancies and a lower education level [39]. The risk of miscarriage was adjusted to an OR of 1.38 for women who consumed alcohol in Ethiopia [19]. Our study revealed a greater risk of pregnancy loss because alcohol use disorder was identified by more severity codes in claims data.

The OR for the risk of miscarriage was 1.25 in patients with depressive disorders in Norway [40]. A higher education level and socioeconomic status and greater stress were associated with an increased risk of abortion in Iran. Serotonin reuptake inhibitors for antidepressant treatment induce placental insufficiency and increase the risk of miscarriage, with an HR of 1.27 [41]; our study showed similar findings. The discontinuation of treatment before pregnancy was suggested.

Fibromyalgia and chronic fatigue syndrome induce inflammation [42] and increase the risk of pregnancy loss, with an HR of 1.4 in our study. Chronic fatigue syndrome is associated with oxidative stress and immune dysregulation [43,44], and increased the risk of pregnancy loss, with an HR of 1.8 in our study. A mother with asthma has increased chronic inflammation, altered hormonal balance, and medication effects; these factors increase oxidative stress and impair placental function. The risk of pregnancy loss in mothers with asthma had an adjusted HR of 1.21 in Sweden [45]. Our study showed similar results.

The pathophysiology of irritable bowel syndrome involves complex mechanisms, including visceral hypersensitivity and immunoinflammatory disturbances. Inflammation induces the apoptosis pathway, resulting in pregnancy loss. Maternal irritable bowel syndrome is associated with a risk of miscarriage, with an OR of 1.21, and ectopic pregnancy, with an OR of 1.28 [46]. Our study showed similar results. Women with more

severe disease and a higher CCI are at greater risk. Our study revealed a lower risk of pregnancy loss, with an HR of 0.7 in women with frequent medical center visits, indicating that better pregnancy care was provided in medical centers. More vigilance is needed regarding the risks associated with diabetes during pregnancy. Good control of DM with HbA1c can reduce adverse pregnancy outcomes [47]. Understanding and addressing the multifaceted risks associated with these conditions can improve pregnancy outcomes for affected women.

There was no significant increase in the risk of pregnancy loss in women with low incomes. High blood sugar levels in diabetic patients also contribute to the accumulation of lipids in the body, leading to hyperlipidemia and obesity. Mothers with pregestational T2DM had greater body weights than mothers without diabetes did in England [48]. The risk of early miscarriage in obese women has an OR of 1.2 [49], but our study revealed no significant risk of obesity due to the lower prevalence of a body mass index greater than 25 kg/m<sup>2</sup> in women ( $23.1 \pm 0.24$  kg/m<sup>2</sup> in the 19- to 44-year-old group [50]).

There is no significant increase in the risk of hyperlipidemia in the USA [5]. The majority of patients received antilipidemic treatment, which reduced the risk of pregnancy loss in claim data. In Iran, mothers with hypertension had a lower risk of abortion, with an adjusted OR of 0.6, and they received better healthcare to prevent abortion [21]. Our study revealed no significant findings. Abortion increased chronic obstructive pulmonary disease, with an OR of 1.12, with increased inflammation in China [12]. Chronic obstructive pulmonary disease is characterized by increased smoke exposure with hypoxia resulting in lower ovum activity, a lower pregnancy rate and severe symptoms, with asthma attack significantly increasing risk. The OR for the risk of miscarriage was 1.25 in patients with anxiety disorders in Norway [40], but our study revealed no significant difference in the risk of pregnancy loss associated with the lower toxicity of antianxiety agents. More cases of pregnancy loss were induced by bladder disorders, and there was no risk of pregnancy loss. There was no significant risk of chronic kidney disease or polyneuropathy, possibly because renal or peripheral nerve involvement is an end complication of DM with inflammation, and these patients have less pregnancy willingness and pregnancy rates.

In addition to controlling blood sugar, treatments that target oxidative stress, mitochondrial impairment and hyperinflammation reduce DM complications [51]. These findings suggest that managing oxidative stress could be a potential therapeutic approach. Treatment with the antioxidant N-acetylcysteine improved fetal survival in DHT+insulin-treated pregnant rats [22]. The antioxidant and anti-inflammatory effects of melanin reduce diabetic complications [52]. Suitable exercise to increase parasympathetic activity decreases inflammation and reduces pregnancy complications [53]. A Mediterranean diet is associated with a lower risk of preterm birth in Western countries [54]. Vaginal micronized progesterone has an effect on threatened miscarriage, with a risk ratio of 1.03, and increases the live birth rate, with a risk ratio of 1.08 for women with one or more previous miscarriages and early pregnancy bleeding [55]. Insulin use causes insulin receptor overload, reducing FSH and LH secretion [56]. Metformin and insulin can control blood sugar equally but, compared with insulin, metformin has a lower risk of abortion, with an OR of 0.81 [57]. Metformin and glucagon-like peptide-1 (GLP-1) agonists have anti-inflammatory effects and are potential treatments for controlling diabetes in pregnant women [57,58].

There were several limitations in this study. First, the blood sugar control conditions were unavailable in the claims data. The relationship between diabetes control and pregnancy loss is worthy of investigation, and registry studies are needed in the future. Second, smoking status, pregnancy number and body mass index data were not provided in the NHIRD. Smoking increased the OR of pregnancy loss by 1.31 in China [59]. More than three pregnancies are associated with a greater risk of abortion in Iran [21]. A higher body mass index is associated with a greater risk of abortion [21,49], and this relationship needs to be studied in Chinese women. Third, fetal loss was similar in mothers with type 1 DM or type 2 DM in previous studies [16,60]. The risk of pregnancy loss was higher with adjusted HR of 1.5 in women with type 2 DM than in women with type 1 DM. The medica-



tions used to treat DM were not surveyed, and neither metformin nor GLP-1 agonists had anti-inflammatory effects. However, further studies are needed to address this gap.

## 5. Conclusions

This study revealed that women with DM have an increased risk of pregnancy loss. It is important to educate and aggressively manage blood sugar in women of childbearing age. Older women with other gynecological disorders have a greater risk of pregnancy loss. Early pregnancy at a young age should be encouraged, and gynecological disorders should be managed. Inflammatory conditions caused by other disorders were noted in this study, and reducing inflammation and oxidative stress could reduce the risk of pregnancy complications.

**Author Contributions:** Conceptualization, C.-A.C.; Data curation, C.-H.C.; Formal analysis, C.-H.C.; Funding acquisition, C.-G.C.; Investigation, S.-H.S. and R.C.; Methodology, W.-C.C.; Project administration, W.-C.C.; Resources, W.-C.C.; Software, C.-H.C.; Supervision, C.-A.C.; Validation, S.-H.S. and R.C.; Visualization, R.C.; Writing—original draft, C.-G.C. and S.-H.S.; Writing—review and editing, C.-A.C. All authors have read and agreed to the published version of the manuscript.

**Funding:** This research received no external funding.

**Institutional Review Board Statement:** The study was conducted in accordance with the Declaration of Helsinki and approved by the Institutional Review Board of TSGH (protocol code TSGHIRB-B-110-05 and 16 March 2021 approval).

**Informed Consent Statement:** Not applicable.

**Data Availability Statement:** Restrictions apply to the availability of these data. Data were obtained from the National Health Insurance database and are available from the authors with the permission of the National Health Insurance Administration of Taiwan.

**Acknowledgments:** This study was supported by the Taoyuan Armed Forces General Hospital grant (TYAFGH\_E\_113048) and Tri-Service General Hospital grand (TSGH-B-113025). The sponsor has no role in the study design, data collection and analysis, decision to publish or preparation of the manuscript. We also appreciate the Health and Welfare Data Science Center, Ministry of Health and Welfare (HWDC, MOHW), Taiwan, for providing the National Health Insurance Research Database (NHIRD).

**Conflicts of Interest:** The authors declare no conflicts of interest.

## References

1. Quenby, S.; Gallos, I.D.; Dhillon-Smith, R.K.; Podsek, M.; Stephenson, M.D.; Fisher, J.; Brosens, J.J.; Brewin, J.; Ramhorst, R.; Lucas, E.S.; et al. Miscarriage matters: The epidemiological, physical, psychological, and economic costs of early pregnancy loss. *Lancet* **2021**, *397*, 1658–1667. [CrossRef] [PubMed]
2. Lek, S.M.; Ku, C.W.; Allen, J.C., Jr.; Malhotra, R.; Tan, N.S.; Østbye, T.; Tan, T.C. Validation of serum progesterone < 35 nmol/L as a predictor of miscarriage among women with threatened miscarriage. *BMC Pregnancy Childbirth* **2017**, *17*, 78. [CrossRef]
3. Verheijen, E.C.; Critchley, J.A.; Whitelaw, D.C.; Tuffnell, D.J. Outcomes of pregnancies in women with pre-existing type 1 or type 2 diabetes, in an ethnically mixed population. *BJOG* **2005**, *112*, 1500–1533. [CrossRef] [PubMed]
4. Wei, Y.; Xu, Q.; Yang, H.; Yang, Y.; Wang, L.; Chen, H.; Anderson, C.; Liu, X.; Song, G.; Li, Q.; et al. Preconception diabetes mellitus and adverse pregnancy outcomes in over 6.4 million women: A population-based cohort study in China. *PLoS Med.* **2019**, *16*, e1002926. [CrossRef] [PubMed]
5. Cortés, Y.I.; Zhang, S.; Hussey, J.M. Pregnancy loss is related to body mass index and prediabetes in early adulthood: Findings from Add Health. *PLoS ONE* **2022**, *17*, e0277320. [CrossRef] [PubMed]
6. Crețu, D.; Cernea, S.; Onea, C.R.; Pop, R.M. Reproductive health in women with type 2 diabetes mellitus. *Hormones* **2020**, *19*, 291–300. [CrossRef] [PubMed]
7. Colamatteo, A.; Fusco, C.; Micillo, T.; D’Hooghe, T.; de Candia, P.; Alviggi, C.; Longobardi, S.; Matarese, G. Immunobiology of pregnancy: From basic science to translational medicine. *Trends Mol. Med.* **2023**, *29*, 711–725. [CrossRef] [PubMed]
8. Massimiani, M.; Lacconi, V.; La Civita, F.; Ticconi, C.; Rago, R.; Campagnolo, L. Molecular Signaling Regulating Endometrium-Blastocyst Crosstalk. *Int. J. Mol. Sci.* **2019**, *21*, 23. [CrossRef]
9. Singh, A.; Kukreti, R.; Saso, L.; Kukreti, S. Mechanistic Insight into Oxidative Stress-Triggered Signaling Pathways and Type 2 Diabetes. *Molecules* **2022**, *27*, 950. [CrossRef]

10. Gäreskog, M.; Cederberg, J.; Eriksson, U.J.; Wentzel, P. Maternal diabetes in vivo and high glucose concentration in vitro increases apoptosis in rat embryos. *Reprod. Toxicol.* **2007**, *23*, 63–74. [CrossRef]
11. Wang, M.; Zhang, J.; Yuan, L.; Hu, H.; Li, T.; Feng, Y.; Zhao, Y.; Wu, Y.; Fu, X.; Ke, Y.; et al. Miscarriage and stillbirth in relation to risk of cardiovascular diseases: A systematic review and meta-analysis. *Eur. J. Obstet. Gynecol. Reprod. Biol.* **2024**, *297*, 1–7. [CrossRef]
12. Huang, S.; Hee, J.Y.; Zhang, Y.O.; Gongye, R.; Zou, S.; Tang, K. Association between pregnancy and pregnancy loss with COPD in Chinese women: The China Kadoorie Biobank study. *Front. Public Health* **2022**, *10*, 990057. [CrossRef]
13. Hee, J.Y.; Huang, S.; Leong, K.P.; Chun, L.; Zhang, Y.O.; Gongye, R.; Tang, K. Pregnancy loss and the risk of rheumatoid arthritis in Chinese women: Findings from the China Kadoorie biobank. *BMC Public Health* **2022**, *22*, 1768. [CrossRef]
14. Taiwanese National Health Insurance Dataset. Available online: <https://nhird.nhri.edu.tw> (accessed on 1 February 2024).
15. Das, M.; Patidar, H.; Singh, M. Understanding trimester-specific miscarriage risk in Indian women: Insights from the calendar data of National Family Health Survey (NFHS-5) 2019–21. *BMC Womens Health* **2024**, *24*, 63. [CrossRef] [PubMed]
16. Cundy, T.; Gamble, G.; Neale, L.; Elder, R.; McPherson, P.; Henley, P.; Rowan, J. Differing causes of pregnancy loss in type 1 and type 2 diabetes. *Diabetes Care* **2007**, *30*, 2603–2607. [CrossRef]
17. Chen, X.; Zhang, Y.; Chen, H.; Dou, Y.; Wang, Y.; He, W.; Ma, X.; Sheng, W.; Yan, W.; Huang, G. Association Between Serum Glycated Hemoglobin Levels at Early Gestation and the Risk of Subsequent Pregnancy Loss in Pregnant Women Without Diabetes Mellitus: Prospective Cohort Study. *JMIR Public Health Surveill.* **2023**, *9*, e46986. [CrossRef] [PubMed]
18. Munné, S.; Alikani, M.; Tomkin, G.; Grifo, J.; Cohen, J. Embryo morphology, developmental rates, and maternal age are correlated with chromosome abnormalities. *Fertil. Steril.* **1995**, *64*, 382–391, Corrected and republished in: *Fertil. Steril.* **2019**, *112* (Suppl. S1), e71–e80. [CrossRef]
19. Ayana, G.M.; Raru, T.B.; Deressa, A.; Regassa, L.D.; Gamachu, M.; Negash, B.; Birhanu, A.; Merga, B.T. Association of alcohol consumption with abortion among ever-married reproductive age women in Ethiopia: A multilevel analysis. *Front. Glob. Women's Health* **2022**, *3*, 1028166. [CrossRef]
20. Khadra, M.M.; Suradi, H.H.; Amarín, J.Z.; El-Bassel, N.; Kaushal, N.; Jaber, R.M.; Al-Qutob, R.; Dasgupta, A. Risk factors for miscarriage in Syrian refugee women living in non-camp settings in Jordan: Results from the Women ASPIRE cross-sectional study. *Confl. Health* **2022**, *16*, 32. [CrossRef]
21. Moradinazar, M.; Najafi, F.; Nazar, Z.M.; Hamzeh, B.; Pashar, Y.; Shakiba, E. Lifetime Prevalence of Abortion and Risk Factors in Women: Evidence from a Cohort Study. *J. Pregnancy* **2020**, *2020*, 4871494. [CrossRef]
22. Zhang, Y.; Zhao, W.; Xu, H.; Hu, M.; Guo, X.; Jia, W.; Liu, G.; Li, J.; Cui, P.; Lager, S.; et al. Hyperandrogenism and insulin resistance-induced fetal loss: Evidence for placental mitochondrial abnormalities and elevated reactive oxygen species production in pregnant rats that mimic the clinical features of polycystic ovary syndrome. *J. Physiol.* **2019**, *597*, 3927–3950. [CrossRef]
23. Vidali, A.; Riccio, L.G.C.; Abrao, M.S. Endometriosis and recurrent pregnancy loss: Two manifestations of the same underlying dysfunction? *Fertil. Steril.* **2023**, *119*, 836–837. [CrossRef] [PubMed]
24. Salmeri, N.; Li Piani, L.; Cavoretto, P.I.; Somigliana, E.; Viganò, P.; Candiani, M. Endometriosis increases the risk of gestational diabetes: A meta-analysis stratified by mode of conception, disease localization and severity. *Sci. Rep.* **2023**, *13*, 8099. [CrossRef] [PubMed]
25. Nakhai-Pour, H.R.; Broy, P.; Sheehy, O.; Bérard, A. Use of nonaspirin nonsteroidal anti-inflammatory drugs during pregnancy and the risk of spontaneous abortion. *CMAJ* **2011**, *183*, 1713–1720. [CrossRef] [PubMed]
26. Boje, A.D.; Egerup, P.; Westergaard, D.; Bertelsen, M.M.F.; Nyegaard, M.; Hartwell, D.; Lidegaard, Ø.; Nielsen, H.S. Endometriosis is associated with pregnancy loss: A nationwide historical cohort study. *Fertil. Steril.* **2023**, *119*, 826–835. [CrossRef] [PubMed]
27. Huang, Y.M.; Chien, W.C.; Cheng, C.G.; Chang, Y.H.; Chung, C.H.; Cheng, C.A. Females with Diabetes Mellitus Increased the Incidence of Premenstrual Syndrome. *Life* **2022**, *12*, 777. [CrossRef] [PubMed]
28. Beddig, T.; Reinhard, I.; Kuehner, C. Stress, mood, and cortisol during daily life in women with Premenstrual Dysphoric Disorder (PMDD). *Psychoneuroendocrinology* **2019**, *109*, 104372. [CrossRef] [PubMed]
29. Ko, C.H.; Wong, T.H.; Suen, J.L.; Lin, P.C.; Long, C.Y.; Yen, J.Y. Estrogen, progesterone, cortisol, brain-derived neurotrophic factor, and vascular endothelial growth factor during the luteal phase of the menstrual cycle in women with premenstrual dysphoric disorder. *J. Psychiatr. Res.* **2024**, *169*, 307–317. [CrossRef]
30. Seo, J.; Lee, J.; Kim, S.; Lee, M.; Yang, H. Lipid Polysaccharides have a Detrimental Effect on the Function of the Ovaries and Uterus in Mice through Increased Pro-Inflammatory Cytokines. *Dev. Reprod.* **2022**, *26*, 135–144. [CrossRef]
31. MacKenzie, S.; Montserrat, N.; Mas, M.; Acerete, L.; Tort, L.; Krasnov, A.; Goetz, F.W.; Planas, J.V. Bacterial lipopolysaccharide induces apoptosis in the trout ovary. *Reprod. Biol. Endocrinol.* **2006**, *4*, 46. [CrossRef]
32. Grewal, K.; Lee, Y.S.; Smith, A.; Brosens, J.J.; Bourne, T.; Al-Memar, M.; Kundu, S.; MacIntyre, D.A.; Bennett, P.R. Chromosomally normal miscarriage is associated with vaginal dysbiosis and local inflammation. *BMC Med.* **2022**, *20*, 38. [CrossRef] [PubMed]
33. Singh, M.; Wambua, S.; Lee, S.I.; Okoth, K.; Wang, Z.; Fayaz, F.F.A.; Eastwood, K.A.; Nelson-Piercy, C.; Reynolds, J.A.; Nirantharakumar, K.; et al. Autoimmune diseases and adverse pregnancy outcomes: An umbrella review. *BMC Med.* **2024**, *22*, 94. [CrossRef] [PubMed]
34. Li, P.F.; Li, S.; Zheng, P.S. Reproductive Effect by Rheumatoid Arthritis and Related Autoantibodies. *Rheumatol. Ther.* **2024**, *11*, 239–256. [CrossRef] [PubMed]

35. Nathan, N.O.; Mørch, L.S.; Wu, C.S.; Olsen, J.; Hetland, M.L.; Li, J.; Rom, A.L. Rheumatoid arthritis and risk of spontaneous abortion: A Danish nationwide cohort study. *Rheumatology* **2020**, *59*, 1984–1991. [CrossRef] [PubMed]
36. Yang, Y.; Li, Q.; Wang, Q.; Ma, X. Thyroid antibodies and gestational diabetes mellitus: A meta-analysis. *Fertil. Steril.* **2015**, *104*, 665–671.e3. [CrossRef] [PubMed]
37. Napolitano, G.; Fasciolo, G.; Di Meo, S.; Venditti, P. Vitamin E Supplementation and Mitochondria in Experimental and Functional Hyperthyroidism: A Mini-Review. *Nutrients* **2019**, *11*, 2900. [CrossRef] [PubMed]
38. Andersen, S.L.; Olsen, J.; Wu, C.S.; Laurberg, P. Spontaneous abortion, stillbirth and hyperthyroidism: A danish population-based study. *Eur. Thyroid J.* **2014**, *3*, 164–172. [CrossRef] [PubMed]
39. Corrales-Gutierrez, I.; Mendoza, R.; Gomez-Baya, D.; Leon-Larios, F. Understanding the Relationship between Predictors of Alcohol Consumption in Pregnancy: Towards Effective Prevention of FASD. *Int. J. Environ. Res. Public Health* **2020**, *17*, 1388. [CrossRef] [PubMed]
40. Magnus, M.C.; Havdahl, A.; Morken, N.H.; Wensaas, K.A.; Wilcox, A.J.; Håberg, S.E. Risk of miscarriage in women with psychiatric disorders. *Br. J. Psychiatry* **2021**, *219*, 501–506. [CrossRef]
41. Andersen, J.T.; Andersen, N.L.; Horwitz, H.; Poulsen, H.E.; Jimenez-Solem, E. Exposure to selective serotonin reuptake inhibitors in early pregnancy and the risk of miscarriage. *Obstet. Gynecol.* **2014**, *124*, 655–661. [CrossRef]
42. Polli, A.; Hendrix, J.; Ickmans, K.; Bakusic, J.; Ghosh, M.; Monteyne, D.; Velkeniers, B.; Bekaert, B.; Nijs, J.; Godderis, L. Genetic and epigenetic regulation of Catechol-O-methyltransferase in relation to inflammation in chronic fatigue syndrome and Fibromyalgia. *J. Transl. Med.* **2022**, *20*, 487. [CrossRef] [PubMed]
43. Venturini, L.; Bacchi, S.; Capelli, E.; Lorusso, L.; Ricevuti, G.; Cusa, C. Modification of Immunological Parameters, Oxidative Stress Markers, Mood Symptoms, and Well-Being Status in CFS Patients after Probiotic Intake: Observations from a Pilot Study. *Oxidative Med. Cell. Longev.* **2019**, *2019*, 1684198. [CrossRef] [PubMed]
44. Maes, M.; Kubera, M.; Kortańska, M. Aberrations in the Cross-Talks Among Redox, Nuclear Factor- $\kappa$ B, and Wnt/ $\beta$ -Catenin Pathway Signaling Underpin Myalgic Encephalomyelitis and Chronic Fatigue Syndrome. *Front. Psychiatry* **2022**, *13*, 822382. [CrossRef] [PubMed]
45. Jöud, A.; Nilsson-Condori, E.; Schmidt, L.; Ziebe, S.; Vassard, D.; Mattsson, K. Infertility, pregnancy loss and assisted reproduction in women with asthma: A population-based cohort study. *Hum. Reprod.* **2022**, *37*, 2932–2941. [CrossRef] [PubMed]
46. Khashan, A.S.; Quigley, E.M.; McNamee, R.; McCarthy, F.P.; Shanahan, F.; Kenny, L.C. Increased risk of miscarriage and ectopic pregnancy among women with irritable bowel syndrome. *Clin. Gastroenterol. Hepatol.* **2012**, *10*, 902–909. [CrossRef]
47. Davidson, A.J.F.; Park, A.L.; Berger, H.; Aoyama, K.; Harel, Z.; Cohen, E.; Cook, J.L.; Ray, J.G. Association of Improved Periconception Hemoglobin A1c With Pregnancy Outcomes in Women with Diabetes. *JAMA Netw. Open* **2020**, *3*, e2030207. [CrossRef] [PubMed]
48. Coton, S.J.; Nazareth, I.; Petersen, I. A cohort study of trends in the prevalence of pregestational diabetes in pregnancy recorded in UK general practice between 1995 and 2012. *BMJ Open* **2016**, *6*, e009494. [CrossRef] [PubMed]
49. Lashen, H.; Fear, K.; Sturdee, D.W. Obesity is associated with increased risk of first trimester and recurrent miscarriage: Matched case-control study. *Hum. Reprod.* **2004**, *19*, 1644–1646. [CrossRef]
50. Nutrition Health Survey in Taiwan, 2017–2020. Available online: [https://www.hpa.gov.tw/File/Attach/15562/File\\_18775.pdf](https://www.hpa.gov.tw/File/Attach/15562/File_18775.pdf). (accessed on 1 February 2024).
51. Teodoro, J.S.; Nunes, S.; Rolo, A.P.; Reis, F.; Palmeira, C.M. Therapeutic Options Targeting Oxidative Stress, Mitochondrial Dys-function and Inflammation to Hinder the Progression of Vascular Complications of Diabetes. *Front. Physiol.* **2019**, *9*, 1857. [CrossRef]
52. Yang, H.L.; Zhou, W.J.; Gu, C.J.; Meng, Y.H.; Shao, J.; Li, D.J.; Li, M.Q. Pleiotropic roles of melatonin in endometriosis, recurrent spontaneous abortion, and polycystic ovary syndrome. *Am. J. Reprod. Immunol.* **2018**, *80*, e12839. [CrossRef]
53. Picard, M.; Tauveron, I.; Magdasy, S.; Benichou, T.; Bagheri, R.; Ugbole, U.C.; Navel, V.; Dutheil, F. Effect of exercise training on heart rate variability in type 2 diabetes mellitus patients: A systematic review and meta-analysis. *PLoS ONE* **2021**, *16*, e0251863. [CrossRef] [PubMed]
54. Yang, J.; Song, Y.; Gaskins, A.J.; Li, L.J.; Huang, Z.; Eriksson, J.G.; Hu, F.B.; Chong, Y.S.; Zhang, C. Mediterranean diet and female reproductive health over lifespan: A systematic review and meta-analysis. *Am. J. Obstet. Gynecol.* **2023**, *229*, 617–631. [CrossRef] [PubMed]
55. Devall, A.J.; Papadopoulou, A.; Podeseck, M.; Haas, D.M.; Price, M.J.; Coomarasamy, A.; Gallos, I.D. Progestogens for preventing miscarriage: A network meta-analysis. *Cochrane Database Syst. Rev.* **2021**, *4*, CD013792. [CrossRef] [PubMed]
56. Evans, M.C.; Hill, J.W.; Anderson, G.M. Role of insulin in the neuroendocrine control of reproduction. *J. Neuroendocrinol.* **2021**, *33*, e12930. [CrossRef] [PubMed]
57. Wang, T.; Zhang, W. Application of Gestational Blood Glucose Control During Perinatal Period in Parturients with Diabetes Mellitus: Meta-Analysis of Controlled Clinical Studies. *Front. Surg.* **2022**, *9*, 893148. [CrossRef]
58. Mehdi, S.F.; Pusapati, S.; Anwar, M.S.; Lohana, D.; Kumar, P.; Nandula, S.A.; Nawaz, F.K.; Tracey, K.; Yang, H.; LeRoith, D.; et al. Glucagon-like peptide-1: A multi-faceted anti-inflammatory agent. *Front. Immunol.* **2023**, *14*, 1148209. [CrossRef] [PubMed]

59. Yuan, S.; Liu, J.; Larsson, S.C. Smoking, alcohol and coffee consumption and pregnancy loss: A Mendelian randomization investigation. *Fertil. Steril.* **2021**, *116*, 1061–1067. [CrossRef] [PubMed]
60. Murphy, H.R.; Howgate, C.; O’Keefe, J.; Myers, J.; Morgan, M.; Coleman, M.A.; Jolly, M.; Valabhji, J.; Scott, E.M.; Knighton, P.; et al. Characteristics and outcomes of pregnant women with type 1 or type 2 diabetes: A 5-year national population-based cohort study. *Lancet Diabetes Endocrinol.* **2021**, *9*, 153–164. [CrossRef]

**Disclaimer/Publisher’s Note:** The statements, opinions and data contained in all publications are solely those of the individual author(s) and contributor(s) and not of MDPI and/or the editor(s). MDPI and/or the editor(s) disclaim responsibility for any injury to people or property resulting from any ideas, methods, instructions or products referred to in the content.

Article

# The Role of Neutrophil-to-Lymphocyte Ratio as a Predictor of Ovarian Torsion in Children: Results of a Multicentric Study

Carlos Delgado-Miguel <sup>1,2,\*</sup>, Javier Arredondo-Montero <sup>3</sup>, Julio César Moreno-Alfonso <sup>4</sup>, María San Basilio <sup>5</sup>, Raquel Peña Pérez <sup>6</sup>, Noela Carrera <sup>7</sup>, Pablo Aguado <sup>1</sup>, Ennio Fuentes <sup>1,6,8</sup>, Ricardo Díez <sup>1,6,8,†</sup> and Francisco Hernández-Oliveros <sup>2,5,†</sup>

<sup>1</sup> Pediatric Surgery Department, Fundación Jiménez Díaz University Hospital, Avenida de los Reyes Católicos, 2, 28040 Madrid, Spain

<sup>2</sup> Institute for Health Research IdiPAZ, La Paz University Hospital, 28046 Madrid, Spain

<sup>3</sup> Pediatric Surgery Department, Complejo Asistencial Universitario de León, 24071 Castilla y León, Spain

<sup>4</sup> Pediatric Surgery Department, Navarra University Hospital, 31008 Pamplona, Spain

<sup>5</sup> Pediatric Surgery Department, La Paz University Hospital, 28046 Madrid, Spain

<sup>6</sup> Pediatric Surgery Department, Rey Juan Carlos University Hospital, 28933 Móstoles, Spain

<sup>7</sup> Pediatric Surgery Department, Toledo University Hospital, 45005 Toledo, Spain

<sup>8</sup> Pediatric Surgery Department, Villalba University Hospital, 28400 Villalba, Spain

\* Correspondence: carlosdelgado84@hotmail.com

† These authors contributed equally to this work.

**Abstract:** Introduction: Pediatric ovarian torsion (OT) is an emergency condition that remains challenging to diagnose because of its overall unspecific clinical presentation. The aim of this study was to determine the diagnostic value of clinical, ultrasound, and inflammatory laboratory markers in pediatric OT. Methods: We performed a retrospective multicentric case–control study in patients with clinical and ultrasound suspicion of OT, in whom surgical examination was performed between 2016–2022 in seven pediatric hospitals. Patients were divided into two groups according to intraoperative findings: OT group (ovarian torsion), defined as torsion of the ovarian axis at least 360°, and non-OT group (no torsion). Demographics, clinical, ultrasound, and laboratory features at admission were analyzed. The diagnostic yield analysis was performed using logistic regression models, and the results were represented by ROC curves. Results: We included a total of 110 patients (75 in OT group; 35 in non-OT group), with no demographic or clinical differences between them. OT-group patients had shorter time from symptom onset (8 vs. 12 h;  $p = 0.023$ ), higher ultrasound median ovarian volume (63 vs. 51 mL;  $p = 0.013$ ), and a significant increase in inflammatory markers (leukocytes, neutrophils, neutrophil-to-lymphocyte ratio, C-reactive protein) when compared to the non-OT group. In the ROC curve analysis, the neutrophil-to-lymphocyte ratio (NLR) presented the highest AUC (0.918), with maximum sensitivity (92.4%) and specificity (90.1%) at the cut-off point  $NLR = 2.57$ . Conclusions: NLR can be considered as a useful predictor of pediatric OT in cases with clinical and ultrasound suspicion. Values above 2.57 may help to anticipate urgent surgical treatment in these patients.

**Keywords:** ovarian torsion; neutrophil-to-lymphocyte ratio; predictive factors; children

## 1. Introduction

Ovarian torsion (OT) is a relatively rare cause of acute abdominal pain in children, with challenging diagnosis due to nonspecific clinical presentation and poor specificity of radiologic tests [1,2]. Severe pain and the sudden onset of the pain are highly suggestive but are not always found. However, delay in establishing the diagnosis and treatment in a timely fashion can result in irreversible ovarian ischemia with functional loss of the ovary [3].

Ultrasound is the mainstay of evaluation for OT in the pediatric population, with a sensitivity of around 80% [4], and some findings related to OT have been described, such as the absence of ovarian Doppler flow, although none of them is pathognomonic [5]. Further, there is near-universal agreement that presence of intra-ovarian blood flow does not exclude torsion [6].

Neutrophil-to-lymphocyte ratio (NLR) has been postulated as an inflammatory biomarker in several ischemic diseases in children such as testicular torsion [7]. In addition, few studies have demonstrated its role as a diagnostic predictor in diseases with significant intra-abdominal inflammatory involvement, such as Henoch–Schönlein purpura and acute appendicitis with peritonitis or intra-abdominal abscess [8–10]. Recently, its relationship with adnexal torsion and ovarian tumors in adult women has been investigated, but there is scarce evidence in the pediatric population [11,12]. The aim of this study is to analyze the role of the NLR as a predictor of ovarian torsion in children and adolescents and compare it with other potential clinical, ultrasound, and inflammatory factors.

## 2. Methods

A retrospective multicenter case–control study was performed in patients with clinical and ultrasound OT suspicion, in whom diagnostic laparoscopy was performed at seven pediatric institutions between January 2016 and December 2022. Patients were divided into two groups according to the intraoperative diagnosis of OT, which was defined as the ovary twisting on its axis at least 360 degrees: OT group (ovarian torsion) and non-OT group (no torsion observed).

Demographic variables, clinical features, menstruation status, time since symptoms onset, laboratory variables, ultrasound characteristics, and intraoperative findings were analyzed. Clinical features recorded included the presence of abdominal pain, vomiting, diarrhea or constipation, fever (temperature  $\geq 38.0$  °C), dysuria, anorexia, as well as the occurrence of previous similar episodes. Among ultrasonographic features, imaging features (cystic, solid or mixed), ovarian volumen (measured in mL), ovarian volumen ratio (ratio between the volume of both ovaries), absence of Doppler flow, and the presence of pelvic free fluid were reported. Patients with missing data were excluded from the analysis.

Laboratory data were gathered from blood tests conducted in the Emergency Department (ED) upon the patients' arrival. These tests encompassed a complete blood count, including leukocyte count and absolute counts of neutrophils, lymphocytes, monocytes, basophils, and eosinophils. Additionally, biochemistry parameters such as glucose, fibrinogen, and ion levels were measured, along with C-reactive protein (CRP) levels. NLR was calculated by dividing the absolute number of neutrophils by the absolute number of lymphocytes. Platelet-to-Lymphocyte Ratio (PLR) was obtained by the ratio between the total number of platelets ( $\times 10^9$ /L) and lymphocytes ( $\times 10^9$ /L). Systemic Inflammation Response Index (SIRI) was obtained by the following formula: neutrophil  $\times$  monocytes/lymphocytes [13]. Systemic Immune-Inflammation Index (SII) was obtained by calculating neutrophil  $\times$  platelets/lymphocytes. Serum levels of human chorionic gonadotropin (hCG), alpha-fetoprotein (AFP), CA 125, CA 19-9, CA 15-3, and carcinoembryonic antigen (CEA) were also measured. The study protocol received approval from the Institutional Review Board (IRB number PI-263-23) and adhered to the principles outlined in the Declaration of Helsinki (2013 revision). Due to the retrospective design of the study and the absence of human samples, informed consent was not required, consistent with institutional ethical standards.

Data were collected using Microsoft Excel software version 2010 (Redmond, WA, USA) and analyzed using SPSS Statistics version 25 (Chicago, IL, USA). Normality of variables was assessed using Kolmogorov–Smirnov and Shapiro–Wilk tests. For normally distributed continuous variables, independent samples t-tests were utilized, with results expressed as mean and standard deviation. Mann–Whitney tests were employed for continuous data not following a normal distribution, and results were presented as median and interquartile range (IQR). Discrete variables were presented as frequency and percentage

and analyzed using the Chi-square test or Fisher's test when applicable. Odds ratios (OR) with 95% confidence intervals were calculated. All statistical analyses were two-tailed, and significance was set at  $p < 0.05$ . The OT diagnostic yield analysis was performed using logistic regression models, and the results were represented by receiver operating characteristic (ROC) curves by calculating the area under the curve (AUC). The DeLong method was employed to compare these curves [14]. Optimal cut-off values for maximal diagnostic accuracy of each analytical parameter were determined using the Youden index with this formula "sensitivity + specificity – 1" [15].

### 3. Results

A total of 110 patients were included, with a median age at diagnosis of 11.5 years (IQR 8.2–13.6 years), and a median weight of 43 kg (24.5–53.2). In 75 patients, OT was observed during diagnostic laparoscopy (OT group), and in the remaining 35, no OT was observed (non-OT group). Patients in the OT group had a median age of 10.9 years, which was significantly lower than those in the non-OT group (median 12.1 years;  $p < 0.001$ ), although no differences in menstruation status were observed, most of them being in the premenarcheal stage.

Regarding associated symptoms, abdominal pain was the form of presentation in 70% of both groups. Nausea or vomiting was more frequent in the OT group (74% of patients), compared to only 42% in the non-OT group ( $p < 0.001$ ). Hyperthermia, on the other hand, was more frequent in the non-OT group. Time from symptoms onset to ED consultation was also higher in the non-OT group (median 18 h) compared to 12 h in the OT-group ( $p = 0.029$ ). About 20% of patients in both groups had previous episodes. Table 1 shows the demographic and clinical features in both groups.

**Table 1.** Demographic and clinical features in both groups.

	Group OT ( <i>n</i> = 75)	Group Non-OT ( <i>n</i> = 35)	<i>p</i> -Value	OR (95%CI)
Age (years); median (IQR)	10.9 (7.3–13.2)	12.1 (11.2–13.7)	<0.001	-
Weight (kg); mean (SD)	35.9 (12.1)	49.4 (16.1)	<0.001	-
Menstruation status; <i>n</i> (%)	54 (72)	23 (65.7)		
• Premenarchal			0.449	1.34 (0.56–3.17)
• Postmenarchal	21 (28)	12 (34.3)		
Clinical features; <i>n</i> (%)	59 (78.7)	25 (71.4)	0.405	1.47 (0.58–3.69)
• Abdominal pain	56 (74.7)	15 (42.9)	0.001	3.92 (1.68–9.18)
• Vomiting	2 (2.7)	1 (2.9)	0.577	0.93 (0.08–10.63)
• Diarrhea	10 (13.3)	5 (14.3)	0.892	0.92 (0.29–2.94)
• Constipation	4 (5.3)	6 (17.1)	0.046	0.27 (0.07–1.03)
• Fever	5 (6.7)	5 (14.3)	0.195	0.42 (0.12–1.59)
• Dysuria	7 (9.3)	5 (14.3)	0.438	0.62 (0.18–2.10)
• Anorexia				
Time since symptoms onset (hours); median (IQR)	12 (4–48)	18 (7–72)	0.029	-
Previous episodes; <i>n</i> (%)	15 (20)	6 (17.1)	0.722	1.21 (0.42–3.44)

95% CI, 95% Confidence Interval; OR, odds ratio; IQR, interquartile range; SD standard deviation.

Concerning ultrasound features (Table 2), the right side was the most affected in both groups. More than half of the lesions had cystic characteristics, followed by mixed lesions. Solid lesions were found in 10–14% of patients, with no differences between the two groups. Patients in the OT group had a higher ovarian volume affected and a higher affected/healthy ovarian volume ratio when compared to those in the non-OT group. In more than 90% of cases, no ovarian Doppler flow was identified. The presence of free

fluid in the pelvis was observed in more than half of the patients in both groups, with no differences between them.

**Table 2.** Preoperative ultrasound characteristics in both groups.

	OT Group ( <i>n</i> = 75)	Non-OT Group ( <i>n</i> = 35)	<i>p</i> -Value
Affected side; <i>n</i> (%)			
• Right	45 (60)	29 (82.9)	0.017
• Left	30 (40)	6 (17.1)	
Adnexal mass; <i>n</i> (%)			
• Cystic	38 (50.7)	23 (65.7)	0.064
• Solid	8 (10.7)	5 (14.3)	
• Mixed	29 (38.7)	7 (20.0)	
Ovarian volumen (ml); median (IQR)	63 (42–97)	51 (34–78)	0.013
Ovarian volumen ratio; median (IQR)	2.8 (2.1–3.5)	1.9 (1.5–2.4)	0.021
Absence of Doppler flow; <i>n</i> (%)	72 (96)	32 (91.4)	0.325
Pelvic free fluid; <i>n</i> (%)	40 (53.3)	22 (62.9)	0.348

IQR, interquartile range.

In relation to laboratory data, patients in the OT group presented elevated values of leukocytes, neutrophils, NLR, PLR, SIRI, and SII (all  $p < 0.001$ ). There were no differences in monocyte counts, nor in biochemical parameters such as CRP, glucose, fibrinogen, or ionogram. There were also no differences in tumor markers between the two groups. A summary of the laboratory findings is provided in Table 3.

Finally, the statistically significant quantitative variables in the univariate analysis were represented by ROC curves (Figure 1, Table 4). NLR was the parameter with the highest AUC (0.918), followed by SII (0.895), WBC (0.874), and SIRI (0.824). The cut-off point of NLR = 2.57 was the one with the highest sensitivity (92.4%) and specificity (90.1%).

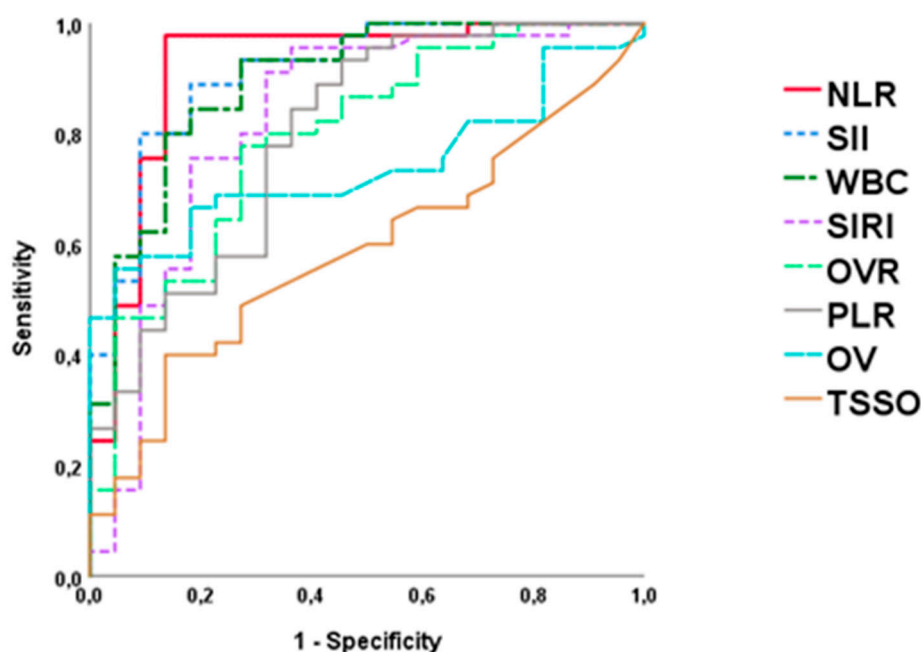


**Figure 1.** ROC curves for OT intraoperative diagnosis. NLR, Neutrophil-to-Lymphocyte Ratio; SII, Systemic Immune-Inflammation Index; SIRI, Systemic Inflammation Response Index; WBC, White Blood Cells; PLR, Platelet-to-Lymphocyte Ratio; OVR, ovarian volumen ratio; OV, ovarian volumen; TSSO, time since symptoms onset.



**Table 3.** Laboratory variables collected in both groups.

	OT Group ( <i>n</i> = 75)	Non-OT Group ( <i>n</i> = 35)	<i>p</i> -Value
Leukocytes ( $\times 10^9$ /L)	10.8 (8.6–13.4)	7.84 (5.73–10.2)	<0.001
Neutrophils ( $\times 10^9$ /L)	8.58 (6.34–13.22)	3.48 (2.81–6.04)	<0.001
Lymphocytes ( $\times 10^9$ /L)	1.64 (1.34–1.99)	2.59 (1.84–3.62)	<0.001
Monocytes ( $\times 10^9$ /L)	0.43 (0.34–0.76)	0.44 (0.32–0.61)	0.942
Platelets ( $\times 10^9$ /L)	289 (243–329)	295 (240–355)	0.785
NLR	4.6 (3.1–7.9)	1.58 (1.02–2.07)	<0.001
PLR	174.4 (126.8–278.4)	185.7 (99.1–295)	<0.001
SIRI ( $\times 10^9$ /L)	2.2 (1.1–3.9)	0.6 (0.4–1.2)	<0.001
SII ( $\times 10^9$ /L)	1385 (796–2542)	391 (265–673)	<0.001
CRP (mg/L)	2.9 (1.5–4.1)	0.9 (0.5–3.5)	0.145
Glucose (mg/dL)	100 (84–114)	98 (83–101)	0.352
Fibrinogen (mg/dL)	337 (255–427)	286 (257–402)	0.589
Ionogram			
• Na+	138 (136–140)	138 (136–140)	0.863
• K+	4 (3.7–4.4)	3.9 (3.8–4.2)	0.599
• Cl−	105 (103–106)	106 (105–108)	0.242
Tumour markers	1.2 (0.2–2)	2 (1.2–2)	0.089
• hCG	1.7 (1.3–3.2)	1.8 (1.3–10.5)	0.415
• AFP	23.7 (15.9–44.7)	14.8 (11.4–26.4)	0.072
• CA 125	17.7 (9.7–26.0)	16.9 (12.1–35.5)	0.949
• CA 19-9	10.4 (9.4–19.8)	10.4 (8.7–15.3)	0.853
• CA 15-3			
• CEA	1.0 (0.5–1.2)	0.5 (0.5–4)	0.600

NLR, Neutrophil-to-Lymphocyte Ratio; PLR, Platelet-to-Lymphocyte Ratio; SIRI, Systemic Inflammation Response Index; SII, Systemic Immune-Inflammation Index; hCG, human chorionic gonadotropin; AFP, alpha-fetoprotein; CA 125, cancer antigen 125; CA 19-9, cancer antigen 19-9; CA 15-3, cancer antigen 15-3; CEA, carcinoembryonic antigen.

**Table 4.** Area under the curve (AUC) values, cut-off point, sensitivity, and specificity for OT intraoperative finding.

	AUC	Cut-Off Point	Sensitivity	Specificity	<i>p</i> Value
NLR	0.918	2.57	92.4	90.1	<0.001
SII ( $\times 10^9$ /L)	0.895	717.8	88.9	81.8	<0.001
WBC ( $\times 10^9$ /L)	0.872	9,235	84.4	81.8	<0.001
SIRI ( $\times 10^9$ /L)	0.824	1.25	75.6	81.8	<0.001
OV (mL)	0.797	58	77.4	75.1	0.025
OVR	0.794	2.3	77.8	72.7	0.012
PLR	0.739	157	73.8	78.2	0.002
TSSO (min)	0.588	296	68.1	79.3	0.245

NLR, Neutrophil-to-Lymphocyte Ratio; SII, Systemic Immune-Inflammation Index; WBC, white blood cells; SIRI, Systemic Inflammation Response Index; OV, ovarian volumen; OVR, ovarian volumen ratio; PLR, Platelet-to-Lymphocyte Ratio; TSSO, time since symptoms onset.

#### 4. Discussion

This study analyzes different clinical, radiological, and laboratory factors as predictors of ovarian torsion in children. Although clinical symptoms and ultrasound data provide the basis for a diagnosis of suspicion, the NLR has the strongest predictive ability for

ovarian torsion in infants. Diagnosis complexity in these patients can cause delays in optimal treatment, and therefore seeking potential predictive biomarkers is important for the prognosis of this disease.

The incidence of ovarian torsion is estimated to be between 0.5 and 2 cases per 10,000 patients, representing approximately 2% to 3% of all visits for abdominal pain in EDs [1,16]. Symptoms can also be very vague and may range from mild to severe pelvic or abdominal pain, nausea, vomiting, or fever, and can even mimic other etiologies of abdominal pain, including acute appendicitis, mesenteric adenitis, constipation, functional ovarian cysts, renal colic, pyelonephritis, and even colitis [17,18]. In postmenarcheal cases, a possible ectopic pregnancy should also be considered [19]. Furthermore, in the pediatric population, reproductive organs lie high in the abdomen and may be difficult to evaluate on physical examination, which may additionally complicate reaching an appropriate diagnosis [20,21]. Abdominal pain is the most common presentation, which was present in more than 70% of patients in both groups. Vomiting and/or nausea are the most common accompanying complaints [4]. In our study, we found that the presence of vomiting was more frequently associated with OT, which may be secondary to the parasympathetic reaction induced by ischemia. In contrast, we observed that hyperthermia was more frequent in patients without OT, more related to abdominal or pelvic infectious causes.

A prolonged interval between the onset of pain and the diagnosis of torsion correlates with a decreased rate of ovarian salvage [16]. However, it is difficult to influence the duration between the first symptoms and consultation in the ED. In our study, patients in the OT group had a shorter time from symptom onset to ED consultation than girls in the non-OT group. The ischemia maintained during the time in the OT may explain that the pain is less bearable in these cases, and that is why the time to go to the ED is shorter. Although ovarian torsion is more common in the postmenarcheal girls due to the increased prevalence of ovarian cysts in these patients, it can also be found in premenarcheal children [22]. Other common acute adnexal pathologies such as simple ovarian cysts with or without rupture are more frequent during menstruation and may be confused with an OT. This may justify the findings found in our study, where the majority of girls in the non-OT group were postmenarcheal, unlike those in the OT group, and consequently, ovarian torsion may still remain a potential diagnosis in both pre- and postmenarcheal girls. The association of vomiting, shorter time from symptom onset and premenarcheal age have been identified by other authors as clinical predictors of OT in girls [23]. However, these studies do not include ultrasound data or inflammatory laboratory parameters.

Ultrasonography is the preferred imaging modality when ovarian pathology is clinically suspected. Signs such as increased ovarian size, the presence of a complex mass, and free fluid can indicate adnexal torsion [5]. However, the ultrasound appearance of ovarian torsion varies depending on factors like the duration and extent of torsion, whether it is complete or incomplete, and the presence or absence of an ovarian mass. Color Doppler sonography has emerged as a potential tool for identifying interruptions in ovarian blood flow in recent years [24,25]. Yet, it is essential to recognize that the presence of vascular flow on Doppler studies does not conclusively exclude torsion, nor does the flow absence confirm OT. Shadinger et al. found arterial flow in 54% and venous flow in 33% of patients with pathologically proven OT [5]. In our study, we found significantly higher ovarian volume and ovarian volume ratio in patients with OT, with no differences in the rates of absence of Doppler flow or pelvic free fluid. We also observed a predominant occurrence of torsion on the right side in both groups, similar to previous studies [26–28]. This might be attributed to the presence of the sigmoid colon in the left iliac fossa, which reduces the mobility of the tubal structure and consequently lowers the risk of left adnexal torsion.

Some laboratory data have been tested to predict OT, although several authors found them unhelpful in the diagnostic process [29,30]. CRP levels rise in response to inflammation and tissue necrosis several hours after torsion, making it of little use for early diagnosis [31]. In addition, alternating CRP concentrations during the menstrual cycle have been reported, although they are not usually as high as that encountered in ovarian torsion,

but this could potentially make interpretation difficult [31]. In OT, tissue ischemia initiates systemic inflammation that can be quantified in peripheral blood. In adults, markers such as interleukin-6, interleukin-8, tumor necrosis factor- $\alpha$ , and E-selectin have been proposed, but low availability and high cost make their use in clinical practice complicated [31]. In contrast, white blood cell data reflect systemic inflammation, being universally available, quickly analyzed, and cost effective. In this context, the usefulness of NLR as a diagnostic marker of OT has been described, mainly in adult women [11,32]. However, there is scarce experience in pediatric patients. Nissen et al. analyzed laboratory data from 18 girls with OT and 58 controls with ovarian pathology other than torsion and observed that NLR and PLR allowed differentiation between the two cohorts [12]. Nonetheless, they did not include ultrasound data in the analysis, so our present study represents a novelty in this aspect. Furthermore, our study is the first to analyze different inflammatory indices (NLR, PLR, SIRI, SII), which are easily calculated from blood count data, and also compares them with clinical and ultrasound data, similar to what occurs in clinical practice. The results obtained demonstrate that the NLR is the most sensitive and specific predictor for the diagnosis of OT in girls. On the one hand, it is a more objective parameter than clinical data such as time from symptom onset, which is sometimes not very accurate since the presentation sometimes begins with progressive pain. In addition, it avoids the explorer-dependent variability of radiological tests such as ultrasound.

Inflammatory response secondary to ovarian ischemia results in neutrophilia due to chemotaxis and increased release of these cells from the bone marrow to the peripheral blood, which is combined with lymphopenia induced by elevated levels of endogenous cortisol due to ischemia [33]. All this leads to an elevation of the NLR by two combined pathways. This may explain the higher AUC with respect to other inflammatory indices such as PLR, SIRI, or SII that involves monocytes or platelets, as NLR translates the combined cellular response of neutrophilia and lymphopenia. These observations may extend beyond female reproductive organs, as the role of NLR as a predictor of testicular torsion in adolescents has also been recently described [7]. Other authors have described the usefulness of NLR for the differentiation of ruptured ovarian cysts and adnexal torsion, although no analysis of additional inflammatory indices has been performed [34]. Tayyar et al. reported a marked reduction of platelets in patients with OT with comparably unaltered lymphocyte counts, which conditioned a low predictive capacity of the PLR, consistent with the results obtained in our study [35]. In summary, the main advantage of NLR is that it incorporates the informative aspects of two variables representing contrasting immune pathways through the leukocyte subtype ratio, which provides a more accurate depiction of the overall impact of alterations in ovarian torsion. NLR demonstrated superior discriminatory power compared to leukocytes, neutrophils, PLR, SIRI, and SII, as evidenced by higher AUC values in ROC curves analysis.

The main strength of this study is the inclusion of clinical, ultrasound, and laboratory data, which allows ovarian torsion to be analyzed from a holistic perspective, which constitutes a novelty in this aspect. This translates into high applicability, as it includes the same parameters that are used in routine clinical practice in this type of patient. This translates into the need for urgent diagnostic laparoscopy in cases with NLR values above 2.57, avoiding delays in the management of these patients, while in cases with low inflammatory parameters, initial conservative management can be considered, with subsequent clinical, ultrasound, and analytical reevaluation. However, our study has limitations that should be taken into account. The retrospective design is the main limitation, since it only allows us to analyze the data previously collected in the medical record. In addition, the absence of similar studies in pediatric patients makes it difficult to compare the results obtained. The sample size is also limited, despite the multicenter participation, due to the relatively low incidence of this pathology. Therefore, caution should be adopted when extrapolating or generalizing these results. Prospective studies are required to validate these findings.

## 5. Conclusions

NLR can be considered as a useful predictor of pediatric OT in cases with clinical and ultrasound suspicion. Values above 2.57 may help to anticipate urgent surgical treatment in these patients, avoiding delays in surgical care in these cases. In patients with low inflammatory values, an initial conservative management can be considered, with clinical, ultrasound, and analytical reevaluation. However, prospective studies are required to validate these findings.

**Author Contributions:** Conceptualization, C.D.-M.; methodology, J.A.-M., J.C.M.-A., M.S.B. and N.C.; software, J.A.-M.; validation, F.H.-O.; formal analysis, R.D.; investigation, C.D.-M.; resources, C.D.-M.; data curation, J.A.-M., J.C.M.-A., M.S.B. and N.C.; writing—original draft preparation, C.D.-M.; writing—review and editing, J.A.-M. and J.C.M.-A.; visualization, R.P.P., E.F. and P.A.; supervision, R.D.; project administration, F.H.-O. All authors have read and agreed to the published version of the manuscript.

**Funding:** This research did not receive any specific grant from funding agencies in the public, commercial, or not-for-profit sectors.

**Institutional Review Board Statement:** The study was conducted in accordance with the Declaration of Helsinki, and approved by the Institutional Review Board of Fundación Jiménez Díaz Hospital (IRB number PI-263-23).

**Informed Consent Statement:** Patient consent was waived due to the retrospective design of the study and the absence of human samples.

**Data Availability Statement:** The data generated and analysed in this study will be made available upon reasonable request to the authors.

**Conflicts of Interest:** The authors declare no conflict of interest.

## References

- Guthrie, B.D.; Adler, M.D.; Powell, E.C. Incidence and trends of pediatric ovarian torsion hospitalizations in the United States, 2000–2006. *Pediatrics* **2010**, *125*, 532–538. [CrossRef] [PubMed]
- Breech, L.L.; Hillard, P.J. Adnexal torsion in pediatric and adolescent girls. *Curr. Opin. Obstet. Gynecol.* **2005**, *17*, 483–489. [CrossRef] [PubMed]
- Nur Azurah, A.G.; Zainol, Z.W.; Zainuddin, A.A.; Lim, P.S.; Sulaiman, A.S.; Ng, B.K. Update on the management of ovarian torsion in children and adolescents. *World J. Pediatr.* **2015**, *11*, 35–40. [CrossRef] [PubMed]
- Rey-Bellet Gasser, C.; Gehri, M.; Joseph, J.M.; Pauchard, J.Y. Is It Ovarian Torsion? A Systematic Literature Review and Evaluation of Prediction Signs. *Pediatr. Emerg. Care* **2016**, *32*, 256–261. [CrossRef]
- Shadinger, L.L.; Andreotti, R.F.; Kurian, R.L. Preoperative sonographic and clinical characteristics as predictors of ovarian torsion. *J. Ultrasound Med.* **2008**, *27*, 7–13. [CrossRef] [PubMed]
- Hurh, P.J.; Meyer, J.S.; Shaaban, A. Ultrasound of a torsed ovary: Characteristic gray-scale appearance despite normal arterial and venous flow on Doppler. *Pediatr. Radiol.* **2002**, *32*, 586–588. [CrossRef] [PubMed]
- Delgado-Miguel, C.; García, A.; Muñoz-Serrano, A.J.; López-Pereira, P.; Martínez-Urrutia, M.J.; Martínez, L. The role of neutrophil-to-lymphocyte ratio as a predictor of testicular torsion in children. *J. Pediatr. Urol.* **2022**, *18*, e1–e697. [CrossRef] [PubMed]
- Yakut, H.I.; Kurt, T.; Uncu, N.; Semsä Cayci, F.; Celikel Acar, B. Predictive role of neutrophil to lymphocyte ratio and mean platelet volume in Henoch-Schönlein purpura related gastrointestinal and renal involvement. *Arch. Argent. Pediatr.* **2020**, *118*, 139–142. [PubMed]
- Delgado-Miguel, C.; Muñoz-Serrano, A.J.; Barrera Delfa, S.; Núñez Cerezo, V.; Estefanía, K.; Velayos, M.; Serradilla, J.; Martínez Martínez, L. Neutrophil-to-lymphocyte ratio as a predictor of peritonitis in acute appendicitis in children. *Cir. Pediatr.* **2019**, *32*, 185–189.
- Delgado-Miguel, C.; Muñoz-Serrano, A.J.; Núñez, V.; Estefanía, K.; Velayos, M.; Miguel-Ferrero, M.; Barrera, S.; Martínez, L. Neutrophil-to-Lymphocyte Ratio as a Predictor of Postsurgical Intraabdominal Abscess in Children Operated for Acute Appendicitis. *Front. Pediatr.* **2019**, *7*, 424. [CrossRef]
- Khanzadeh, S.; Tahernia, H.; Hernandez, J.; Sarcone, C.; Lucke-Wold, B.; Salimi, A.; Tabatabaei, F. Predictive Role of Neutrophil to Lymphocyte Ratio in Adnexal Torsion: A Systematic Review and Meta-Analysis. *Mediat. Inflamm.* **2022**, *2022*, 9680591. [CrossRef]
- Nissen, M.; Sander, V.; Rogge, P.; Alrefai, M.; Tröbs, R.B. Neutrophil to Lymphocyte Ratio and Platelet to Lymphocyte Ratio Might Predict Pediatric Ovarian Torsion: A Single-Institution Experience and Review of the Literature. *J. Pediatr. Adolesc. Gynecol.* **2021**, *34*, 334–340. [CrossRef]

13. Siki, F.Ö.; Sarıkaya, M.; Gunduz, M.; Sekmenli, T.; Korez, M.K.; Ciftci, I. Evaluation of the systemic immune inflammation index and the systemic inflammatory response index as new markers for the diagnosis of acute appendicitis in children. *Ann. Saudi Med.* **2023**, *43*, 329–338. [CrossRef] [PubMed]
14. DeLong, E.R.; DeLong, D.M.; Clarke-Pearson, D.L. Comparing the areas under two or more correlated receiver operating characteristic curves: A nonparametric approach. *Biometrics* **1988**, *44*, 837–845. [CrossRef]
15. Fluss, R.; Faraggi, D.; Reiser, B. Estimation of the Youden Index and its associated cutoff point. *Biometr. J.* **2005**, *47*, 458–472. [CrossRef]
16. Schmitt, E.R.; Ngai, S.S.; Gausche-Hill, M.; Renslo, R. Twist and shout! Pediatric ovarian torsion clinical update and case discussion. *Pediatr. Emerg. Care* **2013**, *29*, 518–523. [CrossRef]
17. Kurtoglu, E.; Kokcu, A.; Danaci, M. Asynchronous bilateral ovarian torsion. A case report and mini review. *J. Pediatr. Adolesc. Gynecol.* **2014**, *27*, 12244. [CrossRef] [PubMed]
18. Damigos, E.; Johns, J.; Ross, J. An update on the diagnosis and management of ovarian torsion. *Obstet. Gynaecol.* **2012**, *14*, 229–236. [CrossRef]
19. Kokoska, E.R.; Keller, M.S.; Weber, T.R. Acute ovarian torsion in children. *Am. J. Surg.* **2000**, *180*, 462–465. [CrossRef]
20. Huchon, C.; Staraci, S.; Fauconnier, A. Adnexal torsion: A predictive score for pre-operative diagnosis. *Hum. Reprod.* **2010**, *25*, 2276–2280. [CrossRef]
21. Oelsner, G.; Shashar, D. Adnexal torsion. *Clin. Obstet. Gynecol.* **2006**, *49*, 459. [CrossRef] [PubMed]
22. Ashwal, E.; Hirsch, L.; Krissi, H.; Eitan, R.; Less, S.; Wiznitzer, A.; Peled, Y. Characteristics and Management of Ovarian Torsion in Premenarchal Compared With Postmenarchal Patients. *Obstet. Gynecol.* **2015**, *126*, 514–520. [CrossRef] [PubMed]
23. Bolli, P.; Schädelin, S.; Holland-Cunz, S.; Zimmermann, P. Ovarian torsion in children: Development of a predictive score. *Medicine* **2017**, *96*, e8299. [CrossRef] [PubMed]
24. Ben-Ami, M.; Perlitz, Y.; Haddad, S. The effectiveness of spectral and color Doppler in predicting ovarian torsion. A prospective study. *Eur. J. Obstet. Gynecol. Reprod. Biol.* **2002**, *104*, 64–66. [CrossRef] [PubMed]
25. Albayram, F.; Hamper, U.M. Ovarian and adnexal torsion: Spectrum of sonographic findings with pathologic correlation. *J. Ultrasound Med.* **2001**, *20*, 1083–1089. [CrossRef]
26. Cass, D.L.; Hawkins, E.; Brandt, M.L.; Chintagumpala, M.; Bloss, R.S.; Milewicz, A.L.; Minifee, P.K.; Wesson, D.E.; Nuchtern, J.G. Surgery for ovarian masses in infants, children, and adolescents: 102 consecutive patients treated in a 15-year period. *J. Pediatr. Surg.* **2001**, *36*, 693–699. [CrossRef] [PubMed]
27. Anders, J.F.; Powell, E.C. Urgency of evaluation and outcome of acute ovarian torsion in pediatric patients. *Arch. Pediatr. Adolesc. Med.* **2005**, *159*, 532–535. [CrossRef] [PubMed]
28. Poonai, N.; Poonai, C.; Lim, R.; Lynch, T. Pediatric ovarian torsion: Case series and review of the literature. *Can. J. Surg.* **2013**, *56*, 103–108. [CrossRef] [PubMed]
29. Pepys, M.B.; Hirschfield, G.M. C-reactive protein: A critical update. *J. Clin. Investig.* **2003**, *111*, 1805–1812. [CrossRef]
30. Wander, K.; Brindle, E.; O'Connor, K.A. C-reactive protein across the menstrual cycle. *Am. J. Phys. Anthropol.* **2008**, *136*, 138–146. [CrossRef]
31. Daponte, A.; Pournaras, S.; Hadjichristodoulou, C.; Lialios, G.; Kallitsaris, A.; Maniatis, A.N.; Messinis, I.E. Novel serum inflammatory markers in patients with adnexal mass who had surgery for ovarian torsion. *Fertil. Steril.* **2006**, *85*, 1469–1472. [CrossRef] [PubMed]
32. Ercan, Ö.; Köstü, B.; Bakacak, M.; Coşkun, B.; Tohma, A.; Mavigök, E. Neutrophil to Lymphocyte ratio in the diagnosis of adnexal torsion. *Int. J. Clin. Exp. Med.* **2015**, *8*, 16095–16100. [PubMed]
33. Buck, B.H.; Liebeskind, D.S.; Saver, J.L.; Bang, O.Y.; Yun, S.W.; Starkman, S.; Ali, L.K.; Kim, D.; Villablanca, J.P.; Salamon, N.; et al. Early neutrophilia is associated with volume of ischemic tissue in acute stroke. *Stroke* **2008**, *39*, 355–360. [CrossRef] [PubMed]
34. Soysal, S.; Baki, R.B. Diagnostic value of neutrophil to lymphocyte ratio in differentiation of ruptured ovarian cysts and adnexal torsion. *Turk. J. Obstet. Gynecol.* **2018**, *15*, 91–94. [CrossRef]
35. Tayyar, A.T.; Özkaya, E.; Yayla, Ç.A.; Şentürk, M.B.; Selçuk, S.; Polat, M.; Cündübay, C.R.; Tayyar, M. Evaluation of complete blood count parameters to predict ovarian torsion in women with adnexal mass. *Gynecol. Obstet. Reprod. Med.* **2017**, *23*, 1. [CrossRef]

**Disclaimer/Publisher’s Note:** The statements, opinions and data contained in all publications are solely those of the individual author(s) and contributor(s) and not of MDPI and/or the editor(s). MDPI and/or the editor(s) disclaim responsibility for any injury to people or property resulting from any ideas, methods, instructions or products referred to in the content.

Review

# Abdominal Parietal Metastasis from Cervical Cancer: A Review of One of the Most Uncommon Sites of Recurrence Including a Report of a New Case

Irinel-Gabriel Dicu-Andreescu <sup>1,2</sup>, Marian-Augustin Marincas <sup>1,2,\*</sup>, Anca-Angela Simionescu <sup>1,3,\*</sup>, Ioana Dicu-Andreescu <sup>1</sup>, Virgiliu-Mihail Prunoiu <sup>1,2</sup>, Sânziana-Octavia Ionescu <sup>1,2</sup>, Ștefania-Ariana Neicu <sup>4</sup>, Gabriela-Mădălina Radu <sup>4</sup>, Eugen Brătucu <sup>1,2</sup> and Laurențiu Simion <sup>1,2</sup>

<sup>1</sup> Clinical Department No 10, General Surgery, University of Medicine and Pharmacy “Carol Davila”, 050474 Bucharest, Romania; irinel-gabriel.andreescu@rez.umfcd.ro (I.-G.D.-A.)

<sup>2</sup> Department of Oncological Surgery, Oncological Institute “Prof. Dr. Alexandru Trestioreanu”, 022328 Bucharest, Romania

<sup>3</sup> Department of Obstetrics and Gynecology, Filantropia Clinical Hospital, 011171 Bucharest, Romania

<sup>4</sup> Department of Pathological Anatomy, Oncological Institute “Prof. Dr. Alexandru Trestioreanu”, 022328 Bucharest, Romania

\* Correspondence: marian.marincas@umfcd.ro (M.-A.M.); anca.simionescu@umfcd.ro (A.-A.S.)

**Abstract:** Introduction: Cervical cancer is the fourth most common cancer in women, the highest mortality being found in low- and middle-income countries. Abdominal parietal metastases in cervical cancer are a very rare entity, with an incidence of 0.1–1.3%, and represent an unfavorable prognostic factor with the survival rate falling to 17%. Here, we present a review of cases of abdominal parietal metastasis in recent decades, including a new case of a 4.5 cm abdominal parietal metastasis at the site of the scar of the former drain tube 28 months after diagnosis of stage IIB cervical cancer (adenosquamous carcinoma), treated by external radiotherapy with concurrent chemotherapy and intracavitary brachytherapy and subsequent surgery (type B radical hysterectomy). The tumor was resected within oncological limits with the histopathological result of adenosquamous carcinoma. The case study highlights the importance of early detection and appropriate treatment of metastases in patients with cervical cancer. The discussion explores the potential pathways for parietal metastasis and the impact of incomplete surgical procedures on the development of metastases. The conclusion emphasizes the poor prognosis associated with this type of metastasis in cervical cancer patients and the potential benefits of surgical resection associated with systemic therapy in improving survival rates.

**Keywords:** parietal; metastasis; cervical cancer; HPV; hysterectomy; radiotherapy; lymph node

## 1. Introduction

Cervical cancer is the fourth most frequent cancer in women worldwide, with about 604,000 new cases and 342,000 deaths reported in 2020 [1]. Almost 90% of cases take place in low- and middle-income countries [2]. The most prevalent cause is chronic infection with human papillomavirus (HPV) [3], favored by a series of additional risk factors such as a weaker immune system caused by coinfection with HIV/AIDS [4,5], obesity [6], smoking [7], multiple sexual partners, multiparity [8], and a diet poor in fruits and vegetables [9]. Also, some studies have shown that women with a first-degree relative who has had cervical cancer may have a higher risk of developing the disease themselves [10].

The treatment options for this type of cancer vary depending on its stage, established by the International Federation of Gynecology and Obstetrics (FIGO). In the early stages (IA1, IA2), the patient can opt for fertility preservation methods such as cervical conization or radical trachelectomy, or, if fertility preservation is not desired, an extrafascial

hysterectomy can be performed (also known as hysterectomy type A according to the Querleu–Morrow classification) for stage IA1 or a modified radical hysterectomy (hysterectomy type B) for stage IA2. For stages IB1, IB2, and IIA1, in which the tumor does not exceed 4 cm in diameter and is limited to the cervix, the recommended intervention is a radical hysterectomy type C with pelvic lymphadenectomy [11].

For stages IB3 and IIA2, external radiotherapy combined with concurrent platinum-based chemotherapy followed by intracavitary brachytherapy is recommended. Another alternative is external pelvic radiotherapy associated with concurrent chemotherapy and brachytherapy followed by a complementary radical hysterectomy (type C), but only for certain selected cases. Starting with stage IIB, the NCCN recommends concurrent chemoradiotherapy with the possibility of additional external beam irradiation with 5–10 Gy in case of parametrial invasion, as well as irradiation of the para-aortic lymph nodes [11].

The local guideline of the Bucharest Oncological Institute follows the ESGO/ESTRO/ESP [12] and NCCN treatment guidelines but also provides an alternative treatment option for selected cases of patients with stages considered locoregionally advanced (Stages IIB, III, and IVA) but nonmetastatic. In these cases, our guideline recommends that the concurrent radio-chemotherapy be followed, after an interval of 6–8 weeks, by open radical surgery [13].

The abdominal wall is a complex structure consisting of connective tissue, muscle, fat, and skin. Parietal metastases from internal malignancies range in frequency from 1–4.6% [14], a number that is even lower when it comes to cervical cancer—0.1 to 1.3% [15].

Parietal metastases can involve the skin and can invade conjunctive tissue, and muscles typically appear near metastatic lymph nodes, surgical scars, such as laparoscopic port sites [16], or the umbilicus [17]. They are often a late indicator of the disease, although occasionally they might be the first indication of internal cancers like lung, renal, and ovarian cancers [17]. The most common initial tumors that present parietal metastasis are the breast and ovaries in women and the lung and colon in men [18].

Parietal metastases are divided into two main categories based on the location of the lesion and the past surgical history of the patients: Sister (Mary) Joseph Nodules (SJNs), which are metastatic umbilical tumors [19], and non-SJN skin metastases. SJNs usually develop in patients with gastrointestinal and gynecological cancers [20]. However, umbilical metastases that appear as a port-site recurrence following laparoscopic surgery are not included in the SJNs group. Also, in individuals with peritoneal dissemination, an SJN may appear as the initial presentation of a tumor or as a marker of recurrence [21]. Although chemotherapy can resolve peritoneal dissemination, an SJN may still arise even in the absence of other concomitant peritoneal recurrences [22]. Furthermore, patients with severe involvement of the superficial lymph nodes, such as the axillary and inguinal nodes, may develop SJNs [23].

Based on previous medical treatments or situations, non-SJN parietal metastases can be further classified into three major patterns such as parietal metastasis following surgery, injury, or the presence of lymphadenopathy. After surgery, parietal metastases frequently appear at the location of the incisions following surgery for gynecological and gastrointestinal malignancies and it is claimed that about 1–2% of patients who have undergone laparoscopic surgery for malignant illness have port-site recurrences [24].

Non-SJN metastasis following injury can appear even when the location of a traumatic injury is far from the source of the primary tumor. The literature describes a few such cases: skin metastases occurred at the injection site in a patient with advanced prostate cancer receiving subcutaneous goserelin treatment [25]; also, a patient with colon cancer developed skin metastases at the site of the inflammatory reaction to skin test antigen (Dinitrochlorobenzene) [26]. Last, but not least, a patient with laryngeal cancer who did not have lymph node metastases experienced the development of many superficial nodules encircling the region that previously had the body spica cast applied on from an earlier incident [27].

Finally, skin metastases may appear in the region of the metastatic superficial lymphadenopathy. In some cases, patients with breast cancer experienced skin metastases in the chest wall after axillary node metastases [28]. In patients with prostate cancer, inguinal node metastasis was followed by skin metastases in the lower abdomen, scrotum, and penis [29]. Moreover, in patients with cervical cancer, skin metastases to the vulva, upper thigh, and lower abdomen appeared after inguinal node metastasis [30,31].

During surgical intervention, certain steps must be taken to prevent the dissemination of tumor cells, such as clamping fallopian tubes at the start of the surgery, washing the abdominal cavity with sodium chloride 0.9% at the end of the operation, and obtaining all lymph nodes and lymphadenectomy specimens without lymph node fragmentation [32]. In Figure 1, there is a brief description of the main pathways of dissemination of tumor cells.

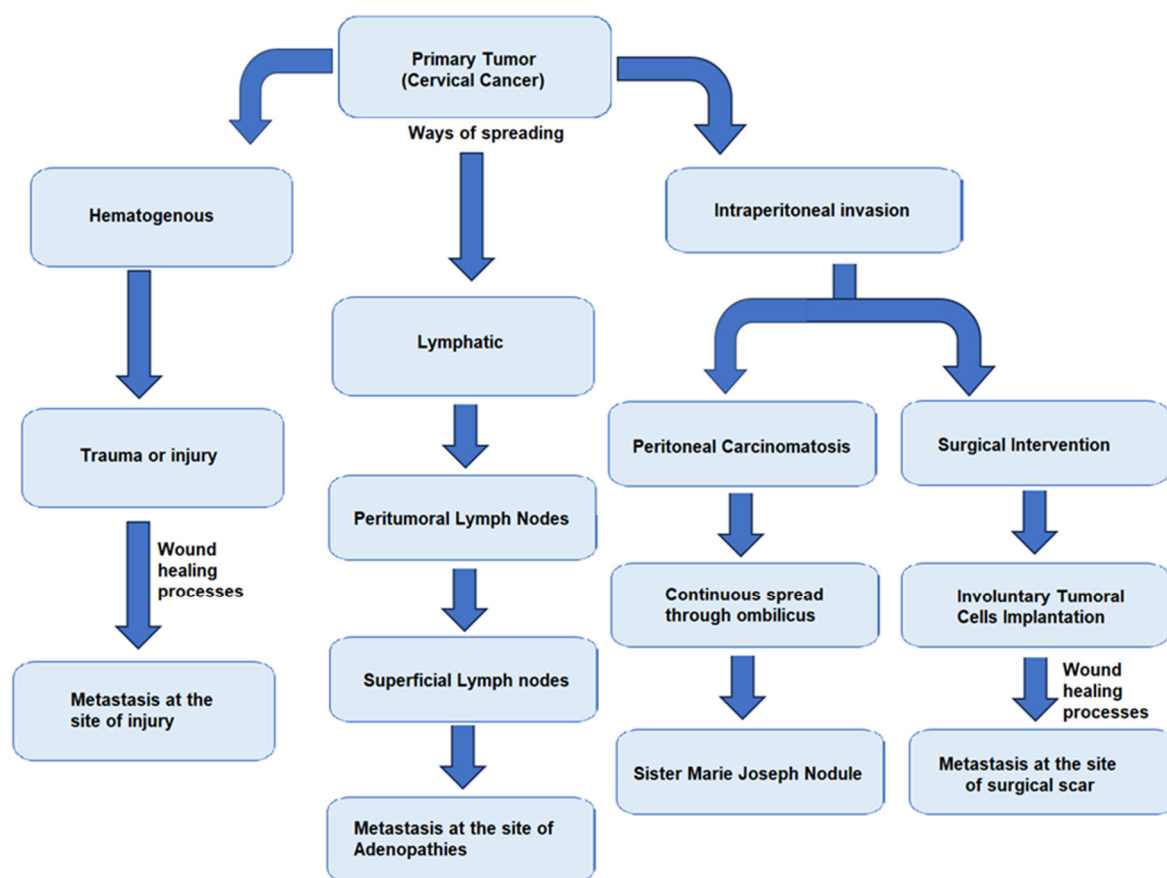


**Figure 1.** Schematic description of tumor dissemination pathways.

Here, we also present a rare case of abdominal parietal metastasis that occurred 28 months after treatment for stage IIB cervical carcinoma and a review of other similar cases. Informed consent for the research and publication of the data was obtained from the patient according to the Declaration of Helsinki, revised in 2000 in Edinburgh.

## 2. Case Description

A 47-year-old patient was admitted to the Department of Oncological Surgery of the Bucharest Oncological Institute in November 2019 for vaginal bleeding and leucorrhea and was diagnosed with stage IIB adenosquamous carcinoma. From her medical history, we found that she was nulliparous and had frequent episodes of depression that have intensified in the last 3 years, for which she did not take medication.

A multidisciplinary committee consisting of a surgeon, an oncologist, and a radiotherapist was convened, who decided to perform radiotherapy with concurrent chemotherapy as the first step of treatment. Six weeks after the neoadjuvant treatment was completed, only if



the patient had a good response, meaning that the tumor had significantly decreased in size or had completely disappeared, radical hysterectomy type C with pelvic lymphadenectomy was recommended.

The patient was directed to the radiotherapy department to perform neoadjuvant radiotherapy with concurrent chemotherapy. The preirradiation CT examinations revealed: an enlarged uterus of 11/7.5 cm, a tumorous cervix of 7/3.5 cm with fine irregular external contour especially on the left lateral circumference, and apparent left parametrial invasion. Some small infracentimetric inguinal and external iliac adenopathies were also described. Twenty-five sessions of external radiotherapy with a total dose of 50 Gray (Gy) and five sessions of concurrent chemotherapy (Cisplatin) (until February 2020) were performed, followed by three sessions of endocavitary brachytherapy (until March 2020).

At the imaging examinations after the completion of radiotherapy treatment (April 2020), the patient showed a favorable response with a decrease in the size of the uterus and the complete disappearance of the cervical tumor, leaving an area of 9 mm of fibrous tissue at the site of the former tumor. Small bilateral external iliac and inguinal lymph nodes were still present. However, the PET-CT examination did not reveal any metabolically active lesions with an oncological substrate.

Although the internal guide recommends that the operation should be performed 6 weeks after the end of the neoadjuvant treatment, it was performed after 12 weeks because of the patient's hesitation, in August 2020. Intraoperatively, a uterus of quasinormal size was visualized, with the bladder intimately adherent to the cervix, (as shown in Figure 2), with slight retraction of the parameter and the left paracolpium. At the level of both ilio-obturator fossae, a fibroinflammatory remodeling process was observed, probably postradiation, without palpable adenopathies.

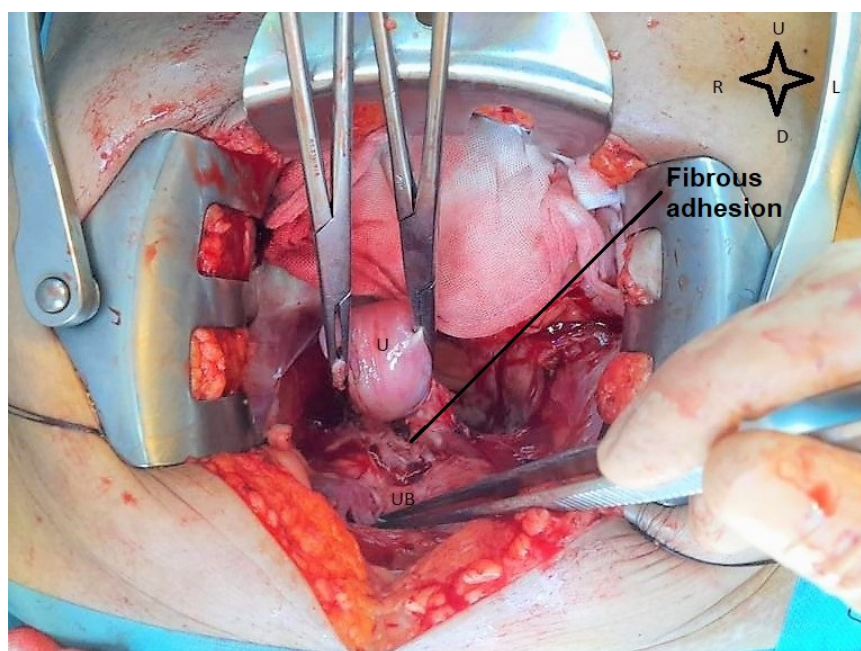


**Figure 2.** Intraoperative view during radical hysterectomy. The cervix is adherent to the urinary bladder. U—uterus; UB—urinary bladder (image from video archive of Bucharest Oncological Institute, personal collection of Dr. Marincaş).

A radical hysterectomy type B2 according to the Querleu–Morrow Classification (classical “modified” radical hysterectomy) was performed, consisting of excision of the uterus and both adnexa, with the lateral mobilization of the ureter and resection of the nodes of the lateral part of the paracervix with a vaginal cuff of 10 mm. The resection margin was free of tumor cells. Radical lymphadenectomy could not be performed due to fibrotic changes developed postirradiation, but we managed to take biopsies from both

ilio-obturator lymph node tissue. To prevent tumor dissemination, both fallopian tubes were clamped at the beginning of the operation, the pelvic cavity was washed at the end, and the sampling of lymph nodes was performed without lymph node fragmentation. At the histopathological examination of the resection piece, no residual tumor was identified at the level of the cervix.

Postoperative, the clinical evolution was favorable and the patient was discharged after five days. No immediate complications were noted. A periodic check-up, including clinical examinations, vaginal swab cytology, and CT and MRI examinations was performed.

Until December 2022, no signs of locoregional tumor recurrence, distant metastasis, or abdominopelvic tumoral adenopathy were detected. However, in March 2023, 28 months after surgery, the patient presented in the clinic complaining of slight pain in the right iliac fossa and the appearance of a 4 cm palpable tumor in the same place, with skin retraction and erythema, a hard consistency, being fixed to the muscle plane, and also painful when the right abdominal muscle was contracted.

An abdominopelvic CT scan revealed a 37/28 mm tumor in the right iliac fossa in the full thickness of the abdominal wall (Figure 3). Also, there were numerous pelvic lymph nodes in the left ilio-obturator fossa with a tendency to form adenopathic blocks (Figure 4).



**Figure 3.** Abdomino-pelvin CT scan shows the parietal tumor in the right iliac fossa (yellow circles).

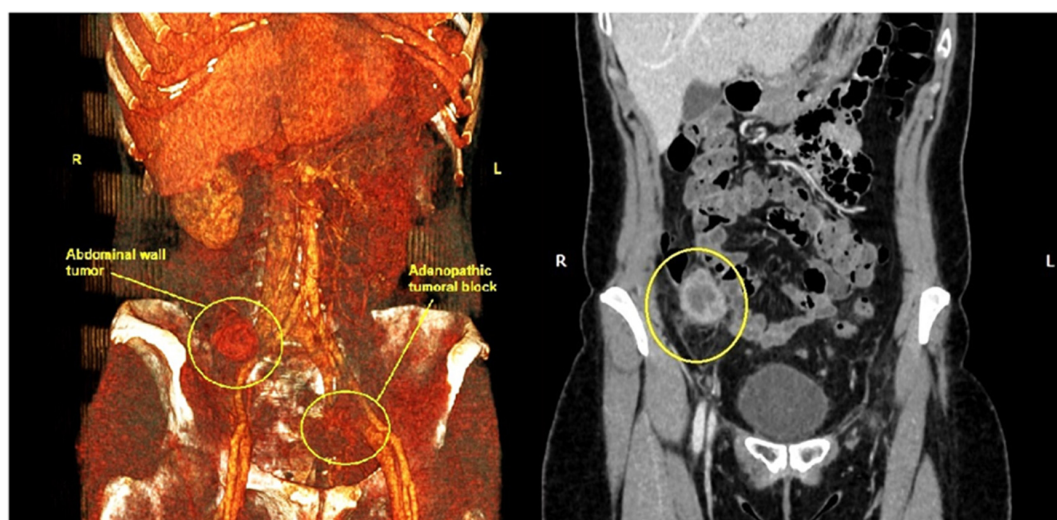


**Figure 4.** Abdominal CT scan with 3D reconstruction shows the parietal tumor from the right iliac fossa and the left iliac adenopathic block (yellow circles). (R—right, L—Left).

The multidisciplinary committee decided that surgery should be the next step of treatment due to the benefits it can bring on the histological result and also through the removal of the painful right iliac fossa tumor. Intraoperative findings included a 4.5 cm parietal tumor, corresponding to the scar of the former abdominal drain tube at the level of the right iliac fossa, with the great omentum adhering to it, without any other intraperitoneal metastases. We also found a left iliac adenopathic tumor block surrounding the left external iliac vein (Figure 5), which was biopsied, as it could not be completely resected due to the vascular risks involved. A pelvic drain tube was placed at this level as shown in Figure 5.

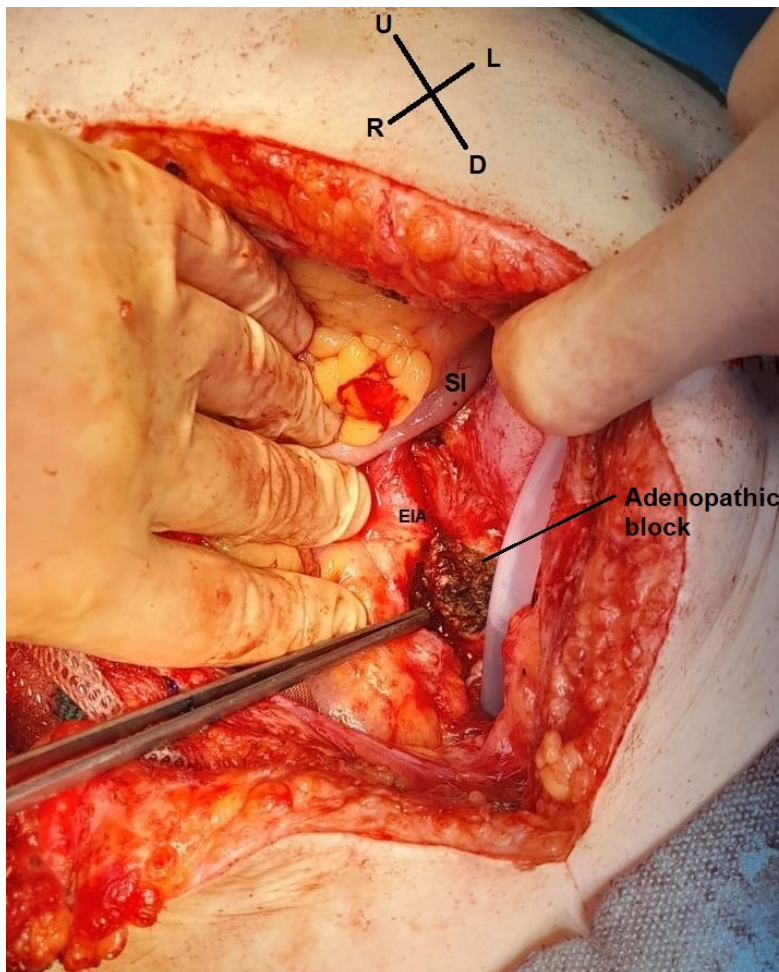


**Figure 5.** Intraoperative view. The left adenopathic block surrounds the external iliac artery (EIA). SI—small intestine (image from video archive of Bucharest Oncological Institute, personal collection of Dr. Marincaș).

Unfortunately, relevant pre-excisional images of the parietal tumor could not be taken as it crossed the entire abdominal wall with a small area of skin retraction and intense adhesions to the omentum. Excision of the parietal tumor was performed with 1 cm safety margins around and the abdominal wall was reconstructed using a textile Dual Mesh prosthesis. Below in Figure 6, we present the parietal defect left after tumor excision.



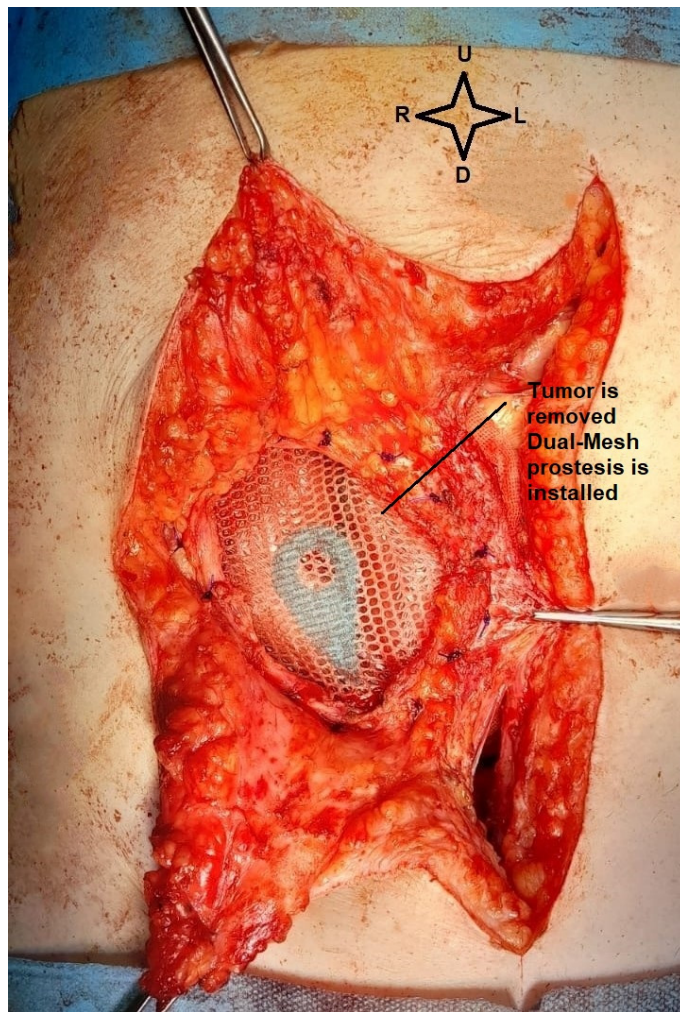


**Figure 6.** Intraoperative view. The dual mesh prosthesis, with the small intestine below (image from video archive of Bucharest Oncological Institute, personal collection of Dr. Marincas).

The intraoperative histopathological result of the parietal tumor was an adenosquamous carcinoma with areas of ossification. The left iliac adenopathic block shared the same histopathological result. Figure 7 below shows various sections of the parietal tumor in different magnifications.

The postoperative recovery was favorable again with the drainage tube suppressed on the third day after surgical intervention. The patient was discharged home six days later in good general condition, with the wound healing. However, when she returned at 30 days for re-evaluation taking into account the final histological result of adenosquamous carcinoma metastasis, the multidisciplinary committee recommended the continuation of the chemotherapy treatment, an option that the patient firmly refused.

After another 36 days, she presented to the emergency room asthenic, underweight, and complaining of moderate joint and bone pain. The next day, unfortunately, the patient requested to be discharged for personal reasons before any further evaluation. In the following week, we tried several times to contact her by phone but without success. After ten days from discharge, we found out that she died at home.

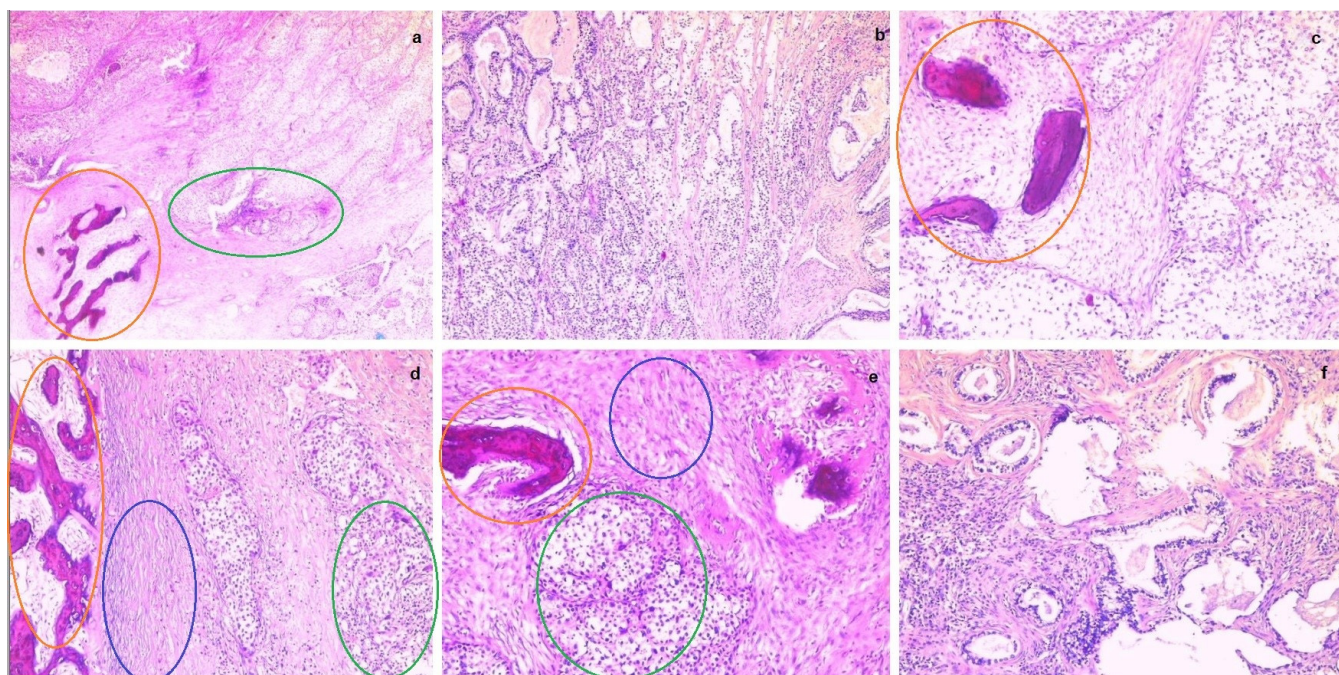


**Figure 7.** From (a–f) parietal tumor fragments in different magnifications, showing malignant infiltration (adenosquamous carcinoma) with areas of ossification. (Ossification areas—orange circles, glandular tumor cells—green circles, squamous tumor cells—blue circles).

### 3. Discussion

Parietal abdominal metastases in cervical cancer are very rare with less than 20 cases reported in recent decades. Implementing HPV vaccines for females and males, early detection of cervical dysplasia including the Pap smear, liquid-based cytology, and high-risk HPV identification test has been shown to reduce the incidence and mortality of cervical cancer in the United States of America [33,34].

A way to avoid the reluctance of patients to screening through classical methods (cervical cytology) can be the wide spread of self-testing devices for HPV detection [35]. Also, the education of patients regarding the risks and benefits of screening methods is deficient. Moreover, genital diseases are often seen as shameful topics for discussion so the stages of presentation are usually advanced, and associated with symptoms such as vaginal bleeding, vaginal pain, or abnormal vaginal discharge.

Table 1 presents a summary report of some of the most representative cases of abdominal parietal metastasis. We can observe that the most frequent places of occurrence of metastases are the pelvis, chest, and lower limbs. Also, the stages usually associated with skin metastases are IIB and above, and, in most cases, they involve multiple areas of the body.

**Table 1.** Summary of reported cases of cervical cancer with abdominal parietal metastasis.

No	Author	Age	Neoadjuvant Therapy	Surgery	Stage of Disease	Time of Recurrence (Months)	Location of Metastasis	Survival after Metastasis (Months)
1	Agrawal et al. [36]	66	Yes	No	IVA	2	Pelvis	6
2	Basu et al. [37]	60	Yes	Yes	IIA	12	Pelvis, lower thigh	7
3	Benoulaid et al. [38]	63	Yes	No	IIIB	6	Chest, Pelvis	2
4	Malfetano et al. [39]	59	Yes	No	IIIB	1	Pelvis	1
5	Malfetano et al. [39]	58	Yes	Yes	IB	60	Pelvis	1
6	Katiyar et al. [40]	60	Yes	No	IIA	86	Pelvis, back, thigh	1

In addition, as expected, the more advanced the stage of the disease, the shorter the period of occurrence of metastases, with a period of 1–2 months in stage IIIB. The prognosis

is very poor, with a survival period of 1 and 7 months at most after the appearance of metastases, with an overall 5-year survival of 17% [41].

We also discussed the case of a 47-year-old patient who initially presented with vaginal bleeding and leucorrhea. These are usually the most common symptoms when it comes to genital neoplasia [42]. The result of the patient's cervical biopsy was cervical adenosquamous carcinoma. This histological type is quite rare, with an incidence of only 5–10% of the total number of cases, and it is also associated with a poorer response to neoadjuvant treatment [43]. According to some studies, the response of this histological type is only 55–60%, so after neoadjuvant treatment, 45% of patients will still have residual tumor cells at the level of the cervix [44].

This case, in particular, emphasizes the importance of pelvic lymphadenectomy in assessing the lymph node status in patients with cervical cancer. Lymph nodes can act as a potential reservoir of tumor cells even after neoadjuvant treatment. It also shows the importance of the time recommended by the local guidelines (six weeks after the nonadjuvant treatment) in order to avoid post-irradiation fibrosis, which may limit the optimal extent of surgical intervention.

The imaging examinations before neoadjuvant treatment showed a cervical tumor with a diameter greater than 4 cm with an apparent invasion of the left parameter without reaching the pelvic wall, which is consistent with stage IIB. The reported 5-year survival rate at this stage is 63.9% [45].

The Guide of the Oncological Institute of Bucharest follows the ESGO/ESTRO/ESP [12] and NCCN treatment guidelines but also maintains a treatment alternative for locoregionally advanced (IIB, III, IVA) but nonmetastatic cervical cancers. This is represented by the performing of open surgical intervention six weeks after the completion of neoadjuvant treatment (radio-chemotherapy), consisting of radical hysterectomy type C whenever possible [13]. In this case, the entire neoadjuvant treatment scheme (radio-chemotherapy and brachytherapy) was carried out according to international guidelines. However, due to the patient's hesitation and other personal issues, the surgical intervention was performed 12 weeks after neoadjuvant treatment. Due to post-radiation sclero-inflammatory changes, only a type B hysterectomy was performed (the uterus and both ovaries were excised with lateral mobilization of the ureter and resection of the nodes of the lateral part of the paracervix, with a vaginal cuff of 10 mm).

The impossibility of performing the surgical intervention in its entirety due to postirradiation fibrosis is a relatively common adverse reaction; according to some studies, grade 1 and 2 perivaginal fibrosis and stenosis are found in 21.7% of patients with EBRT (external beam radiotherapy) [46]. In this case, the surgery was limited to lymph node sampling with the excision of only three or four lymph nodes on each side, which is considered insufficient to reflect the real state of lymph node invasion. This can represent a negative prognostic factor since the sampling of at least 10 pelvic lymph nodes can help to better stage the disease [47].

As suggested by the imaging investigations after neoadjuvant treatment and later by intraoperative anatomopathological examination, no residual tumor could be identified, which means that the patient had a complete therapeutic response. However, given the fact that the patient presented perivaginal fibrosis that did not allow the resection of the upper third of the vagina and the impossibility of performing pelvic lymphadenectomy, although there was no more tumor tissue, we can consider that the absolute radicality of the intervention was not reached [48].

The patient was in perfect health without any signs of recurrences for almost two and a half years of follow-up but after she presented directly with a parietal mass localized in the right iliac fossa, the imaging investigations also described a left iliac adenopathic block. According to some studies, this is the typical period of tumor recurrence, local or metastatic, which occurs between the second and third year post-treatment [49]. On the other hand, it is a very rare situation for metastasis to appear firstly subcutaneously, in cervical cancer the prevalence being between 0.1–1.3% [15].



Usually, there are two phases in the process of parietal metastasis: the first is the dissemination of the tumor cells to the abdominal wall and the second is the growth of the tumor cells at the new location, which is favored by inflammation, wound healing, and the presence of adipose tissue. Some studies show that tumor cells exploit the healing mechanisms of surgical wounds or other injuries [50]. Mesenchymal, epithelial, endothelial, and immune cells interact through cytokines and growth factors for tissue restoration but tumor cells use these stimuli for their own proliferation [51]. Another factor is the presence of adipose tissue. Some studies claim that around metastases, adipocytes are smaller in size and have a lower lipid content; the tumoral cells use them as a source of energy [52,53]. This fact can explain the rapid progression of metastases for our patient in just 3 months after the periodical check-up, with the abdominal wall having a well represented adipose tissue. In addition, because the tumor was on the site of the old drain tube, it can be argued that the healing mechanism after the drain tube was removed also enabled the recurrence.

Another aspect that has to be discussed is that, in some cases, young patients who want to avoid the unwanted side effects of irradiation on the ovaries and those of early menopause induced by treatment can opt for ovarian transposition intervention, which involves preserving ovarian function by repositioning the ovaries out of the field of radiation. This intervention is generally performed laparoscopically. However, laparoscopic interventions, especially in advanced locoregional stages (IIB and above) have increased risks of tumor cell dissemination [54]. We did not opt for this therapeutic strategy in our patient because she understood all the risks and benefits and accepted radio-chemotherapy as the first treatment.

However, the fact that, after the recurrence of the disease, the patient refused the chemotherapy treatment can be attributed, in part, to the depression that she has had since she was first diagnosed with cervical cancer, with the worsening of symptoms in the last period. According to the latest studies, the prevalence of depression in patients with cervical cancer who received neoadjuvant treatment is 72%, this relation varying according to the quality of life and marital relations [55]. Depressed patients may have problems in compliance with treatment and also it can influence their general clinical condition and quality of life [56].

We believe it is of great importance to provide cancer patients with a variety of resources for multidisciplinary care, such as the aid of psychosocial services during and after the completion of cancer treatment [57]. According to some studies, cancer patients have stated that they generally tend to get oncology-related information or psychological support on their own, rather than from medical staff, after treatment is completed [58]. Therefore, the medical teams should provide more comprehensive post-treatment care through referrals to appropriate psychosocial services.

#### 4. Conclusions

Surgery after neoadjuvant treatment for patients with advanced locoregional non-metastatic cervical cancer (stages IB3–IIB) is practiced in some countries in Eastern Europe with a high incidence of this type of cancer. In our Oncological Surgery Department, an open Type C radical hysterectomy is recommended six weeks after the neoadjuvant treatment if the patient has a complete response to the treatment and good physiological status. However, the fibroinflammatory changes after neoadjuvant treatment can represent an impediment to the radicality of the surgical intervention. Also, a fact of utmost importance, but also limited by the fibrous and inflammatory changes, is the proper evaluation of the lymph node status as they can represent a reservoir for tumor cells and, therefore, the starting point for subsequent dissemination.

Parietal metastases are a very rare entity, especially for gynecological cancers such as cervical cancer. The occurrence of metastasis is also related to the histological type of cancer, some types being more aggressive than others. In the case of our patient, adenosquamous carcinoma, although not so common, is associated with a poorer response to neoadjuvant treatment.

The spreading pathways of parietal metastasis are varied and include dissemination by contiguity, hematogenous, lymphatic, or direct involuntary implantation of tumor cells during surgery. Local factors such as cytokines or growth factors secreted after injuries promote tumor proliferation. Adipose tissue also contributes to tumor growth, being a source of energy. The average time duration of occurrence of metastases is between two and three years after treatment, as was the case of our patient. The overall survival rate is poor, falling to 17% at 5 years, a fact that should encourage further research in order to find the optimal therapeutic strategies.

**Author Contributions:** Conceptualization: I.-G.D.-A., M.-A.M., E.B. and L.S.; Data curation: I.-G.D.-A. and I.D.-A.; Formal analysis: I.-G.D.-A. and I.D.-A.; Investigation: I.-G.D.-A. and I.D.-A.; Methodology: I.-G.D.-A., M.-A.M. and E.B.; Project administration: M.-A.M., S.-O.I., V.-M.P., E.B. and L.S.; Resources: M.-A.M., Ş.-A.N. and G.-M.R.; Software: I.-G.D.-A. and I.D.-A.; Supervision: M.-A.M., A.-A.S., S.-O.I., V.-M.P., E.B. and L.S.; Validation: I.-G.D.-A., M.-A.M., A.-A.S., S.-O.I., Ş.-A.N., G.-M.R., E.B. and L.S.; Visualization: I.-G.D.-A., M.-A.M., A.-A.S. and S.-O.I.; Writing—original draft: I.-G.D.-A.; Writing—review and editing: I.-G.D.-A., A.-A.S. and I.D.-A. All authors have read and agreed to the published version of the manuscript.

**Funding:** This research received no external funding.

**Institutional Review Board Statement:** The study was conducted in accordance with the Declaration of Helsinki and approved by the Ethics Committee of the Bucharest Oncological Institute (protocol code 3C and date of approval 25 March 2024).

**Informed Consent Statement:** Written informed consent has been obtained from the patient to publish this paper.

**Data Availability Statement:** The patient's data were obtained from the medical documents of the Bucharest Oncological Institute and they cannot be made publicly available as they contain personal and confidential data of the patient but any information about these documents can be obtained on request from the corresponding author.

**Acknowledgments:** Publication of this paper was supported by the University of Medicine and Pharmacy Carol Davila through the institutional program Publish not Perish.

**Conflicts of Interest:** The authors declare no conflict of interest.

## References

1. Sung, H.; Ferlay, J.; Siegel, R.L.; Laversanne, M.; Soerjomataram, I.; Jemal, A.; Bray, F. Global Cancer Statistics 2020: GLOBOCAN Estimates of Incidence and Mortality Worldwide for 36 Cancers in 185 Countries. *CA Cancer J. Clin.* **2021**, *71*, 209–249. [CrossRef] [PubMed]
2. Mullapally, S.K.; Digumarti, L.; Digumarti, R. Cervical Cancer in Low- and Middle-Income Countries: A Multidimensional Approach to Closing the Gaps. *JCO Oncol. Pract.* **2022**, *18*, 423–425. [CrossRef] [PubMed]
3. Crosbie, E.J.; Einstein, M.H.; Franceschi, S.; Kitchener, H.C. Human Papillomavirus and Cervical Cancer. *Lancet* **2013**, *382*, 889–899. [CrossRef] [PubMed]
4. Gilles, C.; Konopnicki, D.; Rozenberg, S. The Recent Natural History of Human Papillomavirus Cervical Infection in Women Living with HIV: A Scoping Review of Meta-analyses and Systematic Reviews and the Construction of a Hypothetical Model. *HIV Med.* **2023**, *24*, 877–892. [CrossRef] [PubMed]
5. Ghebrey, R.G.; Grover, S.; Xu, M.J.; Chuang, L.T.; Simonds, H. Cervical Cancer Control in HIV-Infected Women: Past, Present and Future. *Gynecol. Oncol. Rep.* **2017**, *21*, 101–108. [CrossRef] [PubMed]
6. Wichmann, I.A.; Cuello, M.A. Obesity and Gynecological Cancers: A Toxic Relationship. *Int. J. Gynecol. Obstet.* **2021**, *155*, 123–134. [CrossRef] [PubMed]
7. Roura, E.; Castellsagué, X.; Pawlita, M.; Travier, N.; Waterboer, T.; Margall, N.; Bosch, F.X.; de Sanjosé, S.; Dillner, J.; Gram, I.T.; et al. Smoking as a Major Risk Factor for Cervical Cancer and Pre-Cancer: Results from the EPIC Cohort. *Int. J. Cancer* **2014**, *135*, 453–466. [CrossRef] [PubMed]
8. Tekalegn, Y.; Sahiledengle, B.; Woldeyohannes, D.; Atlaw, D.; Degno, S.; Desta, F.; Bekele, K.; Aseffa, T.; Gezahegn, H.; Kene, C. High Parity Is Associated with Increased Risk of Cervical Cancer: Systematic Review and Meta-Analysis of Case-Control Studies. *Womens Health* **2022**, *18*, 17455065221075904. [CrossRef] [PubMed]
9. Ghosh, C.; Baker, J.A.; Moysich, K.B.; Rivera, R.; Brasure, J.R.; McCann, S.E. Dietary Intakes of Selected Nutrients and Food Groups and Risk of Cervical Cancer. *Nutr. Cancer* **2008**, *60*, 331–341. [CrossRef]



10. Haug, U.; Riedel, O.; Cholmakow-Bodechtel, C.; Olsson, L. First-Degree Relatives of Cancer Patients: A Target Group for Primary Prevention? A Cross-Sectional Study. *Br. J. Cancer* **2018**, *118*, 1255–1261. [CrossRef]
11. NCCN Guidelines for Cervical Cancer. Available online: [https://www.nccn.org/professionals/physician\\_gls/pdf/cervical.pdf](https://www.nccn.org/professionals/physician_gls/pdf/cervical.pdf) (accessed on 18 June 2023).
12. Cibula, D.; Raspollini, M.R.; Planchamp, F.; Centeno, C.; Chargari, C.; Felix, A.; Fischerová, D.; Jahnn-Kuch, D.; Joly, F.; Kohler, C.; et al. ESGO/ESTRO/ESP Guidelines for the Management of Patients with Cervical Cancer—Update 2023 \*. *Int. J. Gynecol. Cancer* **2023**, *33*, 649–666. [CrossRef]
13. Nagy, V.; Rancea, A.; Coza, O.; Kacso, G.; Aldea, B.; Eniu, A. Ghid MS Conduita Cancer Col Uterin. Available online: <http://old.ms.ro/index.php?pag=181&pg=5> (accessed on 4 March 2024).
14. Hu, S.C.-S.; Chen, G.-S.; Wu, C.-S.; Chai, C.-Y.; Chen, W.-T.; Lan, C.-C.E. Rates of Cutaneous Metastases from Different Internal Malignancies: Experience from a Taiwanese Medical Center. *J. Am. Acad. Dermatol.* **2009**, *60*, 379–387. [CrossRef] [PubMed]
15. Dai, Y.; Zhang, Y.; Ke, X.; Liu, Y.; Zang, C. Cutaneous Metastasis from Cervical Cancer to the Scalp and Trunk: A Case Report and Review of the Literature. *J. Med. Case Rep.* **2023**, *17*, 435. [CrossRef]
16. Martínez, A.; Querleu, D.; Leblanc, E.; Narducci, F.; Ferron, G. Low Incidence of Port-Site Metastases after Laparoscopic Staging of Uterine Cancer. *Gynecol. Oncol.* **2010**, *118*, 145–150. [CrossRef] [PubMed]
17. Schwartz, R.A. Cutaneous Metastatic Disease. *J. Am. Acad. Dermatol.* **1995**, *33*, 161–185. [CrossRef]
18. Lookingbill, D.P.; Spangler, N.; Sexton, F.M. Skin Involvement as the Presenting Sign of Internal Carcinoma. *J. Am. Acad. Dermatol.* **1990**, *22*, 19–26. [CrossRef] [PubMed]
19. Majmudar, B.; Wiskind, A.K.; Croft, B.N.; Dudley, A.G. The Sister (Mary) Joseph Nodule: Its Significance in Gynecology. *Gynecol. Oncol.* **1991**, *40*, 152–159. [CrossRef] [PubMed]
20. Kouira, M.; Bannour, I.; Ben Abdesslem, M.R.; Abdessayed, N.; Bannour, B. Ovarian Cancer Was Discovered in Sister Mary Joseph’s Nodule. *Case Rep. Med.* **2022**, *2022*, 5131705. [CrossRef]
21. Leyrat, B.; Bernadach, M.; Ginzac, A.; Lusho, S.; Durando, X. Sister Mary Joseph Nodules: A Case Report about a Rare Location of Skin Metastasis. *Case Rep. Oncol.* **2021**, *14*, 664–670. [CrossRef]
22. Otsuka, I.; Matsuura, T. Skin Metastases in Epithelial Ovarian and Fallopian Tube Carcinoma. *Medicine* **2017**, *96*, e7798. [CrossRef]
23. Otsuka, I. Cutaneous Metastases in Ovarian Cancer. *Cancers* **2019**, *11*, 1292. [CrossRef] [PubMed]
24. Gao, Q.; Guo, L.; Wang, B. The Pathogenesis and Prevention of Port-Site Metastasis in Gynecologic Oncology. *Cancer Manag. Res.* **2020**, *12*, 9655–9663. [CrossRef] [PubMed]
25. Mbaeri, T.; Orakwe, J.; Ezejiolor, O. Unsuspected Skin Metastasis of Adenocarcinoma of the Prostate in a Patient on Goserelin (Zoladex). *Niger. J. Surg.* **2018**, *24*, 138. [CrossRef]
26. Shine, T.; Wallack, M.K. Inflammatory Oncotaxis after Testing the Skin of the Cancer Patient. *Cancer* **1981**, *47*, 1325–1328. [CrossRef] [PubMed]
27. Cohen, H.J.; Laszlo, J. Influence of Trauma on the Unusual Distribution of Metastases from Carcinoma of the Larynx. *Cancer* **1972**, *29*, 466–471. [CrossRef]
28. de, S. Weimann, E.T.; Botero, E.B.; Mendes, C.; dos Santos, M.A.S.; Stelini, R.F.; Zelenika, C.R.T. Cutaneous Metastasis as the First Manifestation of Occult Malignant Breast Neoplasia. *An. Bras. Dermatol.* **2016**, *91*, 105–107. [CrossRef]
29. Dills, A.; Obi, O.; Bustos, K.; Jiang, J.; Gupta, S. Cutaneous Metastasis of Prostate Adenocarcinoma: A Rare Presentation of a Common Disease. *J. Investig. Med. High. Impact Case Rep.* **2021**, *9*, 2324709621990769. [CrossRef] [PubMed]
30. Kim, W.-J.; Park, H.-J.; Kim, H.-S.; Kim, S.-H.; Ko, H.-C.; Kim, B.-S.; Kim, M.-B. Vulval Metastasis from Squamous Cell Carcinoma of the Cervix Clinically Presenting as Lymphangioma Circumscriptum. *Ann. Dermatol.* **2011**, *23*, S64. [CrossRef] [PubMed]
31. Otsuka, I. Cutaneous Metastasis after Surgery, Injury, Lymphadenopathy, and Peritonitis: Possible Mechanisms. *Int. J. Mol. Sci.* **2019**, *20*, 3286. [CrossRef]
32. Bebia, V.; Monreal-Clua, S.; Pérez-Benavente, A.; Franco-Camps, S.; Díaz-Feijoo, B.; Gil-Moreno, A. Potential Strategies for Prevention of Tumor Spillage in Minimally Invasive Radical Hysterectomy. *J. Gynecol. Oncol.* **2020**, *31*, e73. [CrossRef]
33. Tabibi, T.; Barnes, J.M.; Shah, A.; Osazuwa-Peters, N.; Johnson, K.J.; Brown, D.S. Human Papillomavirus Vaccination and Trends in Cervical Cancer Incidence and Mortality in the US. *JAMA Pediatr.* **2022**, *176*, 313–316. [CrossRef] [PubMed]
34. Simms, K.T.; Keane, A.; Nguyen, D.T.N.; Caruana, M.; Hall, M.T.; Lui, G.; Gauvreau, C.; Demke, O.; Arbyn, M.; Basu, P.; et al. Benefits, Harms and Cost-Effectiveness of Cervical Screening, Triage and Treatment Strategies for Women in the General Population. *Nat. Med.* **2023**, *29*, 3050–3058. [CrossRef] [PubMed]
35. Ertik, F.C.; Kampers, J.; Hülse, F.; Stolte, C.; Böhmer, G.; Hillemanns, P.; Jentschke, M. CoCoss-Trial: Concurrent Comparison of Self-Sampling Devices for HPV-Detection. *Int. J. Environ. Res. Public Health* **2021**, *18*, 10388. [CrossRef] [PubMed]
36. Agrawal, A.; Yau, A.; Magliocco, A.; Chu, P. Cutaneous Metastatic Disease in Cervical Cancer: A Case Report. *J. Obstet. Gynaecol. Can.* **2010**, *32*, 467–472. [CrossRef]
37. Elamurugan, T.P.; Agrawal, A.; Dinesh, R.; Aravind, R.; Naskar, D.; Kate, V.; Reddy, R.; Elamurugan, S.; Siddaraju, Basu, D.; et al. Palmar Cutaneous Metastasis from Carcinoma Cervix. *Indian. J. Dermatol. Venereol. Leprol.* **2011**, *77*, 252. [CrossRef] [PubMed]
38. Benoulaid, M.; Elkacemi, H.; Bourhafour, I.; Khalil, J.; Elmajjaoui, S.; Khannoussi, B.; Kebdani, T.; Benjaafar, N. Skin Metastases of Cervical Cancer: Two Case Reports and Review of the Literature. *J. Med. Case Rep.* **2016**, *10*, 265. [CrossRef] [PubMed]
39. Malfetano, J.H. Skin Metastases from Cervical Cancer: A Fatal Event. *Gynecol. Oncol.* **1986**, *24*, 177–182. [CrossRef] [PubMed]

40. Katiyar, V.; Araujo, T.; Majeed, N.; Ree, N.; Gupta, S. Multiple Recurrences from Cervical Cancer Presenting as Skin Metastasis of Different Morphologies. *Gynecol. Oncol. Rep.* **2019**, *28*, 61–64. [CrossRef] [PubMed]
41. Zhou, S.; Peng, F. Patterns of Metastases in Cervical Cancer: A Population-Based Study. *Int. J. Clin. Exp. Pathol.* **2020**, *13*, 1615–1623.
42. Cervical Cancer Signs and Symptoms. Available online: [https://www.who.int/news-room/fact-sheets/detail/cervical-cancer?gad\\_source=1&gclid=Cj0KCQjw2PSvBhDjARIsAKc2cgNV-vCzxygp2l00eiIzNe9fqzUUiSIG3rf0M-J0Gwutk7Jpoj8qiRYaArXDEALw\\_wcB](https://www.who.int/news-room/fact-sheets/detail/cervical-cancer?gad_source=1&gclid=Cj0KCQjw2PSvBhDjARIsAKc2cgNV-vCzxygp2l00eiIzNe9fqzUUiSIG3rf0M-J0Gwutk7Jpoj8qiRYaArXDEALw_wcB) (accessed on 22 March 2024).
43. Rohan, T.E. The Epidemiology of Adenocarcinoma of the Cervix. In *Cervical Cancer: From Etiology to Prevention. Cancer Prevention—Cancer Causes*; Rohan, T.E., Shah, K.V., Eds.; Springer: Dordrecht, The Netherlands, 2004; Volume 2. [CrossRef]
44. Voinea, S.; Herghelegiu, C.; Sandru, A.; Ioan, R.; Bohiltea, R.; Bacalbaşa, N.; Chivu, L.; Furtunescu, F.; Stanica, D.; Neacşu, A. Impact of Histological Subtype on the Response to Chemoradiation in Locally Advanced Cervical Cancer and the Possible Role of Surgery. *Exp. Ther. Med.* **2020**, *21*, 93. [CrossRef]
45. Dicu-Andrescu, I.-G.; Marincas, A.-M.; Ungureanu, V.-G.; Ionescu, S.-O.; Prunoiu, V.-M.; Brătucu, E.; Simion, L. Current Therapeutic Approaches in Cervical Cancer Based on the Stage of the Disease: Is There Room for Improvement? *Medicina* **2023**, *59*, 1229. [CrossRef] [PubMed]
46. Hofsjö, A.; Bohm-Starke, N.; Blomgren, B.; Jahren, H.; Steineck, G.; Bergmark, K. Radiotherapy-Induced Vaginal Fibrosis in Cervical Cancer Survivors. *Acta Oncol.* **2017**, *56*, 661–666. [CrossRef] [PubMed]
47. Wang, R.; Tao, X.; Wu, X.; Jiang, H.; Xia, H. Number of Removed Pelvic Lymph Nodes as a Prognostic Marker in FIGO Stage IB1 Cervical Cancer with Negative Lymph Nodes. *J. Minim. Invasive Gynecol.* **2020**, *27*, 946–952. [CrossRef] [PubMed]
48. Gray, H.J.; Seifert, E.; Sal y Rosas, V.G.; Nicandri, K.F.; Koh, W.-J.; Goff, B.A. The Abandoned Radical Hysterectomy for Cervical Cancer: Clinical Predictors and Outcomes. *Obstet. Gynecol. Int.* **2010**, *2010*, 743794. [CrossRef] [PubMed]
49. Linhares Moreira, A.S.; Cunha, T.M.; Esteves, S. Cervical Cancer Recurrence—Can We Predict the Type of Recurrence? *Diagn. Interv. Radiol.* **2020**, *26*, 403–410. [CrossRef] [PubMed]
50. Sundaram, G.M.; Quah, S.; Sampath, P. Cancer: The Dark Side of Wound Healing. *FEBS J.* **2018**, *285*, 4516–4534. [CrossRef] [PubMed]
51. Ceelen, W.; Pattyn, P.; Mareel, M. Surgery, Wound Healing, and Metastasis: Recent Insights and Clinical Implications. *Crit. Rev. Oncol. Hematol.* **2014**, *89*, 16–26. [CrossRef]
52. Duong, M.N.; Geneste, A.; Fallone, F.; Li, X.; Dumontet, C.; Muller, C. The Fat and the Bad: Mature Adipocytes, Key Actors in Tumor Progression and Resistance. *Oncotarget* **2017**, *8*, 57622–57641. [CrossRef]
53. Nieman, K.M.; Romero, I.L.; Van Houten, B.; Lengyel, E. Adipose Tissue and Adipocytes Support Tumorigenesis and Metastasis. *Biochim. Biophys. Acta (BBA)—Mol. Cell Biol. Lipids* **2013**, *1831*, 1533–1541. [CrossRef]
54. Picone, O.; Aucouturier, J.S.; Louboutin, A.; Coscas, Y.; Camus, E. Abdominal Wall Metastasis of a Cervical Adenocarcinoma at the Laparoscopic Trocar Insertion Site after Ovarian Transposition: Case Report and Review of the Literature. *Gynecol. Oncol.* **2003**, *90*, 446–449. [CrossRef]
55. Ding, X.; Zhang, Y.; Wang, J.; Huang, A.; Liu, Y.; Han, Y.; Hu, D. The Association of Adverse Reactions and Depression in Cervical Cancer Patients Treated with Radiotherapy and/or Chemotherapy: Moderated Mediation Models. *Front. Psychol.* **2023**, *14*, 1207265. [CrossRef] [PubMed]
56. DiMatteo, M.R.; Lepper, H.S.; Croghan, T.W. Depression Is a Risk Factor for Noncompliance with Medical Treatment. *Arch. Intern. Med.* **2000**, *160*, 2101. [CrossRef] [PubMed]
57. Shyu, I.-L.; Hu, L.-Y.; Chen, Y.-J.; Wang, P.-H.; Huang, B.-S. Risk Factors for Developing Depression in Women with Cervical Cancer: A Nationwide Population-Based Study in Taiwan. *Int. J. Womens Health* **2019**, *11*, 135–141. [CrossRef] [PubMed]
58. Edgar, L.; Remmer, J.; Rosberger, Z.; Fournier, M.A. Resource Use in Women Completing Treatment for Breast Cancer. *Psychooncology* **2000**, *9*, 428–438. [CrossRef]

**Disclaimer/Publisher’s Note:** The statements, opinions and data contained in all publications are solely those of the individual author(s) and contributor(s) and not of MDPI and/or the editor(s). MDPI and/or the editor(s) disclaim responsibility for any injury to people or property resulting from any ideas, methods, instructions or products referred to in the content.

## Review

# From Satirical Poems and Invisible Poisons to Radical Surgery and Organized Cervical Cancer Screening—A Historical Outline of Cervical Carcinoma and Its Relation to HPV Infection

Leonard Jung <sup>1,2,\*</sup>, Gilbert Georg Klamminger <sup>2,3</sup>, Bert Bier <sup>1</sup> and Elke Eltze <sup>1,2</sup>

<sup>1</sup> Institute of Pathology, Saarbrücken-Rastpfuhl, 66113 Saarbrücken, Germany

<sup>2</sup> Department of General and Special Pathology, Saarland University (USAAR), 66424 Homburg, Germany

<sup>3</sup> Department of General and Special Pathology, Saarland University Medical Center (UKS), 66424 Homburg, Germany

\* Correspondence: s9ldjung@stud.uni-saarland.de

**Abstract:** Over the last century, the narrative of cervical cancer history has become intricately tied to virus research, particularly the human papillomavirus (HPV) since the 1970s. The unequivocal proof of HPV's causal role in cervical cancer has placed its detection at the heart of early screening programs across numerous countries. From a historical perspective, sexually transmitted genital warts have been already documented in ancient Latin literature; the remarkable symptoms and clinical descriptions of progressed cervical cancer can be traced back to Hippocrates and classical Greece. However, in the new era of medicine, it was not until the diagnostic–pathological accomplishments of Aurel Babeş and George Nicolas Papanicolaou, as well as the surgical accomplishments of Ernst Wertheim and Joe Vincent Meigs, that the prognosis and prevention of cervical carcinoma were significantly improved. Future developments will likely include extended primary prevention efforts consisting of better global access to vaccination programs as well as adapted methods for screening for precursor lesions, like the use of self-sampling HPV-tests. Furthermore, they may also advantageously involve additional novel diagnostic methods that could allow for both an unbiased approach to tissue diagnostics and the use of artificial-intelligence-based tools to support decision making.

**Keywords:** cervical cancer; HPV; cervical cancer screening

## 1. Introduction

From an epidemiological perspective, cervical cancer is a global disease with pronounced regional variations. Being the fourth most common neoplasm and, therefore, the second most common cause of cancer-related deaths globally [1,2], incidences vary drastically per region, affecting public health systems predominantly in developing countries. Although in Eswatini, incidence rates of up to 95.9/100,000 per year have been reported [3], European incidence rates are 10.6/100,000 per year [3], and an even lower incidence rate has been reported in Palestine (2/100,000 per year). In Germany, it is ‘solely’ the 14th most frequent tumor in women and, therefore, only the fourth most common gynecological malignancy [4,5]. Its political dimension is extremely diverse in itself: in a way, it reflects differences between social standards (The socioeconomic factor is a major risk factor for the development of cervical cancer [6]) as well as health and economic issues relating to adequate screening services. With the overall aim of mortality reduction, organized screening programs have proven to reduce incidence rates as well as cervical-cancer-dependent mortality rates in Northern Europe. To this day, the clear advantage of organized screening programs is widely evident [4,7–10].

The medical–therapeutic dimension is subject to constant change; nowadays, diagnostic dogmas of cytology are increasingly replaced by primary gene amplification testing.

Moreover, therapeutic strategies are constantly being improved [11–13]. In the present review, we touch on all these aspects merely, thereby supplementing the body of known literature on this disease with a historical perspective. Despite it being worth reading reviews of the historical development of cervical cancer screening, our report aims to honor achieved surgical, pathological, virological, and potential future milestones in equal measure, providing a comprehensive overview for gynecologists, pathologists, and scientists involved in cervical cancer research.

## 2. Materials and Methods

A literature search was conducted via the online databases PubMed and Google Scholar. Using the Boolean AND/OR operators, we combined the tags “history”, “cervical cancer”, “cervical neoplasm”, “HPV”, “oncogenic virus”, “Harald zur Hausen”, “Pap-smear”, “HPV-test”, and “cervical cancer screening”, along with associated mesh terms. Affiliated literature as well as references of semantically consistent articles were considered and included at our convenience. After the initial title/abstract screening, relevant papers were discussed and individually selected upon the agreement of all the authors. Literary works written in languages other than English, German, French, Italian, and Latin, as well as solely brief historical summaries, were excluded.

## 3. From Ancient Promiscuity to Microscopic Diagnosis

The first description of cervical cancer and its symptomatic irregular bleedings was written 400 years BC by Hippocrates, who, recognizing the fatal course of the disease, prescribed a palliative concept [14]. However, the phylogenetic development of papillomavirus genomes and, thus, the main risk factor for the development of cervical cancer (id est infection with HPV), can be traced back several hundred million years; as a result, an affection of women since early human history seems quite plausible [15]. Early written evidence proves that sexually transmitted diseases have been recognized already in ancient Rome, where genital warts were interpreted as a sign of promiscuity. The warts were called *figus*, corresponding to their fig-like appearance. The suspected connection between anal warts and anal intercourse is revealed by satirical poems of that time [16]:

*“Ut pueros emeret Labienus vendidit hortos.*

*Nil nisi ficetum nunc Labienus habet.”*

*“In order to buy boys, Labienus sold his gardens,  
but now Labienus only possesses a fig tree.”*

(M. Valerii Martialis Epigrammaton Libri XII, XXXIII)

*“Ficosa est uxor, ficosus et ipse maritus,*

*Filia ficosa est et gener atque nepos,*

*Nec dispensator nec vilicus ulcere turpi*

*Nec rigidus fossor, sed nec arator eget.*

*Cum sint ficosi pariter iuvenesque senesque,*

*Res mira est, ficos non habet unus ager.”*

*“The wife is full of genital warts; even the husband is full of genital warts.*

*The daughter is full of genital warts as well as the son-in-law and the grandson.*

*Neither the steward nor the farm bailiff is free from the distasteful ulcer;*

*nor even the harsh digger or the ploughman is without.*

*Since both the young and the old are full of genital warts,*

*the incident is astonishing; the acre does not have figs.”*

(M. Valerii Martialis Epigrammaton Libri VII, LXXI)

It was not until the beginning of the 19th century and the rise of modern gynecology, that the epidemiologic risk factors as well as the diagnostic and treatment capabilities of cervical cancer improved. As a key factor, the expansive use of the vaginal speculum, supported by the French gynecologist Joseph Récamier between 1801 and 1819, provided deeper clinical and anatomical insights into the internal female reproductive organs and the

associated possibility for initiating further diagnostic and therapeutic measures [17]. Historically, finds of ancient specula in the ruins of Pompeii prove the longstanding tradition of this particular examination tool, even though up to this time, it was largely associated with prostitution as well as venereal diseases and was, therefore, socially stigmatized [15,18]. Following the successful removal of the cervix by Nikolaas Tulp in the 17th century [15], Friedrich Benjamin Osiander from Göttingen amputated a cancerous cervix in 1801 [19]. In 1813, Bernhard von Langenbeck successfully performed a vaginal hysterectomy in a patient with cervical carcinoma [20].

Apart from these therapeutic successes, the Italian doctor Domenico Rigoni-Stern was one of the first to study the epidemiology of cervical cancer by analyzing the death certificates of women who died between 1760 and 1839 in 1842. He thereby recognized that cervical cancer was more common in widows and prostitutes—whereas virgins and nuns were rarely affected—and drew the conclusion that cancer of this type must be associated with sexual contact [21]. The German pathologist Carl Arnold Ruge and the German gynecologist Johann Veit laid the foundation for further systematic research into cervical carcinoma by investigating and describing gynecological surgical specimens removed by the gynecologist Karl Schröder (He suggested high cervical resection as a treatment option at the time.) [15]; in 1877, they described cervical carcinoma as an independent disease and highlighted the impact of presurgical biopsies [15,22].

Though surgical therapies at the time were chosen intuitively, the advantage of uterus removal in terms of overall survival was pointed out consecutively. Early works, such as *“Uterus Amputation am vaginalen Wege”* (1830) and *“Ca colli uteri”* (1878, *Wiener medizinische Wochenschrift*), focused on (radical) vaginal uterus removal [23]. The first radical abdominal hysterectomies were performed in 1878 by the German gynecologist Wilhelm Alexander Freund and in 1880 in Prague by Karel Pawlik [24,25]; subsequently, this procedure of a ‘radical hysterectomy’ was summarized in 1898 by the Austrian gynecologist Ernst Wertheim, who assumed a spread of neoplastic cells into the lymphatic tissue and, therefore, added a systematic pelvic curative lymphadenectomy to the surgical protocol, using individualized forceps made for dissecting the dorsal parametria (*“Wertheim Klemme”*). This modification would be, later on, further developed by the American Joe Vincent Meigs [26]. Such radical approaches were accompanied by an improvement in the long-term prognosis compared to the vaginal hysterectomy introduced by Frederich Schauta, whereby the latter had the advantage of a lower perioperative mortality rate in the 19th century [15]. An ongoing dispute between Schauta and Wertheim (so-called *“Drüsenstreit”*, the nodule dispute) regarding the importance of lymphadenectomy filled the professional European literature for decades and was not resolved until Wertheim’s death and the introduction of radiation as a method of treatment [27].

In the late twentieth century, Daniel Dargent and Marc Possover proposed a combined laparoscopic lymphadenectomy with vaginal specimen removal, including a nerve sparing technique [28,29], within the overall concept of TRLH (total radical laparoscopic hysterectomy). Furthermore, Michael Hoeckel and Rainer Kimmig suggested the TMMR (total mesometrial resection) method as a potential treatment option [30,31]. Within the last century, radical hysterectomies have been divided into distinct subtypes based on the extent of the resection of the parametria/paracervix, and systematic pelvic lymphadenectomies have mostly been replaced by the concept of the sentinel lymph node mapping (SLNM). Recently, the LACC (Laparoscopic Approach to Cervical Cancer) trial provided a paradigm shift by demonstrating the advantage of open abdominal surgery in cervical cancer patients over laparoscopic tumor resection [32].

To date, surgical therapy (abdominal open radical hysterectomy combined with SLNM or/and systematic pelvic lymphadenectomy) is considered as a first-line treatment of locally advanced cervical cancer, although definitive radiotherapy with concomitant chemotherapy is favored in the progressed disease. Current treatment strategies avoid the combination of radical surgery and radiotherapy owing to its high morbidity rate [6]. To reduce post-operative morbidity and complications, experimental setups nowadays question the need

for radical surgical therapy in patients with 1A2 or 1B1 low-risk cervical carcinomas with lesions smaller than or equal to the size of 2 cm [33].

Another diagnostic milestone in the early detection of cervical carcinoma was the invention of colposcopy by the German gynecologist Hans Hinselmann in 1925 [34]. Despite his involvement in Nazi Germany and the resulting slowdown in the spread of his medical achievement, he was undoubtedly an expert in the field of the clinical detection of cervical neoplasia; he was flown to Argentina as a consultant shortly before Eva Perón's death [35]. Two years later, a differentiation between normal cervical mucosa and pathologically altered mucosa based on an iodine reaction (Lugol's solution) was achieved by the Austrian gynecologist and pathologist Walter Schiller [36]. Following up the discovery of the British doctor Hayle Walsh in the middle of the 18th century that a distinct identification of cancerous cells was possible using solely a light microscope [37,38], the Romanian doctor Aurel Babeş examined cells from a female cervix in 1927, which he obtained using a platinum loop, under a microscope. Thereby, he succeeded in detecting the presence of cervical cancer [38]. At the same time, the Greek physician George Nicolas Papanicolaou was conducting research in America after completing his doctorate in Germany (Munich) [39]. He transferred his research findings on menstruation-related cytological changes in the vaginal mucosa of guinea pigs to humans and discovered—with the active support of his wife as a repeated volunteer—the same cyclical cellular estrogen dependency and, by chance, neoplastic cell forms [40]. In 1928, he presented his work for the first time [41,42], which, after technical improvements by the Canadian gynecologist J. Ernest Ayre, provides an efficient tool for the early detection of cervical cancer as it is used today [43].

See Figure 1 for an overview of historical diagnostic and surgical achievements and Figure 2 for an assessment of HPV infection during today's routine cervical cancer screening via light microscopy.

#### Timeline: From ancient promiscuity to microscopic diagnosis

- 400 years BC:** Hippocrates: Phenomenological descriptions and non-surgical therapy
- ~ **AD 86 to 103:** M. Valerii Martialis: Lyrical interpretation of genital warts and anal intercourse
- ~ **1801:** Joseph Récamier: Redefinition of vaginal examination (speculum)
- ~ **1801:** Friedrich Benjamin Osiander: Amputation of a cancerous cervix
- 1813:** Bernhard von Langenbeck: Vaginal hysterectomy in a patient with cervical carcinoma
- 1842:** Domenico Rigoni-Stern: The prevalence of cervical cancer in Italian nuns
- 1877:** Carl Arnold Ruge and Johann Veit: The diagnostic value of biopsy in cervical cancer
- 1880:** Karel Pawlik: Radical hysterectomy
- ~ **1890:** Ernst Wertheim and Frederick Schauta: The importance of lymphadenectomy
- 1925:** Hans Hinselmann: Colposcopic diagnoses
- 1927:** Aurel Babeş: Cytological aspects of cervical cells
- 1928:** George Nicolas Papanicolaou: Cytological detection of cervical lesions

**Figure 1.** Overview of diagnostic and surgical achievements from Hippocrates to Papanicolaou.

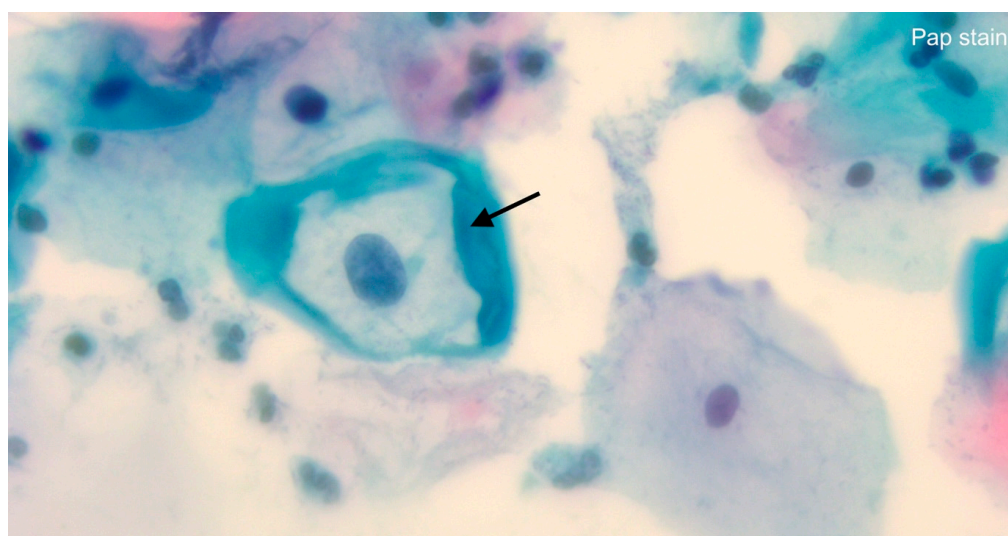


**Figure 2.** Distinct cytopathological features (slightly enlarged acentric nucleus, perinuclear cytoplasmic vacuolization, surrounding prominent cytoplasm) mark koilocytotic atypia, an HPV-related transformation from squamous cells to ‘koilocytes’ (black arrow); lens magnification:  $\times 63$ .

#### 4. The Presence of Oncogenic Viruses: From “Invisible Poison” to Viral Genetics

Although scientifically supported by epidemiological studies showing higher incidences in women who (themselves or their husbands) had a high number of sexual partners ( $n > 2$ ) [44,45] or were regularly involved in prostitution [46,47], all the attempts linking cervical cancer to sexually transmitted infections remained unsuccessful within the second half of the 19th century. Strikingly, the prevalence was lower among Jewish women and in women married to circumcised males [48]. Viruses came into question as a possible sexually transmitted pathogen, whereas at that time, the history and study of viruses was a comparatively young research field. In 1894, Dmitri Ivanovsky succeeded in transmitting the mosaic disease of tobacco from infected to healthy tobacco plants by pressing leaves infected with the mosaic disease of tobacco through a filter that only allowed a pass through for pathogens smaller than bacteria. As the final cause of the disease, he suspected an “invisible poison” [49]. In accordance, Martinus Beijerinck achieved the same results in 1898, and he called the pathogenic agent a *virus* (*poison/sap/mucus*). Furthermore, Beijerinck defined two further characteristics of a virus, namely, the ability to pass through a filter that only allowed a pass through for particles smaller than bacteria and the necessary presence of living cells to grow [50]. The proof that this new infectious agent may also infect humans and thereby even cause disease was obtained by Walter Reed in 1902. The yellow fever virus is considered as the first proven human pathogenic virus [51], and the acceptance of the scientific world that infectious diseases in humans could be caused by viruses as well as bacteria provided the basis for upcoming research tasks in the field of virology. In addition to research of viral infectious diseases, the potential involvement of viruses in the development of neoplasia was investigated already at an early stage. In 1911, Peyton Rous succeeded in triggering a tumor in chickens with the help of a virus. Three years earlier, two Danish researchers, namely, Vilhelm Ellerman and Oluf Bang, were able to provoke leukemia in chickens using a cell-free extract, which served as the first evidence suggesting a link between viruses and tumors [52]. Peyton Rous once more and J.W. Beard were successful in 1936 in transferring the same warts from infected to healthy areas of skin by subcutaneous injection using a cell-free extract of existing lesions. Their efforts were based on observations made by Richard E. Shope, who found warts on the heads of American wild rabbits and concluded that they were caused by a wart virus. As Beard and Rous described, they first recognized benign tissue growths, which appeared at the injection site. These irregularities then turned malignant, spread, and finally killed the rabbit [53]. In 1961, Yohei Ito and Alfred Evans demonstrated the role of genetic viral material as a decisive

factor in the development of skin cancer in rabbits [54]. Up to this point, research into links between neoplasia and viruses had been limited to animal studies. Finally, Michael Anthony Epstein, Yvonne Barr, and Bert Achong succeeded in detecting the Epstein–Barr virus in Burkitt’s lymphoma in 1964 [55] and linked neoplasia in humans and a human pathogenic virus for the first time. That said, a final link between human papillomaviruses and cervical cancer was inconceivable until the research findings of Harald zur Hausen. In 1965, June Almeida proposed the existence of different human wart viruses [56], and in 1968, Rawls et al. (among others) emphasized herpes simplex type 2 as a possible causative agent of cervical cancer [57,58]—an assertion that was not only disproved by zur Hausen’s abortive attempts to isolate genetic material from herpes simplex viruses in cervical tumors [59] but also refuted by a prospective study in the mid-1980s [60]. Alternatively, zur Hausen et al. began to hypothesize a conditional relation between cervical cancer and human papillomaviruses in the early 1970s, based on reports in the medical literature of the rare, malignant transformation from genital warts (*Condyloma acuminata*) to squamous cell carcinomas [59,61,62]. HPVs were finally detected in cervical carcinomas in 1983 [63,64]. Approximately 50% of the tissues that were examined contained the genetic material of HPV 16, whereas in 1984, HPV type 18 was detected in 20% of the examined tumors [65,66]; subsequently, papillomaviruses 16 and 18 were categorized as high-risk variants. Consecutive studies provided increasingly precise and incontrovertible evidence of the role of high-risk HPVs in the development of cervical carcinoma: This included, among others, the decisive discovery that the genetic material of papillomaviruses can be incorporated into the host cell’s genome of cancer cells and that specific viral genes (coding oncoproteins E6 and E7) thereby switch off antiproliferative cell mechanisms [67,68]. In 1991, McDougall et al. demonstrated that immortalized human keratinocytes spontaneously developed malignant degeneration after long-term cultivation in the laboratory [69]. Additional epidemiological evidence of an HPV association with cervical carcinoma was provided in the late 1980s and early 1990s [70,71]. As a result of this growing body of evidence, the International Agency for Research on Cancer classified HPVs 16 and 18 as carcinogenic, HPVs 31 and 33 as probably carcinogenic, and other HPV types as possibly carcinogenic agents in 1995 [72]. The involvement of HPVs in cervical cancer, viz., the group of HPV-positive tumors, changed over the course of time as further HPV types were characterized. The proportion of HPV-positive tumors of the cervix uteri was estimated at 72% at the beginning of the 1980s [63] and was raised to 99.7% in 1999 [73]. Consequently, researchers were starting to call for a rethink of cytology as a routine examination method in cervical carcinoma screening: The idea for a combination of cytology and HPV testing or single HPV testing was born [73]. Up to now, over 200 genetically differentiated HPV types have been detected [74] (of which 40 can infect the genital tract via the mucosal epithelium, and 12 virus types are categorized as high-risk variants in the development of cervical cancer [75,76]), although solely 60 different HPV types were identified toward the end of the 1980s [77]. In 2008, Harald zur Hausen (\*11.03.1936; † 29.05.2023) was honored with the Nobel Prize in physiology and medicine for his most valuable research [78]. Table 1 summarizes the HPV types associated with cervical cancer and their capabilities to infect the genital area.

**Table 1.** HPV types and their classification according their malignancy potential by the IARC.

HPV Types	IARC Classification (2012)
16; 18; 31; 33; 35; 39; 45; 51; 52; 56; 58; 59	1 (carcinogenic; high risk)
68	2a (probably carcinogenic)
26; 30; 34; 53; 66; 67; 69; 70; 73; 82; 85; 97	2b (possibly carcinogenic)
Gamma-HPV; Beta-HPV; 6; 11	3 (not classifiable)
40; 42; 43; 44; 54; 61; 72; 81	low-risk types



The established role of the human papillomavirus in cervical cancer has sparked the interest of the pharmaceutical industry to develop a vaccine against HPV. Before Gardasil<sup>®</sup>, a recombinant, quadrivalent vaccine against HPVs 6, 11, 16, and 18, was approved by the FDA (Food And Drug Administration, USA) on 8 June 2006 [79] and Cervarix<sup>®</sup>, a recombinant vaccine against HPV high-risk types 16 and 18, was authorized by the European Medicines Agency in 2007 [80], as well as Gardasil<sup>®</sup>-9, the successor of Gardasil<sup>®</sup>, which, in addition to the aforementioned virus types, also covers virus variants 31, 33, 45, 52, and 58, was finally approved by the FDA in December 2014 [81], the foundations for the successful introduction of the vaccine were laid back in the 1990s, when Kirnbauer and associates used papillomavirus clones to successfully produce HPV 16 virus-like particles and attested to their strong immune response [82]. By 2023, the pharmaceutical company Merck & Co., Inc. (Rahway, NJ, USA), which sells Gardasil, is expected to generate sales of up to \$2.5 billion—and the forecasts for the next years are still rising [83]. Cecolin<sup>®</sup> (Xiamen Innovax Biotech Co., Ltd., Xiamen, China)—another vaccine that was approved in China in 2020—is a bivalent vaccine and, thus, covers HPV types 16 and 18. Because its immunogenicity and properties are yet to be investigated, approval by US and European authorities are uncertain so far [84]; nevertheless, it was already prequalified by the WHO in 2021 [85]. In the near future, an Indian vaccine should be available, after its permission by the Indian administration [76]. To date, 120 million women have been vaccinated with a minimum of one dose, mainly in high-income countries [86]. As new vaccines aim to show lower costs [87], broader coverage of administered vaccinations in low-income countries could strengthen the WHO's goal for eliminating cervical cancer [88]. However, to date, official screening recommendations do include all women, regardless of their vaccination status, because HPV vaccination is not able to provide sufficient protection against all the cancerogenous HPV virus types [4]. For a visualization of the history of HPV research in cervical cancer, refer to Figure 3.

#### Timeline: From "invisible poison" to viral genetics

- 1894:** Dmitri Ivanovsky: Mosaic disease of tobacco is caused by pathogens smaller than bacteria
- 1898:** Martinus Beijerinck: Defines an infectious agent *virus*
- 1902:** Walter Reed: Viruses cause human diseases (yellow fever)
- 1936:** Peyton Rous and J.W. Beard: Transfer of skin warts causing neoplasia in rabbits
- 1961:** Yohei Ito and Alfred Evans: The role of genetic viral material in the development of skin cancer
- 1964:** Michael Anthony Epstein, Yvonne Barr, and Bert Achong: First link between human pathogenic virus and neoplasia (Epstein-Barr virus in Burkitt's lymphoma)
- 1965:** June Almeida: Proposes existence of different human wart viruses
- 1968:** Herpes simplex type 2 is discussed as a possible causative agent of cervical cancer
- 1974:** Harald zur Hausen: First attempts to link cervical cancer to HPV
- 1983:** HPV is detected in cervical cancer (Harald zur Hausen)
- 1984:** Elisabeth Schwartz and Harald zur Hausen: HPV-DNA is integrated in the cellular host genome
- 1990:** Bruce A. Werness, Arnold J. Levine and Peter M. Howley: Viral proteins E6 and E7 interact with tumor suppressor proteins
- 1991:** McDougall: Malignant degeneration of human keratinocytes
- 1995:** The International Agency for Research on Cancer classifies HPV 16 and 18 as carcinogenic, HPV 31 and 33 as probably carcinogenic, and other HPV types as possibly carcinogenic agents
- 1999:** Jan M. Walboomers: HPV detection rate in cervical cancers of 99.7%
- 2006:** Gardasil<sup>®</sup>, a recombinant, quadrivalent vaccine against HPV 6, 11, 16 and 18 is approved by the FDA (Food And Drug Administration, USA)
- 2007:** Cervarix<sup>®</sup>, a recombinant vaccine against HPV high-risk types 16 and 18, is authorized by the European Medicines Agency (EMA)
- 2008:** Harald zur Hausen is honored with the Nobel Prize in Physiology and Medicine
- 2014:** Gardasil<sup>®</sup>-9 (additionally covering virus variants 31, 33, 45, 52 and 58) is approved by the FDA

**Figure 3.** Overview of historical virological milestones from Beijerinck to zur Hausen.

## 5. The HPV Test and Its Role in Cancer Screening

The first efforts to establish a commercial HPV test took place just 18 months after the eminent role of HPVs in the pathophysiology of cervical carcinomas gained attention [89]. The first steps in the development of a commercial HPV test can be traced back to the

USA, with the first official FDA approval recorded in 1988 (FDA premarket approval P880009). However, the ViraPap<sup>®</sup> kit from BRL–Life Technologies (Bethesda Research Laboratories–Life Technologies, Bethesda, MD, USA), in cooperation with Georgetown University (Washington, DC, USA), did not achieve a clinical breakthrough because there were insufficient data that could demonstrate a direct patient benefit [90]. As the test was radioactive, it had a limited shelf life and was potentially dangerous to the staff using it. Subsequently, Digene’s (Gaithersburg, MD, USA) Hybrid Capture<sup>®</sup> 2 high-risk HPV DNA test was officially approved by the FDA in 1999 as a triage test for atypical squamous epithelial cells of undetermined significance (ASC-US) [91]. In 2001, the American Society for Colposcopy and Cervical Pathology published the consensus guidelines for the management of women with cervical cytological abnormalities, in which Digene’s Hybrid Capture<sup>®</sup> 2 high-risk HPV DNA test was proposed as a secondary test for atypical squamous epithelial cells of uncertain significance (ASC-US) [92]. This recommendation was based on the advantages of the HPV test, filling the missing space between a possible overtreatment as well as missed neoplasms owing to non-compliance with repetitive cytological testing follow-ups in the case of a single suspicious cytological-screening result. Therefore, the American Society for Colposcopy and Cervical Pathology recommended an HPV test after a suspicious cytological result before women should receive a colposcopic examination. This approach was not without controversy. The *ASCUS/LISL Triage Study for Cervical Cancer* (ATLS) [93], the research of which was used to develop guidelines for the American Society for Colposcopy and Cervical Pathology and which confirmed that the HPV test had a sensitivity of 96.3% in detecting CIN III, was called into question fairly quickly after its publication [93]—opponents complained that routine clinical use did not provide certainty in the detection of cellular atypia [94,95]. In 2002, the American Cancer Society recommended HPV testing using the Digene HC2 high-risk HPV DNA test (QIAGEN, Venlo, The Netherlands) as an additional test option, namely, as a primary co-test every three years, for women over the age of 30. This was confirmed by the FDA in 2003 and was included in the American College of Obstetricians and Gynecologists’ practice bulletin [91,96–98]. Opposite to that, the United States Preventive Services Task Force (USPSTF) interpreted the scientific data and the derived value of HPV testing as being insufficient and did not recommend its routine use as a primary tool in the screening program [99]. To counter stagnating economic growth in 2005, Digene penned the concise slogans “You’re not failing your Pap test, but it might be failing you.” and “If you’re a gambling woman, then getting just a Pap test is fine.” [100] with success! According to a consumer survey, this precautionary advertising led to a significant increase in interest in HPV testing and the cervical-cancer-screening program—within a six-month observation period following the advertisement, a 42% increase in revenue for the HPV test was recorded [101]. Owing to the high negative predictive value of HPV testing, the USPSTF, the American College of Gynecologists and Obstetricians, and the American Cancer Society recommended co-testing with HPV testing and cytology at five-year intervals as a primary screening algorithm in 2005, overcoming past contradictions [102–104]. In 2014, the FDA approved the HPV test COBAS from Roche (Basel, Switzerland) as a primary screening tool for cervical cancer screening in women over 25 [105].

To date, numerous commercially available HPV-testing systems have received approval by the FDA and EMA. The presence of viral infections can be determined either by means of direct genome detection or DNA/RNA amplification. Related to the mode of the HPV detection as well as the specific test system, different HPV types (low risk/high risk) are simultaneously screened. Even though polymerase chain reaction (PCR)-based methods allow for a high degree of sensitivity, the clinical ability of single testing in detecting high-grade squamous lesions remains to be resolved [106]. In comparison, the predictive value of hybrid-based methods is inherently correlated with the quality and quantity of the specimens [107]. Finally, the selection of individual test systems should furthermore be made in accordance with regional approvals by federal agencies as well as the capabilities and infrastructures of hospitals’ local screening programs.

The integration of HPV testing into the cervical-cancer-screening program took a little longer in Germany. Introduced in 1971, the German cervical-cancer-screening program consisted initially of annual pap tests. The first attempts to establish HPV testing within the German screening program were made in 2006 but failed at such an early time. Regulated by the framework conditions of the German legal system and, in particular, ‘*Sozialgesetzbuch V*’, every upcoming change in cancer screening is associated with a change in the German law. Potential modifications to early-cancer-screening programs must be proposed by the Federal Joint Committee to be brought to a binding legal form by the legislature. The Institute for Quality and Efficiency in Health Care (IQWiG), which is responsible for submitting scientific assessments and scientific methods to the Federal Joint Committee, was commissioned in spring 2010 to assess the benefits of the HPV test in primary screening for cervical carcinoma; the report was published in 2012 and postulated a benefit for HPV testing with regard to reductions in high-grade cervical intraepithelial neoplasia and the incidence of cervical carcinoma [108]. In response, the Federal Joint Committee commissioned IQWiG to develop a letter of invitation for screening programs and an information package on cervical cancer that women aged from 20 to 60 should receive from their health insurers. Additionally, women > 30 years should receive an HPV test every five years, and cytology should be reserved as a triage, with the overall aim to collect data during a six-year transition phase, which could then ultimately be analyzed to establish a superior screening strategy [109]. The early detection program was adjusted again on 22 November 2018: Women > 35 years should be offered a co-test consisting of a pap smear and HPV testing at three-year intervals; the annual single cytology test remained as a part of the cancer-screening program for women aged between 20 and 34 [110]. Following the national German guideline on the prevention of cervical cancer, the cancer-testing systems used in clinical routines should be able to identify high-risk HPV types and should cover a sensitivity of at least 95% (The specificity should be 98% at a minimum) in detecting cervical intraepithelial neoplasia grade II (CIN II, high-grade squamous intraepithelial lesions). Nationwide, commonly implemented test systems include, for example, the BD Onclarity™ HPV test (Becton Dickinson, NJ, USA) or the PapilloCheck® HPV test (Greiner Bio-One, Kremsmünster, Austria) [4]. Table 2 offers a synopsis of the approved and commercially available HPV tests that meet the criteria of the German guideline to prevent cervical cancer.

**Table 2.** Commercially available HPV tests, which meet the criteria of the German guideline to prevent cervical cancer.

HPV Test	HPV Types	Technique
Digene Hybrid Capture 2 High-Risk HPV DNA Test (QIAGEN, Gaithersburg, Inc.)	16; 18; 31; 33; 35; 39; 45; 51; 52; 56; 58; 59; 68	DNA: whole genome
COBAS HPV Test (Roche Diagnostics)	16; 18; 31; 33; 35; 39; 45; 51; 52; 56; 58; 59; 66; 68	DNA: L1
Cervista™ HPV HR and GenFind™ DNA Extraction Kit (Hologic)	16; 18; 31; 33; 35; 39; 45; 51; 52; 56; 58; 59; 66; 68	DNA E6/E7/L1
APTIMA HPV Assay (Hologic)	16; 18; 31; 33; 35; 39; 45; 51; 52; 56; 58; 59; 66; 68	RNA E6/E7
Abbot RT High-Risk HPV Test	16; 18; 31; 33; 35; 39; 45; 51; 52; 56; 58; 59; 66; 68	DNA L1
BD Onclarity HPV Test	16; 18; 31; 45; 51; 52; 33–58; 56–59–66; 35; 39–68	DNA E6/E7
PapilloCheck® HPV Test	16; 18; 31; 33; 35; 39; 45; 51; 52; 53; 56; 58; 59; 66; 68; 70; 73; 82; 6; 11; 40; 42; 43; 44	DNA E1

According to the ‘WHO Guideline for the Screening and Treatment of Cervical Pre-Cancer Lesions for Cervical Cancer Prevention’, only a globally applying screening algorithm favoring HPV testing has been established to date [111]. Still, largely different recommendations across American and European guidelines exist, considering not only regional differences in resources, such as laboratory landscapes and testing capabilities, but also the available access to health systems among different socioeconomic groups, even in high-income countries and, therefore, diverging proposed starting ages and HPV test/pap smear intervals within individual screening programs [112–116]. Besides the modern approach for the dual staining of cytological specimens (a p16/Ki67 staining marks HPV association as well as cell proliferation [117]), a meta-analysis carried out by Ogilvie et al. advantageously shows that an HPV test can also be carried out independently by the patient (self-collected vaginal specimens) in self-sampling, with comparable test reliability, rendering the possibility to potentially better include access-limited populations as well as patients with trauma history within screening programs [118].

## 6. The Future of Cervical Cancer Screening—Quo Vadimus?

Despite the urge for quick offers and straightforward access to HPV vaccination (primary prevention), the benefits of an unbiased approach to tissue diagnosis will remain the key in upcoming diagnostic developments. Therefore, novel screening techniques as well as methods for analysis could find their way from research uses to clinical applications in the near future. Because vibrational spectroscopy generates an individual molecular spectroscopic signature of tissues, it provides a quick, inexpensive, and non-destructive way for observer-independent tissue analysis [119]. It has been already successfully employed at a single-cell level to differentiate between normal cells and cells deriving from cervical intraepithelial neoplasia, using Raman spectroscopy on regular cervical cytology samples [120] as well as on tissue samples to distinguish between adenocarcinoma and squamous cell carcinoma [121] or among cervicitis, precursor lesions, and invasive carcinoma [122]. Additionally, the future employment of AI (artificial intelligence) applications and machine learning may lead to objective, independent, and simple diagnostic methods and, therefore, expand the fields of the screening and early diagnosis of cervical cancer [123]. Deep-learning software and suitable algorithms that evaluate images from the cervix could, at a certain point, outperform the current diagnostic ability in terms of the accuracy and reproducibility of colposcopy-guided diagnosis [124,125]. Furthermore, it could reduce costs by lowering the need for laboratory equipment and highly skilled staff [126]. In progressed disease, AI may be capable to improve the workflow of MRI image segmentation [127] and may noninvasively be used to identify lymph node metastasis in cervical cancer [128]. Another potential future improvement could make use of the prognostic impact of DNA methylation patterns. Epigenetic structures may, therefore, provide a new approach in diagnostics and individualized medicine to distinguish the risk patterns of the transformation. Hypermethylated genes seen in precancerous lesions could possibly be taken into account when it comes to the triage of women with a higher risk for developing cancer [129,130]. In the next step, this could lead to new pharmacological therapies in cervical neoplasia: Trichosanthin, the main substance in a Chinese medical herb, for instance, is able to reactivate tumor suppressor genes by inhibiting DNA methyltransferase in cervical cancer cells [131]. To date, modern treatment options include immunotherapeutic drugs such as pembrolizumab, which is yet to be approved for cervical cancer patients [132]. In addition, ongoing research trials examine inter alia the combination of immunotherapeutic and vaccination approaches [133] as well as the combination of checkpoint inhibitors with radiation therapy [134], providing hope for patients with, so far, limited treatment options.

As research continues, both the early detection as well as therapeutic options of cervical cancer could be revolutionized; however, the future path of the development can only be critically evaluated retrospectively. The WHO’s ambitious future goal is clearly defined: to eliminate the worldwide burden of cervical cancer by 2030 through the vigorous implementation of primary, secondary, and tertiary prevention strategies [88].

**Author Contributions:** Conceptualization, L.J., G.G.K. and E.E.; methodology, L.J. and G.G.K.; investigation, L.J. and G.G.K.; resources, PubMed and Google Scholar; data curation, L.J.; writing—original draft preparation, L.J.; writing—review and editing, G.G.K., E.E., L.J. and B.B.; supervision, E.E. and B.B.; project administration, E.E. All authors have read and agreed to the published version of the manuscript.

**Funding:** This research received no external funding.

**Acknowledgments:** Figures 1 and 3 were created with BioRender.com.

**Conflicts of Interest:** The authors declare no conflicts of interest.

## References

1. Sung, H.; Ferlay, J.; Siegel, R.L.; Laversanne, M.; Soerjomataram, I.; Jemal, A.; Bray, F. Global Cancer Statistics 2020: GLOBOCAN Estimates of Incidence and Mortality Worldwide for 36 Cancers in 185 Countries. *CA A Cancer J. Clin.* **2021**, *71*, 209–249. [CrossRef]
2. Daniyal, M.; Akhtar, N.; Ahmad, S.; Fatima, U.; Akram, M.; Asif, H.M. Update Knowledge on Cervical Cancer Incidence and Prevalence in Asia. *Asian Pac. J. Cancer Prev.* **2015**, *16*, 3617–3620. [CrossRef]
3. Ferlay, J.; Ervik, M.; Lam, F.; Laversanne, M.; Colombet, M.; Mery, L.; Piñeros, M.; Znaor, A.; Soerjomataram, I.; Bray, F. Cancer Today. Available online: <https://gco.iarc.who.int/today/> (accessed on 22 February 2024).
4. Leitlinienprogramm Onkologie (Deutsche Krebsgesellschaft, Deutsche Krebshilfe, AWMF) Prävention Des Zervixkarzinoms, Langversion 1.1. Available online: <http://www.leitlinienprogramm-onkologie.de/leitlinien/zervixkarzinom-praevention/> (accessed on 17 January 2024).
5. Gesellschaft der epidemiologischen Krebsregister in Deutschland e.V.; Robert Koch-Institut. Krebs in Deutschland Für 2019/2020. Available online: [https://www.krebsdaten.de/Krebs/DE/Content/Publikationen/Krebs\\_in\\_Deutschland/krebs\\_in\\_deutschland\\_node.html](https://www.krebsdaten.de/Krebs/DE/Content/Publikationen/Krebs_in_Deutschland/krebs_in_deutschland_node.html) (accessed on 17 January 2024).
6. AWMF; Deutsche Krebshilfe; Deutsche Krebsgesellschaft. S3-Leitlinie Diagnostik, Therapie Und Nachsorge Der Patientin Mit Zervixkarzinom, Langversion, 2.2. Available online: <https://register.awmf.org/de/leitlinien/detail/032-033OL> (accessed on 17 January 2024).
7. IARC. *Cervix Cancer Screening*; IARC: Lyon, France, 2005; Volume 10, ISBN 978-92-832-3010-6.
8. Day, N.E. Review Article: Screening for Cancer of the Cervix. *J. Epidemiol. Community Health* (1979-) **1989**, *43*, 103–106. [CrossRef] [PubMed]
9. Läärä, E.; Day, N.; Hakama, M. Trends in mortality from cervical cancer in the nordic countries: association with organised screening programmes. *Lancet* **1987**, *329*, 1247–1249. [CrossRef]
10. Sankila, R.; Démaret, E.; Hakama, M.; Lynge, E.; Schouten, L.J.; Parkin, D.M. *Evaluation and Monitoring of Screening Programmes*; European Commission: Luxembourg, 2001; ISBN 978-92-894-0253-8.
11. Rose, P.G.; Mahdi, H. Landmark Studies of Therapeutic Vaccination in Cervical and Ovarian Cancers. *Lancet Oncol.* **2020**, *21*, 1549–1550. [CrossRef]
12. Burmeister, C.A.; Khan, S.F.; Schäfer, G.; Mbatani, N.; Adams, T.; Moodley, J.; Prince, S. Cervical Cancer Therapies: Current Challenges and Future Perspectives. *Tumour Virus Res.* **2022**, *13*, 200238. [CrossRef]
13. Gottschlich, A.; van Niekerk, D.; Smith, L.W.; Gondara, L.; Melnikow, J.; Cook, D.A.; Lee, M.; Stuart, G.; Martin, R.E.; Peacock, S.; et al. Assessing 10-Year Safety of a Single Negative HPV Test for Cervical Cancer Screening: Evidence from FOCAL-DECADE Cohort. *Cancer Epidemiol. Biomark. Prev.* **2021**, *30*, 22–29. [CrossRef] [PubMed]
14. Hajdu, S.I. A Note from History: Landmarks in History of Cancer, Part 1. *Cancer* **2011**, *117*, 1097–1102. [CrossRef]
15. Jenkins, D. Chapter 1—A Brief History of Cervical Cancer. In *Human Papillomavirus*; Jenkins, D., Bosch, F.X., Eds.; Academic Press: Cambridge, MA, USA, 2020; pp. 1–12, ISBN 978-0-12-814457-2.
16. Oriel, J.D. Anal Warts and Anal Coitus. *Br. J. Vener. Dis.* **1971**, *47*, 373–376. [CrossRef] [PubMed]
17. Renner, C. À propos du spéculum d’étain de Récamier. *Hist. Des Sci. Médicales* **2006**, *40*, 345–350. [PubMed]
18. Bliquez, L.J. Gynecology in Pompeii. In *Ancient Medicine in Its Socio-Cultural Context*; Brill: Leiden, The Netherlands, 1995; Volume 1, pp. 209–223, ISBN 978-90-04-41837-0.
19. Osiander, F.B. Observations on the Cure of Cancer of the Womb by Excision. *Edinb. Med. Surg. J.* **1816**, *12*, 286–294. [PubMed]
20. Senn, N. The early history of vaginal hysterectomy. *J. Am. Med. Assoc.* **1895**, *XXV*, 476–482. [CrossRef]
21. DiMaio, D. Nuns, Warts, Viruses, and Cancer. *Yale J. Biol. Med.* **2015**, *88*, 127–129.
22. Ebert, A.D.; David, M. „Was ihn vor allem charakterisierte, war seine . . . ungewöhnliche Klugheit“—Zum 100. Todestag von Johann Veit (1852–1917). *Geburtshilfe Frauenheilkd.* **2017**, *77*, 949–951. [CrossRef]
23. Zander, J. *Milestones in Gynecology and Obstetrics*; Ludwig, H., Thomsen, K., Eds.; Springer: Berlin/Heidelberg, Germany, 1986.
24. Freund, W.A. *Zu Meiner Methode der Totalen Uterus-Exstirpation*; Breitkopf und Härtel: Leipzig, Germany, 1878; Volume 12, pp. 265–269.
25. Toellner, R. *Illustrierte Geschichte der Medizin*; Andreas Verlag: Vaduz, Liechtenstein, 1992; pp. 1307–1308, ISBN 3-86070-204-1.
26. Dursun, P.; Gultekin, M.; Ayhan, A. The History of Radical Hysterectomy. *J. Low. Genit. Tract. Dis.* **2011**, *15*, 235. [CrossRef] [PubMed]

27. Yumpu.com Hysterektomie von der Antike bis Heute—Frauenarzt. Available online: <https://www.yumpu.com/de/document/read/8470067/hysterektomie-von-der-antike-bis-heute-frauenarzt> (accessed on 22 February 2024).
28. Dargent, D.; Mathevet, P. 4 Schauta's Vaginal Hysterectomy Combined with Laparoscopic Lymphadenectomy. *Baillière's Clin. Obstet. Gynaecol.* **1995**, *9*, 691–705. [CrossRef] [PubMed]
29. Possover, M. Options for Laparoscopic Surgery in Cervical Carcinomas. *Eur. J. Gynaecol. Oncol.* **2003**, *24*, 471–472.
30. Höckel, M.; Horn, L.-C.; Hentschel, B.; Höckel, S.; Naumann, G. Total Mesometrial Resection: High Resolution Nerve-Sparing Radical Hysterectomy Based on Developmentally Defined Surgical Anatomy. *Int. J. Gynecol. Cancer* **2003**, *13*, 791–803. [CrossRef]
31. Kimmig, R. "Robotic surgery" beim Zervixkarzinom. *Gynäkologe* **2012**, *45*, 707–713. [CrossRef]
32. Ramirez, P.T.; Frumovitz, M.; Pareja, R.; Lopez, A.; Vieira, M.; Ribeiro, R.; Buda, A.; Yan, X.; Shuzhong, Y.; Chetty, N.; et al. Minimally Invasive versus Abdominal Radical Hysterectomy for Cervical Cancer. *N. Engl. J. Med.* **2018**, *379*, 1895–1904. [CrossRef]
33. Plante, M.; Kwon, J.S.; Ferguson, S.; Samouëlian, V.; Ferron, G.; Maulard, A.; de Kroon, C.; Van Driel, W.; Tidy, J.; Marth, C.; et al. An International Randomized Phase III Trial Comparing Radical Hysterectomy and Pelvic Node Dissection (RH) vs. Simple Hysterectomy and Pelvic Node Dissection (SH) in Patients with Low-Risk Early-Stage Cervical Cancer (LRESCC): A Gynecologic Cancer Intergroup Study Led by the Canadian Cancer Trials Group (CCTG CX.5-SHAPE). *JCO* **2023**, *41*, LBA5511. [CrossRef]
34. Hinselmann, H. Verbesserung Der Inspektionsmöglichkeiten von Vulva, Vagina Und Portio. *Münch Med. Wschr* **1925**, *72*, 1733.
35. Hübner, J. Kolposkopie ohne Menschlichkeit?! Hinselmann und die Versuche an Frauen in Auschwitz. *Geburtshilfe Frauenheilkd.* **2016**, *76*, A11. [CrossRef]
36. Reich, O.; Pickel, H. 100 Years of Iodine Testing of the Cervix: A Critical Review and Implications for the Future. *Eur. J. Obstet. Gynecol. Reprod. Biol.* **2021**, *261*, 34–40. [CrossRef] [PubMed]
37. Diamantis, A.; Magiorkinis, E. Pioneers of Exfoliative Cytology in the 19th Century: The Predecessors of George Papanicolaou. *Cytopathology* **2014**, *25*, 215–224. [CrossRef] [PubMed]
38. Tan, S.Y.; Tatsumura, Y. George Papanicolaou (1883–1962): Discoverer of the Pap Smear. *Singap. Med. J.* **2015**, *56*, 586–587. [CrossRef] [PubMed]
39. Swailes, A.L.; Hossler, C.E.; Kesterson, J.P. Pathway to the Papanicolaou Smear: The Development of Cervical Cytology in Twentieth-Century America and Implications in the Present Day. *Gynecol. Oncol.* **2019**, *154*, 3–7. [CrossRef]
40. Stockard, C.R.; Papanicolaou, G.N. The Existence of a Typical Oestrous Cycle in the Guinea-Pig—With a Study of Its Histological and Physiological Changes. *Am. J. Anat.* **1917**, *22*, 225–283. [CrossRef]
41. Race Betterment Foundation. Race Betterment Foundation Proceedings of the Third Race Betterment Conference.; Battle Creek, MI, 1928. In *Proceedings of the Third Race Betterment Conference, Battle Creek, MI, USA, 2 January 1928*; Race Betterment Foundation: Battle Creek, MI, USA, 2 January 1928.
42. Chantziantoniou, N.; Donnelly, A.D.; Mukherjee, M.; Boon, M.E.; Austin, R.M. Inception and Development of the Papanicolaou Stain Method. *Acta Cytol.* **2017**, *61*, 266–280. [CrossRef]
43. Shaw, P.A. The History of Cervical Screening I: The Pap. Test. *J. SOGC* **2000**, *22*, 110–114. [CrossRef]
44. Martin, C.E. Epidemiology of Cancer of the Cervix. II. Marital and Coital Factors in Cervical Cancer. *Am. J. Public Health Nations Health* **1967**, *57*, 803–814. [CrossRef]
45. Buckley, J.D.; Doll, R.; Harris, R.W.C.; Vessey, M.P.; Williams, P.T. Case-control study of the husbands of women with dysplasia or carcinoma of the cervix uteri. *Lancet* **1981**, *318*, 1010–1015. [CrossRef]
46. Elliott, R.I.K. On the prevention of carcinoma of the cervix. *Lancet* **1964**, *283*, 231–235. [CrossRef] [PubMed]
47. Beral, V. Cancer of the cervix: A sexually transmitted infection? *Lancet* **1974**, *303*, 1037–1040. [CrossRef] [PubMed]
48. Hochman, A.; Ratzkowski, E.; Schreiber, H. Incidence of Carcinoma of the Cervix in Jewish Women in Israel. *Br. J. Cancer* **1955**, *9*, 358–364. [CrossRef] [PubMed]
49. Lechevalier, H. Dmitri Iosifovich Ivanovski (1864–1920). *Bacteriol. Rev.* **1972**, *36*, 135–145. [CrossRef] [PubMed]
50. Sankaran, N. On the Historical Significance of Beijerinck and His Contagium Vivum Fluidum for Modern Virology. *Hist. Philos. Life Sci.* **2018**, *40*, 41. [CrossRef]
51. Ryu, W.-S. Discovery and Classification. *Mol. Virol. Hum. Pathog. Viruses* **2017**, *3*–20. [CrossRef]
52. Van Epps, H.L. Peyton Rous. *J. Exp. Med.* **2005**, *201*, 320. [CrossRef]
53. Rous, P.; Kidd, J.G.; Beard, J.W. Observations on the relation of the virus causing rabbit papillomas to the cancers deriving therefrom. *J. Exp. Med.* **1936**, *64*, 385–400. [CrossRef]
54. Ito, Y.; Evans, C.A. Induction of tumors in domestic rabbits with nucleic acid preparations from partially purified Shope papilloma virus and from extracts of the papillomas of domestic and cottontail rabbits. *J. Exp. Med.* **1961**, *114*, 485–500. [CrossRef]
55. Epstein, M.A.; Achong, B.G.; Barr, Y.M. Virus particles in cultured lymphoblasts from burkitt's lymphoma. *Lancet* **1964**, *1*, 702–703. [CrossRef]
56. Almeida, J.; Goffe, A. Antibody to wart virus in human sera demonstrated by electron microscopy and precipitin tests. *Lancet* **1965**, *286*, 1205–1207. [CrossRef] [PubMed]
57. Rawls, W.E.; Tompkins, W.A.; Figueroa, M.E.; Melnick, J.L. Herpesvirus Type 2: Association with Carcinoma of the Cervix. *Science* **1968**, *161*, 1255–1256. [CrossRef] [PubMed]
58. Naib, Z.M.; Nahmias, A.J.; Josey, W.E.; Kramer, J.H. Genital Herpetic Infection Association with Cervical Dysplasia and Carcinoma. *Cancer* **1969**, *23*, 940–945. [CrossRef] [PubMed]

59. Hausen, H.Z.; Meinhof, W.; Scheiber, W.; Bornkamm, G.W. Attempts to Detect Virus-Specific DNA in Human Tumors. I. Nucleic Acid Hybridizations with Complementary RNA of Human Wart Virus. *Int. J. Cancer* **1974**, *13*, 650–656. [CrossRef] [PubMed]
60. Vonka, V.; Kaňka, J.; Jelínek, J.; Šubrt, I.; Suchánek, A.; Havráňková, A.; Váchal, M.; Hirsch, I.; Domorázková, E.; Závadová, H.; et al. Prospective Study on the Relationship between Cervical Neoplasia and Herpes Simplex Type-2 Virus. I. Epidemiological Characteristics. *Int. J. Cancer* **1984**, *33*, 49–60. [CrossRef] [PubMed]
61. zur Hausen, H. Condylomata Acuminata and Human Genital Cancer. *Cancer Res.* **1976**, *36*, 794. [PubMed]
62. zur Hausen, H. Human Papillomaviruses and Their Possible Role in Squamous Cell Carcinomas. In *Current Topics in Microbiology and Immunology*; Arber, W., Henle, W., Hofschneider, P.H., Humphrey, J.H., Klein, J., Koldovský, P., Koprowski, H., Maaløe, O., Melchers, F., Rott, R., et al., Eds.; Springer: Berlin/Heidelberg, Germany, 1977; pp. 1–30, ISBN 978-3-642-66800-5.
63. Dürst, M.; Gissmann, L.; Ikenberg, H.; zur Hausen, H. A Papillomavirus DNA from a Cervical Carcinoma and Its Prevalence in Cancer Biopsy Samples from Different Geographic Regions. *Proc. Natl. Acad. Sci. USA* **1983**, *80*, 3812–3815. [CrossRef] [PubMed]
64. zur Hausen, H. Papillomaviruses—To Vaccination and Beyond. *Biochem. Mosc.* **2008**, *73*, 498–503. [CrossRef]
65. Boshart, M.; Gissmann, L.; Ikenberg, H.; Kleinheinz, A.; Scheurlen, W.; zur Hausen, H. A New Type of Papillomavirus DNA, Its Presence in Genital Cancer Biopsies and in Cell Lines Derived from Cervical Cancer. *EMBO J.* **1984**, *3*, 1151–1157. [CrossRef]
66. Gissmann, L.; Boshart, M.; Dürst, M.; Ikenberg, H.; Wagner, D.; Hausen, H.Z. Presence of Human Papillomavirus in Genital Tumors. *J. Investig. Dermatol.* **1984**, *83*, S26–S28. [CrossRef]
67. Werness, B.A.; Levine, A.J.; Howley, P.M. Association of Human Papillomavirus Types 16 and 18 E6 Proteins with P53. *Science* **1990**, *248*, 76–79. [CrossRef]
68. Schwarz, E.; Freese, U.K.; Gissmann, L.; Mayer, W.; Roggenbuck, B.; Stremlau, A.; Hausen, H. zur Structure and Transcription of Human Papillomavirus Sequences in Cervical Carcinoma Cells. *Nature* **1985**, *314*, 111–114. [CrossRef]
69. Hurlin, P.J.; Kaur, P.; Smith, P.P.; Perez-Reyes, N.; Blanton, R.A.; McDougall, J.K. Progression of Human Papillomavirus Type 18-Immortalized Human Keratinocytes to a Malignant Phenotype. *Proc. Natl. Acad. Sci. USA* **1991**, *88*, 570–574. [CrossRef]
70. Reeves, W.C.; Rawls, W.E.; Brinton, L.A. Epidemiology of Genital Papillomaviruses and Cervical Cancer. *Rev. Infect. Dis.* **1989**, *11*, 426–439. [CrossRef]
71. Muñoz, N.; Bosch, F.X. HPV and Cervical Neoplasia: Review of Case-Control and Cohort Studies. *IARC Sci. Publ.* **1992**, *119*, 251–261. [PubMed]
72. IARC. *Human Papillomaviruses*; IARC Publications: Lyon, France, 1995; ISBN 978-92-832-1264-5.
73. Walboomers, J.M.M.; Jacobs, M.V.; Manos, M.M.; Bosch, F.X.; Kummer, J.A.; Shah, K.V.; Snijders, P.J.F.; Peto, J.; Meijer, C.J.L.M.; Muñoz, N. Human Papillomavirus Is a Necessary Cause of Invasive Cervical Cancer Worldwide. *J. Pathol.* **1999**, *189*, 12–19. [CrossRef]
74. Choi, S.; Ismail, A.; Pappas-Gogos, G.; Boussios, S. HPV and Cervical Cancer: A Review of Epidemiology and Screening Uptake in the UK. *Pathogens* **2023**, *12*, 298. [CrossRef]
75. Markowitz, L.E.; Schiller, J.T. Human Papillomavirus Vaccines. *J. Infect. Dis.* **2021**, *224*, S367–S378. [CrossRef]
76. Jeannot, E.; Ben Abdeljelil, H.; Viviano, M. HPV Vaccination for Cervical Cancer Prevention in Switzerland. *Encyclopedia* **2023**, *3*, 512–519. [CrossRef]
77. de Villiers, E.M. Heterogeneity of the Human Papillomavirus Group. *J. Virol.* **1989**, *63*, 4898–4903. [CrossRef]
78. The Nobel Prize in Physiology or Medicine. 2008. Available online: <https://www.nobelprize.org/prizes/medicine/2008/hausen/biographical/> (accessed on 11 February 2024).
79. Research, C. for B.E. and Approved Products—June 8, 2006 Approval Letter—Human Papillomavirus Quadrivalent (Types 6, 11, 16, 18) Vaccine, Recombinant. Available online: <http://wayback.archive-it.org/7993/20170722145339/https://www.fda.gov/BiologicsBloodVaccines/Vaccines/ApprovedProducts/ucm111283.htm> (accessed on 20 January 2024).
80. Cervarix | European Medicines Agency. Available online: <https://www.ema.europa.eu/en/medicines/human/EPAR/cervarix#authorisation-details-section> (accessed on 20 January 2024).
81. Research, C. for B.E. and Approved Products—December 10, 2014 Approval Letter-GARDASIL 9. Available online: <https://wayback.archive-it.org/7993/20190425005410/https://www.fda.gov/BiologicsBloodVaccines/Vaccines/ApprovedProducts/ucm426520.htm> (accessed on 20 January 2024).
82. Kirnbauer, R.; Booy, F.; Cheng, N.; Lowy, D.R.; Schiller, J.T. Papillomavirus L1 Major Capsid Protein Self-Assembles into Virus-like Particles That Are Highly Immunogenic. *Proc. Natl. Acad. Sci. USA* **1992**, *89*, 12180–12184. [CrossRef]
83. Erman, M.; Leo, L. Merck Raises 2023 Sales Forecast as Top Drugs Beat Street Estimates. Available online: <https://www.reuters.com/business/healthcare-pharmaceuticals/merck-posts-narrower-than-expected-loss-sales-top-drugs-beat-street-estimates-2023-08-01/> (accessed on 20 January 2024).
84. Akhatova, A.; Azizan, A.; Atageldiyeva, K.; Ashimkhanova, A.; Marat, A.; Iztleuov, Y.; Suleimenova, A.; Shamkeeva, S.; Aimagambe-tova, G. Prophylactic Human Papillomavirus Vaccination: From the Origin to the Current State. *Vaccines* **2022**, *10*, 1912. [CrossRef]
85. New HPV Vaccine from Inovax Receives WHO Prequalification. Available online: <https://www.path.org/our-impact/media-center/new-hpv-vaccine-inovax-receives-who-prequalification/> (accessed on 8 February 2024).
86. Bruni, L.; Diaz, M.; Barrionuevo-Rosas, L.; Herrero, R.; Bray, F.; Bosch, F.X.; de Sanjosé, S.; Castellsagué, X. Global Estimates of Human Papillomavirus Vaccination Coverage by Region and Income Level: A Pooled Analysis. *Lancet Glob. Health* **2016**, *4*, e453–e463. [CrossRef]

87. Zou, Z.; Fairley, C.K.; Ong, J.J.; Hocking, J.; Canfell, K.; Ma, X.; Chow, E.P.F.; Xu, X.; Zhang, L.; Zhuang, G. Domestic HPV Vaccine Price and Economic Returns for Cervical Cancer Prevention in China: A Cost-Effectiveness Analysis. *Lancet Glob. Health* **2020**, *8*, e1335–e1344. [CrossRef]
88. WHO Global Strategy to Accelerate the Elimination of Cervical Cancer as a Public Health Problem. Available online: <https://www.who.int/publications-detail-redirect/9789240014107> (accessed on 21 January 2024).
89. Hogarth, S.; Hopkins, M.; Rotolo, D. Technological Accretion in Diagnostics: HPV Testing and Cytology in Cervical Cancer Screening. In *Medical Innovation: Science, Technology and Practice*; Consoli, D., Mina, A., Nelson, R.R., Ramlogan, R., Eds.; Wellcome Trust–Funded Monographs and Book Chapters; Routledge: New York, NY, USA, 2015; ISBN 978-1-138-86034-6.
90. Corliss, J. Utility of ViraPap Remains to Be Established. *JNCI J. Natl. Cancer Inst.* **1990**, *82*, 252–253. [CrossRef]
91. Saraiya, M.; Steben, M.; Watson, M.; Markowitz, L. Evolution of Cervical Cancer Screening and Prevention in United States and Canada: Implications for Public Health Practitioners and Clinicians. *Prev. Med.* **2013**, *57*, 426–433. [CrossRef]
92. Wright, J.; Thomas, C.; Cox, J.T.; Massad, L.S.; Twiggs, L.B.; Wilkinson, E.J. 2001 ASCCP-Sponsored Consensus Conference 2001 Consensus Guidelines for the Management of Women With Cervical Cytological Abnormalities. *JAMA* **2002**, *287*, 2120–2129. [CrossRef]
93. Solomon, D.; Schiffman, M.; Tarone, R.; For the ALTS Group. Comparison of Three Management Strategies for Patients With Atypical Squamous Cells of Undetermined Significance: Baseline Results From a Randomized Trial. *JNCI J. Natl. Cancer Inst.* **2001**, *93*, 293–299. [CrossRef]
94. Cain, J.M.; Howett, M.K. Preventing Cervical Cancer. *Science* **2000**, *288*, 1753–1755. [CrossRef]
95. Herbst, A.L.; Pickett, K.E.; Follen, M.; Noller, K.L. The Management of ASCUS Cervical Cytologic Abnormalities and HPV Testing: A Cautionary Note. *Obstet. Gynecol.* **2001**, *98*, 849–851. [CrossRef]
96. Premarket Approval (PMA). Available online: <https://www.accessdata.fda.gov/scripts/cdrh/cfdocs/cfpma/pma.cfm?id=P890064S009> (accessed on 20 January 2024).
97. ACOG Practice Bulletin. *Int. J. Gynecol. Obstet.* **2003**, *83*, 237–247. [CrossRef]
98. Saslow, D.; Runowicz, C.D.; Solomon, D.; Moscicki, A.-B.; Smith, R.A.; Eyre, H.J.; Cohen, C. American Cancer Society Guideline for the Early Detection of Cervical Neoplasia and Cancer. *CA A Cancer J. Clin.* **2002**, *52*, 342–362. [CrossRef]
99. U.S. Preventive Services Task Force Screening for Cervical Cancer: Recommendations and Rationale. *Am. J. Nurs.* **2003**, *103*, 101–102, 105–106, 108–109.
100. Rosenwald, M.S. *Digene's Ads Take Their Case to Women*; Washington Post: Washington, DC, USA, 2005.
101. Luechtefeld, L. Driving Awareness. Available online: <https://www.mddionline.com/medical-device-markets/driving-awareness> (accessed on 20 January 2024).
102. Committee on Practice Bulletins—Gynecology ACOG Practice Bulletin Number 131: Screening for Cervical Cancer. *Obstet. Gynecol.* **2012**, *120*, 1222–1238. [CrossRef]
103. Saslow, D.; Solomon, D.; Lawson, H.W.; Killackey, M.; Kulasingam, S.L.; Cain, J.M.; Garcia, F.A.R.; Moriarty, A.T.; Waxman, A.G.; Wilbur, D.C.; et al. American Cancer Society, American Society for Colposcopy and Cervical Pathology, and American Society for Clinical Pathology Screening Guidelines for the Prevention and Early Detection of Cervical Cancer. *J. Low. Genit. Tract. Dis.* **2012**, *16*, 175–204. [CrossRef]
104. Moyer, V.A. Screening for Cervical Cancer: U.S. Preventive Services Task Force Recommendation Statement. *Ann. Intern. Med.* **2012**, *156*, 880–891. [CrossRef] [PubMed]
105. Roche Roche's Cobas HPV Test Receives FDA Approval for First-Line Cervical Cancer Screening Using SurePath Preservative Fluid. Available online: <https://www.prnewswire.com/news-releases/roches-cobas-hpv-test-receives-fda-approval-for-first-line-cervical-cancer-screening-using-surepath-preservative-fluid-300688266.html> (accessed on 20 January 2024).
106. Luu, H.N.; Adler-Storthz, K.; Dillon, L.M.; Follen, M.; Scheurer, M.E. Comparing the Performance of Hybrid Capture II and Polymerase Chain Reaction (PCR) for the Identification of Cervical Dysplasia in the Screening and Diagnostic Settings. *Clin. Med. Insights Oncol.* **2013**, *7*, 247–255. [CrossRef]
107. Qiagen. *Qiagen Digene® HC2 Sample Conversion Kit Instructions for Use*; QIAGEN Sciences Inc.: Germantown, MD, USA, 2013.
108. IQWiG HPV-Test: Hinweise auf Nutzen im Primärscreening | IQWiG.de. Available online: [https://www.iqwig.de/presse/pressemitteilungen/pressemitteilungen-detailseite\\_10827.html](https://www.iqwig.de/presse/pressemitteilungen/pressemitteilungen-detailseite_10827.html) (accessed on 21 January 2024).
109. IQWiG Einladung und Entscheidungshilfe Zervixkarzinom-Screening: IQWiG Legt Finale Fassung vor. Available online: [https://www.iqwig.de/presse/pressemitteilungen/pressemitteilungen-detailseite\\_10228.html](https://www.iqwig.de/presse/pressemitteilungen/pressemitteilungen-detailseite_10228.html) (accessed on 21 January 2024).
110. Gemeinsamer Bundesausschuss Richtlinie Für Organisierte Krebsfrüherkennungsprogramme Und Krebsfrüherkennungs-Richtlinie: Programm zur Früherkennung von Zervixkarzinomen—Gemeinsamer Bundesausschuss. Available online: <https://www.g-ba.de/beschluesse/3597/> (accessed on 21 January 2024).
111. WHO. WHO Guideline for Screening and Treatment of Cervical Pre-Cancer Lesions for Cervical Cancer Prevention. Available online: <https://www.who.int/publications-detail-redirect/9789240030824> (accessed on 21 January 2024).
112. European Commission Proposal for a Council Recommendation (CR) on Strengthening Prevention through Early Detection: A New Approach on Cancer Screening Replacing CR 2003/878/EC—European Commission. Available online: [https://health.ec.europa.eu/publications/proposal-council-recommendation-cr-strengthening-prevention-through-early-detection-new-approach\\_en](https://health.ec.europa.eu/publications/proposal-council-recommendation-cr-strengthening-prevention-through-early-detection-new-approach_en) (accessed on 21 January 2024).



113. US Preventive Services Task Force Screening for Cervical Cancer: US Preventive Services Task Force Recommendation Statement. *JAMA* **2018**, *320*, 674–686. [CrossRef]
114. ACOG Updated Cervical Cancer Screening Guidelines. Available online: <https://www.acog.org/clinical/clinical-guidance/practice-advisory/articles/2021/04/updated-cervical-cancer-screening-guidelines> (accessed on 21 January 2024).
115. Fontham, E.T.H.; Wolf, A.M.D.; Church, T.R.; Etzioni, R.; Flowers, C.R.; Herzig, A.; Guerra, C.E.; Oeffinger, K.C.; Shih, Y.-C.T.; Walter, L.C.; et al. Cervical Cancer Screening for Individuals at Average Risk: 2020 Guideline Update from the American Cancer Society. *CA A Cancer J. Clin.* **2020**, *70*, 321–346. [CrossRef]
116. Shastri, S.S.; Temin, S.; Almonte, M.; Basu, P.; Campos, N.G.; Gravitt, P.E.; Gupta, V.; Lombe, D.C.; Murillo, R.; Nakisige, C.; et al. Secondary Prevention of Cervical Cancer: ASCO Resource–Stratified Guideline Update. *JCO Glob. Oncol.* **2022**, *8*, e2200217. [CrossRef]
117. Shi, Q.; Xu, L.; Yang, R.; Meng, Y.; Qiu, L. Ki-67 and P16 Proteins in Cervical Cancer and Precancerous Lesions of Young Women and the Diagnostic Value for Cervical Cancer and Precancerous Lesions. *Oncol. Lett.* **2019**, *18*, 1351–1355. [CrossRef]
118. Ogilvie, G.S.; Patrick, D.M.; Schulzer, M.; Sellors, J.W.; Petric, M.; Chambers, K.; White, R.; FitzGerald, J.M. Diagnostic Accuracy of Self Collected Vaginal Specimens for Human Papillomavirus Compared to Clinician Collected Human Papillomavirus Specimens: A Meta-Analysis. *Sex. Transm. Infect.* **2005**, *81*, 207–212. [CrossRef]
119. Shaikh, R.; Daniel, A.; Lyng, F.M. Raman Spectroscopy for Early Detection of Cervical Cancer, a Global Women’s Health Issue—A Review. *Molecules* **2023**, *28*, 2502. [CrossRef]
120. Ramos, I.R.; Meade, A.D.; Ibrahim, O.; Byrne, H.J.; McMenamin, M.; McKenna, M.; Malkin, A.; Lyng, F.M. Raman Spectroscopy for Cytopathology of Exfoliated Cervical Cells. *Faraday Discuss.* **2016**, *187*, 187–198. [CrossRef]
121. Zheng, C.; Qing, S.; Wang, J.; Lü, G.; Li, H.; Lü, X.; Ma, C.; Tang, J.; Yue, X. Diagnosis of Cervical Squamous Cell Carcinoma and Cervical Adenocarcinoma Based on Raman Spectroscopy and Support Vector Machine. *Photodiagnosis Photodyn. Ther.* **2019**, *27*, 156–161. [CrossRef]
122. Wang, J.; Zheng, C.-X.; Ma, C.-L.; Zheng, X.-X.; Lv, X.-Y.; Lv, G.-D.; Tang, J.; Wu, G.-H. Raman Spectroscopic Study of Cervical Precancerous Lesions and Cervical Cancer. *Lasers Med. Sci.* **2021**, *36*, 1855–1864. [CrossRef]
123. Hou, X.; Shen, G.; Zhou, L.; Li, Y.; Wang, T.; Ma, X. Artificial Intelligence in Cervical Cancer Screening and Diagnosis. *Front. Oncol.* **2022**, *12*, 851367. [CrossRef] [PubMed]
124. Hu, L.; Bell, D.; Antani, S.; Xue, Z.; Yu, K.; Horning, M.P.; Gachuhi, N.; Wilson, B.; Jaiswal, M.S.; Befano, B.; et al. An Observational Study of Deep Learning and Automated Evaluation of Cervical Images for Cancer Screening. *JNCI J. Natl. Cancer Inst.* **2019**, *111*, 923–932. [CrossRef] [PubMed]
125. Xue, P.; Ng, M.T.A.; Qiao, Y. The Challenges of Colposcopy for Cervical Cancer Screening in LMICs and Solutions by Artificial Intelligence. *BMC Med.* **2020**, *18*, 169. [CrossRef] [PubMed]
126. Vargas-Cardona, H.D.; Rodriguez-Lopez, M.; Arrivillaga, M.; Vergara-Sanchez, C.; García-Cifuentes, J.P.; Bermúdez, P.C.; Jaramillo-Botero, A. Artificial Intelligence for Cervical Cancer Screening: Scoping Review, 2009–2022. *Int. J. Gynecol. Obstet.* **2023**. [CrossRef]
127. Liang, P.; Sun, G.; Wei, S. Application of Deep Learning Algorithm in Cervical Cancer MRI Image Segmentation Based on Wireless Sensor. *J. Med. Syst.* **2019**, *43*, 156. [CrossRef] [PubMed]
128. Wu, Q.; Wang, S.; Zhang, S.; Wang, M.; Ding, Y.; Fang, J.; Wu, Q.; Qian, W.; Liu, Z.; Sun, K.; et al. Development of a Deep Learning Model to Identify Lymph Node Metastasis on Magnetic Resonance Imaging in Patients With Cervical Cancer. *JAMA Netw. Open* **2020**, *3*, e2011625. [CrossRef] [PubMed]
129. Albulescu, A.; Plesa, A.; Fudulu, A.; Iancu, I.V.; Anton, G.; Botezatu, A. Epigenetic Approaches for Cervical Neoplasia Screening (Review). *Exp. Ther. Med.* **2021**, *22*, 1481. [CrossRef] [PubMed]
130. Dueñas-González, A.; Lizano, M.; Candelaria, M.; Cetina, L.; Arce, C.; Cervera, E. Epigenetics of Cervical Cancer. An Overview and Therapeutic Perspectives. *Mol. Cancer* **2005**, *4*, 38. [CrossRef]
131. Huang, Y.; Song, H.; Hu, H.; Cui, L.; You, C.; Huang, L. Trichosanthin Inhibits DNA Methyltransferase and Restores Methylation-Silenced Gene Expression in Human Cervical Cancer Cells. *Mol. Med. Rep.* **2012**, *6*, 872–878. [CrossRef]
132. Cervical Cancer Immunotherapy | Immune Checkpoint Inhibitors. Available online: <https://www.cancer.org/cancer/types/cervical-cancer/treating/immunotherapy.html> (accessed on 22 February 2024).
133. Ding, H.; Zhang, J.; Zhang, F.; Xu, Y.; Yu, Y.; Liang, W.; Li, Q. Effectiveness of Combination Therapy with ISA101 Vaccine for the Treatment of Human Papillomavirus-Induced Cervical Cancer. *Front. Oncol.* **2022**, *12*, 990877. [CrossRef]
134. Ladbury, C.; Germino, E.; Novak, J.; Liu, J.; Horne, Z.; Dyer, B.; Glaser, S. Combination Radiation and Immunotherapy in Gynecologic Malignancies—A Comprehensive Review. *Transl. Cancer Res.* **2021**, *10*, 2609–2619. [CrossRef]

**Disclaimer/Publisher’s Note:** The statements, opinions and data contained in all publications are solely those of the individual author(s) and contributor(s) and not of MDPI and/or the editor(s). MDPI and/or the editor(s) disclaim responsibility for any injury to people or property resulting from any ideas, methods, instructions or products referred to in the content.

# Second Trimester Amniotic Fluid Angiotensinogen Levels Linked to Increased Fetal Birth Weight and Shorter Gestational Age in Term Pregnancies

Dionysios Vrachnis <sup>1</sup>, Alexandros Fotiou <sup>1</sup>, Aimilia Mantzou <sup>2</sup>, Vasilios Pergialiotis <sup>3</sup>, Panagiotis Antsaklis <sup>3</sup>, George Valsamakis <sup>4</sup>, Sofoklis Stavros <sup>5</sup>, Nikolaos Machairiotis <sup>5</sup>, Christos Iavazzo <sup>6</sup>, Christina Kanaka-Gantenbein <sup>2</sup>, George Mastorakos <sup>7</sup>, Petros Drakakis <sup>5</sup>, Nikolaos Vrachnis <sup>5,8</sup> and Nikolaos Antonakopoulos <sup>9,\*</sup>

- <sup>1</sup> National and Kapodistrian University of Athens Medical School, 11527 Athens, Greece; dionisisvrachnis@gmail.com (D.V.); alexandrosfotiou92@gmail.com (A.F.)
- <sup>2</sup> Aghia Sophia Children's Hospital, National and Kapodistrian University of Athens, 11527 Athens, Greece; amantzou@med.uoa.gr (A.M.); chriskan@med.uoa.gr (C.K.-G.)
- <sup>3</sup> First Department of Obstetrics and Gynecology, National and Kapodistrian University of Athens Medical School, Alexandra Hospital, 11527 Athens, Greece; pergialiotis.vp@gmail.com (V.P.); panosant@gmail.com (P.A.)
- <sup>4</sup> Second Department of Obstetrics and Gynecology, National and Kapodistrian University of Athens Medical School, Aretaieion Hospital, 11527 Athens, Greece; gedvalsamakis@yahoo.com
- <sup>5</sup> Third Department of Obstetrics and Gynecology, National and Kapodistrian University of Athens Medical School, Attikon Hospital, 11527 Athens, Greece; sfstavrou@yahoo.com (S.S.); nikolaosmachairiotis@gmail.com (N.M.); pdrakakis@hotmail.com (P.D.)
- <sup>6</sup> Department of Gynecologic Oncology, Metaxa Memorial Cancer Hospital of Piraeus, 18537 Piraeus, Greece; christosiavazzo@gmail.com
- <sup>7</sup> Unit of Endocrinology, Diabetes Mellitus and Metabolism, National and Kapodistrian University of Athens Medical School, Aretaieion Hospital, 11527 Athens, Greece; mastorakg@gmail.com
- <sup>8</sup> Vascular Biology, Molecular and Clinical Sciences Research Institute, St George's University of London, London SW17 0RE, UK
- <sup>9</sup> Department of Obstetrics and Gynecology, University Hospital of Patras, Medical School, University of Patras, 26504 Patra, Greece
- \* Correspondence: antonakopoulos2002@yahoo.gr

**Abstract:** Background: Despite the considerable progress made in recent years in fetal assessment, the etiology of fetal growth disturbances is not as yet well understood. In an effort to enhance our knowledge in this area, we investigated the associations of the amniotic fluid angiotensinogen of the renin–angiotensin system with fetal growth abnormalities. Methods: We collected amniotic fluid samples from 70 pregnant women who underwent amniocentesis during their early second trimester. Birth weight was documented upon delivery, after which the embryos corresponding to the respective amniotic fluid samples were categorized into three groups as follows: small for gestational age (SGA), appropriate for gestational age (AGA), and large for gestational age (LGA). Amniotic fluid angiotensinogen levels were determined by using ELISA kits. Results: Mean angiotensinogen values were 3885 ng/mL (range: 1625–5375 ng/mL), 4885 ng/mL (range: 1580–8460 ng/mL), and 4670 ng/mL (range: 1995–7250 ng/mL) in the SGA, LGA, and AGA fetuses, respectively. The concentrations in the three groups were not statistically significantly different. Although there were wide discrepancies between the mean values of the subgroups, the large confidence intervals in the three groups negatively affected the statistical analysis. However, multiple regression analysis revealed a statistically significant negative correlation between the angiotensinogen levels and gestational age and a statistically significant positive correlation between the birth weight and angiotensinogen levels. Discussion: Our findings suggest that fetal growth abnormalities did not correlate with differences in the amniotic fluid levels of angiotensinogen in early second trimester pregnancies. However, increased angiotensinogen levels were found to be consistent with a smaller gestational age at birth and increased BMI of neonates.

**Keywords:** angiotensinogen; renin–angiotensin system (RAS); amniotic fluid; second trimester of pregnancy; third trimester of pregnancy; small for gestational age (SGA); large for gestational age (LGA); fetal growth; birth weight

## 1. Introduction

The fetal growth centile estimated at 24–42 weeks is based on birth weight and can vary depending on the ethnicity and geographic region of the population under study. The fetal growth curves used today have therefore been created by utilizing normative data from diverse populations and geographic regions. The rate of fetal growth velocity can be estimated through the use of sequential sonographic measurements of specific fetal body parts prior to delivery [1]. Small for gestational age (SGA) infants are neonates whose birth weight is less than the 10th percentile for gestational age [2]. Macrosomia is used to describe a large fetus or newborn, while large for gestational age (LGA) is the term used for fetuses or newborns with a weight above the 90th percentile for gestational age [3]. Appropriate for gestational age (AGA) are fetuses between the 10th and the 90th percentile.

However, not all fetuses classified as SGA or LGA are growth-restricted once maternal ethnicity, parity, maternal body mass index, and/or other parameters have been considered [3]. Notably, approximately 70% of SGA fetuses have normal perinatal outcomes despite their small weight at birth [4]. On the other hand, FGR (fetal growth-restricted) fetuses, that is, those that do not attain their complete growth potential due to pathological fetal or maternal factors, are more frequently correlated with unfavorable perinatal outcomes. The mortality rate of FGR was estimated to be from 1 to 6%, while those with AGA have a lower mortality rate of 0.2% [5,6].

FGR impacts a number of SGA fetuses, affecting approximately 3 to 6% of all deliveries [7,8]. A fairly extensive amount of data point to the possibility that an adverse prenatal environment and impaired fetal growth may result in fetal programming that predisposes the fetus to such conditions as hypertension, diabetes, and cardiovascular disease later in life [9].

Fetuses that experience fetal growth disorders, i.e., either SGA or LGA, have an increased risk of perinatal morbidity and mortality. Meanwhile, severe SGA fetuses (below the 3rd centile) as well as FGR fetuses face the greatest risk of perinatal complications, such as perinatal demise, intraventricular hemorrhage, hypoxic ischemic encephalopathy, sepsis, or bronchopulmonary dysplasia [5]. LGA fetuses have a heightened risk of adverse outcomes during labor, such as shoulder dystocia and/or perinatal brachial plexus palsy [10]. Despite the significant progress that has been achieved in the field of fetal monitoring and high-risk pregnancy management, the precise mechanisms and the underlying cause(s) of impaired fetal growth are yet to be fully elucidated [11,12].

The renin–angiotensin system (RAS), a circulating endocrine system and homeostatic signaling pathway, controls blood pressure and regulates fluid balance. Every element of the RAS is present in the placenta as early as the 6th week of gestation. Regarding the placental expression of these components, they may potentially function separately from the systemic RAS, influencing various functions such as villous and extravillous cytotrophoblast proliferation, extravillous cytotrophoblast migration, invasion, and development of placental blood vessels [13]. Disturbance of the placental RAS and the equilibrium between the vasoactive peptides, which are components of the RAS, may influence placental blood circulation, resulting in an insufficiency of nutrient delivery, thus leading to SGA and FGR [14].

Several published studies have investigated the ability of several biomarkers to detect abnormalities in fetal growth, including angiotensinogen [15,16]. Angiotensinogen, an  $\alpha_2$ -globulin precursor of angiotensin, is a yin hormone produced in the fetal brain, heart, and blood vessels, liver, kidney, adipose tissue, and adrenal glands, which regulates blood pressure via vasoconstriction, one of the main functions of the RAS. The RAS, and particularly angiotensin II, play an important role in blood pressure regulation through the

circulating fluid volume. A number of published studies, though presenting conflicting results, have highlighted the potential role of angiotensinogen in the development and establishment of preeclampsia [17–20], while a limited number of studies have sought to correlate this precursor hormone with fetal growth abnormalities with regard to its expression in the placenta [21,22]. Furthermore, there is no literature on the amniotic levels of angiotensinogen among these pregnancies in any trimester. Of interest, published research shows that polymorphisms in the angiotensinogen gene in both maternal and fetal DNA could be associated with an increased risk of adverse pregnancy outcomes, including preeclampsia and intrauterine FGR [23].

The aim of our prospective observational study is to examine angiotensinogen in the amniotic fluid of early second trimester gestations, to investigate any correlations among groups, and to study its role in fetal growth abnormalities.

## 2. Material and Methods

This observational prospective cohort study included pregnant women who underwent amniocentesis during the early second trimester (17–21 weeks of gestation): the diagnostic test was performed due to such indications as previous history of birth defects, increased nuchal translucency, advanced maternal age, or detection of an anatomical anomaly in the ultrasound examination of the first or second trimester. The exclusion criteria were as follows: pregnancies with chromosomal abnormalities or major abnormalities diagnosed by fetal karyotype, in vitro fertilization pregnancies, and multiple pregnancies. All pregnant women who were diagnosed with hypertensive disorders (pre-existing or gestational) or diabetes (pre-existing or gestational) were excluded from our cohort population. Cases affected by such pathologies are known to be at high risk of fetal growth disturbances and are monitored closely during the pregnancy. Greater scientific lack of knowledge surrounds other groups of unpredictable cases with fetal growth disturbances who may suffer an unexpected unfavorable outcome. For this reason, our investigation focuses on the correlation between angiotensinogen's amniotic fluid levels and fetal growth disturbances in an otherwise healthy pregnant population.

Gestational age was calculated based on the crown–rump length (CRL) measurement at the first trimester ultrasound, between the 11th and 14th week of gestation [24]. Follow-up was carried out until labor. Birth weight was documented at the time of delivery and thus the neonates were characterized as SGA, AGA, and LGA. Birth weight reflects the growth velocity in utero during the third trimester, so the same labeling can be attributed to the fetuses prior to delivery and be given to the amniotic fluid samples obtained in the second trimester. Thus, the samples were also categorized into three groups, namely, SGA, AGA, and LGA, meaning that the SGA samples are derived from the fetuses proved to be SGA as neonates at birth, the AGA samples are derived from the fetuses proved to be AGA as neonates at birth, and the LGA samples are derived from the fetuses proved to be LGA neonates at birth.

It was anticipated that some SGA fetuses would have FGR, while a number of LGA fetuses might exhibit severe macrosomia, which could result in early delivery, whether spontaneous or medically induced [1].

After amniocentesis, the collected samples underwent centrifugation, and the resulting supernatants were subsequently preserved in polypropylene tubes at a temperature of  $-80^{\circ}\text{C}$  until all samples were collected and analyzed. Amniotic fluid angiotensinogen concentrations were measured using the Human Angiotensinogen ELISA Kit (Life Technologies Corporation, Thermo Fisher Scientific Inc., Carlsbad, CA, USA) according to the manufacturer's instructions. This concerns a solid-phase sandwich ELISA, which is designed to detect and quantify angiotensinogen levels in cell culture supernatants, plasma, and serum. The sensitivity of lower calibrators was evaluated, and the minimum detachable dose of human angiotensinogen was observed to be 1.22, based on the manufacturer's product information sheet.

Statistical analysis was conducted using the Statistical Package for Social Sciences (SPSS) version 21 (IBM Corp., Armonk, NY, USA; Released 2021. IBM SPSS Statistics for Windows, Version 21), with the choice between parametric and nonparametric methods being dependent on the specific circumstances or requirements [25]. The distribution of the sample values was evaluated by regression analysis (Kolmogorov–Smirnov test). The results include the presentation of the median and interquartile range for quantitative variables. As per our study design, confounding factors taken into account include maternal age, body mass index, pregnancy duration, fetal sex, and multiparity. We established the threshold for statistical significance at a *p*-value lower than 0.05.

Approval by the Ethical Committee for Research of the Aretaieion University Hospital, Athens, Greece, was obtained with reference number 542-1310202. Moreover, all women participating in this study were informed, and a signed informed consent was obtained.

Table 1 presents the descriptive characteristics of both maternal and fetal aspects. There was no statistically significant difference observed among the three groups in terms of maternal age, maternal weight, and maternal height. However, statistical analysis found a significantly higher percentage of cesarean sections in the SGA group. As expected, statistically significant differences were observed between the groups in terms of gestational age at birth, birth weight, and centile.

**Table 1.** Maternal and fetal characteristics.

	AGA [Mean (Upper and Lower Extreme)]	SGA [Mean (Upper and Lower Extreme)]	LGA [Mean (Upper and Lower Extreme)]	<i>p</i> -Value
<b>Maternal age (years)</b>	37 (28–43)	36 (26–41)	35 (29–43)	0.060
<b>Maternal weight (Kgr)</b>	60 (48–93)	62 (47–100)	59 (49–105)	0.650
<b>Maternal height (cm)</b>	165 (156–174)	167 (150–174)	166 (160–174)	0.070
<b>Gestational age (days)</b>	275 (261–285)	267 (261–283)	274 (268–282)	<b>0.011</b>
<b>Neonatal birth weight (gr)</b>	3290 (2860–3750)	2630 (1750–2860)	3800 (3550–4330)	<b>&lt;0.001</b>
<b>Neonatal sex (female/all)</b>	19/33	3/18	10/19	<b>&lt;0.001</b>

### 3. Results

In this study, we assessed the concentrations of angiotensinogen present in the amniotic fluid of pregnancies undergoing amniocentesis in the early second trimester. In total, the angiotensinogen levels of 70 amniotic fluid samples were measured. Figure 1 represents the angiotensinogen levels for all subgroups.

More specifically, the AGA subgroup's mean angiotensinogen levels were found to be 4670 ng/mL (values from 1995 to 7250 ng/mL). Respectively, the SGA group's mean level was 3885 ng/mL (values from 1625 to 5375 ng/mL), while the LGA group's mean level was 4885 ng/mL (values from 1580 to 8460 ng/mL). Differences among the values of these three groups were not statistically significant ( $p = 0.676$ ). Post-hoc analysis among these three groups did not find any statistically significant difference (Table 2).

Furthermore, we conducted multiple logistic regression analysis on independent parameters such as maternal age, maternal weight and height, gestational age, fetal birth weight, and percentile of birth weight. Table 3 summarizes the results of this multiple regression analysis. The multiple regression analysis revealed that increased angiotensinogen levels were correlated with lower gestational age at birth. Moreover, the same analysis highlighted the fact that the angiotensinogen levels increased in proportion to the fetal birth weight increase.

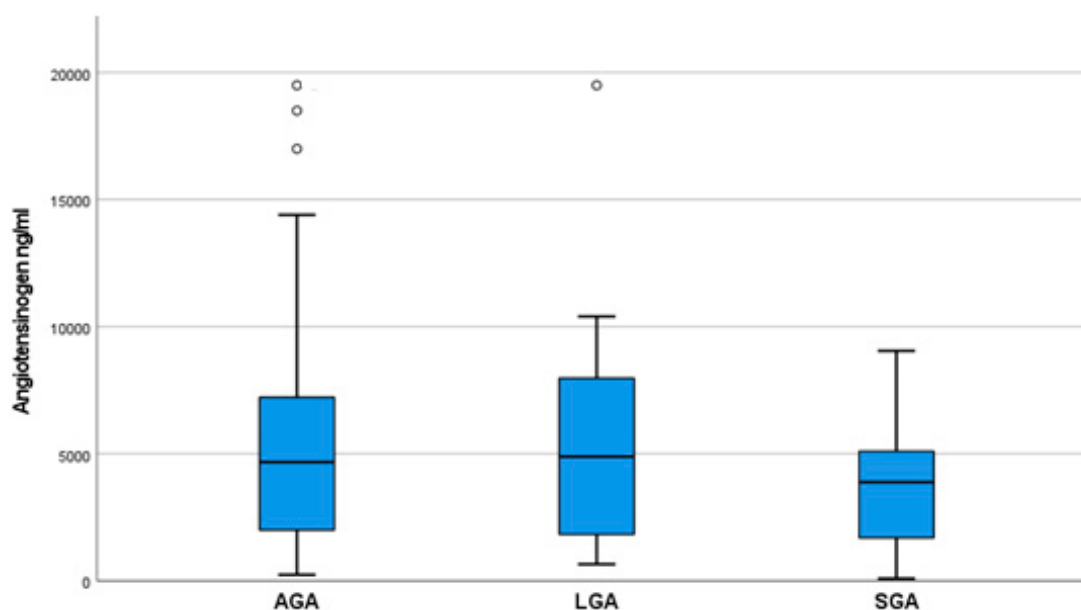


**Figure 1.** Angiotensinogen levels in AGA, LGA, and SGA groups. Box and whisker plots indicate box limits: Q1 and Q3. The dots in the upper part of the figure represent samples that brought back out-of-range increased measurements, located above the standard deviation of the mean value.

**Table 2.** Two-sided test. Each row tests the null hypothesis that the values of two groups are the same. Asymptotic significances (two-sided tests) are displayed. The significance level is 0.050.

Mean Values Compared between Groups	Significance (Two-Sided Test)
SGA-AGA	0.441
LGA-AGA	0.889
SGA-LGA	0.429

**Table 3.** Multiple regression analysis of independent parameters.

	Angiotensinogen	Age	Weight	Gestational Age	Birth Weight	Percentile
Angiotensinogen	1	0.208	0.139	−0.420 *	0.950 **	0.148
Age		1	0.035	0.76	0.148	0.088
Weight			1	−0.152	0.118	0.139
Gestational age				1	−0.157	−0.420 *
Birth weight					1	0.950
Percentile						1

\* Correlation is significant at a level <0.05, \*\* Correlation is significant at a level <0.001.

#### 4. Discussion

Our study included pregnant women who underwent amniocentesis in the first half of the second trimester and were closely monitored until labor. While several amniotic fluid hormones or endocrine disruptors have previously been investigated in order to determine whether there is a possible correlation with fetal growth disturbances [26,27], the primary objective of our study was to determine whether there was potentially any correlation between the levels of angiotensinogen in the amniotic fluid and fetal growth disturbances.

Other authors have suggested the possible role of the placental RAS in the maturation and function of the placenta [28–32]. Although the extent of the RAS component expression has been investigated in placentas affected by FGR, either idiopathic or due to preeclampsia,

there has, to our knowledge, been no investigation of angiotensinogen in the amniotic fluid. This research work is, as far as we know, the first to investigate the possible role of the RAS, and specifically of angiotensinogen, in the amniotic fluid of pregnancies with abnormal growth velocity in pregnancy. Our findings imply that angiotensinogen might play a role in compromising fetal blood circulation in cases of idiopathic SGA and FGR, as is shown below.

Our analysis did not reveal any statistically significant difference between the levels of angiotensinogen in the three subgroups. However, the statistical analysis reveals wide discrepancies in the mean values of angiotensinogen among the SGA, AGA, and LGA subgroups. More specifically, these differences reached a mean value of approximately 1000 ng/mL. Nevertheless, the large confidence intervals that were observed and were used for our statistical analysis resulted in a non-statistically significant difference among these groups, indicating that this hormone cannot be used as an amniotic fluid characteristic biomarker with high diagnostic accuracy. This finding has also been reported in other studies [33,34]. As demonstrated in our study and other previous ones, the larger the width of the confidence interval, the lower the diagnostic accuracy of the substance studied.

Despite the fact that our analysis did not find any statistically significant differences among the three subgroups, multiple regression analysis revealed a significant positive correlation between the levels of amniotic fluid angiotensinogen and birth weight. These highly interesting findings are in accordance with published research studies in adults. More specifically, a study in an African population by Cooper et al. found that the higher the BMI was, the higher the levels of serum angiotensinogen were [35]. A study by Engeli et al. reported that not only were the angiotensinogen levels in obese menopausal women higher than those of women with normal weight, but also that women who achieved a 5% reduction in their weight were observed to have 27% lower serum angiotensinogen levels than they had had previously ( $p < 0.05$ ) [36].

Additionally, our multiple regression analysis revealed a negative correlation between the gestational age and amniotic fluid angiotensinogen levels. Similar results have been shown in the aforementioned study by Cooper et al. More specifically, the researchers revealed a negative correlation of angiotensinogen levels beyond middle age (over 34 years in women and 44 in men) [35]. These results are similar to our findings regarding the correlation between angiotensinogen levels and gestational age, third trimester in utero life, which, in fact, resemble late middle age and late adulthood when angiotensinogen levels drop.

Increased angiotensinogen could comprise one of several biological pathways leading to earlier delivery in cases with reduced growth velocity and may also contribute to advanced birth weight in other cases where the fetal weight is above the 50th centile. Thus, the correlation with the birth weight centile is ultimately minor. This could explain why there is no association between angiotensinogen and fetal growth extremes, which define the SGA and LGA groups.

Several researchers have investigated the role of the RAS in fetal growth. A recently published article investigated the role of the RAS in pregnancies complicated by FGR. The latter study reported a positive correlation between the levels of the m-RNA expression of angiotensinogen and birth weight in AGA fetuses; the authors further report that this correlation was not found in pregnancies with FGR, indicating that a lack of placental angiotensinogen expression could lead to FGR [37]. In our study, the angiotensinogen levels appeared to be lower in the amniotic fluid of SGA pregnancies: it is thus clear that future studies are required to investigate whether the m-RNA expression of the angiotensinogen gene is deficient in low-birth-weight pregnancies.

There is, moreover, evidence in the literature that some polymorphisms in the angiotensinogen gene such as AGT M235T could be associated with fetal growth disturbances, including SGA and FGR [38,39]. Another study found a statistically significant higher prevalence of this gene mutation in idiopathic FGR pregnancies compared to control pregnancies in a cohort population in Utah, USA [40]. Moreover, women carrying this

allele gene were found to have higher levels of serum angiotensinogen even during the postpartum period [41]. In addition, other researchers concluded that fetal AGT M235T polymorphism was associated with low birth weight [42]. Our study did not aim to analyze these hypotheses; however, we anticipate that future research carried out in our cohort or a similar SGA population can investigate their incidence and their correlation with fetal growth disturbances.

The long-term effects of SGA and FGR on adult life have been extensively investigated [11,43–45]. A recently published study has explored the correlation between FGR, including SGA cases and preterm birth, and kidney size and kidney function by measuring several biochemical markers, such as the renin–angiotensin–aldosterone system (RAAS), in adolescents. Although the researchers observed that FGR and preterm birth were associated with smaller total kidney volume, no statistical difference in the biochemical markers of kidney function or RAAS components, including angiotensinogen, was found in this study, which is in accordance with our own angiotensinogen findings [46]. Moreover, these findings were consistent with the previous results of research into fetal growth-restricted sheep wherein the researchers reported significant reductions in the sheep’s kidney weight but no evidence of alteration in the renal RAS components [47]. All the above data revealed that fetal growth disturbances had no impact on the renal angiotensinogen levels in adolescents or adults who had experienced fetal growth disturbances at birth.

It should be pointed out that collecting amniotic fluid is a particularly challenging procedure given the considerable difficulty of dealing with this biological material and assembling the needed number of cases. Therefore, one limitation of the current study is the small number of included cases, which consequently leads to a small sample size within the study subgroups. As far as we know, this is the first examination of amniotic fluid angiotensinogen levels during the second trimester. Previous researchers have investigated only the presence of the angiotensinogen gene or its expression in the placenta of FGR fetuses. This emphasizes the necessity for more extensive studies on amniotic fluid so as to clarify potential links between fetal growth irregularities and the different expression and mode of action of the RAS. It is hypothesized that many other factors influence the renin–angiotensin system and its numerous interactions in human and fetal physiology. Hence, it is hoped that our study may trigger further investigation in this direction.

## 5. Conclusions

This is the first study, to our knowledge, to investigate the presence of and possible correlation between angiotensinogen and fetal growth disorders in the amniotic fluid of early second trimester pregnancies. Our findings did not reveal any correlation between the levels of angiotensinogen in the amniotic fluid and, thus, in fetal growth disturbances. However, there were large discrepancies between the mean values of angiotensinogen in the three subgroups, a highly interesting finding that can be employed as the basis for further research. The mean value of SGA differs greatly from the AGA and LGA values. Moreover, multiple regression analysis identified a statistically significant correlation between the amniotic fluid angiotensinogen levels, gestational age, and birth weight. There are strong indications that angiotensinogen could constitute one of several biological pathways leading to earlier delivery in some cases and may also contribute to advanced birth weight in other cases. These correlations highlight a possible dual role of an RAS component in fetal growth velocity.

**Author Contributions:** Conceptualization, D.V., G.M. and N.A.; methodology, D.V., G.M., N.A., P.A., A.M. and V.P.; validation, G.V., A.M. and C.K.-G.; formal analysis, N.V., P.A. and V.P.; investigation, V.P., S.S., N.M., C.I. and P.D.; research, V.P., P.A., C.I., P.D. and C.K.-G.; data curation, N.V., G.M., N.M. and N.A.; writing of original draft, D.V., A.F., N.V., G.M., V.P. and N.A.; writing of review and editing, D.V., A.F., N.V., G.M. and N.A. All authors have read and agreed to the published version of the manuscript.



**Funding:** This research received no external funding.

**Institutional Review Board Statement:** The study was conducted in accordance with the Declaration of Helsinki, and approved by the Ethical Committee for Research of Aretaieion University Hospital (542-1310202) for studies involving humans.

**Informed Consent Statement:** Informed consent was obtained from all subjects involved in this study.

**Data Availability Statement:** The data presented in this study are available on request from the corresponding author.

**Conflicts of Interest:** The authors declare no conflicts of interest.

## References

- Salomon, L.J.; Alfievic, Z.; Da Silva Costa, F.; Deter, R.L.; Figueras, F.; Ghi, T.; Glanc, P.; Khalil, A.; Lee, W.; Napolitano, R.; et al. ISUOG Practice Guidelines: Ultrasound assessment of fetal biometry and growth. *Ultrasound Obs. Gynecol.* **2019**, *53*, 715–723. [CrossRef] [PubMed]
- Vrachnis, N.; Botsis, D.; Iliodromiti, Z. The fetus that is small for gestational age. *Ann. N. Y. Acad. Sci.* **2006**, *1092*, 304–309. [CrossRef] [PubMed]
- Gordijn, S.J.; Beune, I.M.; Thilaganathan, B.; Papageorgiou, A.; Baschat, A.A.; Baker, P.N.; Silver, R.M.; Wynia, K.; Ganzevoort, W. Consensus definition of fetal growth restriction: A Delphi procedure. *Ultrasound Obstet. Gynecol.* **2016**, *48*, 333–339. [CrossRef]
- Unterscheider, J.; O'Donoghue, K.; Malone, F.D. Guidelines on fetal growth restriction: A comparison of recent national publications. *Am. J. Perinatol.* **2015**, *32*, 307–316. [CrossRef] [PubMed]
- Powel, J.E.; Zantow, E.W.; Bialko, M.F.; Farley, L.G.; Lawlor, M.L.; Mullan, S.J.; Vricella, L.K.; Tomlinson, T.M. Predictive index for adverse perinatal outcome in pregnancies complicated by fetal growth restriction. *Ultrasound Obstet. Gynecol.* **2023**, *61*, 367–376. [CrossRef] [PubMed]
- Unterscheider, J.; Daly, S.; Geary, M.P.; Kennelly, M.M.; McAuliffe, F.M.; O'Donoghue, K.; Hunter, A.; Morrison, J.J.; Burke, G.; Dicker, P.; et al. Definition and management of fetal growth restriction: A survey of contemporary attitudes. *Eur. J. Obstet. Gynecol. Reprod. Biol.* **2014**, *174*, 41–45. [CrossRef] [PubMed]
- Miller, S.L.; Huppi, P.S.; Mallard, C. The consequences of fetal growth restriction on brain structure and neurodevelopmental outcome. *J. Physiol.* **2016**, *594*, 807–823. [CrossRef] [PubMed]
- Figueras, F.; Gratacós, E. Update on the diagnosis and classification of fetal growth restriction and proposal of a stage-based management protocol. *Fetal Diagn. Ther.* **2014**, *36*, 86–98. [CrossRef]
- Burton, G.J.; Fowden, A.L.; Thornburg, K.L. Placental Origins of Chronic Disease. *Physiol. Rev.* **2016**, *96*, 1509–1565. [CrossRef] [PubMed]
- Pergialiotis, V.; Bellos, I.; Fanaki, M.; Vrachnis, N.; Doumouchtsis, S.K. Risk factors for severe perineal trauma during childbirth: An updated meta-analysis. *Eur. J. Obstet. Gynecol. Reprod. Biol.* **2020**, *247*, 94–100. [CrossRef]
- Nardozza, L.M.; Caetano, A.C.; Zamarian, A.C.; Mazzola, J.B.; Silva, C.P.; Marçal, V.M.; Lobo, T.F.; Peixoto, A.B.; Araujo Júnior, E. Fetal growth restriction: Current knowledge. *Arch. Gynecol. Obstet.* **2017**, *295*, 1061–1077. [CrossRef] [PubMed]
- Botsis, D.; Vrachnis, N.; Christodoulakos, G. Doppler assessment of the intrauterine growth-restricted fetus. *Ann. N. Y. Acad. Sci.* **2006**, *1092*, 297–303. [CrossRef] [PubMed]
- Pringle, K.G.; Tadros, M.A.; Callister, R.J.; Lumbers, E.R. The expression and localization of the human placental prorenin/renin-angiotensin system throughout pregnancy: Roles in trophoblast invasion and angiogenesis? *Placenta* **2011**, *32*, 956–962. [CrossRef] [PubMed]
- Shibata, E.; Powers, R.W.; Rajakumar, A.; von Versen-Höynck, F.; Gallaher, M.J.; Lykins, D.L.; Roberts, J.M.; Hubel, C.A. Angiotensin II decreases system A amino acid transporter activity in human placental villous fragments through AT1 receptor activation. *Am. J. Physiol. Endocrinol. Metab.* **2006**, *291*, E1009–E1016. [CrossRef] [PubMed]
- Vrachnis, N.; Loukas, N.; Vrachnis, D.; Antonakopoulos, N.; Christodoulaki, C.; Tsonis, O.; George, M.; Iliodromiti, Z. Phthalates and fetal growth velocity: Tracking down the suspected links. *J. Matern. Fetal Neonatal Med.* **2021**, *35*, 4985–4993. [CrossRef]
- Loukas, N.; Vrachnis, D.; Antonakopoulos, N.; Pergialiotis, V.; Mina, A.; Papoutsis, I.; Iavazzo, C.; Fotiou, A.; Stavros, S.; Valsamakis, G.; et al. Prenatal Exposure to Bisphenol A: Is There an Association between Bisphenol A in Second Trimester Amniotic Fluid and Fetal Growth? *Medicina* **2023**, *59*, 882. [CrossRef]
- Valias, G.R.; Gomes, P.R.L.; Amaral, F.G.; Alnuaimi, S.; Monteiro, D.; O'Sullivan, S.; Zangaro, R.; Cipolla-Neto, J.; Acuna, J.; Baltatu, O.C.; et al. Urinary Angiotensinogen-Melatonin Ratio in Gestational Diabetes and Preeclampsia. *Front. Mol. Biosci.* **2022**, *9*, 800638. [CrossRef]
- Colón, N.S.; Pantho, A.F.; Afroze, S.H.; Ashraf, A.; Akter, R.; Kuehl, T.J.; Uddin, M.N. Reduced urinary angiotensinogen excretion in preeclampsia. *Pregnancy Hypertens.* **2022**, *27*, 1–5. [CrossRef]
- Yilmaz, Z.; Yildirim, T.; Yilmaz, R.; Aybal-Kutlugun, A.; Altun, B.; Kucukozkan, T.; Erdem, Y. Association between urinary angiotensinogen, hypertension and proteinuria in pregnant women with preeclampsia. *J. Renin Angiotensin Aldosterone Syst.* **2015**, *16*, 514–520. [CrossRef]

20. Tamanna, S.; Morosin, S.K.; Delforce, S.J.; van Helden, D.F.; Lumbers, E.R.; Pringle, K.G. Renin-angiotensin system (RAS) enzymes and placental trophoblast syncytialisation. *Mol. Cell. Endocrinol.* **2022**, *547*, 111609. [CrossRef]
21. Narita, T.; Ichihara, A.; Matsuoka, K.; Takai, Y.; Bokuda, K.; Morimoto, S.; Itoh, H.; Seki, H. Placental (pro)renin receptor expression and plasma soluble (pro)renin receptor levels in preeclampsia. *Placenta* **2016**, *37*, 72–78. [CrossRef] [PubMed]
22. Itakura, A.; Mizutani, S. Involvement of placental peptidases associated with renin-angiotensin systems in preeclampsia. *Biochim. Biophys. Acta* **2005**, *1751*, 68–72. [CrossRef]
23. He, D.; Peng, X.; Xie, H.; Peng, R.; Li, Q.; Guo, Y.; Wang, W.; He, H.; Chen, Y. Genetic Variations in Angiotensinogen Gene and Risk of Preeclampsia: A Pilot Study. *J. Clin. Med.* **2023**, *12*, 1509. [CrossRef] [PubMed]
24. Salomon, L.J.; Alfirevic, Z.; Bilardo, C.M.; Chalouhi, G.E.; Ghi, T.; Kagan, K.O.; Lau, T.K.; Papageorgiou, A.T.; Raine-Fenning, N.J.; Stirnemann, J.; et al. ISUOG practice guidelines: Performance of first-trimester fetal ultrasound scan. *Ultrasound Obstet. Gynecol.* **2013**, *41*, 102–113. [CrossRef]
25. IBM Corp. Released 2012. *IBM SPSS Statistics for Windows*; Version 21.0; IBM Corp.: Armonk, NY, USA, 2012.
26. Vrachnis, D.; Antonakopoulos, N.; Fotiou, A.; Pergialiotis, V.; Loukas, N.; Valsamakis, G.; Iavazzo, C.; Stavros, S.; Maroudias, G.; Panagopoulos, P.; et al. Is There a Correlation between Apelin and Insulin Concentrations in Early Second Trimester Amniotic Fluid with Fetal Growth Disorders? *J. Clin. Med.* **2023**, *12*, 3166. [CrossRef] [PubMed]
27. Vrachnis, N.; Zygouris, D.; Vrachnis, D.; Antonakopoulos, N.; Fotiou, A.; Panagopoulos, P.; Kolialexi, A.; Pappa, K.; Mastorakos, G.; Iliodromiti, Z. Effects of Hormone Therapy and Flavonoids Capable on Reversal of Menopausal Immune Senescence. *Nutrients* **2021**, *13*, 2363. [CrossRef] [PubMed]
28. Anton, L.; Merrill, D.C.; Neves, L.A.; Gruver, C.; Moorefield, C.; Brosnihan, K.B. Angiotensin II and angiotensin-(1-7) decrease sFlt1 release in normal but not preeclamptic chorionic villi: An in vitro study. *Reprod. Biol. Endocrinol.* **2010**, *8*, 135. [CrossRef]
29. Anton, L.; Brosnihan, K.B. Systemic and uteroplacental renin-angiotensin system in normal and pre-eclamptic pregnancies. *Ther. Adv. Cardiovasc. Dis.* **2008**, *2*, 349–362. [CrossRef]
30. Wu, W.B.; Xu, Y.Y.; Cheng, W.W.; Yuan, B.; Zhao, J.R.; Wang, Y.L.; Zhang, H.J. Decreased PGF may contribute to trophoblast dysfunction in fetal growth restriction. *Reproduction* **2017**, *154*, 319–329. [CrossRef] [PubMed]
31. Lumbers, E.R.; Delforce, S.J.; Arthurs, A.L.; Pringle, K.G. Causes and Consequences of the Dysregulated Maternal Renin-Angiotensin System in Preeclampsia. *Front. Endocrinol.* **2019**, *10*, 563. [CrossRef] [PubMed]
32. Wang, Y.; Lumbers, E.R.; Arthurs, A.L.; Corbisier de Meaultsart, C.; Mathe, A.; Avery-Kiejda, K.A.; Roberts, C.T.; Pipkin, F.B.; Marques, F.Z.; Morris, B.J.; et al. Regulation of the human placental (pro)renin receptor-prorenin-angiotensin system by microRNAs. *Mol. Hum. Reprod.* **2018**, *24*, 453–464. [CrossRef]
33. Thombs, B.D.; Rice, D.B. Sample sizes and precision of estimates of sensitivity and specificity from primary studies on the diagnostic accuracy of depression screening tools: A survey of recently published studies. *Int. J. Methods Psychiatr. Res.* **2016**, *25*, 145–152. [CrossRef]
34. Rutjes, A.W.; Reitsma, J.B.; Di Nisio, M.; Smidt, N.; van Rijn, J.C.; Bossuyt, P.M. Evidence of bias and variation in diagnostic accuracy studies. *CMAJ* **2006**, *174*, 469–476. [CrossRef]
35. Cooper, R.; Forrester, T.; Ogunbiyi, O.; Muffinda, J. Angiotensinogen levels and obesity in four black populations. ICSHIB Investigators. *J. Hypertens.* **1998**, *16*, 571–575. [CrossRef] [PubMed]
36. Engeli, S.; Böhnke, J.; Gorzelniak, K.; Janke, J.; Schling, P.; Bader, M.; Luft, F.C.; Sharma, A.M. Weight loss and the renin-angiotensin-aldosterone system. *Hypertension* **2005**, *45*, 356–362. [CrossRef] [PubMed]
37. Delforce, S.J.; Lumbers, E.R.; Ellery, S.J.; Murthi, P.; Pringle, K.G. Dysregulation of the placental renin-angiotensin system in human fetal growth restriction. *Reproduction* **2019**, *158*, 237–245. [CrossRef]
38. Pfab, T.; Stirnberg, B.; Sohn, A.; Krause, K.; Slowinski, T.; Godes, M.; Guthmann, F.; Wauer, R.; Halle, H.; Hoher, B. Impact of maternal angiotensinogen M235T polymorphism and angiotensin-converting enzyme insertion/deletion polymorphism on blood pressure, protein excretion and fetal outcome in pregnancy. *J. Hypertens.* **2007**, *25*, 1255–1261. [CrossRef] [PubMed]
39. Kim, Y.J.; Park, M.H.; Park, H.S.; Lee, K.S.; Ha, E.H.; Pang, M.G. Associations of polymorphisms of the angiotensinogen M235 polymorphism and angiotensin-converting-enzyme intron 16 insertion/deletion polymorphism with preeclampsia in Korean women. *Eur. J. Obstet. Gynecol. Reprod. Biol.* **2004**, *116*, 48–53. [CrossRef]
40. Zhang, X.Q.; Varner, M.; Dizon-Townson, D.; Song, F.; Ward, K. A molecular variant of angiotensinogen is associated with idiopathic intrauterine growth restriction. *Obstet. Gynecol.* **2003**, *101*, 237–242. [CrossRef]
41. Rotimi, C.; Cooper, R.; Ogunbiyi, O.; Morrison, L.; Ladipo, M.; Tewksbury, D.; Ward, R. Hypertension, serum angiotensinogen, and molecular variants of the angiotensinogen gene among Nigerians. *Circulation* **1997**, *95*, 2348–2350. [CrossRef]
42. Schlemm, L.; Haumann, H.M.; Ziegner, M.; Stirnberg, B.; Sohn, A.; Alter, M.; Pfab, T.; Kalache, K.D.; Guthmann, F.; Hoher, B. New evidence for the fetal insulin hypothesis: Fetal angiotensinogen M235T polymorphism is associated with birth weight and elevated fetal total glycated hemoglobin at birth. *J. Hypertens.* **2010**, *28*, 732–739. [CrossRef] [PubMed]
43. Melamed, N.; Baschat, A.; Yinon, Y.; Athanasiadis, A.; Mecacci, F.; Figueras, F.; Berghella, V.; Nazareth, A.; Tahlak, M.; McIntyre, H.D.; et al. FIGO (international Federation of Gynecology and obstetrics) initiative on fetal growth: Best practice advice for screening, diagnosis, and management of fetal growth restriction. *Int. J. Gynaecol. Obstet.* **2021**, *152* (Suppl. S1), 3–57. [CrossRef] [PubMed]
44. Iyengar, A.; Bonilla-Félix, M. Effects of Prematurity and Growth Restriction on Adult Blood Pressure and Kidney Volume. *Adv. Chronic Kidney Dis.* **2022**, *29*, 243–250. [CrossRef] [PubMed]

45. Sulyok, E.; Farkas, B.; Bodis, J. Pathomechanisms of Prenatally Programmed Adult Diseases. *Antioxidants* **2023**, *12*, 1354. [CrossRef]
46. Liefke, J.; Heijl, C.; Steding-Ehrenborg, K.; Morsing, E.; Arheden, H.; Ley, D.; Hedström, E. Fetal growth restriction followed by very preterm birth is associated with smaller kidneys but preserved kidney function in adolescence. *Pediatr. Nephrol.* **2023**, *38*, 1855–1866. [CrossRef] [PubMed]
47. Zohdi, V.; Moritz, K.M.; Bubb, K.J.; Cock, M.L.; Wreford, N.; Harding, R.; Black, M.J. Nephrogenesis and the renal renin-angiotensin system in fetal sheep: Effects of intrauterine growth restriction during late gestation. *Am. J. Physiol. Regul. Integr. Comp. Physiol.* **2007**, *293*, R1267–R1273. [CrossRef]

**Disclaimer/Publisher’s Note:** The statements, opinions and data contained in all publications are solely those of the individual author(s) and contributor(s) and not of MDPI and/or the editor(s). MDPI and/or the editor(s) disclaim responsibility for any injury to people or property resulting from any ideas, methods, instructions or products referred to in the content.

Review

# Artificial Intelligence in Obstetric Anomaly Scan: Heart and Brain

Iuliana-Alina Enache <sup>1,2</sup>, Cătălina Iovoaița-Rădescu <sup>1,2</sup>, Ștefan Gabriel Ciobanu <sup>1,2,\*</sup>,  
Elena Iuliana Anamaria Berbecaru <sup>1,2</sup>, Andreea Vochin <sup>2</sup>, Ionuț Daniel Băluță <sup>2</sup>, Anca Maria Istrate-Ofițeru <sup>2,3,4</sup>,  
Cristina Maria Comănescu <sup>2,3,5</sup>, Rodica Daniela Nagy <sup>2,3</sup> and Dominic Gabriel Iliescu <sup>2,3,6</sup>

- <sup>1</sup> Doctoral School, University of Medicine and Pharmacy of Craiova, 200349 Craiova, Romania; alinadica34@gmail.com (I.-A.E.); catalina.ramescu@yahoo.com (C.I.-R.); iuliaberbecaru@gmail.com (E.I.A.B.)
- <sup>2</sup> Department of Obstetrics and Gynecology, University Emergency County Hospital, 200642 Craiova, Romania; dea\_andreea05@yahoo.com (A.V.); ionutdanielbaluta@gmail.com (I.D.B.); ancaofiteru92@yahoo.com (A.M.I.-O.); cristinacomanescu85@gmail.com (C.M.C.); rodica.nagy25@gmail.com (R.D.N.); dominic.iliescu@yahoo.com (D.G.I.)
- <sup>3</sup> Ginecho Clinic, Medgin SRL, 200333 Craiova, Romania
- <sup>4</sup> Research Centre for Microscopic Morphology and Immunology, University of Medicine and Pharmacy of Craiova, 200642 Craiova, Romania
- <sup>5</sup> Department of Anatomy, University of Medicine and Pharmacy of Craiova, 200349 Craiova, Romania
- <sup>6</sup> Department of Obstetrics and Gynecology, University of Medicine and Pharmacy of Craiova, 200349 Craiova, Romania
- \* Correspondence: ciobanustefangabriel1@gmail.com; Tel.: +40-0769019727

**Abstract:** Background: The ultrasound scan represents the first tool that obstetricians use in fetal evaluation, but sometimes, it can be limited by mobility or fetal position, excessive thickness of the maternal abdominal wall, or the presence of post-surgical scars on the maternal abdominal wall. Artificial intelligence (AI) has already been effectively used to measure biometric parameters, automatically recognize standard planes of fetal ultrasound evaluation, and for disease diagnosis, which helps conventional imaging methods. The usage of information, ultrasound scan images, and a machine learning program create an algorithm capable of assisting healthcare providers by reducing the workload, reducing the duration of the examination, and increasing the correct diagnosis capability. The recent remarkable expansion in the use of electronic medical records and diagnostic imaging coincides with the enormous success of machine learning algorithms in image identification tasks. Objectives: We aim to review the most relevant studies based on deep learning in ultrasound anomaly scan evaluation of the most complex fetal systems (heart and brain), which enclose the most frequent anomalies.

**Keywords:** deep learning; artificial intelligence; pregnancy; ultrasound; anomaly scan; fetal heart; fetal brain

## 1. Introduction

Congenital fetal anomalies, which cause a high infant mortality rate worldwide, are identified as fetal structural abnormalities at standard morphology ultrasound scans, which involve standard planes of visible organs or body parts [1]. A fetal structural anomaly can be identified on the ultrasound in about 3% of pregnancies, which can range from a minor defect to severe multisystem anomalies [2]. Congenital heart disorders (CHDs) are increasingly diagnosed during pregnancy in developed countries. Prenatal diagnosis of CHDs is helpful in cases with severe abnormalities, such as hypoplastic left heart syndrome, transposition of the great arteries, and total anomalous pulmonary venous. Knowing the diagnosis during pregnancy improves treatment outcomes, quickening postpartum intervention and preserving the long-term neurodevelopment of the newborn [3]. The frequency of fetal central nervous system (CNS) abnormalities is second to cardiac malformations. A precise

prenatal diagnosis with ultrasound is crucial for the right postpartum therapy for fetal CNS disorders, which significantly cause in utero mortality and postnatal morbidity [4].

Early fetal ultrasound is now a well-recognized technique for detecting fetal abnormalities and monitoring the evolution or development of intrauterine congenital diseases [5]. However, the Eurofetus study [6] that involved 61 obstetrical ultrasound units from 14 European countries showed that only 55% of significant anomalies were identified before 24 weeks of gestation.

The fundamentals of artificial intelligence (AI) as a discipline were established in the 1950s, under the hypothesis formulated by John McCarthy as “Every aspect of learning or any other feature of intelligence can in principle be so precisely described that a machine can be made to simulate it” [7]. Deep learning (DL) is a part of a more prominent family of machine learning techniques built on artificial neural networks (ANNs). The levels of supervision can vary from unsupervised, semi-supervised, and supervised, all being possible [8].

Although medical errors are the third most significant cause of death in the United States [9], AI can reduce this number by improving interpretation accuracy and reducing workload, which can cause critical details to be overlooked. The information processing and distributed communication nodes in biological systems inspired ANNs [10,11]. ANNs and biological structures like the fetal brain differ in many ways. Mainly, ANNs frequently exhibit static and symbolic behavior, whereas fetal organs exhibit dynamic (plastic) and analog behavior.

Rapid advancements in DL algorithms have made them a powerful tool for examining medical images. Numerous types of deep neural networks effectively handle medical picture segmentation [12]. AI in medical science involves classification, localization, detection, segmentation, and registration of medical images. Convolutional neural networks (CNNs) represent one of the main three types of deep learning algorithms, with remarkable progress in image recognition [13].

AI-assisted obstetric ultrasound may automatically identify particular fetal structures based on the gestational age of the pregnancy [14]. Also, AI-based automatic measures and evaluations have been implemented in the last decades to decrease intra- and inter-observer measurement variability and to increase diagnosis accuracy [15]. Moreover, AI progress in recent years enabled the development of AI-based techniques to detect fetal anomalies. We need to remember that AI is based on mathematical algorithms, and the accuracy of the information provided depends not only on the algorithm but also on the quality and quantity of the data [16].

Our review aims to highlight the performance of AI detection of normal and abnormal aspects of the most prevalent congenital malformations concerning fetal cardiovascular and central nervous systems.

## 2. Method

We conducted a search on PubMed, Elsevier, and Scopus using the keywords “deep learning”, “pregnancy”, “Artificial intelligence”, “anomaly scan”, “fetal heart”, “fetal brain”, and “ultrasound”, yielding 265 results from 2015 to 2023. Eligible studies for inclusion had to be in English and focus on discussing the utilization of artificial intelligence in ultrasound and fetal scanning. Two evaluators independently reviewed each study based on the title, abstract, and full text. Studies meeting the selection criteria were included. Each included study underwent assessment and was categorized as 0 = not relevant, 1 = possibly relevant, and 2 = very relevant. Only publications scoring at least 1 point were incorporated into our study. Any discrepancies were deliberated and resolved by a third researcher. Specific exclusion criteria were applied to identify the most pertinent studies. These criteria included excluding studies conducted in languages other than English, those not utilizing artificial intelligence, articles lacking fully available texts, and studies examining systems unrelated to the heart and brain or other medical fields outside of obstetrics and gynecology.

After applying the exclusion criteria, we identified 20 relevant articles specifically about the fetal heart and brain along the skull, as shown in Figure 1.

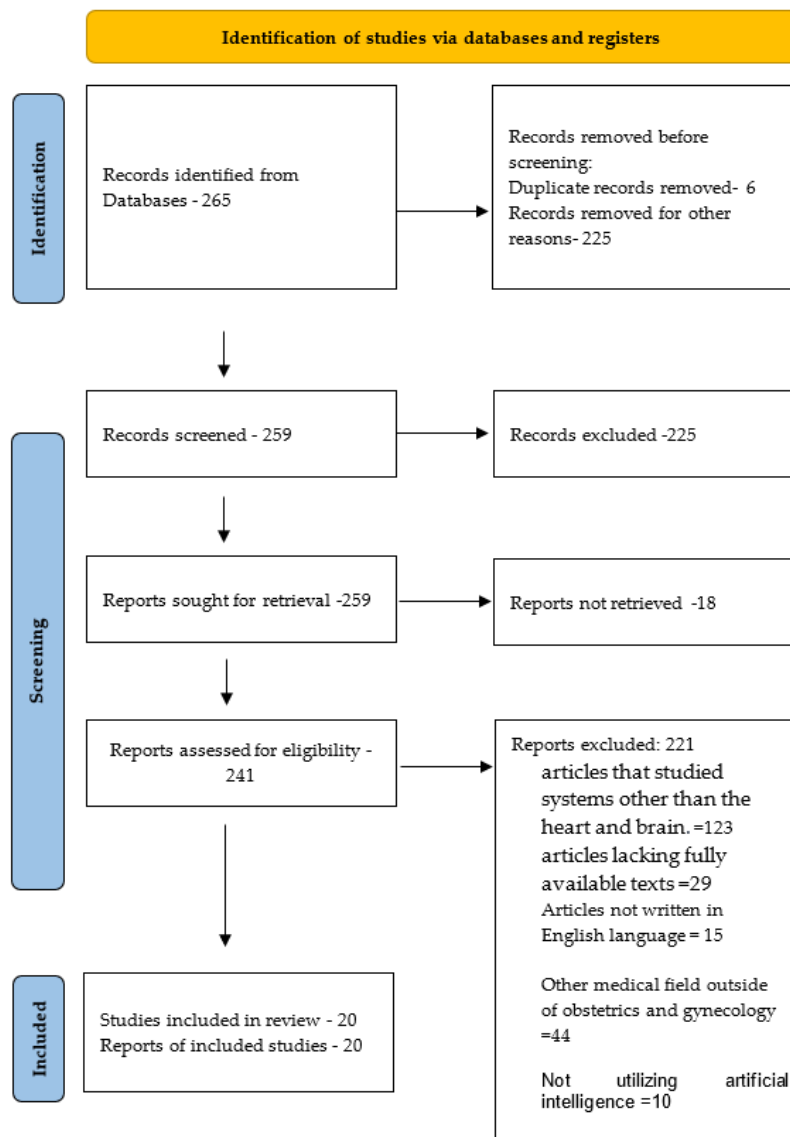


**Figure 1.** Flow diagram of the method for study selection.

Out of the 20 selected articles, 6 addressed the central nervous system, 7 studied the heart, 3 examined the fetal heart rhythm, 2 focused on fetal biometry, and 2 studied nuchal translucency. The working methods are illustrated in Figure 2.

In Figure 2, CNN—convolutional neural network; DL—deep learning; SONO—supervised object detection with normal data Only, AUC—area under the receiver operating characteristic curve; CAD—computer-aided detection; U-NET—network’s U-shaped architecture; VGG-Net—visual geometry group network; PAICS—prenatal ultrasound diagnosis artificial intelligence conduct system; SFTA—segmentation-based fractal texture analysis; MLA-ANFIS—multi-layer architecture of a sub-adaptive neuro-fuzzy inference system; for SVM—support vector machine; MLP—multilayer perceptron; FUVAI—spatio-temporal fetal US video analysis; MFP-Unet—multi-feature pyramid Unet network; MAPSE—mitral valve annular planes systolic excursion; TAPSE—tricuspid valve annular planes systolic excursion; DSC—Dice similarity coefficient; VS—volume similarity; HD95—Hausdorff95 distance; HD—head circumference; BPD—biparietal diameter; AC—abdomen circumference; FL—femur length; HD—Hausdorff coefficient; APD—average perpendicular distance.

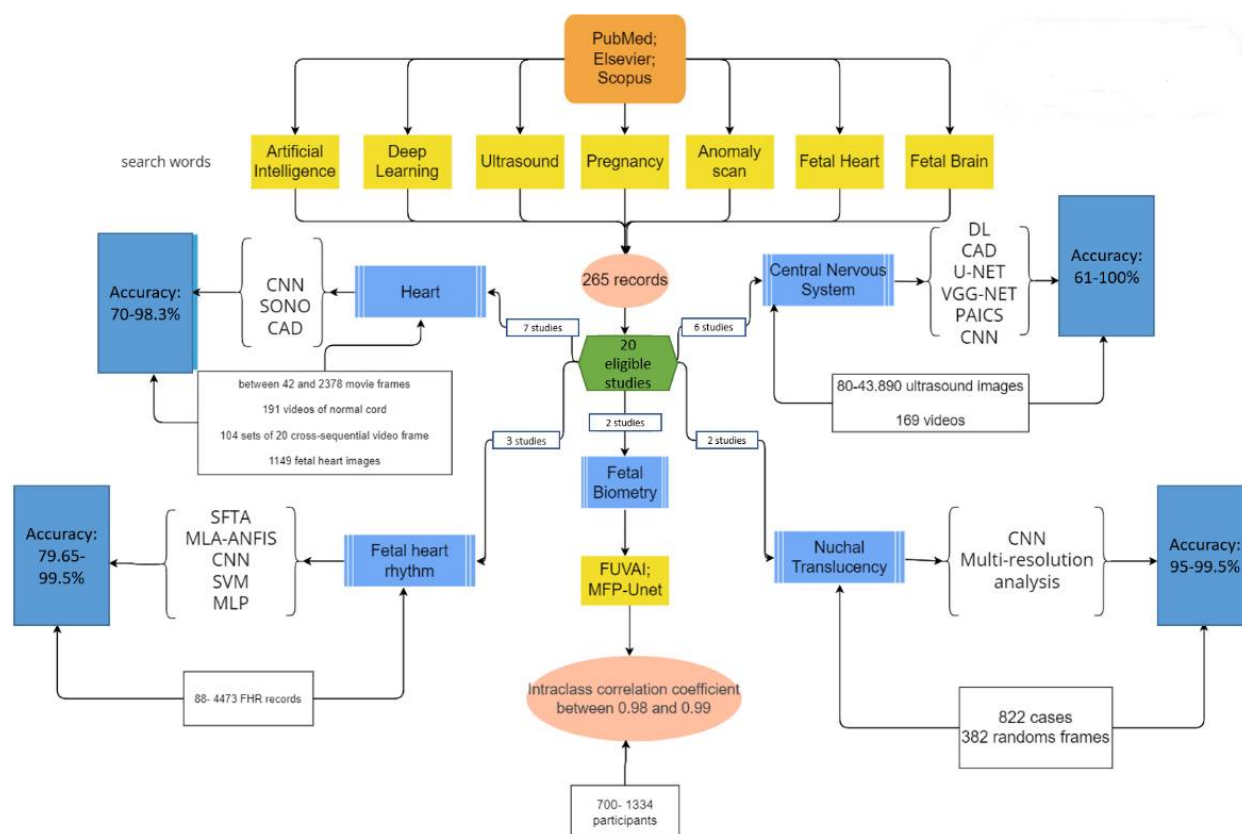


**Figure 2.** A diagram illustrating the working methods.

### 3. Results

#### 3.1. Heart

The fetal heart is a complex organ to analyze and follow because of its nature, continuous movement, and small size. As stated before, congenital heart diseases are the most common [17] fetal malformations. During the first or second trimester scan, sonographers perform an ultrasound anomaly scan as a tool for prenatal diagnosis regarding fetal malformations. Still, the reported detection rates for congenital heart disease remain low [18]. Due to these challenges, a novel concept that seeks to integrate AI into ultrasound (US) fetal evaluations to improve the detection rates and overall fetal heart evaluation accuracy has emerged, as shown in Figure 3.

Pregnant women are advised to undergo fetal screening in the second trimester of pregnancy. The fetal heart scan involves examining five standard recommended planes during the cardiac sweep, which enables physicians to diagnose up to 90% of complex congenital heart defects [19].

In a study conducted by Arnaout et al., echocardiographic and second-trimester screening images of fetuses with gestational age between 18 and 24 weeks were analyzed with the help of a variety of neuronal networks, and the authors found that it was possible to distinguish between normal heart development and the presence of inborn cardiac anomalies. The obtained results indicate predictive performances similar to those made by clinical experts, namely, a sensitivity of 95% (95% confidence interval, 84–99%), specificity of 96% (95% confidence interval, 95–97%), and a predictive negative value of 100% [20].

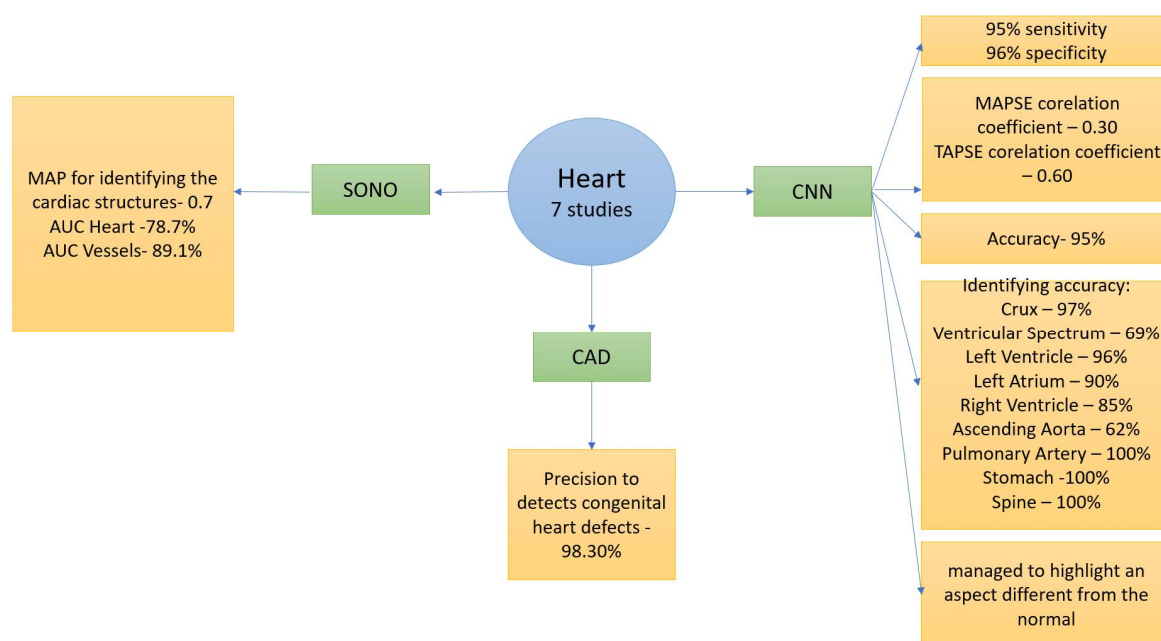


**Figure 3.** AI studies regarding fetal heart structures.

To identify the five screening cardiac plans from fetal ultrasound scans, including three-vessel trachea (3VT), three-vessel view (3VV), left-ventricular outflow tract (LVOT), axial four-chamber (A4C), and abdomen (ABDO) [21], Arnaout et al. [20] used CNNs to categorize the images. Their results showed that the model's sensitivity is comparable to the physician's and succeeds at external datasets and lower-quality images. All the images that did not fit the criteria were categorized as non-target images (for example, head, foot, placenta).

Philip M et al. [22] demonstrated the efficacy of CNNs in the detection and measurement of mitral and tricuspid valve annular planes systolic excursion (MAPSE/TAPSE) for the evaluation of cardiac function with the usage of two separate networks based on the same method, one for mitral valve segmentation and the other for tricuspid valve segmentation. Bland–Altman diagrams were used to analyze differences between measurements made by two experts and the automated method. The TAPSE automatic measurement obtained a correlation coefficient of  $r = 0.61$ , while the expert coefficient was  $r = 0.89$ . The root mean squared error (RMSE) between the automated and reference measurement systems was 0.14. The R-value for the automated MAPSE measurement was 0.30, for the expert measurement was 0.77, and for the RMSE was 0.18. It was observed that the correlation coefficient, both for the expert and the proposed method for MAPSE, was lower than that of TAPSE. This was due to the rotation movement of MA, which is caused by the circular orientation of the muscle fibers in the left ventricle, which makes MAPSE measurement more challenging than TAPSE measurement [22].

Matsuoka et al. [23] used 2378 movie frames from 51 fetal cardiac screening scans with normal anatomy at 18–20 weeks as the training dataset and 701 movie frames from 28 routine fetal cardiac screening scans as test data. The authors aimed to develop AI to identify the normal position of the heart and aspect of the cardiovascular structures as follows: crux, ventricular septum, right atrium, tricuspid valve, right ventricle, left atrium, mitral valve, left ventricle, pulmonary artery, ascending aorta, superior vena cava, descending aorta, stomach spine, umbilical vein, inferior vena cava, pulmonary vein, ductus arteriosus. The accuracy with which AI managed to identify the heart structures was 97.1% for the crux, 69.3% for the ventricular septum, 96.6% for the left ventricle, 90.6% for the left atrium, 84.8% for the right ventricle, 96.9% for right atrium, 61.9% for the ascending aorta; and 100% for the pulmonary artery, stomach, and spine [23].



Komatsu R et al. [24] used 42 movie frames of a normal heart as a training database from second-trimester scans and identified 18 different plans of the heart and peripheral organs, such as the atrium, ventricle, blood vessels, and stomach. Movie frames with pathologies were introduced in the study, such as Tetralogy of Fallot (TOF) and transposition of great arteries (TGA). The pulmonary artery was not clearly demonstrated in the case of TOF, and the outflow tract and blood vessel detection patterns in TGA were inconsistent compared with a normal fetus. The program failed to highlight the pathology but successfully highlighted the aspects different from normal anatomy, according to the receiver operating characteristic (ROC) curves [24].

In a similar study, Komatsu M et al. [25] proposed a novel architecture of supervised object detection with normal data only (SONO) to detect fetal heart structures and cardiac abnormalities. The correct position of 18 fetal structures was annotated. For this program, 191 videos were used for training, 22 for validation, and 34 for testing. SONO achieved a mean value average precision (mAP) of 0.70 in the testing phase. According to each structure's average precision (AP), the crux, ventricular septum, ventricles, atria, outflow tract, pulmonary artery, and ascending aorta were well detected. The tricuspid valve, mitral valve, inferior vena cava, pulmonary vein, and ductus arteriosus identification performed poorly in correct detection. To evaluate the detection of abnormal cardiac structures, 104 sets of 20 sequential cross-sectional video frames around a 4CV and a 3VTV obtained from 40 normal and 14 CHD cases were used. In normal cases, the diagnostic components were well-detected and localized, whereas in CHD cases, the detection of fetal structures was very poor. The ROC analyses were used to assess the performance of detecting cardiac structural anomalies in the heart and vessels. The area under the ROC curves (AUC) produced with SONO was 0.787 in the heart and 0.891 in vessels. Therefore, SONO demonstrated the abnormalities more accurately in vessels than in heart chambers.

Nurmaini et al. [26] investigated the use of deep learning-based computer-aided fetal echocardiography for heart standard view segmentation in detecting congenital heart defects. Their study aimed to develop an automated system that can assist medical professionals in detecting congenital heart defects early on. For this purpose, they used 1149 fetal heart images and included three cases of congenital heart defects. The program managed to detect congenital heart defect cases with a precision of 98.30%.

Ungureanu A et al. [18] published a study protocol to develop an automated intelligent decision support system for early fetal echocardiography using deep learning architectures. The authors used ultrasound images from the first-trimester morphology scan using two-dimensional heart loop videos showing a four-chamber view, left and right ventricular outflow tracts, and a three-vessel view. The sample videos were divided into training (60%), validation (20%), and test sets (20%). The primary outcome of their study was an Intelligent Decision Support System (IS) that can assist early-stage sonographers in training for the accurate detection of the four first-trimester cardiac key planes. Another important outcome was an increase in satisfactory heart key-plane evaluations by inexperienced and newly trained sonographers in first-trimester scans. It also resulted in a reduced rate of diagnosis discrepancies between evaluators with different experiences. The study offers the first standardized AI method for fetal echocardiography weeps in the first trimester of fetal heart anomaly detection.

In contrast to previous studies that used AI in the second trimester of pregnancy, Stoean et al. [27] used CNNs in the first trimester of pregnancy and were able to identify four key planes for fetal heart assessment in the first trimester of pregnancy (the aorta, the arches, the atrioventricular flows, and the crossing of the great vessels) with 95% accuracy.

### 3.2. Brain and Skull

Central nervous system abnormalities are some of the most common congenital fetal malformations, with an incidence rate of 1% [28]. Examining the fetal cranium in standard reference plans, i.e., transventricular, transcerebellar, and transtaminal, represents an essential part of the second-trimester anomaly scan [29,30] Figure 4.

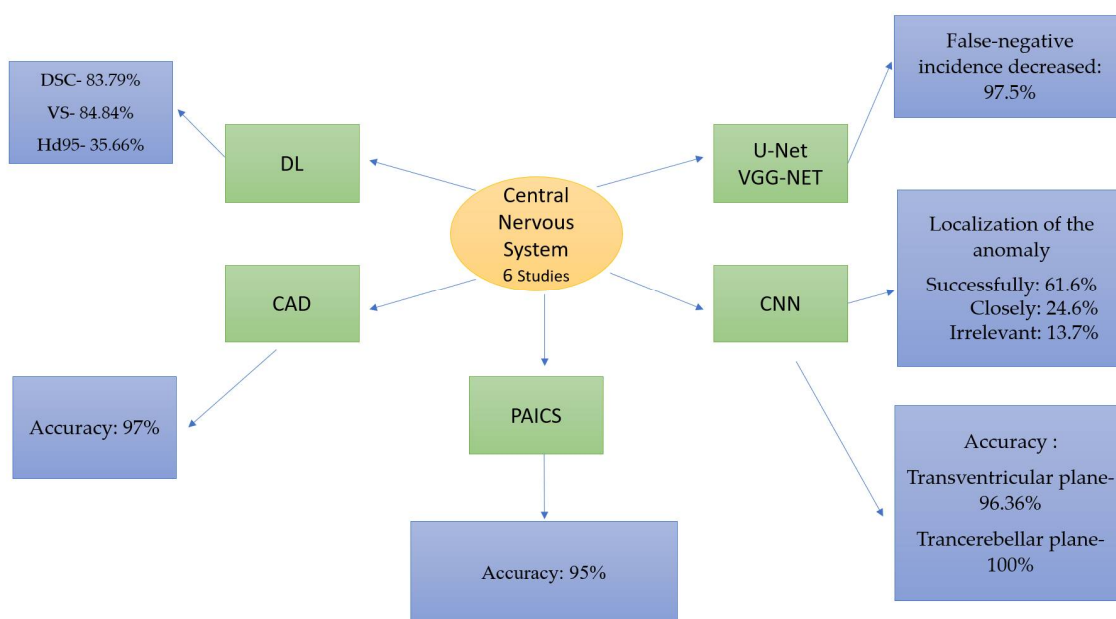


**Figure 4.** AI studies regarding central nervous system anatomy.

The progress of AI-assisted ultrasound diagnosis enabled a 92.93% accuracy in detecting fetal morphology standard planes; therefore, AI was expected to become an alternative screening method for central nervous system fetal malformations [31].

Huang et al. [32] investigated the use of deep learning algorithms for segmenting brain structures imagined with fetal MRI. Their study provides an accurate and efficient method for brain tissue segmentation in fetal MRIs, which is essential for quantifying the presence of congenital disorders. Manual segmentation of fetal brain tissue is cumbersome and time-consuming, so automatic segmentation can significantly simplify the process. The group analyzed 80 fetal brain MRI scans at gestational ages from 20 to 35 weeks. A 6:1:1 ratio was used to divide the dataset into training, validation, and test sets. Dice accuracy, sensitivity, and specificity were used to evaluate the method objectively. The results indicated an average Dice similarity coefficient (DSC) of 83.79%, average volume similarity (VS) of 84.84%, and average Hausdorff95 distance (HD95) of 35.66 mm. The authors compared their approach with several others and demonstrated the superiority of their method.

Heuvel et al. [33] presented a computer-aided detection (CAD) system for automated measurement of the fetal head circumference (HC) in 2D ultrasound images for all trimesters of pregnancy. The CAD system was tested on an independent test set of 335 photos from all trimesters after being trained on 999 images. A skilled sonographer and a medical researcher personally annotated the test set. The outcomes of 0.98 accuracy on the validation set and 0.97 on the test set demonstrate that the CAD system performs as well as a skilled sonographer.

Xie B. et al. [34] utilized the first algorithm for prenatal ultrasonographic diagnosis of central nervous system malformations. Xie et al. utilized U-Net for the cranium region segmentation and the VGG-NET network to differentiate the images of the normal and abnormal structures. Thus, the group decreased false-negative results in fetal brain anomalies by 97.5%.

Xie H.N. et al. [35] used DL-based CNNs to classify ultrasound images as normal or abnormal in standard axial neurosonographic planes. Their study included 15,373 typical images and 14,047 abnormal images of the fetal brain, identified correctly using the program in a proportion of 96.9% and 95.9%, respectively. The exact location of the anomaly was identified correctly in 61.6% of the abnormal ultrasound images, closely in 24.6% of the cases, and irrelevantly in 13.7%. Even though these algorithms can perform simple diagnosis, Yaqub et al. [36] assembled a system that identifies septum cavum pellucidum on the transventricular cerebral plane. Baumgartner et al. [37] assembled a CNN-based

system, which helped them automatically and in real time determine 13 standard fetal plans, including the transventricular and transcerebellar sections with an accuracy of 96.36% and 100%, respectively.

Lin et al. [38] developed an AI system based on CNN (PAICS—prenatal ultrasound diagnosis artificial intelligence conduct system) capable of identifying nine different cerebral malformations based on standard, real-time ultrasound examination images, with an average accuracy of 95%. Using the PAICS system reduced the examination time, and the system's performances were compared with examinations performed by highly experienced practitioners.

### 3.3. Fetal Cardiotocography

Cardiotocography (CTG) is crucial for determining fetal status by monitoring the fetal heart rate (FHR) and uterine contractions. The fetal heart rate (FHR) shows remarkable patterns for evaluating fetal physiology and common stress situations, and according to a vast meta-analysis, continuous CTG monitoring is correlated to a 50% decrease in newborn seizures [39] (Figure 5).

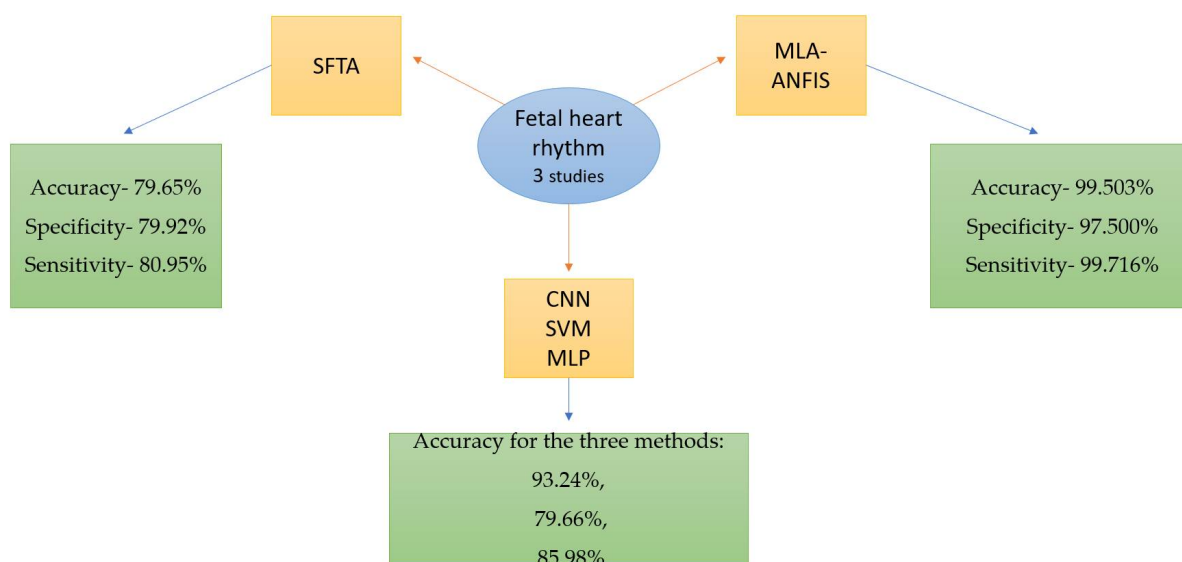


**Figure 5.** AI studies regarding fetal heart rhythm interpretation.

Z. Cömert and A. F. Kocamaz used segmentation-based fractal texture analysis (SFTA) to identify normal and hypoxic records. In total, 44 normal and 44 hypoxic fetuses instances were analyzed, resulting in a 79.65% accuracy, 79.92% specificity, and 80.95% sensitivity to distinguish normal and hypoxic fetuses [40].

On a CTG dataset, different topologies of the multi-layer architecture of a sub-adaptive neuro-fuzzy inference system (MLA-ANFIS) were constructed using multiple input features, neural networks (NNs), deep stacked sparse auto-encoders (DSSAEs), and deep-ANFIS models. In a study conducted by Iraj MS, the results obtained with DSSAE were more accurate than other suggested techniques to predict fetal well-being. The method showed a sensitivity of 99.716%, a specificity of 97.500%, and an accuracy of 99.503% [41]. AI has been used with contemporary computer systems to interpret CTG to overcome human limitations, and numerous trials are being conducted in this area.

CNNs are often used in medicine to create screening systems that automatically aid physicians because of the apparent advantages. Li et al. [42] collected 4473 FHR records and categorized them into three classes: normal, suspicious, and abnormal, based on the electronic fetal monitoring (EFM) system. To improve classification accuracy, the researchers divided the high-resolution 1-dimensional FHR records into ten d-window segments and used CNNs to process the data in parallel. Their study also conducted a comparative experiment. This experiment extracted features from the FHR data using basic statistics.

These features were then used as inputs for support vector machine (SVM) and multilayer perceptron (MLP) classifiers. The accuracy of classification was reported for SVM (79.66%), MLP (85.98%), and CNN (93.24%). These percentages represent each classification method's accuracy rates, with CNN showing the highest accuracy [42].

### 3.4. Fetal Biometry

Accurate fetal biometric measurements of head circumference (HC), biparietal diameter (BPD), abdomen circumference (AC), and femur length (FL) are used to estimate gestational age (GA) and fetal weight (EFW), which are essential for proper delivery management [43] (Figure 6).

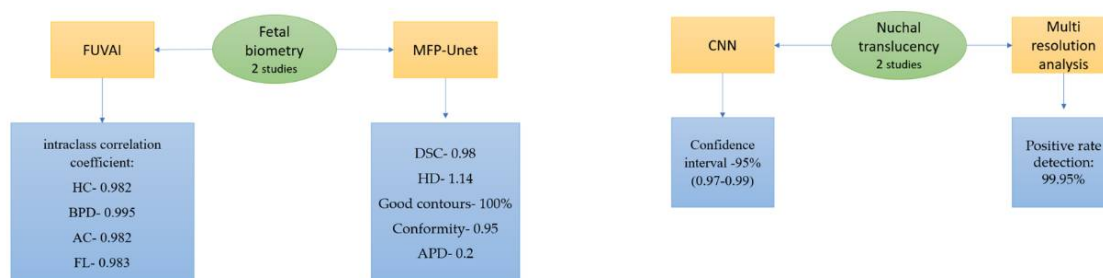


**Figure 6.** AI studies regarding fetal biometry parameters and nuchal translucency estimations.

Szymon Płotka et al. [44] used a novel multi-task CNN-based spatiotemporal fetal US feature extraction and standard plane detection algorithm (FUVAI). They used video recordings from 700 pregnancies and compared the FUVAI fetal biometric measurements with those of experienced sonographers. Clinical studies have revealed that errors are less than 15%, which is acceptable in clinical practice [45]. In the same study, the authors found intraclass correlation coefficients (ICCs) between FUVAI and junior readers of 0.982, 0.989, 0.985, and 0.981 for HC, BPD, AC, and FL, respectively, and ICCs between FUVAI and seniors of 0.987, 0.991, 0.987, and 0.986 for HC, BPD, AC, and FL, respectively. Those results show us that FUVAI results are better correlated with senior examiners. For the second and third trimesters of pregnancy, the corresponding values were 0.982, 0.994, 0.980, and 0.981, and 0.982, 0.995, 0.982, and 0.983, for HC, BPD, AC, and FL, respectively, with no notable differences between the second and third trimester of pregnancy [44].

In a study by Oghli MG et al. [46], CNNs were utilized for automatic measurement and segmentation of fetal biometric parameters, including biparietal diameter (BPD), head circumference (HC), abdominal circumference (AC), and femur length (FL) using a multi-feature pyramid Unet (MFP-Unet) network. They trained this algorithm on 1334 subjects and achieved 0.98, 1.14, 100%, 0.95, and 0.2 mm for the Dice similarity coefficient (DSC), Hausdorff (HD), satisfactory contours, conformity, and average perpendicular distance (APD), respectively.

### 3.5. Nuchal Translucency

AI can assist sonographers in automatically identifying the neck region in ultrasound images and measuring the nuchal translucency (NT). Zhang L et al. [47] used CNNs to screen the trisomy 21 by measuring the NT. They enrolled 822 cases in their study, including 550 participants in the training set and 272 participants in the validation set, with a similar mean age. The DL model showed good performance in both sets for trisomy 21 screening with a 95% confidence interval of 0.92–0.95.

Sciortino G et al. [48] proposed a methodology based on wavelet and multi-resolution analysis. They obtained a positive rate of 99.95% concerning nuchal region detection, and about 64% of scans presented an error of 0.1 mm Figure 4.

Table 1 gives an overview and summary of the results obtained from the research we reviewed and contrasts the analysis performed using AI with that performed by conventional sonographers.

**Table 1.** Results summary.

Authors	Method	Objective	Pregnancy Trimesters	Results
Arnaout et al. [20]	CNN	Heart	Second	Sensitivity to distinguish normal heart development—95% Specificity to distinguish normal heart development—96%
Philip, M. et al. [22]	CNN	Heart	Second	MAPSE correlation coefficient = 0.30 TAPSE correlation coefficient = 0.61
Matsuoka et al. [23]	CNN	Heart	Second	The accuracy with which AI managed to identify the heart: Crux—97.1%; Ventricular septum—69.3%; Left ventricle—96.6%; Left atrium—90.6%; Right ventricle—84.8%; Ascending aorta—61.9%; Pulmonary artery—100%; Stomach—100%; Spine—100%.
Komatsu R et al. [24]	CNN	Heart	Second	Managed to highlight an aspect different from normal
Komatsu M et al. [25]	SONO	Heart	Second	Median average precision for identifying the cardiac structures—70% AUC heart—78.7% AUC vessels—89.1%
Nurmaini et al. [26]	CAD	Heart	Second	Precision—98.30%
Stoean et al. [27]	CNN	Heart	First	Accuracy—95%
Huang et al. [32]	DL	Brain	Second Third	DSC—83.79% VS—84.84% Hd95—35.66%
Heuvel et al. [33]	CAD	Brain	All trimesters	Accuracy: 97%
Xie B. et al. [34]	U-Net VGG-NET	Brain		False-negative incidence decreased by 97.5%
Xie H.N. et al. [35]	CNN	Brain	Second Third	Localization of the anomaly Correctly—61.6% Closely—24.6% Irrelevant—13.7%
Baumgartner et al. [37]	CNN	Brain	Second	Accuracy of identifying: Transventricular plane—96.36%. Trancerebellar plane—100%.
Lin et al. [38]	PAICS	Brain	Second Third	Accuracy for identifying different cerebral malformations—95%
Z. Cömert and A. F. Kocamaz [40]	SFTA	Fetal heart rate	Third	Accuracy—79.65% Specificity—79.92% Sensitivity—80.95%
Iraji MS [41]	MLA-ANFIS	Fetal heart rate	Third	Accuracy—99.503% Specificity—97.500% Sensitivity—99.716%
Li et al. [42]	CNN SVM MLP	Fetal heart rate	Third	Accuracy of the three methods: 93.24%; 79.66%; 85.98%.
Szymon Płotka et al. [44]	FUVAI	Fetal biometry	Second Third	Intraclass correlation coefficient: HC—0.982. BPD—0.995. AC—0.982. FL—0.983.

Table 1. Cont.

Authors	Method	Objective	Pregnancy Trimesters	Results
Oghli, M. G. et al. [46]	MFP-Unet	Fetal biometry	Second	DSC—0.98 HD—1.14 Good contours—100% Conformity—0.95 APD—0.2
Zhang L et al. [47]	CNN	NT	First	Confidence interval—95% (0.92–0.95)
Sciortino G [48]	Multi resolution analysis	NT	First	Positive rate of detection: 99.95%

### 3.6. Results Summary Table 1

In Table 1, CNN—convolutional neural network; DL—deep learning; SONO—supervised object detection with normal data Only, AUC—area under the receiver operating characteristic curve; CAD—computer-aided detection; U-NET—network’s U-shaped architecture; VGG-Net—visual geometry group network; PAICS—prenatal ultrasound diagnosis artificial intelligence conduct system; SFTA—segmentation-based fractal texture analysis; MLA-ANFIS—the multi-layer architecture of a sub-adaptive neuro-fuzzy inference system; SVM—support vector machine; MLP—multilayer perceptron; FUVAI—spatio-temporal fetal US video analysis; MFP-Unet—multi-feature pyramid Unet network; MAPSE—mitral valve annular planes systolic excursion; TAPSE—tricuspid valve annular planes systolic excursion; DSC—Dice similarity coefficient; VS—volume similarity; HD95—Hausdorff95 distance; HD—head circumference; BPD—biparietal diameter; AC—abdomen circumference; FL—femur length; HD—Hausdorff coefficient; APD—average perpendicular distance.

### 3.7. Results of Syntheses

The predictive values of the AI methods used in the included studies were divided into groups according to the system analyzed and evaluated. The results are summarized in Tables 2–6.

Table 2. Cord studies—synthesized records.

Arnaout et al. [20]	Boston	107,823 images	Gestational age between 18 and 24 weeks	CNN	Sensitivity of 95% Specificity of 96% Predictive negative value of 100%
Philip M et al. [22]	New South Wales	95 participants	Mean gestational age of 30.7 Gestational age between 22.9 and 38.0	CNN	RMSE for TAPSE—0.14 RMSE for MAPSE—0.18
Matsuoka et al. [23]	Japan	2378 movie frames from 51 fetal cardiac screening scans used as the training dataset 701 movie frames from fetal cardiac screening used as test data	Gestational age between 18 and 20	CNN	The accuracy with which AI managed to identify the heart was between 61.9 and 100%
Komatsu R et al. [24]	Japan	42 movie frames for database	Second trimester	CNN	Managed to highlight an aspect different from normal
Komatsu M et al. [25]	Japan	191 videos of normal cord used for training 22 videos used for validation 34 videos used for testing	Second trimester	SONO	Mean value average precision (mAP) of 0.70

**Table 2.** *Cont.*

Komatsu M et al. [25]	Japan	104 sets of 20 sequential cross-sectional video-frames	Second trimester	SONO	AUC for heart—0.787 AUC for vessels—0.891
Nurmaini et al. [26]	Indonesia	1149 fetal heart images	Second trimester	CAD	Precision: 98.3%
Stoean et al. [27]	Romania	7251 fetal heart images	First trimester	CNN	Accuracy: 95%

**Table 3.** Brain studies—synthesized records.

Huang et al. [32]	China	80 fetal brain scans	20–35 gestational age	DL	Dice coefficient—83.79% VS—84.84% Hd95—35.66%
Heuvel et al. [33]	Netherlands	999 images for the training set 335 images for test data	All trimesters	CAD	Accuracy on the validation set—0.98 Accuracy on the test set—0.97
Xie B. et al. [34]	China	13.350 images	18–32 gestational weeks	U-net VGG-Net	False-negative incidence decreased by 97.5%
Xie HN et al. [35]	China	13.373 normal pregnancies 14.047 abnormal pregnancies	Second trimesters	CNN	Located lesions: Precisely in 61.6%; Closely in 24.6%; Irrelevantly in 13.7%.
Baumgartner et al. [37]	UK	2694 ultrasound examinations	18–22 gestational weeks	CNN	Accuracy to identify the correct plans between 96.36% and 100%
Lin et al. [38]	China	43.890 ultrasound images 169 ultrasound videos	18–40 gestational weeks	PAICS	Accuracy to identify the correct plans—95%

**Table 4.** Fetal heart rhythm studies—synthesized records.

Z. Cömert and A. F. Kocamaz [40]	Turkey	44 normal fetuses 44 hypoxic fetuses	Third trimester	SFTA	Distinguished normal and hypoxic fetuses with: Accuracy—79.65%; Specificity—79.92%; Sensitivity—80.95%.
Iraji MS [41]	Iran		Third trimester	MLA-ANFIS DSSAEs Deep-ANFIS	Predicted fetal well-being with: Specificity—97.500%; Accuracy—99.503%; Sensitivity—99.716%.
Li et al. [42]	China	4473 FHR records	Third trimester	SVM MLP CNN	Accuracy for classification in three classes: normal, suspicious, and abnormal SVM—79.66%

**Table 5.** Fetal biometry studies—synthesized records.

Szymon Płotka et al. [44]	Poland	700 pregnancies	Second and third trimester	FUVAI	Intraclass correlation coefficient: HC—0.982; BPD—0.995; AC—0.982; FL—0.983.
Oghli, M. G. et al. [46]	Iran	1334 subject	Second	MFP-Unet	DSC—0.98 HD—1.14 Good contours—100% Conformity—0.95 APD—0.2

**Table 6.** Nuchal translucency studies—synthesized records.

Zhang L et al. [47]	China	822 cases	11–14 gestational weeks	CNN	Confidence interval—95% (0.92–0.95)
Sciortino G [48]	Italy	382 cases	FIRST	Multi resolution analysis	Positive rate of detection—99.95%

#### 4. Discussion

This review encompasses several articles focusing on using AI in fetal ultrasound assessment. The objective of developing these neural networks is to enhance the process of ultrasound assessment by automating the identification of fetal structures, thereby maximizing the accuracy of the technique and minimizing examination time.

Numerous programs were outlined in the reviewed studies, all of which successfully attained their objectives by achieving accuracy rates exceeding 90% in identifying fetal brain and heart structures or their biometric measurements [27]. These findings have exhibited promising outcomes in enhancing the precision and automation of fetal parameter estimations.

Congenital heart diseases are the most common fetal malformations [4]. The incorporation of AI into ultrasound assessments is directed at enhancing both detection rates and precision. Research studies have showcased the efficacy of AI applications applicable across any gestational age, demonstrating the capability to identify fetal structures as early as the first trimester of pregnancy [14,18]. These studies delineated four established fetal heart assessment key plans and expanded to identify up to nine fetal heart structures in the second trimester [23]. Additionally, a protocol for developing an automated intelligent decision support system for early fetal echocardiography using DL architectures was developed and successfully implemented. The goal is to aid sonographers in identifying correctly the key cardiac planes during the first trimester.

The development of specialized systems, such as those determining various fetal plans, emphasizes the versatility of AI in fetal ultrasound examinations. The potential of AI to enhance prenatal care by providing more accurate and efficient methods for identifying and diagnosing fetal anomalies is evident. These advancements underline the transformative impact of AI on the field, offering a promising avenue for future improvements in fetal healthcare [37].

Central nervous system abnormalities are the second most common congenital fetal malformations, with an incidence rate of 1% [28]. AI-assisted ultrasound diagnosis has achieved high accuracy rates of up to 100% in detecting fetal brain standard planes, making it a potential alternative screening method for central nervous system fetal malformations. Notably, specialized software was developed, exhibiting the ability to accurately identify up to 13 fetal brain planes, such as the transventricular plane and the transcerebellar plane, with a remarkable 96.36% and 100% accuracy rate, respectively [37].



Beyond identifying standard fetal planes, AI demonstrated proficiency in distinguishing between typical and abnormal images, effectively pinpointing the location of abnormalities within the fetal brain. AI was able to precisely identify different types of brain abnormalities in real time during ultrasound tests using the PAICS system (95% accuracy) (ventriculomegaly, non-visualization of Cavum septum pellucidum, septum pellucidum, crescent-shaped single ventricle, non-intraventricular cyst, intraventricular cyst, open four ventricles, and mega cisterna magna) [37].

Certain programs have utilized cases involving congenital brain anomalies (neural tube defect, holoprosencephaly, lissencephaly, microcephalus, posterior fossa anomaly, sparse occupying lesion, intracranial hemorrhage, or ventriculomegaly) as part of the training data, leading to the capability to detect fetal anomalies at an impressive rate of over 96%. Moreover, AI has successfully located an anomaly with an accuracy rate of 61.6% in the cases, closely in 24.6%, and irrelevantly in 13.7% [35].

This approach underlines the efficiency of using AI-based programs as valuable tools for less experienced medical professionals that can significantly support improving diagnostic competence [18].

The use of AI can support sonographers in automatically identifying the neck region in ultrasound images and measuring the nuchal translucency in cases with Down Syndrome. The deep learning model performed well in training and validation sets, achieving a 95% confidence interval by measuring NT [47]. Also, good outcomes were obtained in studies that utilized normal cases for identifying nuchal translucency (99.95% detection of the nuchal region) [48].

Our comprehensive review encompasses diverse AI-based evaluation methodologies, recent studies, their associated advantages and disadvantages, potential obstacles, and the anticipated applications of AI in obstetrics. With this thorough investigation, it becomes evident that AI holds significant promise in prenatal diagnosis [14]. It has the potential to surmount diagnostic challenges, enhance treatment options, and ultimately contribute to improved patient outcomes in fetal medicine.

## 5. Conclusions

AI has seamlessly integrated into various facets of our daily lives and emerged as a pivotal source of innovation in healthcare. It plays a substantial role in supporting clinical decision-making and providing high-quality assistance. AI solutions prove to be highly advantageous, particularly in healthcare domains where professionals such as radiographers and sonographers heavily depend on information derived from images. DL, a subset of AI, excels in image pattern recognition, making it particularly effective for practitioners relying on image-based data for diagnosis and decision-making in healthcare settings.

AI-assisted ultrasound diagnosis addresses certain limitations associated with traditional ultrasound examinations. The substantial progress made in recent years, coupled with enhanced capabilities in detecting prenatal fetal malformations, positions AI as a prospective adjunct or alternative screening method for identifying fetal anomalies. This includes the assessment of complex systems like the brain and heart.

Studies highlight AI's potential in accurately detecting heart structures. AI, particularly CNNs, effectively distinguishes normal development from cardiac anomalies, with studies showing comparable and predictive performances to experts.

AI technologies, such as DL algorithms and CNNs, have demonstrated impressive accuracy in identifying brain planes and structures and automated fetal head biometry measurements. Also, comparable performance to the skilled sonographers in anomaly detection and a reduction in false-negative results in diagnosing fetal brain anomalies were obtained.

The development of specialized systems, such as those determining various fetal plans, emphasizes the versatility of AI in fetal ultrasound examinations. The potential of AI to enhance prenatal care by providing more accurate and efficient methods for identifying and diagnosing fetal anomalies is evident. These advancements underline the transfor-

mative impact of AI on the field, offering a promising avenue for future improvements in fetal healthcare.

**Author Contributions:** Conceptualization, I.-A.E., Ș.G.C. and C.I.-R.; investigation, E.I.A.B., A.V. and I.D.B.; writing—original draft preparation, I.-A.E.; writing—review and editing, A.M.I.-O., C.M.C., R.D.N. and D.G.I.; supervision, D.G.I. All authors have read and agreed to the published version of the manuscript.

**Funding:** The article processing charges were funded by the Doctoral School of the University of Medicine and Pharmacy of Craiova, Romania.

**Informed Consent Statement:** Informed consent was obtained from all subjects involved in this study.

**Data Availability Statement:** Data sharing is not applicable to this article.

**Acknowledgments:** This work was supported by a grant from the Ministry of Research Innovation and Digitization, CSNC-UEFISCDI, project number PN-III-P4-PCE-2021-0057, within PNCDI III.

**Conflicts of Interest:** The authors declare no conflicts of interest.

## References

1. Corsello, G.; Giuffrè, M. Congenital malformations. *J. Matern. Fetal Neonatal Med.* **2012**, *25* (Suppl. S1), 25–29. [CrossRef] [PubMed]
2. Persson, M.; Cnattingius, S.; Villamor, E.; Söderling, J.; Pasternak, B.; Stephansson, O.; Neovius, M. Risk of major congenital malformations in relation to maternal overweight and obesity severity: Cohort study of 1.2 million singletons. *BMJ* **2017**, *357*, j2563. [CrossRef] [PubMed]
3. Bonnet, D. Impacts of prenatal diagnosis of congenital heart diseases on outcomes. *Transl. Pediatr.* **2021**, *10*, 2241–2249. [CrossRef] [PubMed]
4. Cater, S.W.; Boyd, B.K.; Gbate, S.V. Abnormalities of the Fetal Central Nervous System: Prenatal US Diagnosis with Postnatal Correlation. *RadioGraphics* **2020**, *40*, 1458–1472. [CrossRef]
5. McBrien, A.; Hornberger, L.K. Early fetal echocardiography. *Birth Defects Res.* **2019**, *111*, 370–379. [CrossRef]
6. Grandjean, H.; Larroque, D.; Levi, S. The performance of routine ultrasonographic screening of pregnancies in the Eurofetus Study. *Am. J. Obstet. Gynecol.* **1999**, *181*, 446–454. [CrossRef]
7. McCarthy, J.; Minsky, M.L.; Rochester, N.; Shannon, C.E. A Proposal for the Dartmouth Summer Research Project on Artificial Intelligence: August 31, 1955. *AI Mag.* **2006**, *27*, 12.
8. LeCun, Y.; Bengio, Y.; Hinton, G. Deep learning. *Nature* **2015**, *521*, 436–444. [CrossRef]
9. Makary, M.A.; Daniel, M. Medical error—The third leading cause of death in the US. *BMJ* **2016**, *353*, i2139. [CrossRef]
10. Marblestone, A.H.; Wayne, G.; Kording, K.P. Toward an Integration of Deep Learning and Neuroscience. *Front. Comput. Neurosci.* **2016**, *10*, 94. [CrossRef]
11. Bengio, Y.; Lee, D.H.; Bornschein, J.; Mesnard, T.; Lin, Z. Towards Biologically Plausible Deep Learning. *arXiv* **2016**, arXiv:1502.04156.
12. Aljabri, M.; AlGhamdi, M. A review on the use of deep learning for medical images segmentation. *Neurocomputing* **2022**, *506*, 311–335. [CrossRef]
13. Li, X.; Zhang, S.; Zhang, Q.; Wei, X.; Pan, Y.; Zhao, J.; Xin, X.; Qin, C.; Wang, X.; Li, J.; et al. Diagnosis of thyroid cancer using deep convolutional neural network models applied to sonographic images: A retrospective, multicohort, diagnostic study. *Lancet Oncol.* **2019**, *20*, 193–201. [CrossRef] [PubMed]
14. Chen, Z.; Liu, Z.; Du, M.; Wang, Z. Artificial Intelligence in Obstetric Ultrasound: An Update and Future Applications. *Front. Med.* **2021**, *8*, 733468. [CrossRef] [PubMed]
15. Pramanik, M.; Gupta, M.; Krishnan, K.B. Enhancing reproducibility of ultrasonic measurements by new users. In Proceedings of the Medical Imaging 2013: Image Perception, Observer Performance, and Technology Assessment, Lake Buena Vista, FL, USA, 9–14 February 2013; p. 86730Q. Available online: <http://proceedings.spiedigitallibrary.org/proceeding.aspx?doi=10.1117/12.2008032> (accessed on 8 December 2023).
16. Dawood, Y.; Buijendijk, M.F.; Shah, H.; Smit, J.A.; Jacobs, K.; Hagoort, J.; Oostra, R.-J.; Bourne, T.; van den Hoff, M.J.v.D.; de Bakker, B.S. Imaging fetal anatomy. *Semin. Cell Dev. Biol.* **2022**, *131*, 78–92. [CrossRef] [PubMed]
17. Carvalho, J.S.; Axt-Flidner, R.; Chaoui, R.; Copel, J.A.; Cuneo, B.F.; Goff, D.; Kopylov, L.G.; Hecher, K.; Lee, W.; Moon-Grady, A.J.; et al. ISUOG Practice Guidelines (updated): Fetal cardiac screening. *Ultrasound Obstet. Gynecol.* **2023**, *61*, 788–803. [CrossRef]
18. Ungureanu, A.; Marcu, A.S.; Patru, C.L.; Ruican, D.; Nagy, R.; Stoean, R.; Stoean, C.; Iliescu, D.G. Learning deep architectures for the interpretation of first-trimester fetal echocardiography (LIFE)—A study protocol for developing an automated intelligent decision support system for early fetal echocardiography. *BMC Pregnancy Childbirth* **2023**, *23*, 20. [CrossRef]
19. Sklansky, M.; DeVore, G.R. Fetal Cardiac Screening: What Are We (and Our Guidelines) Doing Wrong? *J. Ultrasound Med.* **2016**, *35*, 679–681. [CrossRef]

20. Arnaout, R.; Curran, L.; Zhao, Y.; Levine, J.C.; Chinn, E.; Moon-Grady, A.J. An ensemble of neural networks provides expert-level prenatal detection of complex congenital heart disease. *Nat. Med.* **2021**, *27*, 882–891. [CrossRef]
21. International Society of Ultrasound in Obstetrics and Gynecology Null; Carvalho, J.S.; Allan, L.D.; Chaoui, R.; Copel, J.A.; DeVore, G.R.; Hecher, K.; Lee, W.; Munoz, H.; Paladini, D.; et al. ISUOG Practice Guidelines (updated): Sonographic screening examination of the fetal heart. *Ultrasound Obstet. Gynecol. Off. J. Int. Soc. Ultrasound Obstet. Gynecol.* **2013**, *41*, 348–359. [CrossRef]
22. Philip, M.E.; Sowmya, A.; Avnet, H.; Ferreira, A.; Stevenson, G.; Welsh, A. Convolutional Neural Networks for Automated Fetal Cardiac Assessment using 4D B-Mode Ultrasound. In Proceedings of the 2019 IEEE 16th International Symposium on Biomedical Imaging (ISBI 2019), Venice, Italy, 8–11 April 2019; pp. 824–828. Available online: <https://ieeexplore.ieee.org/document/8759377/> (accessed on 8 December 2023).
23. Matsuoka, R.; Komatsu, M.; Sakai, A.; Yasutomi, S.; Arakaki, T.; Tokunaka, M.; Komatsu, R.; Hamamoto, R.; Sekizawa, A. P08.01: A novel deep learning based system for fetal cardiac screening. *Ultrasound Obstet. Gynecol.* **2019**, *54*, 177–178. [CrossRef]
24. Komatsu, R.; Matsuoka, R.; Arakaki, T.; Tokunaka, M.; Komatsu, M.; Sakai, A.; Yasutomi, S.; Hamamoto, R.; Sekizawa, A. OP15.04: Novel AI-guided ultrasound screening system for fetal heart can demonstrate findings in timeline diagram. *Ultrasound Obstet. Gynecol.* **2019**, *54*, 134. [CrossRef]
25. Komatsu, M.; Sakai, A.; Komatsu, R.; Matsuoka, R.; Yasutomi, S.; Shozu, K.; Dozen, A.; Machino, H.; Hidaka, H.; Arakaki, T.; et al. Detection of Cardiac Structural Abnormalities in Fetal Ultrasound Videos Using Deep Learning. *Appl. Sci.* **2021**, *11*, 371. [CrossRef]
26. Nurmaini, S.; Rachmatullah, M.N.; Sapitri, A.I.; Darmawahyuni, A.; Tutuko, B.; Firdaus, F.; Partan, R.U.; Bernolian, N. Deep Learning-Based Computer-Aided Fetal Echocardiography: Application to Heart Standard View Segmentation for Congenital Heart Defects Detection. *Sensors* **2021**, *21*, 8007. [CrossRef] [PubMed]
27. Stoean, R.; Iliescu, D.; Stoean, C.; Ilie, V.; Patru, C.; Hotoleanu, M.; Nagy, R.; Ruican, D.; Trocan, R.; Marcu, A.; et al. Deep Learning for the Detection of Frames of Interest in Fetal Heart Assessment from First Trimester Ultrasound. In *Advances in Computational Intelligence*; Rojas, I., Joya, G., Català, A., Eds.; Lecture Notes in Computer Science; Springer International Publishing: Cham, Switzerland, 2021; Volume 12861, pp. 3–14. Available online: [https://link.springer.com/10.1007/978-3-030-85030-2\\_1](https://link.springer.com/10.1007/978-3-030-85030-2_1) (accessed on 22 December 2023).
28. Paladini, D.; Malinger, G.; Birnbaum, R.; Monteagudo, A.; Pilu, G.; Salomon, L.J.; Timor-Tritsch, I.E. ISUOG Practice Guidelines (updated): Sonographic examination of the fetal central nervous system. Part 2: Performance of targeted neurosonography. *Ultrasound Obstet. Gynecol.* **2021**, *57*, 661–671. [CrossRef]
29. ISUOG Education Committee. ISUOG Education Committee recommendations for basic training in obstetric and gynecological ultrasound: ISUOG Recommendations. *Ultrasound Obstet. Gynecol.* **2014**, *43*, 113–116. [CrossRef]
30. Malinger, G.; Paladini, D.; Haratz, K.K.; Monteagudo, A.; Pilu, G.L.; Timor-Tritsch, I.E. ISUOG Practice Guidelines (updated): Sonographic examination of the fetal central nervous system. Part 1: Performance of screening examination and indications for targeted neurosonography. *Ultrasound Obstet. Gynecol.* **2020**, *56*, 476–484. [CrossRef]
31. Xiao, S.; Zhang, J.; Zhu, Y.; Zhang, Z.; Cao, H.; Xie, M.; Zhang, L. Application and Progress of Artificial Intelligence in Fetal Ultrasound. *J. Clin. Med.* **2023**, *12*, 3298. [CrossRef]
32. Huang, X.; Liu, Y.; Li, Y.; Qi, K.; Gao, A.; Zheng, B.; Liang, D.; Long, X. Deep Learning-Based Multiclass Brain Tissue Segmentation in Fetal MRIs. *Sensors* **2023**, *23*, 655. [CrossRef]
33. Van Den Heuvel, T.L.A.; De Bruijn, D.; De Korte, C.L.; Ginneken, B.V. Automated measurement of fetal head circumference using 2D ultrasound images. *PLoS ONE* **2018**, *13*, e0200412. [CrossRef]
34. Xie, B.; Lei, T.; Wang, N.; Cai, H.; Xian, J.; He, M.; Zhang, L.; Xie, H. Computer-aided diagnosis for fetal brain ultrasound images using deep convolutional neural networks. *Int. J. Comput. Assist. Radiol. Surg.* **2020**, *15*, 1303–1312. [CrossRef] [PubMed]
35. Xie, H.N.; Wang, N.; He, M.; Zhang, L.H.; Cai, H.M.; Xian, J.B.; Lin, M.F.; Zheng, J.; Yang, Y.Z. Using deep-learning algorithms to classify fetal brain ultrasound images as normal or abnormal. *Ultrasound Obstet. Gynecol.* **2020**, *56*, 579–587. [CrossRef] [PubMed]
36. Yaqub, M.; Kelly, B.; Papageorgiou, A.T.; Noble, J.A. A Deep Learning Solution for Automatic Fetal Neurosonographic Diagnostic Plane Verification Using Clinical Standard Constraints. *Ultrasound Med. Biol.* **2017**, *43*, 2925–2933. [CrossRef] [PubMed]
37. Baumgartner, C.F.; Kamnitsas, K.; Matthew, J.; Fletcher, T.P.; Smith, S.; Koch, L.M.; Kainz, B.; Rueckert, D. SonoNet: Real-Time Detection and Localisation of Fetal Standard Scan Planes in Freehand Ultrasound. *IEEE Trans. Med. Imaging* **2017**, *36*, 2204–2215. [CrossRef] [PubMed]
38. Lin, M.; He, X.; Guo, H.; He, M.; Zhang, L.; Xian, J.; Lei, T.; Xu, Q.; Zheng, J.; Feng, J.; et al. Use of real-time artificial intelligence in detection of abnormal image patterns in standard sonographic reference planes in screening for fetal intracranial malformations. *Ultrasound Obstet. Gynecol.* **2022**, *59*, 304–316. [CrossRef]
39. Alfrevic, Z.; Devane, D.; Gyte, G.M.; Cuthbert, A. Continuous cardiotocography (CTG) as a form of electronic fetal monitoring (EFM) for fetal assessment during labour. *Cochrane Database Syst. Rev.* **2017**, *2*, CD006066. [CrossRef]
40. Comert, Z.; Kocamaz, A.F. Cardiotocography analysis based on segmentation-based fractal texture decomposition and extreme learning machine. In Proceedings of the 2017 25th Signal Processing and Communications Applications Conference (SIU), Antalya, Turkey, 15–18 May 2017; pp. 1–4. Available online: <http://ieeexplore.ieee.org/document/7960397/> (accessed on 8 December 2023).
41. Iraj, M.S. Prediction of fetal state from the cardiotocogram recordings using neural network models. *Artif. Intell. Med.* **2019**, *96*, 33–44. [CrossRef]

42. Li, J.; Chen, Z.-Z.; Huang, L.; Fang, M.; Li, B.; Fu, X.; Wang, H.; Zhao, Q.; Shen, Z.; Zhang, Y. Automatic Classification of Fetal Heart Rate Based on Convolutional Neural Network. *IEEE Internet Things J.* **2019**, *6*, 1394–1401. [CrossRef]
43. Salomon, L.; Alfirevic, Z.; Da Silva Costa, F.; Deter, R.; Figueras, F.; Ghi, T.; Glanc, P.; Khalil, A.; Lee, W.; Napolitano, R.; et al. ISUOG Practice Guidelines: Ultrasound assessment of fetal biometry and growth. *Ultrasound Obstet. Gynecol.* **2019**, *53*, 715–723. [CrossRef]
44. Plotka, S.; Klasa, A.; Lisowska, A.; Seliga-Siwecka, J.; Lipa, M.; Trzciński, T.; Sitek, A. Deep learning fetal ultrasound video model match human observers in biometric measurements. *Phys. Med. Biol.* **2022**, *67*, 045013. [CrossRef]
45. Sarris, I.; Ioannou, C.; Chamberlain, P.; Ohuma, E.; Roseman, F.; Hoch, L.; Altman, D.G.; Papageorgiou, A.T. Intra- and interobserver variability in fetal ultrasound measurements. *Ultrasound Obstet. Gynecol.* **2012**, *39*, 266–273. [CrossRef] [PubMed]
46. Oghli, M.G.; Shabanzadeh, A.; Moradi, S.; Sirjani, N.; Gerami, R.; Ghaderi, P.; Taheri, M.S.; Shiri, I.; Arabi, H.; Zaidi, H. Automatic fetal biometry prediction using a novel deep convolutional network architecture. *Phys. Med.* **2021**, *88*, 127–137. [CrossRef] [PubMed]
47. Zhang, L.; Dong, D.; Sun, Y.; Hu, C.; Sun, C.; Wu, Q.; Tian, J. Development and Validation of a Deep Learning Model to Screen for Trisomy 21 During the First Trimester From Nuchal Ultrasonographic Images. *JAMA Netw. Open* **2022**, *5*, e2217854. [CrossRef] [PubMed]
48. Sciortino, G.; Tegolo, D.; Valenti, C. Automatic detection and measurement of nuchal translucency. *Comput. Biol. Med.* **2017**, *82*, 12–20. [CrossRef]

**Disclaimer/Publisher’s Note:** The statements, opinions and data contained in all publications are solely those of the individual author(s) and contributor(s) and not of MDPI and/or the editor(s). MDPI and/or the editor(s) disclaim responsibility for any injury to people or property resulting from any ideas, methods, instructions or products referred to in the content.

## Review

# Hydatidiform Mole—Between Chromosomal Abnormality, Uniparental Disomy and Monogenic Variants: A Narrative Review

Andreea Florea <sup>1</sup>, Lavinia Caba <sup>1,\*</sup>, Ana-Maria Grigore <sup>1</sup>, Lucian-Mihai Antoci <sup>1</sup>, Mihaela Grigore <sup>2</sup>, Mihaela I. Gramescu <sup>1</sup> and Eusebiu Vlad Gorduza <sup>1</sup>

- <sup>1</sup> Department of Medical Genetics, Faculty of Medicine, “Grigore T. Popa” University of Medicine and Pharmacy, 700115 Iasi, Romania; andreeaflorea97@gmail.com (A.F.); anagrigore2626@gmail.com (A.-M.G.); lucian-mihai.antoci@email.umfiasi.ro (L.-M.A.); mihaelagramescu@yahoo.ro (M.I.G.); vgord@mail.com (E.V.G.)
- <sup>2</sup> Department of Obstetrics and Gynecology, “Grigore T. Popa” University of Medicine and Pharmacy, 700115 Iasi, Romania; mihaela.grigore@edr.ro
- \* Correspondence: lavinia.caba@umfiasi.ro

**Abstract:** A hydatidiform mole (HM) or molar pregnancy is the most common benign form of gestational trophoblastic disease characterized by a proliferation of the trophoblastic epithelium and villous edema. Hydatidiform moles are classified into two forms: complete and partial hydatidiform moles. These two types of HM present morphologic, histopathologic and cytogenetic differences. Usually, hydatidiform moles are a unique event, but some women present a recurrent form of complete hydatidiform moles that can be sporadic or familial. The appearance of hydatidiform moles is correlated with some genetic events (like uniparental disomy, triploidy or diandry) specific to meiosis and is the first step of embryo development. The familial forms are determined by variants in some genes, with *NLRP7* and *KHDC3L* being the most important ones. The identification of different types of hydatidiform moles and their subsequent mechanisms is important to calculate the recurrence risk and estimate the method of progression to a malign form. This review synthesizes the heterogeneous mechanisms and their implications in genetic counseling.

**Keywords:** hydatidiform mole; uniparental disomy; triploidy; androgenetic; monogenic variant

## 1. Introduction and Objectives

Gestational trophoblastic disease (GTD) comprises a series of gestational disorders that vary from benign to malignant forms. The benign form of GTD is represented by a hydatidiform mole (HM), which is the most common. The malignant forms of GTD are represented by trophoblastic tumors (with two forms—epithelial trophoblastic and placental site trophoblastic tumors), choriocarcinoma and invasive moles [1].

Moles have been described since antiquity by Hippocrates, but the term mole was introduced in 1752 by William Smellie [2]. The hydatidiform mole, commonly known as a molar pregnancy, is a rare complication in gestation, mainly caused by a genetic error during fertilization or gametogenesis [3,4]. This is characterized by a disordered proliferation of the trophoblastic epithelium and villous edema [5,6].

Morphologic, histopathologic and cytogenetic criteria can identify two types of hydatidiform moles: a complete hydatidiform mole (CHM) and partial hydatidiform mole (PHM) [7]. In the majority of cases with a CHM, the genetic material has paternal origin, being generated by errors of meiosis or fertilization, or during the first steps of embryo development. Usually, a complete hydatidiform mole is a unique event during the reproductive period of women. Although unusual, when recurrence occurs, it is indicative of a genetic predisposition. In partial hydatidiform moles, an imbalance is present between the

maternal and paternal genomes with a preponderance of the male genome [2]. The main characteristics of CHMs and PHMs are presented in Table 1.

**Table 1.** Differences between CHMs and PHMs [8–11].

Characteristics	CHM	PHM
<b>Histological findings</b>	<ul style="list-style-type: none"> <li>- Abnormal chorionic villi (enlarged, irregular, polyploid or lobular aspect) which form the “cisterns” with stromal fluid trophoblastic inclusion.</li> <li>- Cytological atypia.</li> <li>- Apoptotic bodies.</li> <li>- Fetal stromal blood vessels are absent.</li> </ul>	<ul style="list-style-type: none"> <li>- Some of the villi are large and hydropic and others are small and fibrotic; the edges of the villi are irregular.</li> <li>- Small trophoblastic inclusions.</li> <li>- An irregular maze-like appearance given with a sketch of the formation of the central cistern is noticeable.</li> </ul>
<b>Immunohistochemical findings</b>	Absence of p57 expression	Presence of p57 expression
<b>hCG</b>	Very high levels (>100,000)	Normal range/lower
<b>Uterine size</b>	Larger related to the expected gestational date of the pregnancy	Smaller than the suggested date
<b>Fetal parts</b>	Lack of embryonic or fetal structures	Fetal structures present
<b>Recurrence</b>	1 in 100	Small
<b>Risk of choriocarcinoma</b>	3%	Low

Epidemiological studies have revealed variable incidence rates of molar pregnancies across different global regions (0.2–9.9 per 1000 pregnancies) [6]. In North America and Europe, the frequency is estimated within the range of 60 to 120 cases per 100,000 pregnancies [8]. However, the incidence is more elevated in other geographic regions, particularly in Asia (especially in Southeast Asia) and Africa, with rates up to ten times higher compared with those of developed countries [2,6]. In developed countries, the incidence of complete hydatidiform moles is approximated at one to three cases per 1000 pregnancies, while those of PHMs hover at about three cases per 1000 pregnancies [2].

In rare situations, a twin pregnancy is affected by a mole. There are two distinct categories of twin molar pregnancies. The most frequent one is a dizygotic twin pregnancy with a coexistence between a CHM in one twin and a normal fetus and placenta in the other twin, which occurs in 1 per 22,000–100,000 pregnancies. In these cases, the placental mass has two components: the normal placenta that serves the normal fetus and the molar placenta [12].

The rate of favorable evolution of such pregnancies is about 40%. The second variant entails an analogous twin configuration, but with a partial hydatidiform mole in one twin, which evolves into a viable fetus in fewer than 25% of instances [13].

The classic complications of hydatidiform moles during pregnancy are spontaneous abortions, intrauterine death, hyperthyroidism and preeclampsia [12]. Whatever the prognosis of hydatidiform moles is worth, the majority of such pregnancies generate a miscarriage or an intrauterine death [3,5].

It is important to differentiate between complete hydatidiform moles, partial hydatidiform moles and non-molar pregnancies for several reasons: the different management in cases of hydatidiform moles and non-molar pregnancies and the risk of recurrence of molar pregnancies in the same individual and in the family is also different [14]. In medical practice, serum  $\beta$ -hCG (human chorionic gonadotropin) and ultrasound are used to identify hydatidiform moles. Histological criteria and genetic analyses are used to discriminate between the two types of HMs and hydropic abortion (HA) [9].

The microscopic appearance is different in complete hydatidiform moles, partial hydatidiform moles and HAs. There are overlaps in histological signs between the two types of moles, but also between molar and non-molar pregnancies. In this last case,

differential diagnosis problems may arise when there are pregnancies with abnormal villous morphology or hyperplastic ones, products of mosaic conception or those cases where there is a chimeric conception [9,15].

An proportion of 50% of the partial hydatidiform mole cannot be diagnosed by routine histological examination. This occurs for at least two reasons: there are no specific histological signs and there is a significant inter- and intra-observer variability [16].

Some morphological criteria depend on the gestational age. Thus, ultrasonographic signs of an abnormal pregnancy can lead to therapeutic abortion, but the histopathological examination may not reveal histological signs characteristic of molar pregnancy, because they have not yet appeared [9,15,17].

Sarmadi et al. analyzed various histological criteria belonging to the following category of histological diagnosis criteria: trophoblastic proliferation, villous stroma, villous shape and presence of fetal structures [9]. Using Kappa statistics, the authors concluded that there are morphological criteria with high specificity such as “cistern formation” and “hydropic change” (Kappa value: 0.746 and 0.686, respectively). Kappa values between 0.549 and 0.412 are associated with moderate agreement rates. This category included atypia in trophoblastic cells, trophoblastic-free cell cluster, predominantly syncytiotrophoblastic proliferation, predominantly cytotrophoblastic proliferation, polypoid/lobulated villus, chorionic membrane and nucleated red blood cells. Other histological criteria had a slight agreement rate: a round inclusion (Kappa = 0.174) and an irregular inclusion (Kappa = 0.136). The other criteria used had a fair degree of agreement rate: nuclear debris in the villous stroma, stromal fibrosis (fibrotic chorionic villi), scalloping villus and round villus [9].

Immunohistochemical tests (IHC) are applied for stromal and cytotrophoblastic cells. P57 IHC cannot discriminate between a diploid non-molar hydropic abortion (HA), a partial hydatidiform mole, triploid digynic–monoandric gestations and a trisomy. In all these situations, maternal alleles are present. In this case, in order to increase the detection rate, complementary methods should be applied [17]. The short tandem repeat (STR) profile with the presence of paternal alleles in at least two loci establishes the diagnosis of a CHM [18].

The treatment in gestational trophoblastic disease is different depending on the classification in 1 of the 4 entities: hydatidiform mole, trophoblastic tumor, choriocarcinoma and invasive mole. The standard treatment includes combinations of chemotherapy, dilation and curettage, and hysterectomy. When choosing the treatment option, the woman’s wish to preserve her fertility will also be considered. In all cases, a post-treatment follow-up is necessary to exclude the recurrence of the disease. Management can be challenging in some cases. For example, there is no consensus regarding the application of a prophylactic treatment in cases of a hydatidiform mole with a risk of persistence of the disease or an attitude of following the levels of human chorionic gonadotropin and the application of treatment measures when the criteria of persistence of the disease are met [4].

**Objectives:** The main objectives of this review are to synthesize the heterogeneous mechanisms (chromosomal abnormality, uniparental disomy and monogenic variants) involved in the pathogenesis of the hydatidiform mole and their implications in genetic counselling.

## 2. Materials and Methods

This narrative review centers on the etiology of the hydatidiform mole and its connection to genetic factors. A comprehensive literature search was conducted through the PubMed and Web of Science/Clarivate Analytics databases. The search included articles published in the last 20 years, but we tried to select the most recent ones as research in the genetics field is continuously growing. Only articles available as full-text and in English have been included. The exclusion criteria were conference abstracts, editorials, non-English publications. The electronic search was conducted following different combinations of five keywords: hydatidiform mole, uniparental disomy, triploidy, androgenetic and monogenic variant.

### 3. Results and Discussion

#### 3.1. Mechanisms in Hydatidiform Mole

The mechanisms of the hydatidiform mole are different in the complete hydatidiform mole and in the partial hydatidiform mole. In the complete hydatidiform mole, a complete paternal uniparental disomy is implied. In a PHM, a form of polyploidy is present [2].

##### 3.1.1. Genetic Particularities of the Complete Hydatidiform Mole

In the case of a complete hydatidiform mole, the amount of genetic material is normal (with a diploid normal chromosomal formula 46,XX or 46,XY), but the origin of all chromosomes is only paternal. The 46,XX karyotype is identified in 90% of cases [19]. There are two possible mechanisms: endoreduplication and dispermia. In the first case, an enucleated egg is fertilized by a normal sperm, and then the genetic material of paternal origin is duplicated (15% of cases). In the second case, a fertilization error occurs: one enucleate oocyte is fertilized by two genetically normal sperms or by a diploid sperm (resulting from an error of male meiosis—diandry) (Figure 1). Another possible mechanism concerns an error of fertilization—dispermia—with the formation of a triploid embryo, followed by the loss of maternal genetic material [20]. In 15–25% of complete hydatidiform moles, the mechanism is dispermia [14]. Thus, in 80–90% of complete hydatidiform moles, there is a diploid androgenetic genome and, in 10–20%, the genetic contribution is biparental [2,11,21]. In cases with paternal origin, there are some abnormal genetic phenomena called paternal complete uniparental disomy, characterized by the presence of all chromosomal pairs with paternal uniparental origin.

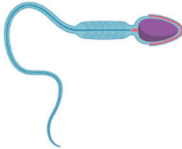



Other genetic changes implied in complete hydatidiform moles are the presence of a maternal mutation that affects imprinting in the offspring. In this situation, the genetic material has a biparental origin, with a normal 46,XX or 46,XY karyotype [20].

Genomic imprinting is an important event in normal embryonic development [22,23]. The phenomenon of parental or genomic imprinting involves epigenetic changes that allow a uniparental allelic expression, either maternal or paternal. The human genome contains about 200 imprinted genes, located on different chromosomes which represent less than 1% of all genes. Some imprinted genes have roles in growth, viability and physiological functions [23]. The *CDKN1C* gene (Cyclin-dependent kinase inhibitor 1C) (alias symbols P57; KIP2), located at 11p15.5, encodes p57<sup>KIP2</sup>, a Cyclin-dependent kinase inhibitor 1C (Cyclin-dependent kinase inhibitor p57). The chromosomal region 11p15.5 is one of the main chromosomal regions characterized by parental imprinting. The *CDKN1C* gene presents a paternal imprinting pattern and thus, normally, only the maternal allele is expressed [22,24]. The immunohistochemistry studies on embryonic tissues show a loss of p57<sup>KIP2</sup> staining in cytotrophoblast and villous stromal cells in CHMs that is concordant with the absence of this protein, generated by the absence of a maternal allele. On the other hand, P57<sup>KIP2</sup> immunohistochemistry in PHMs revealed no loss of p57 staining, confirming the presence of an active maternal allele [25].

##### 3.1.2. Chromosomal Abnormality—Triploidy

A partial hydatidiform mole is associated with a polyploid status in the embryo. Usually, there is a triploidy with a paternal extra haploid set of chromosomes. The triploidy is generated in the majority of cases by dispermia, while the rest are produced by a diandry. The most frequent chromosomal formula is 69,XXX karyotype (90% of cases) [19] (Figure 1). In a PHM, both parental genomes are expressed, but this expression is unbalanced with an excess of one of the genomes, maternal or paternal. This imbalance produces anomalies of development that concern the embryo and the placenta. Paternal triploidy is characterized by an abnormal development of the placenta, with the presence of a partial hydatidiform mole in association with relatively minor changes in the embryo (usually microcephaly) [5,19]. Other karyotypes (diploid biparental, triploid digenic, tetraploid triandric) have occasionally been identified [2].



Sperm	Egg		Zygote	Phenotype
				
23,X or 23,Y	23,X	→	46,XX or 46,XY	Normal
46,XX* (endoreduplication)		→	46,XX	CHM
23,X+23,X (dispermia)			46,XX	
23,X+23,Y (dispermia)			46,XY	
23,X+23,X (dispermia)	23,X	→	69,XXX	PHM
23,X+23,Y (dispermia)			69,XXY	
23,Y+23,Y (dispermia)			69,XYY	
46,XX or 46,YY (lack of separations of cells in 2 <sup>nd</sup> meiosis)			69,XXX or 69,XXY	

**Figure 1.** Main mechanisms in the hydatidiform mole: chromosomal abnormality and uniparental disomy. \* Result of endoreduplication of the paternal genome; blue—paternal genome; red—maternal genome; yellow—abnormal genetic material quantity/phenomena. Created with Biorender.com (accessed on 19 September 2023).

### 3.1.3. Monogenic Variants and Recurrent Hydatidiform Mole

A recurrent hydatidiform mole (RHM) is a rare form of the complete hydatidiform mole, being discovered in less of 1% of all cases of complete hydatidiform moles. This disorder is characterized by the occurrence of two or more molar pregnancies in the same patient [26]. RHMs can be isolated or familial. The isolated (sporadic) form is generated by a dispermic triploid or androgenetic diploid. In the familial forms, the origin is monogenic, and the embryonic genome is a biparental diploid [20].

Table 2 synthesizes genes involved in RHMs. The most common mutant variants concern the *NLRP7* gene (55% of cases) and the *KHDC3L* gene (5% of cases) [20].

**Table 2.** Genes involved in recurrent hydatidiform mole [20,27–29].

No	Approved/Alias (Previous), Gene Symbol	Approved Gene Name	Location	Approved Protein Name	Gene/Locus MIM Number	Gene Frequency
1	<i>NLRP7</i> / <i>PYPAF3</i> , <i>NOD12</i> , <i>PAN7</i> , <i>CLR19.4</i> ( <i>NALP7</i> )	NLR family pyrin domain containing 7	19q13.42	NACHT, LRR and PYD domains-containing protein 7	609661	55%
2	<i>KHDC3L</i> / <i>ECAT1</i> ( <i>C6orf221</i> )	KH domain containing 3 like, subcortical maternal complex member	6q13	KH domain-containing protein 3	611687	5%
3	<i>PADI6</i>	Peptidyl arginine deiminase 6	1p36.13	Protein-arginine deiminase type-6	610363	1%
4	<i>NLRP5</i> / <i>PYPAF8</i> , <i>MATER</i> . <i>PAN11</i> , <i>CLR19.8</i> ( <i>NALP5</i> )	NLR family pyrin domain containing 5	19q13.43	NACHT, LRR and PYD domains-containing protein 5	609658	0.5%
5	<i>MEI1</i> / <i>MGC4004.2</i> <i>SPATA38</i>	meiotic double-stranded break formation protein 1	22q13.2	Meiosis inhibitor protein 1	608797	0.5%
6	<i>TOP6BL</i> / <i>FLJ22531</i> , <i>TOPOVIBL</i> ( <i>C11orf80</i> )	TOP6B like initiator of meiotic double strand breaks	11q13.2	Type 2 DNA topoisomerase 6 subunit B-like	616109	0.5%
7	<i>REC114</i> / <i>LOC283677</i> , <i>FLJ27520</i> , <i>FLJ36860</i> , <i>FLJ44083</i> , <i>CT147</i> ( <i>C15orf60</i> )	REC114 meiotic recombination protein	15q24.1	Meiotic recombination protein REC114	618421	0.5%

In familial RHMs, the fertilization is normal, but the haploid ovum carries a mutation in either the *NLRP7* or *KHDC3L* gene. Both genes present a monoallelic pattern of expression, produced by parental imprinting. In cases with RHMs, there are mutations in the *NLRP7* or *KHDC3L* genes that produce an inactivation of the maternal allele. Thus, only the paternal allele remains active and its effect on the placenta is similar to that of a male monopaternal diploid genomic expression. Probably, *NLRP7* or *KHDC3L* mutations disrupt defective placental-specific imprinting mechanisms with an unbalanced expression between maternal and paternal alleles. Therefore, we see a biparental recurrent diploid CHM appear [2].

The *NLRP7* gene belongs to the NLR family gene. Members of this gene family are immunoregulatory proteins characterized by the presence of the NACHT nucleotide-binding domain (NBD) and leucine-rich repeats (LRRs). This family contains 25 genes with a role in inflammation and apoptosis [27,30]. *NLRP7* is the first gene whose mutations have been associated with RHMs in over 55% of cases [20]. The *NLRP7* gene is expressed in the oocyte's stages and the pre-implantation stages of the embryo, but also in the endometrium, placenta and hematopoietic cells. In the embryo, the protein level is different in different stages with a minimum in the blastocyst stage (day 3) and a sudden increase on days 3–5 [31]. Also, this protein has a crucial role in oocyte maturation and in placental development. *NLRP7* allows trophoblast proliferation but has a negative regulatory role in trophoblast differentiation. Thus, the abnormal level of *NLRP7* expression is associated with excessive trophoblast differentiation [32,33].

To date, more than 275 variants in the *NLRP7* gene have been identified. They are reported in the INFEVERS database. Figures 2 and 3 summarize the pathogenic and likely pathogenic variants in the *NLRP7* gene [34–38].

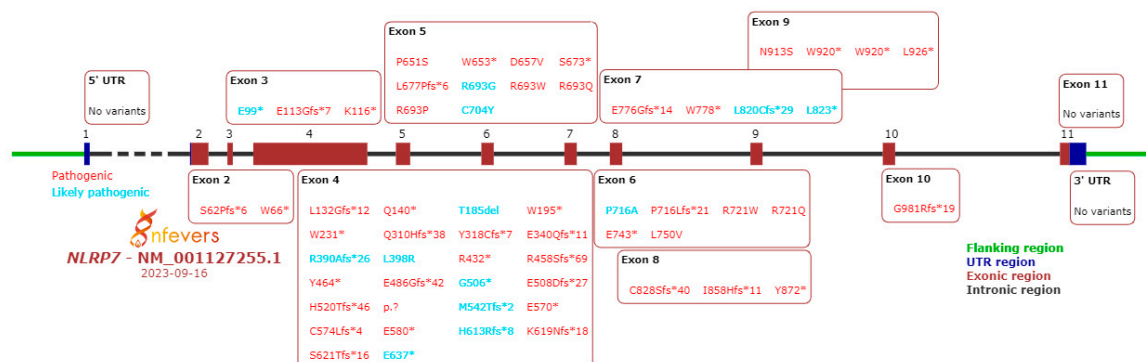


**Figure 2.** Pathogenic and likely pathogenic variants in *NLRP7* gene exons (“\*” name as first published/submitted to Infervers database).

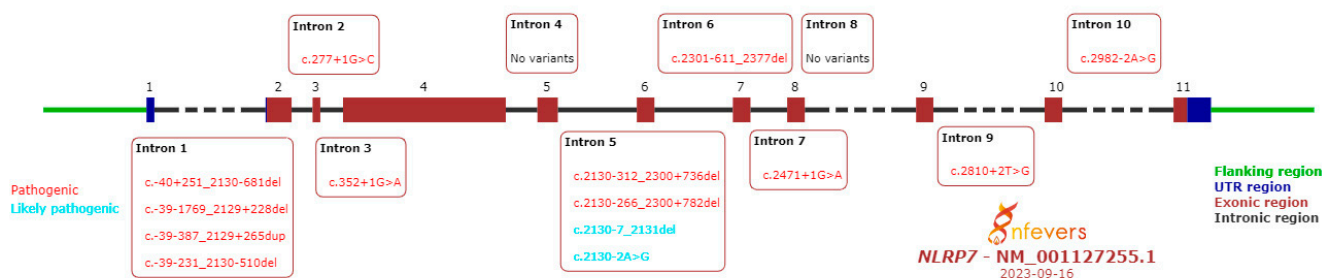


**Figure 3.** Pathogenic and likely pathogenic variants in *NLRP7* gene introns.

Slim et al. analyzed variants in the *NLRP7* gene. Thus, it was observed that there are variants associated with the disease in all exons except exon 11. The most frequent variants are p.Leu750Val (24%), p.Arg693Pro (8.8%) and p.Leu825\* (5%). Most variants (73.2%) determined the truncation of the protein and, in 26.7% of cases, they are missense variants. The distribution of these two types of variants is different: protein-truncating variants are dispersed throughout the gene, while missense variants are found especially in the leucine-rich repeat. Protein-truncating variants have a more severe phenotypic effect. Some missense variants are not pathogenic and their presence was associated with normal pregnancy [20]. Some of the mutations of the *NLRP7* gene are characterized by a founder effect. Thus, p.Leu750Val (79% of the alleles) and p.Arg937\_Leu938ins54 are specific to Mexicans cases, p.Arg693Trp are frequent in Caucasians and Turks, p.Arg693Trp represents 39% of the mutant alleles in the Indo-Pakistani population, p.Arg693Gln is characteristic of the Chinese population, while p.Glu710Aspfs (32% of the alleles) was found in Egyptians [20,39].

Pathogenic variants in the *NLRP7* gene can induce diploid biparental molar conception, early embryo cleavage abnormalities, non-molar abortions, stillbirths and intrauterine growth retardation [40–43].

The androgenetic CHMs and the diploid biparental mole determined by *NLRP7* variants have the same phenotype. The difference is that in the second situation, the phenotype is the milder one [20].

The *KHDC3L* gene encodes KH domain-containing protein 3. Transcripts of this gene have been highlighted in hematopoietic cells, all oocytes' stages and preimplantation embryos that play a role in the development of the ovaries and embryo [31,44]. Like *NLRP7*, KH domain-containing protein 3 is a constituent of the oocyte cytoskeleton located mainly in the cortical region [45]. Mutations in the *KHDC3L* gene cause an abnormal development of oocytes and molar pregnancies after fertilization [31,44].

The *PADI6* gene is another maternal-effect gene. It encodes an enzyme called protein-arginine deiminase type-6 involved in citrullination. Citrullination (deamination) represents the conversion of the arginine into citrulline, the post-translational process taking place in a protein. This process plays a role in the formation of rigid structures (e.g., hair, skin) and is also a member of the subcortical maternal complex [46]. Recessive variants in *PADI6* genes have been associated with primary female infertility, with an early arrest during embryonic stages after ART (Assisted Reproductive Technology) and with a hydatidiform mole [46–48]. Missense variants and protein-truncating variants have been described, the first with milder effects than the last. Missense variants allow the stopping of the evolution after blastocyte implantation and differentiation [46].

The coexistence of molar changes with an apparently unaffected fetus is an atypical phenomenon within the familial recurrent hydatidiform mole cases. Overall, the maternal and fetal prognosis, in molar pregnancies accompanied by a viable fetus, is unfavorable [5].

Nguyen and Slim proposed an algorithm for DNA testing and the subsequent genetic counselling of patients with recurrent HM. Patients with at least two HM should be tested first for mutations in the *NLRP7* gene. If the testing is positive for biallelic mutations, genetic advice is given as follows: 7% may have a normal live birth (LB), while another possibility is ovum donation. If the *NLRP7* mutation analysis is negative, the next step is *KHDC3L* testing. If the test is positive, the genetic counseling is the same. If the *KHDC3L* testing is negative, it is recommended to review the histopathology and to establish their parental distribution. For the cases with two CHM biparental diploids, the genetic counselling is the same as in the previous cases. For cases with androgenetic diploids or dispermic triploids, the chances of getting an LB from one's own eggs are high, and ART increases the chances of an LB [31].

### 3.2. Risk Factors for Hydatidiform Mole and Progression to GTN

#### 3.2.1. Risk Factors for Hydatidiform Mole

Several risk factors have been implicated in elevating the prevalence of molar pregnancies. The risk factors are represented by age, ethnicity, antecedent molar pregnancies and family history [4]. Among the extensively researched factors, the extremes of maternal age are the most well-known factor, particularly maternal age below 20 years and over 35 years old; the latter confers a risk escalation ranging from fivefold to tenfold [2,6,8]. Triploidy resulting from fertilization between a diploid sperm (generated by diandry) and a normal egg is more common in young patients [2].

The risk profile of a complete hydatidiform mole exhibits notable variations in response to age changes. In contrast, the risk associated with a partial hydatidiform mole appears to display relatively minor fluctuations in conjunction with age, while it does not exhibit heightened occurrence among adolescents [2,7,36]. These observations are in concordance with the hypothesis that the process leading to molar pregnancy, stemming from fertilization of an aberrant oocyte, is more prone to manifest at the extremes of reproductive age. This could be attributed to higher chances of ovulating an empty ovum due to reproductive immaturity or senescence, as opposed to the probability of abnormal fertilization by two sperms [36]. While there are well-documented associations between chromosome anomalies and advanced maternal age, instances of chromosome defects in oocytes of adolescents have not been identified [7].

Additionally, antecedent molar pregnancies contribute to an increased risk of 1 to 2% for future pregnancies [6,8]. The likelihood of recurrence is on the rise with every previous molar gestation and reaches an apex in the second year after the initial event [10]. The probability of encountering a third molar pregnancy experiences a notable surge to approximately 15–20%, remaining unaffected by changes in partners, and possibly retaining a connection to either familial or sporadic instances of biparental molar disease [2]. It should be noted that patients with a partial hydatidiform mole are more likely to develop another one, as opposed to patients with a complete hydatidiform mole [10]. A woman

with a previous pregnancy with a hydatidiform mole will have a 10–20% risk of having a pregnancy loss from a non-molar cause [32].

The impact of race/ethnicity on the development of molar pregnancies has also been subject to investigation. Multiple studies indicated that Asian women manifest the most pronounced susceptibility for complete moles, being over twice as likely as the white population to develop them, while concurrently displaying a diminished propensity for the development of partial moles. Furthermore, a diminished proclivity for partial mole occurrence was noted among Hispanic and black women in relation to white women [37].

Further contributing to the risk profile are factors encompassing a medical history characterized by previous instances of spontaneous abortions or infertility, dietary considerations (encompassing deficiencies in carotene and animal fats), smoking, blood group B, paternal age, maternal genetic anomalies and oral contraceptives [2,8,10]. Deficiencies in vitamins A and B9 during the first gestational weeks could deteriorate the oocytes' differentiation in female fetuses. The insufficiency of vitamin A leads to an incomplete development of oocytes and prevents the accurate progression of meiosis II. Folate deficiencies disturb the normal proteins and DNA synthesis, which have an impact on the differentiation of the oocyte and zygote, and, additionally, they influence the instability of maternal-origin chromosomes. Both vitamin A and folates also intervene in the DNA methylation process. These methylation irregularities impact the imprinted genes within the oocyte, where the maternal methylation vanishes and is substituted by the paternal one. This phenomenon explains why affected women may develop an HM with different partners [2,49].

### 3.2.2. Risk of GTN Progression

The placenta has its origin in the two layers of the blastocyst (cytotrophoblast and syncytiotrophoblast) associated with extra-embryonic mesoderms [2]. The hydatidiform mole is a particular condition because it originates in gestational tissue rather than maternal tissue [8]. The hydatidiform mole is in most cases benign but can become malignant and invasive [4,8]. The risk of GTN progression is different in the two forms of hydatidiform moles: 15–20% for CHMs and 0.5–1% for PHMs [25,50]. Several risk factors have been identified in correlation with the increased risk of GTN: elevated levels of hCG (over 100,000 mIU/mL), a uterus size larger than normal for gestational age and large cysts of theca lutein. Maternal age has been associated with a 3-fold risk of GTN if exceeding 50 years [51].

Since it is known that microRNA molecules are involved in various stages in the pathogenesis of cancers, the question naturally arises whether there are microRNAs involved in the progression to GTN, a hypothesis that has been the subject of several studies. A microRNA profile associated with the risk of progression to GTN was involved in complete hydatidiform moles [51].

One such factor is represented by the members of the miR-181 family. It appears that they are well expressed in the moles that will become complicated with GTN. Their function is to inhibit the expression of Apoptosis regulator Bet-2. This protein (encoded by *BCL2* genes) plays a role in suppressing apoptosis, it regulates cell death and it acts as an inhibitor of autophagy [27,28]. In the complete moles that progress to GTN, these proteins have very low levels [51].

Zhao et al. analyzed a number of microRNA molecules and identified a profile of six microRNAs with varying expression in GTN and hydatidiform moles that do not progress to GTN: miR-370-3p, miR-371a-5p, miR-518a-3p, miR-519d-3p, miR-520a3p and miR-934. The authors showed the involvement of miR-371a-5p and miR-518a-3p in the proliferation, the migration and the invasion of choriocarcinoma cells. miR-371a-5p correlated negatively with proteins encoded by the following genes: *BCCIP* (BRCA2 and CDKN1A interacting protein), *SOX2* (SRY-box transcription factor 2) and *BNIP3L* (BCL2 interacting protein 3 like). miR-518a-3p negatively correlated with proteins encoded by *MST1* (macrophage stimulating 1) and *EFNA4* (ephrin A4) [52].

The strengths of the review are the inclusion of information about various characteristics of the disease, not just the genetic part, and the highlighting of the mechanisms in correlation with the risk factors for hydatidiform moles and progression to GTN. Potential limitations of this review could be the lack of articles relevant to the topic but not identified by the search strategy. Another limitation is the paucity of studies focused on cytogenetics or molecular genetics of the hydatidiform mole.

#### 4. Conclusions

Although it is a rare pathology, the hydatidiform mole is important due to its genetic heterogeneity. In this context, for proper subsequent management, it is desirable to establish the type of mole and the mechanism of its occurrence. Hydatidiform moles can be diagnosed using histopathological criteria, but in the cases of early pregnancy/borderline/difficult cases, cytogenetic techniques and, more recently, molecular biology techniques play a special role in diagnosis. The correct management is desirable to avoid the situation in which treatment is not given/an insufficient treatment is given in those cases that have a high malignant potential. Also, this approach avoids cases in which an unjustified excess treatment is given for low-risk lesions. The gestational history in conjunction with the diagnosis of the type of mole can direct the management towards testing for mutations in *NLRP7* or *KHDC3L* genes. Patients who had androgenetic and triploid dispermic moles could benefit from in vitro fertilization and preimplantation genetic screening.

The identification and knowledge of mutational mechanisms (chromosomal/genic), as well as the extension of research on the involvement of epigenetic factors in the pathogenesis of hydatidiform moles, is a prerequisite for validating diagnostic and prognostic biomarkers in various types of HM. This way, it will be possible to apply a personalized treatment associated with general management, a part of personalized medicine.

**Author Contributions:** Conceptualization, A.F., L.C. and E.V.G.; formal analysis, A.-M.G., L.-M.A. and M.I.G.; resources, A.-M.G., L.-M.A. and M.I.G.; writing—original draft preparation, A.F. and L.C.; writing—review and editing, A.F., L.C., M.G. and E.V.G.; visualization, A.F., L.C., E.V.G. and M.G.; supervision, E.V.G. All authors have read and agreed to the published version of the manuscript.

**Funding:** This research received no external funding.

**Institutional Review Board Statement:** Not applicable.

**Informed Consent Statement:** Not applicable.

**Data Availability Statement:** Not applicable.

**Conflicts of Interest:** The authors declare no conflict of interest.

#### References

1. Beltrão, M.; Mota, M.; Bacha, E.; Barros, L.; Brandão, L.; Mascarenhas, N.; Silva, T.; Souza, M.; Braga, S.; Borges, V. Management of Gestational Trophoblast Disease: An Integrative Review of National and International Guidelines. *Health* **2022**, *14*, 1321–1333. [CrossRef]
2. Candelier, J.J. The hydatidiform mole. *Cell Adhes. Migr.* **2016**, *10*, 226–235. [CrossRef] [PubMed]
3. Kawasaki, K.; Kondoh, E.; Minamiguchi, S.; Matsuda, F.; Higasa, K.; Fujita, K.; Mogami, H.; Chigusa, Y.; Konishi, I. Live-born diploid fetus complicated with partial molar pregnancy presenting with pre-eclampsia, maternal anemia, and seemingly huge placenta: A rare case of confined placental mosaicism and literature review. *J. Obstet. Gynaecol. Res.* **2016**, *42*, 911–917. [CrossRef]
4. Ning, F.; Hou, H.; Morse, A.N.; Lash, G.E. Understanding and management of gestational trophoblastic disease. *F1000Research* **2019**, *8*, 428. [CrossRef] [PubMed]
5. Hemida, R.; Khashaba, E.; Zalata, K. Molar pregnancy with a coexisting living fetus: A case series. *BMC Pregnancy Childbirth* **2022**, *22*, 681. [CrossRef] [PubMed]
6. Tantengco, O.A.G.; De Jesus, F.C.C., II; Gampoy, E.F.S.; Ornos, E.D.B.; Vidal, M.S., Jr.; Cagayan, M. Molar pregnancy in the last 50 years: A bibliometric analysis of global research output. *Placenta* **2021**, *112*, 54–61. [CrossRef]
7. Soares, R.R.; Maesta, I.; Colon, J.; Braga, A.; Salazar, A.; Charry, R.C.; Sun, S.Y.; Goldstein, D.P.; Berkowitz, R.S. Complete molar pregnancy in adolescents from North and South America: Clinical presentation and risk of gestational trophoblastic neoplasia. *Gynecol. Oncol.* **2016**, *142*, 496–500. [CrossRef]

8. Ghassemzadeh, S.; Farci, F.; Kang, M. Hydatidiform Mole. Available online: <https://www.ncbi.nlm.nih.gov/pubmed/29083593> (accessed on 22 July 2023).
9. Sarmadi, S.; Izadi-Mood, N.; Sanii, S.; Motevalli, D. Inter-observer variability in the histologic criteria of diagnosis of hydatidiform moles. *Malays. J. Pathol.* **2019**, *41*, 15–24.
10. Eagles, N.; Sebire, N.J.; Short, D.; Savage, P.M.; Seckl, M.J.; Fisher, R.A. Risk of recurrent molar pregnancies following complete and partial hydatidiform moles. *Hum. Reprod.* **2015**, *30*, 2055–2063. [CrossRef]
11. Lurain, J.R. Gestational trophoblastic disease I: Epidemiology, pathology, clinical presentation and diagnosis of gestational trophoblastic disease, and management of hydatidiform mole. *Am. J. Obstet. Gynecol.* **2010**, *203*, 531–539. [CrossRef]
12. Libretti, A.; Longo, D.; Faiola, S.; De Pedrini, A.; Troia, L.; Remorgida, V. A twin pregnancy with partial hydatidiform mole and a coexisting normal fetus delivered at term: A case report and literature review. *Case Rep. Women's Health* **2023**, *39*, e00544. [CrossRef]
13. Suksai, M.; Suwanrath, C.; Kor-Anantakul, O.; Geater, A.; Hanprasertpong, T.; Atjimakul, T.; Pichatechaiyoot, A. Complete hydatidiform mole with co-existing fetus: Predictors of live birth. *Eur. J. Obstet. Gynecol. Reprod. Biol.* **2017**, *212*, 1–8. [CrossRef]
14. Fisher, R.A.; Maher, G.J. Genetics of gestational trophoblastic disease. *Best Pract. Res. Clin. Obstet. Gynaecol.* **2021**, *74*, 29–41. [CrossRef]
15. Vang, R.; Gupta, M.; Wu, L.S.; Yemelyanova, A.V.; Kurman, R.J.; Murphy, K.M.; Descipio, C.; Ronnett, B.M. Diagnostic reproducibility of hydatidiform moles: Ancillary techniques (p57 immunohistochemistry and molecular genotyping) improve morphologic diagnosis. *Am. J. Surg. Pathol.* **2012**, *36*, 443–453. [CrossRef] [PubMed]
16. Hui, P.; Buza, N.; Murphy, K.M.; Ronnett, B.M. Hydatidiform Moles: Genetic Basis and Precision Diagnosis. *Annu. Rev. Pathol.* **2017**, *12*, 449–485. [CrossRef] [PubMed]
17. Meng, Y.; Yang, X.; Yin, H. Application of short tandem repeat (STR) genotyping in partial hydatidiform mole. *Am. J. Transl. Res.* **2023**, *15*, 3731–3738.
18. Murphy, K.M.; McConnell, T.G.; Hafez, M.J.; Vang, R.; Ronnett, B.M. Molecular genotyping of hydatidiform moles: Analytic validation of a multiplex short tandem repeat assay. *J. Mol. Diagn.* **2009**, *11*, 598–605. [CrossRef]
19. Capozzi, V.A.; Butera, D.; Armano, G.; Monfardini, L.; Gaiano, M.; Gambino, G.; Sozzi, G.; Merisio, C.; Berretta, R. Obstetrics outcomes after complete and partial molar pregnancy: Review of the literature and meta-analysis. *Eur. J. Obstet. Gynecol. Reprod. Biol.* **2021**, *259*, 18–25. [CrossRef]
20. Slim, R.; Fisher, R.; Milhavet, F.; Hemida, R.; Rojas, S.; Rittore, C.; Bagga, R.; Aguinaga, M.; Touitou, I. Biallelic NLRP7 variants in patients with recurrent hydatidiform mole: A review and expert consensus. *Hum. Mutat.* **2022**, *43*, 1732–1744. [CrossRef] [PubMed]
21. Slim, R.; Mehio, A. The genetics of hydatidiform moles: New lights on an ancient disease. *Clin. Genet.* **2007**, *71*, 25–34. [CrossRef]
22. Creff, J.; Besson, A. Functional Versatility of the CDK Inhibitor p57(Kip2). *Front. Cell Dev. Biol.* **2020**, *8*, 584590. [CrossRef]
23. Tucci, V.; Isles, A.R.; Kelsey, G.; Ferguson-Smith, A.C.; Erice Imprinting, G. Genomic Imprinting and Physiological Processes in Mammals. *Cell* **2019**, *176*, 952–965. [CrossRef]
24. Chia, W.K.; Chia, P.Y.; Abdul Aziz, N.H.; Shuib, S.; Mustangin, M.; Cheah, Y.K.; Khong, T.Y.; Wong, Y.P.; Tan, G.C. Diagnostic Utility of TSSC3 and RB1 Immunohistochemistry in Hydatidiform Mole. *Int. J. Mol. Sci.* **2023**, *24*, 9656. [CrossRef] [PubMed]
25. Joyce, C.M.; Fitzgerald, B.; McCarthy, T.V.; Coulter, J.; O'Donoghue, K. Advances in the diagnosis and early management of gestational trophoblastic disease. *BMJ Med.* **2022**, *1*, e000321. [CrossRef]
26. Kalogiannidis, I.; Kalinderi, K.; Kalinderis, M.; Miliaras, D.; Tarlatzis, B.; Athanasiadis, A. Recurrent complete hydatidiform mole: Where we are, is there a safe gestational horizon? Opinion and mini-review. *J. Assist. Reprod. Genet.* **2018**, *35*, 967–973. [CrossRef]
27. HGNC. HUGO Gene Nomenclature Committee Home Page. Available online: <http://www.genenames.org/> (accessed on 15 July 2023).
28. UniProt: The Universal Protein Knowledgebase in 2023. Available online: <https://www.uniprot.org/> (accessed on 29 July 2023).
29. Online Mendelian Inheritance in Man, OMIM. Available online: <https://omim.org/> (accessed on 15 August 2023).
30. Nguyen, N.M.P.; Ge, Z.J.; Reddy, R.; Fahiminiya, S.; Sauthier, P.; Bagga, R.; Sahin, F.I.; Mahadevan, S.; Osmond, M.; Breguet, M.; et al. Causative Mutations and Mechanism of Androgenetic Hydatidiform Moles. *Am. J. Hum. Genet.* **2018**, *103*, 740–751. [CrossRef]
31. Nguyen, N.M.; Slim, R. Genetics and Epigenetics of Recurrent Hydatidiform Moles: Basic Science and Genetic Counselling. *Curr. Obstet. Gynecol. Rep.* **2014**, *3*, 55–64. [CrossRef]
32. Abi Nahed, R.; Reynaud, D.; Borg, A.J.; Traboulsi, W.; Wetzel, A.; Sapin, V.; Brouillet, S.; Dieudonné, M.N.; Dakouane-Giudicelli, M.; Benharouga, M.; et al. NLRP7 is increased in human idiopathic fetal growth restriction and plays a critical role in trophoblast differentiation. *J. Mol. Med.* **2019**, *97*, 355–367. [CrossRef]
33. Carriere, J.; Dorfleutner, A.; Stehlik, C. NLRP7: From inflammasome regulation to human disease. *Immunology* **2021**, *163*, 363–376. [CrossRef]
34. Infevers: An Online Database for Autoinflammatory Mutations. Copyright. Available online: <https://infevers.umai-montpellier.fr/> (accessed on 16 September 2023).
35. Milhavet, F.; Cuisset, L.; Hoffman, H.M.; Slim, R.; El-Shanti, H.; Aksentijevich, I.; Lesage, S.; Waterham, H.; Wise, C.; Sarrauste de Menthiere, C.; et al. The infevers autoinflammatory mutation online registry: Update with new genes and functions. *Hum. Mutat.* **2008**, *29*, 803–808. [CrossRef]

36. Sarrauste de Menthier, C.; Terriere, S.; Pugner, D.; Ruiz, M.; Demaille, J.; Touitou, I. INFEVERS: The Registry for FMF and hereditary inflammatory disorders mutations. *Nucleic Acids Res.* **2003**, *31*, 282–285. [CrossRef]
37. Touitou, I.; Lesage, S.; McDermott, M.; Cuisset, L.; Hoffman, H.; Dode, C.; Shoham, N.; Aganna, E.; Hugot, J.P.; Wise, C.; et al. Infevers: An evolving mutation database for auto-inflammatory syndromes. *Hum. Mutat.* **2004**, *24*, 194–198. [CrossRef]
38. Van Gijn, M.E.; Ceccherini, I.; Shinar, Y.; Carbo, E.C.; Slofstra, M.; Arostegui, J.I.; Sarabay, G.; Rowczenio, D.; Omoyimni, E.; Balci-Peynircioglu, B.; et al. New workflow for classification of genetic variants' pathogenicity applied to hereditary recurrent fevers by the International Study Group for Systemic Autoinflammatory Diseases (INSAID). *J. Med. Genet.* **2018**, *55*, 530–537. [CrossRef]
39. Aguinaga, M.; Rezaei, M.; Monroy, I.; Mechtouf, N.; Perez, J.; Moreno, E.; Valdespino, Y.; Galaz, C.; Razo, G.; Medina, D.; et al. The genetics of recurrent hydatidiform moles in Mexico: Further evidence of a strong founder effect for one mutation in NLRP7 and its widespread. *J. Assist. Reprod. Genet.* **2021**, *38*, 1879–1886. [CrossRef]
40. Andreasen, L.; Christiansen, O.B.; Niemann, I.; Bolund, L.; Sunde, L. NLRP7 or KHDC3L genes and the etiology of molar pregnancies and recurrent miscarriage. *Mol. Hum. Reprod.* **2013**, *19*, 773–781. [CrossRef]
41. Deveault, C.; Qian, J.H.; Chebaro, W.; Ao, A.; Gilbert, L.; Mehio, A.; Khan, R.; Tan, S.L.; Wischmeijer, A.; Coullin, P.; et al. NLRP7 mutations in women with diploid androgenetic and triploid moles: A proposed mechanism for mole formation. *Hum. Mol. Genet.* **2009**, *18*, 888–897. [CrossRef]
42. Dixon, P.H.; Trongwongsa, P.; Abu-Hayyah, S.; Ng, S.H.; Akbar, S.A.; Khawaja, N.P.; Seckl, M.J.; Savage, P.M.; Fisher, R.A. Mutations in NLRP7 are associated with diploid biparental hydatidiform moles, but not androgenetic complete moles. *J. Med. Genet.* **2012**, *49*, 206–211. [CrossRef] [PubMed]
43. Messaied, C.; Chebaro, W.; Di Roberto, R.B.; Rittore, C.; Cheung, A.; Arseneau, J.; Schneider, A.; Chen, M.F.; Bernishke, K.; Surti, U.; et al. NLRP7 in the spectrum of reproductive wastage: Rare non-synonymous variants confer genetic susceptibility to recurrent reproductive wastage. *J. Med. Genet.* **2011**, *48*, 540–548. [CrossRef] [PubMed]
44. Laviola, G.M.; Fortini, A.S.; Salles, D.; da Silva Lourenco, C.; Ribeiro, D.A.; Sun, S.Y.; Ishigai, M.M.; Iwamura, E.S.M.; Alves, M.T.S.; Malinverni, A.C.M. Complementary tool in diagnosis of hydatidiform mole: Review. *Pathol. Res. Pract.* **2022**, *237*, 154041. [CrossRef] [PubMed]
45. Moein-Vaziri, N.; Fallahi, J.; Namavar-Jahromi, B.; Fardaei, M.; Momtahan, M.; Anvar, Z. Clinical and genetic-epigenetic aspects of recurrent hydatidiform mole: A review of literature. *Taiwan. J. Obstet. Gynecol.* **2018**, *57*, 1–6. [CrossRef]
46. Qian, J.; Nguyen, N.M.P.; Rezaei, M.; Huang, B.; Tao, Y.; Zhang, X.; Cheng, Q.; Yang, H.; Asangla, A.; Majewski, J.; et al. Biallelic PADI6 variants linking infertility, miscarriages, and hydatidiform moles. *Eur. J. Hum. Genet.* **2018**, *26*, 1007–1013. [CrossRef]
47. Maddirevula, S.; Coskun, S.; Awartani, K.; Alsaif, H.; Abdulwahab, F.M.; Alkuraya, F.S. The human knockout phenotype of PADI6 is female sterility caused by cleavage failure of their fertilized eggs. *Clin. Genet.* **2017**, *91*, 344–345. [CrossRef]
48. Xu, Y.; Shi, Y.; Fu, J.; Yu, M.; Feng, R.; Sang, Q.; Liang, B.; Chen, B.; Qu, R.; Li, B.; et al. Mutations in PADI6 Cause Female Infertility Characterized by Early Embryonic Arrest. *Am. J. Hum. Genet.* **2016**, *99*, 744–752. [CrossRef] [PubMed]
49. Anvar, Z.; Chakchouk, I.; Demond, H.; Sharif, M.; Kelsey, G.; Van den Veyver, I.B. DNA Methylation Dynamics in the Female Germline and Maternal-Effect Mutations That Disrupt Genomic Imprinting. *Genes* **2021**, *12*, 1214. [CrossRef]
50. Seckl, M.J.; Sebire, N.J.; Berkowitz, R.S. Gestational trophoblastic disease. *Lancet* **2010**, *376*, 717–729. [CrossRef] [PubMed]
51. Lin, L.H.; Maestá, I.; St Laurent, J.D.; Hasselblatt, K.T.; Horowitz, N.S.; Goldstein, D.P.; Quade, B.J.; Sun, S.Y.; Braga, A.; Fisher, R.A.; et al. Distinct microRNA profiles for complete hydatidiform moles at risk of malignant progression. *Am. J. Obstet. Gynecol.* **2021**, *224*, 372.e1–372.e30. [CrossRef] [PubMed]
52. Zhao, J.R.; Cheng, W.W.; Wang, Y.X.; Cai, M.; Wu, W.B.; Zhang, H.J. Identification of microRNA signature in the progression of gestational trophoblastic disease. *Cell Death Dis.* **2018**, *9*, 94. [CrossRef]

**Disclaimer/Publisher's Note:** The statements, opinions and data contained in all publications are solely those of the individual author(s) and contributor(s) and not of MDPI and/or the editor(s). MDPI and/or the editor(s) disclaim responsibility for any injury to people or property resulting from any ideas, methods, instructions or products referred to in the content.



Review

# The Task Matters: A Comprehensive Review and Proposed Literature Score of the Effects of Chemical and Physical Parameters on Embryo Developmental Competence

Alessandro Bartolacci <sup>1,\*</sup>, Francesca Tondo <sup>2</sup>, Alessandra Alteri <sup>1</sup>, Lisett Solano Narduche <sup>3</sup>, Sofia de Girolamo <sup>1</sup>, Giulia D'Alessandro <sup>1</sup>, Elisa Rabellotti <sup>1</sup>, Enrico Papaleo <sup>1</sup> and Luca Pagliardini <sup>3</sup>

- <sup>1</sup> Obstetrics and Gynaecology Unit, IRCCS San Raffaele Scientific Institute, Via Olgettina, 60, 20132 Milan, Italy; alteri.alessandra@hsr.it (A.A.); degirolamo.sofia@hsr.it (S.d.G.); dalessandro.giulia@hsr.it (G.D.); rabellotti.elisa@hsr.it (E.R.); papaleo.enrico@hsr.it (E.P.)
- <sup>2</sup> Infertility Unit, Fondazione IRCCS Ca' Granda Ospedale Maggiore Policlinico, 20122 Milan, Italy; francesca.tondo@policlinico.mi.it
- <sup>3</sup> Reproductive Sciences Laboratory, Obstetrics and Gynaecology Unit, IRCCS San Raffaele Scientific Institute, Via Olgettina 60, 20132 Milan, Italy; solano.lisett@hsr.it (L.S.N.); pagliardini.luca@hsr.it (L.P.)
- \* Correspondence: bartolacci.alessandr@hsr.it

**Abstract:** To explore the effects of chemical and physical parameters on embryo developmental competence, we conducted a systematic search on PubMed for peer-reviewed original papers using specific keywords and medical subject heading terms. Studies of interest were selected from an initial cohort of 4141 potentially relevant records retrieved. The most relevant publications were critically evaluated to identify the effect of these parameters on embryo development. Moreover, we generated a literature score (LS) using the following procedure: (i) the number of studies favoring a reference group was expressed as a fraction of all analyzed papers; (ii) the obtained fraction was multiplied by 10 and converted into a decimal number. We identified and discussed six parameters (oxygen, temperature, humidity, oil overlay, light, pH). Moreover, we generated a LS according to five different comparisons (37 °C vs. <37 °C; 5% vs. 20% oxygen; 5–2% vs. 5% oxygen; humidity conditions vs. dry conditions; light exposure vs. reduced/protected light exposure). Only two comparisons (37 °C vs. <37 °C and 5% vs. 20% oxygen) yielded a medium-high LS (8.3 and 7, respectively), suggesting a prevalence of studies in favor of the reference group (37 °C and 5% oxygen). In summary, this review and LS methodology offer semi-quantitative information on studies investigating the effects of chemical and physical parameters on embryo developmental competence.

**Keywords:** temperature; oxygen; humidity; light; oil overlay; pH; embryo development; IVF outcomes

## 1. Introduction

In the field of assisted reproductive technology (ART), human embryo culture plays a pivotal role in the success of in vitro fertilization (IVF) treatments. The delicate and intricate nature of preimplantation human development demands a meticulously controlled environment. During human embryo culture, chemical and physical parameters play a crucial role in embryo development and viability [1–3]. These parameters encompass a range of environmental conditions, including temperature, oxygen concentration, humidity conditions (HC), the use of oil overlay, and light exposure, all of which are carefully regulated within the laboratory setting. Moreover, these parameters directly influence the embryo metabolic activities [4–18]. It is well established that temperature ensures proper enzymatic reactions and cellular functions [4]. In addition, oxygen plays a vital role in supporting embryo metabolism and development [5]. While a consensus has been reached regarding the utilization of 5% oxygen levels compared to atmospheric levels (20%) [6],

conflicting results have emerged when employing biphasic oxygen conditions (5–2%). Although the use of biphasic oxygen conditions appears to offer advantages in terms of blastulation, inconsistent findings have been reported in relation to clinical pregnancy [7,8].

Oil overlay has several important functions and benefits: (i) gas exchange, (ii) temperature stability, (iii) pH regulation, (iv) preventing contamination, and (v) minimizing disturbance. The inherent chemical and physical properties of the oil exert a significant influence on this vital aspect. These properties play a crucial role in shaping and determining the outcome, emphasizing the importance of understanding and considering them when working with human embryo culture [9]. Light exposure during mammalian embryo culture has garnered significant interest. However, despite several investigations, the impact of light on embryos remains a subject of ongoing debate, with inconclusive findings [10,11]. Recently, due to the introduction of dry incubators, several studies have investigated the impact of humidity conditions (HC) and dry conditions (DC) on IVF outcomes. While basic research studies show increased osmolality in culture medium under DC [12–14], these conditions do not seem to have negative effects on biological and clinical outcomes such as blastulation and pregnancy rates [16,17]. By carefully controlling these parameters, embryologists create an environment that mimics the natural conditions required for healthy embryo development. Nevertheless, despite these efforts, our culture conditions are unlikely to mirror precisely the dynamic environment experienced by embryos *in vivo*. Concerns exist that sub-optimal culture conditions could affect embryo developmental competence. Therefore, the meticulous quality control of these parameters is critical in maximizing the efficiency of our treatments. This comprehensive review explores the effects of chemical and physical parameters on mammalian embryo culture and their crucial roles in enhancing embryo development, implantation potential, and the overall success rates of IVF procedures.

## 2. Materials and Methods

### 2.1. Literature Search Methodology

A systematic search was conducted on PubMed to identify peer-reviewed original research articles related to the effects of chemical and physical parameters on development and clinical outcomes. The search strategy involved using relevant keywords and Medical Subject Heading (MeSH) terms. These keywords and Mesh terms were combined in various overlapping combinations to ensure the identification of publications specifically relevant to the topic: (“temperature” OR “oxygen” OR “humidity” OR “oil overlays” OR “light” OR “pH”) AND (“embryo quality” OR “IVF outcomes” OR “pregnancy” OR “live birth”). Furthermore, additional studies were identified by meticulously examining the reference lists of the selected publications. Full manuscripts were obtained for all the selected papers, and a thorough evaluation of the articles was conducted to make a final decision regarding their inclusion in the review. The most relevant publications, *i.e.*, those concerning the effects of chemical and physical parameters on embryo development, as well as clinical outcome, were critically evaluated and discussed.

### 2.2. Study Selection

Two reviewers (AB and FT) independently assessed all studies for inclusion or exclusion. Disagreements were solved in discussion with a last author (LP). During the first screening, titles and abstracts were investigated and studies with a lack of any relevance were excluded; review articles were also excluded (Figure 1). The remaining articles were retrieved in their full length and assessed according to the eligibility criteria. The following information of such studies was collected: first author’s last name, year of publication, research objective, design of the study, outcomes investigated, and conclusions. No time restrictions were applied. Full-length articles were considered eligible if written in English. Data extraction was performed in 62 papers. A summary of the extraction results is shown in Table 1. In the following step, we generated a literature score (LS) using 4 parameters (oxygen, temperature, humidity and light) and 5 different comparisons [37 °C vs. <37 °C;

5% vs. 20% oxygen; biphasic oxygen (5–2%) vs. 5% oxygen; HC vs. DC; light exposure (LE) vs. reduced/protected LE]. The reference groups identified were HC for humidity, 37 °C for the temperature, LE for light, 5% and 5–2% for low vs. atmospheric (5% vs. 20%) and biphasic vs. monophasic (5–2% vs. 5%) oxygen, respectively. The LS was obtained from the percentage of papers reporting a positive correlation [improved outcomes for temperature, humidity, and oxygen (5% in 20% vs. 5% comparison and 5–2% in 5% vs. 5–2% comparison)] or negative correlation (compromised outcomes for LE) between a specific reference group and at least one biological/clinical outcome, as described below. Specifically, this score was calculated using the following procedure: (i) the number of studies favoring a specific reference group was expressed as a fraction of all analyzed papers; (ii) the obtained fraction was multiplied by 10 and converted into a decimal number. A score ranging from 1 to 5 indicates no evidence, 6 indicates low evidence, 7 indicates medium evidence, and 8–9 indicates high evidence of superiority for the reference group over the contrasting group. On the other hand, a score of 0 means that no study found a correlation between such reference groups and IVF outcomes, while 10 indicates that all studies converged towards a unanimous decision. To ensure consistency and reduce potential operator subjectivity in assessing outcomes, i.e., embryo quality, the authors collectively identified principal outcomes for analysis, focusing on objective measures such as fertilization, blastulation, euploid blastocyst formation, ongoing pregnancy, and live birth. Studies that did not report a correlation with the aforementioned outcomes were excluded from the LS calculation, but their findings were appropriately discussed if deemed relevant.

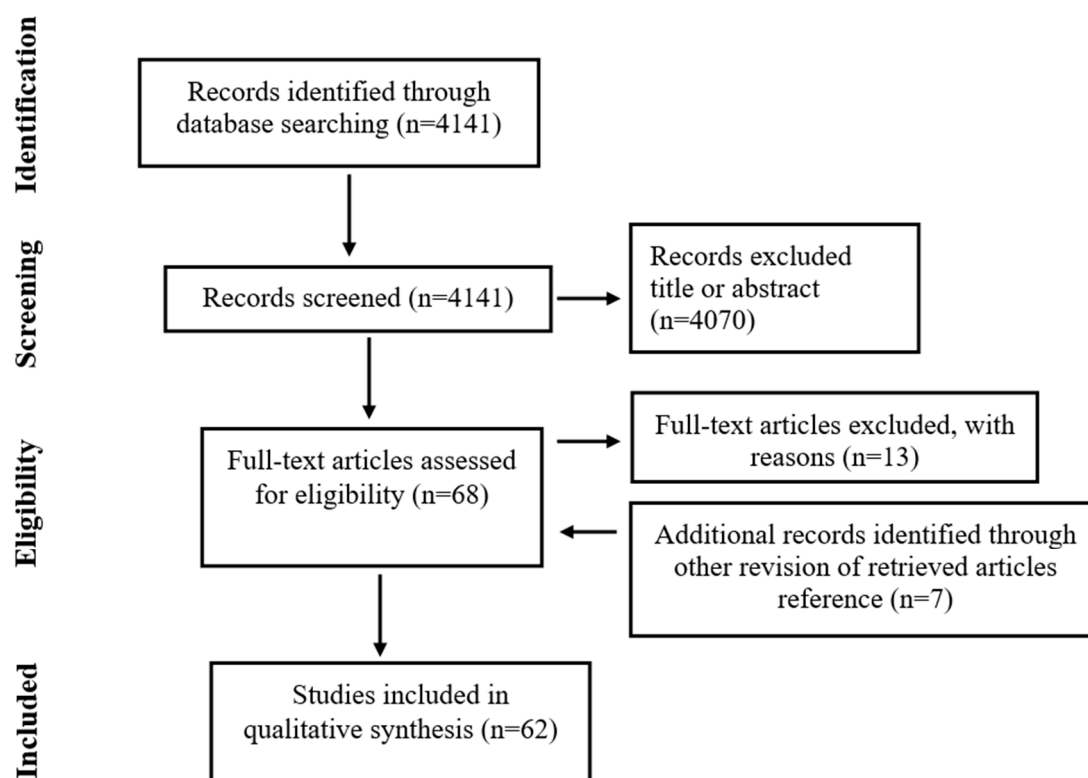


Figure 1. Flow diagram of study selection for review.

**Table 1.** Summary of the results from 62 papers identified in a review of the literature.

Study	Type of Study	Parameter	Comparison	Outcome	Results and Conclusions
Waldenström et al., 2009 [19]	Randomized	Oxygen	5% vs. 19%	LB	Improved in favor of 5%
Kea et al., 2007 [20]	Randomized	Oxygen	5% vs. 20%	OP	No significant difference
Dumoulin et al., 1995 [21]	Randomized	Oxygen	5% vs. 20%	OP	No significant difference
Dumoulin et al., 1999 [22]	Randomized	Oxygen	5% vs. 20%	OP	No significant difference
Ciray et al., 2009 [23]	Randomized	Oxygen	5% vs. 20%	BL	Improved in favor of 5%
Kovacic et al., 2008 [24]	Prospective	Oxygen	5% vs. 20%	BL	Improved in favor of 5%
Kovacic et al., 2010 [25]	Randomized	Oxygen	5% vs. 20%	LB	Improved in favor of 5%
Guo et al., 2014 [26]	Randomized	Oxygen	5% vs. 20%	LB	Improved in favor of 5%
Meintjes et al., 2009 [27]	Randomized	Oxygen	5% vs. 20%	LB	Improved in favor of 5%
Bontekoe et al., 2012 [6]	Meta-analysis	Oxygen	5% vs. 20%	LB	Improved in favor of 5%
Kaser et al., 2018 [7]	Randomized	Oxygen	5% vs. 5–2%	BL	Improved in favor of 5–2%
Yang et al., 2016 [8]	Experimental	Oxygen	5% vs. 20% vs. 2%	BL	No significant difference
De Munck et al., 2019 [28]	Randomized	Oxygen	5% vs. 5–2%	BL	No significant difference
Ferrieres-Hoa et al., 2017 [29]	Retrospective	Oxygen	5% vs. 5–2%	BL	Improved in favor of 5–2%
Li et al., 2022 [30]	Retrospective	Oxygen	5% vs. 5–2%	BL	Improved in favor of 5–2% in low quality embryos
Papadopoulou et al., 2022 [31]	Retrospective	Oxygen	5% vs. 3%	ER	No significant difference
Chen et al., 2023 [32]	Retrospective	Oxygen	5% vs. 5–2%	ER	Improved in favor of 5–2%
Brouillet et al., 2021 [33]	Retrospective	Oxygen	5% vs. 5–2%	BL, CLB	Improved in favor of 5–2%
Bahat et al., 2005 [34]	Experimental	Temperature	n.a.	TI	Temperature at the storage and fertilization sites are time and ovulation dependent
Higdon et al., 2008 [35]	Retrospective	Temperature	<37 °C vs. >37 °C	CP	Higher pregnancy at <37 °C
Zenzes et al., 2001 [36]	Experimental	Temperature	n.a.	SM	Alteration meiotic spindle at 0 °C
Wang et al., 2002 [37]	Experimental	Temperature	37 °C vs. 34 °C vs. 33 °C	CP	Higher pregnancy at 37 °C
Wang et al., 2001 [38]	Experimental	Temperature	n.a.	SM	Alteration meiotic spindle at <37 °C
Hong et al., 2014 [39]	Randomized	Temperature	37 °C vs. 36 °C	IR	Improved in favor of 37 °C
De Munk et al., 2019 [40]	Prospective	Temperature	37.1 °C vs. 36.6 °C	CP	Improved in favor of 37.1 °C
Fawzy et al., 2018 [41]	Randomized	Temperature	37 °C vs. 36.5 °C	BL	Improved in favor of 37 °C
Baak et al., 2019 [42]	Meta-analysis	Temperature	37 °C vs. <37 °C	LB	Improved in favor of 37 °C
Chi et al., 2020 [43]	Retrospective	Humidity	HC vs. DC	OP	Improved in favor of HC
Fawzy et al., 2017 [15]	Randomized	Humidity	HC vs. DC	OP	Improved in favor of HC
Swain et al., 2018 [44]	Prospective	Humidity	HC vs. DC	OSM	Increased in DC
Yumoto et al., 2019 [14]	Experimental	Humidity	HC vs. DC	OSM	Increased in DC
Mestres et al., 2021 [45]	Experimental	Humidity	HC vs. DC	OSM	Increased in DC
Swain et al., 2016 [46]	Experimental	Humidity	HC vs. DC	OSM	Increased in DC
Holmes et al., 2018 [13]	Prospective	Humidity	HC vs. DC	OSM	Increased in DC
Del Gallego et al., 2018 [47]	Randomized	Humidity	HC vs. DC	BL	Increased in HC
Valera et al., 2022 [16]	Retrospective	Humidity	HC vs. DC	LB	No significant difference
Bartolacci et al., 2023 [17]	Retrospective	Humidity	HC vs. DC	OP	No significant difference
Yumoto et al., 2019 [14]	Experimental	Oil	Oil comparison	OSM	Increase osmolality in oil with lower viscosity and density, and higher water content
Swain et al., 2016 [46]	Experimental	Oil	3 mL vs. 5 mL	OSM	Lower in 5 mL group
Mestres et al., 2022 [48]	Experimental	Oil	Oil comparison	OSM	Increase osmolality in oil with lower viscosity and density
Swain et al., 2018 [44]	Prospective	Oil	Oil comparison	OSM	Increase osmolality in light oil
Mestres et al., 2021 [45]	Experimental	Oil	High vs. low volume	OSM	Increased in low volume
Schumacher et al., 1998 [49]	Experimental	Light	Light exposure	DP	No negative impact
Fisher et al., 1988 [50]	Experimental	Light	Light exposure	CI	Vacuolization, lamellar bodies after 24 h
Barlow et al., 1992 [51]	Experimental	Light	Light exposure	IR	No negative impact
Bedford et al., 1989 [52]	Experimental	Light	Light exposure	CP	No negative impact
Kruger et al., 1985 [53]	Experimental	Light	Light exposure	CR	No negative impact
Hegele-Hartung et al., 1988 [54]	Experimental	Light	Light exposure	ULTR	Negative impact on day 1 embryos; no impact on day 3 embryos
Nakayama et al., 1994 [55]	Experimental	Light	Light exposure	ORP	Negative impact
Hegele-Hartung et al., 1991 [56]	Experimental	Light	Light exposure	ULTR	Increased cytoplasmic electron density and fragmentation after 8 h

Table 1. Cont.

Study	Type of Study	Parameter	Comparison	Outcome	Results and Conclusions
Li et al., 2014 [57]	Experimental	Light	Effect of red light	BL	No negative impact
Bognar et al., 2019 [11]	Experimental	Light	Light exposure	IR	Decreased implantation
Daniel et al., 1964 [58]	Experimental	Light	Light exposure	CR	Negative time-dependent impact
Korhonen et al., 2009 [59]	Experimental	Light	Green filtered exposure	ED	No negative impact
Oh et al., 2007 [60]	Experimental	Light	Blue light exposure	BL	Negative impact
Sakharove et al., 2014 [61]	Experimental	Light	Blue light exposure	BL	Negative impact
Jeon et al., 2022 [62]	Experimental	Light	Yellow light exposure	BL	Improved BL
Soares et al., 2014 [10]	Experimental	Light	Laser light	ED	No negative impact with use of low-level laser irradiation
Dinkins et al., 2001 [63]	Experimental	Light	Laser light	BL	No negative impact
Bodis et al., 2020 [64]	Prospective	Light	Light exposure	FR, BL, CP	Negative impact
Squirrell et al., 2001 [65]	Experimental	pH	Alteration pH	ED	reduce ED
Phillips et al., 2000 [66]	Experimental	pH	pHi	pHi range	Mature oocytes: $6.98 \pm 0.02$ ; Cleavage stage embryos: $7.12 \pm 0.01$
Lane et al., 1999 [67]	Experimental	pH	Alteration pH	ED	Impaired ED
Hentemann et al., 2011 [68]	Comparative study	pH	pH range	ED	7.30 before the pronuclear stage and pH 7.15 at the cleavage stage
Dale et al., 1998 [69]	Experimental	pH	pHi	FR, ED	Insemination in the human is pH-sensitive
Edwards et al., 1998 [70]	Experimental	pH	pHi	AM	30 mM DMO in the presence of non-essential amino acids and 1 mM glutamine did not block at the 2-cell stage

LB, Live birth; CLB, Cumulative live birth; CP, Clinical pregnancy; CI, Cell Injury; OP, Ongoing pregnancy; IR, Implantation rate; CR, Cleavage rate; ED, Embryo development; BL, Blastulation; ER, Euploidy rate; SM, Spindle morphology; OSM, Osmolality; HC, Humidity conditions; DC, Dry conditions; ORP, Oxygen radical production; VIS, Viscosity; DENS, Density; TI, Temperature identification; DP, DNA ploidy; ULTR, Ultrastructure; pHi, intracellular pH; AM, Amino-acids; DMO, 5,5-dimethyl-2,4-oxazol-idinedione; mM, millimolar; n.a., not applicable.

The major limitation of our LS is that it does not take into consideration the variable number of patients/embryos per study to which a different weight should be attributed. Moreover, another limitation is its inability to consider whether or not embryos are taken in and out of the incubator for embryo assessment. It is important to note that our approach does not seek to replace the results yielded using a meta-analysis, but rather serves as a complementary elaboration, enriching the written information presented in the manuscript.

### 3. Results

#### 3.1. Oxygen

Oxygen plays a vital role in supporting embryo metabolism and development. In the female reproductive tract, oxygen concentration is typically around 2–8% [18]. Thus, in vivo, the oxygen concentration is different from the atmospheric levels. Several studies have investigated oxygen concentration during human embryo culture. One study showed higher blastulation, pregnancy, and live birth rates using 5% oxygen concentration [19], in contrast to another study that showed no improvements on fertilization, blastulation, and pregnancy rates [20]. Previous studies showed no significant difference in terms of fertilization, pregnancy, and implantation rates between 5% and 20% oxygen concentrations at the cleavage stage [21,22]. On the other hand, several studies showed higher top quality embryos, blastulation rate, and live birth in favor of 5% oxygen than 20% [23–25]. No difference was found in fertilization rate between 5% and 20% oxygen tension, but an increased number of top quality embryos on day 3, higher blastocyst formation, clinical pregnancy, and implantation rates in favor of 5% [26], according to one study that showed an overall increase in live birth when embryos were cultured in low oxygen tension [27]. Finally, a meta-analysis showed an improvement in the live birth rate of 43% during embryo

culture in 5% oxygen concentration [6]. Accordingly, the latest recommendations provided from the ESHRE guidelines suggest the use of low oxygen concentration [1].

Interestingly, recent studies investigated the use of sequential oxygen tension (5% until day 3 and, subsequently, 2% from day 3 to day 5). This is probably to mimic the natural conditions of in vivo embryo development. A sibling zygote randomized control trial showed, although a small sample size, better blastulation rate when oxygen tension is reduced from 5% to 2% on day 3 for extended embryo culture (day 5) [7], in contrast to two studies that showed a similar blastocyst formation rate between 2%, 5% and 20% oxygen tension [8,28]. One report showed that blastocyst utilization rate is higher in 2% oxygen tension group [29], according to another study that showed improvement in blastocyst formation but only in low-quality human embryos cultured with 2% oxygen [30]. No significant difference were found between 5% and 3% oxygen tension in fertilization, blastulation and euploid blastocyst [31]. Recently, two studies suggested that biphasic oxygen culture could be an alternative strategy to increase the euploid blastocyst [32], blastocyst formation, and cumulative live birth rate [33].

We analyzed 18 studies for the LS calculation, 10 focused on comparing between 5% and a 20% oxygen concentration, resulting in a LS of 7. Additionally, eight studies examined the comparison between monophasic (5%) and biphasic (5–2%) culture oxygen tension, resulting in a LS of 5. These findings suggest there is no evidence that biphasic culture (5–2%) is better than monophasic culture (5%), especially in terms of clinical outcomes (Table 2).

**Table 2.** Literature score of different chemical and physical parameters.

Parameters	Comparison	Reference Group	Studies in Favor of Reference Group	Overall Studies	Literature Score
Temperature	37 °C vs. <37 °C	37 °C	5	6	8.3
Oxygen	5% vs. 20%	5%	7	10	7
Oxygen	5–2% vs. 5%	5–2%	4	8	5
Humidity	HC vs. DC	HC	2	4	5
Light	LE vs. r/p LE	LE	3	7	4.3

HC, Humidity conditions: DC, Dry conditions; LE, Light exposure; r/p, Reduced/protected.

### 3.2. Temperature

Maintaining the correct temperature is essential for proper gamete function and/or embryo metabolism and development [4]. Deviation from the optimal temperature can have detrimental effects on gamete function and embryo development, resulting in reduced viability and lower success rates in ART. Typically, the temperature is set at approximately 37 degrees Celsius (°C) to emulate the natural temperature found within the female reproductive tract. However, certain studies have suggested that a temperature of 36 °C may be more suitable to mimic the conditions of the female reproductive tract, potentially leading to improved fertilization and implantation rates [34,35]. Several studies have investigated the impact of temperature on IVF outcomes, yielding contradictory results. There has been evidence supporting negative consequences on the stability of the oocyte's meiotic spindle when the temperature decreases [36,37], resulting in delayed embryo development [38], lower fertilization, and pregnancy rates [37]. A particular study found that the temperatures measured in the oviducts of non-mated, pre-ovulatory, peri-ovulatory, and post-ovulatory rabbits ranged from approximately 34.8 to 35.8 °C and from 35.9 to 36.6 °C in the sperm storage and fertilization site, respectively. These findings suggest that working at these temperatures (around 36 °C) may better mimic the human female reproductive tract [34], according to Higdon and colleagues, who showed a higher pregnancy rate when the incubator environment was cooler than 37 °C [35]. On the contrary, one randomized control trial showed that 36 °C does not improve embryo developmental competence and implantation rate [39]. A recent prospective sibling oocyte study suggests that culture

temperature at 36.6 °C or 37.1 °C did not affect embryo development. However, it was observed that the clinical pregnancy rate was higher when the culture temperature was set at 37.1 °C [40], according to Fawzy and colleagues, who showed improvement in embryo development when the incubator was set at 37 °C [41]. Finally, one meta-analysis [42] showed no evidence that embryo culture at a lower temperature than 37 °C improves biological and clinical outcomes.

We analyzed six studies for the LS calculation, obtaining a high LS of 8.3 (Table 2), suggesting a prevalence of studies in favor of 37 °C.

### 3.3. Humidity Conditions

Humidity plays a significant role in the incubator environment. Maintaining optimal humidity levels is crucial to prevent excessive evaporation from the culture medium, which can affect embryo development by altering osmolality and pH [13]. However, it is important to acknowledge that humidity conditions in the incubator can have drawbacks as well. One notable concern is the increased risk of microbial contamination [12,71]. Advancements in IVF technology have led to significant improvements in incubator design. The latest generation of incubators now feature smaller individual chambers, specifically designed to minimize oscillations that may occur when the chambers are opened. However, the introduction of these new incubators, with their smaller individual chambers, has initiated a shift towards utilizing a DC atmosphere, as opposed to the conventional humidified environment. While this innovation offers advantages in minimizing oscillations during the opening of the chambers [72], there are concerns among scientists regarding the potential negative impact of DC on embryo developmental competence and clinical outcomes [15,43]. Two studies showed that significant evaporation occurs during single-step medium culture after 6 days in a dry incubator [14,44]. The humidity levels within incubators have a significant impact on the stabilization of osmolality [45], according to a previous study [46], suggesting that incubating the medium in a non-humidified environment leads to an increase in osmolality. The osmolality and pH of the culture media increase significantly over the course of 6 days of culture in both DC and HC, although the change was less with HC [13]. Nonetheless, evidence relevant to the impact of HC on biological and clinical outcomes are scarce and conflicting. A randomized controlled trial revealed a statistically significant decrease in implantation rates, as well as clinical and ongoing pregnancy rates, in DC [15], while another study found a difference in terms of ongoing pregnancy in the day 3 but not in the day 5 transfer policy [43]. Embryos developing under DC produced lower blastulation rates [47], in contrast to Valera and colleagues, who showed a comparable blastocyst formation rate and usable blastocyst [16]. The same authors showed a higher clinical pregnancy rate under HC in PGT cycles, but not in egg donation or autologous cycles. Moreover, the authors observed a negative impact of DC only on clinical pregnancy but not on ongoing pregnancy and live birth with use of single-step medium [16], according to a previous report that showed similar pregnancy and miscarriage rates [47]. Interestingly, another recent study using sequential medium yielded similar results. The authors suggest that HC do not enhance the rate of ongoing pregnancy and several embryological outcomes when employing a day 3 medium change-over [17]. These recent results [16,17] are reinforced by the control approach (the same incubator under two different conditions).

In conclusion, while basic research studies consistently indicate alterations in pH and osmolality of the culture medium under DC (although a relatively large volume of medium and a thick oil overlay cooperate in reducing evaporation), it is important to note that this consensus does not align with the clinical evidence. For the LS calculation, we analyzed four studies and obtained a LS of 5 (Table 2), suggesting no evidence of superiority for HC over DC.

### 3.4. Oil Overlay

In human embryo culture, an oil overlay is often used as a covering layer on top of the culture medium to create a specific environment for the embryos. One of the primary purposes of an oil overlay is to facilitate appropriate gas exchange within the embryo culture system, to minimize evaporation, and help maintain a stable environment. Despite this, evaporation could also occur with the use of a mineral oil overlay [44,46,73]. A study discovered that the osmolality of the medium (microdrops ranging from 50 to 200  $\mu$ L) increased significantly when it was covered with mineral oil during a 5-day incubation period in a dry incubator. However, no such increase was observed when the incubation took place in a humidified atmosphere [14]. Furthermore, one study showed that one particular oil (oil B) exhibited a greater increase in osmolality compared to the three other oils (oils A, C, and D), which displayed similar increases in osmolality. This discrepancy can be attributed to the distinct physical oils composition. Specifically, oil B had lower viscosity and density, while its water content and activity were significantly higher [14]. Furthermore, denser oils have been observed to effectively reduce evaporation. In this context, a slight density difference of 0.04 g/mL can have a considerable influence on the rate of evaporation [46]. Another report indicated that using a 5 mL oil overlay resulted in lower osmolality compared to when only 3 mL was used [46]. Interestingly, a comparison of various brands of oil proposed that commercial oils exhibit variations in their ability to maintain the stability of osmolality and pH. Furthermore, the authors found differences in the total number of cells and the number of inner cell mass (ICM) of the obtained blastocysts across different oils [48]. To mitigate evaporation and prevent an increase in osmolality, employing a large volume of oil can effectively counteract these phenomena [45]. Indeed, higher evaporation occurs when using 3 mL of oil compared to using 5 or 7 mL in the same type of dish [73]. In this scenario, the volume of oil used to prepare the culture dishes plays a significant role in preventing medium evaporation and ensuring temperature stability. Using higher volumes of oil and ensuring a thicker layer can effectively minimize evaporation and maintain stable medium osmolality, particularly in single-step medium culture. Due to the specific inclusion criteria, calculating LS in relation to oil was not feasible.

### 3.5. Light

In vivo embryos, which develop inside the female reproductive system, are not directly exposed to light. However, during IVF treatments, embryos may be exposed to light, albeit in a controlled and regulated manner. There is scientific literature available on light exposure and its potential effects on embryo development; nevertheless, contradictory results have been obtained. In a study focusing on pre-implantation rabbit embryos, researchers found that subjecting the embryos to 24 h of visible light exposure did not lead to a significant increase in DNA ploidy abnormalities [49], in contrast to another study that showed how exposure to light for 24 h induced vacuolization, lamellar bodies, and increased electron density in the cytoplasm [50]. Moreover, the same authors suggested that the susceptibility of embryos to light might vary depending on their developmental stage [50]. Several studies have shed light on the potential effects of direct and prolonged exposure to visible light on oocyte's rabbit. Light exposure does not interfere with the normal oocyte's maturation process, embryos implantation, and cleavage rate [51–53]. A study examining pre-implantation rabbit embryos at different developmental stages investigated the effects of a 24 h exposure to light. The results of this study revealed contrasting outcomes for day 1 and day 3 embryos. In the case of day 1 embryos, exposure to light for 24 h led to noticeable cell degeneration, indicating a negative impact on their viability. On the other hand, day 3 embryos showed signs of apoptosis, albeit to a lesser extent compared to day 1 embryos. This suggests that the vulnerability to light-induced damage varies between different stages of embryo development [54]. Interestingly, one study, conducted on hamster and mouse embryos, showed that with just 3 min of exposure to microscope light, there was a significant increase in hydrogen peroxide levels [55]. Increased cytoplasmic



electron density and fragmentation were found after an 8 h exposure to light [56]. Recently, white light has been reported to potentially decrease the implantation capacity of mouse embryos [11], in contrast to another two studies that showed no compromised fertilization rate, embryo development as well as clinical pregnancy with the use of a red filter light protection [57,64]. Moreover, prolonged exposure to light reduced the cleavage ability of rabbit embryos in a time-dependent manner, suggesting the use of red filtered light for prolonged exposure [58]. On the other hand, the use of a green filter on a microscope did not significantly improve bovine embryo development [59]. Two studies have investigated the probable harmful effects of blue light, showing that it has a negative impact on the blastulation rate of hamster and mouse embryos [60,61]. More recently, there has been evidence supporting the beneficial effects of yellow light irradiation on preimplantation development of mouse embryos during in vitro blastocyst production, regardless of the stage of the embryo [62]. Two studies investigated the potential detrimental effects of laser light on embryos, demonstrating no negative impact on embryo development, survival, and blastulation rates [10,63]. There exist differing perspectives regarding the potential adverse effects of light and our data suggest low scientific evidence for negative impacts with prolonged exposure to light. Moreover, we analyzed seven studies for the LS calculation, resulting in a low LS of 4.3 (Table 2).

### 3.6. pH

Culture media pH is a critical factor in human embryo culture. pH is closely correlated with carbon dioxide (CO<sub>2</sub>) levels due to the bicarbonate buffering system, in which changes in CO<sub>2</sub> concentrations impact the production of carbonic acid, consequently leading to variations in pH. Adjusting the percentage of CO<sub>2</sub> gas in the incubator is a fundamental method for precise pH control in the culture medium, which is essential for embryo development [65]. While embryos exhibit an impressive capacity to tolerate a wide range of pH values, it is crucial to note that deviations from the optimal pH range can have adverse effects on developmental competence [65]. In zygotes and embryos, intracellular pH (pHi) plays a pivotal role in maintaining cellular homeostasis, governing a myriad of cellular processes, including enzymatic reactions, cell division, and differentiation [65]. Fluctuations in the extracellular pH of the culture media directly influence the pHi of embryos, consequently affecting their homeostasis and developmental competence [69]. Although human embryos possess several intracellular mechanisms to regulate their pHi [66], any fluctuations can lead to cellular stress, impairing embryo developmental competence [67]. In comparison to embryos, oocytes exhibit heightened fragility due to their limited intrinsic capacity for robust pHi regulation, rendering them more susceptible to pH fluctuations [68]. Mammalian embryos at the morula and blastocyst stages appear to exhibit enhanced capabilities in regulating their pH levels due to the presence of tight junctions that are less permeable to H<sup>+</sup> ions [69,70]. The optimal extracellular pH (pHe) was determined to be slightly higher than the pHi. Deviations in either direction, whether towards higher or lower pHe values, were observed to have inhibitory effects [66]. An ideal pH range of approximately 7.30 was identified for the pronuclear stage, followed by a lower pH value of 7.15 for cleaving embryos [71]. The pH of the culture medium pH can also be influenced by various additional factors, such as the laboratory's geographical altitude. Altitude and air pressure can influence pH levels in embryo culture media due to variations in the solubility of CO<sub>2</sub>. Therefore, it is essential to consider altitude and air pressure to maintain a stable and optimal pH for embryo development.

## 4. Discussion

The purpose of this review was to evaluate studies focusing on the effects of chemical and physical parameters on mammalian embryo culture, with the aim of understanding their importance for human IVF treatments. Out of the 4141 initial studies, only 62 met the selection criteria. A summary of the main findings are shown in Figure 2.

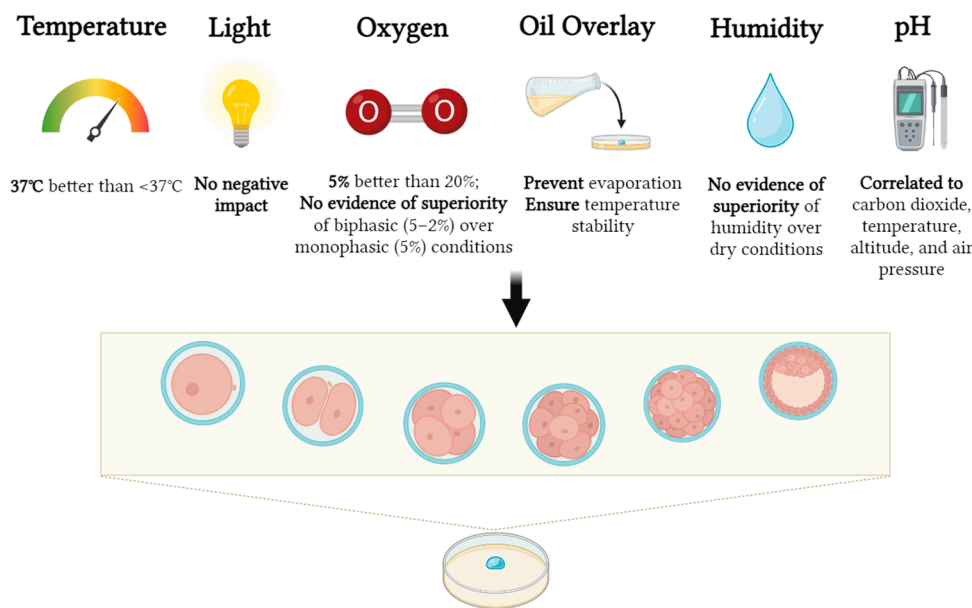


**Figure 2.** Summary of the main findings.

Moreover, to provide further details, we have chosen to employ an alternative methodology. We generated a semi-quantitative outcome LS for the parameters that allowed it. Specifically, we identified four parameters (oxygen, temperature, humidity, and LE) and five different comparisons (37 °C vs. <37 °C; 5% vs. 20% oxygen; 5–2% vs. 5% oxygen; HC vs. DC; LE vs. reduced/protected LE) (Table 2). By adopting this approach, our intention was to bolster the objectivity of our conclusions, going beyond the limitations of a standard review. In relation to oxygen, we conducted an analysis of 18 papers that encompassed studies comparing low oxygen tension with atmospheric oxygen, as well as investigations into the efficacy of biphasic oxygen utilization. Numerous studies have consistently highlighted the advantages of employing low oxygen concentrations in embryo culture, particularly during extended culture periods [19,23–25]. These findings are supported by a recent meta-analysis, which demonstrated a substantial 43% improvement in live birth rates when embryos were cultured under low oxygen concentrations [6]. Notably, the latest recommendations from the ESHRE guidelines also endorse the use of low oxygen levels in embryo culture [1]. Regarding the use of low oxygen tension, we analyzed 10 studies, generating a LS of 7, suggesting medium evidence of superiority for 5% over 20% oxygen tension. On the other hand, assessing the efficacy of biphasic (5–2%) compared to monophasic (5%) culture, despite the use of biphasic oxygen, seems to have benefits in terms of blastulation; we obtained a low LS of 5, suggesting no evidence of superiority for biphasic over monophasic culture [29–33]. In our temperature analysis, we reviewed a total of 9 [34–42] studies, 6 of which were used to calculate the LS. We obtained a LS of 8.3, showing high evidence of superiority for 37 °C over cooler temperatures (36 < 37). According to a recent meta-analysis [42], our findings suggest that, currently, there is no compelling evidence supporting that embryo culture at temperatures lower than 37 °C leads to improved IVF outcomes. We analyzed 10 studies on humidity. It is evident that a humid environment plays a crucial role in reducing medium evaporation, leading to increased osmolality and pH [12–14]. While basic research studies show increased osmolality in culture medium under DC [12–14], these conditions do not seem to have negative effects on biological and clinical outcomes such as blastulation and pregnancy rates [16,17]. In the LS calculation, we analyzed four studies obtaining a low LS of 5, suggesting contradictory results (Table 2). Nevertheless, we analyzed a limited number of studies (four); consequently, further randomized controlled trials are needed to investigate this parameter. Due to the specific inclusion criteria, calculating the LS in relation to oil and pH were not feasible, but their findings were appropriately discussed. Our analysis

of the papers related to oil emphasized its significance in preventing evaporation from the culture medium and in providing greater temperature stability. This crucial aspect is heavily influenced by the inherent properties of the oil, including water content, viscosity, and density. However, it is important to acknowledge that other factors, such as the culture conditions (humid or dry) and the volume of the drop medium, also play an important role in mitigating evaporation. Culture media pH is a critical factor in human embryo culture. While embryos exhibit an impressive capacity to tolerate a wide range of pH values, it is crucial to note that deviations from the optimal pH range can have adverse effects on developmental competence [65]. Furthermore, the pH of the culture medium can also be influenced by various additional factors, such as temperature [74] and the geographical altitude of the laboratory. For this reason, it is essential to consider temperature, altitude, and air pressure to maintain stable and optimal pH for embryo development. In our investigation into light exposure, we have examined 18 studies reaching contradictory results. Moreover, we analyzed seven studies for the LS calculation, resulting in a low LS of 4.3 (Table 2), suggesting limited clarity and no evidence regarding the potential negative impact of light on embryos, particularly in the context of human embryos. All studies on the toxic effects of light were experimental, so they may not accurately reflect real working conditions in an IVF lab. Furthermore, it is worth noting that a majority of these studies are conducted on animal models—i.e., rabbits—which may not be a good model reflecting human oocytes/embryos. Nevertheless, employing light filters can mitigate the adverse impact of light within IVF laboratories [57–64]. Moreover, it is important to note that the static nature of our current culture conditions does not accurately reflect the dynamic environment experienced by embryos in the human body [75,76]. Finally, in the longer term, large studies based on national birth registries are needed to clarify possible adverse effects for the newborn.

## 5. Conclusions

In summary, this review and proposed LS methodology offer semi-quantitative information on studies investigating the effects of chemical and physical parameters on mammalian embryo culture in order to minimize them in the practice of human IVF. Overall, we identified and critically discussed six parameters (oxygen, temperature, humidity, oil overlay, light, and pH). Furthermore, we generated a LS of five different comparisons (37 °C vs. <37 °C; 5% vs. 20% oxygen; 5–2% vs. 5% oxygen; HC vs. DC; LE vs. reduced/protected LE). Among these, two comparisons (37 °C vs. <37 °C and 5% vs. 20% oxygen) yielded medium-high literature scores, suggesting a prevalence of studies in favor of the reference group (37 °C and 5% oxygen). Conversely, the other three comparisons (5–2% vs. 5% oxygen, HC vs. DC, and LE vs. reduced/protected LE) produced a low score for 5–2% oxygen, HC, and LE.

**Author Contributions:** All authors contributed to the conception of this review. A.B. and F.T. designed the study, collected and interpreted the data, and drafted the manuscript. L.S.N., S.d.G. and G.D. were involved in drafted the manuscript. L.P. revised the manuscript. A.A., E.R. and E.P. critical reading of manuscript. All authors have read and agreed to the published version of the manuscript.

**Funding:** This research received no external funding.

**Institutional Review Board Statement:** Not applicable.

**Informed Consent Statement:** Not applicable.

**Data Availability Statement:** Not applicable.

**Conflicts of Interest:** The authors declare no conflict of interest.

## References

1. ESHRE Guideline Group on Good Practice in IVF Labs; De los Santos, M.J.; Apter, S.; Coticchio, G.; Debrock, S.; Lundin, K.; Plancha, C.E.; Prados, F.; Rienzi, L.; Verheyen, G.; et al. Revised guidelines for good practice in IVF laboratories (2015). *Hum. Reprod.* **2016**, *31*, 685–686. [PubMed]

2. Wale, P.L.; Gardner, D.K. The effects of chemical and physical factors on mammalian embryo culture and their importance for the practice of assisted human reproduction. *Hum. Reprod. Update* **2016**, *22*, 2–22. [CrossRef] [PubMed]
3. Swain, J.E.; Carrell, D.; Cobo, A.; Meseguer, M.; Rubio, C.; Smith, G.D. Optimizing the culture environment and embryo manipulation to help maintain embryo developmental potential. *Fertil. Steril.* **2016**, *105*, 571–587. [CrossRef] [PubMed]
4. Leese, H.J.; Baumann, C.G.; Brison, D.R.; McEvoy, T.G.; Sturmey, R.G. Metabolism of the viable mammalian embryo: Quietness revisited. *Mol. Hum. Reprod.* **2008**, *14*, 667–672. [CrossRef]
5. Bedaiwy, M.A.; Falcone, T.; Mohamed, M.S.; Aleem, A.A.; Sharma, R.K.; Worley, S.E.; Thornton, J.; Agarwal, A. Differential growth of human embryos in vitro: Role of reactive oxygen species. *Fertil. Steril.* **2004**, *82*, 593–600. [CrossRef]
6. Bontekoe, S.; Mantikou, E.; van Wely, M.; Seshadri, S.; Repping, S.; Mastenbroek, S. Low oxygen concentrations for embryo culture in assisted reproductive technologies. *Cochrane Database Syst. Rev.* **2012**, *11*, CD008950. [CrossRef] [PubMed]
7. Kaser, D.J.; Bogale, B.; Sarda, V.; Farland, L.V.; Williams, P.L.; Racowsky, C. Randomized controlled trial of low (5%) versus ultralow (2%) oxygen for extended culture using bipronucleate and tripronucleate human preimplantation embryos. *Fertil. Steril.* **2018**, *109*, 1030–1037. [CrossRef]
8. Yang, Y.; Xu, Y.; Ding, C.; Khoudja, R.Y.; Lin, M.; Awonuga, A.O.; Dai, J.; Puscheck, E.E.; Rappolee, D.A.; Zhou, C. Comparison of 2, 5, and 20 % O<sub>2</sub> on the development of post-thaw human embryos. *J. Assist. Reprod. Genet.* **2016**, *33*, 919–927. [CrossRef]
9. Scarica, C.; Monaco, A.; Borini, A.; Pontemuzzo, E.; Bonanni, V.; De Santis, L.; Zacà, C.; Coticchio, G. Use of mineral oil in IVF culture systems: Physico-chemical aspects, management, and safety. *J. Assist. Reprod. Genet.* **2022**, *39*, 883–892. [CrossRef]
10. Soares, C.A.; Annes, K.; Dreyer, T.R.; Magrini, T.; Sonoda, M.T.; da Silva Martinho, H.; Nichi, M.; Ortiz d’Ávila Assumpção, M.E.; Milazzotto, M.P. Photobiological effect of low-level laser irradiation in bovine embryo production system. *J. Biomed. Opt.* **2014**, *19*, 35006. [CrossRef]
11. Bogнар, Z.; Csabai, T.J.; Pallinger, E.; Balassa, T.; Farkas, N.; Schmidt, J.; Görgey, E.; Berta, G.; Szekeres-Bartho, J.; Bodis, J. The effect of light exposure on the cleavage rate and implantation capacity of preimplantation murine embryos. *J. Reprod. Immunol.* **2019**, *132*, 21–28. [CrossRef]
12. Swain, J.E. Decisions for the IVF laboratory: Comparative analysis of embryo culture incubators. *Reprod. Biomed. Online* **2014**, *28*, 535–547. [CrossRef] [PubMed]
13. Holmes, R.; Swain, J.E. Humidification of a dry benchtop IVF incubator: Impact on culture media parameters. *Fertil. Steril.* **2018**, *110*, 52–53. [CrossRef]
14. Yumoto, K.; Iwata, K.; Sugishima, M.; Yamauchi, J.; Nakaoka, M.; Tsuneto, M.; Shimura, T.; Flaherty, S.; Mio, Y. Unstable osmolality of microdrops cultured in non-humidified incubators. *J. Assist. Reprod. Genet.* **2019**, *36*, 1571–1577. [CrossRef] [PubMed]
15. Fawzy, M.; AbdelRahman, M.Y.; Zidan, M.H.; Abdel Hafez, F.F.; Abdelghafar, H.; Al-Inany, H.; Bedaiwy, M.A. Humid versus dry incubator: A prospective, randomized, controlled trial. *Fertil. Steril.* **2017**, *108*, 277–283. [CrossRef]
16. Valera, M.Á.; Albert, C.; Marcos, J.; Larreategui, Z.; Bori, L.; Meseguer, M. A propensity score-based, comparative study assessing humid and dry time-lapse incubation, with single-step medium, on embryo development and clinical outcomes. *Hum. Reprod.* **2022**, *37*, 1980–1993. [CrossRef] [PubMed]
17. Bartolacci, A.; Borini, A.; Cimadomo, D.; Fabozzi, G.; Maggiulli, R.; Lagalla, C.; Pignataro, D.; dell’Aquila, M.; Parodi, F.; Patria, G.; et al. Humidified atmosphere in a time-lapse embryo culture system does not improve ongoing pregnancy rate: A retrospective propensity score model study derived from 496 first ICSI cycles. *J. Assist. Reprod. Genet.* **2023**, *40*, 1429–1435. [CrossRef] [PubMed]
18. Fischer, B.; Bavister, B.D. Oxygen tension in the oviduct and uterus of rhesus monkeys, hamsters and rabbits. *J. Reprod. Fertil.* **1993**, *99*, 673–679. [CrossRef]
19. Waldenström, U.; Engström, A.B.; Hellberg, D.; Nilsson, S. Low-oxygen compared with high-oxygen atmosphere in blastocyst culture, a prospective randomized study. *Fertil. Steril.* **2009**, *91*, 2461–2465. [CrossRef]
20. Kea, B.; Gebhardt, J.; Watt, J.; Westphal, L.M.; Lathi, R.B.; Milki, A.A.; Behr, B. Effect of reduced oxygen concentrations on the outcome of in vitro fertilization. *Fertil. Steril.* **2007**, *87*, 213–216. [CrossRef]
21. Dumoulin, J.C.; Vanvuchelen, R.C.; Land, J.A.; Pieters, M.H.; Geraedts, J.P.; Evers, J.L. Effect of oxygen concentration on in vitro fertilization and embryo culture in the human and the mouse. *Fertil. Steril.* **1995**, *63*, 115–119. [CrossRef]
22. Dumoulin, J.C.; Meijers, C.J.; Bras, M.; Coonen, E.; Geraedts, J.P.; Evers, J.L. Effect of oxygen concentration on human in-vitro fertilization and embryo culture. *Hum. Reprod.* **1999**, *14*, 465–469. [CrossRef] [PubMed]
23. Ciray, H.N.; Aksoy, T.; Yaramanci, K.; Karayaka, I.; Bahceci, M. In vitro culture under physiologic oxygen concentration improves blastocyst yield and quality: A prospective randomized survey on sibling oocytes. *Fertil. Steril.* **2009**, *91*, 1459–1461. [CrossRef] [PubMed]
24. Kovacic, B.; Vlaisavljević, V. Influence of atmospheric versus reduced oxygen concentration on development of human blastocysts in vitro: A prospective study on sibling oocytes. *Reprod. Biomed. Online* **2008**, *17*, 229–236. [CrossRef]
25. Kovacic, B.; Sajko, M.C.; Vlaisavljević, V. A prospective, randomized trial on the effect of atmospheric versus reduced oxygen concentration on the outcome of intracytoplasmic sperm injection cycles. *Fertil. Steril.* **2010**, *94*, 511–519. [CrossRef]
26. Guo, N.; Li, Y.; Ai, J.; Gu, L.; Chen, W.; Liu, Q. Two different concentrations of oxygen for culturing precompaction stage embryos on human embryo development competence: A prospective randomized sibling-oocyte study. *Int. J. Clin. Exp. Pathol.* **2014**, *15*, 6191–6198.

27. Meintjes, M.; Chantilis, S.J.; Douglas, J.D.; Rodriguez, A.J.; Guerami, A.R.; Bookout, D.M.; Barnett, B.D.; Madden, J.D. A controlled randomized trial evaluating the effect of lowered incubator oxygen tension on live births in a predominantly blastocyst transfer program. *Hum. Reprod.* **2009**, *24*, 300–307. [CrossRef] [PubMed]
28. De Munck, N.; Janssens, R.; Segers, I.; Tournaye, H.; Van de Velde, H.; Verheyen, G. Influence of ultra-low oxygen (2%) tension on in-vitro human embryo development. *Hum. Reprod.* **2019**, *34*, 228–234. [CrossRef] [PubMed]
29. Ferrieres-Hoa, A.; Roman, K.; Mullet, T.; Gala, A.; Hamamah, S. Ultra-low (2%) oxygen tension significantly improves human blastocyst development and quality. *Hum. Reprod.* **2017**, *32*, i26.
30. Li, M.; Xue, X.; Shi, J. Ultralow Oxygen Tension (2%) Is Beneficial for Blastocyst Formation of In Vitro Human Low-Quality Embryo Culture. *Biomed. Res. Int.* **2022**, *1*, 9603185. [CrossRef]
31. Papadopoulou, M.I.; Karagianni, M.; Vorniotaki, A.; Oraipoulou, C.; Christophoridis, N.; Papatheodorou, A.; Chatziparasidou, A. Low 5% vs. ultra-low 3% O<sub>2</sub> concentration on embryo culture: Is there any difference in quality and ploidy? *Hum. Reprod.* **2022**, *37*, 270. [CrossRef]
32. Chen, H.H.; Lee, C.I.; Huang, C.C.; Cheng, E.H.; Lee, T.H.; Lin, P.Y.; Chen, C.H.; Lee, M.S. Biphasic oxygen tension promotes the formation of transferable blastocysts in patients without euploid embryos in previous monophasic oxygen cycles. *Sci. Rep.* **2023**, *13*, 4330. [CrossRef]
33. Brouillet, S.; Baron, C.; Barry, F.; Andreeva, A.; Haouzi, D.; Gala, A.; Ferrières-Hoa, A.; Loup, V.; Anahory, T.; Ranisavljevic, N.; et al. Biphasic (5–2%) oxygen concentration strategy significantly improves the usable blastocyst and cumulative live birth rates in in vitro fertilization. *Sci. Rep.* **2021**, *11*, 22461. [CrossRef]
34. Bahat, A.; Eisenbach, M.; Tur-Kaspa, I. Periovulatory increase in temperature difference within the rabbit oviduct. *Hum. Reprod.* **2005**, *20*, 2118–2121. [CrossRef]
35. Higdon, H.L.; Blackhurst, D.W.; Boone, W.R. Incubator management in an assisted reproductive technology laboratory. *Fertil. Steril.* **2008**, *89*, 703–710. [CrossRef] [PubMed]
36. Zenzes, M.T.; Bielecki, R.; Casper, R.F.; Leibo, S.P. Effects of chilling to 0 degrees C on the morphology of meiotic spindles in human metaphase II oocytes. *Fertil. Steril.* **2001**, *75*, 769–777. [CrossRef] [PubMed]
37. Wang, W.H.; Meng, L.; Hackett, R.J.; Oldenbourg, R.; Keefe, D.L. Rigorous thermal control during intracytoplasmic sperm injection stabilizes the meiotic spindle and improves fertilization and pregnancy rates. *Fertil. Steril.* **2002**, *77*, 1274–1277. [CrossRef] [PubMed]
38. Wang, W.H.; Meng, L.; Hackett, R.J.; Oldenbourg, R.; Keefe, D.L. Limited recovery of meiotic spindles in living human oocytes after cooling-rewarming observed using polarized light microscopy. *Hum. Reprod.* **2001**, *16*, 2374–2378. [CrossRef]
39. Hong, K.H.; Lee, H.; Forman, E.J.; Upham, K.M.; Scott, R.T. Examining the temperature of embryo culture in in vitro fertilization: A randomized controlled trial comparing traditional core temperature (37 °C) to a more physiologic, cooler temperature (36 °C). *Fertil. Steril.* **2014**, *102*, 767–773. [CrossRef] [PubMed]
40. De Munck, N.; Janssens, R.; Santos-Ribeiro, S.; Tournaye, H.; Van de Velde, H.; Verheyen, G. The effect of different temperature conditions on human embryos in vitro: Two sibling studies. *Reprod. Biomed. Online* **2019**, *38*, 508–515.
41. Fawzy, M.; Emad, M.; Gad, M.A.; Sabry, M.; Kasem, H.; Mahmoud, M.; Bedaiwy, M.A. Comparing 36.5 °C with 37 °C for human embryo culture: A prospective randomized controlled trial. *Reprod. Biomed. Online* **2018**, *36*, 620–626. [CrossRef] [PubMed]
42. Baak, N.A.; Cantineau, A.E.; Farquhar, C.; Brison, D.R. Temperature of embryo culture for assisted reproduction. *Cochrane Database Syst. Rev.* **2019**, *9*, CD012192. [CrossRef]
43. Chi, H.J.; Park, J.S.; Yoo, C.S.; Kwak, S.J.; Son, H.J.; Kim, S.G.; Sim, C.H.; Lee, K.H.; Koo, D.B. Effect of evaporation-induced osmotic changes in culture media in a dry-type incubator on clinical outcomes in in vitro fertilization-embryo transfer cycles. *Clin. Exp. Reprod. Med.* **2020**, *47*, 284–292. [CrossRef] [PubMed]
44. Swain, J.E.; Graham, C.; Kile, R.; Schoolcraft, W.B.; Krisher, R.L. Media evaporation in a dry culture incubator; effect of dish, drop size and oil on media osmolality. *Fertil. Steril.* **2018**, *110*, e363–e364. [CrossRef]
45. Mestres, E.; García-Jiménez, M.; Casals, A.; Cohen, J.; Acacio, M.; Villamar, A.; Matia-Alguè, Q.; Calderón, G.; Costa-Borges, N. Factors of the human embryo culture system that may affect media evaporation and osmolality. *Hum. Reprod.* **2021**, *36*, 605–613. [CrossRef] [PubMed]
46. Swain, J.E.; Schoolcraft, W.B.; Bossert, N.; Batcheller, A.E. Media osmolality changes over 7 days following culture in a non-humidified benchtop incubator. *Fertil. Steril.* **2016**, *106*, 362. [CrossRef]
47. Del Gallego, R.; Albert, C.; Marcos, J.; Larreategui, Z.; Alegre, L.; Meseguer, M. Humid vs. dry embryo culture conditions on embryo development: A continuous embryo monitoring assessment. *Fertil. Steril.* **2018**, *110*, e362–e363. [CrossRef]
48. Mestres, E.; Matia-Alguè, Q.; Villamar, A.; Casals, A.; Acacio, M.; García-Jiménez, M.; Martínez-Casado, A.; Castelló, C.; Calderón, G.; Costa-Borges, N. Characterization and comparison of commercial oils used for human embryo culture. *Hum. Reprod.* **2022**, *37*, 212–225. [CrossRef]
49. Schumacher, A.; Kesdogan, J.; Fischer, B. DNA ploidy abnormalities in rabbit preimplantation embryos are not increased by conditions associated with in vitro culture. *Mol. Reprod. Dev.* **1998**, *50*, 30–34. [CrossRef]
50. Fischer, B.; Schumacher, A.; Hegele-Hartung, C.; Beier, H.M. Potential risk of light and room temperature exposure to preimplantation embryos. *Fertil. Steril.* **1988**, *50*, 938–944. [CrossRef]
51. Barlow, P.; Puissant, F.; Van der Zwalmen, P.; Vandromme, J.; Trigaux, P.; Leroy, F. In vitro fertilization, development, and implantation after exposure of mature mouse oocytes to visible light. *Mol. Reprod. Dev.* **1992**, *33*, 297–302. [CrossRef] [PubMed]

52. Bedford, J.M.; Dobrenis, A. Light exposure of oocytes and pregnancy rates after their transfer in the rabbit. *J. Reprod. Fertil.* **1989**, *85*, 477–481. [CrossRef] [PubMed]
53. Kruger, T.F.; Stander, F.S. The effect on cleavage of two-cell mouse embryos after a delay in embryo retrieval in a human in vitro fertilization programme. *S. Afr. Med. J.* **1985**, *68*, 743–744.
54. Hegele-Hartung, C.; Schumacher, A.; Fischer, B. Ultrastructure of preimplantation rabbit embryos exposed to visible light and room temperature. *Anat. Embryol.* **1988**, *178*, 229–241. [CrossRef] [PubMed]
55. Nakayama, T.; Noda, Y.; Goto, Y.; Mori, T. Effects of visible light and other environmental factors on the production of oxygen radicals by hamster embryos. *Theriogenology* **1994**, *41*, 499–510. [CrossRef] [PubMed]
56. Hegele-Hartung, C.; Schumacher, A.; Fischer, B. Effects of visible light and room temperature on the ultrastructure of preimplantation rabbit embryos: A time course study. *Anat. Embryol.* **1991**, *183*, 559–571. [CrossRef]
57. Li, R.; Pedersen, K.S.; Liu, Y.; Pedersen, H.S.; Lægdsmand, M.; Rickelt, L.F.; Kühl, M.; Callesen, H. Effect of red light on the development and quality of mammalian embryos. *J. Assist. Reprod. Genet.* **2014**, *31*, 795–801. [CrossRef]
58. Daniel, J.C. Cleavage of mammalian ova inhibited by visible light. *Nature* **1964**, *201*, 316–317. [CrossRef]
59. Korhonen, K.; Sjövall, S.; Viitanen, J.; Ketoja, E.; Makarevich, A.; Peippo, J. Viability of bovine embryos following exposure to the green filtered or wider bandwidth light during in vitro embryo production. *Hum. Reprod.* **2009**, *24*, 308–314. [CrossRef] [PubMed]
60. Oh, S.J.; Gong, S.P.; Lee, S.T.; Lee, E.J.; Lim, J.M. Light intensity and wavelength during embryo manipulation are important factors for maintaining viability of preimplantation embryos in vitro. *Fertil. Steril.* **2007**, *88*, 1150–1157. [CrossRef]
61. Sakharova, N.Y.; Mezhevnikina, L.M.; Smirnov, A.A.; Vikhlyantseva, E.F. Analysis of the effects of blue light on morphofunctional status of in vitro cultured blastocysts from mice carrying gene of enhanced green fluorescent protein (EGFP). *Bull. Exp. Biol. Med.* **2014**, *157*, 162–166. [CrossRef] [PubMed]
62. Jeon, Y.R.; Baek, S.; Lee, E.S.; Lee, S.T. Effects of light wavelength exposure during in vitro blastocyst production on preimplantation development of mouse embryos. *Reprod. Fertil. Dev.* **2022**, *34*, 1052–1057. [CrossRef] [PubMed]
63. Dinkins, M.B.; Stallknecht, D.E.; Howerth, E.W.; Brackett, B.G. Photosensitive chemical and laser light treatments decrease epizootic hemorrhagic disease virus associated with in vitro produced bovine embryos. *Theriogenology* **2001**, *55*, 1639–1655. [CrossRef]
64. Bodis, J.; Gödöny, K.; Várnagy, Á.; Kovács, K.; Koppán, M.; Nagy, B.; Erostyák, J.; Herczeg, R.; Szekeres-Barthó, J.; Gyenesei, A.; et al. How to reduce the potential harmful effects of light on blastocyst development during IVF. *Med. Princ. Pract.* **2020**, *29*, 558–564. [CrossRef]
65. Squirrel, J.M.; Lane, M.; Bavister, B.D. Altering intracellular pH disrupts development and cellular organization in preimplantation hamster embryos. *Biol. Reprod.* **2001**, *64*, 1845–1854. [CrossRef]
66. Phillips, K.P.; Léveillé, M.C.; Claman, P.; Baltz, J.M. Intracellular pH regulation in human preimplantation embryos. *Hum. Reprod.* **2000**, *15*, 896–904. [CrossRef] [PubMed]
67. Lane, M.; Bavister, B.D. Regulation of intracellular pH in bovine oocytes and cleavage stage embryos. *Mol. Reprod. Dev.* **1999**, *54*, 396–401. [CrossRef]
68. Hentemann, M.; Mousavi, K.; Bertheussen, K. Differential pH in embryo culture. *Fertil. Steril.* **2011**, *95*, 1291–1294. [CrossRef]
69. Dale, B.; Menezo, Y.; Cohen, J.; Di Matteo, L.; Wilding, M. Intracellular pH regulation in the human oocyte. *Hum. Reprod.* **1998**, *13*, 964–970. [CrossRef] [PubMed]
70. Edwards, L.J.; Williams, D.A.; Gardner, D.K. Intracellular pH of the mouse preimplantation embryo: Amino acids act as buffers of intracellular pH. *Hum. Reprod.* **1998**, *13*, 3441–3448. [CrossRef]
71. Geraghty, R.J.; Capes-Davis, A.; Davis, J.M.; Downward, J.; Freshney, R.I.; Knezevic, I.; Lovell-Badge, R.; Masters, J.R.W.; Meredith, J.; Stacey, J.N.; et al. Guidelines for the use of cell lines in biomedical research. *Br. J. Cancer* **2014**, *111*, 1021–1046. [CrossRef] [PubMed]
72. Fujiwara, M.; Takahashi, K.; Izuno, M.; Duan, Y.R.; Kazono, M.; Kimura, F.; Noda, Y. Effect of micro-environment maintenance on embryo culture after in-vitro fertilization: Comparison of top-load mini incubator and conventional front-load incubator. *J. Assist. Reprod. Genet.* **2007**, *24*, 5–9. [CrossRef] [PubMed]
73. Swain, J.E. Controversies in ART: Considerations and risks for uninterrupted embryo culture. *Reprod. Biomed. Online* **2019**, *39*, 19–26. [CrossRef] [PubMed]
74. Lane, M. Mechanisms for managing cellular and homeostatic stress in vitro. *Theriogenology* **2001**, *55*, 225–236. [CrossRef] [PubMed]
75. Gardner, D.K.; Lane, M.; Calderon, I.; Leeton, J. Environment of the preimplantation human embryo in vivo: Metabolite analysis of oviduct and uterine fluids and metabolism of cumulus cells. *Fertil. Steril.* **1996**, *65*, 349–353. [CrossRef] [PubMed]
76. Thouas, G.A.; Dominguez, F.; Green, M.P.; Vilella, F.; Simon, C.; Gardner, D.K. Soluble ligands and their receptors in human embryo development and implantation. *Endocr. Rev.* **2015**, *36*, 92–130. [CrossRef]

**Disclaimer/Publisher’s Note:** The statements, opinions and data contained in all publications are solely those of the individual author(s) and contributor(s) and not of MDPI and/or the editor(s). MDPI and/or the editor(s) disclaim responsibility for any injury to people or property resulting from any ideas, methods, instructions or products referred to in the content.

## Article

# Risk Prediction Model of Early-Onset Preeclampsia Based on Risk Factors and Routine Laboratory Indicators

Yuting Xue <sup>1,†</sup>, Nan Yang <sup>2,†</sup>, Xunke Gu <sup>3</sup>, Yongqing Wang <sup>3,\*</sup>, Hua Zhang <sup>4</sup> and Keke Jia <sup>1,\*</sup>

<sup>1</sup> Department of Laboratory Medicine, Peking University Third Hospital, Beijing 100191, China; 2011210372@bjmu.edu.cn

<sup>2</sup> Department of Blood Transfusion, Peking University Third Hospital, Beijing 100191, China; yangnan@bjmu.edu.cn

<sup>3</sup> Department of Obstetrics and Gynecology, Peking University Third Hospital, Beijing 100191, China; guxunke@163.com

<sup>4</sup> Research Center of Clinical Epidemiology, Peking University Third Hospital, Beijing 100191, China; zhanghua824@163.com

\* Correspondence: mddoctor@163.com (Y.W.); jiakeke76@126.com (K.J.); Tel.: +86-10-82264403 (Y.W.); +86-10-82267621 (K.J.)

† These authors contributed equally to this work.

**Abstract: Background:** Globally, 10–15% of maternal deaths are statistically attributable to preeclampsia. Compared with late-onset PE, the severity of early-onset PE remains more harmful with higher morbidity and mortality. **Objective:** To establish an early-onset preeclampsia prediction model by clinical characteristics, risk factors and routine laboratory indicators were investigated from pregnant women at 6 to 10 gestational weeks. **Methods:** The clinical characteristics, risk factors, and 38 routine laboratory indicators (6–10 weeks of gestation) including blood lipids, liver and kidney function, coagulation, blood count, and other indicators of 91 early-onset preeclampsia patients and 709 normal controls without early-onset preeclampsia from January 2010 to May 2021 in Peking University Third Hospital (PUTH) were retrospectively analyzed. A logistic regression, decision tree model, and support vector machine (SVM) model were applied for establishing prediction models, respectively. ROC curves were drawn; area under curve ( $AUC^{ROC}$ ), sensitivity, and specificity were calculated and compared. **Results:** There were statistically significant differences in the rates of diabetes, antiphospholipid syndrome (APS), kidney disease, obstructive sleep apnea (OSAHS), primipara, history of preeclampsia, and assisted reproductive technology (ART) ( $p < 0.05$ ). Among the 38 routine laboratory indicators, there were no significant differences in the levels of PLT/LYM, NEU/LYM, TT, D-Dimer, FDP, TBA, ALP, TP, ALB, GLB, UREA, Cr, P, Cystatin C, HDL-C, Apo-A<sub>1</sub>, and Lp(a) between the two groups ( $p > 0.05$ ). The levels of the rest indicators were all statistically different between the two groups ( $p < 0.05$ ). If only 12 risk factors of PE were analyzed with the logistic regression, decision tree model, and support vector machine (SVM), and the  $AUC^{ROC}$  were 0.78, 0.74, and 0.66, respectively, while 12 risk factors of PE and 38 routine laboratory indicators were analyzed with the logistic regression, decision tree model, and support vector machine (SVM), and the  $AUC^{ROC}$  were 0.86, 0.77, and 0.93, respectively. **Conclusions:** The efficacy of clinical risk factors alone in predicting early-onset preeclampsia is not high while the efficacy increased significantly when PE risk factors combined with routine laboratory indicators. The SVM model was better than logistic regression model and decision tree model in early prediction of early-onset preeclampsia incidence.

**Keywords:** early-onset preeclampsia; risk factors; routine laboratory indicators; risk prediction model; machine learning

## 1. Introduction

Globally, 10–15% of all maternal deaths can be attributed to preeclampsia or eclampsia, a placentally derived disease of pregnancy [1,2]. Maternal complications associated with

preeclampsia include placental abruption, acute kidney disease, pulmonary edema, and heart failure. In severe cases, preeclampsia leads to eclamptic seizures and life-threatening hemolysis, elevated liver enzymes, and low platelet count (HELLP) syndrome [3]. Moreover, fetal complications related to preeclampsia include impaired fetal growth, neonatal respiratory distress syndrome, and stillbirth. Preeclampsia can be classified as early-onset preeclampsia, which develops before 34 weeks' gestation, and the more common late-onset preeclampsia, which develops at or after 34 weeks' gestation [4]. Compared with late-onset PE, the severity of early-onset PE remains more harmful with higher morbidity and mortality [5].

Despite the serious clinical consequences, there is no effective preventive measure for preeclampsia currently. Timely identification and management of preeclampsia can significantly improve maternal and perinatal outcomes [6]. Therefore, risk prediction of preeclampsia and preeclampsia-related disorders has received considerable attention over the past two decades. A practical prediction model would allow for increased surveillance of at-risk patients and reduce the surveillance of patients who are less likely to develop preeclampsia, which makes medical resources fully and reasonably allocated and utilized. Although previous studies have analyzed clinical features and evaluated biomarkers for effective prediction, few have demonstrated clinically sufficient properties [7–11].

Machine learning (ML) techniques provide the possibility to infer important connections between items from different data sets that would otherwise be difficult to correlate [12,13]. Due to the vast amount and complexity of medical information, ML is considered a promising method for diagnosing diseases or predicting clinical outcomes. Multiple ML techniques have been used in clinical settings and shown to be more accurate than traditional methods in predicting disease [14].

This study was aimed to develop ML models to predict early-onset preeclampsia by using risk factors and routine laboratory indicators and to compare the performance of different models.

## 2. Materials and Methods

### 2.1. Study Population

Pregnant women with non-singleton, miscarriage or fetal death, intrauterine chromosomal disorders or fetal malformations, and missing laboratory data were excluded. Preeclampsia (PE) is defined as systolic blood pressure at  $\geq 140$  mm Hg and/or diastolic blood pressure at  $\geq 90$  mm Hg on at least two occasions measured 4 h apart in previously normotensive women and is accompanied by one or more of the following new-onset conditions at or after 20 weeks of gestation: 1. Proteinuria (i.e.,  $\geq 30$  mg/mol protein:creatinine ratio;  $\geq 300$  mg/24 h; or  $\geq 2+$  dipstick); 2. Evidence of other maternal organ dysfunction, including acute kidney injury (creatinine  $\geq 90$   $\mu$ mol/L; 1 mg/dL); liver involvement (elevated transaminases, e.g., alanine aminotransferase or aspartate aminotransferase  $>40$  IU/L) with or without right upper quadrant or epigastric abdominal pain; neurological complications (e.g., eclampsia, altered mental status, blindness, stroke, clonus, severe headaches, and persistent visual scotomata); or hematological complications (thrombocytopenia—platelet count  $<150,000/\mu$ L, disseminated intravascular coagulation, hemolysis); 3. Uteroplacental dysfunction (such as fetal growth restriction, abnormal umbilical artery Doppler waveform analysis, or stillbirth) according to the FIGO guidelines [6]. Pregnant women who met the diagnostic criteria for preeclampsia and with delivery at  $<34^{+0}$  weeks of gestation can be subclassified into early-onset preeclampsia. A total of 91 Chinese pregnant women who were diagnosed with early-onset preeclampsia in the Department of Obstetrics and Gynecology of Peking University Third Hospital from January 2010 to May 2021 were included as PE group. Meanwhile, 709 Chinese pregnant women who had normal delivery and single live birth in the department of Obstetrics and Gynecology of Peking University Third Hospital during the same period were selected as the control group (CON). The retrospective study protocol was approved by the Peking University Third Hospital Medical Science Research Ethics Committee (IRB00006761-M2021032).



## 2.2. Clinical and Biochemical Data Collection

Clinical characteristics of patients, such as age of admission, gestational age, disease history, pregnancy history, and blood pressure (1 mmHg = 0.133 kPa), were obtained from electronic medical records. There are 12 risk factors [15] for preeclampsia, which include diabetes, thrombotic diseases, systemic lupus erythematosus (SLE), antiphospholipid syndrome (APS) and kidney diseases, assisted reproductive technology (ART), obstructive sleep apnea, pre-pregnancy body mass index (BMI) > 30 kg/m<sup>2</sup>, age > 35 years old, multiple pregnancies, primipara, and history of eclampsia or preeclampsia. Routine laboratory indicators including albumin (ALB), alanine transaminase (ALT), aspartate transaminase (AST), alkaline phosphatase (ALP), complement C1q, calcium (Ca), creatinine (Cr), C-reactive protein (CRP), cystatin C,  $\gamma$ -glutamyl transpeptidase (GGT), globulin (GLB), triglyceride (TG), total cholesterol (TC), high-density lipoprotein cholesterol (HDL-C), low-density lipoprotein cholesterol (LDL-C), lipoprotein (a) [Lp (a)], apolipoprotein A<sub>1</sub> (ApoA<sub>1</sub>), apolipoprotein B (ApoB), small dense low density lipoprotein (sdLDL-C), total protein (TP), total bile acid (TBA), total bilirubin (T-Bil), direct bilirubin (D-Bil), uric acid (UA), Urea (UREA), phosphorus (P), absolute value of lymphocyte (LYM), absolute value of neutrophil (NEU), platelet count (PLT), NEU /LTM ratio, PLT /LYM ratio, prothrombin time (PT), prothrombin activity (PTA), activated partial thrombin time (APTT), fibrinogen (FIB), D-Dimer, fibrinogen degradation Products (FDP), thrombin time (TT).

## 2.3. Instruments and Reagents

Fasting blood samples of the participants were collected from elbow venous using vacutainer containing separation glue at 6–10 weeks of gestation. The blood samples were centrifuged at  $2793 \times g$  for 5 min. The serum was separated and stored at  $-80^{\circ}\text{C}$  refrigerator for subsequent detection. Serum liver and kidney function, lipid metabolism, and complement indexes were detected by AU5800 automatic biochemical analyzer (Beckman Coulter, Brea, CA, USA).

The peripheral blood samples were obtained with venipuncture and collected into vacuum blood collection tubes containing sodium citrate as the anticoagulant (INSEPACK<sup>®</sup> Sekisui, Beijing, China). The plasma was obtained by centrifuging the samples at  $1500 \times g$  for 5 min. Automatic coagulation analyzer (ACL-TOP 700<sup>®</sup>, Werfen, Barcelona, Spain) was used to detect coagulation items.

The peripheral blood samples were obtained with venipuncture and collected in vacuum blood collection tubes containing EDTA-K2 as the anticoagulant (INSEPACK<sup>®</sup>, Sekisui, Beijing, China). The peripheral leukocytes were counted and classified into neutrophils, eosinophils, basophils, lymphocytes, and monocytes in the traditional five subtype classification method with an automatic blood count analyzer (SYSMEX XN-2000 Automated Hematology Analyzer, Kobe, Japan).

Instrument calibration, calibration, quality control were matched and applied in strict accordance with the standard operation procedure.

## 2.4. Statistical Analysis

SPSS 24.0 and MATLAB software (R2022a) were used for data analysis. The K-S normal distribution was used to detect the normality of data; measurement data conformed to normal distribution with  $\bar{x} \pm s$  description and non-normal distribution with a median (interquartile range). Mann–Whitney U test was used for pairwise comparison of skewed distribution data between groups. The count data were tested with chi-square test, and the number of use cases (percentage) was described.  $p < 0.05$  was considered statistically significant.

### 2.4.1. Logistic Regression Model

All routine laboratory indicators were analyzed with univariate binary Logistic regression; multivariate binary Logistic regression analysis was performed for the variable of  $p < 0.05$ . The maximum Youden index was taken as the cut-off point, the risk degree

was expressed as the OR value [95% confidence interval (CI), 95%CI], and the receiver operating characteristic (ROC) curve was made.

#### 2.4.2. Machine Learning

We used 2 machine learning algorithms: the decision tree model and support vector machine (SVM). For the development of machine learning models, we obtained 12 risk factors and 38 routine laboratory indicators mentioned above. The predictive value of individual risk factors and the models combining risk factors and laboratory indicators were explored, respectively. Machine learning models were trained with all variables as inputs to classify patients likely to have favorable outcomes. Among the study population, 80% were randomly selected for the training set, and the remaining 20% were used as the test set to prevent overfitting of the models. MATLAB version R 2022a was used to train the machine learning models.

##### Decision Tree Model

Decision tree is a commonly used supervised learning algorithm. It uses Gini coefficient, entropy, and other parameters to select features and generate a tree structure, and classifies the original data set into a series of smaller subgroups. This method had the advantages of strong interpretability, low computational costs, and strong robustness. Similarly, the ROC curve was made compared with other models.

##### Support Vector Machine (SVM)

The support vector machine is a learning system that uses a hypothesis space of linear functions in a high-dimensional feature space. This method maximizes the separation boundary of the two classes under the assumption of improving the generalization ability of the classifier. It makes all samples of different classes well discriminated by finding a projection direction and obtaining the optimal hyperplane. In addition, this method can also achieve nonlinear mapping through the kernel function so as to obtain a stronger fitting ability. Among them, the commonly used kernel functions are as follows: gaussian kernel function, polynomial kernel function, sigmoid kernel function, etc. In this study, considering the strong linear relationship between laboratory indicators and predicted results and the objective situation due to limited sample size, a linear kernel with lower complexity was used. We used the ten-fold cross-validation method to verify the ability of the model, and the results of the sensitivity, specificity, and other indicators were good and consistent, which proved that the model had good fitting and generalization ability.

### 3. Results

#### 3.1. Participants' Clinical Characteristics

There were significant differences in maternal age and pre-pregnancy BMI between the two groups ( $p < 0.05$ ), and the PE group had a higher pre-pregnancy BMI compared with the control group (Table 1).

**Table 1.** Clinical characteristics and risk factors of Control group and early-onset PE group.

Variables	Control Group (n = 709)	PE Group (n = 91)	Statistical Magnitude	p Value
Age, year	35 (32–38) <sup>a</sup>	33 (31–35.5) <sup>a</sup>	4.32 <sup>b</sup>	<0.001 *
Body mass index, BMI	21.71 (19.93–23.81) <sup>a</sup>	23.73 (23.12–24.43) <sup>a</sup>	−4.68 <sup>b</sup>	<0.001 *
Medical history, n (%)				
Diabetes	155 (21.86)	29 (31.87)	4.56 <sup>c</sup>	0.033 *
Thrombotic disease	2 (0.28)	0 (0.00)	<0.001 <sup>c</sup>	0.998
Systemic lupus erythematosus (SLE)	5 (0.71)	3 (3.30)	3.17 <sup>c</sup>	0.075
Antiphospholipid syndrome (APS)	20 (2.82)	7 (7.69)	7.31 <sup>c</sup>	0.026 *
Kidney disease	5 (0.71)	6 (6.59)	16.51 <sup>c</sup>	<0.001 *
Obstructive sleep apnea hypopnea syndrome (OSAHS)	0 (0.00)	2 (2.20)	8.05 <sup>c</sup>	0.005 *

Table 1. Cont.

Variables	Control Group (n = 709)	PE Group (n = 91)	Statistical Magnitude	p Value
History of eclampsia or preeclampsia	4 (0.56)	6 (6.59)	19.12 <sup>c</sup>	<0.001 *
History of gestation, n (%)	591 (83.36)	51 (56.04)	46.69 <sup>c</sup>	<0.001 *
Primipara, n (%)	238 (33.57)	72 (79.12)	74.97 <sup>c</sup>	<0.001 *
Fertilization way, n (%)				
Assisted reproductive technology (ART)	119 (16.78)	32 (35.16)		
Natural conception	590 (83.22)	59 (64.84)	16.61 <sup>c</sup>	<0.001 *

<sup>a</sup> Expressed as the median (interquartile range). <sup>b</sup> Rank sum test: Z value <sup>c</sup> Chi-square value \* p values were statistically different,  $p < 0.05$ .

### 3.2. Comparison of Risk Factors

There was no significant difference in the proportion of pregnant women with thrombotic disease or systemic lupus erythematosus (SLE) between the two groups ( $p > 0.05$ ). However, there were statistically significant differences in the rates of diabetes, antiphospholipid syndrome (APS), kidney disease, obstructive sleep apnea (OSAHS), primipara, history of preeclampsia, and assisted reproductive technology (ART) ( $p < 0.05$ ). The proportion of thrombotic diseases in the PE group was lower than that in the control group, and the other proportions were higher than that in the control group (Table 1).

### 3.3. Comparison of Routine Laboratory Indicators

Among the 38 routine laboratory indicators, there were no significant differences in the levels of PLT/LYM, NEU/LYM, TT, D-Dimer, FDP, TBA, ALP, TP, ALB, GLB, UREA, Cr, P, Cystatin C, HDL-C, Apo-A<sub>1</sub>, and Lp(a) between the two groups ( $p > 0.05$ ). The levels of the rest indicators were all statistically different ( $p < 0.05$ ) (Table 2).

**Table 2.** Routine laboratory indicators at 6–10 weeks of gestation between Control group and early-onset PE group.

Variable	Control Group (n = 709)	PE Group (n = 91)	Statistical Magnitude	p Value
Blood cell count				
PLT, $\times 10^9/L$	244 (211–283) <sup>a</sup>	256.5 (226.25–300.5) <sup>a</sup>	−2.58 <sup>b</sup>	<0.001 *
LYM, $\times 10^9/L$	1.79 (1.48–2.1) <sup>a</sup>	1.98 (1.74–2.40) <sup>a</sup>	−3.56 <sup>b</sup>	<0.001 *
NEU, $\times 10^9/L$	5.24 (4.28–6.55) <sup>a</sup>	6.25 (5.24–8.35) <sup>a</sup>	−4.63 <sup>b</sup>	<0.001 *
PLT/LYM	135.19 (114.35–163.73) <sup>a</sup>	125.46 (106.26–158.16) <sup>a</sup>	1.51 <sup>b</sup>	0.13
NEU/LYM	2.95 (2.29–3.73) <sup>a</sup>	2.97 (2.42–4.14) <sup>a</sup>	−0.97 <sup>b</sup>	0.33
Index of coagulation function				
PT, s	11.3 (11–11.7) <sup>a</sup>	10.9 (10.5–11.3) <sup>a</sup>	5.53 <sup>b</sup>	<0.001 *
PTA, %	91 (88–96) <sup>a</sup>	97 (92–102) <sup>a</sup>	−5.15 <sup>b</sup>	<0.001 *
APTT, s	31.2 (29.3–33.1) <sup>a</sup>	29.6 (27.7–31.3) <sup>a</sup>	4.30 <sup>b</sup>	<0.001 *
TT, s	13.5 (12.9–14) <sup>a</sup>	13.4 (12.7–14) <sup>a</sup>	1.06 <sup>b</sup>	0.29
FIB, g/L	3.27 (2.92–3.66) <sup>a</sup>	3.51 (3.1–3.98) <sup>a</sup>	−3.38 <sup>b</sup>	<0.001 *
D-Dimer, mg/L	0.15 (0.15–0.18) <sup>a</sup>	0.15 (0.15–0.17) <sup>a</sup>	1.13 <sup>b</sup>	0.26
FDP, $\mu g/mL$	2.5 (2.5–2.5) <sup>a</sup>	2.5 (2.5–2.5) <sup>a</sup>	−0.79 <sup>b</sup>	0.43
Liver function index				
ALT, U/L	13 (10–18) <sup>a</sup>	18 (13–27.5) <sup>a</sup>	−4.67 <sup>b</sup>	<0.001 *
AST, U/L	16 (14–19) <sup>a</sup>	19 (15–25) <sup>a</sup>	−4.70 <sup>b</sup>	<0.001 *

Table 2. Cont.

Variable	Control Group (n = 709)	PE Group (n = 91)	Statistical Magnitude	p Value
T-Bil, umol/L	12 (10–14.8) <sup>a</sup>	10 (8.9–12.6) <sup>a</sup>	4.71 <sup>b</sup>	<0.001 *
D-Bil, umol/L	1.3 (1–1.8) <sup>a</sup>	1.1 (0.6–1.8) <sup>a</sup>	2.27 <sup>b</sup>	0.02 *
TBA, umol/L	1.6 (1–2.3) <sup>a</sup>	1.4 (1–2.35) <sup>a</sup>	0.54 <sup>b</sup>	0.59
ALP, U/L	49 (43–58) <sup>a</sup>	53 (44–64) <sup>a</sup>	−1.92 <sup>b</sup>	0.05
TP, g/L	72.4 (70.1–74.7) <sup>a</sup>	72 (70.9–74.9) <sup>a</sup>	−0.24 <sup>b</sup>	0.81
ALB, g/L	43.01 ± 2.42 <sup>c</sup>	43.04 ± 3.00 <sup>c</sup>	−0.08 <sup>d</sup>	0.94
GGT, U/L	14 (11–18) <sup>c</sup>	17 (14–28) <sup>c</sup>	−4.86 <sup>b</sup>	<0.001 *
GLB, g/L	29 (27–31) <sup>c</sup>	30 (28–32) <sup>c</sup>	−1.12 <sup>b</sup>	0.26
Renal function index				
UREA, mmol/L	3.1 (2.7–3.7) <sup>a</sup>	3.2 (2.8–3.7) <sup>a</sup>	−1.09 <sup>b</sup>	0.28
Cr, umol/L	59 (54–63) <sup>a</sup>	60 (54–65) <sup>a</sup>	−0.87 <sup>b</sup>	0.39
Ca, mmol/L	2.3 (2.24–2.35) <sup>a</sup>	2.33 (2.27–2.4) <sup>a</sup>	−3.40 <sup>b</sup>	<0.001 *
P, mmol/L	1.232 ± 0.136 <sup>c</sup>	1.228 ± 0.138 <sup>c</sup>	0.21 <sup>d</sup>	0.83
UA, umol/L	210 (184–239) <sup>a</sup>	238 (214–279.75) <sup>a</sup>	−5.57 <sup>b</sup>	<0.001 *
Cystatin C, mg/L	0.62 (0.57–0.68) <sup>a</sup>	0.59 (0.54–0.66) <sup>a</sup>	1.18 <sup>b</sup>	0.24
Blood lipid indicators				
TCHO, mmol/L	4.01 (3.56–4.48) <sup>a</sup>	4.27 (3.87–4.79) <sup>a</sup>	−3.09 <sup>b</sup>	<0.001 *
TG, mmol/L	1.06 (0.8–1.43) <sup>a</sup>	1.39 (1.15–1.83) <sup>a</sup>	−5.00 <sup>b</sup>	<0.001 *
HDL-C, mmol/L	1.43 (1.24–1.63) <sup>a</sup>	1.33 (1.14–1.58) <sup>a</sup>	1.40 <sup>b</sup>	0.16
LDL-C, mmol/L	2.16 (1.79–2.53) <sup>a</sup>	2.38 (2.11–2.93) <sup>a</sup>	−3.84 <sup>b</sup>	<0.001 *
ApoA <sub>1</sub> , g/L	1578 (1355–1893) <sup>a</sup>	1508 (1293–2057) <sup>a</sup>	0.10 <sup>b</sup>	0.92
ApoB, g/L	621 (519–738) <sup>a</sup>	702 (520–828) <sup>a</sup>	−2.35 <sup>b</sup>	0.02 *
Lp(a), mg/L	87 (44–188) <sup>a</sup>	87 (42–188.5) <sup>a</sup>	0.29 <sup>b</sup>	0.77
sdLDL-C, mmol/L	0.7 (0.56–0.87) <sup>a</sup>	0.93 (0.77–1.00) <sup>a</sup>	−3.33 <sup>b</sup>	<0.001 *
Complement/inflammatory markers				
CRP, mg/dL	1.04 (0.5–2.6) <sup>a</sup>	1.71 (0.895–3.68) <sup>a</sup>	−2.68 <sup>b</sup>	0.007 *
C1q, mg/L	184 (166–211) <sup>a</sup>	194 (171.75–224.75) <sup>a</sup>	−2.11 <sup>b</sup>	0.03 *

<sup>a</sup> Expressed as the median (interquartile range). <sup>b</sup> Rank sum test: Z value; <sup>c</sup> Expressed as mean ± standard deviation (SD); <sup>d</sup> Student's *t*-test: *t*-value; \* *p*-values were statistically different, *p* < 0.05.

### 3.4. Results of Each Model and Receiver Operating Curve (ROC) Analysis

#### a. Logistic regression analysis

When the risk factors were analyzed with a univariate logistic regression, the results were shown in Supplementary Table S1 (*p* < 0.05).

If only 12 risk factors of PE were analyzed with a multivariate binary logistic regression and an ROC curve analysis was performed, the maximum Youden index of logistic regression was 0.110, the sensitivity of the model was 12.1%, the specificity was 98.9%, and the AUC<sup>ROC</sup> = 0.78.

Multivariate binary logistic regression analysis was performed on 12 risk factors of PE and 38 routine laboratory indicators. An ROC curve analysis was performed according to the above methods, the maximum Youden index of logistic regression was 0.701, the sensitivity of the model was 73.6%, the specificity was 96.5%, and the AUC<sup>ROC</sup> = 0.86.

### b. Decision tree model analysis

Using a decision tree learning algorithm, if only 12 risk factors of PE were included in the model, the maximum Youden index of logistic regression was 0.130, the sensitivity of the model was 15.4%, the specificity was 97.6%, and the  $AUC^{ROC} = 0.74$ ; when 12 risk factors of PE and 38 routine laboratory indicators were included in the model, the maximum Youden index of logistic regression was 0.616, the sensitivity of the model was 64.8%, the specificity was 96.8%, and the  $AUC^{ROC} = 0.77$ .

### c. Support vector machine (SVM) analysis

Using SVM learning system, if only 12 risk factors of PE were included in the model, the maximum Youden index of logistic regression was 0.055, the sensitivity of model was 6.6%, the specificity of model was 98.9%, and the  $AUC^{ROC} = 0.66$ . When 12 risk factors of PE and 38 routine laboratory indicators were included in the model, the maximum Youden index of logistic regression was 0.669, the sensitivity of the model was 67.0%, the specificity was 99.9%, and the  $AUC^{ROC} = 0.93$ .

The results of the ROC analysis based on 12 risk factors of PE are shown in Figure 1, and the results of the ROC analysis based on 12 risk factors of PE combining with 38 routine laboratory indicators are shown in Figure 2.

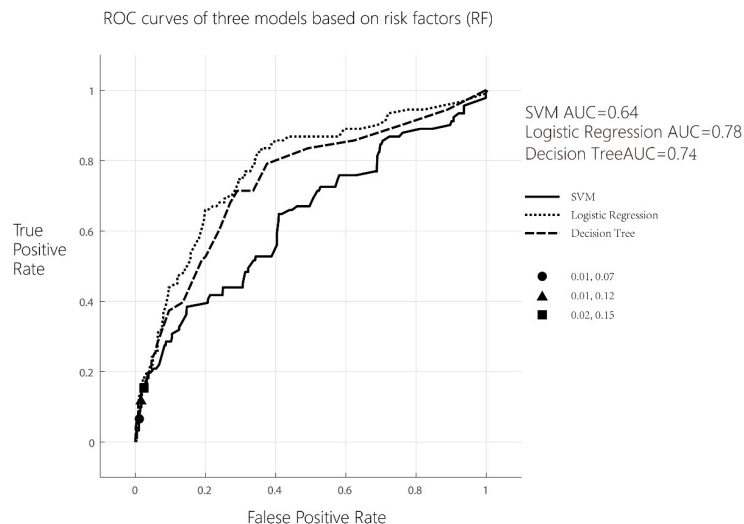


**Figure 1.** ROC curves of three models based on 12 risk factors (RF).

ROC curves of three models based on risk factors (RF) and routine laboratory indicators

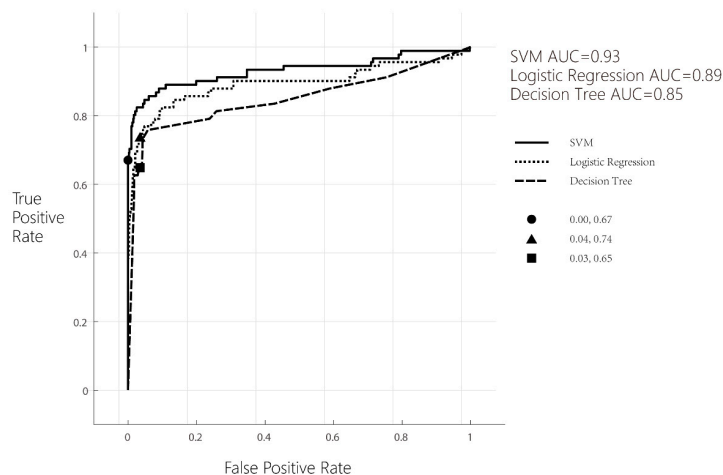


**Figure 2.** ROC curves of three models based on 12 risk factors (RF) and 38 routine laboratory indicators.

## d. Delong test of ROCs differ between models

Delong tests were used to explore whether there were statistical differences in the area under the curve between the three models. If only 12 risk factors of PE were included in the models, the results of the pairwise comparison of ROC curves between support vector machine and decision tree models and those between support vector machine and logistic regression models were statistically different. The results are shown in Table 3 ( $p < 0.05$ ).

While 12 risk factors of PE and 38 routine laboratory indicators were included in the models, the results of pairwise comparison of ROC curves between support vector machine and decision tree models and that between support vector machine and logistic regression models were also statistically different. The results are shown in Table 4 ( $p < 0.05$ ).

**Table 3.** Delong test of ROCs differ between models (12 risk factors). Pairwise comparison of ROC curves.

SVM~Decision Tree	
Difference between areas	0.08
Standard Error <sup>a</sup>	0.044
95% Confidence Interval	0.047 to 0.220
z statistic	3.02
Significance level	$p = 0.0025$
Logistic Regression~Decision Tree	
Difference between areas	0.04
Standard Error <sup>a</sup>	0.025
95% Confidence Interval	−0.009 to 0.088
z statistic	1.57
Significance level	$p = 0.1162$
Logistic Regression~SVM	
Difference between areas	0.12
Standard Error <sup>a</sup>	0.034
95% Confidence Interval	0.106 to 0.238
z statistic	5.08
Significance level	$p < 0.0001$

**Table 4.** Delong test of ROCs differ between models (12 risk factors and 38 routine laboratory indicators).

SVM~Decision Tree	
Difference between areas	0.07
Standard Error <sup>a</sup>	0.027
95% Confidence Interval	0.026 to 0.132
z statistic	2.92
Significance level	$p = 0.0035$
Logistic Regression~Decision Tree	
Difference between areas	0.09
Standard Error <sup>a</sup>	0.033
95% Confidence Interval	−0.050 to 0.077

Table 4. Cont.

SVM~Decision Tree	
z statistic	0.41
Significance level	$p = 0.6837$
Logistic Regression~SVM	
Difference between areas	0.07
Standard Error <sup>a</sup>	0.023
95% Confidence Interval	0.020 to 0.112
z statistic	2.82
Significance level	$p = 0.0049$

#### 4. Discussion

The incidence of PE is related to spiral artery remodeling disorder, endothelial dysfunction, vasospasm, oxidative stress, and micro-embolism. Therefore, factors affecting placenta formation and endothelial function damage are the risk factors for PE [16]. Consistent with other studies [17–19], previous history of preeclampsia, diabetes mellitus, thrombotic disease, systemic lupus erythematosus (SLE), antiphospholipid syndrome (APS), kidney disease, assisted reproductive technology, obstructive sleep apnea hypopnea syndrome (OSAHS), BMI > 30 kg/m<sup>2</sup>, age over 35, multiple pregnancies, and primipara were included as risk factors in the model. In this study, there was no thrombotic disease in the PE group, which may be because pregnant women with thrombotic disease tendency continued to take anticoagulant drugs, such as aspirin in the first trimester, effectively preventing abnormal blood flow status and thrombosis and reducing the risk of PE.

The pathologic lesions of preeclampsia and eclampsia are characterized by widespread endothelial lesions in various organ beds [20], such as liver lesions with periportal and portal necrosis and hepatic arterial medial necrosis, based on an autopsy series of 317 mothers who died of eclampsia. Therefore, when PE has not progressed in the first trimester of pregnancy, slight changes in liver vessels may have occurred in pregnant women, and the liver function is affected, which is manifested as elevated liver enzymes, abnormal coagulation function, and abnormal substance metabolism. Similarly, renal tissue demonstrated hallmarks of glomerular endotheliosis reported in previous studies [21]. Glomerular endothelial cell lesions, impaired mechanical barrier and charge barrier, and increased filtration membrane permeability lead to abnormal renal function and proteinuria in PE patients [22].

Previous studies have shown an association between abnormal lipid metabolism and inflammatory activation with preeclampsia [23–26]. In this study, except for HDL-C and ApoA<sub>1</sub>, the other blood lipid indicators in the PE group were higher than those in the control group. HDL is involved in the reverse transport of cholesterol (as a vascular protective factor that has an anti-atherosclerosis effect while ApoA<sub>1</sub> is a tool to carry HDL), is also a component of HDL, and has a relatively important role in preventing the occurrence of atherosclerosis. HDL-C and ApoA<sub>1</sub> levels of the PE group were lower than those of the control group, which was consistent with previous studies [27].

In this study, it is not hard to see that the models established combining routine laboratory indicators with risk factors improve the accuracy of prediction rather than only with risk factors. In this study, the SVM model had the best prediction ability of early-onset PE. Machine learning has received a lot of attention in recent years. The advantages and disadvantages of machine learning and traditional statistical models vary with different research questions, research designs, and research data. Compared to the other machine learning methods, the SVM is very powerful at recognizing subtle patterns in complex datasets, greatly improves the prediction performance of the model, and has a good clinical application prospect [28]. The SVM loss function has its own regular term, so SVM is a

structural risk minimization algorithm. The so-called structural risk minimization means to seek a balance between a training error and model complexity to prevent overfitting so as to minimize the real error. In order to better minimize structural risks, regular terms were added to the SVM model construction to further reduce potential overfitting.

In previous studies, mean arterial pressure, uterine arterial pulse index, and serum placental growth factor were selected as biomarkers for early-onset PE prediction [29,30]. Although the accuracy and specificity are relatively high, the collection cost is high, and the operation is difficult. Similar to this study, Jong et al. used logistic regression, decision tree model, naive Bayes classification, support vector machine, random forest algorithm, and stochastic gradient boosting method to build a prediction model for delayed preeclampsia by collecting general clinical data, medical history and biochemical laboratory data. The stochastic gradient boosting model had the best prediction performance with an accuracy and false positive rate of 0.973 and 0.009 [31]. Although different from the variables included in this study, it also shows that machine learning algorithms can effectively predict preeclampsia to a certain extent. The routine laboratory indicators adopted in this study are included in the routine prenatal examination, which is convenient to obtain, simple and rapid, and at the same time reduces the extra cost for patients and the prediction cost. However, the deficiency also lies in this; the established model lacks the specific index of early-onset PE, and the specificity of the model is not high. The sample size of the PE group is smaller than that of the control group, which may have a certain impact on the model. Subsequent studies will improve upon this. The sample size of this study is small, which does not meet the requirements of EPV (Event Per Variable), so the results of the logistic regression may not be robust enough. However, considering that this type of patient is rare and that the results are somewhat interpretable, it is still presented. Further research is needed to confirm the reliability of the results.

## 5. Conclusions

The performance of clinical risk factors alone in predicting early-onset PE is poor, and the performance significantly improved when combining risk factors with routine laboratory indicators. The support vector machine (SVM) model showed the best  $AUC^{ROC}$ , specificity, and sensitivity compared with the logistic regression model and decision tree model.

**Supplementary Materials:** The following supporting information can be downloaded at: <https://www.mdpi.com/article/10.3390/life13081648/s1>, The univariate logistic regression analysis of risk factors for PE was shown in Supplementary Table S1 ( $p < 0.05$ ).

**Author Contributions:** Y.X.: Conceptualization, Investigation, Visualization, Writing—original draft. N.Y.: Investigation, Data curation. X.G.: Investigation, Data curation. Y.W.: Writing—review & editing, Project administration, Funding acquisition. H.Z.: Data curation. K.J.: Conceptualization, Writing—review & editing, Project administration and Funding acquisition. All authors have read and agreed to the published version of the manuscript.

**Funding:** This work was supported by the General Project of National Natural Science Foundation of China (Project No.62071007).

**Institutional Review Board Statement:** The study was conducted in accordance with the Declaration of Helsinki, and approved by the Ethics Committee of Peking University Third Hospital (protocol code IRB00006761-M2016122, date of approval 22 September 2016).

**Informed Consent Statement:** Not applicable.

**Data Availability Statement:** The data used to support the findings of this study are available from the corresponding author upon request.

**Acknowledgments:** We would like to thank all study participants who were involved in this investigation but are not in the author list.



**Conflicts of Interest:** We declare that we have no financial and personal relationships with other people or organizations that can inappropriately influence our work, there is no professional or other personal interest of any nature or kind in any product, service and/or company that could be construed as influencing the position presented in, or the review of, the manuscript entitled.

## Abbreviations

PE: preeclampsia; ML, machine learning; BMI, body mass index; SLE, systemic lupus erythematosus; APS, antiphospholipid syndrome; ART, assisted reproductive technology; OSAHS, obstructive sleep apnea; ALB, albumin; ALT, alanine transaminase; AST, aspartate transaminase; ALP, alkaline phosphatase; C1q, complement C1q; Ca, calcium; Cr, creatinine; CRP, C-reactive protein; GGT,  $\gamma$ -glutamyl transpeptidase; GLB, globulin; TG, triglyceride; TC, total cholesterol; HDL-C, high-density lipoprotein cholesterol; LDL-C, low-density lipoprotein cholesterol; Lp (a), lipoprotein (a); ApoA<sub>1</sub>, apolipoprotein A1; ApoB, apolipoprotein B; sdLDL-C, small dense low density lipoprotein; TP, total protein; TBA, total bile acid; T-Bil, total bilirubin; D-Bil, direct bilirubin; UA, uric acid; UREA, urea; P, phosphorus; LYM, absolute value of lymphocyte; NEU, absolute value of neutrophil; PLT, platelet count; PT, prothrombin time; PTA, prothrombin activity; APTT, activated partial thrombin time; FIB, fibrinogen; FDP, fibrinogen degradation Products; TT, thrombin time; SVM, support vector machine, CI, confidence interval.

## References

1. Khan, K.S.; Wojdyla, D.; Say, L.; Gülmezoglu, A.M.; Van Look, P.F. WHO analysis of causes of maternal death: A systematic review. *Lancet* **2006**, *367*, 1066–1074. [CrossRef]
2. Duley, L. The Global Impact of Pre-eclampsia and Eclampsia. *Semin. Perinatol.* **2009**, *33*, 130–137. [CrossRef]
3. Habli, M.; Eftekhari, N.; Wiebracht, E.; Bombrys, A.; Khabbaz, M.; How, H.; Sibai, B. Long-term maternal and subsequent pregnancy outcomes 5 years after hemolysis, elevated liver enzymes, and low platelets (HELLP) syndrome. *Am. J. Obs. Gynecol.* **2009**, *201*, 381–385. [CrossRef]
4. Nelson, D.B.; Ziadie, M.S.; McIntire, D.D.; Rogers, B.B.; Leveno, K.J. Placental pathology suggesting that preeclampsia is more than one disease. *Am. J. Obs. Gynecol.* **2014**, *210*, 61–66. [CrossRef]
5. De Kat, A.C.; Hirst, J.; Woodward, M.; Kennedy, S.; Peters, S.A. Prediction models for preeclampsia: A systematic review. *Pregnancy Hypertens.* **2019**, *16*, 48–66. [CrossRef]
6. Poon, L.C.; Shennan, A.; Hyett, J.A.; Kapur, A.; Hadar, E.; Divakar, H.; McAuliffe, F.; da Silva Costa, F.; von Dadelszen, P.; McIntyre, H.D.; et al. The International Federation of Gynecology and Obstetrics (FIGO) initiative on pre-eclampsia: A pragmatic guide for first-trimester screening and prevention. *Int. J. Gynaecol. Obstet.* **2019**, *145* (Suppl. S1), 1–33. [CrossRef]
7. Payne, B.A.; Hutcheon, J.A.; Ansermino, J.M.; Hall, D.R.; Bhutta, Z.A.; Bhutta, S.Z.; Biryabarema, C.; Grobman, W.A.; Groen, H.; Haniff, F.; et al. A risk prediction model for the assessment and triage of women with hypertensive disorders of pregnancy in low-resourced settings: The miniPIERS (Pre-eclampsia Integrated Estimate of RiSk) multi-country prospective cohort study. *PLoS Med.* **2014**, *11*, e1001589. [CrossRef]
8. Thangaratinam, S.; Allotey, J.; Marlin, N.; Mol, B.W.; Von Dadelszen, P.; Ganzevoort, W.; Akkermans, J.; Ahmed, A.; Daniels, J.; Deeks, J.; et al. Development and validation of Prediction models for Risks of complications in Early-onset Pre-eclampsia (PREP): A prospective cohort study. *Health Technol. Assess.* **2017**, *21*, 1–100. [CrossRef]
9. Chappell, L.C.; Duckworth, S.; Seed, P.T.; Griffin, M.; Myers, J.; Mackillop, L.; Simpson, N.; Waugh, J.; Anumba, D.; Kenny, L.C.; et al. Diagnostic accuracy of placental growth factor in women with suspected preeclampsia: A prospective multicenter study. *Circulation* **2013**, *128*, 2121–2131. [CrossRef]
10. Zeisler, H.; Llurba, E.; Chantraine, F.; Vatish, M.; Staff, A.C.; Sennström, M.; Olovsson, M.; Brennecke, S.P.; Stepan, H.; Allegranza, D.; et al. Predictive Value of the sFlt-1:PlGF Ratio in Women with Suspected Preeclampsia. *N. Engl. J. Med.* **2016**, *374*, 13–22. [CrossRef]
11. North, R.A.; McCowan, L.M.; Dekker, G.A.; Poston, L.; Chan, E.H.; Stewart, A.W.; Black, M.A.; Taylor, R.S.; Walker, J.J.; Baker, P.N.; et al. Clinical risk prediction for pre-eclampsia in nulliparous women: Development of model in international prospective cohort. *BMJ* **2011**, *342*, d1875. [CrossRef]
12. Obermeyer, Z.; Emanuel, E.J. Predicting the Future—Big Data, Machine Learning, and Clinical Medicine. *N. Engl. J. Med.* **2016**, *375*, 1216–1219. [CrossRef]
13. Darcy, A.M.; Louie, A.K.; Roberts, L.W. Machine Learning and the Profession of Medicine. *JAMA* **2016**, *315*, 551–552. [CrossRef]

14. Frizzell, J.D.; Liang, L.; Schulte, P.J.; Yancy, C.W.; Heidenreich, P.A.; Hernandez, A.F.; Bhatt, D.L.; Fonarow, G.C.; Laskey, W.K. Prediction of 30-Day All-Cause Readmissions in Patients Hospitalized for Heart Failure: Comparison of Machine Learning and Other Statistical Approaches. *JAMA Cardiol.* **2017**, *2*, 204–209. [CrossRef]
15. Gestational Hypertension and Preeclampsia: ACOG Practice Bulletin Summary, Number 222. *Obstet. Gynecol.* **2020**, *135*, 1492–1495. [CrossRef]
16. Ives, C.W.; Sinkey, R.; Rajapreyar, I.; Tita, A.T.N.; Oparil, S. Preeclampsia—Pathophysiology and Clinical Presentations: JACC State-of-the-Art Review. *J. Am. Coll. Cardiol.* **2020**, *76*, 1690–1702. [CrossRef]
17. Phipps, E.A.; Thadhani, R.; Benzing, T.; Karumanchi, S.A. Pre-eclampsia: Pathogenesis, novel diagnostics and therapies. *Nat. Rev. Nephrol.* **2019**, *15*, 275–289. [CrossRef]
18. Good clinical practice advice: First trimester screening and prevention of pre-eclampsia in singleton pregnancy. *Int. J. Gynaecol. Obstet.* **2019**, *144*, 325–329. [CrossRef]
19. ACOG Practice Bulletin No. 202: Gestational Hypertension and Preeclampsia. *Obs. Gynecol.* **2019**, *133*, 1.
20. Hecht, J.L.; Ordi, J.; Carrilho, C.; Ismail, M.R.; Zsengeller, Z.K.; Karumanchi, S.A.; Rosen, S. The pathology of eclampsia: An autopsy series. *Hypertens. Pregnancy* **2017**, *36*, 259–268. [CrossRef]
21. Gaber, L.W.; Spargo, B.H.; Lindheimer, M.D. Renal pathology in pre-eclampsia. *Baillieres Clin. Obs. Gynaecol.* **1994**, *8*, 443–468. [CrossRef] [PubMed]
22. Garovic, V.D.; Wagner, S.J.; Turner, S.T.; Rosenthal, D.W.; Watson, W.J.; Brost, B.C.; Rose, C.H.; Gavrilova, L.; Craig, P.; Bailey, K.R.; et al. Urinary podocyte excretion as a marker for preeclampsia. *Am. J. Obs. Gynecol.* **2007**, *196*, 320–321. [CrossRef] [PubMed]
23. Dey, M.; Arora, D.; Narayan, N.; Kumar, R. Serum Cholesterol and Ceruloplasmin Levels in Second Trimester can Predict Development of Pre-eclampsia. *N. Am. J. Med. Sci.* **2013**, *5*, 41–46. [CrossRef] [PubMed]
24. van Rijn, B.B.; Veerbeek, J.H.; Scholtens, L.C.; Post, U.E.; Koster, M.P.; Peeters, L.L.; Koenen, S.V.; Bruinse, H.W.; Franx, A. C-reactive protein and fibrinogen levels as determinants of recurrent preeclampsia: A prospective cohort study. *J. Hypertens.* **2014**, *32*, 408–414. [CrossRef]
25. Alma, L.J.; Bokslag, A.; Maas, A.; Franx, A.; Paulus, W.J.; de Groot, C. Shared biomarkers between female diastolic heart failure and pre-eclampsia: A systematic review and meta-analysis. *ESC Heart Fail.* **2017**, *4*, 88–98. [CrossRef]
26. Mary, S.; Kulkarni, M.J.; Malakar, D.; Joshi, S.R.; Mehendale, S.S.; Giri, A.P. Placental Proteomics Provides Insights into Pathophysiology of Pre-Eclampsia and Predicts Possible Markers in Plasma. *J. Proteome Res.* **2017**, *16*, 1050–1060. [CrossRef]
27. Wang, Y.; Shi, D.; Chen, L. Lipid profile and cytokines in hypertension of pregnancy: A comparison of preeclampsia therapies. *J. Clin. Hypertens.* **2018**, *20*, 394–399. [CrossRef]
28. Huang, S.; Cai, N.; Pacheco, P.P.; Narrandes, S.; Wang, Y.; Xu, W. Applications of Support Vector Machine (SVM) Learning in Cancer Genomics. *Cancer Genom. Proteom.* **2018**, *15*, 41–51.
29. Serra, B.; Mendoza, M.; Scazzocchio, E.; Meler, E.; Nolla, M.; Sabrià, E.; Rodríguez, I.; Carreras, E. A new model for screening for early-onset preeclampsia. *Am. J. Obs. Gynecol.* **2020**, *222*, 601–608. [CrossRef]
30. Akolekar, R.; Syngelaki, A.; Poon, L.; Wright, D.; Nicolaides, K.H. Competing Risks Model in Early Screening for Preeclampsia by Biophysical and Biochemical Markers. *Fetal Diagn. Ther.* **2013**, *33*, 8–15. [CrossRef]
31. Jhee, J.H.; Lee, S.; Park, Y.; Lee, S.E.; Kim, Y.A.; Kang, S.-W.; Kwon, J.-Y.; Park, J.T. Prediction model development of late-onset preeclampsia using machine learning-based methods. *PLoS ONE* **2019**, *14*, e221202. [CrossRef] [PubMed]

**Disclaimer/Publisher’s Note:** The statements, opinions and data contained in all publications are solely those of the individual author(s) and contributor(s) and not of MDPI and/or the editor(s). MDPI and/or the editor(s) disclaim responsibility for any injury to people or property resulting from any ideas, methods, instructions or products referred to in the content.

## Article

# Outcomes of Pregnancy in COVID-19-Positive Mothers in a Tertiary Centre

Vigneshwaran Subramaniam, Beng Kwang Ng \*, Su Ee Phon, Hamizan Muhammad Rafi'uddin, Abd Razak Wira Sorfan, Abd Azman Siti Hajar and Mohamed Ismail Nor Azlin

Department of Obstetrics and Gynaecology, Faculty of Medicine, Universiti Kebangsaan Malaysia, Jalan Yaacob Latiff, Bandar Tun Razak, Cheras, Kuala Lumpur 56000, Malaysia; kinet246@gmail.com (V.S.); sephon88@yahoo.com (S.E.P.); rafinofee@gmail.com (H.M.R.); wirasorfan@gmail.com (A.R.W.S.); sitihsajar.abdazman@gmail.com (A.A.S.H.); azlinm@ppukm.ukm.edu.my (M.I.N.A.)

\* Correspondence: nbk9955@ppukm.ukm.edu.my

**Abstract:** Background: COVID-19 is an emerging global pandemic with potential adverse effects during pregnancy. This study aimed to determine the adverse maternal and foetal outcomes due to COVID-19 infection. We also compared maternal and neonatal outcomes with regard to the timing of diagnosis (first and second trimester vs. third and fourth trimester); early COVID-19 (stage I and II) vs. severe-stage COVID-19 (III, IV, and V); and lastly, women who were partially vaccinated vs. unvaccinated. Methods: This was a retrospective study conducted in HCTM from January 2021 to January 2022. All pregnant women admitted for COVID-19 infections were recruited. The patients' records were traced. Adverse maternal and neonatal outcomes were documented and analysed. Results: There were 172 pregnant women recruited into this study. We excluded twenty-four patients with incomplete data and nine women who delivered elsewhere. The final 139 patients were available for data analysis. The majority of women were in their third trimester of pregnancy (87.8%); however, only 5.0% and 7.2% were in the first and second trimesters, respectively. The study population had a median BMI of 29.1 kg/m<sup>2</sup> and almost half of them had never received a COVID-19 vaccination. A sub-analysis of data concerning adverse maternal and foetal outcomes comparing early vs. severe stages of COVID-19 infection showed that severe-stage disease increased the risk of preterm birth (54.5% vs. 15.4%,  $p < 0.001$ ) and preterm birth before 34 weeks (31.9% vs. 2.6%,  $p < 0.001$ ) significantly. The severe-stage disease also increased NICU admission (40.9% vs. 15.4%,  $p = 0.017$ ) with lower birth weight (2995 g vs. 2770 g,  $p = 0.017$ ). The unvaccinated mothers had an increased risk of preterm birth before 34 weeks and this was statistically significant (11.6% vs. 2.9%,  $p = 0.048$ ). Conclusions: Adverse pregnancy outcomes such as ICU admission or patient death could occur; however, the clinical course of COVID-19 in most women was not severe and the infection did not significantly influence the pregnancy. The risk of preterm birth before 34 weeks was higher in a more severe-stage disease and unvaccinated mother. The findings from this study can guide and enhance antenatal counselling of women with COVID-19 infection, although they should be interpreted with caution in view of the very small number of included cases of patients in the first and second trimesters.

**Keywords:** COVID-19; pregnancy; maternal; perinatal; infection; vaccination

## 1. Introduction

The world was shaken in 2019 by the spread of an unknown virus causing pneumonia-like symptoms. Starting from a small city in Wuhan, China, the virus spread like wildfire and led to a global pandemic. The outbreak was caused by a novel coronavirus known as severe acute respiratory syndrome coronavirus-2 (SARS-CoV-2) and the disease is now named coronavirus disease 2019 (COVID-19) [1]. Due to the increasing mortalities from COVID-19 globally, the WHO announced this highly infectious disease as a global pandemic on 11th March 2020 [1]. Pregnant and non-pregnant women had the same risk

of acquiring COVID-19 [1]. Due to physiologic, anatomic, and immunologic changes in pregnancy, there was an increased risk of complications during pregnancy and the management of pregnant women was more challenging and complicated. Pregnant women with COVID-19 were 5.4 times more likely to be hospitalised, 1.5 times more likely to be admitted to the ICU, and 1.7 times at higher risk of requiring mechanical ventilation [1].

Malaysia was not exempt from this global pandemic, with the first three imported cases confirmed on 25th January 2020. Since then, Malaysia has reported 2.75 million cases and 31,485 deaths as of 31 December 2021 [2]. The first large outbreak in Malaysia was managed successfully using movement restrictions between March and April 2020 [3]. Following the implementation of the MCO, all Malaysians were primarily instructed to stay indoors. Other imposed restrictions included a prohibition of mass gatherings, health screening and quarantine for Malaysians coming from abroad, restriction on foreigners entering the country, and closure of all facilities except primary and essential services such as health services, water, electricity, telecommunication, and food supply companies [3]. However, since September 2020, institutional outbreaks, state elections, and an inconsistent implementation of public health and social measures have led to large periodic outbreaks [4]. Hospital Canselor Tuanku Muhriz (HCTM) started seeing COVID-19 patients during pregnancy in January 2021.

Several studies conducted in Europe observed adverse pregnancy outcomes in COVID-19-infected women. Adverse pregnancy outcomes were associated with infection acquired at early gestational age, more symptomatic presentation, and use of oxygen support therapy. Maternal and neonatal outcomes include caesarean section, premature birth, low birth weight, COVID-19 transmission in neonates, maternal ICU admission, mechanical ventilation rates, and maternal death. Little evidence suggests that COVID-19 infection in early pregnancy causes preterm delivery and low birth weight in certain countries [5–12]. A recent systematic review regarding the effect of COVID-19 on maternal, perinatal, and neonatal outcomes among 324 pregnant women concluded that gestational age upon admission ranged from 5 weeks to 41 weeks, and up to 14% of women presented with severe pneumonia. There were four cases of spontaneous miscarriage, and gestational age upon delivery ranged from 28 weeks to 41 weeks. The majority of women delivered via caesarean section, and in those with severe disease, almost all required ICU admission [13].

Unfortunately, local data about the effect of COVID-19 infection on adverse maternal and neonatal outcomes are limited. This study will allow us to increase our knowledge about the effect of COVID-19 during pregnancy among the local population and help to redistribute resources in the management of COVID-19-related issues in the local setting. We aimed to determine the adverse maternal outcomes such as miscarriage, preterm birth, preterm prelabour rupture of membrane, SGA, IUGR, emergency caesarean section, post-partum haemorrhage, and maternal death. We also aimed to determine the adverse neonatal outcomes such as low birth weight, NICU admission, baby requiring mechanical intubation, neonatal COVID-19 infection, and neonatal death. In the sub-analysis, we also compared maternal and neonatal outcomes with regard to the timing of diagnosis (before 28 weeks vs. after 28 weeks); early COVID-19 (stage I and II) vs. severe-stage COVID-19 (III, IV, and V); and lastly, partially vaccinated women vs. unvaccinated women.

## 2. Materials and Methods

### 2.1. Study Design

This was a retrospective study conducted in HCTM from January 2021 to January 2022. All pregnant women admitted for COVID-19 infection were recruited. Patients' records were traced from the record office unit, which includes the patient's social characteristics (age, parity, gestational age upon admission, body mass index, and pre-existing antenatal co-morbidity (e.g., diabetes mellitus, hypertension, and hyperthyroidism)), their presenting complaint (asymptomatic, fever, cough, chest tightness, sore throat, SOB, diarrhoea, loss of smell, loss of taste, myalgia, fatigue, and headache), and laboratory testing performed during admission (TWC, lymphocyte count, CRP, ALT, and AST). Adverse maternal out-

comes such as miscarriage, preterm birth, preterm prelabour rupture of membrane, SGA, IUGR, emergency caesarean section, post-partum haemorrhage, ICU admission, need for mechanical ventilation, antiviral therapy used, required antibiotic therapy, LMWH used, corticosteroid used, and maternal death were documented on the data collection sheet. Lastly, adverse neonatal outcomes such as low birth weight, poor Apgar score, NICU admission, mechanical intubation, oxygen support, neonatal COVID-19 infection, and neonatal death were also documented.

The diagnosis of COVID-19 was based on the results of real-time reverse transcriptase polymerase chain reaction (rRT-PCR) or RTK Ag detection and positive saliva test. The samples were collected from upper respiratory nasopharyngeal swabs to confirm COVID-19 either from government hospitals or private hospitals. Patients' medical records with incomplete data or who delivered elsewhere were excluded from the study. We included all of the pregnant women who were admitted to HCTM for COVID-19 infection and delivered in our hospital. Exclusion criteria were patients with incomplete data and who delivered elsewhere.

## 2.2. Sample Size Calculation

This study reports the rates or prevalence of clinical manifestations (symptoms, laboratory, and radiological findings) and risk factors of maternal and perinatal outcomes (preterm birth, foetal distress, and low birth weight) in pregnancies of women with COVID-19 and admitted to HCTM. Following the formula calculator that Epitools used, we used a prevalence calculator similar to the prevalence used by Smith et al. [9]. Therefore, based on the calculated sample size, about 139 patients were needed for this study.

## 2.3. Data Analysis

The Statistical Package of Social Sciences (SPSS) Version 22.0 (IBM Corp., Armonk, NY, USA) was used to analyse the study data. Data that were not normally distributed were expressed as median (quartile). Other statistical tests included Mann–Whitney U and Fisher exact/chi-square tests. A probability value of <0.05 was considered to be statistically significant.

## 3. Results

There were 172 pregnant women recruited into this study. We excluded twenty-four patients with incomplete data and nine women who delivered elsewhere. The final 139 patients were available for data analysis. The median maternal age was 32 years old, Para two, and the median gestational age upon admission was 38 weeks gestation. The majority of women were in their third trimester of pregnancy (87.8%), with only 5.0% and 7.2% being in the first and second trimesters, respectively. The ethnicity distribution followed the Malaysian population with the majority of the women being Malay (87.1%), followed by others (7.2%), and then Chinese and Indian (2.9% each). More than half of the women were professional in occupation, followed by housewives (34.5%). Most women received tertiary education and belonged to the M40 group according to household income in Malaysia. The study population had a median BMI of 29.1 kg/m<sup>2</sup> and almost half of them had never received a COVID-19 vaccination (Table 1).

Almost three quarters of patients diagnosed with COVID-19 were diagnosed using COVID-19 PCR testing. The majority presented in the early stages (stages 1 and 2), but 16.8% of patients were diagnosed with COVID-19 stage 3A and above. Sixty percent of them were symptomatic upon diagnosis. Symptoms such as cough, sore throat, and fever were among the most common symptoms experienced by patients. Other symptoms included myalgia (28.8%), fatigue (20.1%), headache (8.6%), loss of smell (23.3%), and loss of taste (28.8%). Almost 60% of patients were given LMWH for the prevention of pulmonary embolism, but only 13.6% were given steroids (Table 2).

Upon admission, laboratory testing was performed that included a median white blood count of 10.3, a lymphocyte count of 16.3, and a CRP of 2.1. Both median ALT and AST were 15.0 and 14.0, respectively. There were 107 chest radiographs performed: 6.5%

revealed ground-glass opacity and 12.1% observed pneumonia changes. Only ten CT scans were performed, and only one patient was diagnosed with pulmonary embolism (Table 3).

**Table 1.** Maternal characteristics.

Maternal Characteristic	N (%)
Age (years)	32.0 (28.0, 35.0)
Parity	2 (1, 3)
Gestational age upon admission	38.0 (33.0, 39.1)
Trimester	
• First	7 (5.0)
• Second	10 (7.2)
• Third	122 (87.8)
Ethnicity	
• Malay	121 (87.1)
• Chinese	4 (2.9)
• Indian	4 (2.9)
• Other (non-Malaysian)	10 (7.1)
Occupation	
• Professional	72 (51.8)
• Non-professional	19 (13.7)
• Housewife	48 (34.5)
Educational level	
• Primary	6 (4.3)
• Secondary	48 (34.5)
• Tertiary	80 (57.6)
• No formal education	5 (3.6)
Household income	
• B40 (<RM 4360)	55 (39.5)
• M40 (>RM 4360–RM9619)	71 (51.1)
• T20 (>RM9616)	13 (9.4)
Body mass index (kg/m <sup>2</sup> )	29.1 (25.5, 32.4)
• Medical comorbid	37 (26.6)
• Diabetes	13 (40.6)
• Hypertension	8 (25.0)
• Hyperthyroidism	2 (6.2)
• Bronchial asthma	9 (28.1)
Status vaccination of mother	
• Completed the first dose	24 (17.9)
• Completed the second dose	44 (32.8)
• Completed the first booster	2 (1.5)
• Not vaccinated	64 (47.8)

Data presented as median (quartile) unless otherwise specified.

With regard to pregnancy outcomes, there were five miscarriages (3.6%) and 22.4% of the pregnancies were delivered before 37 weeks. Upon further analysis, 7.5% of the patients delivered preterm before 34 weeks, with 1.4% of SGA and 2.9% of IUGR. Almost 60% of patients delivered via lower segment caesarean section (LSCS), followed by vaginal delivery (32.4%) and instrumental delivery (3.6%). Of the caesarean deliveries, 85.7% were emergency, and 14.3% were elective. The reasons for elective caesarean section included being COVID-19-positive (58.3%), followed by other obstetrics indications such as two previous scars, refused trial of scar, and placenta praevia. Almost half of the patients underwent emergency LSCS due to COVID-19 in labour, and only 5.3% of deliveries were complicated with PPH (Table 4).

**Table 2.** Diagnosis and clinical presentation.

	N (%)
Type of test performed	
• Saliva RTK antigen	16 (11.5)
• Rapid mole PCR	16 (11.5)
• PCR	107 (77.0)
COVID-19 category	
• 1	55 (39.6)
• 2A	39 (28.1)
• 2B	23 (16.5)
• 3A	5 (3.6)
• 3B	1 (0.7)
• 4A	6 (4.3)
• 4B	6 (4.3)
• 5	4 (2.9)
Clinical presentation	
• Symptomatic	84 (60.4)
• Fever	58 (41.7)
• Cough	66 (47.5)
• Chest tightness	9 (6.5)
• Sore throat	64 (46.0)
• Shortness of breath	20 (14.4)
• Vomiting	17 (12.2)
• Diarrhoea	21 (15.1)
• Loss of smell	28 (20.1)
• Loss of taste	32 (23.0)
• Myalgia	40 (28.8)
• Fatigue	28 (20.1)
• Headache	12 (8.6)
Drug used	
• Antiviral	9 (6.5)
• Antibiotic	26 (18.7)
• LMWH (enoxaparin)	83 (59.7)
• Steroids	19 (13.7)

RTK: rapid test kit, PCR: polymerase chain reaction, LMWH: low-molecular-weight heparin.

**Table 3.** Laboratory testing and radiological imaging.

Laboratory Testing	N (%)
WBC ( $n = 139$ ), $\times 10^9/L$	10.3 (7.9, 12.2)
Lymphocyte ( $n = 139$ ), $\times 10^9/L$	16.3 (11.2, 21.9)
CRP ( $n = 139$ ), mg/dL	2.1 (1.1, 3.8)
ALT ( $n = 139$ )	15.0 (11.0, 21.0)
AST ( $n = 61$ )	14.0 (11.0, 20.0)
Chest radiograph ( $n = 107$ )	
• Ground-glass opacity	7 (6.5)
• Observed pneumonia changes	13 (12.1)
• Clear CXR	87 (81.3)
CT thorax ( $n = 10$ )	
• PE	1 (10)
• No PE	9 (90)

WBC: white blood count, CRP: C-reactive protein, AST: Aspartate Aminotransferase, ALT: Alanine Transaminase, PE: pulmonary embolism. Data presented as median (quartile) unless otherwise specified.

**Table 4.** Pregnancy outcomes.

Pregnancy Outcome	N (%)
Miscarriage	5 (3.6)
Preterm birth less than 37 weeks	30 (22.4)
Preterm birth less than 34 weeks	10 (7.5)
Preterm prelabour rupture of membrane	3 (2.2)
SGA	2 (1.4)
IUGR	4 (2.9)
Mode of delivery	
• SVD	45 (32.4)
• Instrumental delivery	5 (3.6)
• LSCS	84 (60.4)
Nature of LSCS	
• Elective	12 (14.3)
• Emergency	72 (85.7)
Reason for elective LSCS	
• COVID-19-positive	7 (58.3)
• Two previous scars	2 (16.7)
• Refused VBAC	2 (16.7)
• Placenta praevia major	1 (8.3)
Reason for emergency LSCS	
• COVID-19-positive in labour	34 (47.2)
• Foetal distress	19 (26.4)
• Poor progress	1 (1.4)
• Maternal indication	9 (12.5)
• Abnormal lie in labour	8 (11.1)
• Bleeding placenta praevia	1 (1.4)
Post-partum complication	
• PPH	7 (5.3)

SGA: small for gestational age; IUGR: intrauterine growth restriction; SVD: spontaneous vertex delivery; LSCS: lower segment caesarean section; VBAC: vaginal delivery after caesarean; PPH: post-partum haemorrhage; maternal indications include a higher stage of COVID-19, e.g., stage 4B and stage 5.

The median birth weight was 2990 g and almost 20.1% were admitted to the NICU due to various reasons such as presumed sepsis (11.1%), respiratory distress (29.7%), and prematurity (59.3%). There were a total of 16 out of 27 babies admitted to the NICU who required oxygen support, half of the babies required mechanical ventilation, and the other half were given oxygen support such as CPAP or nasal oxygen. There were no neonatal deaths in our study population (Table 5).

There were no statistically significant differences when comparing the timing of diagnosis of COVID-19 infection in each trimester (first and second trimester and third trimester onward) with regard to maternal and foetal outcomes, except for the miscarriage (Table 6).

A sub-analysis of data concerning adverse maternal and foetal outcomes comparing early vs. severe stages of COVID-19 infection showed that severe-stage disease increased the risk of preterm birth (54.5% vs. 15.4%,  $p < 0.001$ ) and preterm birth before 34 weeks (31.9% vs. 2.6%,  $p < 0.001$ ) significantly. Severe-stage disease also increases NICU admission (40.9% vs. 15.4%,  $p = 0.017$ ) and lower birth weight (2995 g vs. 2770 g,  $p = 0.017$ ) (Table 7).

Lastly, unvaccinated mothers had an increased risk of preterm birth before 34 weeks and this was statistically significant (11.6% vs. 2.9%,  $p = 0.048$ ) (Table 8).



**Table 5.** Neonatal outcomes.

Neonatal Outcome	N (%)
Birth weight (gram)	2990 (2547, 3282)
NICU admission	27 (20.1)
Reason for admission, <i>n</i> = 27	
• Presumed sepsis	3 (11.1)
• Respiratory distress	8 (29.6)
• Prematurity	18 (59.3)
Oxygen support, <i>n</i> = 16	
• Mechanical ventilation	8 (50.0)
• Oxygen other than mechanical ventilation	8 (50.0)
Baby COVID-19-positive, <i>n</i> = 134	5 (3.7)
Neonatal death	0

Data presented as median (quartile) unless otherwise specified.

**Table 6.** Comparison of maternal and neonatal outcomes based on the diagnosis of COVID-19.

Pregnancy Outcome	First and Second Trimester <i>n</i> = 16	Third Trimester Onward <i>n</i> = 123	<i>p</i> (Value)
Miscarriage, <i>n</i> (%)	5 (31.3)	0	<0.001
Preterm birth, <i>n</i> (%)	4 (26)	20 (16.2)	0.109
Preterm birth less than 34 weeks, <i>n</i> (%)	2 (12.5)	8 (6.5)	0.192
Preterm prelabour rupture of membrane, <i>n</i> (%)	0	3 (2.4)	1.000
SGA, <i>n</i> (%)	0	3 (2.4)	1.000
IUGR, <i>n</i> (%)	0	4 (3.3)	1.000
Mode of delivery, <i>n</i> (%)			
• SVD	6 (37.5)	39 (31.7)	0.275
• Instrumental delivery	0	5 (4.1)	
• LSCS	5 (31.3)	79 (64.2)	
Post-partum complication			
• PPH, <i>n</i> (%)	1 (6.3)	6 (4.9)	0.459
Neonatal outcome			
Baby weight (gram)	2900 (2400, 3160)	2990 (2560, 3320)	0.305
NICU admission, <i>n</i> (%)	3 (18.8)	24 (19.5)	0.694
Mechanical intubation, <i>n</i> (%)	2 (12.5)	6 (4.9)	0.467
COVID-19-positive, <i>n</i> (%)	0	5 (4.1)	1.000

Data presented as median (quartile) unless otherwise specified.

**Table 7.** Comparison of maternal and neonatal outcomes based on the diagnosis of COVID-19 in early vs. severe stage.

Pregnancy Outcome	Early Stage (I, II) <i>n</i> = 117	Severe Stage (III, IV, V) <i>n</i> = 22	<i>p</i> (Value)
Miscarriage, <i>n</i> (%)	5 (4.3)	0	1.000
Preterm birth, <i>n</i> (%)	18 (15.4)	12 (54.5)	<0.001
Preterm birth less than 34 weeks, <i>n</i> (%)	3 (2.6)	7 (31.9)	<0.001
Preterm prelabour rupture of membrane, <i>n</i> (%)	1 (0.9)	2 (9.1)	0.070
SGA, <i>n</i> (%)	3 (2.6)	0	1.000
IUGR, <i>n</i> (%)	3 (2.6)	1 (4.5)	0.516

**Table 7.** *Cont.*

Pregnancy Outcome	Early Stage (I, II) <i>n</i> = 117	Severe Stage (III, IV, V) <i>n</i> = 22	<i>p</i> (Value)
Mode of delivery, <i>n</i> (%)			
• SVD	38 (32.5)	7 (31.8)	0.567
• Instrumental delivery	5 (4.3)	0	
• LSCS	69 (59.0)	15 (68.2)	
Post-partum complication			
• PPH, <i>n</i> (%)	7 (6.0)	0	0.599
Neonatal outcome			
Baby weight (gram)	2995 (2602, 3342)	2700 (2027, 3210)	0.047
NICU admission, <i>n</i> (%)	18(15.4)	9 (40.9)	0.017
Mechanical intubation, <i>n</i> (%)	4 (3.4)	4 (18.2)	1.000
COVID-19-positive, <i>n</i> (%)	5 (4.3)	0	0.591

Data presented as median (quartile) unless otherwise specified.

**Table 8.** Comparison of maternal and neonatal outcomes based on the diagnosis of COVID-19 according to vaccination stage.

Pregnancy Outcome	At Least Partially Vaccinated <i>n</i> = 70	Unvaccinated <i>n</i> = 69	<i>p</i> (Value)
Miscarriage, <i>n</i> (%)	0	5 (7.2)	0.028
Preterm birth, <i>n</i> (%)	11 (15.7)	19 (27.5)	0.053
Preterm birth less than 34 weeks, <i>n</i> (%)	2 (2.9)	8 (11.6)	0.048
Preterm prelabour rupture of membrane, <i>n</i> (%)	1 (1.4)	2 (2.9)	0.606
SGA, <i>n</i> (%)	3 (4.3)	0	0.246
IUGR, <i>n</i> (%)	2 (2.8)	2 (2.9)	1.000
Mode of delivery, <i>n</i> (%)			
• SVD	22 (31.4)	23 (37.7)	0.826
• Instrumental delivery	3 (4.3)	2 (2.9)	
• LSCS	45 (64.2)	39 (56.5)	
Post-partum complication			
• PPH, <i>n</i> (%)	5 (7.1)	2 (2.9)	0.444
Neonatal outcome			
Baby weight (gram)	3100 (2607, 3352)	2885 (2525, 3200)	0.059
NICU admission, <i>n</i> (%)	12 (17.1)	15 (21.7)	0.395
Mechanical intubation, <i>n</i> (%)	3 (4.3)	5 (7.2)	1.000
COVID-19-positive, <i>n</i> (%)	2 (2.8)	3 (4.3)	0.669

Data presented as median (quartile) unless otherwise specified.

#### 4. Discussion

The COVID-19 pandemic has been the greatest communicable disease outbreak. Malaysia has experienced several waves of infection, leading to a devastated health system. Malaysia reported 2.75 million cases and 31,485 deaths as of 30 December 2021. The disease burden studied by Jayaraj et al. showed that approximately 32.8% of the total population in Malaysia was estimated to have been infected with COVID-19 by the end of December 2021 [14]. The proportion of COVID-19 infections in ages 0–11, 12–17, 18–50, 51–65, and

above 65 years were 19.9% ( $n = 1,982,000$ ), 2.4% ( $n = 236,000$ ), 66.1% ( $n = 6,577,000$ ), 9.1% ( $n = 901,000$ ), and 2.6% ( $n = 256,000$ ), respectively [14]. The Malaysian MOH, since the outset, prepared for the worst-case scenarios and outlined the plan in clear and easily accessible guidelines. The mitigation strategies that have been in place for disease containment have included movement control order (MCO), enhanced MCO, social distancing, flattening the epidemic curve, vaccination, and achieving herd immunity [15,16].

Pregnant women are susceptible to COVID-19 complications due to gestation-related physiological changes. A cross-sectional study conducted during the Malaysian MCO showed that the majority of women (95%) demonstrated an adequate level of knowledge on COVID-19, whilst 99% had good practice [17]. Women with adequate knowledge also reported a more positive perception of MCO and better obstetric care experience. Additionally, the author also found that tertiary education, employment status, and higher household income were independent predictors of adequate maternal knowledge of COVID-19. Younger and nulliparous women demonstrated greater anxiety levels [17]. Our study population was young women with a median age of 32 years old, Para two. More than half of the women were professional and received a tertiary level education, with 60% of them being M40 and above.

Currently, the results of different studies on the asymptomatic proportion vary significantly from country to country, by at least 1.4% up to 80% [18,19]. On the other hand, among these COVID-19 patients who experience symptoms, about 80% of them develop mild to moderate symptoms. In comparison, 10–20% of cases present severe symptoms throughout the disease, and about 5–6% become critically ill with ARDS, multi-organ failure, and/or septic shock [20]. In our study, 15.8% of the women presented at least stage 3 of the disease and 60.4% were symptomatic. We had three maternal deaths due to COVID-19 among the study population. They were aged between 28 and 37 years old, and presented between 27 and 33 weeks. All three of them were obese, came in with stage 5 disease, and were admitted to the ICU. Two of them were not vaccinated at all and another one only received one dose of the vaccine. All of the babies were delivered before 34 weeks, with babies weighing between 700 and 1600 g. However, none of the babies were COVID-19-positive.

The implementation of lockdowns or MCO over a long period of time in several countries, including Malaysia, has caused an economic crisis, either at the individual or national level. The impact of the economic burden, rates of unemployment, loss of income, and increased mental health issues were found to increase steadily, especially among the young, women, and poor families [21]. Thus, constant lockdowns were not the best way to combat the spread of COVID-19. The Malaysian government established the National COVID-19 Immunisation Program (PICK), which served as a coping strategy or mechanism to increase the Malaysian population's herd immunity in dealing with the COVID-19 hazard. This initiative aimed to vaccinate 80 percent (23.6 million) of Malaysia's population by February 2022 [22]. Unfortunately, until mid-2022, the number of PICK registrations (particularly for booster doses) in Malaysia remained low and unsatisfactory due to some vaccine hesitancy [23,24].

In our study, almost half (47.8%) of the pregnant women remained unvaccinated. A total of 17.9% of women had received one dose, 32.8% had completed two doses of vaccine, and only two women had had their first booster dose. All five miscarriages in our study were from the unvaccinated group. We also found that the unvaccinated group had a higher risk of preterm birth before 34 weeks. This contradicts a study by Wainstock et al., in which there were no differences found between the groups in terms of pregnancy, delivery, and newborn complications, including gestational age at delivery, the incidence of SGA, and newborn respiratory complications [25]. However, we could not demonstrate any correlation between vaccination status vs. stages of COVID-19. This is in contrast with the more recently published systematic review and meta-analysis (2023), where the rate of COVID-19 infections among vaccinated pregnant women compared to unvaccinated is significantly reduced by 43% [12].

With regard to the effects of COVID-19 infection during pregnancy, adverse pregnancy outcomes were associated with infection acquired at early gestational age, severe COVID-19 stage, and use of oxygen support therapy [5–12]. In this study, we could not demonstrate the adverse pregnancy outcome if the patient presented earlier gestation, as the sample size for patients in the first trimester and second trimester was only 5.0% and 7.2%, respectively. This is probably due to the fact that quite a number of patients presented earlier at our institution and were discharged or home monitored, but never delivered in our centre. However, we managed to demonstrate that the presentation of COVID-19 at stage 3 and above (severe stage) was associated with preterm birth, preterm birth before 34 weeks, higher risk of NICU admission, and lower birth weight.

Looking at the data from our neighbour, Singapore, where a prospective cohort study was performed among 16 patients, 37.5%, 43.8%, and 18.7% were infected in the first, second, and third trimesters, respectively. Two patients aged  $\geq 35$  years (12.5%) developed severe pneumonia; one patient (body mass index:  $32.9 \text{ kg/m}^2$ ) required transfer to intensive care. There were no maternal mortalities. Five pregnancies produced term live births, while two spontaneous miscarriages occurred at 11 and 23 weeks [26].

In the earlier systematic review and meta-analysis by Di Mascio D et al. (2019), which included nineteen studies with 79 hospitalised women, preterm birth (24.3%) was the most common adverse pregnancy outcome. COVID-19 infection was associated with a higher rate of PPROM (20.7%), preeclampsia (16.2%), IUGR (11.7%), caesarean section delivery (84%), and perinatal death (11.1%) [6]. In another systematic review by Di Toro F et al., which included 24 studies and 1100 pregnancies, the prevalence of pneumonia was 89%, and 8% of women were admitted to the ICU. Three stillbirths and five maternal deaths were reported. The prevalence of COVID-19-related admission to the neonatal intensive care unit was 2%. Nineteen out of four hundred and forty-four neonates were positive for COVID-19 at birth [7]. In our study, we had a total of three maternal deaths but no cases of neonatal death. There were five babies who were confirmed to be COVID-19-positive in our study.

Lastly, the issue of vertical transmission of severe acute respiratory syndrome coronavirus 2 (SARS-CoV-2) is still not well established. In a review that involved fifty-one studies reporting 336 newborns screened for COVID-19, only 15 (4.4%) were positive for throat swab RT-PCR [27]. Among neonates who were SARS-CoV-2-positive after throat swab, only five (33.3%) had concomitant placenta, amniotic fluid, and cord blood samples tested, and of which, only one amniotic fluid sample was positive via RT PCR [27]. Thus, it is still debatable whether vertical transmission occurred during the first trimester of pregnancy. Additionally, there is no evidence to support caesarean delivery, abstaining from breastfeeding, or mother and infant separation [27,28].

The strength of this study is that this is probably the first local study looking at maternal and foetal outcomes due to COVID-19 infection during pregnancy with a relatively good sample size. Besides reporting the profile of patients and the clinical features, we also looked at the effect of early diagnosis, stages of COVID-19, and vaccination status on pregnancy outcomes. However, there were a few limitations in this study. We did not have enough samples or representative cases from the first and second trimesters; thus, the data on the outcomes of pregnancy should be analysed with caution. We lost the follow-up when the patient was diagnosed early but did not deliver in our centre. We could not assess and further analyse the placental involvement in all of these cases, as there was another project looking at placental histo-morphological patterns, disease severity, and perinatal outcomes.

## 5. Conclusions

Adverse pregnancy outcomes such as ICU admission or death could occur; however, the clinical course of COVID-19 in most women was not severe, and the infection did not significantly influence the pregnancy. The risk of preterm birth before 34 weeks was higher in those with more severe-stage disease and unvaccinated mothers. The findings from this study can guide and enhance antenatal counselling of women with COVID-19 infection,

although they should be interpreted with caution in view of the very small number of cases in the first and second trimesters.

**Author Contributions:** Conceptualisation, V.S., B.K.N., S.E.P. and M.I.N.A.; methodology, V.S., B.K.N. and M.I.N.A.; software, V.S. and B.K.N.; validation, V.S., B.K.N. and M.I.N.A.; formal analysis, V.S. and B.K.N.; investigation, A.A.S.H., A.R.W.S. and B.K.N.; resources, V.S., B.K.N., H.M.R. and M.I.N.A.; data curation, V.S. and B.K.N.; writing—original draft preparation, V.S. and B.K.N.; writing—review and editing, V.S., M.I.N.A. and B.K.N.; visualisation, V.S., S.E.P., A.A.S.H., H.M.R. and B.K.N.; supervision, B.K.N. and M.I.N.A.; project administration, V.S., B.K.N. and M.I.N.A. All authors have read and agreed to the published version of the manuscript.

**Funding:** This research received no external funding.

**Institutional Review Board Statement:** The study was conducted according to the guidelines of the Declaration of Helsinki, and approved by the Medical Research and Ethics Committee of Universiti Kebangsaan Malaysia Medical Centre (UKMMC) (research code: FF2022-271).

**Informed Consent Statement:** Not applicable as this was a retrospective study.

**Data Availability Statement:** The data presented in this study are available upon request from the corresponding author. The data are not publicly available due to ownership belonging to the institution where the study was conducted.

**Acknowledgments:** We would like to thank all of the staff from the record office who helped. Their contributions are sincerely appreciated and gratefully acknowledged.

**Conflicts of Interest:** The authors declare no conflict of interest.

## References

- Overton, E.E.; Goffman, D.; Friedman, A.M. The Epidemiology of COVID-19 in Pregnancy. *Clin. Obstet. Gynecol.* **2022**, *65*, 110–122. [CrossRef] [PubMed]
- Department of Social and Preventive Medicine. COVID-19 Epidemiology for Malaysia. 2020. Available online: <https://spm.um.edu.my/knowledgecentre/covid19-epid-live/> (accessed on 19 April 2021).
- Aziz, N.A.; Othman, J.; Lugova, H.; Suleiman, A. Malaysia's approach in handling COVID-19 onslaught: Report on the Movement Control Order (MCO) and targeted screening to reduce community infection rate and impact on public health and economy. *J. Infect. Public Health* **2020**, *13*, 1823–1829. [CrossRef]
- Rampal, L.; Liew, B.S. Malaysia's third COVID-19 wave—A paradigm shift required. *Med. J. Malays.* **2021**, *76*, 1–4.
- Zaigham, M.; Andersson, O. Maternal and perinatal outcomes with COVID-19: A systematic review of 108 pregnancies. *Acta Obstet. Gynecol. Scand.* **2020**, *99*, 823–829. [CrossRef] [PubMed]
- Di Mascio, D.; Khalil, A.; Saccone, G.; Rizzo, G.; Buca, D.; Liberati, M.; Vecchiet, J.; Nappi, L.; Scambia, G.; Berghella, V.; et al. Outcome of coronavirus spectrum infections (SARS, MERS, COVID-19) during pregnancy: A systematic review and meta-analysis. *Am. J. Obstet. Gynecol. MFM* **2020**, *2*, 100107. [CrossRef]
- Di Toro, F.; Gjoka, M.; Di Lorenzo, G.; De Santo, D.; De Seta, F.; Maso, G.; Risso, F.M.; Romano, F.; Wiesenfeld, U.; Levi-D'Ancona, R.; et al. Impact of COVID-19 on maternal and neonatal outcomes: A systematic review and meta-analysis. *Clin. Microbiol. Infect.* **2021**, *27*, 36–46. [CrossRef]
- De Medeiros, K.S.; Sarmiento, A.C.A.; Costa, A.P.F.; Macêdo, L.T.A.; da Silva, L.A.S.; de Freitas, C.L.; Simões, A.C.Z.; Gonçalves, A.K. Consequences and implications of the coronavirus disease (COVID-19) on pregnancy and newborns: A comprehensive systematic review and meta-analysis. *Int. J. Gynaecol. Obstet.* **2022**, *156*, 394–405. [CrossRef]
- Smith, V.; Seo, D.; Warty, R.; Payne, O.; Salih, M.; Chin, K.L.; Ofori-Asenso, R.; Krishnan, S.; da Silva Costa, F.; Vollenhoven, B.; et al. Maternal and neonatal outcomes associated with COVID-19 infection: A systematic review. *PLoS ONE* **2020**, *15*, e0234187. [CrossRef]
- Simbar, M.; Nazarpour, S.; Sheidaei, A. Evaluation of pregnancy outcomes in mothers with COVID-19 infection: A systematic review and meta-analysis. *J. Obstet. Gynaecol.* **2023**, *43*, 2162867. [CrossRef]
- Mirbeyk, M.; Saghazadeh, A.; Rezaei, N. A systematic review of pregnant women with COVID-19 and their neonates. *Arch. Gynecol. Obstet.* **2021**, *304*, 5–38. [CrossRef]
- Kontovazainitis, C.G.; Katsaras, G.N.; Gialamprinou, D.; Mitsiakos, G. COVID-19 vaccination and pregnancy: A systematic review of maternal and neonatal outcomes. *J. Perinat. Med.* **2023**, 1–17. [CrossRef] [PubMed]
- Juan, J.; Gil, M.M.; Rong, Z.; Zhang, Y.; Yang, H.; Poon, L.C. Effect of coronavirus disease 2019 (COVID-19) on maternal, perinatal and neonatal outcome: Systematic review. *Ultrasound Obstet. Gynecol.* **2020**, *56*, 15–27. [CrossRef] [PubMed]
- Jayaraj, V.J.; Ng, C.W.; Bulgiba, A.; Appannan, M.R.; Rampal, S. Estimating the infection burden of COVID-19 in Malaysia. *PLoS Negl. Trop. Dis.* **2022**, *16*, e0010887. [CrossRef] [PubMed]

15. Hashim, J.H.; Adman, M.A.; Hashim, Z.; Mohd Radi, M.F.; Kwan, S.C. COVID-19 Epidemic in Malaysia: Epidemic Progression, Challenges, and Response. *Front. Public Health* **2021**, *9*, 560592. [CrossRef] [PubMed]
16. Shah, A.U.M.; Safri, S.N.A.; Thevadas, R.; Noordin, N.K.; Rahman, A.A.; Sekawi, Z.; Ideris, A.; Sultan, M.T.H. COVID-19 outbreak in Malaysia: Actions taken by the Malaysian government. *Int. J. Infect. Dis.* **2020**, *97*, 108–116. [CrossRef]
17. Syed Anwar Aly, S.A.; Abdul Rahman, R.; Sharip, S.; Shah, S.A.; Abdullah Mahdy, Z.; Kalok, A. Pregnancy and COVID-19 Pandemic Perception in Malaysia: A Cross-Sectional Study. *Int. J. Environ. Res. Public Health* **2021**, *18*, 5762. [CrossRef]
18. Alene, M.; Yismaw, L.; Assemie, M.A.; Ketema, D.B.; Mengist, B.; Kassie, B.; Birhan, T.Y. Magnitude of asymptomatic COVID-19 cases throughout the course of infection: A systematic review and meta-analysis. *PLoS ONE* **2021**, *16*, e0249090. [CrossRef] [PubMed]
19. Huang, C.; Wang, Y.; Li, X.; Ren, L.; Zhao, J.; Hu, Y.; Zhang, L.; Fan, G.; Xu, J.; Gu, X.; et al. Clinical features of patients infected with 2019 novel coronavirus in Wuhan, China. *Lancet* **2020**, *395*, 497–506. [CrossRef]
20. Wu, Z.; McGoogan, J.M. Characteristics of and Important Lessons from the Coronavirus Disease 2019 (COVID-19) Outbreak in China: Summary of a Report of 72,314 Cases From the Chinese Center for Disease Control and Prevention. *JAMA* **2020**, *323*, 1239–1242. [CrossRef]
21. Wong, L.P.; Alias, H.; Md Fuzi, A.A.; Omar, I.S.; Mohamad Nor, A.; Tan, M.P.; Baranovich, D.L.; Saari, C.Z.; Hamzah, S.H.; Cheong, K.W.; et al. Escalating progression of mental health disorders during the COVID-19 pandemic: Evidence from a nationwide survey. *PLoS ONE* **2021**, *16*, e0248916. [CrossRef]
22. JKJAV (Jawatankuasa Khas Jaminan Akses Bekalan Vaksin COVID-19). Trending Statistics of the National COVID-19 Immunisation Programme. Available online: <https://www.vaksincovid.gov.my/en/> (accessed on 23 April 2022).
23. Jafar, A.; Dambul, R.; Dollah, R.; Sakke, N.; Mapa, M.T.; Joko, E.P. COVID-19 vaccine hesitancy in Malaysia: Exploring factors and identifying highly vulnerable groups. *PLoS ONE* **2022**, *17*, e0270868. [CrossRef]
24. Kalok, A.; Razak Dali, W.; Sharip, S.; Abdullah, B.; Kamarudin, M.; Dasrilayah, R.A.; Abdul Rahman, R.; Kamisan Atan, I. Maternal COVID-19 vaccine acceptance among Malaysian pregnant women: A multicenter cross-sectional study. *Front. Public Health* **2023**, *11*, 1092724. [CrossRef] [PubMed]
25. Wainstock, T.; Yoles, I.; Sergienko, R.; Sheiner, E. Prenatal maternal COVID-19 vaccination and pregnancy outcomes. *Vaccine* **2021**, *39*, 6037–6040. [CrossRef] [PubMed]
26. Mattar, C.N.; Kalimuddin, S.; Sadarangani, S.P.; Tagore, S.; Thain, S.; Thoon, K.C.; Hong, E.Y.; Kanneganti, A.; Ku, C.W.; Chan, G.M.; et al. Pregnancy Outcomes in COVID-19: A Prospective Cohort Study in Singapore. *Ann. Acad. Med. Singap.* **2020**, *49*, 857–869. [CrossRef]
27. Tolu, L.B.; Ezech, A.; Feyissa, G.T. Vertical transmission of Severe Acute Respiratory Syndrome Coronavirus 2: A scoping review. *PLoS ONE* **2021**, *16*, e0250196. [CrossRef] [PubMed]
28. Rodrigues, C.; Baía, I.; Domingues, R.; Barros, H. Pregnancy and Breastfeeding During COVID-19 Pandemic: A Systematic Review of Published Pregnancy Cases. *Front. Public Health* **2020**, *8*, 558144. [CrossRef]

**Disclaimer/Publisher’s Note:** The statements, opinions and data contained in all publications are solely those of the individual author(s) and contributor(s) and not of MDPI and/or the editor(s). MDPI and/or the editor(s) disclaim responsibility for any injury to people or property resulting from any ideas, methods, instructions or products referred to in the content.



MDPI AG  
Grosspeteranlage 5  
4052 Basel  
Switzerland  
Tel.: +41 61 683 77 34

*Life* Editorial Office  
E-mail: [life@mdpi.com](mailto:life@mdpi.com)  
[www.mdpi.com/journal/life](http://www.mdpi.com/journal/life)



Disclaimer/Publisher's Note: The title and front matter of this reprint are at the discretion of the Guest Editors. The publisher is not responsible for their content or any associated concerns. The statements, opinions and data contained in all individual articles are solely those of the individual Editors and contributors and not of MDPI. MDPI disclaims responsibility for any injury to people or property resulting from any ideas, methods, instructions or products referred to in the content.







Academic Open  
Access Publishing

[mdpi.com](http://mdpi.com)

ISBN 978-3-7258-4395-4